frontiers | Research Topics

Identification, function and mechanisms of interferon induced genes associated with viruses

Edited by
Chang Li, Linzhu Ren, Penghua Wang, Fuping You and Jieying Bai

Published in
Frontiers in Immunology

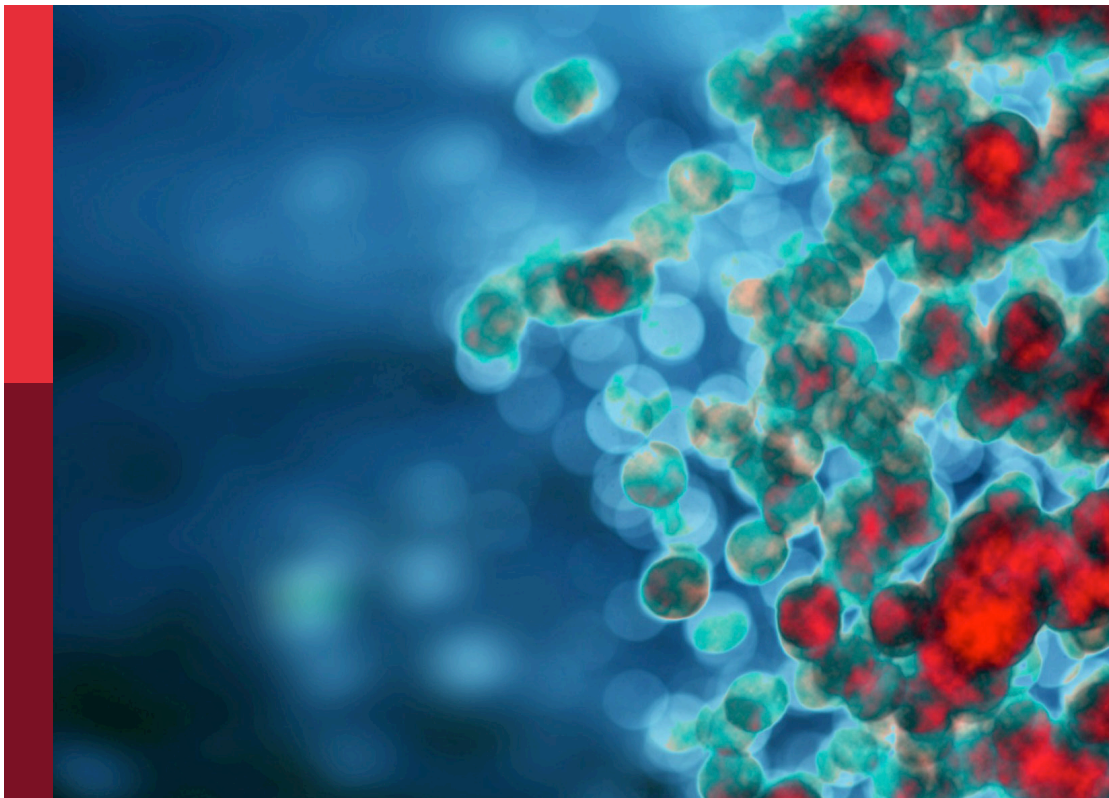

ISSN 1664-8714
ISBN 978-2-83251-469-6
DOI 10.3389/978-2-83251-469-6

About Frontiers

Frontiers is more than just an open access publisher of scholarly articles: it is a pioneering approach to the world of academia, radically improving the way scholarly research is managed. The grand vision of Frontiers is a world where all people have an equal opportunity to seek, share and generate knowledge. Frontiers provides immediate and permanent online open access to all its publications, but this alone is not enough to realize our grand goals.

Frontiers journal series

The Frontiers journal series is a multi-tier and interdisciplinary set of open-access, online journals, promising a paradigm shift from the current review, selection and dissemination processes in academic publishing. All Frontiers journals are driven by researchers for researchers; therefore, they constitute a service to the scholarly community. At the same time, the *Frontiers journal series* operates on a revolutionary invention, the tiered publishing system, initially addressing specific communities of scholars, and gradually climbing up to broader public understanding, thus serving the interests of the lay society, too.

Dedication to quality

Each Frontiers article is a landmark of the highest quality, thanks to genuinely collaborative interactions between authors and review editors, who include some of the world's best academicians. Research must be certified by peers before entering a stream of knowledge that may eventually reach the public - and shape society; therefore, Frontiers only applies the most rigorous and unbiased reviews. Frontiers revolutionizes research publishing by freely delivering the most outstanding research, evaluated with no bias from both the academic and social point of view. By applying the most advanced information technologies, Frontiers is catapulting scholarly publishing into a new generation.

What are Frontiers Research Topics?

Frontiers Research Topics are very popular trademarks of the *Frontiers journals series*: they are collections of at least ten articles, all centered on a particular subject. With their unique mix of varied contributions from Original Research to Review Articles, Frontiers Research Topics unify the most influential researchers, the latest key findings and historical advances in a hot research area.

Find out more on how to host your own Frontiers Research Topic or contribute to one as an author by contacting the Frontiers editorial office: frontiersin.org/about/contact

Identification, function and mechanisms of interferon induced genes associated with viruses

Topic editors

Chang Li — Chinese Academy of Agricultural Sciences (CAAS), China
Linzhu Ren — Jilin University, China
Penghua Wang — University of Connecticut Health Center, United States
Fuping You — Peking University, China
Jieying Bai — Academy of Military Medical Sciences (AMMS), China

Citation

Li, C., Ren, L., Wang, P., You, F., Bai, J., eds. (2023). *Identification, function and mechanisms of interferon induced genes associated with viruses*. Lausanne: Frontiers Media SA. doi: 10.3389/978-2-83251-469-6

The authors declare that the research was conducted in the absence of any commercial or financial relationships that could be construed as a potential conflict of interest.

Table of contents

frontiers | Frontiers in Immunology

TYPE Editorial
PUBLISHED 12 January 2023
DOI 10.3389/fimmu.2022.1126639

OPEN ACCESS

EDITED AND REVIEWED BY
Hiroyuki Oshiumi,
Kumamoto University, Japan

*CORRESPONDENCE
Chang Li
lichang78@163.com

SPECIALTY SECTION
This article was submitted to Molecular Innate Immunity, a section of the journal Frontiers in Immunology

RECEIVED 18 December 2022
ACCEPTED 28 December 2022
PUBLISHED 12 January 2023

CITATION
Ren L, Bai J and Li C (2023) Editorial: Identification, function and mechanisms of interferon induced genes associated with viruses.
Front. Immunol. 13:1126639.
doi: 10.3389/fimmu.2022.1126639

Editorial: Identification, function and mechanisms of interferon induced genes associated with viruses

Linzhu Ren[1], Jieying Bai[2] and Chang Li[3]*

[1]College of Animal Sciences, Key Lab for Zoonoses Research, Ministry of Education, Jilin University, Changchun, China, [2]Non-Human Primate Research Center, Institute of Molecular Medicine, Peking University, Beijing, China, [3]Research Unit of Key Technologies for Prevention and Control of Virus Zoonoses, Chinese Academy of Medical Sciences, Changchun Veterinary Research Institute, Chinese Academy of Agricultural Sciences, Changchun, China

KEYWORDS

interferons, interferon stimulated genes, innate immunity, viral infection, interaction

Editorial on the Research Topic
Identification, function and mechanisms of interferon induced genes associated with viruses

Innate immunity, especially mediated by interferons (IFNs), is regarded as the first line of host immune protection against viral infection. As a strict intracellular parasite, the virus can enter the host cell through its receptor, thus surviving and proliferating in the cell (Figure 1). Since then, viruses and their hosts have been battling incessantly. Over evolutionary time, they have developed sophisticated and complicated regulation interactions (1, 2). The virus is constantly searching for the appropriate host and cells to replicate. Accordingly, the host has evolved strategies to eliminate these "enemies". It uses an array of pattern recognition receptors (PRRs, such as TLRs) to detect unique pathogen-associated molecular patterns (PAMPs), followed by inducing IFNs, including type I interferons (IFNα and IFNβ) and type III interferons (IFNλ1–4). Like marshals, IFNs orchestrate and maneuver the production of hundreds of IFN-stimulated genes (ISGs). As reported, most ISGs exhibit antiviral activities, such as interferon-induced transmembrane proteins (IFITMs), Cholesterol 25-hydroxylase (CH25H), protein kinase R (PKR), etc. (1, 2). Therefore, the ISGs, like generals, are dispatched to the front line of the war to fight and inhibit viral infection in every step, from viral entry, replication, and assembly to egress. However, viruses also evolved multiple mechanisms to evade the inhibition of specific ISGs (Figure 1). To date, accumulating excellent publications have demonstrated the dynamic relationship between virus and host (3). However, many questions still need to be further uncovered.

The goals of this collection are focused on studies of the complex interactions between ISGs and viruses. It is of great significance to elucidate the function and molecular mechanisms of action of known or new ISGs *in vitro* or *in vivo* to provide insights into viral pathogenesis, the scientific basis for novel vaccine design, and new targets for antiviral drug development.

To explore the expression of ISGs against viral infection, Song et al. performed differential transcriptomics. As a result, 90 shared upregulated ISGs were identified in porcine IPEC-J2 cells single or coinfected with porcine epidemic diarrhea virus (PEDV) and/or transmissible gastroenteritis virus (TGEV), among which 27 ISGs have antiviral activities. Furthermore, by

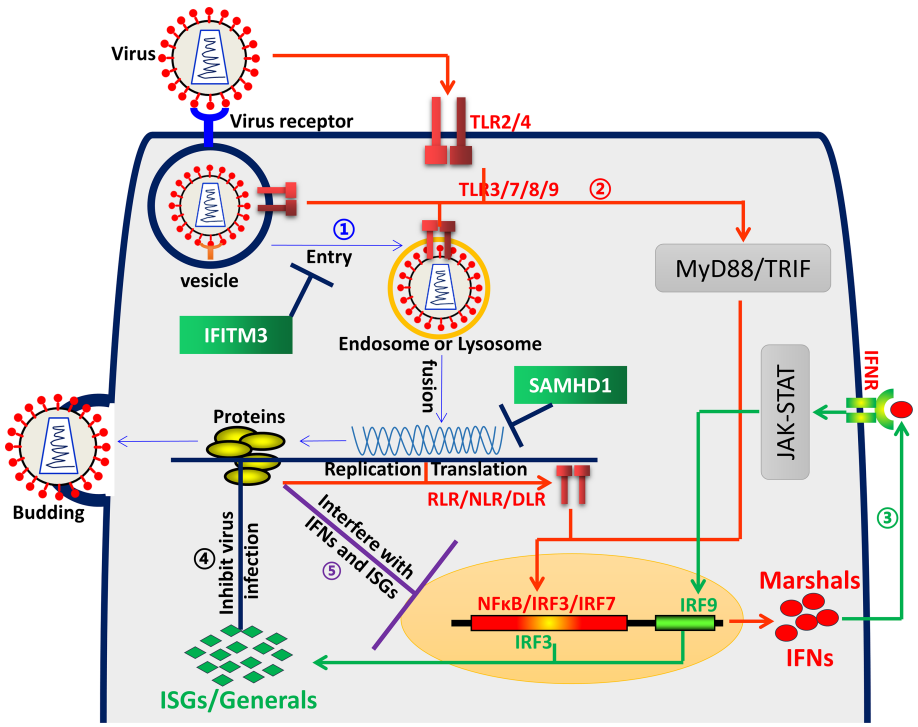

FIGURE 1
Virus and host interaction. ① Blue arrows represent the virus life cycle. A virus first binds to its receptor and entry cells depending on endocytic uptake, then delivers the viral genome into the cytosol and uses a repertoire of cellular processes to complete its replication, assembly and release. ② Red arrows represent the interferon induction process. The host uses an array of pattern recognition receptors (PRRs), such as TLRs, NLRs, etc., to detect unique pathogen-associated molecular patterns (PAMPs), followed by inducing expression of IFNs. ③ Green arrows represent the ISGs induction process. IFNs bind to cell surface receptors (IFNR), triggering a signal transduction cascade, producing hundreds of ISGs. ④ Black lines represent ISGs interfering with virus infection. ISGs delay or inhibit viral infection in different stages, such as entry, viral gene expression and genome amplification, viral particle assembly and egress, etc., with diverse mechanisms. ⑤ Purple lines represent virus antagonism towards ISGs. Viruses have evolved multiple evasion proteins, targeting IFN signal pathways through various sophisticated mechanisms and escaping IFN-ISG-mediated antiviral activities.

analyzing many references and databases, they depicted the activity of ISGs in inhibiting or delaying virus proliferation at different stages of the virus cycle, indicating potential candidate targets for antiviral research. Moreover, swine IFITM3, one of the ISGs, can significantly inhibit the infection of PEDV, TGEV, and vesicular stomatitis virus (VSV) in different cells, indicating that it has broad-spectrum antiviral activity (Song et al.).

In addition, Ding et al. conducted a transcriptome analysis of primary macrophages induced by IFN-γ, a type II interferon that exhibits not only antibacterial but also antiviral activity in the Chinese sturgeon (*Acipenser sinensis*). A total of 4004 differential expression genes (DEGs) were enriched in the GO annotation, many of which were involved in immune-related processes. KEGG enrichment analysis showed that six signaling pathways are related to interferon regulation, emphasizing the importance of IFN-γ. Wang et al. evaluated the proteome in lung tissues of a cynomolgus monkey model in the early stage of severe acute respiratory syndrome coronavirus 2 (SARS-CoV-2) infection. They identified 44 proteins from all 194 significantly altered proteins, most encoded by ISGs. These results strongly indicate that IFN-ISG-mediated signaling pathways are essential in host resistance to viral infection. Besides, Dang et al. also established a high-through screening type I interferon-inducible antiviral effectors platform based on CRISPR/Cas9 knockout library with 1908 sgRNAs targeting 359 ISGs. Using VSV-eGFP as a model virus, a subset of the highest-ranking candidates, including known or novel host factors, were identified, demonstrating useful and promising methods to screen novel ISGs against a panel of porcine viruses.

As mentioned above, research on the functions and mechanisms of ISGs is crucial. Lang et al. provided a macroscopic overview of the characteristics, expressions, and mechanisms of ISGs in the central nervous system (CNS) and neurological diseases, including neurological inflammation, neuropsychiatric disorders, and neurodegenerative diseases, during viral infection. The authors also summarized up-to-date progress on viral infection in neurological disorders, exhibiting the broad promise application vision and high commercial value of ISGs as potential clinical biomarkers and therapeutic targets. Furthermore, IFITM3, a well-studied ISG, can inhibit a diverse range of pathogenic virus infections *in vivo* or *in vitro*. But the precise antiviral mechanisms remain unclear. Wen et al. reviewed the latest progress on the antiviral mechanism of IFITM3, the regulation mechanism by four post-translational modifications (PTMs), especially S-palmitoylation modification, providing helpful information for understanding IFITM3 antiviral mechanism and aiding in the design of therapeutics. An et al. reported that sterile alpha motif and histidine-aspartate domain-containing protein 1 (SAMHD1), another ISG, inhibited lipid bio-metabolic pathway to suppress flavivirus infection. Further studies showed that SAMHD1 could negatively regulate the expression of sterol regulatory element binding protein (SREBP1) and the formation of histidine aspartic acid-containing domain (HD), two critical factors associated with the lipid bio-metabolic

pathway. These results revealed a novel mechanism of SAMHD1 and laid a new target for targeting lipid bio-metabolic pathway against the *Flaviviridae* family and other lipid-dependent viruses.

In summary, more and more antiviral ISGs have been discovered and studied with new technologies, such as unbiased screening approaches, differential transcriptome and proteome, affinity chromatography-mass spectrometry, proximity interactome, etc. The articles on this Research Topic provided new insights into the recent advances in ISGs. However, for most ISGs, the exact mechanisms of virus inhibition have not been clarified. Additionally, the vital importance of evaluating the effectiveness and safety of these ISGs *in vivo* models or human studies is highly summoned beyond mechanism. It may take more effort and time to get there, but it is hoped that many scientists will pay more attention to this field, solving and unveiling the most sophisticated antiviral defense systems to apply these ISGs in transgenic animal breeding or gene therapy as soon as possible.

Author contributions

LR, JB, and CL wrote the draft and revised it critically for important intellectual content. All authors contributed to the article and approved the submitted version.

Funding

This work was supported by the National Key Research and Development Program of China [No. 2021YFD1801103], the National Natural Science Foundation of China [No. 31972719], and the CAMS Innovation Fund for Medical Sciences [2020-12M-5-001].

Conflict of interest

The authors declare that the research was conducted in the absence of any commercial or financial relationships that could be construed as a potential conflict of interest.

Publisher's note

References

1. Borden EC, Sen GC, Uze G, Silverman RH, Ransohoff RM, Foster GR, et al. Interferons At age 50: Past, current and future impact on biomedicine. *Nat Rev Drug Discovery* (2007) 6:975–90. doi: 10.1038/nrd2422

2. Majdoul S, Compton AA. Lessons in self-defence: Inhibition of virus entry by intrinsic immunity. *Nat Rev Immunol* (2022) 22:339–52. doi: 10.1038/s41577-021-00626-8

3. Chen N, Zhang B, Deng L, Liang B, Ping J. Virus-host interaction networks as new antiviral drug targets for iav and sars-Cov-2. *Emerg Microbes Infect* (2022) 11:1371–89. doi: 10.1080/22221751.2022.2071175

frontiers in Immunology

ORIGINAL RESEARCH
published: 17 March 2022
doi: 10.3389/fimmu.2022.854689

Transcriptome Sequencing Reveals the Antiviral Innate Immunity by IFN-γ in Chinese Sturgeon Macrophages

Guangyi Ding[1†], Chuwen Zheng[1†], Bei Wang[2], Lifeng Zhang[1], Dan Deng[1], Qian Li[1], Huizhi Guo[1], Shuhuan Zhang[3] and Qiaoqing Xu[1,2]*

[1] Institute of Chinese Sturgeon Disease, Yangtze University, Jingzhou, China, [2] Guangdong Provincial Key Laboratory of Pathogenic Biology and Epidemiology for Aquatic Economic Animals, Guangdong Ocean University, Zhanjiang, China, [3] Sturgeon Healthy Breeding and Medicinal Value Research Center, Guizhou University of Traditional Chinese Medicine, Guiyang, China

To further study the biological function of interferon-gamma (IFN-γ) in the Chinese sturgeon (*Acipenser sinensis*), we conducted a transcriptome analysis of primary macrophages induced by IFN-γ using Illumina sequencing technology. We obtained 88,879 unigenes, with a total length of 93,919,393 bp, and an average length of 1,057bp. We identified 8,490 differentially expressed genes (DEGs) between the untreated and IFN-γ-treated macrophages, with 4,599 upregulated and 3,891 downregulated. Gene ontology (GO) analysis showed that 4,044 DEGs were enriched in the biological, cellular components, and molecular function categories. Kyoto Encyclopedia of Genes and Genomes (KEGG) identified 278 immunity-related pathways enriched for the DEGs. According to the GO enrichment results, eight key immunity-related genes were screened for verification using qPCR. Results indicate that IFN-γ can activate macrophage Interferon Regulatory Factors (IRFs) and type I interferon (IFN-I), activate RIG-I-like and Toll-like receptor-related pathways, and improve the antiviral ability of macrophages in Chinese sturgeon.

Keywords: ***Acipenser sinensis*, IFN-γ, Illumina sequencing, immunoregulation, antiviral ability**

OPEN ACCESS

Edited by:
Chang Li,
Chinese Academy of Agricultural Sciences (CAAS), China

Reviewed by:
Li Shun Bob,
Institute of Hydrobiology (CAS), China
Chunfu Zheng,
University of Calgary, Canada

***Correspondence:**
Qiaoqing Xu
xuqiaoqing@163.com

[†]These authors have contributed equally to this work and share the first authorship

Specialty section:
This article was submitted to Molecular Innate Immunity, a section of the journal Frontiers in Immunology

Received: *14 January 2022*
Accepted: *21 February 2022*
Published: *17 March 2022*

Citation:
Ding G, Zheng C, Wang B, Zhang L, Deng D, Li Q, Guo H, Zhang S and Xu Q (2022) Transcriptome Sequencing Reveals the Antiviral Innate Immunity by IFN-γ in Chinese Sturgeon Macrophages. Front. Immunol. 13:854689. doi: 10.3389/fimmu.2022.854689

INTRODUCTION

Interferon-gamma (IFN-γ) belongs to the type II interferon (IFN-II) family. IFN-γ is secreted by various cells, such as natural killer (NK cells), NK T cells, macrophages, bone marrow monocytes, T helper type 1 (Th1) cells, cytotoxic T lymphocytes (CTLs), and B cells (1). These cells are functionally divided into two groups that participate in innate or adaptive immune responses. IFN-γ production by NK cells and macrophages might play an important role in early defense against infection, while in adaptive immune responses, IFN-γ is mainly produced by lymphocytes and secreted by Th1 cells.

In contrast to mammals, in bony fish there are two types of IFN-γ. IFN-γ was found in Fugu (*Takifugu rubripes*) by (2), followed by IFN-γrel was described in zebrafish (3). The gene encoding Interferon-gamma related (IFN-γrel) might have been formed by tandem gene replication (4). Although IFN-γrel lacks a classical nuclear localization signal (NLS), it shares many characteristics

with IFN-γ in terms of its protein structure, cell distribution, and immune response. Among all species with duplicate IFN-γ genes, the IFN-γrel gene has more structural similarities with known vertebrate IFN-γ genes. IFN-II gene is highly conserved in most fish and mammals, with a genetic structure of four exons and three introns, and several successive codons for arginine or lysine (5). IFN-γ and IFN-γrel have been identified in at least 20 species of fish, such as Fugu (*Takifugu rubripes*), zebrafish, grass carp (6) and *Anguilla japonica* (7). The sequence homology of IFN-γ in fish and mammals is generally low; however, the tertiary structure of IFN-γ appears to be conserved from fish to mammals and the gene is genetically homologous to higher vertebrates IFN-γ genes.

Belonging to the cytokine receptor family B (CRFB), IFN-γ receptors (IFN-γR) are very conserved in terms of gene structure and loci, as well as their protein functional domains or motifs (8). IFN-γR is composed of two transmembrane proteins, IFN-γR1 and IFN-γR2. IFN-γR1 is a ligand-binding chain, and IFNyR2 is a signal transduction chain. IFN-γR2 has a JAK-2 docking site P263PSIPLQIEEYL274 motif. IFN-γR1 possesses two functionally conserved residue sequences: L266PKS269 binding to JAK-1 and Y440DKPH444 interacting with STAT1 within the receptor's intracellular domain (9). Unlike mammals, there are two copies of IFN-γR1 in bony fish, CRFB17(IFNGR1-1) and CRFB12(IFNGR1-2). The genes encoding the two IFN-γR1 receptors are located at different loci and exhibit conserved collinearity compared to their counterparts in other vertebrates. Two isoforms of IFN-γR1, called IFN-γR1-1and IFN-γR1-2, were described in goldfish and zebrafish, tissue expression analysis showed that IFN-γR1-1 expression was significantly higher than that of IFN-γR1-2 (10). In goldfish, IFN-γR1-1 is highly expressed in the kidneys and spleen, but IFN-γR1-2 is highly expressed in the brain. Microscopic binding studies showed that IFN-γ1 binds to IFN-γR1-1, but not to IFN-γR2, and IFN-γR1-2 preferentially binds to IFN-γrel (11). IFN-γR2, also known as CRFB6, has been identified in grass carp, rainbow trout, and Dabry's sturgeon (12). In vertebrates, including humans, IFN-γR2 is encoded by a single-copy gene, linked to transmembrane protein 50B (TMEM50B) at the conserved site of class II cytokine receptors in vertebrates (9). IFN-γ signaling is caused by the binding of the active form of IFN-γ (a non-covalent homodimer) to a receptor containing complexes (IFN-γR1, IFN-γR2) that activate the intracellular Janus kinase/signal transducer and activator of transcription (JAK/STAT) signaling pathway and initiate the expression of multiple genes in the nucleus (10, 13).

IFN-γ is a typical Th1 cytokine that helps to activate macrophages and promote the Th1 response. Th1 immunity is an important immune defense mechanism against intracellular pathogens such as viruses and bacteria. IFN-γ also induces apoptosis, especially during viral infection, and inhibits cell proliferation (14–16). The antiviral function of IFN-γ has been explored in various fish, and can inhibit the proliferation of a variety of viruses in cells. For example, intramuscular injection of an IFN-γ expression plasmid in turbot (*Scophthalmus maximus*) inhibited the proliferation of viral hemorrhagic septicemia virus, VHSV, *in vivo* and effectively reduced mortality and the expression levels of a large number of pro-inflammatory factors and IFN-I is induced (17). In the Chinese black porgy (*Acanthopagrus schlegelii*), infection with red-spotted grouper nervous necrosis virus (RGNNV) not only induces IFN-γ expression in most tissues *in vivo*, but also significantly induces IFN-γ expression *in vitro*.

Meanwhile, Overexpression of IFN-γ in AsB cells (*Acanthopagrus schlegelii* brain cell) can effectively inhibit RGNNV proliferation in AsB cells and induce Mx1 and ISG15 expression (18, 19). In crucian carp, exposure of crucian carp Hematopoietic necrosis virus (CHNV) directly to infected gill tissue can induce IFN-γ significantly expression in gill and kidney and inhibit CHNV virus replication in gill and kidney (20). In the Chinese sturgeon, recombinant IFN-γ could effectively inhibit the pathological effect in endothelial progenitor cells (EPCs) infected with Spring viremia of carp virus (SVCV) and inhibit the expression of the P, G, and N genes of SVCV (21).

However, the mechanism of IFN-γ regulating the immune system of *Acipenser sinensis* remains unclear. This study used transcriptome sequencing to analyze differential gene expression in macrophages stimulated by IFN-γ. We found that IFN-γ significantly upregulated RIG-I and Toll-like receptor-related pathways and activated macrophages to form antiviral status.

MATERIALS AND METHODS

Experimental Material

Chinese sturgeons (30–500g) were provided by the Yangtze River Fisheries Research Institute (Taihu Lake, Jingzhou, China). Recombinantly expressed Chinese sturgeon IFN-γ protein was preserved in our laboratory (21).

Separation of Primary Macrophages

Chinese sturgeon was euthanized by MS-222, then the body surface of a Chinese sturgeon in a good growth state was swabbed with alcohol, and the head kidney and middle kidney were dissected. The excised kidneys were rinsed three times with 1 × phosphate-buffered saline (PBS). After cleaning, the kidneys were placed in 75% medical alcohol for 45 s. The tissues were ground and filtered into a 15 mL centrifuge tube. M199 complete medium (Invitrogen, Carlsbad, CA, USA) was added while grinding. After grinding, tissues were centrifuged at 500 × *g* for 15 min, and the supernatant was discarded. The centrifugation step was repeated twice, and the cells were resuspended in M199 complete medium. Three new 15 mL centrifuge tubes were taken, and 4 mL of 52% Percoll (Solarbio, Beijing, China) and 4 mL of 34% Percoll were added successively. Finally, the cell suspension was slowly added to the upper layer of 34% Percoll. The cells were centrifuged at 500 × *g* at room temperature for 50 min (with slow increases and decreases in the centrifuge speed). After centrifugation, the cells formed six layers, with the macrophages forming layer four. The supernatant was removed, and the fourth layer was slowly extracted into a new

15 mL centrifugation tube. M199 medium (10 mL) was added, the cells were centrifuged at 500 × *g* for 15 min, the supernatant was discarded, and M199 (containing 10% fetal bovine serum (FBS; Invitrogen)) was added for re-suspension. The cells were successively divided into six-well plates and cultured normally. When the cell coverage reached 80% and growth appeared normal, the experimental groups were treated with 100 ng/mL IFN-γ in PBS (labeled as AM 1, 2, and 3, respectively), and the control groups were treated with an equal volume of PBS (labeled as AMC 1, 2, and 3, respectively); the cells were collected after 24 h of induction.

Total RNA Extraction and Quality Detection

The cells with a coverage rate of more than 80% of the 25 cm^2 cell culture flask and in a good growth state were washed three times with 1 × PBS, the residual liquid was discarded, 1 ml of Trizol (Invitrogen) was added for lysis, and the cells were mixed by aspiration into a 1.5 ml RNase-free EP tube (Axygen, SFO, USA), and left at room temperature for 5 min to fully lyse. Then, 200 μl of chloroform (Sinopharm Chemical Reagent Co. LTD, Shenzhen, China) was added, the mixture was shaken vigorously for 30 s to mix the aqueous phase and organic phases left to stand at room temperature for 5 min, after centrifugation for 10 min at 10000 × *g* at 4°CC, the samples were divided into three layers (upper layer of RNA, middle layer of protein, and lower layer of cell debris). The upper aqueous phase was carefully removed into a new 1.5 ml RNase-Free EP tube, and pre-cooled isopropyl alcohol (Sinopharm Chemical Reagent Co. LTD) was added to the tube. After gentle and full mixing, the tube was stored at -20°CC for 15 min. The supernatant was discarded after centrifugation at 10000 × *g* at 4°CC for 10 min. Pre-cooled 75% ethanol (Sinopharm Chemical Reagent Co. LTD) was added to wash the precipitate 1-2 times (with centrifugation for 10 min at 7500 × *g* and 4 °CC; after adding 75% ethanol, it was only necessary to gently reverse the EP tube to precipitate and float the RNA). Put the RNA precipitation into the ultra-clean workbench, turn on the fan and blow for 2-3 min, so that the alcohol can be quickly swept away. DiethyI pyrocarbonate (DEPC; Takara, Dalian, China) water was added to dissolve the precipitate. The RNA concentration and quality in the samples were determined using a spectrophotometer and agarose gel electrophoresis, and the RNA was stored at −80 °CC for later use. High-quality RNAs were used to synthesize cDNA for quantitative real-time PCR.

Construction of cDNA Libraries

After DNA digestion using DNase, the mRNA was enriched using Oligo(dT) magnetic beads. The fragmentation buffer was added to break the mRNA into short fragments. Reverse transcription PCR and random six-base primers were used to generate first-strand cDNA using the fragmented mRNA as a template, followed by a second-strand synthesis reaction to produce double-stranded cDNA, which was purified using PCR cleanup and gel extraction kits (Takara). After end repair and the addition of poly(A), the short fragments were linked with sequencing adapters, PCR amplification was performed after the fragment size was selected. After the constructed libraries were quantified with Agilent 2100 Bioanalyzer (Agilent, Santa Clara, CA, USA), they were sequenced using Illumina HiSeq 2500 sequencer (Illumina, San Diego, CA, USA) to produce 125 bp or 150 bp paired-end reads.

Data Preprocessing, Quality Control, and Assembly

Raw reads in the FASTA format sequences were subjected to quality filtration to obtain high-quality reads for subsequent analysis. Firstly, Trimmomatic software (22) was used for quality control and removal of adapters. Low-quality bases and N bases were filtered out to obtain high-quality clean reads. Trinity (version: 2.4) (23) was used to splice the clean reads to produce transcript sequences using the paired-end method. The longest transcript was selected as a unigene according to their sequence similarity and length. Then, CD-HIT software (24) clustering was used to remove redundancies to obtain a final set of unigenes, which was used as the reference set for subsequent analysis.

Unigene Functional Annotation

Using BLASTX (http://www.ncbi.nlm.nih.gov/BLAST/) with an E-value threshold of 1e-5 performed the unigene functional annotation. The databases being utilized include non-redundant (NR) (http://www.ncbi.nlm.nih.gov), Clusters of Orthologous Groups (COG)/eukaryotic Orthologous Groups (KOG) (http://ftp://ftp.ncbi.nih.gov/pub/COG/KOG/), and Swiss-Prot protein (http://www.expasy.ch/sprot) databases. Based on the result of Swiss-Prot, we mapped Swiss-Prot IDs to gene ontology (GO) terms to obtain GO annotation of the unigenes. Finally, the unigenes were subjected to Kyoto Encyclopedia of Genes and Genomes (KEGG) (25) using diamond software (26), and HMMER (27) was used to compare the Pfam database (28) for functional analysis of unigene.

Unigene Quantification, Differential Unigene Screening, Functional Enrichment, and Cluster Analysis

The FPKM (fragments per kilobase of transcript per million mapped reads) and count values of the unigene were analyzed using bowtie2 (29) and eXpress (30). The DEGs were identified using the DESeq functions estimate Size Factors and nbinom Test (31). DEGs (P-value < 0.05 and foldchange > 2) were picked out, and DEGs GO enrichment and KEGG pathway enrichment analyses were performed. Unsupervised hierarchical clustering of the DEGs was carried out, and their expression patterns among different samples were displayed in the form of heat maps.

Identification and Expression Analysis of Immunity-Related Genes

The transcript levels of eight immunity-related genes (*As*IFN-e1-3, *As*IFN-γ, IRF1, 2, 3, and 7) were screened using quantitative

real-time RT-PCR (qPCR) for verification. The specific primers are shown in **Supplementary Table 1**.

RESULTS

Transcriptome Data Statistics and *De Novo* Assembly

Raw reads were obtained by high-throughput sequencing, and 268,120,424 and 280,376,796 reads were detected in the experimental group (AM 1, 2, and 3) and the control group (AMC 1, 2, and 3), respectively. After further quality control and filtering of raw reads, high-quality clean reads were obtained by Trimmomatic. There were 272,115,614 reads in the AM group and 273,895,990 reads in the AMC group. The average sequences numbers in the AM and AMC group were 90,705,204 and 210,075,147, respectively. The Q30 of the original data for each sample was 92.99-93.28%, the effective data volume was 12.00-13.40 G, and the average GC content was 46.29% (**Supplementary Table 2**). The filtered clean reads were spliced into 88,879 unigenes, with a total length of 93,916,393 bp, a longest length of 26,838 bp, an average length of 1,057 bp, and an N 50 value of 1,727 bp (**Supplementary Table 3**). The main length distribution was 23,506 (301~400 bp), 13,380 (401~ 500 bp) and 12,525 (>2,000 bp) (**Figure 1**). The above data indicated that the library of primary macrophages induced by Chinese sturgeon IFN-γ is reliable and can be further studied and analyzed.

Unigene Function Annotation

The database annotation results of the unigene were as follows: 27679 (31.14%) genes were annotated to the NR database; 23190 (26.09%) genes were annotated to the Swiss-Prot database; 16011 (18.01%) genes were annotated to the KEGG database; 17081 (19.22%) genes were annotated to the KOG database; 25138 (28.28%) genes were annotated to the eggNOG database; 20900 (23.52%) genes were annotated to the GO database; and 16700 (18.79%) genes were annotated to the Pfam database (**Figure 2A** and **Table 4**). The annotation distribution of NR species showed that the similarity between Chinese sturgeon and *Lepisosteus oculatu* in terms of genomic homology and phylogenetic analysis was the highest, which was consistent with the homology rate of 38.42% of *Lepisosteus oculatus* in this experiment. *Latimeria chalumnae*, *Scleropages formosus*, and Chinese sturgeon all belong to the Osteichthyes, which occupy an extremely important position in the evolutionary history from fish to vertebrates, the homology rates between the two species and the Chinese sturgeon were 4.12% and 5.46%, respectively. Chinese sturgeon, *Cyprinus carpio*, *Salmo salar*, and zebrafish belong to the Actinopterygii, among which, *Cyprinus carpio*, *Salmo salar* and Chinese sturgeon are similar to each other and have a migratory life habit. As a model organism, zebrafish has a higher genetic homology with human, up to 87% (**Figure 2B**). Therefore, the homology of Chinese sturgeon with *Cyprinus carpio*, *Salmo salar* and *Oncorhynchus mykiss* was 1.57%, 1.23%, and 1.61%, respectively. In addition, 40.07% of unigene were homologous to other vertebrate genes.

Analysis of Differentially Expressed Genes

A total of 8490 DEGs were screened out. The distribution of DEGs was represented by a volcano map (**Figure 3A**). Among the DEGs between the experimental group (AM) compared with the control group (AMC) 4599 were upregulated, 3891 were downregulated, and with false discovery rate value of $P < 0.05$ & $|\log_2 FC| > 1$ (**Figure 3B**). There may be differences between different groups under the same experimental conditions. Therefore, we analyzed the correlations among the DEGs in the three replicates in each group, which showed a strong correlation among the AM1, 2, and 3, and most of the genes with high expression were clustered in the same branch. AMC1 and AMC3, but not AMC2, showed very strong correlation in the control group. In addition, the correlation between genes in the AM group and those in the AMC group

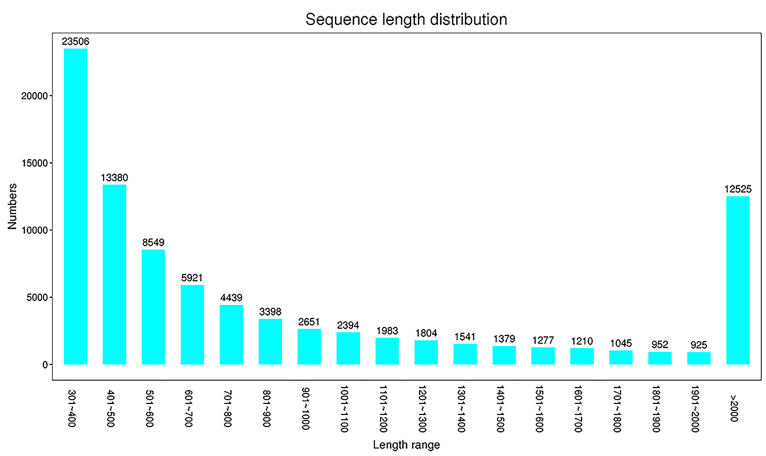

FIGURE 1 | Unigene Length distribution. X-axis is the sequence length range, Y-axis is the number.

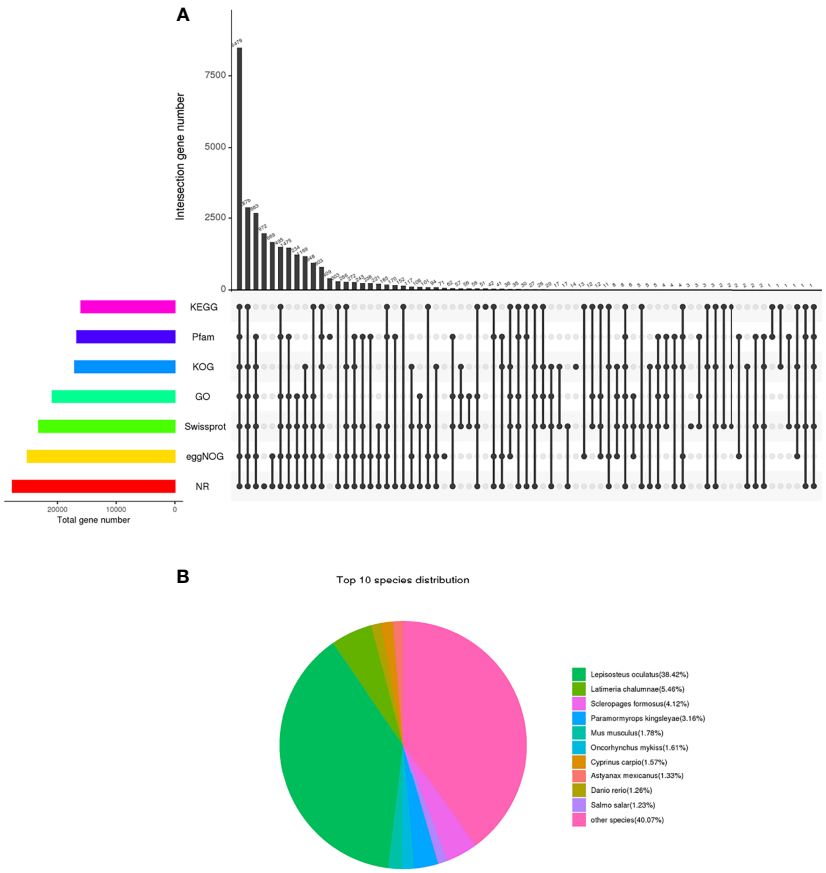

FIGURE 2 | The database annotation results of the unigene. **(A)** Venn diagram of each database annotation. the number on the top of the bar represents the result of the intersection of the databases with black dots in the following matrix, and the column on the left represents the number of unigene annotated in all databases. **(B)** Species comparison distribution of unigenes in NR database.

was low and the difference was large (**Figure 3C**), indicating that the screened DEGs were reliable and convincing.

GO Enrichment Analysis of DEGs

After the DEGs were selected, GO enrichment analysis was performed to determine which biological processes were mainly affected by the DEGs. 4004 DEGs were detected in the GO enrichment, 1300 GO annotations were obtained, 830 were upregulated, and 470 were downregulated. The unigene annotated by the GO database can be divided into biological processes (biological processes, BP), Cellular Component (CC), molecular function (MF). The GO level 2 results were further divided into 64 subcategories. BP was divided into 23 subcategories, among which the three categories with the largest number of DEGs were: cellular process (77.54%), regulation of biological process (53.61%), metabolic process (53.08%); CC was divided into 20 subgroups, and the components with the largest proportion of DEGs were: cell (85.69%), cell part (85.38%), organelle (62.69%), membrane (42.23%); MF was divided into 21 subtypes, and the three most important ones were: binding (71.92%), catalytic activity (41.69%), molecular sensing activity (41.69%) (**Figure 4A**). The differences between the enriched DEGs and all unigenes in BP, CC, and MF were compared and analyzed to maximize the visualization of the regulatory effect of Chinese sturgeon IFN-γ on the transcription of Chinese sturgeon in GO enrichment function annotation. In BP, the expression rate of DEGs enriched in biological functions such as cell process, metabolic process, biological regulatory process, and stimulus-response was greater than 50%; in CC, the differential expression rate of DEGs in cells, cell parts and organelles was the highest; in MF, the expression rate was the highest only in the binding process (**Figure 4B**). The results indicated that Chinese sturgeon IFN-γ is involved in the three biological processes of BP, CC, and MF, and had a certain immune regulation effect in all three categories.

KEGG Enrichment Analysis of the DEGs

KEGG is a major public database related to pathways. Pathway entries with significantly enriched unigenes were found through Pathway analysis of DEGs, providing clues as to which cell pathways might be related to the differences in unigene expression between the samples. In this study, 16011 unigenes

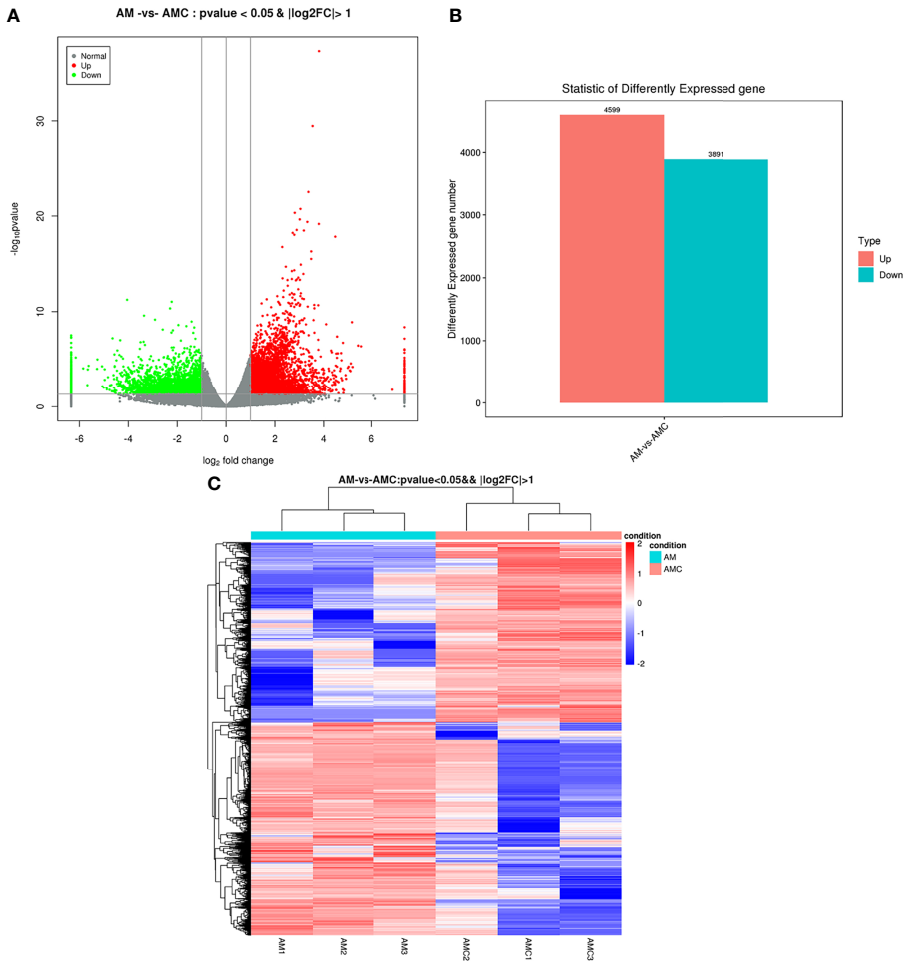

FIGURE 3 | Analysis results of differentially expressed genes. **(A)** Distribution of DEGs volcanoes. X-axis is the display of log2 foldchange, Y-axis is -$\log_{10}$*P*-value; Red represents upregulation unigene, green represents downregulation unigene, gray represents non differentiation unigene. **(B)** Statistical chart of the number of DEGs. The abscissa is DEGs, and the ordinate is the number of difference genes; Red represents upregulation unigene, green represents downregulation unigene. **(C)** Clustering diagram of different groups. Red indicates high expression of unigene and blue indicates low expression of unigene.

annotated by KEGG were combined, 1300 DEGs were enriched for 278 pathways, 222 pathways were significantly downregulated, and 248 pathways were significantly upregulated. The top 20 pathways with the largest number of DEGs were screened. The -$\log_{10}$ *P*-value corresponding to each entry was sorted from large to small (**Figure 5A** and **Supplementary Table 5**). Among them, six signaling pathways related to interferon regulation were identified: The RIGI-like receptor signaling pathway (35 unigenes) and Cytosolic DNA-Sensing Pathway (28 unigenes), NOD-like receptor signaling pathway (41 unigenes), Toll-like receptor signaling pathway (TLR) (27 unigenes), and the JAK-STAT signaling pathway (16 unigenes). Pathways enriched for DEGs and all unigenes at KEGG Level 2 level were divided into six categories: Organic systems (5297, 57.05%), metabolism (3027, 32.59%), human diseases (7187, 77.4%), genetic information processing (2229, 24.01%), environmental information processing (3277, 35.3%), cellular processes (3021, 32.54%) (**Figure 5B**). In terms of the expression trends of the unigenes, 143 unigenes were upregulated in human infectious diseases, followed by 131 unigene that were upregulated in the immune system of the organic system, and 58 unigenes were downregulated in signal transduction in environmental information processing (**Figure 5C**). These results indicated that the recombinant IFN-γ protein of Chinese sturgeon could regulate the immune pathways of Chinese sturgeon to exert its related biological functions, and these data provide a certain theoretical basis for further in-depth studies of the mechanism of IFN-γ related to immune regulation of the Chinese sturgeon.

Identification and Expression Analysis of Immunity-Related Genes

To further analyze the function of IFN-γ in Chinese sturgeon and verify the transcriptome data, eight immunity-related genes were screened from the transcriptome, namely, *As*IFN-e1, 2, 3, *As*IFN-γ, IRF1, 2, 3, and 7, and analyzed using qPCR. The results showed

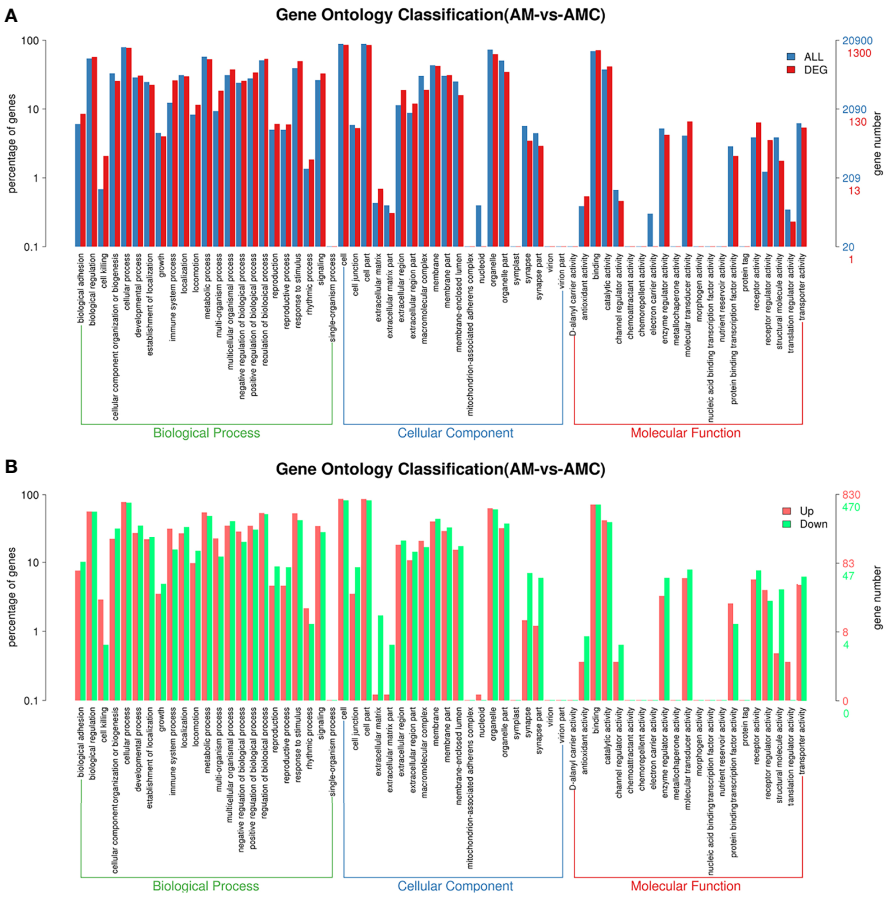

FIGURE 4 | Differential unigenes were analyzed by GO enrichment. **(A)** Comparison of distribution of differentially expressed unigene and all unigene at GO level2. Blue represents all unigene enriched GO level 2 items, red represents differential unigene enriched GO level 2 items, the horizontal axis represents the items name, and the vertical axis represents the number and percentage of unigene of corresponding items. **(B)** Comparison of upregulation and downregulation of unigene at GO level 2. Red indicates up regulation of go level 2 items enriched by DEGs, blue indicates down regulation of go level 2 items enriched by DEGs, the horizontal axis is the item name, and the vertical axis is the number and percentage of unigene of corresponding items.

that IFN-γ could induce the expression of IRF1, 2, 3, and 7 at 1, 8, and 24 h with the same significantly upregulated trend as observed in the transcriptome data. From 1 h to 24 h, their expression increased to a maximum of 20.75 times, 2.76 times, 8.12 times, and 20.63 times, respectively (**Figure 6A**). *As*IFN- e1, 2, 3, and *As*IFN-γ were induced in Chinese sturgeons. Except for *As*IFN-e1, the expression of *As*IFN-e2, 3, and *As*IFN-γ showed the same upregulation trend as observed in the transcriptome data. The expression levels of *As*IFN-e1, 2, 3, and *As*IFN-γ were all lower at 1 h; however, IFN-e1, 2, 3, and IFN-γ expression levels were all upregulated to the highest degree at 24 h, by 6.25 times, 7.84 times, 1.69 times, and 4.88 times respectively (**Figure 6B**); In addition, qPCR results were similar to the up-regulation multiple of transcriptome differential genes (**Figure 6C**). The above results indicated that *As*IFN-γ induced primary macrophages of Chinese sturgeons and had strong immunomodulatory effects on interferon (*As*IFN-e1,2,3 and *As*IFN-γ) and interferon regulatory factors (IRF1, 2, 3, and 7). The qPCR results were similar to the transcriptome data, within the range of allowable error, demonstrating the transcriptome data reliability and validity.

DISCUSSION

Accurately describing the signaling pathways that cause gene expression and activation, and fully exploring the structure, classification, and function of the transcriptome information. As an effective technique to study gene expression and analyze differentially expressed genes and their functions, high-throughput sequencing has been used widely to study a variety of vertebrates, such as soiny mullet (*Liza haematocheila*), grass carp (*Ctenopharyngodon idella*), orange-spotted grouper (*Epinephelus coioides*), and Siamese fighting fish (*Betta Splendens*) (32–35). Based on the protection of genetic resources of the endangered species Chinese sturgeon and the deep exploration of the biological function of IFN-γ in Chinese sturgeon, this study described the effect of IFN-γ on primary macrophages of Chinese sturgeon at 24 h,

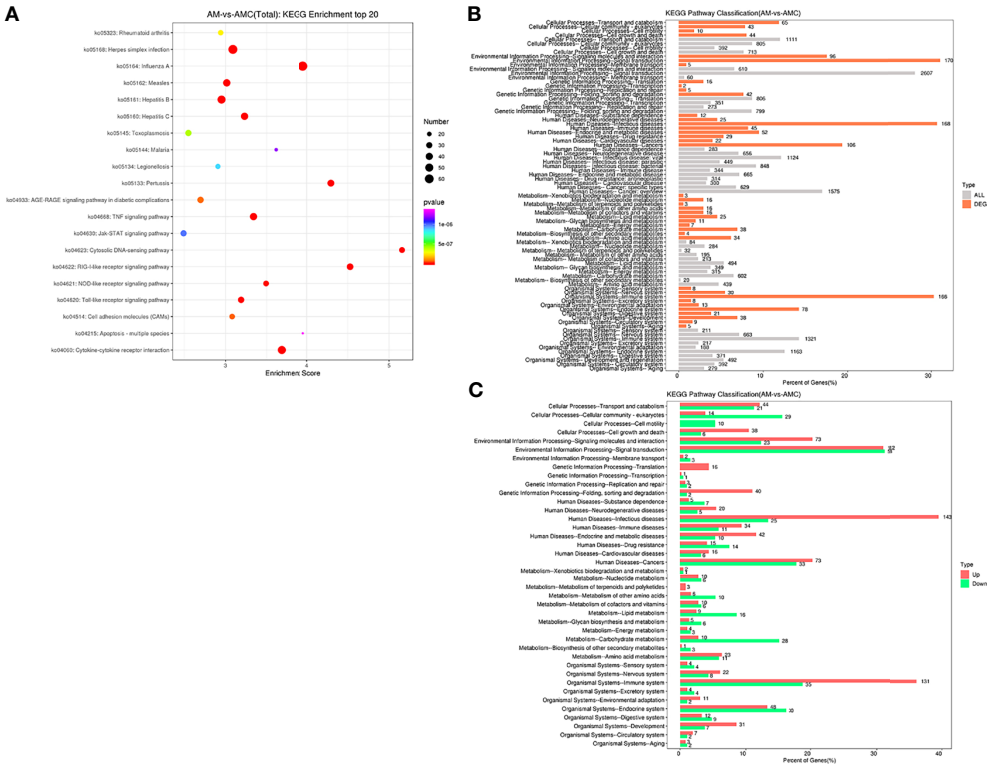

FIGURE 5 | Enrichment analysis of differential gene Unigene. **(A)** KEGG enrichment top20 pathway bubble chart. The X-axis is the enrichment score, the bubble size indicates the number of unigene contained in the item, and the color of the bubble from purple to red indicates *P*-value. **(B)** Distribution comparison of DEGs and all unigene at KEGG level 2. The vertical axis represents the name of level 2 pathway, and the number to the right of the column represents the number of DEGs annotated to that level 2 pathway. **(C)** Distribution of upregulated and downregulated unigene at KEGG level 2.

and analyzed the expression changes of IFN-γ-related, immunity-associated genes and pathways, which is crucial to understanding the immune mechanism of IFN-γ.

Through transcriptomic analysis, 888879 unigene were obtained, 8490 DEGs were screened, and 4004 DEGs were enriched in the GO analysis, many of which were involved in immune-related processes, such as immune response, innate immune response, regulation of apoptosis process, inflammatory response, cytokine-mediated signaling pathway, and viral defense response. These results indicate that IFN-γ has strong immune stimulation or immunomodulatory ability on macrophages. Meanwhile, KEGG annotation results showed that almost all IFN-γ induced DEGs were significantly associated with the three most common pathways, including the immune system, cellular processes, and metabolism. Further analysis of 278 KEGG enriched signaling pathways identified the main pathways as the TNF signaling pathway, the chemokine signaling pathway, the RIG I-like receptor signaling pathway, and the TLR signaling pathway. qPCR verified that the expression patterns of immune pathway-related DEGs were consistent with the transcriptomic results, indicating that the transcriptomic sequencing results were reliable.

TLRs and RIG-I are key molecules to identify pathogens such as ssRNA/dsRNA virus, LPS, Cytosolic DNA, which can be detected in most tissues (36). Recombinant IFN-γ induced upregulation of toll-like receptors TLR2, TLR7, TLR8, and TLR13 in macrophages. In mice, TLR2 plays an important role in Listeria resistance, including enhancing the phagocytosis of macrophages, promoting the production of TNF-α, IL-12, and NO, and promoting the expression of costimulatory molecules CD40 and CD60 (37). TLR7 and TLR8 play a critical role in sensing viral ssRNA in the endosome, in which TLR13 specifically recognizes single-stranded RNA. After recognizing their respective PAMPs, TLRs recruit a set of specific adaptor molecules containing TIR domains, such as MyD88, and initiate downstream signaling events, leading to the secretion of inflammatory cytokines, type I IFN, chemokines, and antimicrobial peptides, the recruitment of neutrophils, the activation of macrophages, and the induction of interferon-stimulating genes, thus killing the infected pathogen directly (38). In this experimental group, TLR4, TRAF6, P38, and AP1 were down-regulated in different degrees, indicating that IFN-γ also had a certain degree of inhibition on TLR4-activated related genes in Chinese sturgeons. In human macrophages, IFN-γ selectively suppresses a subset of TLR4-activated genes and enhancers to potentiate macrophage activation. RIG-I receptor-related genes RIG-I, MDA5, and TRIM25 were also significantly upregulated. As the primary cytoplasmic RNA

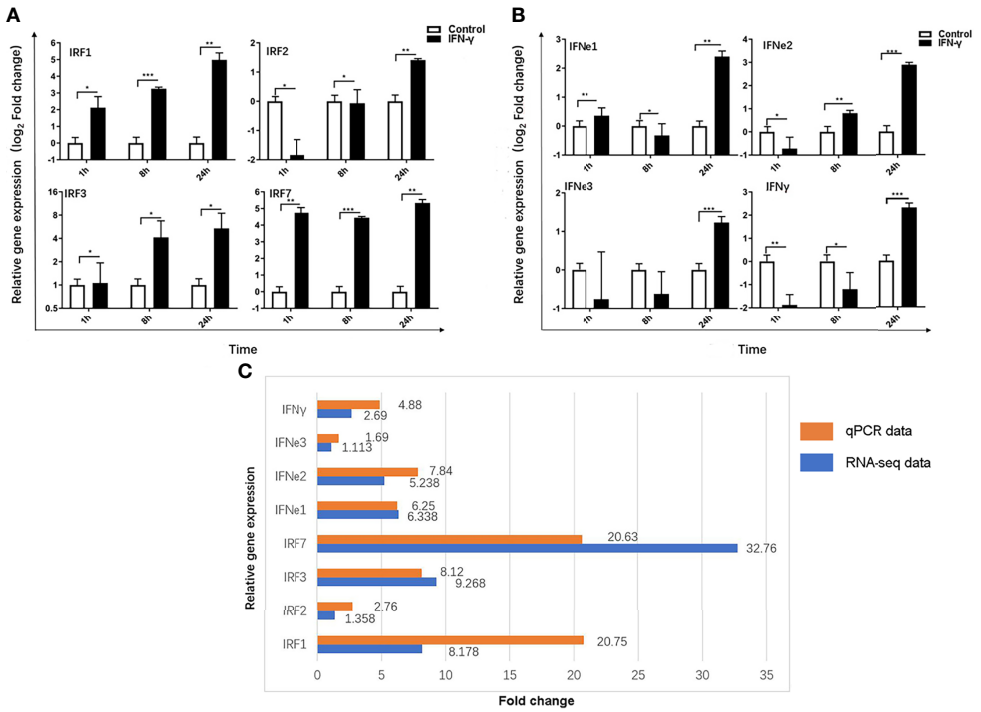

FIGURE 6 | Immunity-related genes expression induced by IFN-γ of Acipenser sinensis. **(A)** Relative expression of IRF1, 2, 3 and 7 induced by IFN-γ of Acipenser sinensis. **(B)** Relative expression of IFN–γ, IFN-e1,2,3 induced by IFN - γ of Acipenser sinensis. **(C)** Fold change of 8 immune genes DEG screened by qPCR and transcriptome. The vertical axis represents the name of the gene and the horizontal axis represents the multiples, red represents qPCR data and blue represents transcriptome data results. *P*-values of less than 0.05 were considered statistically significant (*P<0.05, **P<0.01, ***P<0.001).

monitoring mechanism, the RIG-I-MAVS signaling pathway has been intensively studied as a natural immune protection system for antiviral infection (39). RIG I-like receptors (RLRs), including RIG-I, MDA5, and LGP2, are a series of cytoplasmic RNA helicases that detect the accumulation of multiple viral RNAs during viral infection or replication (40). In most cell types except pDCs, RLRs are essential for antiviral responses. Thus, IFNγ maintains antiviral status in macrophages through RIG-I and Toll-like receptor-related signaling pathways and up-regulation of related enzymes.

Interestingly, Chinese sturgeon IFN-γ can also induce the expression of a large number of C-X-C motif family genes, and these chemokines are involved in the activation, adhesion, and recruitment of leukocytes to inflammatory sites, promoting immune response, stem cell survival, and angiogenesis by binding to G protein-coupled cell surface receptors. Normally undetectable in most non-lymphoid cells, which IFN-γ can strongly induce during infection or inflammation. In mice, IFN-γ can induce the expression of CXCL10 significantly in primary macrophages, reaching a peak at 3–6 h; IFN-γ in rainbow trout can also stimulate the significant expression of CXCL9, CXCL10, and CXCL11 in RTS-11 cells. In addition, the combination of IFN-γ and lipopolysaccharide, IL1β or TNFα produces a synergistic effect in a variety of cell types, which strongly induce the expression of various chemokines (41). In an *in vitro* study of rainbow trout IFN-γ, TNFα combined with IFN-γ induced the expression levels of CXCL9, CXCL10, and CXCL11 in RTS11 cells to more than 50 times higher than that induced by TNFα alone (42).

The result of stimulation of *Acipenser dabryanus* with LPS and polyI:C, type I interferon *Ad*IFNe1, e2 and e3 showed higher antiviral activity than *Ad*IFN-γ, *Ad*IFN-γ showed more antibacterial than type I interferon. The amino acid sequence similarity between (*Ad*IFNe1 and *As*IFNe1, *Ad*IFNe2 and *As*IFNe2, *Ad*IFNe3 and *As*IFNe3, *Ad*IFN-γ and *As*IFN-γ) are more than 95%, which indicated that the two types interferon functions of these two species were very similar.

In this study, transcriptomic data on many key genes and pathways were obtained, revealing that IFN-γ induces the expression of relevant immune genes or proteins, activates intracellular signaling pathways, regulates cellular and humoral immune systems, and is involved in the regulation of metabolism. These data provide a theoretical reference for further study of the biological function of IFN-γ in Chinese sturgeon and the analysis of the biological evolution and immune gene evolution of ancient Chinese sturgeon species.

DATA AVAILABILITY STATEMENT

The datasets presented in this study can be found in online repositories. The names of the repository/repositories and accession number(s) can be found below: https://www.ncbi.nlm.nih.gov/sra; PRJNA801715.

ETHICS STATEMENT

The animal study was reviewed and approved by Animal Ethics Committee of Yangtze University.

AUTHOR CONTRIBUTIONS

GD contributed to the writing of the manuscript. GD and CZ contributed to the data analysis. LZ, DD, QL, and HG contributed to laboratory work. BW and SZ contributed to the text editing. QX contributed to the conception of the idea and design. All authors read and approved the manuscript.

FUNDING

This work research was financially supported by the Research Fund Program of Guangdong Provincial Key Lab of Pathogenic Biology and Epidemiology for Aquatic Economic Animals (No. PBEA2021ZD03) and the Basic Research Project of Guizhou Province.

ACKNOWLEDGMENTS

The authors thank the member of Yangtze River Fisheries Research Institute (Taihu Lake, Jingzhou, China) for their support.

SUPPLEMENTARY MATERIAL

The Supplementary Material for this article can be found online at: https://www.frontiersin.org/articles/10.3389/fimmu.2022.854689/full#supplementary-material

Supplementary Table 1 | Nucleotide sequences of primers.

Supplementary Table 2 | Transcriptome data statistics.

Supplementary Table 3 | Clean reads assembly statistics.

Supplementary Table 4 | Statistical table of database annotation.

Supplementary Table 5 | Pathway enrichment analysis of AM-vs-AMC, statistical table of KEGG enrichment's top 20 signal pathways.

Supplementary Table 6 | Immune signal pathway and screening of differential genes.

REFERENCES

1. Li L, Chen SN, Laghari ZA, Huang B, Huo HJ, Li N, et al. Receptor Complex and Signalling Pathway of the Two typeII IFNs, IFN-γ and IFN-γrel in Mandarin Fish or the So-Called Chinese Perch Siniperca Chuatsi. *Dev Comp Immunol* (2019) 97:98–112. doi: 10.1016/j.dci.2019.03.016
2. Zou J, Yoshiura Y, Dijkstra JM, Sakai M, Ototake M, Secombes C. Identification of an Interferon Gamma Homologue in Fugu, Takifugu Rubripes. *Fish Shellfish Immunol* (2004) 17(4):403–9. doi: 10.1016/j.fsi.2004.04.015
3. Igawa D, Sakai M, Savan R. An Unexpected Discovery of Two Interferon Gamma-Like Genes Along With Interleukin (IL)-22 and -26 From Teleost: IL-22 and -26 Genes Have Been Described for the First Time Outside Mammals. *Mol Immunol* (2006) 43(7):999–1009. doi: 10.1016/j.molimm.2005.05.009
4. Savan R, Ravichandran S, Collins JR, Sakai M, Young HA. Structural Conservation of Interferon Gamma Among Vertebrates. *Cytokine Growth Factor Rev* (2009) 20:115–24. doi: 10.1016/j.cytogfr.2009.02.006
5. Zou J, Tafalla C, Truckle J, Secombes CJ. Identification of a Second Group of Type I IFNs in Fish Sheds Light on IFN Evolution in Vertebrates. *J Immunol* (2007) 179(6):3859–71. doi: 10.4049/jimmunol.179.6.3859
6. Chen WQ, Xu QQ, Chang MX, Zou J, Secombes CJ, Peng KM, et al. Molecular Characterization and Expression Analysis of the IFN-Gamma Related Gene (IFN-γrel) in Grass Carp *Ctenopharyngodon Idella*. *Vet Immunol Immunopathol* (2010) 134(3-4):199–207. doi: 10.1016/j.vetimm.2009.09.007
7. Li X, Huang WS, Huang B, Xu JS, Zhai SW, Liang Y, et al. Prokaryotic Expression and Purification of Type II Interferon Genes (IFN-γ and IFN-γ REL) From Japanese Eel. *Mar Fish* (2019) 5:567–77. doi: 10.13233/j.cnki.mar.fish.2019.05.004
8. Qi JW, Tang N, Wu YB, Chen H, Wang SY, Wang B, et al. The Transcripts of CRF and CRF Receptors Under Fasting Stress in Dabry's Sturgeon (*Acipenser Dabryanus* Dumeril). *Gen Comp Endocrinol* (2019) 280:200–8. doi: 10.1016/j.ygcen.2019.05.005
9. Chen SN, Huang B, Zhang XW, Li Y, Zhao LJ, Li N, et al. IFN-γ and Its Receptors in a Reptile Reveal the Evolutionary Conservation of Type II IFNs in Vertebrates. *Dev Comp Immunol* (2013) 41(4):587–96. doi: 10.1016/j.dci.2013.07.002
10. Bach EA, Aguet M, Schreiber RD. The IFN Gamma Receptor: A Paradigm for Cytokine Receptor Signaling. *Annu Rev Immunol* (1997) 15:563–91. doi: 10.1146/annurev.immunol.15.1.563
11. Mikulecký P, Cerný J, Biedermannová L, Petroková H, Kuchař M, Vondrášek J, et al. Increasing Affinity of Interferon-Receptor 1 to Interferon-By Computer-Aided Design. *BioMed Res Int* (2013) 2013:752514. doi: 10.1155/2013/752514
12. Johnson HM, Noon-Song EN, Dabelic R, Ahmed CM. IFN Signaling: How a Non-Canonical Model Led to the Development of IFN Mimetics. *Front Immunol* (2013) 4:202. doi: 10.3389/fimmu.2013.00202
13. Au-Yeung N, Mandhana R, Horvath CM. Transcriptional Regulation by STAT1 and STAT2 in the Interferon JAK-STAT Pathway. *JAKSTAT* (2013) 2(3):e23931. doi: 10.4161/jkst.23931
14. Stetson DB, Mohrs M, Reinhardt RL, Baron JL, Wang ZE, Gapin L, et al. Constitutive Cytokine mRNAs Mark Natural Killer (NK) and NK T Cells Poised for Rapid Effector Function. *J Exp Med* (2003) 198(7):1069–76. doi: 10.1084/jem.20030630
15. Lin Y, Lu R, Hou J, Zhou GG, Fu W. IFNgamma-Inducible CXCL10/CXCR3 Axis Alters the Sensitivity of HEp-2 Cells to Ionizing Radiation. *Exp Cell Res* (2021) 398(1):112–21. doi: 10.1016/j.yexcr.2020.112382
16. Jorgovanovic D, Song M, Wang L, Zhang Y. Roles of IFN-γ in Tumor Progression and Regression: A Review. *Biomark Res* (2020) 8:49. doi: 10.1186/s40364-020-00228-x
17. Pereiro P, Forn-Cuni G, Figueras A, Novoa B. Pathogen-Dependent Role of Turbot (*Scophthalmus Maximus*) Interferon-Gamma. *Fish Shellfish Immunol* (2016) 59:25–35. doi: 10.1016/j.fsi.2016.10.021
18. Yang Y, Huang Y, Yu Y, Zhou S, Wang S, Yang M, et al. Negative Regulation of the Innate Antiviral Immune Response by TRIM62 From Orange Spotted Grouper. *Fish Shellfish Immunol* (2016) 57:68–78. doi: 10.1016/j.fsi.2016.08.035
19. Xiang Y, Liu W, Jia P, Li Y, Jin Y, Chen L, et al. Molecular Characterization and Expression Analysis of Interferon-Gamma in Black Seabream Acanthopagrus Schlegelii. *Fish Shellfish Immunol* (2017) 70:140–8. doi: 10.1016/j.fsi.2017.08.046
20. Somamoto T, Miura Y, Nakanishi T, Nakao M. Local and Systemic Adaptive Immune Responses Toward Viral Infection *via* Gills in Ginbuna Crucian Carp. *Dev Comp Immunol* (2015) 52(1):81–7. doi: 10.1016/j.dci.2015.04.016
21. Zhen CW, Yuan HW, Tian GM, Li Q, Zhang SH, Xu QQ, et al. Immune Regulation of IFN-γ in Chinese Sturgeon. *J Fish China* (2020) 44(9):1539–48. doi: 10.11964/jfc.20200712346

22. Bolger AM, Lohse M, Usadel B. Trimmomatic: A Flexible Trimmer for Illumina Sequence Data. *Bioinformatics* (2014) 30(15):2114-20. doi: 10.1093/bioinformatics/btu170
23. Grabherr MG, Haas BJ, Yassour M, Levin JZ, Thompson DA, Amit I, et al. Trinity: Reconstructing a Full-Length Transcriptome Without a Genome From RNA-Seq Data. *Nat Biotechnol* (2011) 29(7):644–52. doi: 10.1038/nbt.1883
24. Li W, Jaroszewski L, Godzik A. Clustering of Highly Homologous Sequences to Reduce the Size of Large Protein Databases. *Bioinformatics* (2001) 17 (3):282–3. doi: 10.1093/bioinformatics/17.3.282
25. Simão FA, Waterhouse RM, Ioannidis P, Kriventseva EV, Zdobnov EM. BUSCO: Assessing Genome Assembly and Annotation Completeness With Single-Copy Orthologs. *Bioinformatics* (2015) 31(19):3210–2. doi: 10.1093/bioinformatics/btv351
26. Buchfink B, Xie C, Huson DH. Fast and Sensitive Protein Alignment Using Diamond. *Nat Methods* (2015) 12(1):59–60. doi: 10.1038/nmeth.3176
27. Mistry J, Finn RD, Eddy SR, Bateman A, Punta M. Challenges in Homology Search: HMMER3 and Convergent Evolution of Coiled-Coil Regions. *Nucleic Acids Res* (2013) 41(12):e121–1. doi: 10.1093/nar/gkt263
28. Mistry J, Chuguransky S, Williams L, Qureshi M, Salazar GA, Sonnhammer ELL, et al. Pfam: The Protein Families Database in 2021. *Nucleic Acids Res* (2020) 49(D1):D412–9. doi: 10.1093/nar/gkaa913
29. Langmead B, Salzberg SL. Fast Gapped-Read Alignment With Bowtie 2. *Nat Methods* (2012) 9(4):357–9. doi: 10.1038/nmeth.1923
30. Roberts A. *Ambiguous Fragment Assignment for High-Throughput Sequencing Experiments. PhD Dissertation*. Berkeley: University of California (2013). Available at: https://escholarship.org/uc/item/7zx1s4hr.
31. R Core Team. *R: A Language and Environment for Statistical Computing*. Vienna, Austria: R Foundation for Statistical Computing (2020). Available at: https://www.R-project.org/.
32. Qi ZT, Wu P, Zhang QH, Wei YC, Wang ZS, Qiu M, et al. Transcriptome Analysis of Soiny Mullet (*Liza Haematocheila*) Spleen in Response to Streptococcus Dysgalactiae. *Fish Shellfish Immunol* (2016) 49:194–204. doi: 10.1016/j.fsi.2015.12.029
33. Li G, Zhao Y, Wang J, Liu B, Sun X, Guo S, et al. Transcriptome Profiling of Developing Spleen Tissue and Discovery of Immune-Related Genes in Grass Carp (*Ctenopharyngodon Idella*). *Fish Shellfish Immunol* (2017) 60:400–10. doi: 10.1016/j.fsi.2016.12.012
34. Maekawa S, Byadgi O, Chen YC, Aoki T, Takeyama H, Yoshida T, et al. Transcriptome Analysis of Immune Response Against Vibrio Harveyi Infection in Orange-Spotted Grouper (*Epinephelus Coioides*). *Fish Shellfish Immunol* (2017) 70:628–37. doi: 10.1016/j.fsi.2017.09.052/
35. Amparyup P, Charoensapsri W, Samaluka N, Chumtong P, Yocawibun P, Imjongjirak C. Transcriptome Analysis Identifies Immune-Related Genes and Antimicrobial Peptides in Siamese Fighting Fish (*Betta Splendens*). *Fish Shellfish Immunol* (2020) 99:403–13. doi: 10.1016/j.fsi.2020.02.030
36. Rowland RRR, Joan L, Jack D. Control of Porcine Reproductive and Respiratory Syndrome (PRRS) Through Genetic Improvements in Disease Resistance and Tolerance. *Front Genet* (2012) 3:260. doi: 10.3389/fgene.2012.00260
37. Wang G. *Effects of TLR2 and IFN-γ on Phagocyte Resistance to Listeria Infection. PhD Dissertation*. Jinan: Shandong University (2018). Available at: https://cdmd.cnki.com.cn/Article/CDMD-10422-1019013315.htm.
38. Saitoh T, Satoh T, Yamamoto N, Uematsu S, Takeuchi O, Kawai T, et al. Antiviral Protein Viperin Promotes Toll-Like Receptor 7 and Toll-Like Receptor 9-Mediated Type I Interferon Production in Plasmacytoid Dendritic Cells. *Immunity* (2011) 34(3):285–7. doi: 10.1016/j.immuni.2011.03.010
39. Reikine S, Nguyen JB, Modis Y. Pattern Recognition and Signaling Mechanisms of RIG-I and MDA5. *Front Immunol* (2014) 5:2014.00342. doi: 10.3389/fimmu.2014.00342
40. Loo YM, Gale MJr. Immune Signaling by RIG-I-Like Receptors. *Immunity* (2011) 34(5):680–92. doi: 10.1016/j.immuni.2011.05.003
41. Müller M, Carte S, Hofer MJ and Campbell IL. The Chemokine Receptor CXCR3 and Its Ligands CXCL9, CXCL10 and CXCL11 in Neuroimmunity–A Tale of Conflict and Conundrum. *Neuropathology Appl Neurobiol* (2010) 36 (5):368–87. doi: 10.1111/j.1365-2990.2010.01089.x
42. Laing KJ, Bols N, Secombes CJ. A CXC Chemokine Sequence Isolated From the Rainbow Trout *Oncorhynchus Mykiss* Resembles the Closely Related Interferon-Gamma-Inducible Chemokines CXCL9, CXCL10 and CXCL11. *Eur Cytokine Netw* (2002) 13(4):462–73.

Conflict of Interest: The authors declare that the research was conducted in the absence of any commercial or financial relationships that could be construed as a potential conflict of interest.

Publisher's Note: All claims expressed in this article are solely those of the authors and do not necessarily represent those of their affiliated organizations, or those of the publisher, the editors and the reviewers. Any product that may be evaluated in this article, or claim that may be made by its manufacturer, is not guaranteed or endorsed by the publisher.

frontiers in Immunology

ORIGINAL RESEARCH
published: 25 March 2022
doi: 10.3389/fimmu.2022.844657

Differential Transcriptomics Analysis of IPEC-J2 Cells Single or Coinfected With Porcine Epidemic Diarrhea Virus and Transmissible Gastroenteritis Virus

Lina Song[1,2], Jing Chen[2], Pengfei Hao[2], Yuhang Jiang[2], Wang Xu[2], Letian Li[2], Si Chen[3], Zihan Gao[2], Ningyi Jin[2], Linzhu Ren[3]* and Chang Li[2]**

[1] College of Veterinary Medicine, Key Lab for Zoonoses Research, Ministry of Education, Jilin University, Changchun, China, [2] Research Unit of Key Technologies for Prevention and Control of Virus Zoonoses, Chinese Academy of Medical Sciences, Changchun Institute of Veterinary Medicine, Chinese Academy of Agricultural Sciences, Changchun, China, [3] College of Animal Sciences, Jilin University, Changchun, China

OPEN ACCESS

Edited by:
Chaofeng Han, Second Military Medical University, China

Reviewed by:
Xiangdong Li, Yangzhou University, China
Chunfu Zheng, University of Calgary, Canada

***Correspondence:**
Chang Li
lichang78@163.com
Linzhu Ren
renlz@jlu.edu.cn
Ningyi Jin
ningyik@126.com

Specialty section:
This article was submitted to Molecular Innate Immunity, a section of the journal Frontiers in Immunology

Received: *28 December 2021*
Accepted: *28 February 2022*
Published: *25 March 2022*

Citation:
Song L, Chen J, Hao P, Jiang Y, Xu W, Li L, Chen S, Gao Z, Jin N, Ren L and Li C (2022) Differential Transcriptomics Analysis of IPEC-J2 Cells Single or Coinfected With Porcine Epidemic Diarrhea Virus and Transmissible Gastroenteritis Virus. Front. Immunol. 13:844657. doi: 10.3389/fimmu.2022.844657

Porcine epidemic diarrhea (PED) and transmissible gastroenteritis (TGE) caused by porcine epidemic diarrhea virus (PEDV) and transmissible gastroenteritis virus (TGEV) are two highly contagious intestinal diseases in the swine industry worldwide. Notably, coinfection of TGEV and PEDV is common in piglets with diarrhea-related diseases. In this study, intestinal porcine epithelial cells (IPEC-J2) were single or coinfected with PEDV and/or TGEV, followed by the comparison of differentially expressed genes (DEGs), especially interferon-stimulated genes (ISGs), between different groups *via* transcriptomics analysis and real-time qPCR. The antiviral activity of swine interferon-induced transmembrane protein 3 (sIFITM3) on PEDV and TGEV infection was also evaluated. The results showed that DEGs can be detected in the cells infected with PEDV, TGEV, and PEDV+TGEV at 12, 24, and 48 hpi, and the number of DEGs was the highest at 24 hpi. The DEGs are mainly annotated to the GO terms of protein binding, immune system process, organelle part, and intracellular organelle part. Furthermore, 90 ISGs were upregulated during PEDV or TGEV infection, 27 of which were associated with antiviral activity, including ISG15, OASL, IFITM1, and IFITM3. Furthermore, sIFITM3 can significantly inhibit PEDV and TGEV infection in porcine IPEC-J2 cells and/or monkey Vero cells. Besides, sIFITM3 can also inhibit vesicular stomatitis virus (VSV) replication in Vero cells. These results indicate that sIFITM3 has broad-spectrum antiviral activity.

Keywords: porcine epidemic diarrhea virus (PEDV), transmissible gastroenteritis virus (TGEV), differential transcriptomics, coinfection, interferon-stimulated genes (ISGs), interferon-induced transmembrane protein (IFITM)

INTRODUCTION

Porcine epidemic diarrhea (PED) and transmissible gastroenteritis (TGE) caused by porcine epidemic diarrhea virus (PEDV) and transmissible gastroenteritis virus (TGEV), respectively, are two highly contagious intestinal diseases in the swine industry worldwide, which are characterized by acute gastroenteritis, watery diarrhea, and vomiting in pigs of almost all ages. Both viruses belong to the family *Coronaviridae* and genus *Alphacoronavirus* (1), with a positive-sense single-stranded RNA genome of about 28 kb encoding at least six open reading frames (ORFs): ORF1a, ORF1b, spike (S), envelope (E), membrane (M), and nucleocapsid (N) (2, 3).

TGEV has been spread in pigs for decades, whereas PEDV is considered as a new coronavirus detected in pigs (2, 3), especially the highly virulent PEDV that has recently emerged and caused great losses worldwide. Furthermore, coinfection of TGEV and PEDV is common in piglets with diarrhea (4–7). During infection, TGEV mainly infects the small intestine by interacting with host receptor amino peptidase N (APN, also named as CD13), sialic acid, and/or other cofactors (1, 8, 9). PEDV can directly infect the villous intestinal epithelial cells of the small intestine or nasal epithelial cells followed by dissemination from the nasal cavity to the intestinal mucosa by binding with sialic acid and other receptors (1, 10, 11). However, whether porcine APN is a functional receptor for PEDV infection is still controversial (1). Moreover, TGEV can damage the barrier integrity of intestinal porcine epithelial cells (IPEC-J2) in the early stage of infection by downregulating proteins related to tight and adhesion junction, while PEDV impairs the integrity of the cellular epithelial barrier (12). Both viruses can also affect the remodeling of microfilaments in IPEC-J2 cells, and the coinfection of PEDV and TGEV can increase the damage of tight junction and the remodeling of microfilaments (12). Besides, TGEV or PEDV infection reduced NHE3 activity and Na^+ uptake of IPEC-J2 cells, which may be associated with the imbalance of Na^+ in intestinal tissues, thus resulting in diarrhea in the infected animals (13). The differentially expressed genes (DEGs) in IPEC-J2 cells infected with virulent PEDV virus are mainly related to autophagy and apoptosis, while the DEGs were strongly enriched in immune responses/inflammation in the avirulent PEDV group (14). TLR3 inhibited the replication of avirulent PEDV by increasing the IFIT2 expression (14). Notably, a recent investigation showed that coinfection of TEGV and PEDV leads to recombinant chimeric swine enteric coronavirus (SeCoV) in Italy, Germany, and Slovakia (15–18), which implies the urgency of prevention and control of virus-related diseases. It was reported that viral nucleocapsid from different porcine enteric coronaviruses can differentially modulate PEDV replication by competitively interacting with PEDV nucleocapsid (19). Nucleocapsid from porcine deltacoronavirus (PDCoV) can significantly decrease PEDV replication, while overexpression of the TGEV nucleocapsid enhanced the virus replication (19). These results indicate that coinfection of different enteric coronaviruses may have different results on virus infection and host responses. However, little is known about the cell responses, especially host immune responses, after single or coinfection of PEDV and TGEV.

The ability of the host to inhibit virus infection largely depends on the effectiveness of the antiviral innate immune response, which leads to the upregulation of interferon (IFN), followed by activation of signal transduction cascades, and thus leading to the induction of hundreds of interferon-stimulated genes (ISGs) (20, 21). ISGs work alone or cooperatively to achieve one or more cellular outcomes, including antiviral defense, antiproliferative activity, and stimulation of adaptive immunity (20, 21). However, although the specific antiviral functions of some ISGs have been characterized, the functions of other ISGs have yet to be determined. Moreover, Zhao et al. found that IFN-λ1 has a stronger ability to induce ISGs against PEDV infection than IFN-α (22). TGEV infection stimulates the JAK-STAT1 signaling pathway and ISG expressions (23). However, the expression of ISGs after the infection of PEDV and TGEV alone or together remains to be studied.

In the present study, porcine IPEC-J2 cells were single or coinfected with PEDV and/or TGEV, followed by the comparison of differentially expressed genes, especially ISGs, between different groups *via* transcriptomics analysis and real-time qPCR. The antiviral activity of interferon-induced transmembrane protein 3 (IFITM3) on PEDV and TGEV infection was also evaluated.

MATERIALS AND METHODS

Cells and Viruses

IPEC-J2 cells (kindly provided by Dr. Shuqi Xiao), Vero E6 cells, and ST cells were maintained in Dulbecco's modified Eagle medium (DMEM) (HyClone, Logan, UT, USA), supplemented with 10% fetal bovine serum (FBS, Gibco, Grand Island, NY, USA) and penicillin–streptomycin mixtures at 37°C and 5% CO_2 atmosphere. Human lung epithelial (A549) cells, Baby hamster kidney cells (BHK-21), and chicken fibroblast cells (DF-1) were grown in complete DMEM with 10% fetal bovine serum (Gibco, USA) at 37°C in a 5% CO_2 incubator (24, 25).

The PEDV strain (GenBank No.: OM814174) and the TGEV strain (GenBank No.: OM802899) were isolated in our laboratory previously. The PEDV was cultured in Vero cells supplemented with 5 μg/ml trypsin. Moreover, the TGEV was cultured in ST cells with DEME (2% FBS without penicillin–streptomycin). Vesicular Stomatitis Virus carrying green fluorescent protein gene (rVSV-GFP) was kindly provided by Professor Zhigao Bu as described previously (24, 25).

Antibodies and Reagents

Mouse anti-PEDV N mAb (FITC) was purchased from Medgene Labs (Brookings, SD, USA). Mouse anti-PEDV S and Mouse anti-TGEV S polyclonal antibodies were prepared in our laboratory. Rabbit anti-IFITM3 polyclonal antibody was purchased from Proteintech (Wuhan, China). Rabbit anti-β-actin mAb was purchased from Cell Signaling Technology (Danvers, MA, USA). Lipofectamine 3000 Transfection

Reagent and Lipofectamine™ RNAiMAX Transfection Reagent were purchased from Invitrogen (Carlsbad, CA, USA).

pLV-sIFITM3-Flag was constructed by our laboratory. Briefly, swine interferon-induced transmembrane protein 3 (sIFITM3) was amplified using primers sIFITM3-F and sIFITM3-R (**Supplemental Table 1**) and subcloned into pLV-EGFP (Inovogen Tech, Beijing, China) with *Eco*R I and *Xho* I, resulting in pLV-sIFITM3-Flag. Furthermore, sIFITM3 was also amplified using primers sIFITM3-F2 and sIFITM3-R2 (**Supplemental Table 1**), and subcloned into pCAGGS-Flag (Inovogen Tech, Beijing, China) with *Eco*R I and *Xho* I, resulting in pCAGGS-sIFITM3-Flag. The recombinant plasmids were verified by PCR and sequencing.

TRIzol reagent was purchased from Sangon Biotech (Shanghai, China). M-MLV Reverse Transcriptase RNase and GoTaq® were purchased from Promega (Madison, WI, USA). HRP-labeled Goat Anti-Rabbit IgG (H+L) purchased from Beyotime (Shanghai, China) Pierce ECL Western Blotting Substrate was purchased from Thermo Scientific (Waltham, MA, USA).

One-Step Growth Curve

IPEC-J2 cells were infected with 1 MOI (multiplicity of infection) of PEDV or TGEV at 12, 24, 36, 48, and 60 hpi. The supernatant was collected, followed by the 50% tissue culture infectious dose ($TCID_{50}$) evaluation with the Reed Muench method as follows.

Briefly, Vero (for PEDV) or ST (for TGEV) cells were cultured in 96-well plates at a density of 1×10^5 cells/well for 12 h, followed by washing with PBS three times. The collected supernatant was 10-fold diluted (10^{-1} to 10^{-10}) with cell maintenance solution containing trypsin (final concentration of 10 μg/ml). Thereafter, cells were inoculated with the diluted virus at 37°C, 5% CO_2 for 12, 24, 36, 48, and 60 hpi, and the cytopathic effect (CPE) was observed daily using an inverted microscope. $TCID_{50}$ of each virus was calculated as described by Reed and Muench (26).

Virus Infection

IPEC-J2 cells (2×10^5/ml) were plated in 6-well plates, incubated overnight to reach 70%–80% confluency. Then, cells were inoculated with PEDV (MOI = 1), TGEV (MOI = 1), or PEDV +TGEV (MOI = 1 for each virus) supplemented with 10 μg/ml trypsin and cultured at 37, 5% CO_2 for 12, 24, and 48 h. Cells were collected for lysis and extraction of RNA.

A549, BHK21, and DF-1 cells were transfected with pCAGGS-sIFITM3-Flag using Lipofectamine 3000 reagent (Thermo Fisher Scientific, USA) according to the manufacturer's instruction. 24 h post-transfection, the expression of IFITM3 was examined by Western blot with anti-FLAG antibody. Then the cells were infected with rVSV-GFP at 0.1 MOI and the replication of rVSV-GFP was analyzed by examining *via* fluorescence microscope and flow cytometry at 24 hpi.

RNA Extraction

Total RNA was extracted from virus-infected cells or mock cells using TRIzol Reagent according to the manufacturer's instruction. The total RNA was dissolved in 50 μl of RNase-free ddH_2O and stored at -20°C.

Real-Time Quantitative PCR

Reverse transcription was performed using M-MLV Reverse Transcriptase RNase according to the manufacturer's instruction. Thereafter, SYBR Green quantitative real-time PCR was performed using the ABI7500 Real-Time PCR Detection System and the GoTaq® kit. The real-time PCR primers are listed in **Supplemental Table 1**. For each sample, the GAPDH gene was amplified and used as an internal control. The relative transcript levels of target genes were equal to the $2^{(-\Delta\Delta Ct)}$ threshold method and were shown as fold changes relative to the respective untreated control samples.

RNA-Seq Analysis

To prepare the cDNA library, total RNA was treated with RNase-free DNase I. Then, mRNA was purified using magnetic oligo (dT) beads and evaluated using the Agilent 2100 bioanalyzer (Agilent Technologies, Santa Clara, CA, USA) for RNA integrity. mRNAs with RNA integrity numbers (RINs) > 8 were subjected to subsequent analysis. The purified mRNA was used to construct libraries using TruSeq PE Cluster Kit v3-cBot-HS (Illumina, San Diego, CA, USA) according to the manufacturer's instructions. Then, these libraries were sequenced on an Illumina Novaseq platform (Illumina, USA).

GO and KEGG Enrichment Analysis

Gene Ontology (GO) enrichment and Kyoto The Encyclopedia of Genes and Genomes (KEGG) pathway analysis of DEGs were conducted according to the protocols described by Cao et al. and Xie et al. previously (27, 28). Briefly, GO functional enrichment was performed using the Blast2GO software; the enriched genes were further classified by the GO analysis, with a p-value < 0.05.

The KEGG pathway database was accessed using the KOBAS software *via* a hypergeometric distribution test with the Phyper function in the R software package. Significantly enriched unigenes were selected based on a corrected p-value < 0.05. The distribution of DEGs within each GO/pathway category was determined by mapping all DEGs to terms in the GO and KEGG databases.

STRING Pathway Analysis

GO and KEGG pathway enrichment analyses were analyzed by STRING (https://string-db.org/). The protein list was submitted for multiple protein searches. GO terms and KEGG pathway results were exported in the STRING analysis module. Terms and pathways with p <0.05 were significantly enriched. Appropriate terms and pathways were manually selected for visualization.

Overexpression or Knockdown of IFITM3

IPEC-J2 cells were seeded in 6-well plates at a density of 2×10^5/ml overnight to reach 70%–80% confluency. Then, cells were transfected with 4 μg of pLV-sIFITM3-Flag using Lipofectamine 3000 or 50 μM siRNAs targeting sIFITM3 (si-ssc-IFITM3_001, si-ssc-IFITM3_002, si-ssc-IFITM3_003) (**Supplemental Table 1**) using Lipofectamine RNAiMAX Reagent for 48 h.

For Vero cells, cells were transfected with 4 μg of pLV-sIFITM3-Flag using Lipofectamine 3000 or 50 μM siRNAs targeting monkey IFITM3 (si-csa-IFITM3_001, si-csa-IFITM3_002, si-csa-IFITM3_003) (**Supplemental Table 1**).

Western Blot

Cells were harvested in IP lysis buffer containing the proteinase inhibitor cocktail (Sigma), frozen-thawed, and centrifuged to remove insoluble components. The total protein concentration was determined using a BCA protein assay kit (Beyotime Biotechnology, China). Protein samples were separated with 12% sodium dodecyl sulfate-polyacrylamide gel electrophoresis (SDS-PAGE) and transferred onto PVDF membranes, followed by blocking in 5% non-fat milk. Then, the membranes were incubated with antibodies in TBST containing 5% non-fat milk overnight at 4°C or 1 h at room temperature. After washing three times with TBST, the membranes were incubated with HRP-labeled goat anti-rabbit (or anti-mouse) IgG(H+L) IgG secondary antibodies (Beyotime Biotechnology) at room temperature for 30 min. Followed by washing, the membrane was visualized using Pierce ECL Western Blotting Substrate (Thermo Scientific).

Flow Cytometry (FCM) Analysis

After trypsin incubation, the transfected cells were collected and washed with PBS twice. The cells were centrifuged at 3,000 rmp, at 4°C for 5 min, and subsequently resuspended in 5% PBS buffer at 4°C for 30 min. After centrifugation, the cells were incubated with the mouse anti-PEDV N mAb (FITC) in PBS buffer at 4°C for 30 min. After washing with PBS 3 times, the cells were resuspended in 200 ml PBS buffer at least 2.0×10^4 cells per sample. Fluorescent intensity was determined and analyzed on CytoFLEX (Beckman, Brea, CA, USA).

Crystal Violet Staining Assay

The Vero cells were washed with distilled water 3 times, fixed with 4% paraformaldehyde at room temperature for 20 min. After washing with distilled water 3 times, cells were stained with 0.1% crystal violet at room temperature for 15 min. The stained cells were washed with distilled water and air-dried for taking macrographic images.

Statistical Analysis

The Student's t-test was used for all experiment analyses. Data are presented as the mean ± standard deviation (SD) of 3 times experiments. p-values < 0.05 were considered statistical significance.

RESULTS

Phylogenetic Analysis and Proliferation Kinetics of PEDV and TGEV in IPEC-J2 Cells

Phylogenetic analysis of the PEDV and TGEV strains from our lab was constructed based on the S gene and is depicted in **Figure 1**. The PEDV strain was clustered with the PEDV classic strains (G1 cluster) (**Figure 1A**), whereas the TGEV strain was clustered into group III (**Figure 1B**).

To determine the infectivity and kinetics of the PEDV and TGEV propagation in the IPEC-J2 cells, levels of viral genes and viral titers were monitored after the virus infection. As shown in **Figures 1C, D**, both viruses were gradually increased in IPEC-J2 cells (**Figure 1C**). The results of Western blot showed that spike proteins of PEDV and TGEV were detected at 48 and 60 hpi (**Figure 1D**). Moreover, the titer of two strains was evaluated in Vero (for PEDV) or ST (for TGEV) cells, respectively. These results demonstrated that the titer of two strains at 48 hpi exceeded 10^6/0.1 ml of $TCID_{50}$ (**Figure 1E**). These results indicate that both viruses can effectively replicate in IPEC-J2 cells.

Transcriptional Profile in IPEC-J2 Cells Induced by PEDV, TGEV, and PEDV+TGEV

Cells were infected with PEDV, TGEV, and PEDV+TGEV, followed by sampling at 12, 24, and 48 hpi for whole genomic transcriptomics analysis (NCBI Accession No.: PRJNA796631, **Figure 2A**).

In total, 24,617 different genes were annotated from the transcriptome data, including 12,731 upregulated genes and 11,886 downregulated genes (**Supplemental Table 2**). As shown in **Figure 2B** and **Supplemental Table 2**, the total differential genes of PEDV, TGEV, and PEDV+TGEV were 1,400, 1,590, and 1,415 in three groups at 12 hpi, respectively, which was more than previously reported by Hu et al. (29). This shows that the amount of data in this study is more abundant than previous reports. At 24 hpi, the total differential genes of PEDV, TGEV, and PEDV+TGEV were 7,350, 5,878, and 4,005, respectively, while at 48 hpi, the total differential genes of PEDV, TGEV, and PEDV+TGEV were 597, 858, and 1,524, respectively. Notably, no matter the single infection or co-infection, the numbers of up- and downregulated DEGs in 24 hpi were more than that in 12 and 48 hpi, demonstrating that the interaction between virus and cell reached the maximized at 24 hpi.

Furthermore, the DEGs of the different viruses at different times were different. The shared DEGs were the most at 24 hpi, which was consistent with the above results (**Figure 2C**). Moreover, at the same time point, the shared DEGs of PEDV +TGEV-coinfected cells, including 78 upregulated DEGs and 12 downregulated DEGs, were more than those of the single infected groups (**Figure 2D**), indicating that coinfection of PEDV+TGEV may stimulate more DEGs.

Moreover, unique and shared DEGs in the coinfected group were analyzed *via* a Venn diagram. Both up- (1550) and downregulated (1,274) shared DEGs at 24 hpi were obviously increased in the PEDV+TGEV-coinfected group than that of the coinfected groups at 12 and 48 hpi (**Figure 2E** and **Supplemental Table 2**). Interestingly, the shared DEGs of the same infection groups at different times are less than the former (**Figure 2F** and **Supplemental Table 2**). These results suggest that the time point with the most DEGs was 24 hpi. Therefore, we focused on the DEGs in the coinfected cells at 24 hpi and analyzed the biological

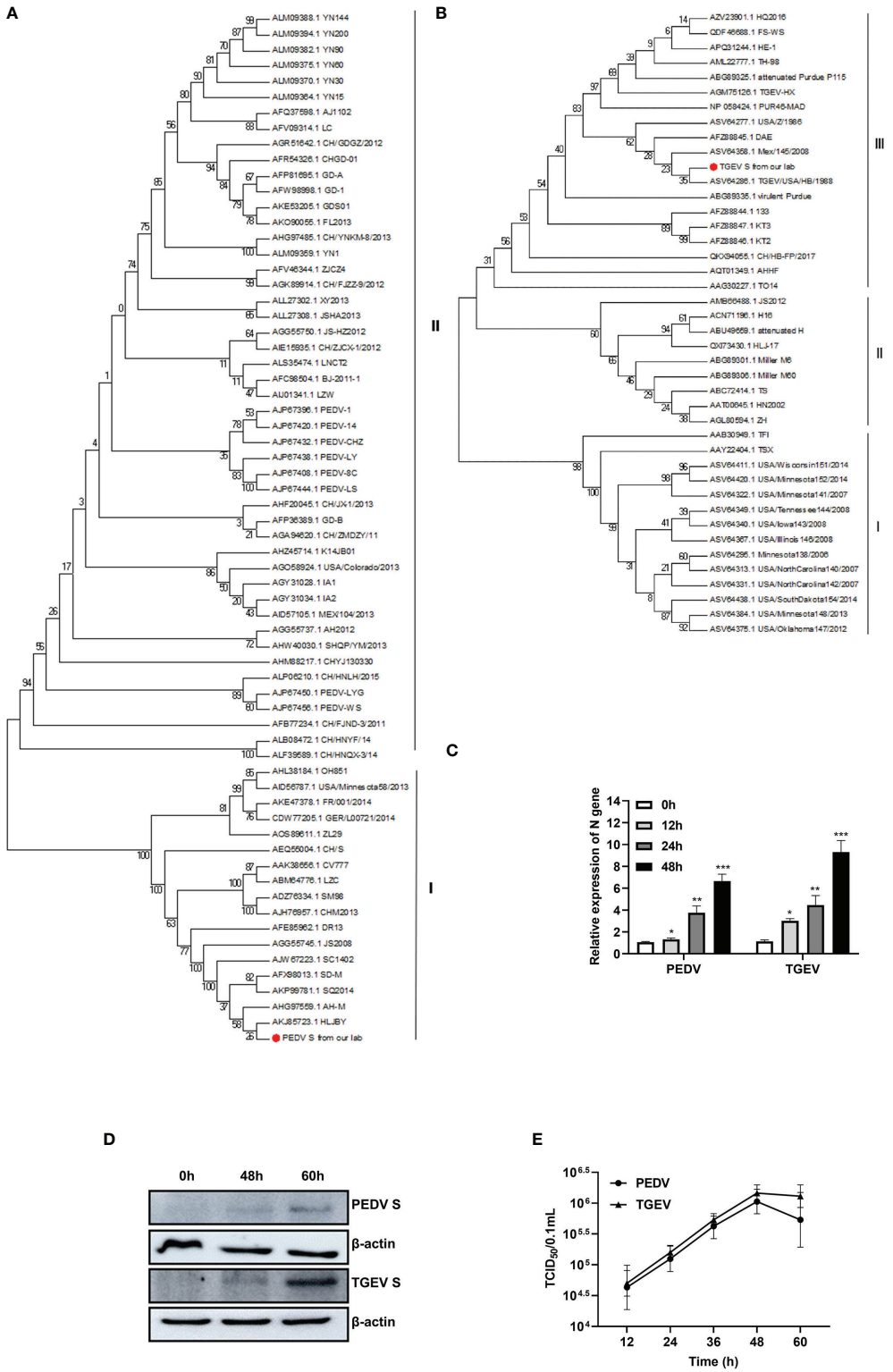

FIGURE 1 | Phylogenetic analysis and proliferation kinetics of PEDV and TGEV in IPEC-J2 cells. **(A)** Phylogenetic trees of PEDV based on the S gene. **(B)** Phylogenetic trees of TGEV based on the S gene. **(C)** qPCR analysis of PEDV and TGEV infection in IPEC-J2 cells. IPEC-J2 cells were infected (MOI = 1) of PEDV or TGEV. The cells were collected at 0, 12, 24, 36, and 48 hpi respectively, followed by RT-PCR analysis. *, p-value <0.05; **, p-value <0.01; ***, p-value <0.001. **(D)** Western blot analysis of PEDV and TGEV replication in IPEC-J2 cells at 48 and 60 hpi. Unprocessed original images is found in **Supplementary Figure S1**. **(E)** One-step growth curve of PEDV and TGEV in Vero or ST cells, respectively. Viruses were collected from IPEC-J2 cells, followed by $TCID_{50}$ evaluation.

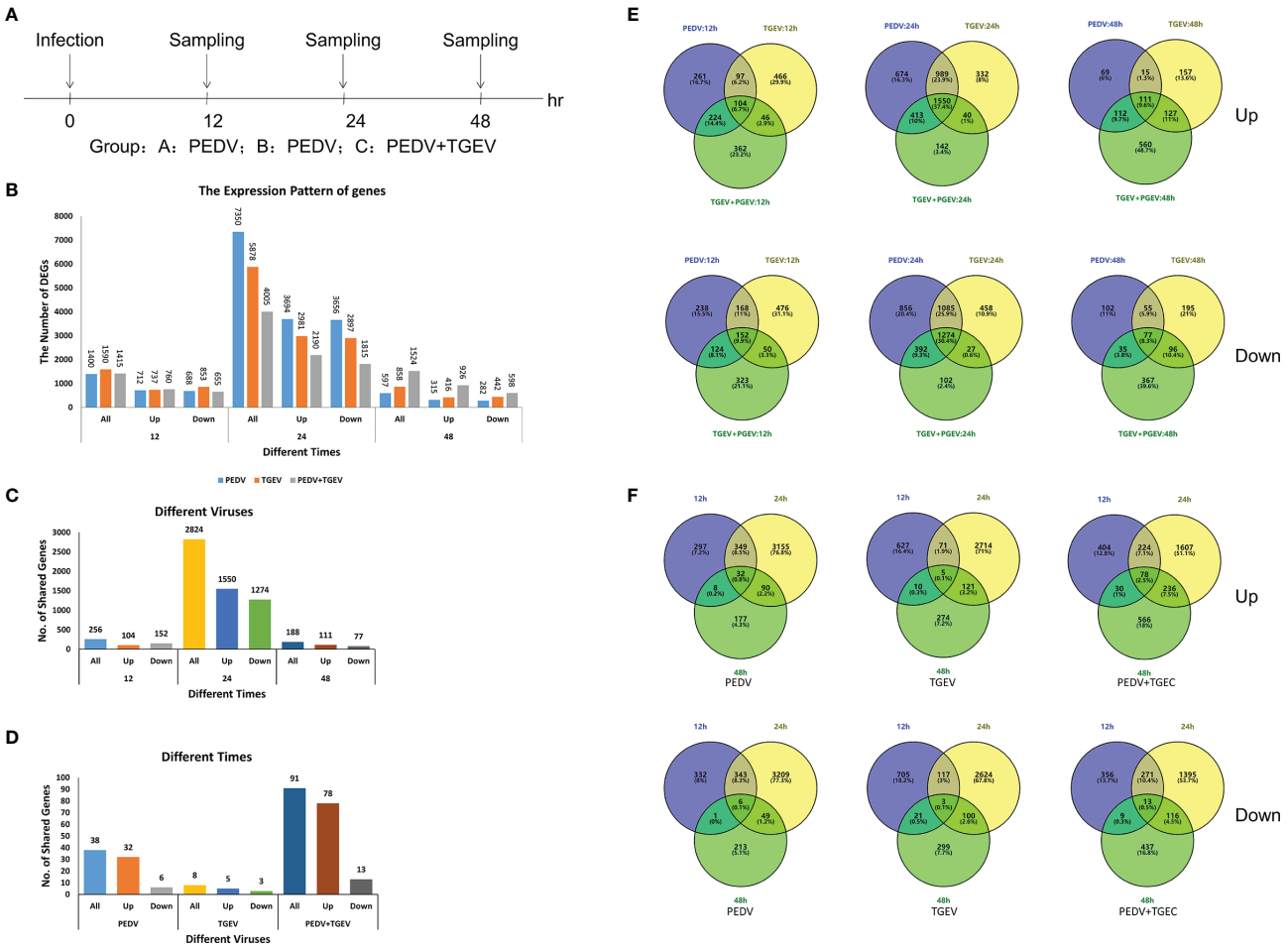

FIGURE 2 | The differentially expressed genes in all transcriptome groups. **(A)** Schematic diagram of sampling. **(B)** The number of DEGs at different times. **(C, E)** DEGs of different groups at different times. **(D, F)** DEGs of the coinfected group at different times.

processes and molecular functions of upregulated genes and downregulated genes in the following studies.

GO and KEGG Pathway Enrichment Analysis of the Shared DEGs

To analyze the function of the shared DEGs in the coinfected cells at 24 hpi, GO enrichments were performed and possible biological interactions of DEGs were examined. The results of GO analysis showed that 2,833 DEGs were identified (**Figure 3A**), including 1,637 upregulated DEGs and 1,196 downregulated DEGs. Furthermore, 2,146 of 2,833 DEGs belonged to the biological process (BP), with 1,264 upregulated and 882 downregulated. 318 of 2,833 DEGs were cellular components (CC), containing 164 upregulated and 154 downregulated. 369 of 2,833 DEGs were molecular function (MF), including 209 upregulated and 160 downregulated. The most annotated GO terms were protein binding (MF), immune system process (BP), organelle part (CC), intracellular organelle part (CC), etc. (**Figures 3A, B**). These results indicate that the biological process and molecular function of the upregulated and downregulated DEGs were different in the coinfected cells at 24 hpi.

Moreover, KEGG classification showed that the upregulated DEGs included Disease-Associated Pathway and Immune Response Associated Pathway, while the downregulated DEGs were annotated to Growth-Associated Pathway, Disease-Associated Pathway, Reproduction-Associated Pathway, and Amino acid metabolism-Associated Pathway (**Figures 3C, D**). The enriched pathways of upregulated DEGs were inconsistent with those of the downregulated DEGs.

Evaluation of the Interferon-Stimulated Genes

Interferon-stimulated genes (ISGs) are molecules regulated by interferon, which has important influences on the host's natural immunity and virus infection. Therefore, we further analyzed the ISGs of the shared genes. Among the upregulated DEGs, 90 ISGs were identified in this study, which were associated with PEDV

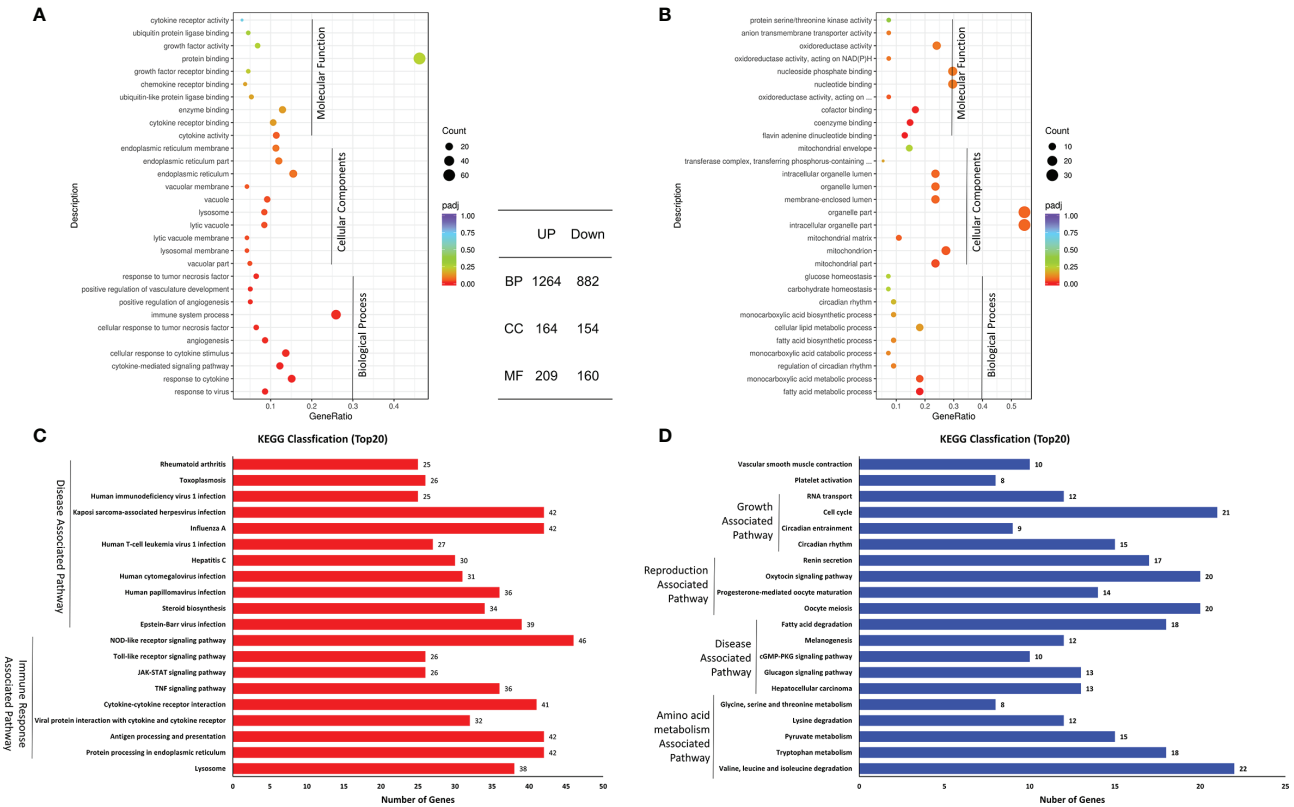

FIGURE 3 | Top 20 pathways of the shared DEGs. **(A, B)** GO annotation of up- **(A)** and downregulated **(B)** DEGs. **(C, D)** KEGG analysis of up- **(C)** and downregulated **(D)** DEGs.

or TGEV infection (**Supplemental Table 3**). Based on the biological function, the identified ISGs can be classified into several groups, including antiviral, antigen presentation, AMP sensing+IFN pathway, miscellaneous, cell signaling and apoptosis, and Ubiquitin-related groups (**Supplemental Table 3**).

Furthermore, the subcellular location of the ISGs demonstrated that most of the ISGs were in the nucleus (68 ISGs) and cytosol (58 ISGs) (**Figure 4A**). Enrichment analysis showed that the ISGs were involved in virus infection and immune response-related pathways, including NOD-like/RIG-I/Toll-like receptor signaling pathways, JAK-STAT signaling pathway, antigen processing and presentation, and pathways induced by other viruses' infection (**Figure 4B**). Especially, 27 ISGs play antiviral roles in these ISGs (**Table 1**). As shown in **Figure 4C**, these ISGs inhibit or delay the process of virus proliferation in different infection stages, such as entry, replication, transcription and translation, packing, and budding. Notably, most of the ISGs mainly target the replication–transcription complex/system. These results indicate that these ISGs are suitable candidate targets for antiviral research.

Moreover, STRING analysis was used to assess the potential interaction network of the ISGs related to response to the virus. As shown in **Figure 5A**, most ISGs interacted with other proteins to form a complex protein–protein interaction network. It is worth noting that interferon-induced transmembrane proteins (IFITMs), especially IFITM1 and IFITM3, were also included in the identified ISGs, which have been widely studied for their antiviral mechanism in the last decade. Among the ISGs, IFITM1 (**Figure 5B**) and IFITM3 (**Figure 5C**) exerted antiviral activities by interacting with various ISGs, which suggests that IFITM1 and IFITM3 are critical in resisting virus immune responses. Therefore, we focused on IFITMs to clarify whether these molecules are involved in the antiviral activities against PEDV and TGEV infection.

Confirmation of the Identified ISGs by Real-Time qPCR

To further confirm the above results, levels of ISGs with antiviral activities, such as IFITM and IRF genes, were evaluated using real-time PCR. As shown in **Figure 6**, IFITM1, IFITM3, IRF1, and IRF7 genes were significantly upregulated at 24 hpi compared with that of the mock-infected group, which were consistent with the RNA-seq data.

Knocking Down IFITMs Enhanced Virus Infection, While Overexpression of IFITMs Inhibited Virus Infection

To evaluate the effect of IFITM3 on PEDV and TGEV infection, porcine IPEC-J2 cells were transfected with si-ssc-IFITM3s or pLV-sIFITM3-Flag for 48 h, followed by infection with PEDV or

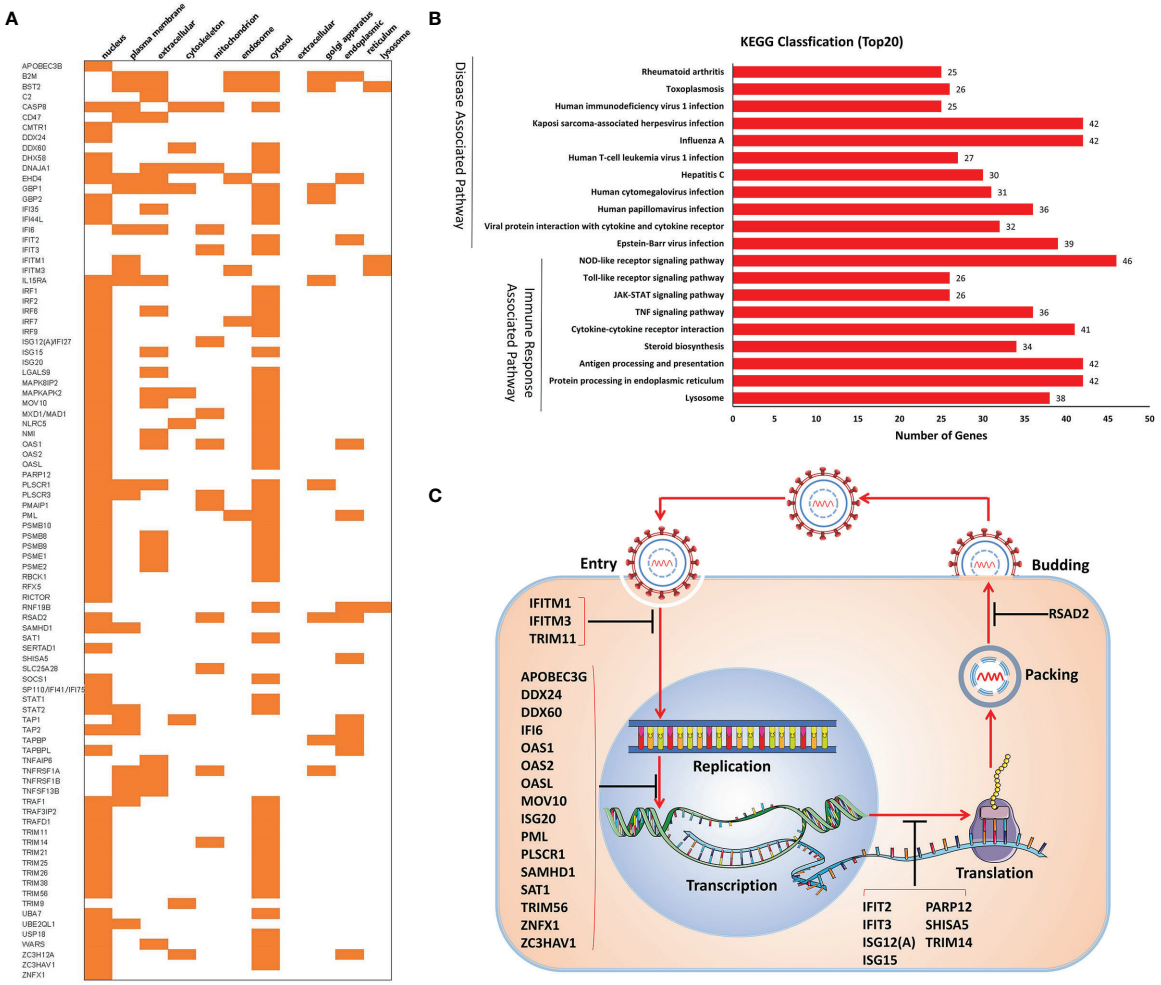

FIGURE 4 | Analysis of 90 ISGs. **(A)** Subcellular localization. **(B)** KEGG classification. **(C)** Antiviral activities of ISGs.

TEGV (MOI = 1). The results showed that the expressions levels of sIFITM3 (sIFITM3) were significantly decreased in the si-ssc-IFITM3s-transfected cells and increased in the pLV-sIFITM3-Flag-transfected cells compared to that of the control groups (**Figures 7A, B**). Expectedly, the expression levels of PEDV and TEGV genes were significantly increased in the si-ssc-IFITM3s-transfected cells (**Figures 7C, D**) and decreased in the pLV-sIFITM3-Flag-transfected cells compared to that of the control groups (**Figures 7E, F**). These results indicate that sIFITM3 has antiviral activity against PEDV and TGEV infection.

To further confirm the above results, Vero cells, a heterogeneous cell line, were transfected with pLV-sIFITM3-Flag or si-csa-IFITM3s for 48 h, followed by infection with PEDV (MOI = 1) for 48 h. As shown in **Figure 8**, the expression levels of IFITM3 were increased in the pLV-sIFITM3-Flag-transfected cells and significantly decreased in the si-csa-IFITM3s-transfected cells compared to that of the control groups (**Figures 8A, B**). Meanwhile, the expression levels of PEDV genes were significantly decreased in the pLV-sIFITM3-Flag-transfected cells and increased in the si-csa-IFITM3s-transfected cells compared to that of the control groups (**Figures 8C, D**). Furthermore, the proliferation of PEDV in IFITM3-overexpressed and knocked-down Vero cells was evaluated using flow cytometry assay and crystal violet staining assay. The results showed consistency with real-time PCR results (**Figures 8E, F**). The cell viability was significantly increased in the sIFITM3-overexpressed and decreased in the knocked-down Vero cells compared with the control groups, respectively (**Figures 8G, H**). These results further confirmed that knocking down IFITM3 enhanced virus infection, while overexpression of sIFITM3 inhibited virus infection.

Additionally, A549, BHK21, and DF-1 cells were transfected with pCAGGS-sIFITM3-Flag, followed by infection with rVSV-GFP. As shown in **Figure 9A**, the sIFITM3 can be efficiently expressed in these cells. The replication of rVSV-GFP was significantly inhibited in the sIFITM3-expressed cells (**Figures 9B, C**). These results further suggest that the antiviral activity of sIFITM3 is broad-spectrum *in vitro*.

TABLE 1 | Antiviral interferon-induced genes in this study.

Gene symbol	PEDV infection		TGEV infection		PEDV+TGEV infection		Gene description	Ref DOI
	log2 fold change	q value	log2 fold change	q value	log2 fold change	q value		
APOBEC3B	0.853622611	3.47E-09	0.716693607	0.002364504	0.953401477	1.82169E-06	Apolipoprotein B mRNA editing enzyme catalytic subunit 3B	10.1038/nature00939
DDX24	0.227246637	0.039698472	0.295532008	0.04570764	0.304417963	0.020049853	DEAD-box helicase 24	10.1016/j.virol.2008.01.025
DDX60	1.110014124	0.048911194	0.998530685	0.032603554	0.955513667	0.013291317	DExD/H-box helicase 60	10.1038/nature09907
IFI6	1.479421789	0.000611615	1.864487534	5.95363E-07	1.377998512	3.09053E-05	Interferon alpha inducible protein 6	10.1038/s41564-018-0244-1
IFIT2	2.292753267	0.005583963	2.170059221	0.010245215	2.269357635	0.007031308	Interferon-induced protein with tetratricopeptide repeats 2	10.1371/journal.pbio.2004086
IFIT3	1.897685589	0.008779897	1.658142819	0.001373656	1.911377054	0.011643211	Interferon-induced protein with tetratricopeptide repeats 3	10.1371/journal.pbio.2004086
IFITM1	2.188304133	7.74E-08	2.519998152	1.35833E-10	1.987652389	1.70188E-10	Interferon-induced transmembrane protein 1	10.1016/j.cell.2009.12.017
IFITM3	1.132823871	4.43E-10	1.434383357	3.99482E-06	1.113465091	9.84344E-07	Interferon-induced transmembrane protein 3	10.3389/fimmu.2018.00228
ISG12(A)	1.822958691	0.00000265	2.186524528	7.21423E-08	1.614782083	3.25923E-07	Putative ISG12(a) protein	10.1128/JVI.00352-16
ISG15	2.302352998	0.00000341	2.663277381	6.77695E-09	2.05115159	3.77527E-08	ISG15 ubiquitin-like modifier	10.1371/journal.pbio.2004086
ISG20	1.742182074	0.000108971	1.948342895	1.72743E-06	1.502146139	3.99749E-06	Interferon stimulated exonuclease gene 20	10.1371/journal.pbio.2004086
MOV10	1.493423741	2.6E-18	1.639326559	1.46511E-08	1.205502595	1.4368E-07	Mov10 RISC complex RNA helicase	10.1371/journal.pbio.2004086
OAS1	1.332989798	2.97E-09	1.421244578	1.39396E-05	1.215590342	1.36733E-05	2′-5′-Oligoadenylate synthetase 1	10.1371/journal.pbio.2004086
OAS2	1.206408548	4.93E-08	1.117235101	0.000354723	1.127790413	5.62295E-05	2′-5′-Oligoadenylate synthetase 2	10.3390/v12040418
OASL	2.319409818	0.000176627	2.883551358	1.62918E-09	2.127805209	0.001844082	2′-5′-pligoadenylate synthetase like	10.1016/j.immuni.2018.12.013
PARP12	1.21350878	0.00365218	1.225430781	0.000345214	1.012772207	0.001336873	Poly(ADP-ribose) polymerase family member 12	10.1371/journal.pbio.2004086
PLSCR1	0.843484336	0.000034	0.81086527	0.004374285	0.825097418	0.001428997	Phospholipid scramblase 1	10.1128/JVI.78.17.8983-8993.2004.
PML	1.110555091	4.43E-08	1.189068424	7.19109E-05	1.117956227	9.76855E-06	Promyelocytic leukemia	10.1371/journal.pbio.2004086
RSAD2	1.739470018	0.025127966	1.263835725	0.026307427	1.743586308	0.032480782	Radical S-adenosyl methionine domain-containing 2	10.1016/j.virusres.2019.01.014
SAMHD1	1.57993947	0.0000295	1.561018618	1.70923E-05	1.419359396	1.79687E-05	SAM and HD domain-containing deoxynucleoside triphosphate triphosphohydrolase 1	10.1016/j.tim.2015.08.002
SAT1	1.234166325	0.000000407	1.816910382	4.24858E-08	1.202642104	0.000799724	Spermidine/spermine N1-acetyltransferase 1	10.1371/journal.pbio.2004086
SHISA5	1.013779953	3.45E-10	1.139773973	9.82032E-06	0.854640948	2.51898E-05	Shisa family member 5	10.1038/ncomms10631
TRIM11	0.79732917	0.000000202	0.859346252	0.000532122	0.642531515	0.000439271	Tripartite motif containing 11	10.1371/journal.ppat.0040016
TRIM14	0.929915084	0.00000209	0.638263983	0.023485833	1.033985153	5.19874E-05	Tripartite motif containing 14	10.3389/fmicb.2019.00344
TRIM56	1.109190465	7.78E-08	0.868601165	0.017945664	0.908904097	0.000233247	Tripartite motif containing 56	10.1371/journal.pntd.0007537
ZC3HAV1	1.260902829	3.74E-09	0.78703522	0.021422393	1.01385866	9.58972E-05	Zinc finger CCCH-type antiviral protein 1	10.1371/journal.pbio.2004086
ZNFX1	1.244001392	0.016690307	0.937197617	0.021673342	1.272066064	0.000428093	Zinc finger NFX1-type containing 1	10.1038/s41556-019-0416-0

DISCUSSION

Porcine diarrhea-associated viruses including PEDV, TGEV, porcine deltacoronavirus (PDCoV), and porcine rotavirus (PoRV) are four common causative agents for viral diarrhea in pigs worldwide (1–3, 6, 7). During 2012–2020, PEDV and TGEV are the top two viruses reported from pig farms in China, responsible for porcine diarrhea and devastating economic losses to the swine industry. It was reported that both TGEV and PEDV infection can activate the JAK-STAT1 signaling

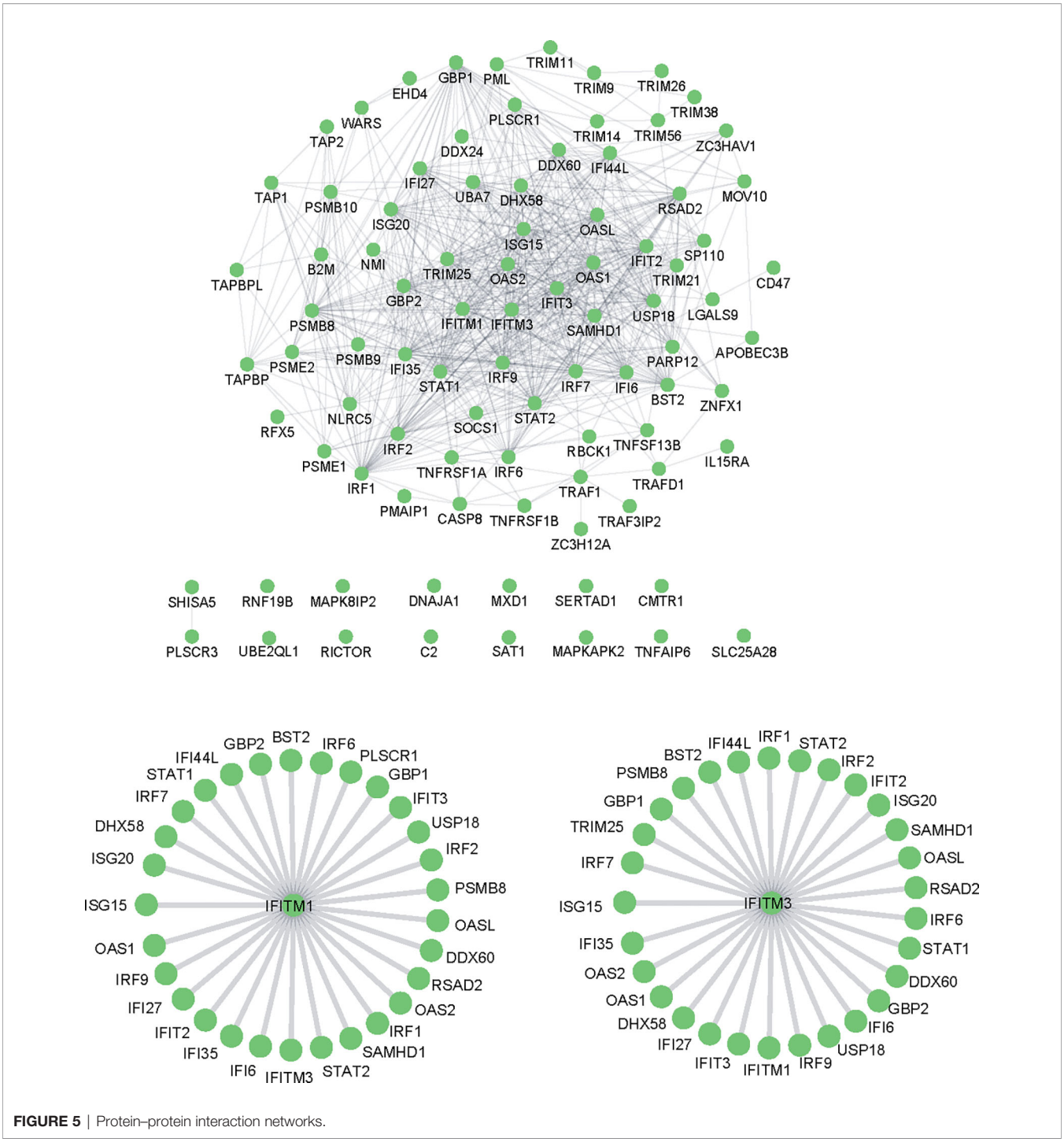

FIGURE 5 | Protein–protein interaction networks.

pathway and ISGs (23, 30). Moreover, differential protein expressions were detected in cells infected with PEDV pandemic and classical strains, including antiviral pathways and proteins, such as RLRs, autophagy, MAPK pathways, and ISGs (30–33). Coinfection of TGEV and enterotoxigenic *Escherichia coli* K88 (ETEC) regulated host proteins, thus enhancing the persistence of pathogen infection, which was partly due to the inhibition of TGEV-induced inflammatory cytokines by ETEC (34). However, differentially expressed genes in cells coinfected with PEDV and TGEV have not been reported to date. In this study, we evaluated the comparative transcriptomics between PEDV and TGEV single and coinfection. The results showed that DEGs can be detected in the cells infected with PEDV, TGEV, and PEDV+TGEV at 12, 24, and 48 hpi, and the number of DEGs was the highest at 24 hpi

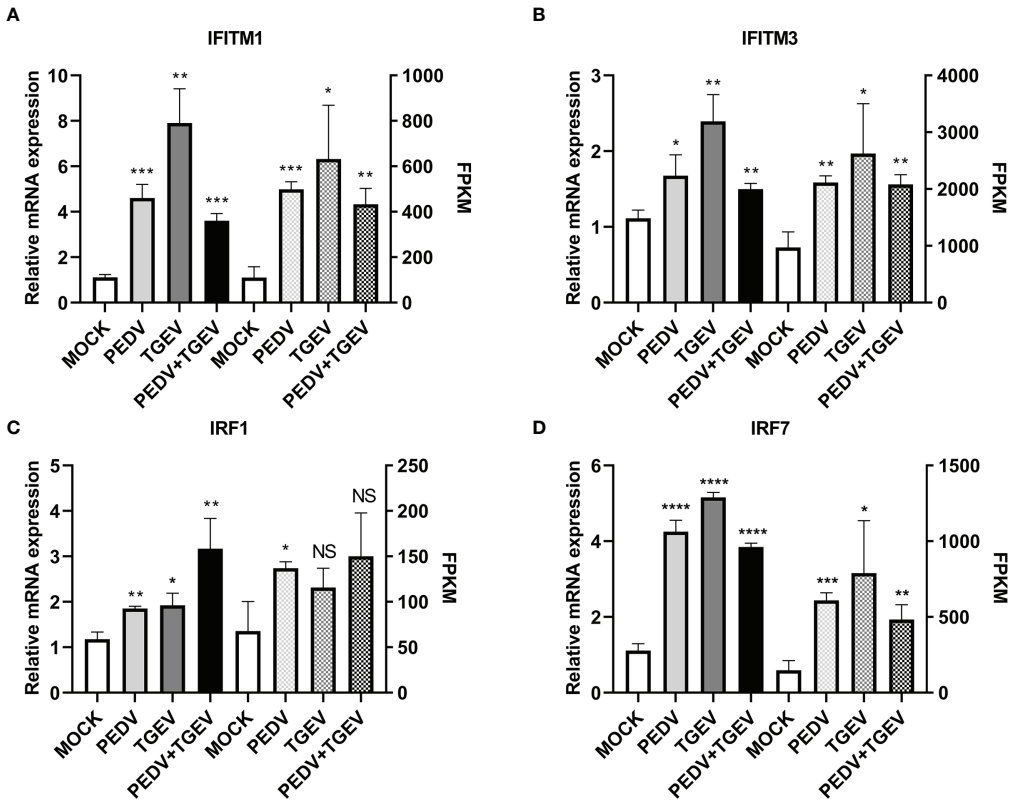

FIGURE 6 | Differentially expressed key genes. IPEC-J2 cells were infected with 1 MOI of PEDV, TGEV, and PEDV+TGEV for 24 hpi. The expression levels of IFITM1 **(A)**, IFITM3 **(B)**, IRF1 **(C)**, and IRF7 **(D)** were compared at 24 hpi with RT-PCR. GAPDH was used as the internal control. *, p-value <0.05; **, p-value <0.01; ***, p-value <0.001; ****, p-value <0.0001. NS, no significant.

(**Figure 2**). Furthermore, coinfection of PEDV+TGEV leads to more DEGs than that of the single infection, which mainly annotated to the GO terms of protein binding (BP), immune system process (MF), organelle part (CC), intracellular organelle part (CC), etc. (**Figure 3**). KEGG classification showed that the upregulated DEGs included Disease-Associated Pathway and Immune Response Associated Pathway (**Figure 3**). Therefore, we chose the shared DEGs associated with immune responses for further study.

Type I interferons, including IFN-α and IFN-β, are critical antiviral cytokines of host immune responses. However, the IFN responses induced by enteric coronaviruses in the intestinal epithelial cells are different from that of the other epithelial cells, which is partly due to the distinct characteristics of the intestinal epithelial mucosal surface and gut microflora (35). Meanwhile, type III interferon (IFN-λ) plays a vital role against infections of enteric coronaviruses (35–37). On the contrary, PEDV, especially nsp1, suppressed IFN-λ activities and interferon regulatory factor 1 (IRF1) signaling *via* inhibiting IRF1 nuclear translocation and reducing the number of peroxisomes, thus blocking the IRF1-mediated type III IFNs (37), suggesting that PEDV can escape the IFN-λ responses in intestinal epithelial cells. Furthermore, TGEV infection can stimulate endoplasmic reticulum (ER) stress and IFN-I production. However, TGEV can also evade the type I IFN antiviral response *via* IRE1α-mediated modulation of the miR-30a-5p/SOCS1/3 axis (38). Here, 90 ISGs were upregulated during PEDV or TGEV infection, which were subcellularly located in the nucleus and cytosol. Among the upregulated ISGs, 27 ISGs, including IRF1, IRF7, IFITM1, and IFITM3, play antiviral roles in different stages of virus proliferation, thus inhibiting or delaying the process of virus infection by interacting with other proteins or ISGs to form a complex protein–protein interaction network.

IFITMs are kinds of small-molecule transmembrane proteins induced by interferon, which are important restriction factors and play broad-spectrum antiviral activities (39–41). IFITMs mainly target viral-to-cellular membrane fusion to block the early stage of virus infection and/or trigger the production of novel virions with decreased infectivity (40). IFITMs can inhibit the feline foamy virus at the late step of viral replication (42). Meanwhile, IFITM1 also exerts antiviral activity by regulating host lipid metabolism (43). We previously found that IFITM3 inhibited vaccinia virus and thrombocytopenia syndrome virus (SFTSV) infection (44, 45). Another group reported that both IFITM1 and IFITM3 can be induced by IFN-α and IFN-λ in IPEC-J2 cells in a dose-dependent

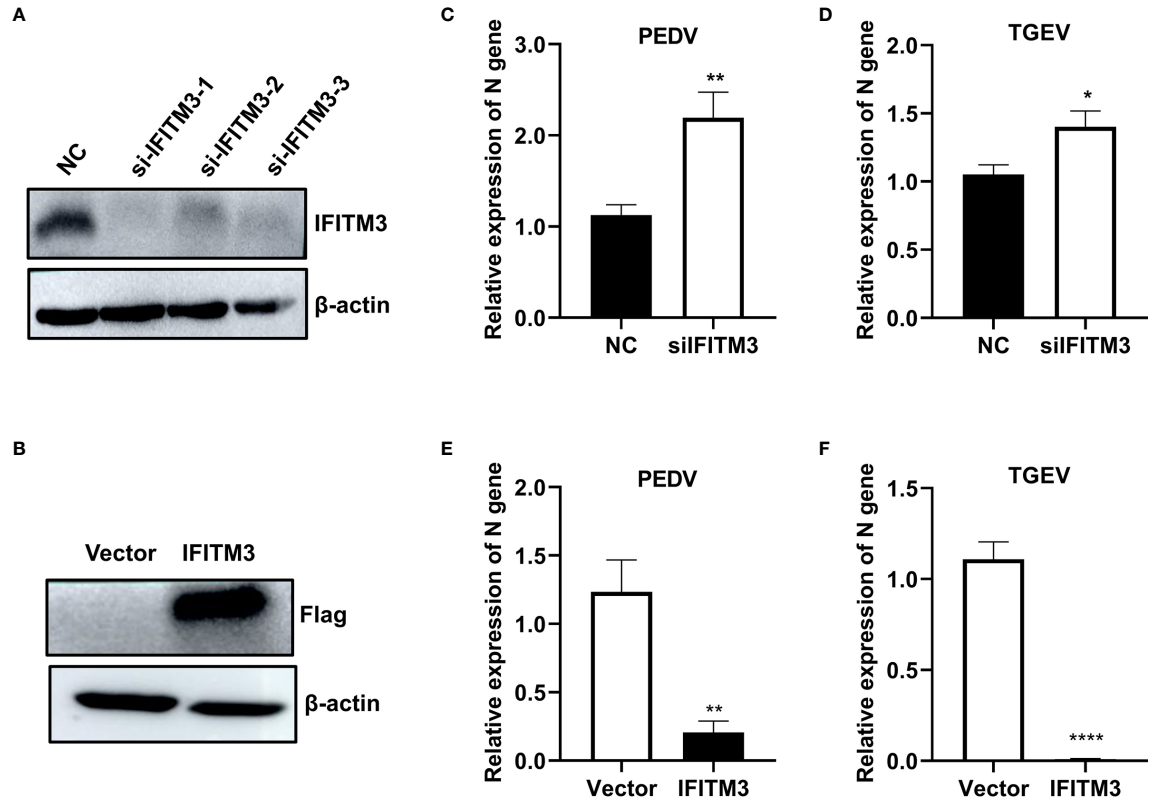

FIGURE 7 | Evaluation of PEDV and TGEV in IFITM3-overexpressed and knocked-down cells. Porcine IPEC-J2 cells were transfected with si-ssc-IFITM3s or pLV-sIFITM3-Flag for 48 h, followed by infection with PEDV or TEGV (MOI = 1). The expressions levels of sIFITM3 were evaluated by Western blot at 48 h post-transfection **(A, B)**, and the levels of viral genes were quantified at 24 h postinfection using real-time PCR **(C–F)**. **(A, C, D)** IPEC-J2 cells transfected with siIFITM3s. **(B, E, F)** IPEC-J2 cells transfected with pLV-sIFITM3-Flag. Unprocessed original images are found in **Supplementary Figure S2**. *, p-value <0.05; **, p-value <0.01; ****, p-value <0.0001.

manner (36). However, functional heterogeneity was detected in mammalian IFITMs, and critical domains of IFITMs with antiviral activity were conserved among mammalian IFITMs (40). As reported, human and mouse IFITM1, IFITM2, and IFITM3 restricted SARS-CoV-2 infections with a distinct mechanism (46). The amphipathic helix and its amphipathic properties of IFITM3 were critical for virus restriction, but its mutation will be converted into an enhancer for SARS-CoV-2 infection and cell-to-cell fusion (46). Moreover, a recent report indicated that several viruses may escape IFN- and IFITM-mediated inhibition, especially cell-to-cell spread, leading to chronic and persistent infections and illness (47). Therefore, we further evaluated the antiviral activity of sIFITM3 in cells infected with PEDV and TGEV. As a result, sIFITM3 can significantly inhibit PEDV and TGEV infection in both porcine IPEC-J2 cells and monkey Vero cells. Also, sIFITM3 can significantly inhibit VSV-EGFP infection in different species cells, such as human A549 cells, mouse BHK21 cells, and avian DF-1 cells. These results further confirm that sIFITM3 has broad-spectrum antiviral activity. In addition, IFITMs are S-palmitoylated proteins in vertebrates that restrict a diverse range of viruses (48–50). S-palmitoylated IFITM3 in particular engages incoming virus particles, prevents their cytoplasmic entry, and accelerates their lysosomal clearance by host cells (48, 50). However, how S-palmitoylation modulates the structure and biophysical characteristics of IFITM3 to promote its antiviral activity remains unclear. The research on the mechanism of sIFITM3 inhibiting virus infection as well as the function of S-palmitoylated sIFITM3 in virus infection is still in progress.

CONCLUSION

In this study, transcriptomes especially shared DEGs and ISGs are different in cells single or co-infected with PEDV and TGEV, suggesting that cells have different responses to virus infection. We firstly identified that sIFITM3 inhibits PEDV, TGEV, and VSV-EGFP, which suggests that sIFITM3 has broad-spectrum antiviral activity. Further studies are needed to elucidate the antiviral function and molecular mechanism of sIFITM3. Our research enriched the knowledge of cells against PEDV and TGEV infection and confirmed that IFITM3 is one of the important antiviral ISGs.

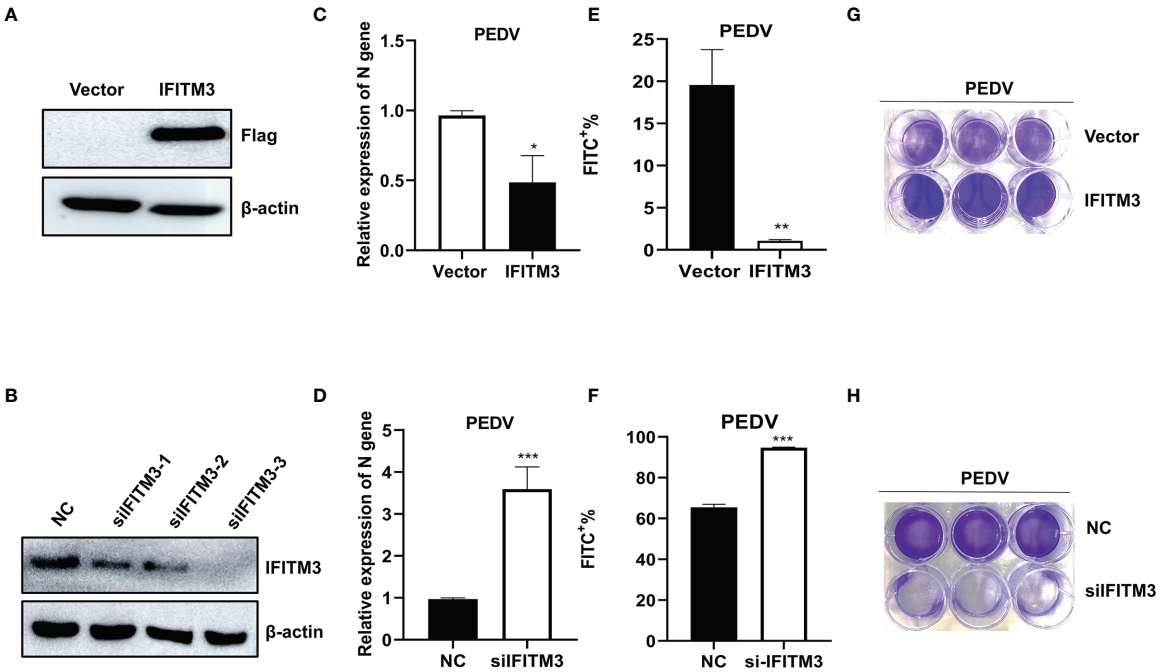

FIGURE 8 | Proliferation of PEDV in IFITM3-overexpressed and knocked-down Vero cells. Vero cells were transfected with pLV-sIFITM3-Flag or si-csa-IFITM3s for 48 h, followed by infection with PEDV (MOI = 1) for 48 h. The proliferation of PEDV in IFITM3-overexpressed and knocked-down Vero cells was evaluated at 24 h postinfection using real-time PCR, flow cytometry assay, and crystal violet staining assay. **(A, B)** Western blot. **(C, D)** Real-time PCR. **(E, F)** flow cytometry assay. **(G, H)** Crystal violet assay. Unprocessed original images are found in **Supplementary Figure S3**. *, p-value <0.05; **, p-value <0.01; ***, p-value <0.001.

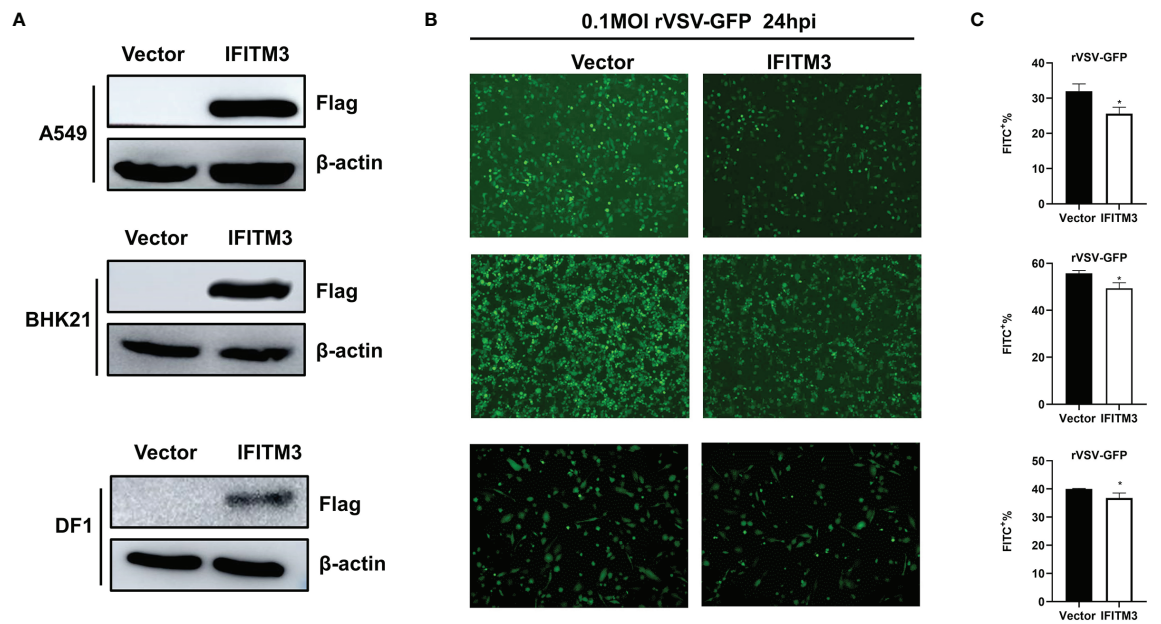

FIGURE 9 | sIFITM3 antagonizes rVSV-GFP proliferation in different cells. A549, BHK21, and DF-1 cells were transfected with pCAGGS-sIFITM3-Flag using Lipofectamine 3000 reagent. 24 h post-transfection, the expression of IFITM3 was examined by Western blot **(A)** with anti-FLAG antibody. Then the cells were infected with rVSV-GFP at 0.1 MOI and the replication of rVSV-GFP was analyzed by examining *via* fluorescence microscopy **(B)** and flow cytometry **(C)** at 24 hpi. *, p-value <0.05.

DATA AVAILABILITY STATEMENT

The datasets presented in this study can be found in online repositories. The names of the repository/repositories and accession number(s) can be found as follows: National Center for Biotechnology Information (NCBI) BioProject database under accession number PRJNA796631.

AUTHOR CONTRIBUTIONS

Conceptualization, NJ, CL, and LR. Methodology, LS and JC. Software, PH and YJ. Validation, WX and LL. Formal analysis, LS and SC. Data curation, LS and ZG. Writing—original draft preparation, LS, CL, and SC. Writing—review and editing, LR, CL, and NJ. Visualization, CL and SC. Supervision, LR, CL, and NJ. Project administration, CL. Funding acquisition, LR and NJ. All authors contributed to the article and approved the submitted version.

FUNDING

This work was supported by the National Key Research and Development Program of China [No. 2021YFD1801103]; the National Natural Science Foundation of China [Nos. 31972719, 31772747]; the Jilin Province Science and Technology Development Project [No. 20200402043NC]; and the Jilin University Science and Technology Innovative Research Team [JLU-STIRT, 2017TD-05]. The funders had no role in study design, data collection and analysis, decision to publish, or preparation of the manuscript.

SUPPLEMENTARY MATERIAL

The Supplementary Material for this article can be found online at: https://www.frontiersin.org/articles/10.3389/fimmu.2022.844657/full#supplementary-material

REFERENCES

1. Liu Q, Wang HY. Porcine Enteric Coronaviruses: An Updated Overview of the Pathogenesis, Prevalence, and Diagnosis. *Vet Res Commun* (2021) 45:75–86. doi: 10.1007/s11259-021-09808-0
2. Wang Q, Vlasova AN, Kenney SP, Saif LJ. Emerging and Re-Emerging Coronaviruses in Pigs. *Curr Opin Virol* (2019) 34:39–49. doi: 10.1016/j.coviro.2018.12.001
3. Turlewicz-Podbielska H, Pomorska-Mol M. Porcine Coronaviruses: Overview of the State of the Art. *Virol Sin* (2021) 36:833–51. doi: 10.1007/s12250-021-00364-0
4. Li ZL, Zhu L, Ma JY, Zhou QF, Song YH, Sun BL, et al. Molecular Characterization and Phylogenetic Analysis of Porcine Epidemic Diarrhea Virus (PEDV) Field Strains in South China. *Virus Genes* (2012) 45:181–5. doi: 10.1007/s11262-012-0735-8
5. Zhu Y, Liang L, Luo Y, Wang G, Wang C, Cui Y, et al. A Sensitive Duplex Nanoparticle-Assisted PCR Assay for Identifying Porcine Epidemic Diarrhea Virus and Porcine Transmissible Gastroenteritis Virus From Clinical Specimens. *Virus Genes* (2017) 53:71–6. doi: 10.1007/s11262-016-1405-z
6. Zhang F, Luo S, Gu J, Li Z, Li K, Yuan W, et al. Prevalence and Phylogenetic Analysis of Porcine Diarrhea Associated Viruses in Southern China From 2012 to 2018. *BMC Vet Res* (2019) 15:470. doi: 10.1186/s12917-019-2212-2
7. Shi Y, Li B, Tao J, Cheng J, Liu H. The Complex Co-Infections of Multiple Porcine Diarrhea Viruses in Local Area Based on the Luminex xTAG Multiplex Detection Method. *Front Vet Sci* (2021) 8:602866. doi: 10.3389/fvets.2021.602866
8. Schwegmann-Wessels C, Zimmer G, Schroder B, Breves G, Herrler G. Binding of Transmissible Gastroenteritis Coronavirus to Brush Border Membrane Sialoglycoproteins. *J Virol* (2003) 77:11846–8. doi: 10.1128/JVI.77.21.11846-11848.2003
9. Hu W, Zhang S, Shen Y, Yang Q. Epidermal Growth Factor Receptor Is a Co-Factor for Transmissible Gastroenteritis Virus Entry. *Virology* (2018) 521:33–43. doi: 10.1016/j.virol.2018.05.009
10. Li W, Hulswit RJG, Kenney SP, Widjaja I, Jung K, Alhamo MA, et al. Broad Receptor Engagement of an Emerging Global Coronavirus may Potentiate Its Diverse Cross-Species Transmissibility. *Proc Natl Acad Sci USA* (2018) 115:E5135–43. doi: 10.1073/pnas.1802879115
11. Li Y, Wu Q, Huang L, Yuan C, Wang J, Yang Q. An Alternative Pathway of Enteric PEDV Dissemination From Nasal Cavity to Intestinal Mucosa in Swine. *Nat Commun* (2018) 9:3811. doi: 10.1038/s41467-018-06056-w
12. Zhao S, Gao J, Zhu L, Yang Q. Transmissible Gastroenteritis Virus and Porcine Epidemic Diarrhoea Virus Infection Induces Dramatic Changes in the Tight Junctions and Microfilaments of Polarized IPEC-J2 Cells. *Virus Res* (2014) 192:34–45. doi: 10.1016/j.virusres.2014.08.014
13. Niu Z, Zhang Y, Kan Z, Ran L, Yan T, Xu S, et al. Decreased NHE3 Activity in Intestinal Epithelial Cells in TGEV and PEDV-Induced Piglet Diarrhea. *Vet Microbiol* (2021) 263:109263. doi: 10.1016/j.vetmic.2021.109263
14. Peng O, Wei X, Ashraf U, Hu F, Xia Y, Xu Q, et al. Genome-Wide Transcriptome Analysis of Porcine Epidemic Diarrhea Virus Virulent or Avirulent Strain-Infected Porcine Small Intestinal Epithelial Cells. *Virol Sin* (2022) 37(1):70–81. doi: 10.1016/j.virs.2022.01.011
15. Akimkin V, Beer M, Blome S, Hanke D, Hoper D, Jenckel M, et al. New Chimeric Porcine Coronavirus in Swine Feces, Germany 2012. *Emerg Infect Dis* (2016) 22:1314–5. doi: 10.3201/eid2207.160179
16. Boniotti MB, Papetti A, Lavazza A, Alborali G, Sozzi E, Chiapponi C, et al. Porcine Epidemic Diarrhea Virus and Discovery of a Recombinant Swine Enteric Coronavirus, Italy. *Emerg Infect Dis* (2016) 22:83–7. doi: 10.3201/eid2201.150544
17. Mandelik R, Sarvas M, Jackova A, Salamunova S, Novotny J, Vilcek S. First Outbreak With Chimeric Swine Enteric Coronavirus (SeCoV) on Pig Farms in Slovakia - Lessons to Learn. *Acta Vet Hung* (2018) 66:488–92. doi: 10.1556/004.2018.043
18. De Nova PJG, Cortey M, Diaz I, Puente H, Rubio P, Martin M, et al. A Retrospective Study of Porcine Epidemic Diarrhoea Virus (PEDV) Reveals the Presence of Swine Enteric Coronavirus (SeCoV) Since 1993 and the Recent Introduction of a Recombinant PEDV-SeCoV in Spain. *Transbound Emerg Dis* (2020) 67:2911–22. doi: 10.1111/tbed.13666
19. Sungsuwan S, Jongkaewwattana A, Jaru-Ampornpan P. Nucleocapsid Proteins From Other Swine Enteric Coronaviruses Differentially Modulate PEDV Replication. *Virology* (2020) 540:45–56. doi: 10.1016/j.virol.2019.11.007
20. Crosse KM, Monson EA, Beard MR, Helbig KJ. Interferon-Stimulated Genes as Enhancers of Antiviral Innate Immune Signaling. *J Innate Immun* (2018) 10:85–93. doi: 10.1159/000484258
21. Schoggins JW. Interferon-Stimulated Genes: What Do They All do? *Annu Rev Virol* (2019) 6:567–84. doi: 10.1146/annurev-virology-092818-015756
22. Zhao M, Li L, Zhai L, Yue Q, Liu H, Ren S, et al. Comparative Transcriptomic and Proteomic Analyses Prove That IFN-Lambda1 is a More Potent Inducer of ISGs Than IFN-Alpha Against Porcine Epidemic Diarrhea Virus in Porcine Intestinal Epithelial Cells. *J Proteome Res* (2020) 19:3697–707. doi: 10.1021/acs.jproteome.0c00164
23. An K, Fang L, Luo R, Wang D, Xie L, Yang J, et al. Quantitative Proteomic Analysis Reveals That Transmissible Gastroenteritis Virus Activates the JAK-STAT1 Signaling Pathway. *J Proteome Res* (2014) 13:5376–90. doi: 10.1021/pr500173p
24. Chen W, Wen Z, Zhang J, Li C, Huang K, Bu Z. Establishing a Safe, Rapid, Convenient and Low-Cost Antiviral Assay of Interferon Bioactivity Based on Recombinant VSV Expressing GFP. *J Virol Methods* (2018) 252:1–7. doi: 10.1016/j.jviromet.2017.08.007

25. Nan FL, Zhang H, Nan WL, Xie CZ, Ha Z, Chen X, et al. Lentogenic NDV V Protein Inhibits IFN Responses and Represses Cell Apoptosis. *Vet Microbiol* (2021) 261:109181. doi: 10.1016/j.vetmic.2021.109181
26. Reed LJ, Muench H. A Simple Method of Estimating Fifty Per Cent Endpoints. *Am J Epidemiol* (1938) 27:493–7. doi: 10.1093/oxfordjournals.aje.a118408
27. Xie J, Zeng Q, Wang M, Ou X, Ma Y, Cheng A, et al. Transcriptomic Characterization of a Chicken Embryo Model Infected With Duck Hepatitis A Virus Type 1. *Front Immunol* (2018) 9:1845. doi: 10.3389/fimmu.2018.01845
28. Cao Y, Zhang K, Liu L, Li W, Zhu B, Zhang S, et al. Global Transcriptome Analysis of H5N1 Influenza Virus-Infected Human Cells. *Hereditas* (2019) 156:10. doi: 10.1186/s41065-019-0085-9
29. Hu Z, Li Y, Du H, Ren J, Zheng X, Wei K, et al. Transcriptome Analysis Reveals Modulation of the STAT Family in PEDV-Infected IPEC-J2 Cells. *BMC Genomics* (2020) 21:891. doi: 10.1186/s12864-020-07306-2
30. Lin H, Li B, Chen L, Ma Z, He K, Fan H. Differential Protein Analysis of IPEC-J2 Cells Infected With Porcine Epidemic Diarrhea Virus Pandemic and Classical Strains Elucidates the Pathogenesis of Infection. *J Proteome Res* (2017) 16:2113–20. doi: 10.1021/acs.jproteome.6b00957
31. Sun D, Shi H, Guo D, Chen J, Shi D, Zhu Q, et al. Analysis of Protein Expression Changes of the Vero E6 Cells Infected With Classic PEDV Strain CV777 by Using Quantitative Proteomic Technique. *J Virol Methods* (2015) 218:27–39. doi: 10.1016/j.jviromet.2015.03.002
32. Guo X, Hu H, Chen F, Li Z, Ye S, Cheng S, et al. iTRAQ-Based Comparative Proteomic Analysis of Vero Cells Infected With Virulent and CV777 Vaccine Strain-Like Strains of Porcine Epidemic Diarrhea Virus. *J Proteomics* (2016) 130:65–75. doi: 10.1016/j.jprot.2015.09.002
33. Li Z, Chen F, Ye S, Guo X, Muhanmmad Memon A, Wu M, et al. Comparative Proteome Analysis of Porcine Jejunum Tissues in Response to a Virulent Strain of Porcine Epidemic Diarrhea Virus and Its Attenuated Strain. *Viruses* (2016) 8(12):323. doi: 10.3390/v8120323
34. Xia L, Dai L, Zhu L, Hu W, Yang Q. Proteomic Analysis of IPEC-J2 Cells in Response to Coinfection by Porcine Transmissible Gastroenteritis Virus and Enterotoxigenic Escherichia Coli K88. *Proteomics Clin Appl* (2017) 11:1600137. doi: 10.1002/prca.201600137
35. Zhang Q, Yoo D. Immune Evasion of Porcine Enteric Coronaviruses and Viral Modulation of Antiviral Innate Signaling. *Virus Res* (2016) 226:128–41. doi: 10.1016/j.virusres.2016.05.015
36. Li L, Fu F, Xue M, Chen W, Liu J, Shi H, et al. IFN-Lambda Preferably Inhibits PEDV Infection of Porcine Intestinal Epithelial Cells Compared With IFN-Alpha. *Antiviral Res* (2017) 140:76–82. doi: 10.1016/j.antiviral.2017.01.012
37. Zhang Q, Ke H, Blikslager A, Fujita T, Yoo D. Type III Interferon Restriction by Porcine Epidemic Diarrhea Virus and the Role of Viral Protein Nsp1 in IRF1 Signaling. *J Virol* (2018) 92:e01677–17. doi: 10.1128/JVI.01677-17
38. Ma Y, Wang C, Xue M, Fu F, Zhang X, Li L, et al. The Coronavirus Transmissible Gastroenteritis Virus Evades the Type I Interferon Response Through IRE1alpha-Mediated Manipulation of the MicroRNA miR-30a-5p/SOCS1/3 Axis. *J Virol* (2018) 92(22):e00728–18. doi: 10.1128/JVI.00728-18
39. Ren L, Du S, Xu W, Li T, Wu S, Jin N, et al. Current Progress on Host Antiviral Factor IFITMs. *Front Immunol* (2020) 11:543444. doi: 10.3389/fimmu.2020.543444
40. Marziali F, Delpeuch M, Kumar A, Appourchaux R, Dufloo J, Tartour K, et al. Functional Heterogeneity of Mammalian IFITM Proteins Against HIV-1. *J Virol* (2021) 95:e0043921. doi: 10.1128/JVI.00439-21
41. Meischel T, Fritzlar S, Villalon-Letelier F, Tessema MB, Brooks AG, Reading PC, et al. IFITM Proteins That Restrict the Early Stages of Respiratory Virus Infection Do Not Influence Late-Stage Replication. *J Virol* (2021) 95:e0083721. doi: 10.1128/JVI.00837-21
42. Kim J, Shin CG. IFITM Proteins Inhibit the Late Step of Feline Foamy Virus Replication. *Anim Cells Syst (Seoul)* (2020) 24:282–8. doi: 10.1080/19768354.2020.1819413
43. Zhang Y, Wang L, Zheng J, Huang L, Wang S, Huang X, et al. Grouper Interferon-Induced Transmembrane Protein 1 Inhibits Iridovirus and Nodavirus Replication by Regulating Virus Entry and Host Lipid Metabolism. *Front Immunol* (2021) 12:636806. doi: 10.3389/fimmu.2021.636806
44. Li C, Du S, Tian M, Wang Y, Bai J, Tan P, et al. The Host Restriction Factor Interferon-Inducible Transmembrane Protein 3 Inhibits Vaccinia Virus Infection. *Front Immunol* (2018) 9:228. doi: 10.3389/fimmu.2018.00228
45. Xing H, Ye L, Fan J, Fu T, Li C, Zhang S, et al. IFITMs of African Green Monkey Can Inhibit Replication of SFTSV But Not MNV *In Vitro*. *Viral Immunol* (2020) 33:634–41. doi: 10.1089/vim.2020.0132
46. Shi G, Kenney AD, Kudryashova E, Zani A, Zhang L, Lai KK, et al. Opposing Activities of IFITM Proteins in SARS-CoV-2 Infection. *EMBO J* (2021) 40:e106501. doi: 10.15252/embj.2020106501
47. Chmielewska AM, Gomez-Herranz M, Gach P, Nekulova M, Bagnucka MA, Lipinska AD, et al. The Role of IFITM Proteins in Tick-Borne Encephalitis Virus Infection. *J Virol* (2022) 96:e0113021. doi: 10.1128/JVI.01130-21
48. Benfield CT, Mackenzie F, Ritzefeld M, Mazzon M, Weston S, Tate EW, et al. Bat IFITM3 Restriction Depends on S-Palmitoylation and a Polymorphic Site Within the CD225 Domain. *Life Sci Alliance* (2020) 3(1):e201900542. doi: 10.26508/lsa.202000747
49. Das T, Yang X, Lee H, Garst E, Valencia E, Chandran K, et al. S-Palmitoylation and Sterol Interactions Mediate Antiviral Specificity of IFITM Isoforms. *Res Sq* (2021) rs.3.rs-1179000. doi: 10.21203/rs.3.rs-1179000/v1
50. Garst EH, Lee H, Das T, Bhattacharya S, Percher A, Wiewiora R, et al. Site-Specific Lipidation Enhances IFITM3 Membrane Interactions and Antiviral Activity. *ACS Chem Biol* (2021) 16:844–56. doi: 10.1021/acschembio.1c00013

Conflict of Interest: The authors declare that the research was conducted in the absence of any commercial or financial relationships that could be construed as a potential conflict of interest.

Publisher's Note: All claims expressed in this article are solely those of the authors and do not necessarily represent those of their affiliated organizations, or those of the publisher, the editors and the reviewers. Any product that may be evaluated in this article, or claim that may be made by its manufacturer, is not guaranteed or endorsed by the publisher.

frontiers | Frontiers in Immunology

REVIEW
published: 13 June 2022
doi: 10.3389/fimmu.2022.919477

Positive Regulation of the Antiviral Activity of Interferon-Induced Transmembrane Protein 3 by S-Palmitoylation

Shubo Wen[1,2†], *Yang Song*[1,2†], *Chang Li*[3], *Ningyi Jin*[3], *Jingbo Zhai*[1,2*] *and Huijun Lu*[3*]

[1] Preventive Veterinary Laboratory, College of Animal Science and Technology, Inner Mongolia Minzu University, Tongliao, China, [2] Key Laboratory of Zoonose Prevention and Control, Universities of Inner Mongolia Autonomous Region, Tongliao, China, [3] Changchun Veterinary Research Institute, Chinese Academy of Agricultural Sciences, Changchun, China

OPEN ACCESS

Edited by:
Xiaoquan Rao,
Case Western Reserve University,
United States

Reviewed by:
Peng Jin,
New York University, United States
Jie Zhang,
Institute of Hydrobiology (CAS), China
Chunfu Zheng,
University of Calgary, Canada

***Correspondence:**
Jingbo Zhai
jbzhai@imun.edu.cn
Huijun Lu
Huijun_lu@126.com

[†]These authors have contributed equally to this work

Specialty section:
This article was submitted to Molecular Innate Immunity, a section of the journal Frontiers in Immunology

Received: 13 April 2022
Accepted: 16 May 2022
Published: 13 June 2022

Citation:
Wen S, Song Y, Li C, Jin N, Zhai J and Lu H (2022) Positive Regulation of the Antiviral Activity of Interferon-Induced Transmembrane Protein 3 by S-Palmitoylation. Front. Immunol. 13:919477. doi: 10.3389/fimmu.2022.919477

The interferon-induced transmembrane protein 3 (IFITM3), a small molecule transmembrane protein induced by interferon, is generally conserved in vertebrates, which can inhibit infection by a diverse range of pathogenic viruses such as influenza virus. However, the precise antiviral mechanisms of IFITM3 remain unclear. At least four post-translational modifications (PTMs) were found to modulate the antiviral effect of IFITM3. These include positive regulation provided by S-palmitoylation of cysteine and negative regulation provided by lysine ubiquitination, lysine methylation, and tyrosine phosphorylation. IFITM3 S-palmitoylation is an enzymatic addition of a 16-carbon fatty acid on the three cysteine residues within or adjacent to its two hydrophobic domains at positions 71, 72, and 105, that is essential for its proper targeting, stability, and function. As S-palmitoylation is the only PTM known to enhance the antiviral activity of IFITM3, enzymes that add this modification may play important roles in IFN-induced immune responses. This study mainly reviews the research progresses on the antiviral mechanism of IFITM3, the regulation mechanism of S-palmitoylation modification on its subcellular localization, stability, and function, and the enzymes that mediate the S-palmitoylation modification of IFITM3, which may help elucidate the mechanism by which this IFN effector restrict virus replication and thus aid in the design of therapeutics targeted at pathogenic viruses.

Keywords: interferon-inducible transmembrane proteins, S-palmitoylation, post-translational modifications, interaction, interferon-stimulated gene

INTRODUCTION

When pathogens invade the host cells, pattern recognition receptors (PRRs), presenting in the host endosomes and within the cytoplasm, could recognize the microbial components as pathogen-associated molecular patterns (PAMPs) to induce an innate immune response.

In total, six PRRs have been discovered so far, including retinoic acid-inducible gene-I-like receptors (RLRs), Toll-like receptors (TLRs), NOD-like receptors (NLRs), C-type lectin receptors (CLRs), cyclic GMP-AMP synthase (cGAS), and absent in melanoma 2 (AIM2). RLRs locate in the

cytoplasm, and they can recognize long or short double-stranded RNAs; TLRs sense double-stranded RNA, single-stranded RNA, double-stranded DNA, and bacterial lipopolysaccharide (1); NLRs could detect microorganisms and parasites; CLRs are a class of calcium-dependent glycol-binding proteins presenting on the surface of immune cells such as macrophages, neutrophils, and immature dendritic cells, and they could distinguish β-glucan and mannan structures in fungal cell walls; cGAS predominantly distributes throughout the cytoplasm and binds to microbial DNA (2); AIM2, a member of the HIN-200 family, mainly responses to cytoplasmic dsDNA (3).

Upon binding to PRRs, PAMPs trigger signaling cascades culminating in the secretion of numerous pro-inflammatory cytokines, including type I interferon that contributes to the host antiviral response. Type I interferon acts in both autocrine and paracrine mode by binding to its receptor to activate Janus kinase (JAK), which results in activation of the downstream STAT proteins (STAT1 and STAT2), by phosphorylating their Tyr residues. The activated STAT proteins bind to IRF9 and the trimeric complex, IFN-stimulated gene factor 3 (ISGF3), translocate into the nucleus (4). ISGF3 in the nucleus induces the transcription of hundreds of IFN- Stimulated genes (ISGs) by binding to their ISRE sequences in the nucleus. These ISGs encode various of known effector proteins with different biological characteristics. They play antiviral roles during different stages of the viral life cycle, including invasion, replication, protein translation, packaging, and release (5, 6). Recent studies on innate immune response mechanisms have suggested hundreds of IFN-stimulated genes (ISGs) that could inhibit the replication of human and animal viruses (7).

For instance, Interferon-stimulated gene 15 (ISG15), which encodes ubiquitin-like proteins, can be strongly upregulated by Type I interferon treatment or pathogen infection. It mainly regulates intracellular innate immune signal transduction, therefore inducing immune tolerance and antiviral immune response through ubiquitination (8). Another example of well-studied ISGs is oligoadenylate synthetase-like proteins (OASL). OASL are a class of protein kinases induced by double-stranded RNA and could inhibit viral protein synthesis depending on their kinase activity (9, 10). Activated OASL induce ATP hydrolysis to produce (2′-5′) oligoadenylate acid and activate endoribonuclease. Once activated, endoribonuclease degrades viral nucleic acid, thereby inhibiting viral protein synthesis and viral replication. It has been shown that down-regulating the expression of OASL restrains RIG-I signaling and promotes viral replication. Conversely, overexpression of OASL can prevent the replication of a range of viruses in a RIG-I-dependent manner and promote RIG-I mediated IFN induction (11).

Among the IGSs endowed with antiviral activity, the interferon-induced transmembrane proteins (IFITMs), especially IFITM3, are the most well-characterized due to their most potent restriction of IAV, Dengue virus, etc. IFITMs are a family of conserved small transmembrane proteins in vertebrates, expressed on cytoplasmic and endolysosomal membranes (5). The human IFITMs family contains five members located on chromosome 11, including *IFITM1*, *IFITM2*, *IFITM3*, *IFITM5* and *IFITM10* genes (12). The five homologous *IFITM* genes in chicken are located on chromosome 5. Whereas in mice, there are seven *IFITM* genes, including *IFITM1-3, IFITM5-7* and *IFITM10*. *IFITM7* is located on chromosome 16 and the other six genes are on chromosome 7. Homologous *IFITM* genes have also been found in many other species, such as fish, cattle, birds, marsupials and reptiles, implicating conserved function for IFITM proteins (12–14).

IFITM proteins are composed of five domains based on their structural characteristics. Human IFITM3 contains a hydrophobic and variable N-terminal (NTD, 1-57 aa), a hydrophobic and conserved intramembrane domain (IMD, 58-80 aa), a conserved intracellular cyclic domain (CIL, 81-104 aa), a hydrophobic transmembrane domain (TMD, 105-126 aa), and a highly variable C-terminal (CTD, 127-133 aa) (15). IMD and CIL together comprise the CD225 domain, which presents in more than 300 proteins (16).

Previous studies showed that there were three models of IFITM topological structure on the membrane. Initially, IFITM was recognized as a kind of transmembrane protein with transmembrane NTD and CTD facing extracellular (**Figure 1**, Model I) (17). Subsequent studies showed that NTD, CTD, and CIL were all located in the cytoplasm, and the two hydrophobic domains (IMD and TMD) folded back in the membrane but did not cross the membrane (**Figure 1**, Model II) (18). Recently, Bailey CC et al. suggested that IFITM3 has a type II transmembrane topology, with its NTD and CIL located in the cytoplasm, while the CTD is located in the extracellular domain (**Figure 1**, Model III) (19). This model was also confirmed by some other researchers (20, 21). However, the precise topological structure of IFITM is still uncertain and needs further confirmation by crystal structure analysis.

IFITM1-3 proteins possess broad-spectrum antiviral activity against partial DNA viruses, enveloped RNA viruses, and non-enveloped RNA viruses (15, 22, 23). They can reduce the fluidity and stability of cell lipid membrane, block the fusion of the viral envelope and cell membrane to inhibit virus invasion (24). Evidence implicating IFITM3 as an innate immune protein with broad-spectrum antiviral activity accumulates rapidly. This review will summarize recent progress on the innate antiviral mechanism of IFITM3, focusing on the regulation mechanism of S-palmitoylation modification on its subcellular localization, stability, and function, and the enzymes that mediate the S-palmitoylation modification of IFITM3. This article may help elucidate how IFITM3 restricts virus replication and thus aid in developing novel therapeutic approaches to enhance the immune response against pathogenic virus infection.

ANTIVIRAL ACTIVITIES OF INTERFERON-INDUCED TRANSMEMBRANE PROTEINS

Interferon-induced transmembrane proteins (IFITM) are widely expressed and highly conserved in mammalian cells. They can be up-regulated by interferon stimulation to participate in antiviral

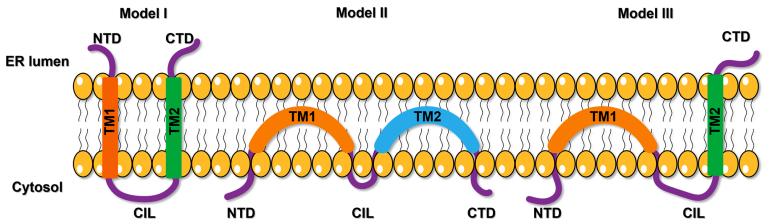

FIGURE 1 | The proposed models of IFITM protein topology. The first model suggests a kind of transmembrane protein with transmembrane NTD and CTD facing extracellular. The second model shows NTD, CTD, and CIL were all located in the cytoplasm, and the two hydrophobic domains (IMD and TMD) folded back in the membrane but did not cross the membrane. The third model proposes a type II transmembrane topology, with its NTD and CIL located in the cytoplasm, while the CTD is located in the extracellular domain. NTD, N-terminal domain; CTD, C-terminal domain; TM, transmembrane domain; CIL, intracellular cyclic loop; ER, endoplasmic reticulum.

immune responses. In recent years, small interfering RNA (15) and overexpression-based screens (25) have confirmed that IFITM1, IFITM2, and IFITM3 possess broad-spectrum antiviral effects. It has been reported that IFITM proteins, when expressed in target cells, significantly inhibit more than ten families of viruses including Alphaviridae (Semliki Forest virus, Sindbis virus) (26), Arteriviridae (Porcine reproductive and respiratory syndrome virus), Asfarviridae (African swine fever virus) (27, 28), Bunyaviridae (Rift valley fever virus, La Crosse virus, Andes virus, Hantaan virus) (29–32), Caliciviridae (Mouse norovirus) (33), Coronaviridae (SARS coronavirus) (22, 30, 34, 35), Filoviridae (Marburg virus, Ebola virus) (22, 36, 37), Flaviviridae (Dengue virus, West Nile virus, Yellow fever virus, Zika virus, Omsk hemorrhagic fever virus, Hepatitis C virus, Classical swine Fever Virus, Japanese encephalitis virus and tick-borne encephalitis virus) (23, 30, 31, 38–44), Iridoviridae (Singapore grouper iridovirus and frog iridovirus) (45–48), Nodaviridae(red spotted grouper nervous necrosis virus) (45, 46), Orthomyxoviridae (Influenza A virus) (49, 50), Paramyxoviridae (Respiratory Syncytial Virus) (51–54), Poxviridae (Vaccina virus) (55) Reoviridae (Reovirus) (56), Retroviridae (HIV-1 and Jaagsiekte sheep retrovirus) (24, 30, 57, 58), Rhabdviridae (Vesicular stomatitis virus) (57, 59, 60), Phenuiviridae (Severe fever with thrombocytopenia syndrome virus) (33).

It has been shown that IFITM1 in mammalian cells is located in the plasma membrane and early endosomes, while IFITM2 and IFITM3 are mainly expressed in the late endosomes and lysosomes (61). Due to different subcellular localization, the antiviral spectrum of the three IFITM molecules also varies. IFITM1 mainly inhibits replication of viruses that enter cells by fusing with the plasma membrane. Whereas, IFITM2 and IFITM3 mainly inhibit viruses invading cells through late endosomal and lysosomal pathways (22). Compared with IFITM1 and IFITM2, IFITM3 is considered to have the strongest antiviral activity (62). Furthermore, IFITM3, when released by the virus-infected cells into the intercellular space as a component of exosomes, could provide antiviral protection to the uninfected cells (63).

The abnormality of the *IFITM3* gene *in vivo* is involved in severe clinical symptoms caused by pathogenic viral infection. Some studies have suggested that the morbidity and mortality of *IFITM3* knockout mice infected by H3N2 or H1N1 increased (64–66). In addition, the naturally occurring single nucleotide polymorphism in IFITM3 (SNP RS12252), which is the truncated N-terminal type of IFITM3 in human may be associated with the severe outcomes following infection by IVA (64, 67), human cytomegalovirus (HCMV) (68), and human enterovirus 71 (69), as well as increased incidence and mortality caused by COVID-19 (70–72). Given the circumstance, some researchers suggested predicting the severity of COVID-19 infection among ethnic minorities based on IFITM3-rs12252 (73). Another IFITM3 SNP rs34481144 identified in the 5 'UTR of the *IFITM3* gene was reported to decrease the transcription level of its mRNA and the $CD8^+$T cell number in the airways of influenza-infected individuals. As a result, it weakens the antiviral effect of IFITM3 and leads to severe illness in adults infected by 2009 IAV (74). These studies further attest to the physiological importance of IFITM3 in the innate immune response to pathogenic viral infections.

The Antiviral Mechanism of IFITM3

IFITM3 may inhibit the release of viral protein and nucleic acid into the cytoplasm and accelerate the trafficking of incoming viral particles to lysosomes for destruction (**Figure 2**). However, the antiviral mechanism of IFITMs remains unclear till now. IFITM3 mainly plays an antiviral role in the early stage of virus infection, and at least four antiviral mechanisms are suggested based on current studies.

The first possible mechanism is that FITM3 clusters on virus-containing vesicles. This IFITM3 oligomerization increases membrane lipid order (increasing rigidity and decreasing fluidity) in cells, thus blocking fusion pore formation following virus-endosome hemifusion and before forming an enlarged fusion pore (75, 76). The overexpression of IFITM3 expands Rab7- and LAMP1-positive late endocytic compartments and accelerates the trafficking of incoming viral particles to lysosomes for destruction (77).

Moreover, IFITM3 may be incorporated into nascent virion particles during viral assembly to decrease their infectivity (39, 78, 79). The third possible mechanism is that IFITM3 may also bind itself to multiple host proteins essential to its antiviral activities. For example, a previous study showed that IFITM3 protein interacts with Vesicle-membrane-protein-associated

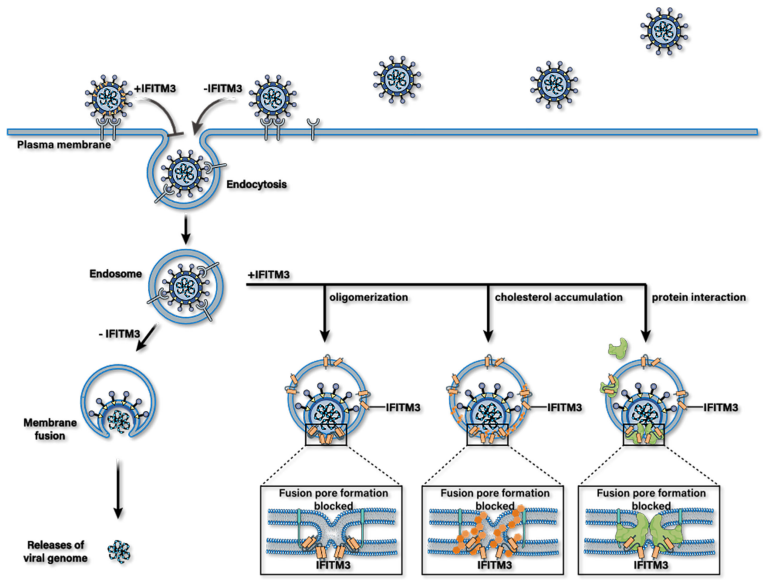

FIGURE 2 | Possible antiviral mechanisms of IFITM3. IFITM3 may inhibit the release of viral protein and nucleic acid into the cytoplasm by blocking the formation of fusion pores following virus-endosome hemifusion and before forming of an enlarged fusion pore. Whereafter, it accelerates the trafficking of incoming viral particles to lysosomes for destruction. IFITM3 can bind itself to multiple host proteins, interact with cholesterol, or packages into virions to reduce their infectious activity.

protein A (VAPA) and inhibits its association with oxysterol-binding protein (OSBP). This effect leads to the accumulation of cholesterol in the late endosomes, and thus inhibits the cytosolic release of virions (80). Likewise, it has been reported that PRRSV was arrested in IFITM3 positive endosomes, followed by the accumulation of cholesterol in endosomes or lysosomes, resulting in obstruction of PRRSV-endosome fusion (79). However, the antiviral mechanism of IFITM3 mediated by VAPA and cholesterol has been questioned by some researchers (81–84). In addition, hABHD6A, capable of inhibiting the influenza virus by itself, has been purported to act as a cofactor required for the anti-IVA effects of IFITM3 during the diseases process (49).

Another example of a putative cofactor for IFITM3 is VCP (valosin-containing protein, also called p97). The hexametric AAA-type ATPase participates in diverse cellular processes, including endoplasmic reticulum-associated degradation (ERAD), membrane fusion, nuclear factor κB (NF-κB) activation, and chromatin-associated degradation. It has been proven to enable the antiviral function of IFITM3 by modulating its intracellular localization (85).

IFITM3 also interact with the Atp6v0b subunit of the v-ATPases within the cell to form a functional v-ATPase complex. This complex contributes to the stability of the v-ATPases and appropriate localization of clathrin, which is required for the antiviral effect of IFITM3 (86). Finally, Zinc metalloproteins STE24 (ZMPSTE24; also known as ACE1), constitutively expressed and localized to the inner nuclear membrane and cytoplasmic organelles, is an intrinsic broad-spectrum antiviral protein, which is suggested to be essential for the antiviral activity of IFITM3 through interacting with IFITM3 (37).

Finally, a recent study showed that cholesterol could change the conformation of IFITM3 in membrane bilayers and interact with S-palmitoylated IFITM3 directly. CARC domain lies on N-terminus of IFITM3, a conserved motif that mediates direct interaction between this transmembrane protein and cholesterol. Further study suggested that the CARCΔ construct of IFITM3 showed a significant loss of antiviral activity against IAV and SARS-CoV-2 infection compared with IFITM3 WT (87). In addition, cholesterol can facilitate the negative membrane curvature induced by IFITM3 resulting in increased lipid order and membrane stiffness (75). Therefore, cholesterol may play a crucial role in blocking virus fusion and the release of genetic material into the cytosol.

The Antiviral Activity of IFITM3 Was Regulated by at Least Four PTMs

IFITM3 is a highly regulated protein with at least four PTMs occurring on multiple residues reported till now (**Figure 3**). For example, ubiquitination, the addition of the 9kDa ubiquitin polypeptide to proteins, occurring on the four lysines has been suggested to be a negative regulator of IFITM3 stability and activity by targeting the protein away from endolysosomes for degradation (18). Once all four lysines were mutated into alanine, IFITM3 became more stable and was completely located in the endosomal membrane. Meanwhile, its co-localization with endoplasmic reticulum markers also disappeared, indicating that ubiquitinated IFITM3 was recruited to the endoplasmic reticulum for degradation.

Another negative regulator of IFITM3 activity has been reported to be the protein-tyrosine kinase FYN-dependent phosphorylation on tyrosine 20 (Tyr20) (88). Mutation of Tyr20 resulted in decreased antiviral activity against vesicular stomatitis virus and

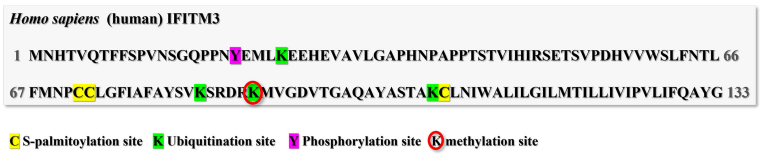

FIGURE 3 | Post-translational modification sites of human IFITM3. The human IFITM3 protein was phosphorylated on tyrosine20; Ubiquitinated on Lysine24, 83, 88 and 104; methylated on Lysine88; and S-palmitoylated on cysteine71,72 and 105.

enrichment of IFITM3 at the plasma membrane (88). Interestingly, cross-regulation of phosphorylation and ubiquitination of IFITM3 was observed in a previous study. It is generally expected that IFITM3 phosphorylation may enhance its ubiquitination level because phosphorylation normally serves as a signal for E3 ubiquitin ligases. However, the opposite was observed in that IFITM3 ubiquitin was attenuated by phosphorylation (89). How ubiquitin and phosphorylation co-regulate the antiviral effect of IFITM3 deserves further study.

Finally, single lysine (Lys88) methylation of IFITM3 mediated by SET7 has also been described to negatively regulate IFITM3 antiviral activity (90). In this study, methylation of IFITM3 was up-regulated by SET7 overexpression leading to a loss of antiviral activity. In contrast, knockdown of SET7 decreased IFITM3 methylation and resulted in enhanced IFITM3 antiviral activity against influenza virus and vesicular stomatitis virus.

Except for the three PTMs, S-palmitoylation of IFITM3 is the only one that can positively regulate its antiviral activity by multiple mechanisms discussed in the following.

PROTEIN S-PALMITOYLATION

Palmitoylation is the posttranslational process by which a 16-carbon palmitic acid is covalently attached to eukaryotic and viral proteins. It is catalyzed by a family of proteins known as DHHC acyltransferases. The most common forms of palmitoylation are S-palmitoylation and N-palmitoylation. S-palmitoylation, a reversible modification, occurs on cysteine residues *via* a thioester bond and is commonly found in most palmitoylated proteins. N-palmitoylation reactions occur on the amino terminus or the epsilon amino group of lysine.

Recently, improved proteomic of cellular proteins has identified tens to hundreds of proteins as substrates for S-palmitoylation. Many lines of evidence suggest that S-Palmitoylation is implicated in various physiological processes, including intracellular trafficking, the activity of ion channels, localization of neuronal scaffolding proteins Ras signaling, and host-pathogen interactions (91–95). As a posttranslational modification, S-palmitoylation was first reported in 1979 (96). However, the enzymes that catalyze protein S-palmitoylation were not discovered until 2002 in yeast (97, 98). A family of low-abundance and polytopic eukaryotic integral membrane enzymes responsible for modifying proteins with palmitate on the cytoplasmic face of cellular membranes is DHHC-palmitoyl transferase. They are so named because they share a signature DHHC (Asp-His-His-Cys) motif, the catalytic center of the enzyme, within a cysteine-rich domain.

Many intracellular soluble and membrane proteins can undergo S-palmitoylation modification, generally occurring in intracellular-membrane contact. S-palmitoylation modifies the hydrophobicity of proteins, affects their membrane-binding properties, intracellular sorting, stability, and thus regulates a series of cellular physiological and pathological processes.

S-Palmitoylation and Viral Infection

It has been suggested that S-palmitoylation modification is also involved in the host defense against pathogens. Some pathogens use palmitoyl transferase of host cells to modify their virulence proteins to enter host cells (95, 99). In 1979, S-palmitoylation of Sindbis virus envelope glycoprotein and vesicular stomatitis virus glycoprotein G were firstly identified (96, 100). With the development of technologies, many other viral proteins have also undergone S-palmitoylation modification as well. Previous studies have shown that S-palmitoylation of influenza virus HA contributes to the recruitment of the viral protein to membrane lipid raft, the budding process of new virus particles, and the fusion of virus particles and membrane to promote virus invasion (101–103). Recent studies have shown that S-palmitoylation modification of HA regulates the membrane curvature and promotes the interaction between HA and matrix protein (M1) during viral particle assembly (104), which promotes the expansion of fusion pores (102). The highly conserved amphiphilic helical region of M2 is also S-palmitoylated to regulate the membrane curvature, promote the separation of the virion from the membrane, and virion release (105, 106).

S-Palmitoylation and Innate Immunity

Chesarino et al. found that S-palmitoylation of TLR2 (a member of the TLR family) mediated its membrane localization, NF-κB activation and inflammatory factor release. Once inhibited, its response to all microbial ligands were restrained. Palmitoyl transferases ZDHHC2, 3, 6, 7, and 15 are responsible for the TLR2 S-palmitoylation (107).

In 2016, Mukai's lab proved that S-palmitoylation of interferon gene stimulator protein (STING) affects its ability to regulate innate immune signals. STING was S-palmitoylated in the Golgi and is restricted to the trans-Golgi network (TGN). The general S-palmitoylation inhibitor 2-BP can selectively inhibit STING-mediated cytoplasmic DNA sensing and its downstream interferon response. In addition, a STING Cys88/91Ser double mutant that significantly reduced S-palmitoylation

could not induce STING-dependent host defense after infection with DNA viruses, and palmitoyl transferases ZDHHC3, 7, and 15 are responsible for STING modification (108).

Studies have shown that S-palmitoylation of Rac1(the Rho family Small Guanosine triphosphatase SE) inhibits the ubiquitination activation of E3 ubiquitin ligase TRIM31 on MAVS, thereby negatively regulating the RLR signaling pathway. However, it remains unclear which ZDHHC protein is responsible for the S-palmitoylation of Rac1 (109).

Recently, Lu and colleagues suggested that targeting NOD1 and NOD2 to bacterial-containing endosomal membranes requires them to be S-palmitoylated by ZDHHC5. They identified pathogenic bacterial-derived peptidoglycan components in the cytoplasm that promote intracellular NOD1/2-mediated immune responses, including autophagy and release of inflammatory factors (110). However, the precise mechanism that ZDHHC5 recruits bacteria to the entry site remains unclear.

It was found that S-palmitoylation of cysteine residues at position 463 near the cytoplasmic end of the IFN AR1 transmembrane region is necessary for phosphorylation activation of STAT1 and STAT2 (downstream of IFNAR1). Blocking S-palmitoylation of IFNAR1 inhibits the nuclear translocation of STAT and thus affects the transcription of ISGs. However, S-palmitoylation of IFNAR1 has no effect on its *in vivo* endocytosis, intracellular distribution, stability on the cell surface, and the formation of IFNAR1-IFNAR2 heterodimer (111).

MECHANISM OF S-PALMITOYLATION TO REGULATE THE ANTIVIRAL CAPACITY OF IFITM3

To date, S-palmitoylation is believed to be essential for the antiviral activity of IFITM3, but the research on the molecular mechanism of how S-palmitoylation regulates its antiviral activity is relatively slow. One of the main reasons is that protein S-palmitoylation was originally studied using radioactive palmitate metabolic labeling methods. However, this approach has the defects of limited sensitivity and poor security. New technologies, such as acy-biotinyl exchange and click-chemistry that allow S-palmitoylation sites to be experimentally-determined have greatly promoted the study of this lipid modification (112). Currently, the research progresses of IFITM3 S-palmitoylation were listed in **Table 1**.

Based on the previous findings, S-palmitoylation of IFITM3 is essential for its antiviral effect, subcellular location, stability, virion trafficking, interaction with cholesterol, and molecular conformation (**Figure 4**).

S-Palmitoylation Affects the Subcellular Location of IFITM3

S-palmitoylation of IFITM3 was first identified by Yount and his colleagues (113) through large-scale profiling of fatty-acylated proteins in the mouse DC line DC2.4 using palmitic acid chemical reporter ALK-16 and CuAAC. Further study revealed that all the three cysteine residues at positions Cys71, Cys72, and Cys105 of IFITM3 were S-palmitoylated. Bioinformatics analysis showed that the S-palmitoylated Cysteine residues are conserved in IFITM isoforms in most vertebrates, suggesting an added layer of regulation of protein S-palmitoylation in innate immunity. Moreover, it was observed that the S-palmitoylation of IFITM3 on membrane-proximal cysteines enhanced its clustering in the membrane compartments. Whereas, the mutation of the three cysteine residues to alanine eliminated the S-palmitoylation of IFITM3, resulting in its spot-like distribution in the endoplasmic reticulum. Additionally, wild-type IFITM3 (WT IFITM3), primarily membrane-associated, also present at lower levels in the cytoplasmic portion. In contrast, IFITM3-PalmΔ mutants are less membrane-associated, suggesting that IFITM3 has an inherent affinity for cell membranes, enhanced by hydrophobic S-palmitoylation (18).

Furthermore, it has been suggested that BODIPY-labeled IFITM3 Cys-to-Ala mutants showed a subcellular localization similar to WT human IFITM3 (116). Meanwhile, a confocal experiment revealed that sIFITM3-PalmΔ (C71,72,105A) was co-located with early/late endosomes and lysosomes in MARC-145 sIFITM3-PalmΔ-Flag cells, consistent with WT IFITM3 (79). Subcellular location change of sIFITM3-PalmΔ was not observed in PK15 as well (38).

Another study proved no change in subcellular location for C71A and C105A, but a more centralized intracellular distribution for C72A compared with WT human IFITM3 (16). Besides, all cysteine mutants of microbat IFITM3 relocalized to perinuclear Golgi-associated sites (117). Together, these studies indicate that S-palmitoylation regulates the subcellular location of human, murine, swine and microbat IFITM3 in different manners.

S-Palmitoylation Affects the Antiviral Activity of IFITM3

Mounting evidence showed that IFITM3 S-palmitoylation was crucial for its antiviral effect. For example, the S-palmitoylation-deficient, triple cysteine-to-alanine IFITM3 mutant significantly weakened its anti-IAV activity (113). A consistent result was observed in another study, in which the antiviral activity of the IFITM3 S-palmitoylation deficient mutant against H1N1 influenza virus (type A, PR8 strain) was significantly reduced (18).

As the analysis of S-palmitoylation levels of endogenous IFITM3 is in need to better elucidate the association between S-palmitoylation and IFITM3 antiviral activity, a mass-tag labeling method termed acyl-PEG exchange (APE) was developed (114). The APE analysis combined with fatty acid metabolic labeling showed that S-palmitoylation occurred in most endogenous IFITM3 in IFN-stimulated cells, and Cys72 was the predominant S-palmitoylation site. Indeed, after the mutation of Cys72 into alanine, the antiviral effect of IFITM3 decreased significantly. Although Cys71 of IFITM3 is highly conserved in mice and humans, its mutation to Ala is reported to have no significant effect on the S-fatty level and antiviral effect of IFITM3. The effect of Cys105 S-palmitoylation on the antiviral activity of IFITM3 varies in different IFITM isoforms, expression levels, and cell types, since mutation of this Cys residue hampers the antiviral activity of IFITM3 in mice but does not affect the activity of human IFITM3.

TABLE 1 | Research progresses of IFITM3 S-palmitoylation.

Year	Progress	Reference
2010	S-palmitoylation of IFITM3 was first identified and this lipid modification controls its clustering in membrane compartments and anti-IVA activity.	(113)
2012	IFITM3 had an inherent affinity for cell membranes, enhanced by hydrophobic S-palmitoylation	(18)
2013	a C72A mutation made human IFITM3 more centralized intracellular distribution	(16)
2016	Acyl-PEG exchange (APE) was developed, and dually S-palmitoylated IFITM3 at Cys72 and Cys105 was suggested to be the most active isoform in mammalian cells	(114)
2017	More than half of the ZDHHCs were capable of increasing IFITM3 palmitoylation with ZDHHCs 3, 7, 15, and 20 having the greatest effect	(115)
2019	S-palmitoylation of IFITM3 at Cys72 is important for its rate of trafficking to IAV particles during infection	(116)
2020	S-palmitoylation has no effect on the subcellular localization of swine IFITM3;	(38)
	S-palmitoylation on the three cysteine residues were all crucial for sIFITM3 to restrict PRRSV replication;	(79)
	All cysteine mutants of microbat IFITM3 relocalized to perinuclear Golgi-associated sites;	(117)
	S-palmitoylation of IFITM3 mediated by ZDHHC1 was indispensible for keeping it from lysosomal degradation.	(39)
2021	modulation of IFITM S-palmitoylation levels and cholesterol interaction may influence host susceptibility to different viruses;	(87)
	S-palmitoylation also enhanced the antiviral activity of IFITM3 by modulating its conformation and interaction with lipid membranes.	(62)

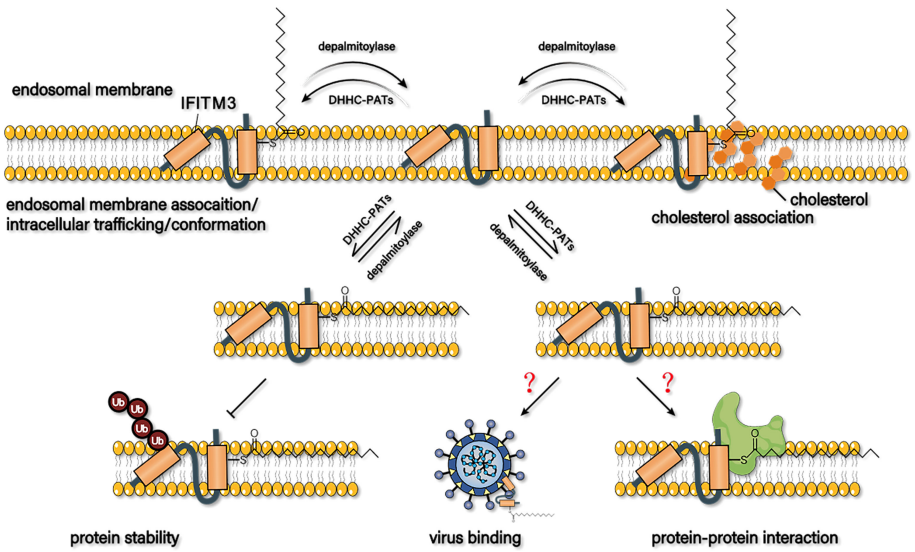

FIGURE 4 | Possible mechanism of s-palmitoylation to regulate the antiviral capacity of IFITM3. S-palmitoylation may affect its membrane proportion, trafficking to virions, stability, interaction with cholesterol, and conformation to regulate the antiviral activity of IFITM3. Whether S-palmitoylation affects the binding of IFITM3 to virus particles or its interaction with host proteins has not been reported yet.

It is also proved that the mutant of Cys72 to Ala significantly reduced its antiviral activity against IAV, while the IFITM3 mutant of Cys71 and Cys105 to Ala retained more activity (116). These results suggest that the antiviral activity of IFITM3 is directly related to the level of S-palmitoylation, and the double S-fatty acylation of IFITM3 on Cys72 and Cys105 may be the most active subtype in mammalian cells. However, when any one of the three cysteines was mutated to alanine, the anti-PRRSV activity of sIFITM3 was almost completely lost (79), indicating that S-palmitoylation on the three cysteine residues were all crucial for sIFITM3 in PRRSV restriction.

S-Palmitoylation Affects the Trafficking of IFITM3 to Virions

S-palmitoylation affects the trafficking of IFITM3 to virions as well. Compared with WT IFITM3 or Ala mutants at Cys71 or Cys105, trafficking and co-localization of IFITM3-C72A mutants with quenched DID-IAV particles was significantly reduced by about 20% through site-specific fluorescent labeling and live-cell imaging analysis. Meanwhile, the trafficking of IFITM3-C72A mutants to DID-IAV particles was also delayed (116). These results suggest that S-palmitoylation at Cys72 is important for the IFITM3 trafficking to IAV particles during infection.

S-Palmitoylation Affects the Stability of IFITM3

S-palmitoylation also affects the stability of IFITM3. It has been revealed that FITM3 protein abundance was significantly decreased in cells treated with the general protein palmitoylation inhibitor (2-brompalmitate, 2-BP), and the inhibition effect is dose- and time-dependent, but IFITM3 mRNA levels were not

affected. The half-life of IFITM3 protein in 2-BP treated cells was significantly reduced to 1.5 h vs 5 h in control cells. Additionally, exogenous IFITM3ΔPalm mutants were degraded rapidly, with a half-life of 2.9 h compared with 7.9 h for WT IFITM3. Moreover, 2-BP-induced IFITM3 degradation in A549 and HCT116 cells can be significantly blocked by lysosome pathway inhibitor (leupeptin and bafilomycin A1) rather than ubiquitin-proteasome pathway inhibitor (MG132), indicating that IFITM3 may be degraded in a lysosome pathway (not ubiquitin-proteasome pathway) when its S-palmitoylation was restrained (39). Nonetheless, IFITM3 PalmΔ mutants were reported to be ubiquitinated effectively in a previous study (114). And it has been suggested that ubiquitinated IFITM3 can be recruited to an ER-proximal site for degradation (18, 89, 118). Therefore, whether the ubiquitin-proteasome pathway is involved in S-palmitoylation deficit-induced IFITM3 degradation needs to be further elucidated.

S-Palmitoylation Affects the Interaction Between IFITM3 and Cholesterol

Of note, the S-palmitoylation level of IFITM2 was significantly lower than IFITM3 by metabolic labeling analysis. High levels of S-palmitoylation enhanced IFITM3 interactions with cholesterol and inhibited viruses like IAV and SARS-CoV2. While with lower levels of S-palmitoylation and fewer interactions with cholesterol, IFITM2 showed more efficient anti-EBOV activity, indicating that S-palmitoylation may inhibit cholesterol-dependent viruses by regulating the interaction between IFITM3 and cholesterol (87).

S-Palmitoylation Affects the Conformation of IFITM3

Compared with S-palmitoylation-deficient IFITM3, Cys72-maleimide palmitate, a reasonable substitute for S-palmitoylation modification, showed a significant structural change both locally and in the disordered N-terminal regions. Meanwhile, the disrupted AH1 region of S-palmitoylation-deficient IFITM3 was stabilized and its association with the membrane bilayer was increased by adding maleimide palmitate to Cys72 in a flotation assay. These results suggest that lipidation can change the biophysical conformation of IFITM3. As the disruption of AH1 attenuates the antiviral activity of IFITM3, it is suggested that the S-palmitoylation at Cys72 directly enhances the antiviral activity of IFITM3 by stabilizing AH1 (62). Besides, stabilization of IFITM3 AH1 by S-palmitoylation of Cys72 may also explain the subcellular distribution of IFITM3 during infection.

ZDHHCs Are Implicated in S-Palmitoylating IFITM3

Although many substrate proteins of ZDHHC transferase have been identified, the mechanism of how transferase recognizes its target protein remains unclear. The distribution of each specific ZDHHC protein in different subcellular locations affects the type of substrate protein. Only a few substrate/ZDHHC pairings have been identified among the hundreds of known S-palmitoylated proteins. For example, ZDHHC9 and ZDHHC17 can only S-palmitoylate HRas and SNAP25, whereas ZDHHC14 has PAT activity toward PSD93 (30).

A variety of ZDHHC proteins are capable of S-palmitoylating IFITM3. To identify the enzyme that performs S-palmitoylation modification for IFITM3, Temet et al. constructed rodent ZDHHC1-23 expression plasmids for overexpression screening. Results showed that ZDHHC1, 2, 5, 6, 9, 14, 23, 24, and 25 could up-regulate IFITM3 S-palmitoylation by 1.7-3 times, whereas ZDHHC3, 7,15, and 20 increased the S-palmitoylation level of IFITM3 by more than 3 times. Importantly, it was reported that the three cysteine residues of IFITM3 protein were not completely modified by S-palmitoylation, which explains why a class of ZDHHC proteins can enhance IFITM3 S-palmitoylation level (115).

Wang et al. reported that p53 up-regulated ZDHHC1 expression and S-palmitoylation level of IFITM3. Overexpression of ZDHHC1 increased the S-palmitoylation level of exogenous IFITM3 and the protein expression level of endogenous IFITM3. The ZDHHC1 mutant with DHHC deficiency could still increase the S-palmitoylation level of exogenous IFITM3, but not the protein expression level of endogenous IFITM3. Meanwhile, ZDHHC1 could not up-regulate endogenous IFITM3 protein expression in the presence of 2-BP. Similar to wild-type ZDHHC1, the ZDHHC1 DHHCΔ mutant can co-precipitate with exogenous IFITM3, suggesting that ZDHHC may interact with IFITM3 independently of the DHHC region and modify it with S-palmitoylation. This study raises the question whether other regions besides DHHC are involved in ZDHHC1 palmitoyltransferase activity (39).

In total, 13 ZDHHCs have been revealed to enhance S-palmitoylation of IFITM3, including 1, 2, 3, 5, 6, 7, 9, 14, 15, 20, 23, 24, and 25. Only ZDHHC1 and ZDHHC20 can enhance the antiviral activity of IFITM3, and further study showed that ZDHHC20 and IFITM3 are co-localized in lysosomes. By contrast, ZDHHC3, ZDHHC7, and ZDHHC15 are co-localized around the nucleus with IFITM3, suggesting that the subcellular localization where hIFITM3 was S-palmitoylated may affect its antiviral activity (115). As ZDHHC2, 5,6,9,14,23,24,25 can also enhance the S-palmitoylation level of IFITM3, it's interesting to explore where the eight ZDHHCs colocalize with IFITM3 and whether these enzymes can enhance its antiviral effect.

CONCLUSIONS AND PERSPECTIVES

In summary, S-palmitoylation of IFITM3 is essential for its antiviral effect, subcellular localization, stability, virion trafficking, interaction with cholesterol, and molecular conformation. IFITM3 can bind directly to the surface of the virus particle to reduce its infective activity or interact directly with host proteins to play an antiviral role. However, whether S-palmitoylation affects the binding of IFITM3 to virus particles or its interaction with host proteins has not been reported yet. This topic is worthy of further research, which could help to reveal the molecular mechanism of how S-palmitoylation regulates the antiviral effect of IFITM3. Furthermore, all the three cysteines

of IFITM3 in murine and humans can be palmitoylated, and Csy72 is the most important palmitoylated site, followed by Csy105. In contrast, The S-palmitoylated modification of Csy71 alone seems to have the least effect on its biological function. However, it has been shown that anyone mutation of the three cysteines to alanine can almost completely abolish the anti-PRRSV activity of porcine IFITM3, suggesting that the dually S-palmitoylated IFITM3 at Cys72 and Cys105 may not necessarily be the most active isoform in mammalian cells.

In this review, we have primarily focused on the classical and novel progress concerning the antiviral mechanism of IFITM3 and the mechanism of how S-palmitoylation regulates its antiviral activity. The role of PTM of proteins involved in regulating of cellular antiviral activity has been a hot topic. Despite recent advances in understanding the mechanism of S-palmitoylated proteins in immune response, little is known about the regulation of natural immune response. Therefore, how S-palmitoylation modification regulates natural immune response could be a research focus in the future. Of note, S-palmitoylation modification participates in virus replication and infection and the regulation of antiviral effect mediated by IFITM3, but the mechanisms of how the host balances these two effects await further elucidation.

As is shown in many studies, the catalytic center of the ZDHHC family is the highly conserved DHHC domain. However, the exogenous ZDHHC1 mutants deficient in the HDDC region can enhance S-palmitoylation of IFITM3. It's worthy of exploring whether other catalytic dominants exit in ZDHHC protein. Moreover, emerging evidence has revealed the interplay between S-palmitoylation and other PTMs. For example, inhibition of S-palmitoylation modification of IFITM3 can significantly up-regulate its ubiquitination level. What effect does S-palmitoylation modification have on the other two posttranslational modifications (methylation and phosphorylation) of IFITM3? The precise molecular mechanisms that govern the synergistic effect of PTMs deserves further exploring.

In general, S-palmitoylation regulates the antiviral activity of IFITM3 through influencing its membrane proportion, trafficking to virions, stability, interaction with cholesterol, and conformation. Future studies are still in need to clarify the regulation mechanism of S-palmitoylation on IFITM3.

AUTHOR CONTRIBUTIONS

Conceptualization: CL and NJ. Writing-original draft preparation: SW and YS. Writing-review: CL, and YS. Figures: SW. Supervision: NJ, JZ, and HL. Funding acquisition: SW, JZ, and HL. All authors contributed to the article and approved the submitted version.

FUNDING

This work was financially supported by the Open Funding Project of Brucellosis Prevention and Treatment Engineering Research Center of Inner Mongolia Autonomous region [No. MDK2021078, MDK2019082], Doctoral Funding of Inner Mongolia Minzu University [No. BS584, BS583], and Key Research and Development Program in Inner Mongolia Autonomous Region [No. 2021ZD001301, 2019ZD006].

REFERENCES

1. Chow KT, Gale M Jr, Loo YM. RIG-I and Other RNA Sensors in Antiviral Immunity. *Annu Rev Immunol* (2018) 36:667–94. doi: 10.1146/annurev-immunol-042617-053309
2. Sun L, Wu J, Du F, Chen X, Chen ZJ. Cyclic GMP-AMP Synthase is a Cytosolic DNA Sensor That Activates the Type I Interferon Pathway. *Science* (2013) 339(6121):786–91. doi: 10.1126/science.1232458
3. Bürckstümmer T, Baumann C, Blüml S, Dixit E, Dürnberger G, Jahn H, et al. An Orthogonal Proteomic-Genomic Screen Identifies AIM2 as a Cytoplasmic DNA Sensor for the Inflammasome. *Nat Immunol* (2009) 10 (3):266–72. doi: 10.1038/ni.1702
4. Stark GR, Darnell JEJr. The JAK-STAT Pathway at Twenty. *Immunity* (2012) 36(4):503–14. doi: 10.1016/j.immuni.2012.03.013
5. Diamond MS, Farzan M. The Broad-Spectrum Antiviral Functions of IFIT and IFITM Proteins. *Nat Rev Immunol* (2013) 13(1):46–57. doi: 10.1038/nri3344
6. Schneider WM, Chevillotte MD, Rice CM. Interferon-Stimulated Genes: A Complex Web of Host Defenses. *Annu Rev Immunol* (2014) 32:513–45. doi: 10.1146/annurev-immunol-032713-120231
7. de Veer MJ, Holko M, Frevel M, Walker E, Der S, Paranjape JM, et al. Functional Classification of Interferon-Stimulated Genes Identified Using Microarrays. *J Leukoc Biol* (2001) 69(6):912–20. doi: 10.1189/jlb.69.6.912
8. Zhang D, Zhang DE. Interferon-Stimulated Gene 15 and the Protein ISGylation System. *J Interferon Cytokine Res* (2011) 31(1):119–30. doi: 10.1089/jir.2010.0110
9. Melchjorsen J, Matikainen S, Paludan SR. Activation and Evasion of Innate Antiviral Immunity by Herpes Simplex Virus. *Viruses* (2009) 1(3):737–59. doi: 10.3390/v1030737
10. Zhu J, Ghosh A, Sarkar SN. OASL-A New Player in Controlling Antiviral Innate Immunity. *Curr Opin Virol* (2015) 12:15–9. doi: 10.1016/j.coviro.2015.01.010
11. Zhu J, Zhang Y, Ghosh A, Cuevas RA, Forero A, Dhar J, et al. Antiviral Activity of Human OASL Protein is Mediated by Enhancing Signaling of the RIG-I RNA Sensor. *Immunity* (2014) 40(6):936–48. doi: 10.1016/j.immuni.2014.05.007
12. Hickford D, Frankenberg S, Shaw G, Renfree MB. Evolution of Vertebrate Interferon Inducible Transmembrane Proteins. *BMC Genomics* (2012) 13:155. doi: 10.1186/1471-2164-13-155
13. Lu G, Ou J, Cai S, Lai Z, Zhong L, Yin X, et al. Canine Interferon-Inducible Transmembrane Protein Is a Host Restriction Factor That Potently Inhibits Replication of Emerging Canine Influenza Virus. *Front Immunol* (2021) 12:710705. doi: 10.3389/fimmu.2021.710705
14. Kim YC, Jeong BH. Phylogenetic and Topological Analyses of the Bovine Interferon-Induced Transmembrane Protein (IFITM3). *Acta Vet Hung* (2021) 69:14–22. doi: 10.1556/004.2021.00010
15. Brass AL, Huang I-C, Benita Y, John SP, Krishnan MN, Feeley EM, et al. IFITM Proteins Mediate the Innate Immune Response to Influenza A H1N1 Virus, West Nile Virus and Dengue Virus. *Cell* (2009) 139(7):1243–54. doi: 10.1016/j.cell.2009.12.017
16. John SP, Chin CR, Perreira JM, Feeley EM, Aker AM, Savidis G, et al. The CD225 Domain of IFITM3 is Required for Both IFITM Protein Association and Inhibition of Influenza A Virus and Dengue Virus Replication. *J Virol* (2013) 87(14):7837–52. doi: 10.1128/jvi.00481-13
17. Weidner JM, Jiang D, Pan XB, Chang J, Block TM, Guo JT. Interferon-Induced Cell Membrane Proteins, IFITM3 and Tetherin, Inhibit Vesicular Stomatitis Virus Infection *via* Distinct Mechanisms. *J Virol* (2010) 84 (24):12646–57. doi: 10.1128/jvi.01328-10

18. Yount JS, Karssemeijer RA, Hang HC. S-Palmitoylation and Ubiquitination Differentially Regulate Interferon-Induced Transmembrane Protein 3 (IFITM3)-Mediated Resistance to Influenza Virus. *J Biol Chem* (2012) 287(23):19631–41. doi: 10.1074/jbc.M112.362095
19. Bailey CC, Kondur HR, Huang IC, Farzan M. Interferon-Induced Transmembrane Protein 3 Is a Type II Transmembrane Protein. *J Biol Chem* (2013) 288(45):32184–93. doi: 10.1074/jbc.M113.514356
20. Ling S, Zhang C, Wang W, Cai X, Yu L, Wu F, et al. Combined Approaches of EPR and NMR Illustrate Only One Transmembrane Helix in the Human IFITM3. *Sci Rep* (2016) 6:24029. doi: 10.1038/srep24029
21. Jia R, Xu F, Qian J, Yao Y, Miao C, Zheng YM, et al. Identification of an Endocytic Signal Essential for the Antiviral Action of IFITM3. *Cell Microbiol* (2014) 16(7):1080–93. doi: 10.1111/cmi.12262
22. Huang IC, Bailey CC, Weyer JL, Radoshitzky SR, Becker MM, Chiang JJ, et al. Distinct Patterns of IFITM-Mediated Restriction of Filoviruses, SARS Coronavirus, and Influenza A Virus. *PLoS Pathog* (2011) 7(1):e1001258. doi: 10.1371/journal.ppat.1001258
23. Savidis G, Perreira JM, Portmann JM, Meraner P, Guo Z, Green S, et al. The IFITMs Inhibit Zika Virus Replication. *Cell Rep* (2016) 15(11):2323–30. doi: 10.1016/j.celrep.2016.05.074
24. Li K, Markosyan RM, Zheng YM, Golfetto O, Bungart B, Li M, et al. IFITM Proteins Restrict Viral Membrane Hemifusion. *PLoS Pathog* (2013) 9(1): e1003124. doi: 10.1371/journal.ppat.1003124
25. Schoggins JW, Wilson SJ, Panis M, Murphy MY, Jones CT, Bieniasz P, et al. A Diverse Range of Gene Products are Effectors of the Type I Interferon Antiviral Response. *Nature* (2011) 472(7344):481–5. doi: 10.1038/nature09907
26. Weston S, Czieso S, White IJ, Smith SE, Wash RS, Diaz-Soria C, et al. Alphavirus Restriction by IFITM Proteins. *Traffic* (2016) 17(9):997–1013. doi: 10.1111/tra.12416
27. Muñoz-Moreno R, Cuesta-Geijo M, Martínez-Romero C, Barrado-Gil L, Galindo I, GarcÍa-Sastre A, et al. Antiviral Role of IFITM Proteins in African Swine Fever Virus Infection. *PLoS One* (2016) 11(4):e0154366. doi: 10.1371/journal.pone.0154366
28. Galindo I, Cuesta-Geijo MA, Hlavova K, Muñoz-Moreno R, Barrado-Gil L, Dominguez J, et al. African Swine Fever Virus Infects Macrophages, the Natural Host Cells, *via* Clathrin- and Cholesterol-Dependent Endocytosis. *Virus Res* (2015) 200:45–55. doi: 10.1016/j.virusres.2015.01.022
29. Mudhasani R, Tran JP, Retterer C, Radoshitzky SR, Kota KP, Altamura LA, et al. IFITM-2 and IFITM-3 But Not IFITM-1 Restrict Rift Valley Fever Virus. *J Virol* (2013) 87(15):8451–64. doi: 10.1128/jvi.03382-12
30. Perreira JM, Chin CR, Feeley EM, Brass AL. IFITMs Restrict the Replication of Multiple Pathogenic Viruses. *J Mol Biol* (2013) 425(24):4937–55. doi: 10.1016/j.jmb.2013.09.024
31. Chiang CF, Flint M, Lin JS, Spiropoulou CF. Endocytic Pathways Used by Andes Virus to Enter Primary Human Lung Endothelial Cells. *PLoS One* (2016) 11(10):e0164768. doi: 10.1371/journal.pone.0164768
32. Xu-Yang Z, Pei-Yu B, Chuan-Tao Y, Wei Y, Hong-Wei M, Kang T, et al. Interferon-Induced Transmembrane Protein 3 Inhibits Hantaan Virus Infection, and Its Single Nucleotide Polymorphism Rs12252 Influences the Severity of Hemorrhagic Fever With Renal Syndrome. *Front Immunol* (2016) 7:535. doi: 10.3389/fimmu.2016.00535
33. Xing H, Ye L, Fan J, Fu T, Li C, Zhang S, et al. IFITMs of African Green Monkey Can Inhibit Replication of SFTSV But Not MNV *In Vitro*. *Viral Immunol* (2020) 33(10):634–41. doi: 10.1089/vim.2020.0132
34. Yánez DC, Ross S, Crompton T. The IFITM Protein Family in Adaptive Immunity. *Immunology* (2020) 159(4):365–72. doi: 10.1111/imm.13163
35. Zhao X, Sehgal M, Hou Z, Cheng J, Shu S, Wu S, et al. Identification of Residues Controlling Restriction Versus Enhancing Activities of IFITM Proteins on Entry of Human Coronaviruses. *J Virol* (2018) 92(6):e01535-17. doi: 10.1128/jvi.01535-17
36. Wrensch F, Karsten CB, Gnirß K, Hoffmann M, Lu K, Takada A, et al. Interferon-Induced Transmembrane Protein-Mediated Inhibition of Host Cell Entry of Ebolaviruses. *J Infect Dis* (2015) 212(Suppl 2):S210–218. doi: 10.1093/infdis/jiv255
37. Fu B, Wang L, Li S, Dorf ME. ZMPSTE24 Defends Against Influenza and Other Pathogenic Viruses. *J Exp Med* (2017) 214(4):919–29. doi: 10.1084/jem.20161270
38. Xu Z, Li X, Xue J, Shen L, Zheng W, Yin S, et al. S-Palmitoylation of Swine Interferon-Inducible Transmembrane Protein is Essential for its Anti-JEV Activity. *Virology* (2020) 548:82–92. doi: 10.1016/j.virol.2020.06.004
39. Wang X, Wu Z, Li Y, Yang Y, Xiao C, Liu X, et al. P53 Promotes ZDHHC1-Mediated IFITM3 Palmitoylation to Inhibit Japanese Encephalitis Virus Replication. *PLoS Pathog* (2020) 16(10):e1009035. doi: 10.1371/journal.ppat.1009035
40. Chmielewska AM, Gómez-Herranz M, Gach P, Nekulova M, Bagnucka MA, Lipińska AD, et al. The Role of IFITM Proteins in Tick-Borne Encephalitis Virus Infection. *J Virol* (2022) 96(1):e0113021. doi: 10.1128/jvi.01130-21
41. Brass AL, Huang IC, Benita Y, John SP, Krishnan MN, Feeley EM, et al. The IFITM Proteins Mediate Cellular Resistance to Influenza A H1N1 Virus, West Nile Virus, and Dengue Virus. *Cell* (2009) 139(7):1243–54. doi: 10.1016/j.cell.2009.12.017
42. Gorman MJ, Poddar S, Farzan M, Diamond MS, et al. The Interferon-Stimulated Gene Ifitm3 Restricts West Nile Virus Infection and Pathogenesis. *J Virol* (2016) 90(18):8212–25. doi: 10.1128/jvi.00581-16
43. Li C, Zheng H, Wang Y, Dong W, Liu Y, Zhang L, et al. Antiviral Role of IFITM Proteins in Classical Swine Fever Virus Infection. *Viruses* (2019) 11 (2):126–43. doi: 10.3390/v11020126
44. Zhang YN, Liu YY, Xiao FC, Liu CC, Liang XD, Chen J, et al. Rab5, Rab7, and Rab11 Are Required for Caveola-Dependent Endocytosis of Classical Swine Fever Virus in Porcine Alveolar Macrophages. *J Virol* (2018) 92(15): e00797-18. doi: 10.1128/jvi.00797-18
45. Zhang Y, Huang Y, Wang L, Huang L, Zheng J, Huang X, et al. Grouper Interferon-Induced Transmembrane Protein 3 (IFITM3) Inhibits the Infectivity of Iridovirus and Nodavirus by Restricting Viral Entry. *Fish Shellfish Immunol* (2020) 104:172–81. doi: 10.1016/j.fsi.2020.06.001
46. Zhang Y, Wang L, Zheng J, Huang L, Wang S, Huang X, et al. Grouper Interferon-Induced Transmembrane Protein 1 Inhibits Iridovirus and Nodavirus Replication by Regulating Virus Entry and Host Lipid Metabolism. *Front Immunol* (2021) 12:636806. doi: 10.3389/fimmu.2021.636806
47. Guo CJ, Liu D, Wu YY, Yang XB, Yang LS, Mi S, et al. Entry of Tiger Frog Virus (an Iridovirus) Into HepG2 Cells *via* a pH-Dependent, Atypical, Caveola-Mediated Endocytosis Pathway. *J Virol* (2011) 85(13):6416–26. doi: 10.1128/jvi.01500-10
48. Zhu R, Wang J, Lei XY, Gui JF, Zhang QY. Evidence for Paralichthys Olivaceus IFITM1 Antiviral Effect by Impeding Viral Entry Into Target Cells. *Fish Shellfish Immunol* (2013) 35(3):918–26. doi: 10.1016/j.fsi.2013.07.002
49. Chen L, Zhu L, Chen J. Human Interferon Inducible Transmembrane Protein 3 (IFITM3) Inhibits Influenza Virus A Replication and Inflammation by Interacting With ABHD16A. *BioMed Res Int* (2021) 2021:6652147. doi: 10.1155/2021/6652147
50. Gerlach T, Hensen L, Matrosovich T, Bergmann J, Winkler M, Peteranderl C, et al. pH Optimum of Hemagglutinin-Mediated Membrane Fusion Determines Sensitivity of Influenza A Viruses to the Interferon-Induced Antiviral State and IFITMs. *J Virol* (2017) 91(11):e00246-17. doi: 10.1128/jvi.00246-17
51. Meischel T, Fritzlar S, Villalon-Letelier F, Tessema MB, Brooks AG, Reading PC, et al. IFITM Proteins That Restrict the Early Stages of Respiratory Virus Infection Do Not Influence Late-Stage Replication. *J Virol* (2021) 95(20): e0083721. doi: 10.1128/jvi.00837-21
52. Zani A, Yount JS. Antiviral Protection by IFITM3 *In Vivo*. *Curr Clin Microbiol Rep* (2018) 5(4):229–37. doi: 10.1007/s40588-018-0103-0
53. Smith SE, Busse DC, Binter S, Weston S, Diaz Soria C, Laksono BM, et al. Interferon-Induced Transmembrane Protein 1 Restricts Replication of Viruses That Enter Cells *via* the Plasma Membrane. *J Virol* (2019) 93(6): e02003-18. doi: 10.1128/jvi.02003-18
54. Zhang W, Zhang L, Zan Y, Du N, Yang Y, Tien P, et al. Human Respiratory Syncytial Virus Infection is Inhibited by IFN-Induced Transmembrane Proteins. *J Gen Virol* (2015) 96(Pt 1):170–82. doi: 10.1099/vir.0.066555-0

55. Li C, Du S, Tian M, Wang Y, Bai J, Tan P, et al. The Host Restriction Factor Interferon-Inducible Transmembrane Protein 3 Inhibits Vaccinia Virus Infection. *Front Immunol* (2018) 9:228. doi: 10.3389/fimmu.2018.00228
56. Anafu AA, Bowen CH, Chin CR, Brass AL, Holm GH. Interferon-Inducible Transmembrane Protein 3 (IFITM3) Restricts Reovirus Cell Entry. *J Biol Chem* (2013) 288(24):17261–71. doi: 10.1074/jbc.M112.438515
57. Ahi YS, Yimer D, Shi G, Majdoul S, Rahman K, Rein A, et al. IFITM3 Reduces Retroviral Envelope Abundance and Function and Is Counteracted by Glycogag. *mBio* (2020) 11(1):e03088-19. doi: 10.1128/mBio.03088-19
58. Li K, Jia R, Li M, Zheng YM, Miao C, Yao Y, et al. A Sorting Signal Suppresses IFITM1 Restriction of Viral Entry. *J Biol Chem* (2015) 290(7):4248–59. doi: 10.1074/jbc.M114.630780
59. Chesarino NM, Compton AA, McMichael TM, Kenney AD, Zhang L, Soewarna V, et al. IFITM3 Requires an Amphipathic Helix for Antiviral Activity. *EMBO Rep* (2017) 18(10):1740–51. doi: 10.15252/embr.201744100
60. Hornick AL, Li N, Oakland M, McCray PB Jr, Sinn PL. Human, Pig, and Mouse Interferon-Induced Transmembrane Proteins Partially Restrict Pseudotyped Lentiviral Vectors. *Hum Gene Ther* (2016) 27(5):354–62. doi: 10.1089/hum.2015.156
61. Ranjbar S, Haridas V, Jasenosky LD, Falvo JV, Goldfeld AE. A Role for IFITM Proteins in Restriction of Mycobacterium Tuberculosis Infection. *Cell Rep* (2015) 13(5):874–83. doi: 10.1016/j.celrep.2015.09.048
62. Garst EH, Lee H, Das T, Bhattacharya S, Percher A, Wiewiora R, et al. Site-Specific Lipidation Enhances IFITM3 Membrane Interactions and Antiviral Activity. *ACS Chem Biol* (2021) 16(5):844–56. doi: 10.1021/acschembio.1c00013
63. Zhu X, He Z, Yuan J, Wen W, Huang X, Hu Y, et al. IFITM3-Containing Exosome as a Novel Mediator for Anti-Viral Response in Dengue Virus Infection. *Cell Microbiol* (2015) 17(1):105–18. doi: 10.1111/cmi.12339
64. Everitt AR, Clare S, Pertel T, John SP, Wash RS, Smith SE, et al. IFITM3 Restricts the Morbidity and Mortality Associated With Influenza. *Nature* (2012) 484(7395):519–23. doi: 10.1038/nature10921
65. Bailey CC, Huang IC, Kam C, Farzan M. Ifitm3 Limits the Severity of Acute Influenza in Mice. *PLoS Pathog* (2012) 8(9):e1002909. doi: 10.1371/journal.ppat.1002909
66. Kenney AD, McMichael TM, Imas A, Chesarino NM, Zhang L, Dorn LE, et al. IFITM3 Protects the Heart During Influenza Virus Infection. *Proc Natl Acad Sci U S A* (2019) 116(37):18607–12. doi: 10.1073/pnas.1900784116
67. Zhang YH, Zhao Y, Li N, Peng YC, Giannoulatou E, Jin RH, et al. Interferon-Induced Transmembrane Protein-3 Genetic Variant Rs12252-C is Associated With Severe Influenza in Chinese Individuals. *Nat Commun* (2013) 4:1418. doi: 10.1038/ncomms2433
68. Wang YS, Luo QL, Guan YG, Fan DY, Luan GM, Jing A. HCMV Infection and IFITM3 Rs12252 are Associated With Rasmussen's Encephalitis Disease Progression. *Ann Clin Transl Neurol* (2021) 8(3):558–70. doi: 10.1002/acn3.51289
69. Li M, Li YP, Deng HL, Wang MQ, Chen Y, Zhang YF, et al. DNA Methylation and SNP in IFITM3 are Correlated With Hand, Foot and Mouth Disease Caused by Enterovirus 71. *Int J Infect Dis* (2021) 105:199–208. doi: 10.1016/j.ijid.2021.02.049
70. Zhang Y, Qin L, Zhao Y, Zhang P, Xu B, Li K, et al. Interferon-Induced Transmembrane Protein 3 Genetic Variant Rs12252-C Associated With Disease Severity in Coronavirus Disease 2019. *J Infect Dis* (2020) 222(1):34–7. doi: 10.1093/infdis/jiaa224
71. Alghamdi J, Alaamery M, Barhoumi T, Rashid M, Alajmi H, Aljasser N, et al. Interferon-Induced Transmembrane Protein-3 Genetic Variant Rs12252 is Associated With COVID-19 Mortality. *Genomics* (2021) 113(4):1733–41. doi: 10.1016/j.ygeno.2021.04.002
72. Gómez J, Albaiceta GM, Cuesta-Llavona E, García-Clemente M, López-Larrea C, Amado-Rodríguez L, et al. The Interferon-Induced Transmembrane Protein 3 Gene (IFITM3) Rs12252 C Variant is Associated With COVID-19. *Cytokine* (2021) 137:155354. doi: 10.1016/j.cyto.2020.155354
73. Mohammed FS, Farooqi YN, Mohammed S. The Interferon-Induced Transmembrane Protein 3 -Rs12252 Allele May Predict COVID-19 Severity Among Ethnic Minorities. *Front Genet* (2021) 12:692254. doi: 10.3389/fgene.2021.692254
74. Allen EK, Randolph AG, Bhangale T, Dogra P, Ohlson M, Oshansky CM, et al. SNP-Mediated Disruption of CTCF Binding at the IFITM3 Promoter is Associated With Risk of Severe Influenza in Humans. *Nat Med* (2017) 23(8):975–83. doi: 10.1038/nm.4370
75. Guo X, Steinkühler J, Marin M, Li X, Lu W, Dimova R, et al. Interferon-Induced Transmembrane Protein 3 Blocks Fusion of Diverse Enveloped Viruses by Altering Mechanical Properties of Cell Membranes. *ACS Nano* (2021) 15(5):8155–70. doi: 10.1021/acsnano.0c10567
76. Rahman K, Coomer CA, Majdoul S, Ding SY, Padilla-Parra S, Compton AA, et al. Homology-Guided Identification of a Conserved Motif Linking the Antiviral Functions of IFITM3 to its Oligomeric State. *Elife* (2020) 9:e58537. doi: 10.7554/eLife.58537
77. Feeley EM, Sims JS, John SP, Chin CR, Pertel T, Chen LM, et al. IFITM3 Inhibits Influenza A Virus Infection by Preventing Cytosolic Entry. *PLoS Pathog* (2011) 7(10):e1002337. doi: 10.1371/journal.ppat.1002337
78. Compton AA, Bruel T, Porrot F, Mallet A, Sachse M, Euvrard M, et al. IFITM Proteins Incorporated Into HIV-1 Virions Impair Viral Fusion and Spread. *Cell Host Microbe* (2014) 16(6):736–47. doi: 10.1016/j.chom.2014.11.001
79. Zhang A, Duan H, Zhao H, Liao H, Du Y, Li L, et al. Interferon-Induced Transmembrane Protein 3 is a Virus-Associated Protein Which Suppresses Porcine Reproductive and Respiratory Syndrome Virus Replication by Blocking Viral Membrane Fusion. *J Virol* (2020) 94:e01350-20. doi: 10.1128/jvi.01350-20
80. Amini-Bavil-Olyaee S, Choi YJ, Lee JH, Shi M, Huang IC, Farzan M, et al. The Antiviral Effector IFITM3 Disrupts Intracellular Cholesterol Homeostasis to Block Viral Entry. *Cell Host Microbe* (2013) 13(4):452–64. doi: 10.1016/j.chom.2013.03.006
81. Narayana SK, Helbig KJ, McCartney EM, Eyre NS, Bull RA, Eltahla A, et al. The Interferon-Induced Transmembrane Proteins, IFITM1, IFITM2, and IFITM3 Inhibit Hepatitis C Virus Entry. *J Biol Chem* (2015) 290(43):25946–59. doi: 10.1074/jbc.M115.657346
82. Wrensch F, Winkler M, Pöhlmann S. IFITM Proteins Inhibit Entry Driven by the MERS-Coronavirus Spike Protein: Evidence for Cholesterol-Independent Mechanisms. *Viruses* (2014) 6(9):3683–98. doi: 10.3390/v6093683
83. Desai TM, Marin M, Chin CR, Savidis G, Brass AL, Melikyan GB. IFITM3 Restricts Influenza A Virus Entry by Blocking the Formation of Fusion Pores Following Virus-Endosome Hemifusion. *PLoS Pathog* (2014) 10(4):e1004048. doi: 10.1371/journal.ppat.1004048
84. Lin TY, Chin CR, Everitt AR, Clare S, Perreira JM, Savidis G. Amphotericin B Increases Influenza A Virus Infection by Preventing IFITM3-Mediated Restriction. *Cell Rep* (2013) 5(4):895–908. doi: 10.1016/j.celrep.2013.10.033
85. Wu X, Spence JS, Das T, Yuan X, Chen C, Zhang Y, et al. Site-Specific Photo-Crosslinking Proteomics Reveal Regulation of IFITM3 Trafficking and Turnover by VCP/p97 ATPase. *Cell Chem Biol* (2020) 27(5):571–85.e576. doi: 10.1016/j.chembiol.2020.03.004
86. Wee YS, Roundy KM, Weis JJ, Weis JH. Interferon-Inducible Transmembrane Proteins of the Innate Immune Response Act as Membrane Organizers by Influencing Clathrin and V-ATPase Localization and Function. *Innate Immun* (2012) 18(6):834–45. doi: 10.1177/1753425912443392
87. Das T, Yang X, Lee H, Garst E, Valencia E, Chandran K, et al. S-Palmitoylation and Sterol Interactions Mediate Antiviral Specificity of IFITM Isoforms. *Res Sq* (2021). doi: 10.21203/rs.3.rs-1179000/v1
88. Jia R, Pan Q, Ding S, Rong L, Liu SL, Geng Y, et al. The N-Terminal Region of IFITM3 Modulates its Antiviral Activity by Regulating IFITM3 Cellular Localization. *J Virol* (2012) 86(24):13697–707. doi: 10.1128/jvi.01828-12
89. Chesarino NM, McMichael TM, Hach JC, Yount JS. Phosphorylation of the Antiviral Protein Interferon-Inducible Transmembrane Protein 3 (IFITM3) Dually Regulates its Endocytosis and Ubiquitination. *J Biol Chem* (2014) 289(17):11986–92. doi: 10.1074/jbc.M114.557694
90. Shan Z, Han Q, Nie J, Cao X, Chen Z, Yin S, et al. Negative Regulation of Interferon-Induced Transmembrane Protein 3 by SET7-Mediated Lysine Monomethylation. *J Biol Chem* (2013) 288(49):35093–103. doi: 10.1074/jbc.M113.511949
91. Huang K, Yanai A, Kang R, Arstikaitis P, Singaraja RR, Metzler M, et al. Huntingtin-Interacting Protein HIP14 is a Palmitoyl Transferase Involved in

Palmitoylation and Trafficking of Multiple Neuronal Proteins. *Neuron* (2004) 44(6):977–86. doi: 10.1016/j.neuron.2004.11.027
92. Hayashi T, Thomas GM, Huganir RL. Dual Palmitoylation of NR2 Subunits Regulates NMDA Receptor Trafficking. *Neuron* (2009) 64(2):213–26. doi: 10.1016/j.neuron.2009.08.017
93. El-Husseini AE, Craven SE, Chetkovich DM, Firestein BL, Schnell E, Aoki C, et al. Dual Palmitoylation of PSD-95 Mediates its Vesiculotubular Sorting, Postsynaptic Targeting, and Ion Channel Clustering. *J Cell Biol* (2000) 148 (1):159–72. doi: 10.1083/jcb.148.1.159
94. Rocks O, Peyker A, Kahms M, Verveer PJ, Koerner C, Lumbierres M, et al. An Acylation Cycle Regulates Localization and Activity of Palmitoylated Ras Isoforms. *Science* (2005) 307(5716):1746–52. doi: 10.1126/science.1105654
95. Hicks SW, Charron G, Hang HC, Galán JE. Subcellular Targeting of Salmonella Virulence Proteins by Host-Mediated S-Palmitoylation. *Cell Host Microbe* (2011) 10(1):9–20. doi: 10.1016/j.chom.2011.06.003
96. Schmidt MF, Schlesinger MJ. Fatty Acid Binding to Vesicular Stomatitis Virus Glycoprotein: A New Type of Post-Translational Modification of the Viral Glycoprotein. *Cell* (1979) 17(4):813–9. doi: 10.1016/0092-8674(79)90321-0
97. Lobo S, Greentree WK, Linder ME, Deschenes RJ. Identification of a Ras Palmitoyltransferase in Saccharomyces Cerevisiae. *J Biol Chem* (2002) 277 (43):41268–73. doi: 10.1074/jbc.M206573200
98. Roth AF, Feng Y, Chen L, Davis NG. The Yeast DHHC Cysteine-Rich Domain Protein Akr1p is a Palmitoyl Transferase. *J Cell Biol* (2002) 159 (1):23–8. doi: 10.1083/jcb.200206120
99. Latz E. The Inflammasomes: Mechanisms of Activation and Function. *Curr Opin Immunol* (2010) 22(1):28–33. doi: 10.1016/j.coi.2009.12.004
100. Schmidt MF, Bracha M, Schlesinger MJ. Evidence for Covalent Attachment of Fatty Acids to Sindbis Virus Glycoproteins. *Proc Natl Acad Sci U S A* (1979) 76(4):1687–91. doi: 10.1073/pnas.76.4.1687
101. Siche S, Brett K, Möller L, Kordyukova LV, Mintaev RR, Alexeevski AV, et al. Two Cytoplasmic Acylation Sites and an Adjacent Hydrophobic Residue, But No Other Conserved Amino Acids in the Cytoplasmic Tail of HA From Influenza A Virus Are Crucial for Virus Replication. *Viruses* (2015) 7 (12):6458–75. doi: 10.3390/v7122950
102. Ujike M, Nakajima K, Nobusawa E. Influence of Acylation Sites of Influenza B Virus Hemagglutinin on Fusion Pore Formation and Dilation. *J Virol* (2004) 78(21):11536–43. doi: 10.1128/jvi.78.21.11536-11543.2004
103. Wagner R, Herwig A, Azzouz N, Klenk HD. Acylation-Mediated Membrane Anchoring of Avian Influenza Virus Hemagglutinin is Essential for Fusion Pore Formation and Virus Infectivity. *J Virol* (2005) 79(10):6449–58. doi: 10.1128/jvi.79.10.6449-6458.2005
104. Chlanda P, Mekhedov E, Waters H, Sodt A, Schwartz C, Nair V, et al. Palmitoylation Contributes to Membrane Curvature in Influenza A Virus Assembly and Hemagglutinin-Mediated Membrane Fusion. *J Virol* (2017) 91 (21):e009147-17. doi: 10.1128/jvi.00947-17
105. Thaa B, Levental I, Herrmann A, Veit M. Intrinsic Membrane Association of the Cytoplasmic Tail of Influenza Virus M2 Protein and Lateral Membrane Sorting Regulated by Cholesterol Binding and Palmitoylation. *Biochem J* (2011) 437(3):389–97. doi: 10.1042/bj20110706
106. Veit M, Serebryakova MV, Kordyukova LV. Palmitoylation of Influenza Virus Proteins. *Biochem Soc Trans* (2013) 41(1):50–5. doi: 10.1042/bst20120210
107. Chesarino NM, Hach JC, Chen JL, Zaro BW, Rajaram MV, Turner J, et al. Chemoproteomics Reveals Toll-Like Receptor Fatty Acylation. *BMC Biol* (2014) 12:91. doi: 10.1186/s12915-014-0091-3
108. Mukai K, Konno H, Akiba T, Uemura T, Waguri S, Kobayashi T, et al. Activation of STING Requires Palmitoylation at the Golgi. *Nat Commun* (2016) 7:11932. doi: 10.1038/ncomms11932
109. Yi L, Zheng C. The Emerging Roles of ZDHHCs-Mediated Protein Palmitoylation in the Antiviral Innate Immune Responses. *Crit Rev Microbiol* (2021) 47(1):34–43. doi: 10.1080/1040841x.2020.1835821
110. Yan Lu YZ, Coyaud Étienne. Palmitoylation of NOD1 and NOD2 Is Required for Bacterial Sensing. *Science* (2019) 366:460–7. doi: 10.1126/science.aau6391
111. Claudinon J, Gonnord P, Beslard E, Marchetti M, Mitchell K, Boularan C, et al. Palmitoylation of Interferon-Alpha (IFN-Alpha) Receptor Subunit IFNAR1 Is Required for the Activation of Stat1 and Stat2 by IFN-Alpha. *J Biol Chem* (2009) 284(36):24328–40. doi: 10.1074/jbc.M109.021915
112. Zhang Y, Qin Z, Sun W, Chu F, Zhou F. Function of Protein S-Palmitoylation in Immunity and Immune-Related Diseases. *Front Immunol* (2021) 12:661202. doi: 10.3389/fimmu.2021.661202
113. Yount JS, Moltedo B, Yang YY, Charron G, Moran TM, Lopez CB, et al. Palmitoylome Profiling Reveals S-Palmitoylation-Dependent Antiviral Activity of IFITM3. *Nat Chem Biol* (2010) 6(8):610–4. doi: 10.1038/nchembio.405
114. Ramakrishnan S. Mass-Tag Labeling Reveals Site-Specific and Endogenous Levels of Protein S-Fatty Acylation. *Proc Natl Acad Sci U S A* (2016) 113 (16):4302. doi: 10.1073/pnas.1602244113
115. McMichael TM, Zhang L, Chemudupati M, Hach JC, Kenney AD, Hang HC, et al. The Palmitoyltransferase ZDHHC20 Enhances Interferon-Induced Transmembrane Protein 3 (IFITM3) Palmitoylation and Antiviral Activity. *J Biol Chem* (2017) 292(52):21517–26. doi: 10.1074/jbc.M117.800482
116. Spence JS, He R, Hoffmann HH, Das T, Thinon E, Rice CM, et al. IFITM3 Directly Engages and Shuttles Incoming Virus Particles to Lysosomes. *Nat Chem Biol* (2019) 15(3):259–68. doi: 10.1038/s41589-018-0213-2
117. Benfield CT, MacKenzie F, Ritzefeld M, Mazzon M, Weston S, Tate EW, et al. Bat IFITM3 Restriction Depends on S-Palmitoylation and a Polymorphic Site Within the CD225 Domain. *Life Sci Alliance* (2020) 3(1): e201900542. doi: 10.26508/lsa.201900542
118. Chesarino NM, Mcmichael TM, Yount JS. Regulation of the Trafficking and Antiviral Activity of IFITM3 by Post-Translational Modifications. *Future Microbiol* (2014) 9(10):1151–63. doi: 10.2217/fmb.14.65

Conflict of Interest: The authors declare that the research was conducted in the absence of any commercial or financial relationships that could be construed as a potential conflict of interest.

Publisher's Note: All claims expressed in this article are solely those of the authors and do not necessarily represent those of their affiliated organizations, or those of the publisher, the editors and the reviewers. Any product that may be evaluated in this article, or claim that may be made by its manufacturer, is not guaranteed or endorsed by the publisher.

frontiers | Frontiers in Immunology

REVIEW
published: 15 June 2022
doi: 10.3389/fimmu.2022.930673

A Vicious Cycle: In Severe and Critically Ill COVID-19 Patients

Peifeng Huang[1‡], Qingwei Zuo[1‡], Yue Li[2‡], Patrick Kwabena Oduro[3‡], Fengxian Tan[1], Yuanyuan Wang[1], Xiaohui Liu[1], Jing Li[2], Qilong Wang[3], Fei Guo[4], Yue Li[3*†] and Long Yang[1,5*]*

[1] School of Integrative Medicine, Tianjin University of Traditional Chinese Medicine, Tianjin, China, [2] School of Department of Clinical Training and Teaching of Traditional Chinese Medicine, Tianjin University of Traditional Chinese Medicine, Tianjin, China, [3] State Key Laboratory of Component-Based Chinese Medicine, Tianjin University of Traditional Chinese Medicine, Tianjin, China, [4] National Health Commission of the People's Republic of China Key Laboratory of Systems Biology of Pathogens, Institute of Pathogen Biology and Center for AIDS Research, Chinese Academy of Medical Sciences & Peking Union Medical College, Beijing, China, [5] Research Center for Infectious Diseases, Tianjin University of Traditional Chinese Medicine, Tianjin, China

OPEN ACCESS

Edited by:
Chang Li,
Chinese Academy of Agricultural Sciences (CAAS), China

Reviewed by:
Zhanbo Zhu,
Heilongjiang Bayi Agricultural University, China
Wentao Qiao,
Nankai University, China

***Correspondence:**
Fei Guo
guofei@ipb.pumc.edu.cn
Yue Li
liyue2018@tjutcm.edu.cn
Long Yang
long.yang@tjutcm.edu.cn

†ORCID:
Yue Li
orcid.org/0000-0001-8198-9911

‡These authors have contributed equally to this work and share first authorship

Specialty section:
This article was submitted to Molecular Innate Immunity, a section of the journal Frontiers in Immunology

Received: 28 April 2022
Accepted: 12 May 2022
Published: 15 June 2022

Citation:
Huang P, Zuo Q, Li Y, Oduro PK, Tan F, Wang Y, Liu X, Li J, Wang Q, Guo F, Li Y and Yang L (2022) A Vicious Cycle: In Severe and Critically Ill COVID-19 Patients. Front. Immunol. 13:930673. doi: 10.3389/fimmu.2022.930673

The coronavirus disease 2019 (COVID-19), caused by the severe acute respiratory syndrome coronavirus 2 (SARS-CoV-2) virus, is one of the fastest-evolving viral diseases that has instigated a worldwide pandemic. Severe inflammatory syndrome and venous thrombosis are commonly noted in COVID-19 patients with severe and critical illness, contributing to the poor prognosis. Interleukin (IL)-6, a major complex inflammatory cytokine, is an independent factor in predicting the severity of COVID-19 disease in patients. IL-6 and tumor necrosis factor (TNF)-α participate in COVID-19-induced cytokine storm, causing endothelial cell damage and upregulation of plasminogen activator inhibitor-1 (PAI-1) levels. In addition, IL-6 and PAI-1 form a vicious cycle of inflammation and thrombosis, which may contribute to the poor prognosis of patients with severe COVID-19. Targeted inhibition of IL-6 and PAI-1 signal transduction appears to improve treatment outcomes in severely and critically ill COVID-19 patients suffering from cytokine storms and venous thrombosis. Motivated by studies highlighting the relationship between inflammatory cytokines and thrombosis in viral immunology, we provide an overview of the immunothrombosis and immunoinflammation vicious loop between IL-6 and PAI-1. Our goal is that understanding this ferocious circle will benefit critically ill patients with COVID-19 worldwide.

Keywords: COVID-19, PAI-1, IL-6, inflammatory reaction, venous thrombosis, tocilizumab, endothelial cells

Abbreviations: ACE, Angiotensin-converting enzyme; COVID-19, Coronavirus disease 2019; ECs, Endothelial cells; EGFR, Epidermal growth factor receptor; HFD, High-fat diet; HPMECs, Human pulmonary microvascular endothelial cells; ICU, Intensive care unit; IL, Interleukin; IL-6R, Interleukin-6 receptor; JAK, Janus kinase; LPS, Lipopolysaccharide; MD2, Myeloid differentiation protein 2; NF-kB, Nuclear factor of kappa B; PAI-1, Plasminogen activator inhibitor 1; STAT3, Signal transducer and activator of transcription 3; TCZ, Tocilizumab; TLR, Toll-like receptors; TNF, Tumor necrosis factor; tPA, Tissue plasminogen activator; uPA, Urokinase-type plasminogen activator.

INTRODUCTION

Since late December, coronavirus disease 2019 (COVID-19) (1) has spread worldwide and instigated a pandemic. Globally, as of April 12, 2022, more than five hundred million people have been diagnosed with COVID-19 disease, including more than 6 million deaths from the disease (WHO, https://covid19.who.int/), posing a great challenge to the health system around the world. The causative agent of the disease is the SARS-CoV-2 virus. Based on the clinical presentation of the COVID-19 disease, the mild-to-moderate disease accounts for 81% of COVID-19 infections and is accompanied by symptoms such as cough, fever, fatigue, and others. Meanwhile, only about 14% of cases have severe symptoms such as dyspnea and hypoxemia, while 5% present with respiratory failure, shock failure, multiple organ failure, and other severe conditions that can result in death. In addition, 14.8% of patients are classified as severe or critically ill patients (**Table 1**) (2). Emerging laboratory and pathological examination data indicate that cytokine storms and thrombosis were closely related to the disease progression, accounting for the poor prognosis in COVID-19 patients (3–8).

A significant reduction in spontaneous clot dissolution after activation of the external clotting pathway and increased resistance to tissue plasminogen activator (tPA) suggests a potential link between fibrinolytic disorder and thrombosis (9). Serum proteomics studies in patients with COVID-19 have found that abnormal increases in IL-6 correlate with increases in the coagulation and complement cascade components (10). PAI-1 is a serine protease inhibitor that acts as a principal inhibitor of tPA and urokinase-type plasminogen activator (uPA) to inhibit fibrinolysis. Based on PAI-1's primary function, diseases, or disorders that increase PAI-1 levels appear to result in high coagulation states (11–13). Interestingly, in patients with mild-to-moderate disease, plasma levels of PAI-1 were normal compared to critically ill COVID-19 patients (14, 15). However, reports from studies suggested that PAI-1 levels significantly increase in critically ill (14) and hospitalized COVID-19 patients (**Figure 1**). In addition, previous analyses on the detection of inflammatory and prethrombotic biomarkers in the blood showed significant differences between IL-6 and PAI-1 levels. The mean concentration of IL-6 in the non-severe COVID-19 group was 430.3 pg/ml, whereas that of the control group was 419.5 pg/ml.

TABLE 1 | The distribution of age, degree, and fatality rate of COVID-19 (2).

Categories	Subgroup	Cases	Distribution
Age	≥80 years	1,408	3%
	30–79 years	38,680	87%
	10–29 years	4,168	6%
	<10 years	416	1%
Degree	Mild	36,160	81%
	Severe	6,168	4%
	Critically ill	**2,087**	**5%**
Fatality rate	44,672 confirmed cases	1,023	2.3%
	Aged ≥80 years	208	14.8%
	70–79 years	312	8.0%
	Critically cases	**1,023**	**49.0%**

Bold values highlight the proportion and mortality of critically ill patients and emphasize the lethality of COVID-19.

Meanwhile, the concentration of IL-6 in severe COVID-19 and death group was 1,463 and 2,200 pg/ml, respectively (14). PAI-1 is a widely recognized biomarker of endothelial dysfunction and has been shown that increased concentration is associated with the severity of the disease (16, 17). The expression of PAI-1 may reflect the severity of SARS-CoV-2 infection to some extent (18). The plasma concentration of PAI-1 detected in patients with severe COVID-19 was 713.3 ng/ml, while in the COVID-19 death group, it was 1,223.5 ng/ml. Then again, in the non-severe COVID-19 group, the plasma concentration of PAI-1 was 465.2 ng/ml and that of healthy donors was 183.7 ng/ml (14). It is important to note that severe and critically ill patients with COVID-19 often suffer from underlying diseases (19, 20). Evidence has also suggested that most of the underlying diseases present with elevated levels of PAI-1 (21). For example, among diabetes and acute cerebral infarction patients without COVID-19, PAI-1 levels averaged 36.5 and 63.95 ng/ml (22, 23). Nonetheless, COVID-19-infected individuals have significantly higher levels of PAI-1 than those with diabetes or acute cerebral infarction, providing indirect evidence that COVID-19 could increase PAI-1 levels (**Table 2**).

Studies on coexpression-induced IL-6 and PAI-1 through the nuclear factor-kappa B (NF-κB) pathway and ligand-dependent epidermal growth factor receptor (EGFR) activation confirmed a significant correlation between IL-6 and PAI-1 (26). The same phenomenon has revealed significant differences between IL-6 and PAI-1 levels in severe and mild-to-moderate COVID-19

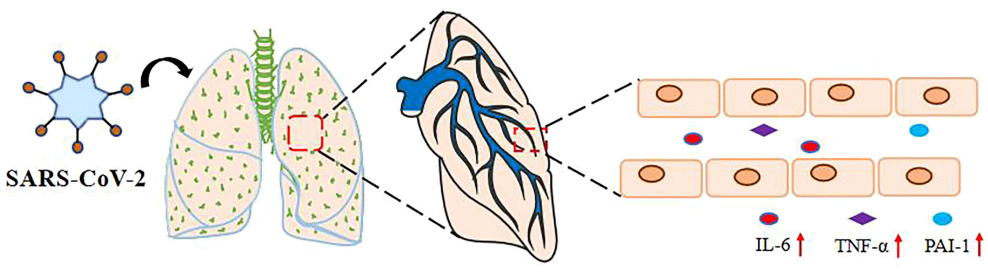

FIGURE 1 | SARS-Co-2 upregulates plasma IL-6, TNF- α, and PAI-1 levels. The levels of IL-6, PAI-1, and TNF-α in the serum of severely and critically ill COVID-19 patients with SARS-CoV-2 pulmonary infection *via* the respiratory tract were significantly increased.

TABLE 2 | The expression of IL-6 and PAI-1 in COVID-19 and underlying diseases.

Disease		IL-6 (mean pg/ml)	PAI-1 (mean ng/ml)
COVID-19	Healthy donors	419.5	183.7
	Non-severe COVID-19 group	430.3	465.2
	Severe COVID-19 group	1463	713.3
	Death group	2200	1,223.5
Type 2 diabetes	–	<20 (24)	36.5
Acute cerebral infarction	–	<1,000 (25)	63.95

patients (14). Treatment with anti-TNFs can reduce the death rate and poor outcomes of COVID-19 patients (27). Below, we review the possible relationship between inflammatory levels and thrombosis in severe and critically ill COVID-19 patients.

SARS-COV-2 RAISES THE EXPRESSION OF PAI-1, IL-6, AND TNF-A

The SARS-CoV-2 infection has a devastating effect on immune regulation, leading to a life-threatening systemic inflammatory syndrome called the cytokine storm. This systemic inflammatory syndrome involves abnormal immune-cell hyperactivation and uncontrolled release of circulatory cytokines. Elegant evidence from the COVID-19 pandemic shows that IL-6 and TNF-α are involved in the COVID-19-induced cytokine storm (28). In severe disease, IL-6 and TNF-α are major contributing factors that worsen the condition and cause poor clinical outcomes and even death (29–31). IL-6 is a multifunctional cytokine capable of transmitting cell signals. It is the main trigger of endothelial cytokine storm and an intervention target for clinical therapy (32, 33). Almost all stromal cells and immune system cells can produce IL-6, and the primary activator is IL-1β or TNF-α (34). Toll-like receptor (TLR)-stimulated monocytes and macrophages can also promote the expression of IL-6 (35).

During propagation of the SARS-CoV-2 virus, the envelope spike glycoprotein of the SARS-CoV-2 virus attaches to the angiotensin-converting enzyme (ACE)-2 on the target cell surface, resulting in ACE-2 loss (36). ACE-2 is a negative regulator that functions by activating tPA. ACE-2 deficiency disrupts the effective ACE-2/angiotensin (1–7)/Mas receptor axis, making Ang II more active and decreasing tPA activity, prompting endothelial and smooth muscle cells to synthesize and release PAI-1, leading to the balance of PAI-1/tPA to revert to its prethrombotic state (37, 38). Studies on intensive care unit (ICU) patients with critically ill COVID-19 found that low fibrinolysis was mainly associated with elevated PAI-1 levels (39). The action of recombinant SARS-CoV-2 on the ACE-2 receptor is comparable to that of live viruses, and its spiking glycoprotein induces the expression of PAI-1 in human pulmonary microvascular endothelial cells (HPMECs) (40). In individuals with severe COVID-19 illness, increased PAI-1 expression reduces tPA activity and increases thrombosis while perhaps worsening the inflammatory response (**Table 3**).

PAI-1 Upregulates the Expressions of IL-6 and TNF-α

In several studies, PAI-1 has been found at the inflammatory site after tissue damage (47, 48). PAI-1 inhibitors reduce TNF-α expression and, at the same time, decrease PAI-1 expression in diabetic mice (49). PAI-1 upregulation may be related to its capacity to activate macrophages. PAI-1 helps to regulate the lipopolysaccharide (LPS)-induced inflammatory response in NR8383 cells, possibly by influencing the TLR4-myeloid differentiation protein 2 (MD-2)/NF-κB signaling transfer pathway (50). PAI-1-induced TLR4 activation causes monocyte macrophages to release significant quantities of IL-6 and TNF-α, exacerbating the inflammatory response (51, 52). This shows that TLR4 is an essential medium for PAI-1 to activate macrophages and promote TNF-α expression. The expression spectrum of macrophages stimulated by PAI-1 occurs 2 h after the peak transcription of PAI-1 (53). PAI-1 can promote macrophage activation and may also be an initial response gene for predicting inflammation. PAI-1 promotes the recruitment of monocytes/macrophages in tumor cells. Its lipoprotein-receptor-related protein 1 interaction domain regulates macrophage migration, whereas its C-terminal uPA interaction domain auto-secretes IL-6 by activating the p38MAPK and NF-κB pathway and inducing macrophage polarization (54). There was a considerable increase in the expression of M1 macrophages in obese mice caused by a high-fat diet (HFD), but PAI-1 deficiency and PAI-039 therapy prevented the development of these markers, demonstrating that PAI-1 is required for macrophage polarization. Meanwhile, PAI-1 activates TLR4, triggering a robust inflammatory response in endothelial cells (ECs), allowing ECs to continuously secrete IL-6 (55). PAI-1 may interact with TLR4 to activate NF-κB, leading ECs to generate

TABLE 3 | The expressions of PAI-1 and IL-6 in severe COVID-19 patients.

Factors	Expressing and working	Reference
PAI-1	rSARS-CoV-2-S1 infect HPMECs exhibited robust induction of PAI-1	(40)
	Circulating levels of PAI-1 upregulate and function as an independent predictor of the severity of COVID-19 disease in patients	(41)
	Decreased the PAI-1 levels and alleviated critical illness in severe COVID-19 patients	(42)
	Significant expression of PAI-1 exists only in severe COVID-19 patients and promotes patient thrombosis	(14)
	Hypercoagulability and hypofibrinolysis are connected to the elevated level of PAI-1 in COVID-19	(39)
IL-6	IL-6 can serve as an independent factor predictor of the severity of COVID-19 disease in patients	(43–46)
	Seroproteomics studies found IL-6 significant upregulation, and IL-6 signal transduction is the most upstream upregulation pathway in severe patients with COVID-19 patients	(10)
	IL-6 is the main trigger of endothelial cytokine storms in COVID-19 patients	(32)

cytokines such as IL-6 (56, 57). This shows that PAI-1 can stimulate macrophages and endothelial cells in various ways, promoting inflammatory responses (**Table 4**).

There is no clinical use of PAI-1 inhibitors in COVID-19 patients. However, it is worth noting that bortezomib upregulates KLF2 to suppress PAI-1 expression and reduce EC damage in HPME cells stimulated with rSARS-CoV-2-S1 glycoprotein (58).

The IL-6 Increases the Expression of the PAI-1

Severe clotting disorder in patients with COVID-19 is closely related to the increased risk of death (59–62). Venous thromboembolism was prevalent in COVID-19 patients, with a total incidence of 31% in 184 patients with severe COVID-19 (63), and a preliminary autopsy on 11 of the COVID-19 patients revealed thrombus in the pulmonary arterioles (64). The D-dimer is a fibrin degradation product used as an alternative marker of fibrinolysis and is often elevated in thrombotic events (65). Relevant studies on COVID-19 report that D-dimer elevation is a prevalent feature (66). Low fibrinolysis is the primary cause of increased blood viscosity and is associated with elevated PAI-1 levels (39). PAI-1 circulating levels may be used as an independent predictor of severity in COVID-19 patients (41), and regulating PAI-1 expression can benefit patients with COVID-19 (42).

Alongside PAI-1, IL-6 is an independent predictor of COVID-19 severity (43–46). IL-6 levels have a substantial predictive value for mortality in COVID-19 ICUs (67). Patients with severe COVID-19 have considerable IL-6 overexpression, and IL-6 signal transduction is the most upregulated pathway in COVID-19 patients (10). IL-6 may have a significant role in the progression of severe COVID-19 disease in patients. PAI-1 expression is only found in severe COVID-19 patients and increases thrombosis (14). PAI-1 is linked to elevated levels of IL-6 in critically ill COVID-19 patients. IL-6 signals through two central pathways. The first is the classic cis signaling, and the second is the trans-signaling. In the classic cis pathway, IL-6 attaches to cells, mainly immune cells, expressing the membrane-bound interleukin-6 receptor (IL-6R) to initiate a downstream signaling response (68, 69). On the other hand, in trans-signaling, IL-6 binds to the soluble form of IL-6R, which is released from IL-6R expressing cell surfaces by proteolysis and IL-6R mRNA to form an exciting complex that associates with membrane-bound gp130 (70–72). In the presence of high circulating levels of IL-6, trans-signaling typically occurs. For instance, ECs express the membrane-bound gp130 but not the membrane-bound IL-6R (73–76), allowing for IL-6/soluble-IL-6R/gp130 downstream signaling activation.

The detection of PAI-1 expression before and after tocilizumab (TCZ) treatment demonstrates that IL-6 signaling transduction can promote PAI-1 expression in ECs (18, 42). LPS stimulates the NF-κB classical pathway to increase the PAI-1 expression and promote alveolar hypercoagulation and fibrinolysis inhibitory states. PAI-1 expression is dramatically reduced following NF-κB knockout (77, 78), indicating that the NF-κB pathway can control PAI-1 expression to some extent. At the same time, elevated plasma IL-6 levels promote NF-κB activation (79), resulting in EC-induced PAI-1 overexpression. In hepatocytes, IL-6 signals *via* the Janus kinase (JAK) pathway to promote C/EBPδ-induced PAI-1 expression (80). In addition, IL-6 signals and activates the IL-6R/signal transducer and activator of transcription 3 (STAT3) pathway (54), which can indirectly upregulate PAI-1 *via* miR-34a (81). TNF-α can also upregulate PAI-1 (82). However, it is less commonly documented in the literature, and the mechanism remains unknown (**Table 5**).

According to the preceding discussion, elevated and persistent IL-6, TNF-α, and PAI-1 levels in severe COVID-19 patients potentially generate a vicious cycle of inflammatory response and thrombosis (**Figure 2**).

CLINICAL SIGNIFICANCE

The probable inflammatory response and thrombus interaction mechanisms are first described in critically ill COVID-19 patients. TCZ is a recombinant human-resistant human IL-6R IgG1 monoclonal antibody (83). The use of TCZ in critically ill COVID-19 patients can decrease PAI-1 levels and improve the condition of severe COVID-19 patients (42). TCZ is authorized for the treatment of rheumatoid arthritis (84) and systemic juvenile idiopathic arthritis (85) because it selectively binds soluble and membrane-bound IL-6 receptors and inhibits IL-6-mediated classic cis and trans-signaling (86). IL-6 levels in severe COVID-19 patients are significantly higher than in other patients, prompting several researchers to recommend TCZ to

TABLE 4 | PAI-1 upregulate the expressions of IL-6 and TNF-α.

Targets	Cell/host	Model	Mechanism	Reference
PAI-1 upregulates TNF-α	NR8383 cells	Inflammatory model induced by LPS	TLR4-MD-2/NF-κB signaling transduction pathway	(50)
	Mouse	Type 2 diabetes mellitus	PAItrap3 decreases the levels of both PAI-1 and TNF-α	(49)
	Mouse	Systemic inflammation model	PAI-1 regulates inflammatory responses through TLR4 mediated macrophage activation	(53)
PAI-1 upregulates IL-6	C57 mouse/HT-1080 fibrosarcoma cancer cell line	$Rag1^{-/-}$ $PAI1^{-/-}$/$Rag1^{-/-}$PAI-1 mice	PAI-1 promotes the recruitment and polarization of macrophages in cancer	(54)
	Microvascular (MIC) and macrovascular (MAC) endothelial cells (ECs)	Inflammatory model induced by LPS	PAI-1 was necessary for macrophage polarization	(55)
	Mice/human aortic endothelial cells (HAECs)	Endotoxemia of mouse/Inflammatory model induced by LPS	PAI-1 combines with TLR4 to promote NF-κB activation so that ECs produce chemokines, such as IL-6	(56, 57)

TABLE 5 | IL-6 and TNF-α promote the expression of PAI-1.

Promote expression	Cell/host	Model	Possible mechanism	Reference
TNF-α upregulates PAI-1	Clinic patients	Atherosclerosis	TNF-α inhibition with infliximab decreases PAI-1 Ag level	(82)
IL-6 upregulates PAI-1	Clinic patients/HUVECs	Patients diagnosed with CRS from sepsis	Tocilizumab treatment decreased the PAI-1 levels and alleviated critical illness in severe COVID-19 patients	(18, 42)
	Human hepatoma/primary mouse hepatocytes	–	IL-6 induces PAI-1 expression through JAK signaling pathways converging on C/EBPδ	(80)
	Human colorectal cancer/breast cancer/prostate cancer	Rag1$^{-/-}$ PAI1$^{-/-}$/Rag1$^{-/-}$PAI-1 mice (54)	IL-6 activates the IL-6/STAT3 pathway and, through miR-34a, upregulates PAI-1	(54, 81)

inhibit IL-6 signaling in patients with severe COVID-19 to improve patient symptoms (35, 87). According to reports, TCZ can be used as an alternative therapy for COVID-19 patients who are at risk of cytokine storms (88). It is advised that in critically ill patients with elevated IL-6 levels, a repeated dose of TCZ will be necessary to reduce IL-6 levels significantly (88). However, TCZ is ineffective for patients with moderate COVID-19 (89) but can improve clinical symptoms in severely and critically ill COVID-19 patients (90). Breathing and bilateral diffuse turbidity disappear by intravenous TCZ in severe COVID-19 patients with pneumonia and acute respiratory distress syndrome (ARDS) (91). Unfortunately, thrombosis in severe COVID-19 patients was not mentioned. PAI-1 inhibition can improve the level of IL-6 and the damage to ECs. Treatment with TM5614 (PAI-1 inhibitor) eliminates the elevated circulating levels of PAI-1 and thrombin in plasma produced by particulate matter (PM) 2.5 (92). Meanwhile, TM5614 significantly reduces the elevated level of IL-6 (92). Bortezomib, a proteasomal degradation inhibitor, enhances KLF2, decreases PAI-1 expression, and reduces EC damage in HPMECs stimulated with rSARS-CoV-2-S1 glycoprotein (58). PAI-1 may have a role in prothrombotic events and inflammation in COVID-19 patients. This asserts the vicious cycle of PAI-1 and IL-6 in COVID-19.

CONCLUSION AND FUTURE PERSPECTIVE

In this review, we briefly discussed the possible link between elevated IL-6 levels and thrombosis in COVID-19 patients. From non-viral contexts, the link between PAI-1 and IL-6 forms an inflammatory–thrombus circuit (42). PAI-1 and IL-6 were not shown to be strongly connected in COVID-19 case reports, although autopsy demonstrated substantial damage to ECs (93). In COVID-19 patients, inflammation and thrombosis are two of the

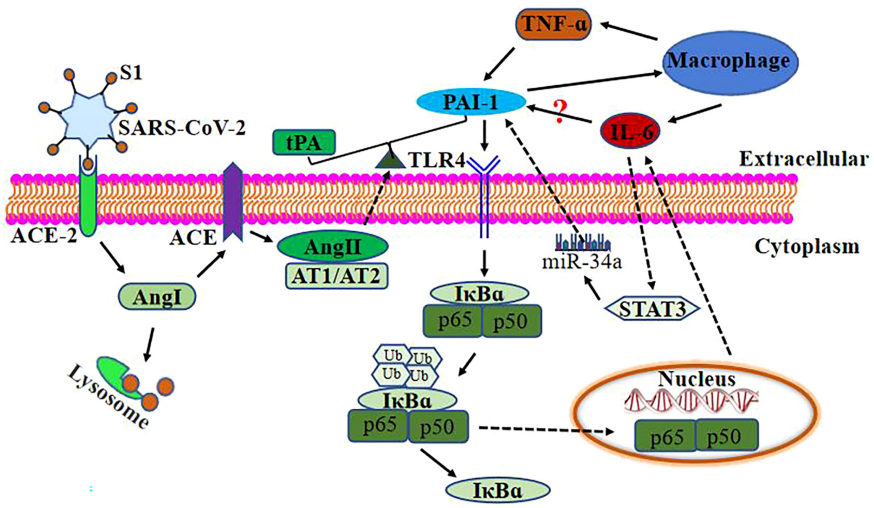

FIGURE 2 | Relationship between PAI-1 and IL-6 after SARS-Co-2 infection. SARS-CoV-2 binds to ACE-2 on the target cell surface, resulting in the loss of ACE-2. ACE-2 is a negative regulator that works by activating tPA. ACE-2 deficiency loses the effective ACE-2/angiotensin (1–7)/Mas receptor axis and increases the level of Ang1. ACE converts Ang I to Ang II and decreases tPA activity, causing endothelial cells and smooth muscle cells to synthesize and release PAI-1. Ang II binds to AT1/AT2 to break the balance of PAI-1/tPA to its prethrombotic state. Elevated levels of PAI-1 in severely and critically ill COVID-19 patients may upregulate IL-6 expression through TLR4/NF-κB pathway and activate macrophages to upregulate IL-6 and TNF-α expression. At the same time, TNF-α can also upregulate PAI-1 expression. IL-6 upregulates the expression of PAI-1 *via* STAT3/miR-29a.

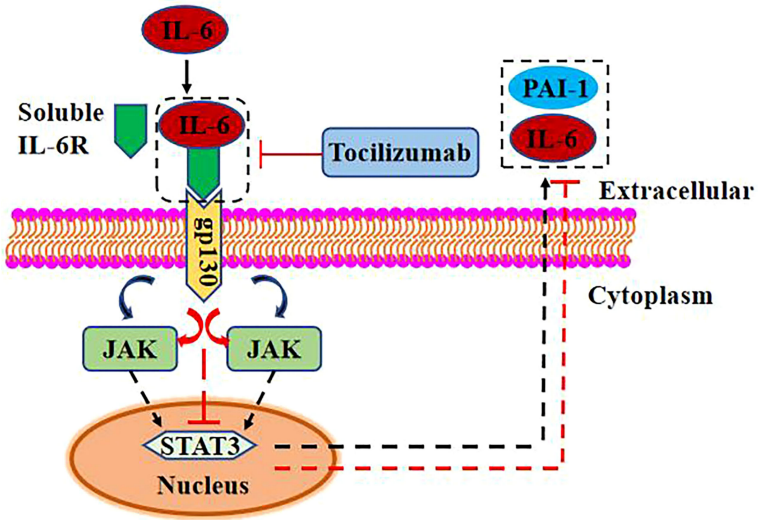

FIGURE 3 | IL-6 promotes PAI-1 expression *via* trans signaling. High concentration of IL-6 combined with soluble IL-6R can activate the JAK/STAT3 signal pathway through gp130 and upregulate the expression of PAI-1 and IL-6. TCZ can reduce the expression of PAI-1 and IL-6 by inhibiting the binding of IL-6 and soluble IL-6R.

most significant deleterious responses (94, 95). The development of blood clots in the heart can be explained by the distribution of ECs in the heart and by the above process (96). In critically ill COVID-19 patients, EC dysfunction increases PAI-1 expression (17) and promotes macrophage recruitment and activation (54). This raises the amount of IL-6 and TNF-α in the blood, increasing the odds of a "cytokine storm" (28). TCZ can decrease IL-6 signal transduction *via* IL-6R and soluble IL-6R. TNF-α, on the other hand, stimulates endothelial PAI-1 production and activates macrophages, exposing ECs to prominent levels of IL-6 and TNF-α and causing sustained tissue and organ damage. In thrombosis, therapeutic use of thrombolytic treatment merely lowers fibrin production. Inability to directly suppress PAI-1 expression and break the vicious cycle between PAI-1 and IL-6 results in serum PAI-1 and IL-6 buildup, facilitating tissue damage and thrombosis development. IL-6 trans-signaling has been shown to increase PAI-1 expression. When IL-6 is coupled with soluble IL-6R and gp130, it activates the downstream JAK/STAT signal pathway and promotes the expression of IL-6 and PAI-1 (54, 97, 98) (**Figure 3**). STAT3-dependent transcription inhibition significantly reduces VEGF-induced vascular permeability in zebrafish, mouse, and human endothelial cells (99). Increased endothelial cell permeability can aggravate pulmonary edema and dyspnea in COVID-19 patients (100). Although the connection between PAI-1 and IL-6 has not yet been shown, the possibility of a malignant interaction between PAI-1 and IL-6 in critically ill COVID-19 patients should not be overlooked. PAI-1 and IL-6 may produce a vicious cycle in which their expression is mutually induced, but the mechanism involved remains unclear. Thrombosis and inflammatory responses in patients with severe COVID-19 are discussed from a new perspective, which provides innovative ideas for future studies.

AUTHOR CONTRIBUTIONS

All authors have read and approved the manuscript. FG, YL (11th author), and LY supervised and edited the final manuscript with comments from co-authors. PH, QZ, YL (3rd author), and PO conceptualized and wrote the initial draft, which was further reviewed and edited by FT, YW, XL, JL, and QW for intellectual content. All authors provided crucial revisions in subsequent drafts.

FUNDING

This work was supported by the Tianjin Municipal Education Commission Scientific Research Project (Natural Science, Grant No. 2019ZD11 to LY), Science and Technology Program of Tianjin (21ZYJDJC00070), the National Key Research and Development Program of China (2019YFC1708803), and Innovation Team and Talents Cultivation Program of National Administration of Traditional Chinese Medicine (ZYYCXTD-C-202203).

ACKNOWLEDGMENTS

We thank LY, YL, and FG for their assistance with conceptualization and helpful discussion. We are also grateful to the Tianjin Municipal Education Commission Scientific Research Project for the funding support.

REFERENCES

1. Li Q, Guan X, Wu P, Wang X, Zhou L, Tong Y, et al. Early Transmission Dynamics in Wuhan, China, of Novel Coronavirus-Infected Pneumonia. *N Engl J Med* (2020) 382(13):1199–207. doi: 10.1056/NEJMoa2001316
2. Wu ZY, McGoogan JM. Characteristics of and Important Lessons From the Coronavirus Disease 2019 (COVID-19) Outbreak in China Summary of a Report of 72 314 Cases From the Chinese Center for Disease Control and Prevention. *Jama-J Am Med Assoc* (2020) 323(13):1239–42. doi: 10.1001/jama.2020.2648
3. Guan WJ, Ni ZY, Hu Y, Liang WH, Ou CQ, He JX, et al. Clinical Characteristics of Coronavirus Disease 2019 in China. *N Engl J Med* (2020) 382(18):1708–20. doi: 10.1056/NEJMoa2002032
4. Liu K, Fang YY, Deng Y, Liu W, Wang MF, Ma JP, et al. Clinical Characteristics of Novel Coronavirus Cases in Tertiary Hospitals in Hubei Province. *Chin Med J (Engl)* (2020) 133(9):1025–31. doi: 10.1097/CM9.0000000000000744
5. Diao B, Wang C, Tan Y, Chen X, Liu Y, Ning L, et al. Reduction and Functional Exhaustion of T Cells in Patients With Coronavirus Disease 2019 (COVID-19). *Front Immunol* (2020) 11:827. doi: 10.3389/fimmu.2020.00827
6. Song F, Shi N, Shan F, Zhang Z, Shen J, Lu H, et al. Emerging 2019 Novel Coronavirus (2019-Ncov) Pneumonia. *Radiology* (2020) 295(1):210–7. doi: 10.1148/radiol.2020200274
7. Tian S, Xiong Y, Liu H, Niu L, Guo J, Liao M, et al. Pathological Study of the 2019 Novel Coronavirus Disease (COVID-19) Through Postmortem Core Biopsies. *Mod Pathol* (2020) 33(6):1007–14. doi: 10.1038/s41379-020-0536-x
8. Belen-Apak FB, Sarialioglu F. Pulmonary Intravascular Coagulation in COVID-19: Possible Pathogenesis and Recommendations on Anticoagulant/Thrombolytic Therapy. *J Thromb Thrombolysis* (2020) 50(2):278–80. doi: 10.1007/s11239-020-02129-0
9. Hammer S, Haberle H, Schlensak C, Bitzer M, Malek NP, Handgretinger R, et al. Severe SARS-CoV-2 Infection Inhibits Fibrinolysis Leading to Changes in Viscoelastic Properties of Blood Clot: A Descriptive Study of Fibrinolysis in COVID-19. *Thromb Haemost* (2021) 121(11):1417–26. doi: 10.1055/a-1400-6034
10. D'Alessandro A, Thomas T, Dzieciatkowska M, Hill RC, Francis RO, Hudson KE, et al. Serum Proteomics in COVID-19 Patients: Altered Coagulation and Complement Status as a Function of IL-6 Level. *J Proteome Res* (2020) 19 (11):4417–27. doi: 10.1021/acs.jproteome.0c00365
11. Cesari M, Pahor M, Incalzi RA. Plasminogen Activator Inhibitor-1 (PAI-1): A Key Factor Linking Fibrinolysis and Age-Related Subclinical and Clinical Conditions. *Cardiovasc Ther* (2010) 28(5):e72–91. doi: 10.1111/j.1755-5922.2010.00171.x
12. Binder BR, Christ G, Gruber F, Grubic N, Hufnagl P, Krebs M, et al. Plasminogen Activator Inhibitor 1: Physiological and Pathophysiological Roles. *News Physiol Sci* (2002) 17:56–61. doi: 10.1152/nips.01369.2001
13. Ghosh AK, Vaughan DE. PAI-1 in Tissue Fibrosis. *J Cell Physiol* (2012) 227 (2):493–507. doi: 10.1002/jcp.22783
14. Lopez-Castaneda S, Garcia-Larragoiti N, Cano-Mendez A, Blancas-Ayala K, Damian-Vazquez G, Perez-Medina AI, et al. Inflammatory and Prothrombotic Biomarkers Associated With the Severity of COVID-19 Infection. *Clin Appl Thromb Hemost* (2021) 27:1076029621999099. doi: 10.1177/1076029621999099
15. Pine AB, Meizlish ML, Goshua G, Chang CH, Zhang H, Bishai J, et al. Circulating Markers of Angiogenesis and Endotheliopathy in COVID-19. *Pulm Circ* (2020) 10(4):2045894020966547. doi: 10.1177/2045894020966547
16. Bernard I, Limonta D, Mahal LK, Hobman TC. Endothelium Infection and Dysregulation by SARS-CoV-2: Evidence and Caveats in COVID-19. *Viruses* (2020) 13(1):29. doi: 10.3390/v13010029
17. Norooznezhad AH, Mansouri K. Endothelial Cell Dysfunction, Coagulation, and Angiogenesis in Coronavirus Disease 2019 (COVID-19). *Microvasc Res* (2021) 137:104188. doi: 10.1016/j.mvr.2021.104188
18. Kellici TF, Pilka ES, Bodkin MJ. Therapeutic Potential of Targeting Plasminogen Activator Inhibitor-1 in COVID-19. *Trends Pharmacol Sci* (2021) 42(6):431–3. doi: 10.1016/j.tips.2021.03.006
19. Vogrig A, Gigli GL, Bna C, Morassi M. Stroke in Patients With COVID-19: Clinical and Neuroimaging Characteristics. *Neurosci Lett* (2021) 743:135564. doi: 10.1016/j.neulet.2020.135564
20. Zhou Y, Chi J, Lv W, Wang Y. Obesity and Diabetes as High-Risk Factors for Severe Coronavirus Disease 2019 (Covid-19). *Diabetes Metab Res Rev* (2021) 37(2):e3377. doi: 10.1002/dmrr.3377
21. Bayomy O, Rao AD, Garg R, Vaidya A, Kotin AR, Reiber B, et al. Plasminogen Activator Inhibitor-1 and Pericardial Fat in Individuals With Type 2 Diabetes Mellitus. *Metab Syndr Relat Disord* (2017) 15(6):269–75. doi: 10.1089/met.2017.0031
22. Sakurai S, Jojima T, Iijima T, Tomaru T, Usui I, Aso Y. Empagliflozin Decreases the Plasma Concentration of Plasminogen Activator Inhibitor-1 (PAI-1) in Patients With Type 2 Diabetes: Association With Improvement of Fibrinolysis. *J Diabetes Complications* (2020) 34(11):107703. doi: 10.1016/j.jdiacomp.2020.107703
23. Li L, Ren S, Hao X, Zhen Z, Ji H. Efficacy of Minimally Invasive Intervention in Patients With Acute Cerebral Infarction. *J Cardiovasc Pharmacol* (2019) 73 (1):22–6. doi: 10.1097/FJC.0000000000000625
24. Mallard AR, Hollekim-Strand SM, Ingul CB, Coombes JS. High Day-to-Day and Diurnal Variability of Oxidative Stress and Inflammation Biomarkers in People With Type 2 Diabetes Mellitus and Healthy Individuals. *Redox Rep* (2020) 25(1):64–9. doi: 10.1080/13510002.2020.1795587
25. Liu Y, Qu M, Wang N, Wang L. Effects of an Evidence-Based Nursing Intervention on Neurological Function and Serum Inflammatory Cytokines in Patients With Acute Cerebral Infarction: A Randomized Controlled Trial. *Restor Neurol Neurosci* (2021) 39(2):129–37. doi: 10.3233/RNN-201080
26. Alberti C, Pinciroli P, Valeri B, Ferri R, Ditto A, Umezawa K, et al. Ligand-Dependent EGFR Activation Induces the Co-Expression of IL-6 and PAI-1 *via* the NFkB Pathway in Advanced-Stage Epithelial Ovarian Cancer. *Oncogene* (2012) 31(37):4139–49. doi: 10.1038/onc.2011.572
27. Robinson PC, Liew DFL, Liew JW, Monaco C, Richards D, Shivakumar S, et al. The Potential for Repurposing Anti-TNF as a Therapy for the Treatment of COVID-19. *Med (NY)* (2020) 1(1):90–102. doi: 10.1016/j.medj.2020.11.005
28. Azevedo RB, Botelho BG, Hollanda JVG, Ferreira LVL, Junqueira de Andrade LZ, Oei S, et al. Covid-19 and the Cardiovascular System: A Comprehensive Review. *J Hum Hypertens* (2021) 35(1):4–11. doi: 10.1038/s41371-020-0387-4
29. Li X, Geng M, Peng Y, Meng L, Lu S. Molecular Immune Pathogenesis and Diagnosis of COVID-19. *J Pharm Anal* (2020) 10(2):102–8. doi: 10.1016/j.jpha.2020.03.001
30. Godeau D, Petit A, Richard I, Roquelaure Y, Descatha A. Return-To-Work, Disabilities and Occupational Health in the Age of COVID-19. *Scand J Work Environ Health* (2021) 47(5):408–9. doi: 10.5271/sjweh.3960
31. Tisoncik JR, Korth MJ, Simmons CP, Farrar J, Martin TR, Katze MG. Into the Eye of the Cytokine Storm. *Microbiol Mol Biol Rev* (2012) 76(1):16–32. doi: 10.1128/MMBR.05015-11
32. Hantoushzadeh S, Norooznezhad AH. Possible Cause of Inflammatory Storm and Septic Shock in Patients Diagnosed With (COVID-19). *Arch Med Res* (2020) 51(4):347–8. doi: 10.1016/j.arcmed.2020.03.015
33. Schett G, Elewaut D, McInnes IB, Dayer JM, Neurath MF. How Cytokine Networks Fuel Inflammation: Toward a Cytokine-Based Disease Taxonomy. *Nat Med* (2013) 19(7):822–4. doi: 10.1038/nm.3260
34. Hunter CA, Jones SA. IL-6 as a Keystone Cytokine in Health and Disease. *Nat Immunol* (2015) 16(5):448–57. doi: 10.1038/ni.3153
35. Zhang C, Wu Z, Li JW, Zhao H, Wang GQ. Cytokine Release Syndrome in Severe COVID-19: Interleukin-6 Receptor Antagonist Tocilizumab may be the Key to Reduce Mortality. *Int J Antimicrob Agents* (2020) 55(5):105954. doi: 10.1016/j.ijantimicag.2020.105954
36. Hoffmann M, Kleine-Weber H, Schroeder S, Kruger N, Herrler T, Erichsen S, et al. SARS-CoV-2 Cell Entry Depends on ACE2 and TMPRSS2 and Is Blocked by a Clinically Proven Protease Inhibitor. *Cell* (2020) 181(2):271–80.e278. doi: 10.1016/j.cell.2020.02.052
37. Nishimura H, Tsuji H, Masuda H, Nakagawa K, Nakahara Y, Kitamura H, et al. Angiotensin II Increases Plasminogen Activator Inhibitor-1 and Tissue Factor mRNA Expression Without Changing That of Tissue Type Plasminogen Activator or Tissue Factor Pathway Inhibitor in Cultured Rat Aortic Endothelial Cells. *Thromb Haemost* (1997) 77(6):1189–95. doi: 10.1055/s-0038-1656136
38. van Leeuwen RT, Kol A, Andreotti F, Kluft C, Maseri A, Sperti G. Angiotensin II Increases Plasminogen Activator Inhibitor Type 1 and Tissue-Type Plasminogen Activator Messenger RNA in Cultured Rat Aortic Smooth Muscle Cells. *Circulation* (1994) 90(1):362–8. doi: 10.1161/01.CIR.90.1.362
39. Nougier C, Benoit R, Simon M, Desmurs-Clavel H, Marcotte G, Argaud L, et al. Hypofibrinolytic State and High Thrombin Generation may Play a Major

Role in SARS-COV2 Associated Thrombosis. *J Thromb Haemost* (2020) 18 (9):2215–9. doi: 10.1111/jth.15016
40. Han M, Pandey D. ZMPSTE24 Regulates SARS-CoV-2 Spike Protein-Enhanced Expression of Endothelial Plasminogen Activator Inhibitor-1. *Am J Respir Cell Mol Biol* (2021) 65(3):300–8. doi: 10.1165/rcmb.2020-0544OC
41. Henry BM, Cheruiyot I, Benoit JL, Lippi G, Prohaszka Z, Favaloro EJ, et al. Circulating Levels of Tissue Plasminogen Activator and Plasminogen Activator Inhibitor-1 Are Independent Predictors of Coronavirus Disease 2019 Severity: A Prospective, Observational Study. *Semin Thromb Hemost* (2021) 47(4):451–5. doi: 10.1055/s-0040-1722308
42. Kang S, Tanaka T, Inoue H, Ono C, Hashimoto S, Kioi Y, et al. IL-6 Trans-Signaling Induces Plasminogen Activator Inhibitor-1 From Vascular Endothelial Cells in Cytokine Release Syndrome. *Proc Natl Acad Sci USA* (2020) 117(36):22351–6. doi: 10.1073/pnas.2010229117
43. Aziz M, Fatima R, Assaly R. Elevated Interleukin-6 and Severe COVID-19: A Meta-Analysis. *J Med Virol* (2020) 92(11):2283–5. doi: 10.1002/jmv.25948
44. Santa Cruz A, Mendes-Frias A, Oliveira AI, Dias L, Matos AR, Carvalho A, et al. Interleukin-6 Is a Biomarker for the Development of Fatal Severe Acute Respiratory Syndrome Coronavirus 2 Pneumonia. *Front Immunol* (2021) 12:613422. doi: 10.3389/fimmu.2021.613422
45. Liu F, Li L, Xu M, Wu J, Luo D, Zhu Y, et al. Prognostic Value of Interleukin-6, C-Reactive Protein, and Procalcitonin in Patients With COVID-19. *J Clin Virol* (2020) 127:104370. doi: 10.1016/j.jcv.2020.104370
46. Henry BM, de Oliveira MHS, Benoit S, Plebani M, Lippi G. Hematologic, Biochemical and Immune Biomarker Abnormalities Associated With Severe Illness and Mortality in Coronavirus Disease 2019 (COVID-19): A Meta-Analysis. *Clin Chem Lab Med* (2020) 58(7):1021–8. doi: 10.1515/cclm-2020-0369
47. Juhan-Vague I, Moerman B, De Cock F, Aillaud MF, Collen D. Plasma Levels of a Specific Inhibitor of Tissue-Type Plasminogen Activator (and Urokinase) in Normal and Pathological Conditions. *Thromb Res* (1984) 33(5):523–30. doi: 10.1016/0049-3848(84)90018-5
48. Kluft C, Verheijen JH, Jie AF, Rijken DC, Preston FE, Sue-Ling HM, et al. The Postoperative Fibrinolytic Shutdown: A Rapidly Reverting Acute Phase Pattern for the Fast-Acting Inhibitor of Tissue-Type Plasminogen Activator After Trauma. *Scand J Clin Lab Invest* (1985) 45(7):605–10. doi: 10.3109/00365518509155267
49. Tang S, Liu W, Pan X, Liu L, Yang Y, Wang D, et al. Specific Inhibition of Plasminogen Activator Inhibitor 1 Reduces Blood Glucose Level by Lowering TNF-A. *Life Sci* (2020) 246:117404. doi: 10.1016/j.lfs.2020.117404
50. Ren W, Wang Z, Hua F, Zhu L. Plasminogen Activator Inhibitor-1 Regulates LPS-Induced TLR4/MD-2 Pathway Activation and Inflammation in Alveolar Macrophages. *Inflammation* (2015) 38(1):384–93. doi: 10.1007/s10753-014-0042-8
51. Kawai T, Akira S. Signaling to NF-kappaB by Toll-Like Receptors. *Trends Mol Med* (2007) 13(11):460–9. doi: 10.1016/j.molmed.2007.09.002
52. Togbe D, Schnyder-Candrian S, Schnyder B, Doz E, Noulin N, Janot L, et al. Toll-Like Receptor and Tumour Necrosis Factor Dependent Endotoxin-Induced Acute Lung Injury. *Int J Exp Pathol* (2007) 88(6):387–91. doi: 10.1111/j.1365-2613.2007.00566.x
53. Gupta KK, Xu Z, Castellino FJ, Ploplis VA. Plasminogen Activator Inhibitor-1 Stimulates Macrophage Activation Through Toll-Like Receptor-4. *Biochem Biophys Res Commun* (2016) 477(3):503–8. doi: 10.1016/j.bbrc.2016.06.065
54. Kubala MH, Punj V, Placencio-Hickok VR, Fang H, Fernandez GE, Sposto R, et al. Plasminogen Activator Inhibitor-1 Promotes the Recruitment and Polarization of Macrophages in Cancer. *Cell Rep* (2018) 25(8):2177–91.e2177. doi: 10.1016/j.celrep.2018.10.082
55. Lu Z, Li Y, Jin J, Zhang X, Lopes-Virella MF, Huang Y. Toll-Like Receptor 4 Activation in Microvascular Endothelial Cells Triggers a Robust Inflammatory Response and Cross Talk With Mononuclear Cells *via* Interleukin-6. *Arterioscler Thromb Vasc Biol* (2012) 32(7):1696–706. doi: 10.1161/ATVBAHA.112.251181
56. Obi AT, Andraska E, Kanthi Y, Kessinger CW, Elfline M, Luke C, et al. Endotoxaemia-Augmented Murine Venous Thrombosis Is Dependent on TLR-4 and ICAM-1, and Potentiated by Neutropenia. *Thromb Haemost* (2017) 117(2):339–48. doi: 10.1160/TH16-03-0218
57. Dasu MR, Devaraj S, Du Clos TW, Jialal I. The Biological Effects of CRP Are Not Attributable to Endotoxin Contamination: Evidence From TLR4 Knockdown Human Aortic Endothelial Cells. *J Lipid Res* (2007) 48(3):509–12. doi: 10.1194/jlr.C600020-JLR200
58. Han M, Pandey D. ZMPSTE24 Regulates SARS-CoV-2 Spike Protein-Enhanced Expression of Endothelial PAI-1. *Am J Respir Cell Mol Biol* (2021) 65(3):300–8. doi: 10.1165/rcmb.2020-0544OC
59. Tang N, Li D, Wang X, Sun Z. Abnormal Coagulation Parameters are Associated With Poor Prognosis in Patients With Novel Coronavirus Pneumonia. *J Thromb Haemost* (2020) 18(4):844–7. doi: 10.1111/jth.14768
60. Chen N, Zhou M, Dong X, Qu J, Gong F, Han Y, et al. Epidemiological and Clinical Characteristics of 99 Cases of 2019 Novel Coronavirus Pneumonia in Wuhan, China: A Descriptive Study. *Lancet* (2020) 395(10223):507–13. doi: 10.1016/S0140-6736(20)30211-7
61. Huang C, Wang Y, Li X, Ren L, Zhao J, Hu Y, et al. Clinical Features of Patients Infected With 2019 Novel Coronavirus in Wuhan, China. *Lancet* (2020) 395(10223):497–506. doi: 10.1016/S0140-6736(20)30183-5
62. Fogarty H, Townsend L, Ni Cheallaigh C, Bergin C, Martin-Loeches I, Browne P, et al. More on COVID-19 Coagulopathy in Caucasian Patients. *Br J Haematol* (2020) 189(6):1060–1. doi: 10.1111/bjh.16791
63. Klok FA, Kruip M, van der Meer NJM, Arbous MS, Gommers D, Kant KM, et al. Incidence of Thrombotic Complications in Critically Ill ICU Patients With COVID-19. *Thromb Res* (2020) 191:145–7. doi: 10.1016/j.thromres.2020.04.013
64. Lax SF, Skok K, Zechner P, Kessler HH, Kaufmann N, Koelblinger C, et al. Pulmonary Arterial Thrombosis in COVID-19 With Fatal Outcome : Results From a Prospective, Single-Center, Clinicopathologic Case Series. *Ann Intern Med* (2020) 173(5):350–61. doi: 10.7326/M20-2566
65. Ordieres-Ortega L, Demelo-Rodriguez P, Galeano-Valle F, Kremers BMM, Ten Cate-Hoek AJ, Ten Cate H. Predictive Value of D-Dimer Testing for the Diagnosis of Venous Thrombosis in Unusual Locations: A Systematic Review. *Thromb Res* (2020) 189:5–12. doi: 10.1016/j.thromres.2020.02.009
66. Lippi G, Plebani M, Henry BM. Thrombocytopenia is Associated With Severe Coronavirus Disease 2019 (COVID-19) Infections: A Meta-Analysis. *Clin Chim Acta* (2020) 506:145–8. doi: 10.1016/j.cca.2020.03.022
67. Gorham J, Moreau A, Corazza F, Peluso L, Ponthieux F, Talamonti M, et al. Interleukine-6 in Critically Ill COVID-19 Patients: A Retrospective Analysis. *PLos One* (2020) 15(12):e0244628. doi: 10.1371/journal.pone.0244628
68. Jones SA, Scheller J, Rose-John S. Therapeutic Strategies for the Clinical Blockade of IL-6/Gp130 Signaling. *J Clin Invest* (2011) 121(9):3375–83. doi: 10.1172/JCI57158
69. Tanaka Y, Martin Mola E. IL-6 Targeting Compared to TNF Targeting in Rheumatoid Arthritis: Studies of Olokizumab, Sarilumab and Sirukumab. *Ann Rheum Dis* (2014) 73(9):1595–7. doi: 10.1136/annrheumdis-2013-205002
70. Rose-John S, Heinrich PC. Soluble Receptors for Cytokines and Growth Factors: Generation and Biological Function. *Biochem J* (1994) 300(Pt 2):281–90. doi: 10.1042/bj3000281
71. Peters M, Jacobs S, Ehlers M, Vollmer P, Mullberg J, Wolf E, et al. The Function of the Soluble Interleukin 6 (IL-6) Receptor *In Vivo*: Sensitization of Human Soluble IL-6 Receptor Transgenic Mice Towards IL-6 and Prolongation of the Plasma Half-Life of IL-6. *J Exp Med* (1996) 183 (4):1399–406. doi: 10.1084/jem.183.4.1399
72. Schobitz B, Pezeshki G, Pohl T, Hemmann U, Heinrich PC, Holsboer F, et al. Soluble Interleukin-6 (IL-6) Receptor Augments Central Effects of IL-6 *In Vivo*. *FASEB J* (1995) 9(8):659–64. doi: 10.1096/fasebj.9.8.7768358
73. Yoshida K, Taga T, Saito M, Suematsu S, Kumanogoh A, Tanaka T, et al. Targeted Disruption of Gp130, a Common Signal Transducer for the Interleukin 6 Family of Cytokines, Leads to Myocardial and Hematological Disorders. *Proc Natl Acad Sci USA* (1996) 93(1):407–11. doi: 10.1073/pnas.93.1.407
74. Kopf M, Baumann H, Freer G, Freudenberg M, Lamers M, Kishimoto T, et al. Impaired Immune and Acute-Phase Responses in Interleukin-6-Deficient Mice. *Nature* (1994) 368(6469):339–42. doi: 10.1038/368339a0
75. Jones GW, McLoughlin RM, Hammond VJ, Parker CR, Williams JD, Malhotra R, et al. Loss of CD4+ T Cell IL-6R Expression During Inflammation Underlines a Role for IL-6 Trans Signaling in the Local Maintenance of Th17 Cells. *J Immunol* (2010) 184(4):2130–9. doi: 10.4049/jimmunol.0901528
76. McElvaney OJ, Curley GF, Rose-John S, McElvaney NG. Interleukin-6: Obstacles to Targeting a Complex Cytokine in Critical Illness. *Lancet Respir Med* (2021) 9(6):643–54. doi: 10.1016/S2213-2600(21)00103-X

77. Wu Y, Wang Y, Liu B, Cheng Y, Qian H, Yang H, et al. SN50 Attenuates Alveolar Hypercoagulation and Fibrinolysis Inhibition in Acute Respiratory Distress Syndrome Mice Through Inhibiting NF-kappaB P65 Translocation. *Respir Res* (2020) 21(1):130. doi: 10.1186/s12931-020-01372-6
78. Katz JM, Tadi P. *Physiology, Plasminogen Activation*. Treasure Island (FL: StatPearls (2021).
79. Li W, Sun L, Lei J, Wu Z, Ma Q, Wang Z. Curcumin Inhibits Pancreatic Cancer Cell Invasion and EMT by Interfering With Tumorstromal Crosstalk Under Hypoxic Conditions *via* the IL6/ERK/NFkappaB Axis. *Oncol Rep* (2020) 44(1):382–92. doi: 10.3892/or.2020.7600
80. Dong J, Fujii S, Imagawa S, Matsumoto S, Matsushita M, Todo S, et al. IL-1 and IL-6 Induce Hepatocyte Plasminogen Activator Inhibitor-1 Expression Through Independent Signaling Pathways Converging on C/EBPdelta. *Am J Physiol Cell Physiol* (2007) 292(1):C209–215. doi: 10.1152/ajpcell.00157.2006
81. Rokavec M, Oner MG, Li H, Jackstadt R, Jiang L, Lodygin D, et al. IL-6r/STAT3/miR-34a Feedback Loop Promotes EMT-Mediated Colorectal Cancer Invasion and Metastasis. *J Clin Invest* (2014) 124(4):1853–67. doi: 10.1172/JCI73531
82. Cigolini M, et al. Expression of Plasminogen Activator Inhibitor-1 in Human Adipose Tissue: A Role for TNF-Alpha?. *Atherosclerosis* (1999) 143(1):81–90. doi: 10.1016/s0021-9150(98)00281-0
83. Alves JD, Marinho A, Serra MJ. Tocilizumab: Is There Life Beyond Anti-TNF Blockade? *Int J Clin Pract* (2011) 65(4):508–13. doi: 10.1111/j.1742-1241.2010.02612.x
84. Kaly L, Rosner I. Tocilizumab - A Novel Therapy for non-Organ-Specific Autoimmune Diseases. *Best Pract Res Clin Rheumatol* (2012) 26(1):157–65. doi: 10.1016/j.berh.2012.01.001
85. Yokota S, Miyamae T, Imagawa T, Iwata N, Katakura S, Mori M, et al. Therapeutic Efficacy of Humanized Recombinant Anti-Interleukin-6 Receptor Antibody in Children With Systemic-Onset Juvenile Idiopathic Arthritis. *Arthritis Rheum* (2005) 52(3):818–25. doi: 10.1002/art.20944
86. Le RQ, Li L, Yuan W, Shord SS, Nie L, Habtemariam BA, et al. FDA Approval Summary: Tocilizumab for Treatment of Chimeric Antigen Receptor T Cell-Induced Severe or Life-Threatening Cytokine Release Syndrome. *Oncologist* (2018) 23(8):943–7. doi: 10.1634/theoncologist.2018-0028
87. Magro G. SARS-CoV-2 and COVID-19: Is Interleukin-6 (IL-6) the 'Culprit Lesion' of ARDS Onset? What is There Besides Tocilizumab? SGP130Fc. *Cytokine X* (2020) 2(2):100029. doi: 10.1016/j.cytox.2020.100029
88. Luo P, Liu Y, Qiu L, Liu X, Liu D, Li J. Tocilizumab Treatment in COVID-19: A Single Center Experience. *J Med Virol* (2020) 92(7):814–8. doi: 10.1002/jmv.25801
89. Stone JH, Frigault MJ, Serling-Boyd NJ, Fernandes AD, Harvey L, Foulkes AS, et al. Efficacy of Tocilizumab in Patients Hospitalized With Covid-19. *N Engl J Med* (2020) 383(24):2333–44. doi: 10.1056/NEJMoa2028836
90. Xu X, Han M, Li T, Sun W, Wang D, Fu B, et al. Effective Treatment of Severe COVID-19 Patients With Tocilizumab. *Proc Natl Acad Sci USA* (2020) 117 (20):10970–5. doi: 10.1073/pnas.2005615117
91. Toniati P, Piva S, Cattalini M, Garrafa E, Regola F, Castelli F, et al. Tocilizumab for the Treatment of Severe COVID-19 Pneumonia With Hyperinflammatory Syndrome and Acute Respiratory Failure: A Single Center Study of 100 Patients in Brescia, Italy. *Autoimmun Rev* (2020) 19 (7):102568. doi: 10.1016/j.autrev.2020.102568
92. Ghosh AK, Soberanes S, Lux E, Shang M, Aillon RP, Eren M, et al. Pharmacological Inhibition of PAI-1 Alleviates Cardiopulmonary Pathologies Induced by Exposure to Air Pollutants PM2.5. *Environ Pollut* (2021) 287:117283. doi: 10.1016/j.envpol.2021.117283
93. Ackermann M, Verleden SE, Kuehnel M, Haverich A, Welte T, Laenger F, et al. Pulmonary Vascular Endothelialitis, Thrombosis, and Angiogenesis in Covid-19. *N Engl J Med* (2020) 383(2):120–8. doi: 10.1056/NEJMoa2015432
94. Gao YD, Ding M, Dong X, Zhang JJ, Kursat Azkur A, Azkur D, et al. Risk Factors for Severe and Critically Ill COVID-19 Patients: A Review. *Allergy* (2021) 76(2):428–55. doi: 10.1111/all.14657
95. Chan NC, Weitz JI. COVID-19 Coagulopathy, Thrombosis, and Bleeding. *Blood* (2020) 136(4):381–3. doi: 10.1182/blood.2020007335
96. Topol EJ. COVID-19 can Affect the Heart. *Science* (2020) 370(6515):408–9. doi: 10.1126/science.abe2813
97. Moore JB, June CH. Cytokine Release Syndrome in Severe COVID-19. *Science* (2020) 368(6490):473–4. doi: 10.1126/science.abb8925
98. Matsuyama T, Kubli SP, Yoshinaga SK, Pfeffer K, Mak TW. An Aberrant STAT Pathway Is Central to COVID-19. *Cell Death Differ* (2020) 27 (12):3209–25. doi: 10.1038/s41418-020-00633-7
99. Wang L, Astone M, Alam SK, Zhu Z, Pei W, Frank DA, et al. Suppressing STAT3 Activity Protects the Endothelial Barrier From VEGF-Mediated Vascular Permeability. *bioRxiv* (2020) 14(11):dmm049029. doi: 10.1101/2020.10.27.358374
100. Barbosa LC, Goncalves TL, de Araujo LP, Rosario LVO, Ferrer VP. Endothelial Cells and SARS-CoV-2: An Intimate Relationship. *Vascul Pharmacol* (2021) 137:106829. doi: 10.1016/j.vph.2021.106829

Conflict of Interest: The authors declare that the research was conducted in the absence of any commercial or financial relationships that could be construed as a potential conflict of interest.

frontiers | Frontiers in Immunology

ORIGINAL RESEARCH
published: 12 July 2022
doi: 10.3389/fimmu.2022.954121

Proteomic and Metabolomic Characterization of SARS-CoV-2-Infected Cynomolgus Macaque at Early Stage

Tiecheng Wang[1,2†], Faming Miao[1,2†], Shengnan Lv[3†], Liang Li[1,2], Feng Wei[3], Lihua Hou[4], Renren Sun[5], Wei Li[6], Jian Zhang[3], Cheng Zhang[1], Guang Yang[1], Haiyang Xiang[1], Keyin Meng[1], Zhonghai Wan[1], Busen Wang[4], Guodong Feng[7], Zhongpeng Zhao[8], Deyan Luo[8], Nan Li[1], Changchun Tu[1,2], Hui Wang[8], Xiaochang Xue[9*], Yan Liu[1,2*] and Yuwei Gao[1,2*]*

[1] Key Laboratory of Jilin Province for Zoonosis Prevention and Control, Changchun Veterinary Research Institute, Chinese Academy of Agricultural Sciences, Changchun, China, [2] Jiangsu Co-innovation Center for Prevention and Control of Important Animal Infectious Disease and Zoonoses, Yangzhou, China, [3] Department of Hepatobiliary and Pancreas Surgery, Jilin University First Hospital, Changchun, China, [4] Vaccine and Antibody Engineering Laboratory, Beijing Institute of Biotechnology, Beijing, China, [5] Key Laboratory of Organ Regeneration & Transplantation of Ministry of Education, and National-Local Joint Engineering Laboratory of Animal Models for Human Diseases, The First Hospital of Jilin University, Changchun, China, [6] The Key Laboratory of Pathobiology, Ministry of Education, College of Basic Medical Sciences, Jilin University, Changchun, China, [7] Department of Neurology, Zhongshan Hospital Fudan University, Shanghai, China, [8] State Key Laboratory of Pathogen and Biosecurity, Beijing Institute of Microbiology and Epidemiology, Beijing, China, [9] National Engineering Laboratory for Resource Development of Endangered Crude Drugs in Northwest China, The Key Laboratory of Medicinal Resources and Natural Pharmaceutical Chemistry, The Ministry of Education, College of Life Sciences, Shaanxi Normal University, Xi'an, China

Although tremendous effort has been exerted to elucidate the pathogenesis of severe COVID-19 cases, the detailed mechanism of moderate cases, which accounts for 90% of all patients, remains unclear yet, partly limited by lacking the biopsy tissues. Here, we established the COVID-19 infection model in cynomolgus macaques (CMs), monitored the clinical and pathological features, and analyzed underlying pathogenic mechanisms at early infection stage by performing proteomic and metabolomic profiling of lung tissues and sera samples from COVID-19 CMs models. Our data demonstrated that innate immune response, neutrophile and platelet activation were mainly dysregulated in COVID-19 CMs. The symptom of neutrophilia, lymphopenia and massive "cytokines storm", main features of severe COVID-19 patients, were greatly weakened in most of the challenged CMs, which are more semblable as moderate patients. Thus, COVID-19 model in CMs is rational to understand the pathogenesis of moderate COVID-19 and may be a candidate model to assess the safety and efficacy of therapeutics and vaccines against SARS-CoV-2 infection.

Keywords: SARS-CoV-2 infection, immune response, cynomolgus macaque, the early stage, proteomics, metabolomics

OPEN ACCESS

Edited by:
Linzhu Ren,
Jilin University, China

Reviewed by:
Ma Mingxiao,
Jinzhou Medical University, China
Shuqi Xiao,
Northwest A&F University, China

****Correspondence:***
Yuwei Gao
yuwei0901@outlook.com
Yan Liu
liu820512@163.com
Xiaochang Xue
xuexch@snnu.edu.cn
Hui Wang
geno0109@vip.sina.com

[†]These authors have contributed equally to this work

Specialty section:
This article was submitted to Molecular Innate Immunity, a section of the journal Frontiers in Immunology

Received: *27 May 2022*
Accepted: *15 June 2022*
Published: *12 July 2022*

Citation:
Wang T, Miao F, Lv S, Li L, Wei F, Hou L, Sun R, Li W, Zhang J, Zhang C, Yang G, Xiang H, Meng K, Wan Z, Wang B, Feng G, Zhao Z, Luo D, Li N, Tu C, Wang H, Xue X, Liu Y and Gao Y (2022) Proteomic and Metabolomic Characterization of SARS-CoV-2-Infected Cynomolgus Macaque at Early Stage. Front. Immunol. 13:954121. doi: 10.3389/fimmu.2022.954121

INTRODUCTION

Coronavirus disease 2019 (COVID-2019), caused by severe acute respiratory syndrome coronavirus 2 (SARS-CoV-2), has spread around the world rapidly, infected over 523 million individuals worldwide, and led to over 6.280 million deaths by June 25, 2022 (https://covid19.who.int). Unfortunately, both numbers are still increasing.

SARS-CoV-2 infection leads to COVID-19 with various severity, ranging from asymptomatic to symptomatic patients, and the latter is usually further classified as severe and moderate cases. Special attention has been given to severe COVID-19 cases who present with high fever and dry cough, pneumonia, uncontrolled inflammatory responses, and are at higher risk of death. Emerging studies have greatly unclosed the clinical and immunological characteristics, epidemiology, and pathology of severe COVID-19 patients (1, 2). For example, an epidemiological study by Ragonnet-Cronin Min et al. showed that early intervention means much lower morbidity and mortality rate of severe COVID-19 (3). Rébillard RM et al. reported that general neutropenia and lymphopenia are not specific predictors of COVID-19, while higher proportions of $ALCAM^+$ monocytes, $ICAM\text{-}1^+$ neutrophils, and $CD38^+$ $CD8^+$ T cells are often associated with higher mortality (4). Guo and colleagues performed proteomic and metabolomics profiling of sera from non-severe and severe COVID-19 patients, revealed characteristic protein and metabolite changes in severe patients (5). However, considering moderate cases account for 90% of COVID-19 patients, and timely and efficient treatment of them means better prognosis and is beneficial to alleviate the burden on medical resources, there is an urgent need to identify the underlying pathological mechanisms and effective prevention strategies for moderate cases.

Establishment of animal models is undoubtedly necessary and a great help for understanding the pathogenesis of COVID-19 (6), evaluating potential vaccines and antiviral agents against SARS-CoV-2 infection before they are used clinically (7, 8). Non-human primate models have been extensively used to investigate pathogenesis of a wide spectrum of viral diseases (9). Previous studies have reported the pathogenesis of COVID-19 in non-human primate models and compared it with MERS and SARS. The data showed that low passage clinical isolate of SARS-CoV-2 caused COVID-19-like disease in both young and aged cynomolgus macaques (CMs), with shedding virus for a prolonged period, although in the absence of overt clinical signs (10). Several groups have used rhesus macaques to simulate SARS-CoV-2 infection and pathogenesis, which usually recapitulates mild to moderate infection in humans (11, 12). These non-human primate COVID-19 models can also be effectively used to evaluate vaccines and drugs for COVID-19 therapy (12–15). Unfortunately, only rare studies performed proteomics and metabolomics analysis in non-human primate models to elucidate the mechanistic details that drive SARS-CoV-2 pathogenesis in humans (11, 16). Additionally, timely and accurate diagnosis of SARS-CoV-2 RNA makes it necessary to study the pathological characteristics of patients with very early infection (14). Thus, in this study, we established COVID-19 model in CMs and performed proteomics and metabolomics to reveal the molecular signature for COVID-19 pathogenesis at very early stages of SARS-CoV-2 infection (7 days post infection).

MATERIALS AND METHODS

Animals and Experimental Procedures

The CMs used in this study were bred and provided by the Laboratory Animal Center, Academy of Military Medical Sciences (Beijing). All animals were confirmed to be specific pathogens (especially SARS-CoV-2) free before the experiment. To establish the model of COVID-19, CMs were anesthetized with Zoletil 50 and inoculated with a dose of 4.7×10^6 $TCID_{50}$/mL SARS-CoV-2 *via* a combined intranasal (0.25 mL per nasal), intratracheal (4.0 mL), and ocular conjunctival routes (0.1 mL per eye). The control CMs were inoculated with an equivalent dose of DMEM. On 2, 4 and 6 days after infection, the nasal, throat, and anal swabs were collected and incubated in 1 mL of PBS containing 1000 μg/mL streptomycin and 1000 U/mL penicillin. The body weight and temperature were measured every other day. The UCT-2112 temperature probes (American Health & Medical Supply International Corp., USA), which were injected interscapularly into the CMs before the experiment, were used to monitor the body temperature. On day 7 post infection, all animals were euthanized and tissues including nasal turbinate, trachea, different lobes of lung, heart, spleen, kidney, colon, brain, liver, and testes were collected to detect the viral loads. All the experiments were done in Animal Biosafety Level 3 (ABSL3) at the Key Laboratory of Jilin Province for Zoonosis Prevention and Control, Institute of Military Veterinary Medicine, according to the protocols approved by the Administrative Committee on Animal Welfare of the Institute of Military Veterinary.

RNA Extraction and qRT-PCR

Total RNA was isolated from 200 μL of samples by using Magnetic Viral DNA/RNA Kit (Tiangen Biotech, Beijing, China). After synthesizing cDNA with reverse transcriptase (Invitrogen, Carlsbad, CA, USA), qPCR was conducted by Bio-Rad CFX96 Real-time PCR system (Bio-Rad, Hercules, CA) following cycling protocol: 50°C for 20 min, followed by 95°C for 3 min and then by 45 cycles of 95°C for 5 s, and 57°C for 45 s. The ORF1ab gene-specific primers (forward, 5'-CCCTGTGGG TTT TACACTTAA-3'; reverse, 5'-ACGATTGTGCATCAGCT GA-3') and probe 5'-FAM-CCGTCTGC GGTATGTGGAAA GGTTATGG-BHQ1-3'. The N gene-specific primers (forward, 5'-GGGGAAC TTCTCCTGCTAGAAT-3'; reverse, 5'-CAGAC ATTTTGCTCTCAAGCTG-3') and probe 5'-FAM-TTGCTGC TGCTTGACAGATT-TAMRA-3' were used according to the information provided by the National Institute for Viral Disease Control and Prevention, China. The gene-specific primers (sgLead-forward: 5'-CGATCTCTTGTAGATCTGTTC TC-3'; reverse: 5'-ATATTGCAGCAGTAC GCACACA-3') and probe 5'-FAM-ACACTAGCCATCCTTACTGCGCTTCG-BHQ1-3' were used for E gene subgenomic mRNA quantitation.

Luminex Assay of Inflammatory Cytokines and Chemokines in Macaque Serum

Peripheral blood samples and sera were collected from all Macaques, the levels of 30 cytokines and chemokines like interleukin (IL)-2, IL-6, IL-8, IL-10, IL12, IL-17, IL-23, MCP-1, IP-10 (CXCL10), MIG, MIP-1β (CCL4), CD40, and SDF-1α etc. were determined by Luminex multi-factor detection platform (eBioscience ProcartaPlex, Thermo Fisher Scientific, Waltham, MA, USA) according to the manufacturer's protocol.

Flow Cytometry and Blood Routine Analysis

Samples of EDTA anticoagulated peripheral blood (6 mL) were collected from control or SARS-CoV-2–infected CMs. Then, diverse cell populations were measured by flow cytometry according to the manufacturer's instructions with the following monoclonal antibodies: anti-CD3-PE-Cy7 (BD Biosciences, 557917), anti-CD4-APC (Biolegend, 317415), anti-CD8-PE (Biolegend, 301008), anti-CD20-PE (Biolegend, 302306), anti-CD16-PE (Biolegend, 302007), and anti-CD56-APC (Biolegend, 318309). Samples were analyzed on a BD FACS Canto II flow cytometry system (BD Biosciences). For blood routine analysis, anticoagulant venous blood collected at indicated time points were subjected to five classification hematologic analyzer (Mindray, China).

Histological Evaluation

For histopathologic examination, tissue samples including lung, trachea, salivary gland, heart, liver, kidney, and brain, were 4%-paraformaldehyde-fixed, paraffin-embedded, sectioned at 5 μm, and subjected to hematoxylin and eosin (H&E) and immunohistochemical (IHC) staining. For IHC staining, the primary antibodies used in the experiments including anti-CD4, CD8, CD14, CD16, CD20, CD64, and Myeloperoxidase (MPO) were all purchased from Abcam. Images of H&E and IHC stained slides were captured with an Olympus BX43 microscope (Olympus).

Proteome Analysis

A 4D-Label free quantitative proteomics analysis was performed using tandem MS/MS in Q Exactive™ Plus coupled online to an EASY-nLC 1000 UPLC system (Thermo) in JingJie Sciences Company (Hangzhou, China). Total proteins were extracted from the frozen lung samples by adding 4 times the volume of 10% TCA/acetone at -20°C and precipitating for more than 4 h. After centrifugation at 4500 g for 5 min, the precipitate was collected and washed 2-3 times with pre-cooled acetone. Then, the pellet from each specimen was reconstituted with lysis buffer (8 M urea, 3 μM TSA, 50 mM NAM, 1% protease inhibitor), and the protein concentration was determined by BCA kit. Equal amount of each protein sample was then enzymatically lysed and adjusted the volume to the same with the lysate. Then, samples were reduced by 5 mM dithiothreitol (DTT) at 56°C for 30 min and alkylated by 11 mM iodoacetamide (IAA) at room temperature for 15 min in the dark, respectively. The alkylated sample was then transferred to an ultrafiltration tube and centrifuged at 12000 g at room temperature for 20 min, followed by replacement with 8 M urea and replacement buffer for 3 times. After that, protein samples were digested by incubation with trypsin at a ratio of 1:50 (protease: protein, m/m) for overnight. Finally, the fragmented peptides were recovered by centrifugation at 12000 g for 10 min at room temperature, and the peptides were recovered with ultrapure water once, and the two peptide solutions were combined. For LC-MS/MS analysis, the tryptic peptides were dissolved in solvent A (0.1% formic acid (FA), 2% acetonitrile in water) and loaded onto a home-made reversed-phase analytical column (25-cm length, 100 μm i.d.). The peptides were separated by eluting the column with a gradient from 6% to 24% solvent B (0.1% FA in 98% acetonitrile) over 70 min, 24% to 35% in 14 min and reached up to 80% in 3 min, then keeping at 80% for 3 min, all at a constant flow rate of 450 nL/min on a nanoElute UHPLC system (Bruker Daltonics). The peptides were then subjected to capillary source followed by the timsTOF Pro MS (Bruker Daltonics). The timsTOF Pro was operated in a parallel accumulation serial fragmentation (PASEF) mode with the electrospray voltage 2.0 kV. Precursors and fragments were analyzed at the TOF detector, and the MS/MS scan ranged from 100 to 1700 m/z. Precursors with charge states 0 to 5 were selected for fragmentation, and 10 PASEF-MS/MS scans were acquired per cycle. The dynamic exclusion was set to 30 s. For database search, The MS/MS data were processed by MaxQuant search engine (v.1.6.6.0). Tandem mass spectra were searched against the *Macaca_mulatta*_9544 database (45179 entries) concatenated with reverse decoy database. Trypsin/P was specified as cleavage enzyme allowing up to 2 missing cleavages. The mass error tolerance for precursor ions was set to 20 ppm in both First search and Main search, and fragment ions mass error tolerance was also set to 20 ppm. Carbamidomethyl on Cys was specified as fixed modification, and acetylation on protein N-terminal and oxidation on Met were specified as variable modifications. The false discovery rate (FDR) (strict) was adjusted to < 1%.

Metabolome Analysis

Plasma/serum samples were thawed on ice, and 3 volumes of ice-cold methanol was added. Samples were agitated for 3 min and centrifuged at 12,000 rpm and 4°C for 10 min. Then the supernatant was collected and centrifuged at 12,000 rpm and 4°C for 5 min. The final supernatant was collected for LC-MS/MS analysis using an LC-ESI-MS/MS system (UPLC, Shim-pack UFLC SHIMADZU CBM A system, https://www.shimadzu.com/; MS, QTRAP® System, https://sciex.com/) in JingJie PTM BioLab Co. Ltd. (Hangzhou, China). The analytical conditions were as follows, UPLC: column, Waters ACQUITY UPLC HSS T3 C18 (1.8 μm, 2.1 mm × 100 mm); column temperature, 40°C; flow rate, 0.4 mL/min; injection volume, 2 μL; solvent system, water (0.1% FA): acetonitrile (0.1% FA); gradient program, 95:5 V/V at 0 min, 10:90 V/V at 11.0 min, 10:90 V/V at 12.0 min, 95:5 V/V at 12.1 min, 95:5 V/V at 14.0 min. Finally, samples were analyzed with ESI-QTRAP-MS/MS. LIT and triple quadrupole (QQQ) scans were acquired on a triple quadrupole-linear ion trap mass spectrometer (QTRAP), QTRAP® LC-MS/MS System, equipped with an ESI Turbo Ion-Spray interface, operating in positive and

negative ion mode, and controlled by Analyst 1.6.3 software (Sciex). The ESI source operation parameters were set as follows: source temperature 500°C; ion spray voltage 5500 V (positive), -4500 V (negative); ion source gas I, gas II, and curtain gas were set at 55, 60, and 25 psi, respectively; the collision gas was high. Instrument tuning and mass calibration were carried out with 10 and 100 μM polypropylene glycol solutions in QQQ and LIT modes. A specific set of MRM transitions was monitored for each period according to the metabolites eluted within this period. For combined omics analysis, we extracted the proteins and metabolites with differential expression and performed pair-wise correlation network analysis to identify co-regulated nodes. Each node in blue circle represented a protein and the box nodes of different colors represented different kinds of metabolites. We calculated the Spearman's correlation coefficient(ρ) between each protein and metabolite based on their abundance levels and then we showed the nodes between which the absolute value of ρ is greater than 0.6.

Statistical Analysis

All data were analyzed with GraphPad Prism 8.0 software. For any test, a P value of < 0.05 was considered to be significant. Statistical significance is shown as $^{*}P < 0.05$, and $^{**}P < 0.01$ compared between indicated groups.

RESULTS

Establishment and Identification of COVID-19 Model in CMs

We inoculated 12 adult CMs (11–17 years old, mean = 14 years) and 2 young CMs (1–3 years old, mean = 2 years) with a dose of 4.7×10^6 $TCID_{50}$/mL SARS-CoV-2 (BetaCoV/Beijing/IME-BJ05/2020) (17), administered by intranasal (IN, 0.25 mL per nasal), intratracheal (IT, 4.0 mL), and conjunctival (CJ, 0.1 mL per eye) routes (18, 19). The detailed information of infection and detection time was demonstrated in **Figures 1A, B**. The body temperature was monitored every other day after SARS-CoV-2 challenge from 0 to 7 days. As shown in **Figure 2A**, an increased body temperature of 0.75°C was observed in 10 out of 14, whereas a decrease of 0.5°C was observed in 3 out of 14 SARS-CoV-2-infected CMs. To determine the infection kinetics, viral load and shedding in swabs and tissues were detected by qRT-PCR at indicated time points. We found that the levels of viral genomic RNA in nasal swab samples from all CMs reached peak at 2 dpi (median: 5.4×10^{11} copies/μL), then 8 of 14 decreased and 6 remained high levels. The peak values were observed in throat swabs at 2 dpi, the values were lower than those in nasal swabs, which decreased to 2.45×10^6 copies/μL (median value) at 6 dpi. Meanwhile, the viral RNA levels in anal swab samples were lower than that in nasal and throat swabs (**Figure 2B**).

Moreover, we evaluated the SARS-CoV-2 viral RNA copies in various tissues of the infected CMs at 7 days after infection. As shown in **Figure 2C**, viral RNA could be detected in 15 of 20 tissues with highest level found in the nasal turbinate, trachea and lung, but much lower viral RNA copies were measured in brain, heart, liver, spleen, kidney, testes, parotid gland, adrenal gland, prostate gland, pulmonary lymph node and tonsil. Moreover, a relatively high level of viral copies could be detected in colon in 7/14 infected CMs.

To verify the active virus replication, the viral E gene subgenomic mRNA were further examined (20). As indicated in **Figure 2D**, except kidney, the viral could replicate in several

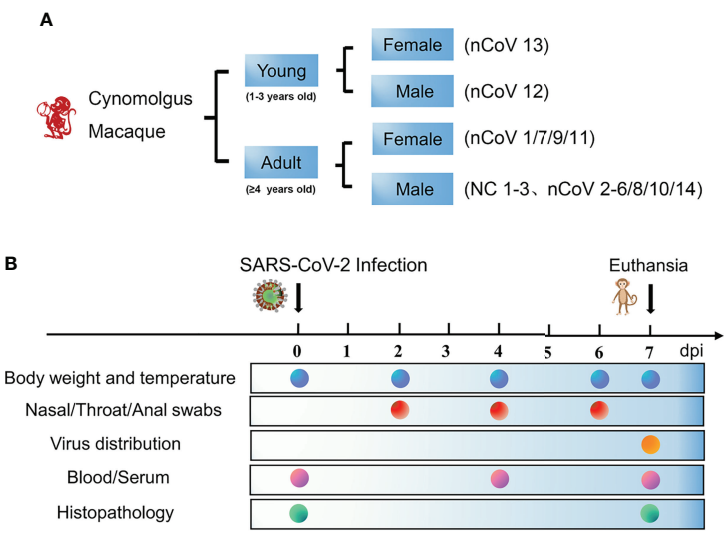

FIGURE 1 | Schematic of the study design and clinical signs of SARS-CoV-2 infection in CMs. **(A)** Two age groups of monkeys (14 in total) were selected for this study to assess their ability to establish COVID-19 model. The monkeys were randomly assigned into two groups, the detail of age and sex were demonstrated. **(B)** The body weight and temperature, swabs, tissues and blood were collected at the indicated time points for evaluation of clinical symptoms, viral shedding and replication, and host responses to SARS-CoV-2. CMs, cynomolgus macaque; NC, negative control; nCoV, SARS-CoV-2.

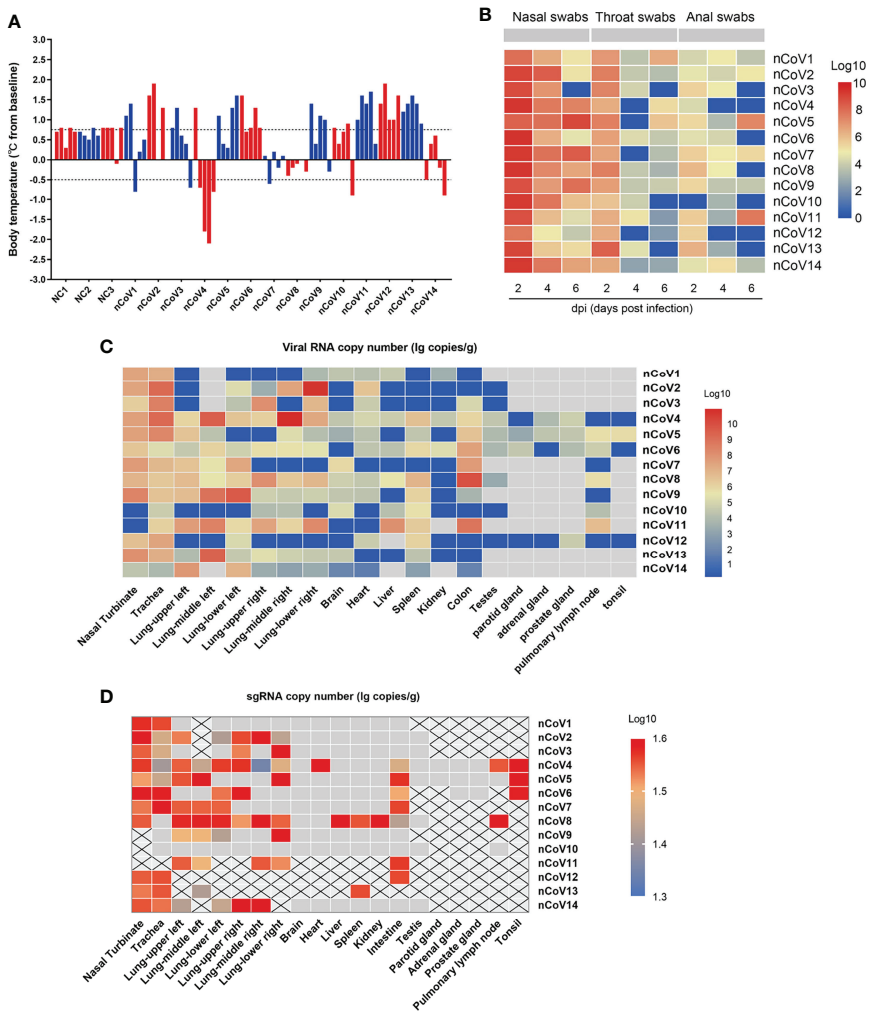

FIGURE 2 | Body temperature, viral shedding and replication in CMs inoculated with SARS-CoV-2. **(A)** The body temperature of each monkey was monitored and recorded at above indicated time points after SARS-CoV-2 inoculation (0, 2, 4, 6, 7dpi). The body temperature changes were calculated by subtracting the baseline (37°C) from each. **(B)** Every two days after virus inoculation, swabs (nasal, throat, and anal) were collected from the monkeys for quantification of virus genomic RNA *via* qRT-PCR. **(C)** Tissue samples were harvested from necropsied animals at 7 dpi for detection of viral load by qRT-PCR. The viral copies were indicated as a $\log_{10}$ value, and the heatmap was prepared *via* heatmap illustrator in TB tools. **(D)** E gene subgenomic viral RNA transcripts were examined by qRT-PCR. qRT-PCR, real-time quantitative-polymerase chain reaction; sgRNA, subgenomic viral RNA.

tissues including nasal turbinate, trachea, lung, spleen, colon, prostate, pulmonary lymph node and tonsil, although with the limited replication efficacy. These results confirmed that SARS-CoV-2 could replicate in multiple tissues of CMs besides the respiratory route, the fecal–oral route may be involved in viral transmission (21, 22), which supported that establishment of COVID-19 in CMs is an ideal model for SARS-CoV-2–associated study.

Clinical Features of COVID-19 in CMs

Several infection markers like alanine aminotransferase (ALT), aminotransferase (AST), lactate dehydrogenase (LDH), high-sensitivity C-reactive protein (CRP), and ferritin were measured to evaluate the severity of COVID-19 in CMs. Results demonstrated that ALT, CRP, and ferritin values were distributed in normal range in almost all the infected CMs, which are similar as those observed in moderate COVID-19 patients (23, 24), but are apparently different from severe ones, in which all these indicators increased significantly (5). As to AST and LDH, significant decreases were found in about 57.1% (4/7) of infected CMs at 7 dpi when compared with control CMs. (**Figure 3A**).

We then isolated peripheral blood mononuclear cell (PBMC) from CMs blood and analyzed the changes of white blood cell count (WBC), lymphocyte count (LYC), monocyte count, absolute neutrophils count (ANC), platelet count (PLT), and hemoglobin (HGB). As shown in **Figure 3B**, WBC decreased slightly from 11.11 to 8.94 × 10^9/L upon SARS-CoV-2 infection. LYC remains unchanged (about 3.74 × 10^9/L) in infected CMs at 7 dpi, which

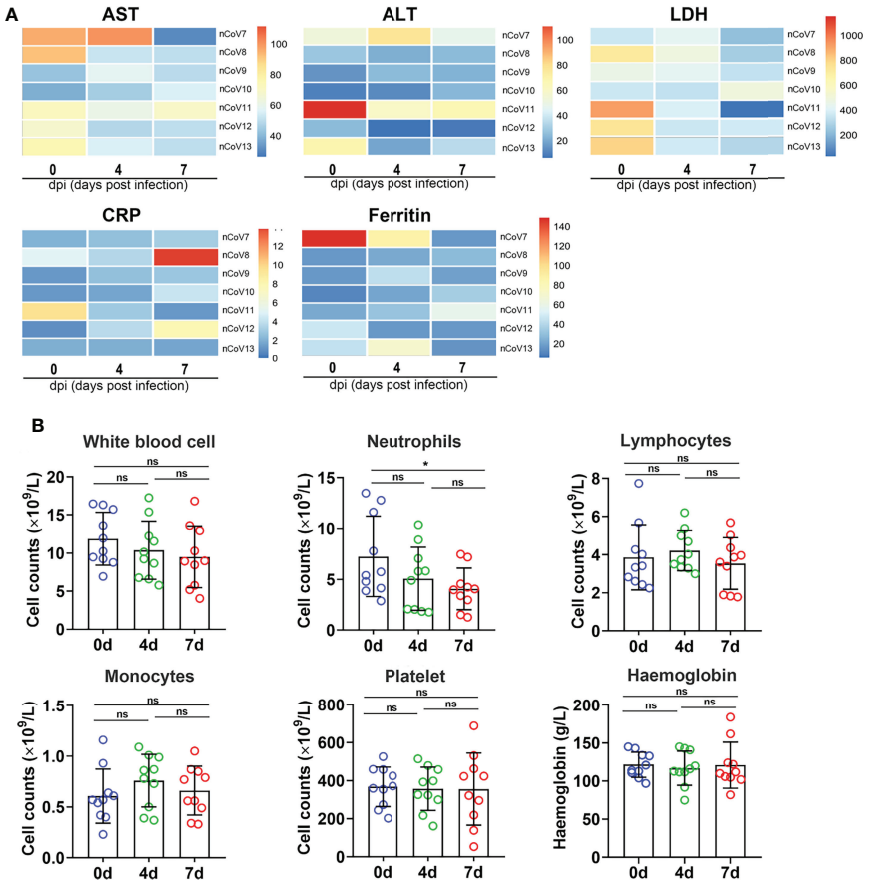

FIGURE 3 | Clinical features in monkeys inoculated with SARS-CoV-2. **(A)** The infection indicators (AST, ALT, LDH, CRP and Ferritin) were examined at indicated time points and compared with each other. The 0 dpi (before infection) of each monkey was put as the control of itself. The heatmap was prepared *via* heatmap illustrator in TB tools. **(B)** The counts and proportion of indicator cells in PBMC were detected at indicated time points in macaques before and after SARS-CoV-2 challenge, and the analysis was plotted in GraphPad Prism 8.0.1. *p<0.05. ns, not significant. AST, aspartate transaminase; ALT, alanine transaminase; LDH, lactate dehydrogenase; CRP, C-reactive protein; nCoV, SARS-CoV-2; PBMC, peripheral blood mononuclear cell.

was consistent with the evidence that lymphopenia (LYC < 0.8 × 10^9/L) was always developed in severe (72.7%) but not in moderate COVID-19 cases (25). ANC were found to be decreased in challenged CMs (4.02 × 10^9/L) when compared with the healthy controls (5.58 × 10^9/L, p<0.05), as reported in moderate COVID-19 patients (2.6-4.4 × 10^9/L) (26). Additionally, monocytes increased slightly, while HGB and PLT appeared almost unchanged in infected CMs.These data collectively suggested that PBMC indicators are more semblable in CMs models at early stage as that in moderate patients, the obvious turbulence of hematological indicators such as lymphopenia and thrombocytopenia that appeared in very severe and severe COVID-19 patients, is obviously weakened in infected CMs.

Immunological Features of COVID-19 Model in CMs

To gain insight into the immunological features of COVID-19 in CMs, we applied a Luminex multi-factor detection to assess the immune cytokines alteration in serum samples of CMs before and post SARS-CoV-2 inoculation. As showed in **Figure 4A**, sCD40L, IL-8, GM-CSF, IP-10, MCP-1, and MIG and IL-10 significantly increased (p<0.01), while IL-6, IL-1β, IL-7 and MIP-1β moderately increased in infected CMs (p<0.05). Notably, IL-10, the traditional Th2 cytokine which usually exerts dual effects on T cells in terms of inhibiting Th1 cell production of IL-2, IFNs as well as TNF-α and enhancing the proliferation and cytolysis activity of NK and $CD8^+$ T cells, elevated in infected CMs, which indicated the susceptibility to COVID-19. Emerging studies also reported that IL-10 is a well-known marker of COVID-19 severity in the clinical setting (27, 28). Several cytokines like IL-12, IL-13, IFN-γ, and IL-1RA, which elevated significantly and predicted severe cases, were unchanged or weakly increase in our CMs model. Therefore, these cytokines may coordinately induce the anti-virus and inflammatory response, explaining why SARS-CoV-2 infection induces moderate symptoms and thoracic injury in CMs.

Then, immune cells populations in PBMC of CMs were investigated by flow cytometry. As showed in **Figure 4B**, the

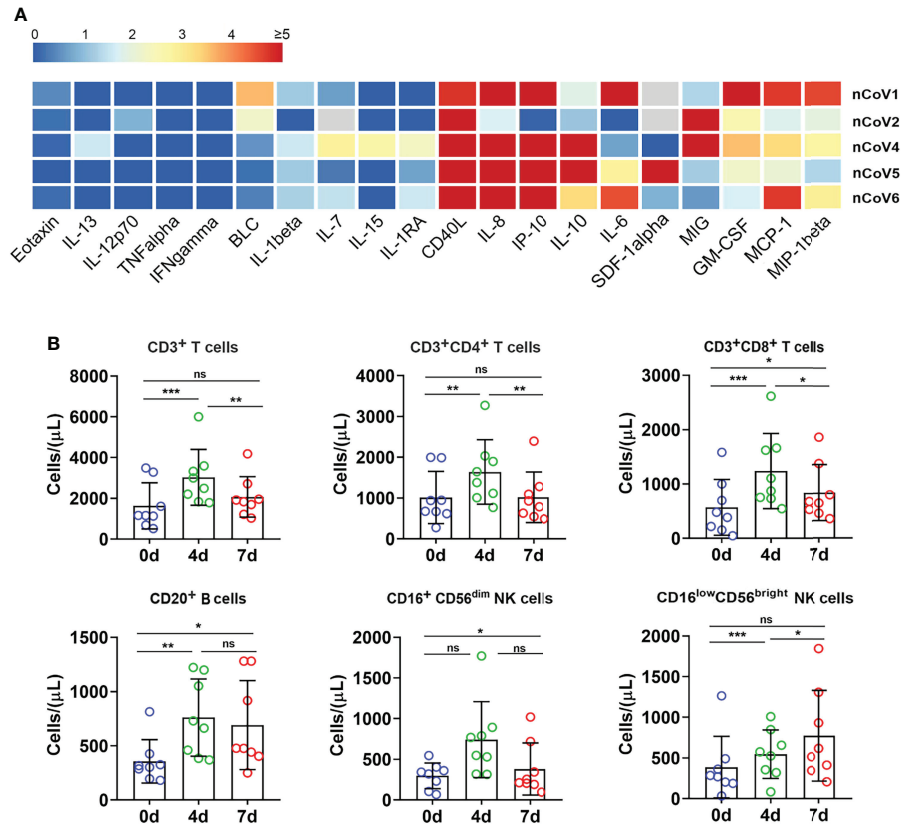

FIGURE 4 | Inflammatory cytokines and immune cell subpopulations in COVID-19 macaques. **(A)** Inflammatory cytokines in serum samples from macaques before and after challenge were measured by Luminex multiplex assays as described in the "Materials and methods" section. The scale bar indicates the change-fold of the cytokines at 7dpi, compared with themselves at before exposure. **(B)** The proportion of immune cells including $CD3^+$, $CD4^+$, and $CD8^+$ T lymphocytes, $CD20^+$ B lymphocytes, and NK cells were analyzed by flow cytometry. *p<0.05; **p<0.01; ***p<0.005. ns, not significant.

absolute numbers of total T lymphocytes, $CD4^+$ T and $CD8^+$ T cells significantly increased at 4 dpi. Then, $CD4^+$ T cells decreased to basal level, while $CD3^+$ and $CD8^+$ T cells hold a slightly higher level than the basal value at 7 dpi. Similar trends were found for $CD20^+$ B lymphocytes. Analysis of NK cells showed an increase of secretory population ($CD16^{low}CD56^{bright}$) upon infection, then decreased to basal level at 7 dpi, while cytotoxic $CD16^+CD56^{dim}$ NK cells remained relatively stable after infection as compared to before infection. These data indicated that SARS-CoV-2 infection stimulated T, B and NK cells proliferation and activation in CMs at very early stage, followed by quickly decrease to the basal level. In contrast, the absolute counts of total T lymphocytes, $CD4^+$, $CD8^+$ T subpopulations and NK cells were all reduced potently in the vast majority of severe COVID-19 patients, even below the lower limit of normal, and these reductions are closely-associated with the severity of COVID-19 cases (29). In addition, the proportion of B cells was significantly higher in severe cases (20.2%) than in moderate ones (10.8%) (30). Thus, these data indicated that SARS-CoV-2 triggered rapid, timely, moderate and controllable immunological response in CMs, and hence avoided excessive immune responses appeared in severe COVID-19 patients.

Histopathological Change and Immune Cells Infiltration

Noting the results of serum cytokines and chemokines, H&E and immunohistochemical (IHC) staining were performed to confirm the inflammatory response and injury in lung tissues of infected CMs. The moderate histopathological characteristic for diffuse alveolar damage were observed in lung tissues, which represented as interstitial pneumonia, widened alveolar septum, hyperemia of alveolar wall capillaries, mainly infiltration of macrophages, neutrophils, accompanied with scattered eosinophils, proliferation of fibroblast-like cells and deposition of powdered matrix (**Figure 5A**). Focal consolidation was frequently observed in some areas, with coagulation necrosis occasionally, and inflammatory exudation in alveolar cavity. Meanwhile, monocytes dominated inflammatory infiltration were observed in heart, and renal interstitium, no significant histopathological changes were observed in other organs, such as salivary gland, liver, brain, tonsil, adrenal gland, prostate, spleen, intestine and testicles (**Figure 5A**).

The SARS-CoV-2-Spike protein was then examined in diverse tissues of CMs. Strong positive staining was predominantly observed in alveolar epithelial cells, vascular

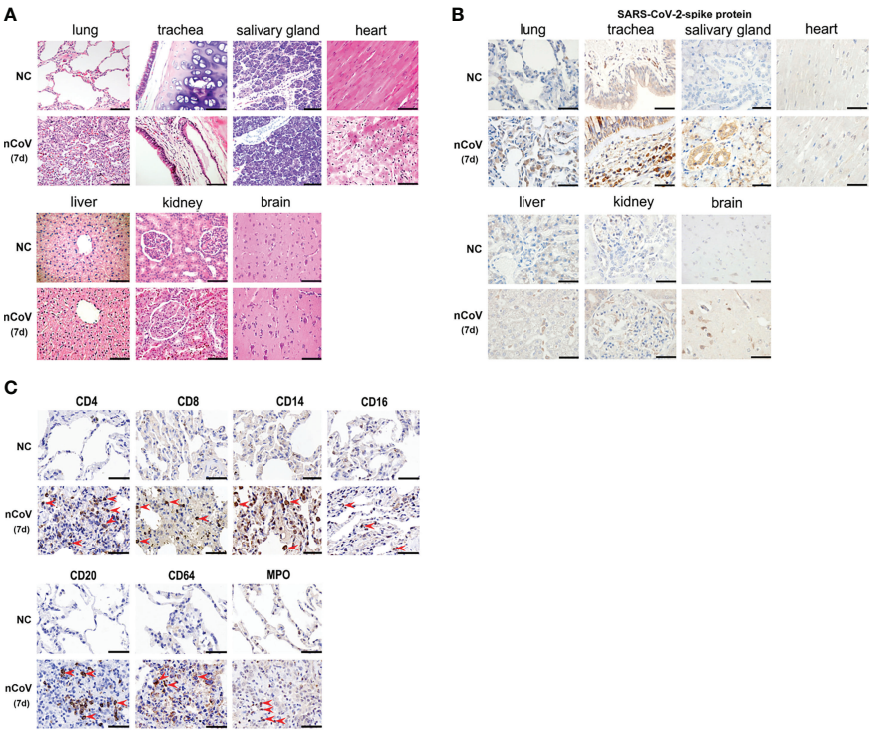

FIGURE 5 | Pathological evaluation, viral distribution and host response in tissues of COVID-19 CMs. **(A)** After necropsy, different tissue samples were cut and fixed in 10% neutral buffered formalin for H&E staining, followed by microscopic inspection. **(B)** SARS-CoV-2–Spike antibody was used to evaluate the viral load and distribution in different tissues. **(C)** Infiltration of immune cells was examined in the lung tissues. The red arrowheads indicate corresponding positive cells in the pulmonary airspace. Scale bar=100 μm. NC, negative control; nCoV, SARS-CoV-2; 7d, 7 days post infection; CMs, cynomolgus macaque.

endothelial cell, alveolar macrophages, salivary gland, hepatic Kupffer cells, and part of glomerulus cells. Weak positive staining was observed in brain and kidney, and no staining was observed in heart (**Figure 5B**). These data were consistent with the results of viral genomic RNA copies in **Figure 2C**.

IHC was further employed to detect infiltration of immune cells in lung tissues of CMs. As showed in **Figure 5C**, moderate infiltration of $CD4^+$ T, $CD8^+$ T cells, $CD14^+$ monocytes, $CD64^+$ and MPO^+ neutrophils, $CD16^+$ NK cells, and $CD169^+$ macrophages were detected in CMs at 7 dpi. Meanwhile, no significant increase of $CD20^+$ B cells were observed in challenged CMs. Most of these are consistent with the distribution of immune cells in PBMC, except neutrophil, which increased apparently in challenged lung tissues ($p<0.05$), whereas decreased in PBMC. These data supported that adequate innate and adaptive immunity play critical anti-viral roles, and recruitment of circulating neutrophils to the infection site is a main characteristic of COVID-19 models in CMs.

Proteomic and Metabolomic Alterations Post SARS-CoV-2 Exposure

Although accumulating proteomics and metabolomics analysis have been performed in COVID-19 patients (5), rare studies paid attention to omics changes at the initial stage of viral infection, especially for moderate cases. Considering the viral detection is becoming more efficient, and timely and efficient treatment of moderate cases (which account for 90% of COVID-19 patients) means better prognosis and alleviation of burden on medical resources, we thus tried to explore the pathogenesis of COVID-19 in CMs models at early stage of infection. We used 4D Label-free proteomics and ultra-performance liquid chromatography/tandem mass spectrometry (UPLC-MS/MS) targeted metabolomics approaches to analyze the lung tissues and sera samples, respectively. Altogether, 4493 proteins and 500 metabolites were identified and quantified.

We found that 194 proteins were differentially expressed in lung tissue of nCoV2 CMs (65 increased *vs* 129 decreased, >1.5-fold, **Figure 6A**) as compared with NC CMs. Target and functional analyses showed that 83 of these proteins belong to four major pathways, namely innate immune response (44 proteins), neutrophil activation and degranulation (33 proteins), platelet degranulation (17 proteins), and viral genome replication (11 proteins). Consistently, the Gene ontology (GO) and Kyoto Encyclopedia of Genes and Genomes (KEGG) analysis data also revealed that innate immune response, neutrophil and platelet activation pathways are involved in moderate COVID-19 onset in CMs (**Figure 6B**). For all differentially expressed proteins, 9 most significantly changed innate immune-associated proteins were shown in **Figure 6C**. most of the differentially expressed genes (DEGs)

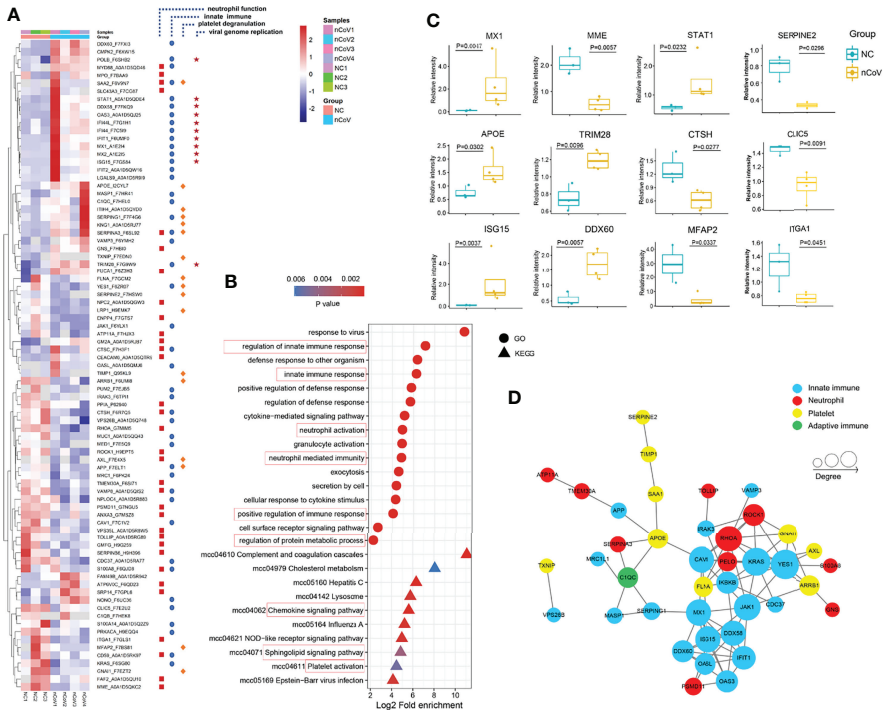

FIGURE 6 | Dysregulated Proteins in lung tissue of monkeys inoculated with SARS-CoV-2, and statistics of functional enrichment. **(A)** Heatmap of 83 selected proteins whose regulation concentrated on four enriched pathways. **(B)** The median CV values was analyzed to confirm the proteomics data with good degree of consistency and reproducibility (median<0.25). **(C)** The expression level change of nine selected proteins with significant difference before and after inoculated with SARS-CoV-2. **(D)** The histogram of GO terms enriched in biological process, cellular component and molecular function. CV, coefficient of variance; GO, Gene Ontology.

in these four signal pathways can form a protein-protein interaction (PPI) network, so as to potently and jointly regulate the process of COVID-19 (**Figure 6D**). In addition, GO analysis was performed to produce a further protein classification and assess gene enrichment sets, in biological process, cellular component, and molecular function.

Meanwhile, 131 metabolites were found to be significantly changed in nCoV2 CMs (**Figures 7A-C**). Among them, 116 metabolites were involved in the four biological processes revealed in the proteomic analysis, and we summarized both proteomics and metabolomics data in the following sections and indicated their function in COVID-19 onset.

SARS-CoV-2 Infection Leads to Neutrophil Recruitment and Activation

As the most abundant white blood cell in humans, neutrophils play critical roles in antiviral defense of innate immune system. But through degranulation and formation of neutrophil extracellular traps (NETs), they can be cytotoxic during severe pneumonia (31). Constantly updated data proved that a fulminant neutrophilia is often observed in severe COVID-19 cases, which could be a symbol of excessive inflammatory response and associated with unfavorable prognosis (26, 32, 33), whereas neutropenia was more common in non-severe group (34, 35), which is consistent with our CM models. Hence, it is urgent to unravel the roles of neutrophils in the moderate cases of COVID-19.

We obtained 33 altered proteins (12 upregulated, 21 downregulated) that are involved in neutrophil recruitment, activation, and degranulation by target-function analysis (**Figure 6A**) in the current model. ATP6V0C, a modulator of neutrophil degranulation and activation, were increased 6.16- and 10.61-fold, respectively. Whereas AXL, which is important for neutrophil infiltration and COVID-19 therapy *via* regulating TGF-β and PI3K signaling pathways (36, 37), also works as a candidate receptor for SARS-CoV-2 entry (38), was significantly reduced about 3-fold in infected CMs as compared with the healthy control. Glia maturation factor-γ (GMFG), decreased by 0.45-fold, could regulate directional migration of neutrophils through regulation of actin cytoskeletal reorganization and integrin-mediated adhesion (39). As known, NETosis is a critical pathologic driver of direct lung injury in COVID-19 patients (40, 41). Of these 33 proteins, LGALS9, MPO, S100A8, C1QC, C1QB, and CTSC were NETs-associated, and their changes were not as obvious as in severe COVID-19 patients (42).

Considering the facts that neutrophil-attracting chemokines like IL-8, MCP-1, and MIP-1β are dramatically upregulated (**Figure 4A**); dozens of neutrophil recruitment, activation, and degranulation-associated genes were significantly changed

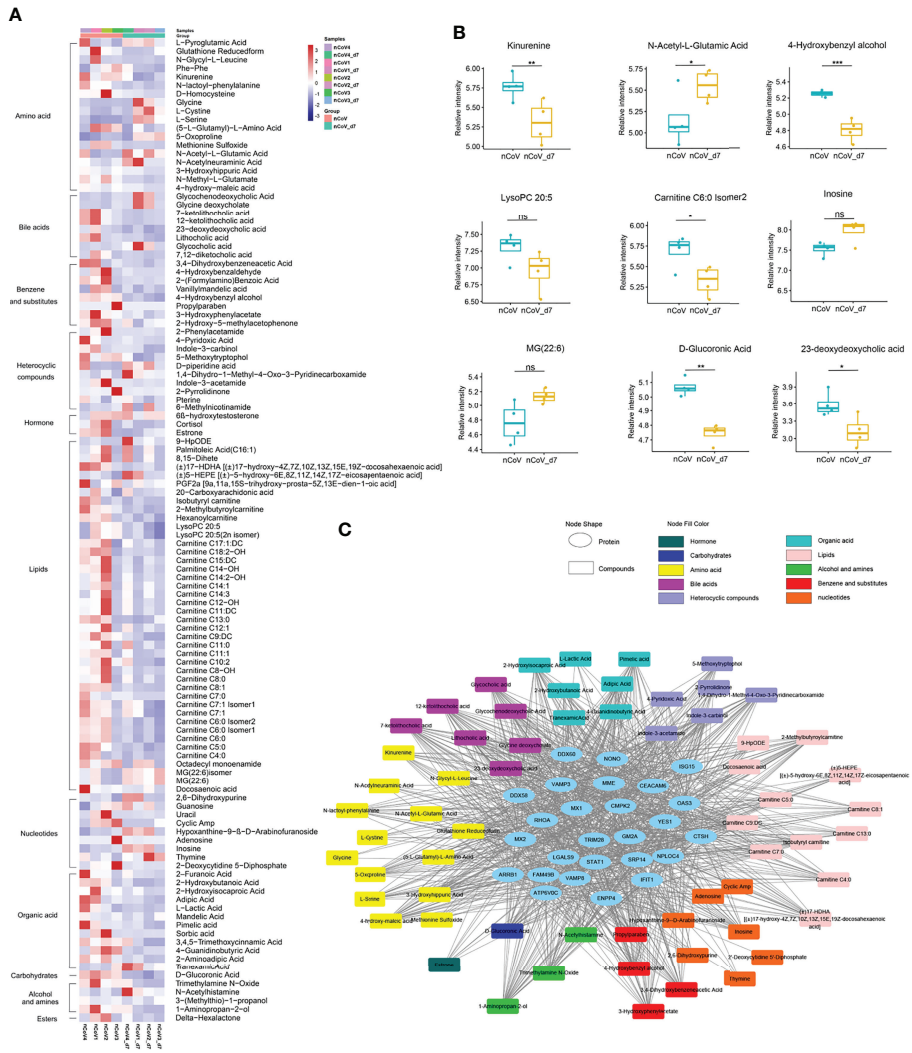

FIGURE 7 | Dysregulated metabolites in sera of CMs inoculated with SARS-CoV-2, and statistics of functional and pathway enrichment. **(A)** Heatmap of 116 most significantly regulated metabolites belonging to 11 major classes as indicated. **(B)** The expression level change of nine selected regulated metabolites with significant difference before and after inoculated with SARS-CoV-2. **(C)** Scatter plot of KEGG enrichment analysis between nCoV *vs.* nCoV-d7 with significant changes. CMs, cynomolgus macaque; nCoV, SARS-CoV-2; nCoV_7d, 7 days post SARS-CoV-2 infection; KEGG, Kyoto encyclopedia of genes and genomes. *p<0.05; **p<0.01; ***p<0.005. ns, not significant.

(**Figure 6A**); neutrophil counts were reduced in PBMC of infected-CMs, these data collectively indicated that the migration and adhesion capacity of neutrophils to lung tissues were tightly- and timely-regulated in infected CMs.

Innate Immune Response Was Potently Activated by SARS-CoV-2 Infection

Activation of innate immunity may assist rapid recognition, suppressed viral evasion and short-term retention of SARS-CoV-2. We identified 44 proteins from all 194 proteins significantly altered in infected-CMs which are known to be responsive to innate immunity. A few representative examples were showed in **Figures 6A, C**. Most of these proteins are encoded by interferon-stimulated genes (ISGs), therefore, our data strongly supported that interferon (IFN) signaling pathway-associated anti-viral action play an essential role in the model. STAT1, a crucial modulator of IFN signaling, can't be avoided in antiviral innate immunity. A study showed that hACE2 transduced STAT1$^{-/-}$ C57BL/6 mice exhibited enhanced inflammatory cell infiltration, and delayed SARS-CoV-2 clearance (43). In our model, STAT1 was significantly upregulated 2.62-fold as compared with the NC CMs. ISG15 was upregulated up to 20.51-fold. MX1 and MX2, downstream targets of ISG15 which play important anti-viral effects on a variety of RNA and DNA viruses, were upregulated 21.44- and 56.85-fold, respectively (44). As a family of IFN-induced antiviral proteins, IFITs potently

restrict viral infection by recognizing virus-derived exogenous RNAs (45, 46). IFIT1 and IFIT2 were upregulated 7.8- and 5.7-fold, respectively. Thus, it is rationale to predict that in moderate cases, SARS-CoV-2 induced ISGs activation, the latter one leaded to the constitutively expression of MX1/2 and IFIT1/2, which then extended and enhanced the anti-viral activity of innate response, thereby alleviate the symptoms of COVID-19 and overcome SARS-CoV-2 viral evasion in CMs.

DDX58 (also known as RIG-I) can initiate a signaling cascade to start an inflammatory and type-1 IFN responses once recognizing pathogen-associated molecular patterns (PAMP), like virus-derived dsRNA. DDX58 was upregulated (3.6-fold) in infected CMs. DDX60, another member of RIG-I signaling pathway, is essential for viral RNA degradation (47), was also remarkably upregulated (3.1-fold, **Figure 6C**). TRIM28, which is involved in innate immunity, has been identified recently to be a regulator of ACE2 expression and SARS-CoV-2 entry (48), also increased significantly in our model.

Although lots of ISGs proteins were potently upregulated in this model, dozens of proteins like MED1, PUM2, MUC1, VPS26B, MRC1, CD59, NPLOC4, S100A14, and S100A8 were significantly downregulated. These data indicated that strong but controllable innate immune response was elicited for SARS-CoV-2 defense and clearance in the COVID-19 model, which provide evidence to explain why CMs mainly present mild symptom after SARS-CoV-2 infection.

No Thrombopenia Was Observed in SARS-CoV-2–Infected CMs

PLTs, as dynamic cells, participate in inflammation and prothrombotic responses in many viral infections (49). Thrombopenia, caused by reduced PLTs production and unrestricted consumption, has been reported to be associated with enhanced risk of severe COVID-19 and mortality (50). Our data demonstrated that no thrombopenia was observed in moderate CMs models.

Platelet factor 4 (PF4) and platelet-expressing chemokines pro-platelet basic protein (PPBP) were reported significantly downregulated in severe COVID-19 patients, which associated with platelet degranulation and potently contributed to thrombopenia (5). Herein, neither PF4 (1.27-fold) nor PPBP (1.78-fold) were decreased in lung tissues of infected CMs. Whereas 17 proteins which associated with platelet aggregation and function were altered significantly. Of them, KNG1, TXNIP, ITIH4, TIMP1 and SERPING1/2/3, which contribute to platelet aggregation and function (51), were increased; whereas ITGA1, CLIC5, ARRB1, MFAP2, and GNAI1 (52–54), which negatively regulate platelet activation, were greatly decreased (**Figure 6A**). As to these proteins, TIMP1 was reported to be overexpressed in anti-inflammatory M2 macrophages upon SARS-CoV-2 infection (55). TXNIP regulates neutrophil platelet aggregates in acute lung injury (ALI), and has been proved to be involved in glucose and lipid metabolism, and NLRP3 inflammasome activation, a known factor for the immunopathogenesis of COVID-19 (56). CLIC5 could be exploited by virus for transportation of new virions (57).

Metabolomic Changes in the Sera of SARS-CoV-2–Infected CMs

Compared with the normal control, more than 116 metabolites, or their derivatives, were significantly decreased in the sera of SARS-CoV-2 infected-CMs. Enriched are 11 metabolites mainly involved in lipids, bile acids, amino acids, and heterocyclic compounds (**Figure 7A**).

According to the aforementioned data, we analyzed the metabolites closely associated with platelet degranulation, innate immune response, neutrophil and macrophage function. We found that several well-known metabolites, such as serotonin, choline, mannose, arachidonate, and eicosanoids (prostaglandins, thromboxanes, and leukotrienes) (58–60), were not changed significantly in infected-CMs. Consistent with previous reports in COVID-19 patients (61, 62), dozens of metabolites like L-cystine, L-glutamic acid, and L-serine were increased in COVID-19 CMs as compared with the healthy control. Notably, for the first time, several lipids, nucleotide, bile acids, and amino acids metabolites were found to be apparently changed, including different products of carnitine, glutathione (0.3-fold), N-acetyl-L-glutamic acid (2.1-fold), adenosine (0.02-fold), and inosine (2.99-fold) (**Figure 7B**).

It is well known that adenosine play critical roles in regulating neutrophil chemotaxis, phagocytosis, and granule release (63, 64). Usually, pathological conditions of inflammation lead to release of adenosine, conferring protection against tissue damage, platelet activation and inflammatory response. In addition, adenosine could be phosphorylated to AMP or deaminated to inosine (65). We found that adenosine decreased to 0.02-fold and inosine increased up to 2.99-fold in SARS-CoV-2 infected CMs. This revealed that adenosine generated and released by neutrophils at sites of inflammation was mainly deaminated to inosine, which was consistent with the increased platelet activation, recruitment and activation of neutrophils and leukocytes observed in the COVID-19 model in CMs. In addition, decreased adenosine-to-inosine ratio indicated elevated adenosine deaminases (ADARs) activity. ADARs can be a pro- or anti-viral factor and has been reported to shape SARS-CoV-2 fate by virus genome editing (66). Thus, these data suggested that elevated ADAR (1.39-fold) are involved in the moderate COVID-19 model.

Carnitine derivatives are the most changed metabolites, among which 38 metabolites were significantly decreased, with lowest down to 0.28-fold. Besides the role in β-oxidation, carnitine also acts in immune regulation as an anti-inflammatory and anti-apoptotic factor (67). It has been reported that carnitine negatively regulated neutrophil and platelet activation (68), and decreased serum carnitine levels usually associated with impaired reactions, metabolic disorders and recurrent infections (69). Thus, significant carnitine reduction in CMs might relieve immune suppression and profit SARS-CoV-2 clearance.

To further uncover the function of DEGs and metabolites in this model, a protein-metabolite interaction regulatory network was done. As shown in **Figure 7C**, most metabolites are associated with metabolic pathways, bile acid biosynthesis and

secretion pathways, and lipid metabolism in SARS-CoV-2 infected CMs, and there are extensive and fine regulations between metabolites and differentially expressed proteins. The detailed mechanism and function of these intermodulations is still under investigation.

DISCUSSION

COVID-19, an unprecedented threat caused by SARS-CoV-2, has been spreading worldwide rapidly. Until now, over 523 million individuals have been infected, leading to over 6.279 million deaths. Epidemiological and clinical characteristics studies have uncovered that most of COVID-19 patients usually recovered with good prognosis who displayed mild or moderate symptoms, or even a higher proportion of asymptomatic symptoms in Delta or Omicron infections (70, 71). However, it is still a great challenge to discriminate cases which will likely become clinically severe and to treat them effectively. Although many specific hematologic indicators have been reported to be strongly associated with severe COVID-19 cases, with low levels of PLTs count, lymphocyte count and percentage, total protein, and high levels of D-dimer, leukocyte count, CRP, creatinine, neutrophil count and percentage, creatine kinase activity, and prolonged prothrombin time to be changed the most (30, 72, 73), the pathogenesis and detailed mechanisms of COVID-19, especially at early stage of infection is still largely unknown.

In the present study, we analyzed the lung tissues and sera samples of SARS-CoV-2–infected CMs *via* 4D Label-free proteomics strategy and UPLC-MS/MS targeted metabolomics approaches. About 4493 proteins and 500 metabolites were identified and quantified. KEGG analysis suggested that most of these differentially expressed proteins focused on innate immune response, neutrophil recruitment, activation and degranulation, and platelet degranulation.

Innate immune response stands as the first line of antiviral defense, the cellular innate immune responses play crucial roles in initiating resistance to virus infection. SARS-CoV-1–infected patients elicited strong innate inflammatory responses, rather than a virus-specific immune response (74). Although only a small percentage of primary endothelial cell were infected, Dengue Virus exerts substantial influence on type I IFN-driven innate immune response induction that can effectively restrict infection (75). Therefore, innate immunity may be the best weapon for flattening the curve of COVID-19 spread, and dysregulated immune response can reduce the ability to detect antigens, blunt the healing process and delay the recovery of patients with COVID-19 (76). In our model, dozens of known host genes that associated with innate immunity and response to viral infections, such as MX1/2, ISG15, IFIT1, DDX58/60, IFI44L, IFI44, OAS3, STAT1, POLB, BANF1, TRIM28, LOC703156, MED1, PUM2, VPS26B, MRC1, CD59, NPLOC4 and S100A14/A8, were greatly changed. Several of these genes can regulate viral genome replication, viral infection process and life cycle. The significant change of ISG15, MX1, MX2, and STAT1 strongly indicated that IFN signaling pathway associated anti-viral action play critical roles in SARS-CoV-2–infected CMs model (77, 78). Which is consistent with a previous report that IFN signaling is significantly induced in rhesus macaque infected lungs (79).

In this moderate COVID-19 model, we found that neutrophils play pivotal roles in host defense against SARS-CoV-2 infection. The proteomics and Luminex data showed that various macrophage and neutrophil related cytokines and chemokines like MCP-1, IP-10 (CXCL10), MIG, MIP-1β (CCL4), CXCL8 (IL-8), SAA2, and AXL were dramatically upregulated at 7 days after infection. This indicated that the circulating or tissue resident macrophages are activated by the intruder/virus at the fastest time and recruited neutrophils to the attack site where they synergistically defense virus infection. IP-10, a chemoattractant for monocytes/macrophages, has been reported as an excellent predictor for the progression of COVID-19 strongly associated with disease severity and ICU admission (80). Our data supported that IP-10 also contributed to the progression of COVID-19 in infected CMs. Most nucleated cells, including neutrophils and monocytes, are the main source of IL-8. So, it is easy to understand the high level of IL-8 after SARS-CoV-2 infection. According to our data, we hypothesize that SARS-CoV-2 infection activates innate immune cells to secrete multi-factors at early stage in CMs, which then exert anti-viral effects. Among them, the sedentary macrophages in lung tissues released abundant IL-8, which acts as a classical neutrophil chemotactic factor, recruiting neutrophil from the blood stream into the infected tissue (alveolar space and airways). IL-8 stimulated the phagocytosis and degranulation of neutrophil to kill virus, and induced the necrosis and exhaustion of neutrophil as well. Neutrophilia is a main feature of severe COVID-19 cases, whereas neutropenia is found in the sera of our model (apparent neutrophil infiltration were also observed in lung tissues). This may be partly due to the significantly regulated metabolites like adenosine, inosine and carnitine derivatives, which take part in regulating neutrophil chemotaxis, phagocytosis, and granule release.

A recent study reported that immature neutrophils with elevated calprotectin S100A8/S100A9 plasma levels can be used as robust biomarkers of COVID-19 severity (81). In the current model, S100A8 was significantly downregulated, and no apparent change was found for S100A9. In addition, the classical inflammatory cytokines secreted by neutrophils and macrophages like TNF-α, IL-1β and IL-2 were not obviously changed, whereas the immunosuppressive IL-10 was significantly upregulated. Which would be helpful to explain the moderate "cytokines storm" and tissue injury in the model and we speculated that potent but controllable spatial and temporal innate immune cell response was essential for SARS-CoV-2 defense and clearance (82), and might be used as potential biomarkers for discriminating severe from mild or moderate COVID-19.

Our Luminex assay data showed that CD40L was significantly increased in CMs, which was also found greatly elevated in ICU patients (83). Although CD40L is a marker of platelet and T-cell

activation, the major source of CD40L present in plasma is derived from platelet, thereby the increase of CD40L here suggested that platelet activation might be an important factor in the pathophysiology of COVID-19–associated coagulopathy and might accelerate the progression of disease. Consistently, proteomic and metabolomics data from CMs revealed several genes (KNG1, TXNIP, ITIH4, TIMP1, SERPING1/2/3, ITGA1, ADAR, and CLIC5 etc.) and molecules (adenosine and inosine) were related with platelet activation, thus, adding antiplatelet might be a possible therapeutic for COVID-19.

As to other viral immunity responses, complement activation can suppress virus invasion and trigger inflammation. Suppression of complement system has successfully ameliorated syndrome of SARS-infected mouse model (84). Upregulation of C1s (1.60-fold), C1q (1.53-fold), C2 (2.76-fold), C3 (1.9-fold), and C4b (2.45-fold) indicated that timely complement activation may contribute to COVID-19 in CMs.

Since some mild patients clear SARS-CoV-2 virus without obvious symptoms stands in sharp contrast to the lethal damage that the virus has brought upon severe patients, early diagnosis and treatment of severe COVID-19 patients remain a major challenge. Therefore, it is necessary to elucidate the pathogenesis and detailed mechanism of mild COVID-19 casels, especially at early stage of SARS-CoV-2 infection. Our data demonstrated that innate immune system, neutrophil and platelet activation and degranulation play central roles in these processes in CMs, which mimicked moderate COVID-19 syndrome. This study shed light on characteristic protein and metabolite changes in COVID-19 and might be used as potential biomarkers reservoir for severity evaluation.

DATA AVAILABILITY STATEMENT

The data presented in the study are deposited in the ProteomeXchange repository, accession number PXD034589.

ETHICS STATEMENT

The animal study was reviewed and approved by the Administrative Committee on Animal Welfare of the Institute of Military Veterinary.

AUTHOR CONTRIBUTIONS

Designed and supervised the project: HW, XX, YL, and YG. Conducted the experiments: TW, FM, LL, LH, JZ, CZ, GY, KM, ZW, BW, RS, WL, NL, and DL. Collected the original data and conduct statistical analysis: SL, FW, ZZ, GF and HX. Conducted proteomic and metabolomics analysis: YL, XX, and YG. Wrote the manuscript with input from co-authors: XX, YL, FW, and YG.

FUNDING

This work was supported by grant from the National Key Research and Development Project of China (No.2021YFC2301701), the National Natural Science Foundation of China (No. 31972720) and the Ministry of Science and Technology of China (No. 2020YFC0846100).

ACKNOWLEDGMENTS

We thank Prof. Chengfeng Qin for providing the SARS-CoV-2 virus. We thank Dr. Chengshi Quan's team for IHC and H&E analysis of CMs tissues.

REFERENCES

1. Zhang F, Mears JR, Shakib L, Beynor JI, Shanaj S, Korsunsky I, et al. Ifn-Gamma and Tnf-Alpha Drive a Cxcl10+ Ccl2+ Macrophage Phenotype Expanded in Severe Covid-19 Lungs and Inflammatory Diseases With Tissue Inflammation. *Genome Med* (2021) 13(1):64. doi: 10.1186/s13073-021-00881-3
2. Zhang F, Gan R, Zhen Z, Hu X, Li X, Zhou F, et al. Adaptive Immune Responses to Sars-Cov-2 Infection in Severe Versus Mild Individuals. *Signal Transduct Target Ther* (2020) 5(1):156. doi: 10.1038/s41392-020-00263-y
3. Ragonnet-Cronin M, Boyd O, Geidelberg L, Jorgensen D, Nascimento FF, Siveroni I, et al. Genetic Evidence for the Association Between Covid-19 Epidemic Severity and Timing of Non-Pharmaceutical Interventions. *Nat Commun* (2021) 12(1):2188. doi: 10.1038/s41467-021-22366-y
4. Rebillard RM, Charabati M, Grasmuck C, Filali-Mouhim A, Tastet O, Brassard N, et al. Identification of Sars-Cov-2-Specific Immune Alterations in Acutely Ill Patients. *J Clin Invest* (2021) 131(8):e145853. doi: 10.1172/JCI145853
5. Shen B, Yi X, Sun Y, Bi X, Du J, Zhang C, et al. Proteomic and Metabolomic Characterization of Covid-19 Patient Sera. *Cell* (2020) 182(1):59–72 e15. doi: 10.1016/j.cell.2020.05.032
6. Lu S, Zhao Y, Yu W, Yang Y, Gao J, Wang J, et al. Comparison of Nonhuman Primates Identified the Suitable Model for Covid-19. *Signal Transduct Target Ther* (2020) 5(1):157. doi: 10.1038/s41392-020-00269-6
7. Yang J, Wang W, Chen Z, Lu S, Yang F, Bi Z, et al. A Vaccine Targeting the Rbd of the S Protein of Sars-Cov-2 Induces Protective Immunity. *Nature* (2020) 586(7830):572–7. doi: 10.1038/s41586-020-2599-8
8. Bao L, Deng W, Huang B, Gao H, Liu J, Ren L, et al. The Pathogenicity of Sars-Cov-2 in Hace2 Transgenic Mice. *Nature* (2020) 583(7818):830–3. doi: 10.1038/s41586-020-2312-y
9. Estes JD, Wong SW, Brenchley JM. Nonhuman Primate Models of Human Viral Infections. *Nat Rev Immunol* (2018) 18(6):390–404. doi: 10.1038/s41577-018-0005-7
10. Rockx B, Kuiken T, Herfst S, Bestebroer T, Lamers MM, Oude Munnink BB, et al. Comparative Pathogenesis of Covid-19, Mers, and Sars in a Nonhuman Primate Model. *Science* (2020) 368(6494):1012–5. doi: 10.1126/science.abb7314
11. Aid M, Busman-Sahay K, Vidal SJ, Maliga Z, Bondoc S, Starke C, et al. Vascular Disease and Thrombosis in Sars-Cov-2-Infected Rhesus Macaques. *Cell* (2020) 183(5):1354–66.e13. doi: 10.1016/j.cell.2020.10.005
12. Hoang TN, Pino M, Boddapati AK, Viox EG, Starke CE, Upadhyay AA, et al. Baricitinib Treatment Resolves Lower-Airway Macrophage Inflammation and Neutrophil Recruitment in Sars-Cov-2-Infected Rhesus Macaques. *Cell* (2021) 184(2):460–75.e21. doi: 10.1016/j.cell.2020.11.007
13. Li Y, Bi Y, Xiao H, Yao Y, Liu X, Hu Z, et al. A Novel DNA and Protein Combination Covid-19 Vaccine Formulation Provides Full Protection Against

Sars-Cov-2 in Rhesus Macaques. *Emerg Microbes Infect* (2021) 10(1):342–55. doi: 10.1080/22221751.2021.1887767
14. Huang Z, Ning B, Yang HS, Youngquist BM, Niu A, Lyon CJ, et al. Sensitive Tracking of Circulating Viral Rna Through All Stages of Sars-Cov-2 Infection. *J Clin Invest* (2021) 131(7):e146031. doi: 10.1172/JCI146031
15. Liu Z, Chan JF, Zhou J, Wang M, Wang Q, Zhang G, et al. A Pan-Sarbecovirus Vaccine Induces Highly Potent and Durable Neutralizing Antibody Responses in Non-Human Primates Against Sars-Cov-2 Omicron Variant. *Cell Res* (2022) 32(5):495–7. doi: 10.1038/s41422-022-00631-z
16. Xiao N, Nie M, Pang H, Wang B, Hu J, Meng X, et al. Integrated Cytokine and Metabolite Analysis Reveals Immunometabolic Reprogramming in Covid-19 Patients With Therapeutic Implications. *Nat Commun* (2021) 12(1):1618. doi: 10.1038/s41467-021-21907-9
17. Gu H, Chen Q, Yang G, He L, Fan H, Deng YQ, et al. Adaptation of Sars-Cov-2 in Balb/C Mice for Testing Vaccine Efficacy. *Science* (2020) 369(6511):1603–7. doi: 10.1126/science.abc4730
18. Deng W, Bao L, Gao H, Xiang Z, Qu Y, Song Z, et al. Ocular Conjunctival Inoculation of Sars-Cov-2 Can Cause Mild Covid-19 in Rhesus Macaques. *Nat Commun* (2020) 11(1):4400. doi: 10.1038/s41467-020-18149-6
19. Yu J, Tostanoski LH, Peter L, Mercado NB, McMahan K, Mahrokhian SH, et al. DNA Vaccine Protection Against Sars-Cov-2 in Rhesus Macaques. *Science* (2020) 369(6505):806–11. doi: 10.1126/science.abc6284
20. Wolfel R, Corman VM, Guggemos W, Seilmaier M, Zange S, Muller MA, et al. Virological Assessment of Hospitalized Patients With Covid-2019. *Nature* (2020) 581(7809):465–9. doi: 10.1038/s41586-020-2196-x
21. Parasa S, Desai M, Thoguluva Chandrasekar V, Patel HK, Kennedy KF, Roesch T, et al. Prevalence of Gastrointestinal Symptoms and Fecal Viral Shedding in Patients With Coronavirus Disease 2019: A Systematic Review and Meta-Analysis. *JAMA Netw Open* (2020) 3(6):e2011335. doi: 10.1001/jamanetworkopen.2020.11335
22. Pawar M, Singh M. Systemic Steroids and Risk of Fecal-Oral Shedding and Increased Transmission of Sars-Cov-2 in Pemphigus Cases. *Clin Dermatol* (2020) 38(6):750–6. doi: 10.1016/j.clindermatol.2020.06.006
23. Huang C, Wang Y, Li X, Ren L, Zhao J, Hu Y, et al. Clinical Features of Patients Infected With 2019 Novel Coronavirus in Wuhan, China. *Lancet* (2020) 395(10223):497–506. doi: 10.1016/S0140-6736(20)30183-5
24. Lei F, Liu YM, Zhou F, Qin JJ, Zhang P, Zhu LH, et al. Longitudinal Association Between Markers of Liver Injury and Mortality in Covid-19 in China. *Hepatology* (2020) 72(2):389–98. doi: 10.1002/hep.31301
25. Zhang G, Hu C, Luo L, Fang F, Chen Y, Li J, et al. Clinical Features and Short-Term Outcomes of 221 Patients With Covid-19 in Wuhan, China. *J Clin Virol* (2020) 127:104364. doi: 10.1016/j.jcv.2020.104364
26. Liu X, Zhang R, He G. Hematological Findings in Coronavirus Disease 2019: Indications of Progression of Disease. *Ann Hematol* (2020) 99(7):1421–8. doi: 10.1007/s00277-020-04103-5
27. Han H, Ma Q, Li C, Liu R, Zhao L, Wang W, et al. Profiling Serum Cytokines in Covid-19 Patients Reveals Il-6 and Il-10 Are Disease Severity Predictors. *Emerg Microbes Infect* (2020) 9(1):1123–30. doi: 10.1080/22221751.2020.1770129
28. Zhao Y, Qin L, Zhang P, Li K, Liang L, Sun J, et al. Longitudinal Covid-19 Profiling Associates Il-1ra and Il-10 With Disease Severity and Rantes With Mild Disease. *JCI Insight* (2020) 5(13):e139834. doi: 10.1172/jci.insight.139834
29. De Biasi S, Meschiari M, Gibellini L, Bellinazzi C, Borella R, Fidanza L, et al. Marked T Cell Activation, Senescence, Exhaustion and Skewing Towards Th17 in Patients With Covid-19 Pneumonia. *Nat Commun* (2020) 11(1):3434. doi: 10.1038/s41467-020-17292-4
30. Chen G, Wu D, Guo W, Cao Y, Huang D, Wang H, et al. Clinical and Immunological Features of Severe and Moderate Coronavirus Disease 2019. *J Clin Invest* (2020) 130(5):2620–9. doi: 10.1172/JCI137244
31. Didangelos A. Covid-19 Hyperinflammation: What About Neutrophils? *mSphere* (2020) 5(3):e00367–20. doi: 10.1128/mSphere.00367-20
32. Laforge M, Elbim C, Frere C, Hemadi M, Massaad C, Nuss P, et al. Tissue Damage From Neutrophil-Induced Oxidative Stress in Covid-19. *Nat Rev Immunol* (2020) 20(9):515–6. doi: 10.1038/s41577-020-0407-1
33. Skendros P, Mitsios A, Chrysanthopoulou A, Mastellos DC, Metallidis S, Rafailidis P, et al. Complement and Tissue Factor-Enriched Neutrophil Extracellular Traps Are Key Drivers in Covid-19 Immunothrombosis. *J Clin Invest* (2020) 130(11):6151–7. doi: 10.1172/JCI141374
34. Zou L, Dai L, Zhang Y, Fu W, Gao Y, Zhang Z, et al. Clinical Characteristics and Risk Factors for Disease Severity and Death in Patients With Coronavirus Disease 2019 in Wuhan, China. *Front Med (Lausanne)* (2020) 7:532. doi: 10.3389/fmed.2020.00532
35. Lutfi F, Benyounes A, Farrukh N, Bork J, Duong V. Agranulocytosis Following Covid-19 Recovery. *Cureus* (2020) 12(7):e9463. doi: 10.7759/cureus.9463
36. Haider C, Hnat J, Wagner R, Huber H, Timelthaler G, Grubinger M, et al. Transforming Growth Factor-Beta and Axl Induce Cxcl5 and Neutrophil Recruitment in Hepatocellular Carcinoma. *Hepatology* (2019) 69(1):222–36. doi: 10.1002/hep.30166
37. Bouhaddou M, Memon D, Meyer B, White KM, Rezelj VV, Correa Marrero M, et al. The Global Phosphorylation Landscape of Sars-Cov-2 Infection. *Cell* (2020) 182(3):685–712.e19. doi: 10.1016/j.cell.2020.06.034
38. Wang S, Qiu ZY, Hou YN, Deng XY, Xu W, Zheng TT, et al. Axl Is a Candidate Receptor for Sars-Cov-2 That Promotes Infection of Pulmonary and Bronchial Epithelial Cells. *Cell Res* (2021) 31(2):126–40. doi: 10.1038/s41422-020-00460-y
39. Aerbajinai W, Liu LH, Zhu JQ, Kumkhaek C, Chin K, Rodgers GP. Glia Maturation Factor- Regulates Monocyte Migration Through Modulation of 1-Integrin. *J Biol Chem* (2016) 291(16):8549–64. doi: 10.1074/jbc.M115.674200
40. Villanueva E, Yalavarthi S, Berthier CC, Hodgin JB, Khandpur R, Lin AM, et al. Netting Neutrophils Induce Endothelial Damage, Infiltrate Tissues, and Expose Immunostimulatory Molecules in Systemic Lupus Erythematosus. *J Immunol* (2011) 187(1):538–52. doi: 10.4049/jimmunol.1100450
41. Narasaraju T, Tang BM, Herrmann M, Muller S, Chow VTK, Radic M. Neutrophilia and Netopathy as Key Pathologic Drivers of Progressive Lung Impairment in Patients With Covid-19. *Front Pharmacol* (2020) 11:870. doi: 10.3389/fphar.2020.00870
42. Wang J, Li Q, Yin Y, Zhang Y, Cao Y, Lin X, et al. Excessive Neutrophils and Neutrophil Extracellular Traps in Covid-19. *Front Immunol* (2020) 11:2063. doi: 10.3389/fimmu.2020.02063
43. Sun J, Zhuang Z, Zheng J, Li K, Wong RL, Liu D, et al. Generation of a Broadly Useful Model for Covid-19 Pathogenesis, Vaccination, and Treatment. *Cell* (2020) 182(3):734–43 e5. doi: 10.1016/j.cell.2020.06.010
44. Zav'yalov VP, Hamalainen-Laanaya H, Korpela TK, Wahlroos T. Interferon-Inducible Myxovirus Resistance Proteins: Potential Biomarkers for Differentiating Viral From Bacterial Infections. *Clin Chem* (2019) 65 (6):739–50. doi: 10.1373/clinchem.2018.292391
45. Li D, Swaminathan S. Human Ifit Proteins Inhibit Lytic Replication of Kshv: A New Feed-Forward Loop in the Innate Immune System. *PloS Pathog* (2019) 15 (2):e1007609. doi: 10.1371/journal.ppat.1007609
46. Diamond MS. Ifit1: A Dual Sensor and Effector Molecule That Detects Non-2 '-O Methylated Viral Rna and Inhibits Its Translation. *Cytokine Growth F R* (2014) 25(5):543–50. doi: 10.1016/j.cytogfr.2014.05.002
47. Kouwaki T, Fukushima Y, Daito T, Sanada T, Yamamoto N, Mifsud EJ, et al. Extracellular Vesicles Including Exosomes Regulate Innate Immune Responses to Hepatitis B Virus Infection. *Front Immunol* (2016) 7:335. doi: 10.3389/fimmu.2016.00335
48. Zhu L, Yang P, Zhao Y, Zhuang Z, Wang Z, Song R, et al. Single-Cell Sequencing of Peripheral Mononuclear Cells Reveals Distinct Immune Response Landscapes of Covid-19 and Influenza Patients. *Immunity* (2020) 53(3):685–96 e3. doi: 10.1016/j.immuni.2020.07.009
49. Salamanna F, Maglio M, Landini MP, Fini M. Platelet Functions and Activities as Potential Hematologic Parameters Related to Coronavirus Disease 2019 (Covid-19). *Platelets* (2020) 31(5):627–32. doi: 10.1080/09537104.2020.1762852
50. Bashash D, Hosseini-Baharanchi FS, Rezaie-Tavirani M, Safa M, Dilmaghani NA, Faranoush M, et al. The Prognostic Value of Thrombocytopenia in Covid-19 Patients; a Systematic Review and Meta-Analysis. *Arch Acad Emerg Med* (2020) 8(1):e75.
51. Meek RL, Urieli-Shoval S, Benditt EP. Expression of Apolipoprotein Serum Amyloid a Mrna in Human Atherosclerotic Lesions and Cultured Vascular Cells: Implications for Serum Amyloid a Function. *Proc Natl Acad Sci U.S.A.* (1994) 91(8):3186–90. doi: 10.1073/pnas.91.8.3186
52. Wang JK, Wang WJ, Cal HY, Du BB, Mai P, Zhang LJ, et al. Mfap2 Promotes Epithelial-Mesenchymal Transition in Gastric Cancer Cells by Activating Tgf-Beta/Smad2/3 Signaling Pathway. *Oncotargets Ther* (2018) 11:4001–17. doi: 10.2147/Ott.S160831

53. Yao J, Liang LH, Zhang Y, Ding J, Tian Q, Li JJ, et al. Gnai1 Suppresses Tumor Cell Migration and Invasion and Is Post-Transcriptionally Regulated by Mir-320a/C/D in Hepatocellular Carcinoma. *Cancer Biol Med* (2012) 9(4):234–41. doi: 10.7497/j.issn.2095-3941.2012.04.003
54. Schaff M, Receveur N, Bourdon C, Ohlmann P, Lanza F, Gachet C, et al. Beta-Arrestin-1 Participates in Thrombosis and Regulates Integrin Aiibbeta3 Signalling Without Affecting P2y Receptors Desensitisation and Function. *Thromb Haemost* (2012) 107(4):735–48. doi: 10.1160/TH11-06-0430
55. Duan F, Guo L, Yang L, Han Y, Thakur A, Nilsson-Payant BE, et al. Modeling Covid-19 With Human Pluripotent Stem Cell-Derived Cells Reveals Synergistic Effects of Anti-Inflammatory Macrophages With Ace2 Inhibition Against Sars-Cov-2. *Res Sq* (2020) 2:rs.3.rs-62758. doi: 10.21203/rs.3.rs-62758/v1
56. Saeedi-Boroujeni A, Mahmoudian-Sani MR. Anti-Inflammatory Potential of Quercetin in Covid-19 Treatment. *J Inflammation (Lond)* (2021) 18(1):3. doi: 10.1186/s12950-021-00268-6
57. Li CW, Jheng BR, Chen BS. Investigating Genetic-And-Epigenetic Networks, and the Cellular Mechanisms Occurring in Epstein-Barr Virus-Infected Human B Lymphocytes *Via* Big Data Mining and Genome-Wide Two-Sided Ngs Data Identification. *PloS One* (2018) 13(8):e0202537. doi: 10.1371/journal.pone.0202537
58. Iba T, Levy JH. Inflammation and Thrombosis: Roles of Neutrophils, Platelets and Endothelial Cells and Their Interactions in Thrombus Formation During Sepsis. *J Thromb Haemostasis* (2018) 16(2):231–41. doi: 10.1111/jth.13911
59. Gould TJ, Vu TT, Swystun LL, Dwivedi DJ, Mai SHC, Weitz JI, et al. Neutrophil Extracellular Traps Promote Thrombin Generation Through Platelet-Dependent and Platelet-Independent Mechanisms. *Arterioscler Thromb Vasc Biol* (2014) 34(9):1977–84. doi: 10.1161/Atvbaha.114.304114
60. Vogel S, Bodenstein R, Chen QW, Feil S, Feil R, Rheinlaender J, et al. Platelet-Derived Hmgb1 Is a Critical Mediator of Thrombosis. *J Clin Invest* (2015) 125 (12):4638–54. doi: 10.1172/JCI81660
61. Shi D, Yan R, Lv L, Jiang H, Lu Y, Sheng J, et al. The Serum Metabolome of Covid-19 Patients Is Distinctive and Predictive. *Metabolism* (2021) 118:154739. doi: 10.1016/j.metabol.2021.154739
62. Thomas T, Stefanoni D, Reisz JA, Nemkov T, Bertolone L, Francis RO, et al. Covid-19 Infection Alters Kynurenine and Fatty Acid Metabolism, Correlating With Il-6 Levels and Renal Status. *JCI Insight* (2020) 5(14): e140327. doi: 10.1172/jci.insight.140327
63. Chen Y, Corriden R, Inoue Y, Yip L, Hashiguchi N, Zinkernagel A, et al. Atp Release Guides Neutrophil Chemotaxis *Via* P2y2 and A3 Receptors. *Science* (2006) 314(5806):1792–5. doi: 10.1126/science.1132559
64. Carmona-Rivera C, Khaznadar SS, Shwin KW, Irizarry-Caro JA, O'Neil LJ, Liu Y, et al. Deficiency of Adenosine Deaminase 2 Triggers Adenosine-Mediated Netosis and Tnf Production in Patients With Dada2. *Blood* (2019) 134(4):395–406. doi: 10.1182/blood.2018892752
65. Borea PA, Gessi S, Merighi S, Varani K. Adenosine as a Multi-Signalling Guardian Angel in Human Diseases: When, Where and How Does It Exert Its Protective Effects? *Trends Pharmacol Sci* (2016) 37(6):419–34. doi: 10.1016/j.tips.2016.02.006
66. Di Giorgio S, Martignano F, Torcia MG, Mattiuz G, Conticello SG. Evidence for Host-Dependent Rna Editing in the Transcriptome of Sars-Cov-2. *Sci Adv* (2020) 6(25):eabb5813. doi: 10.1126/sciadv.abb5813
67. Berard E, Iordache A, Barrillon D, Bayle J. L-Carnitine in Dialysed Patients: The Choice of Dosage Regimen. *Int J Clin Pharmacol Res* (1995) 15(3):127–33.
68. Derin N, Agac A, Bayram Z, Asar M, Izgut-Uysal VN. Effects of L-Carnitine on Neutrophil-Mediated Ischemia-Reperfusion Injury in Rat Stomach. *Cell Biochem Funct* (2006) 24(5):437–42. doi: 10.1002/cbf.1251
69. Famularo G, De Simone C, Trinchieri V, Mosca L. Carnitines and Its Congeners: A Metabolic Pathway to the Regulation of Immune Response and Inflammation. *Ann NY Acad Sci* (2004) 1033:132–8. doi: 10.1196/annals.1320.012
70. Morawietz H, Julius U, Bornstein SR. Cardiovascular Diseases, Lipid-Lowering Therapies and European Registries in the Covid-19 Pandemic. *Cardiovasc Res* (2020) 116(10):E122–E5. doi: 10.1093/cvr/cvaa176
71. Servellita V, Syed AM, Morris MK, Brazer N, Saldhi P, Garcia-Knight M, et al. Neutralizing Immunity in Vaccine Breakthrough Infections From the Sars-Cov-2 Omicron and Delta Variants. *Cell* (2022) 185(9):1539–48.e5. doi: 10.1016/j.cell.2022.03.019
72. Wong JEL, Leo YS, Tan CC. Covid-19 in Singapore-Current Experience: Critical Global Issues That Require Attention and Action. *JAMA* (2020) 323 (13):1243–4. doi: 10.1001/jama.2020.2467
73. Chen N, Zhou M, Dong X, Qu J, Gong F, Han Y, et al. Epidemiological and Clinical Characteristics of 99 Cases of 2019 Novel Coronavirus Pneumonia in Wuhan, China: A Descriptive Study. *Lancet* (2020) 395(10223):507–13. doi: 10.1016/S0140-6736(20)30211-7
74. Reghunathan R, Jayapal M, Hsu LY, Chng HH, Tai D, Leung BP, et al. Expression Profile of Immune Response Genes in Patients With Severe Acute Respiratory Syndrome. *BMC Immunol* (2005) 6:2. doi: 10.1186/1471-2172-6-2
75. Calvert JK, Helbig KJ, Dimasi D, Cockshell M, Beard MR, Pitson SM, et al. Dengue Virus Infection of Primary Endothelial Cells Induces Innate Immune Responses, Changes in Endothelial Cells Function and Is Restricted by Interferon-Stimulated Responses. *J Interferon Cytokine Res* (2015) 35(8):654–65. doi: 10.1089/jir.2014.0195
76. Angka L, Market M, Ardolino M, Auer RC. Is Innate Immunity Our Best Weapon for Flattening the Curve? *J Clin Invest* (2020) 130(8):3954–6. doi: 10.1172/Jci140530
77. Rosa BA, Ahmed M, Singh DK, Choreno-Parra JA, Cole J, Jimenez-Alvarez LA, et al. Ifn Signaling and Neutrophil Degranulation Transcriptional Signatures Are Induced During Sars-Cov-2 Infection. *bioRxiv* (2020) 6:239798. doi: 10.1101/2020.08.06.239798
78. Freitas BT, Scholte FEM, Bergeron E, Pegan SD. How Isg15 Combats Viral Infection. *Virus Res* (2020) 286:198036. doi: 10.1016/j.virusres.2020.198036
79. Rosa BA, Ahmed M, Singh DK, Choreno-Parra JA, Cole J, Jimenez-Alvarez LA, et al. Ifn Signaling and Neutrophil Degranulation Transcriptional Signatures Are Induced During Sars-Cov-2 Infection. *Commun Biol* (2021) 4(1):290. doi: 10.1038/s42003-021-01829-4
80. Petrey AC, Qeadan F, Middleton EA, Pinchuk IV, Campbell RA, Beswick EJ. Cytokine Release Syndrome in Covid-19: Innate Immune, Vascular, and Platelet Pathogenic Factors Differ in Severity of Disease and Sex. *J Leukoc Biol* (2020) 109(1):55–66. doi: 10.1002/JLB.3COVA0820-410RRR
81. Silvin A, Chapuis N, Dunsmore G, Goubet AG, Dubuisson A, Derosa L, et al. Elevated Calprotectin and Abnormal Myeloid Cell Subsets Discriminate Severe From Mild Covid-19. *Cell* (2020) 182(6):1401–18 e18. doi: 10.1016/j.cell.2020.08.002
82. Kacprzyk J, Hughes GM, Palsson-McDermott EM, Quinn SR, Puechmaille SJ, O'Neill LAJ, et al. A Potent Anti-Inflammatory Response in Bat Macrophages May Be Linked to Extended Longevity and Viral Tolerance. *Acta Chiropterol* (2017) 19(2):219–28. doi: 10.3161/15081109acc2017.19.2.001
83. Goshua G, Pine AB, Meizlish ML, Chang CH, Zhang H, Bahel P, et al. Endotheliopathy in Covid-19-Associated Coagulopathy: Evidence From a Single-Centre, Cross-Sectional Study. *Lancet Haematol* (2020) 7(8):e575–82. doi: 10.1016/S2352-3026(20)30216-7
84. Gralinski LE, Sheahan TP, Morrison TE, Menachery VD, Jensen K, Leist SR, et al. Complement Activation Contributes to Severe Acute Respiratory Syndrome Coronavirus Pathogenesis. *mBio* (2018) 9(5):e01753–18. doi: 10.1128/mBio.01753-18

Conflict of Interest: The handling Editor LR declared a shared (parent) affiliation with the authors SL, FW, RS, WL, JZ.

The remaining authors declare that the research was conducted in the absence of any commercial or financial relationships that could be construed as a potential conflict of interest.

Publisher's Note: All claims expressed in this article are solely those of the authors and do not necessarily represent those of their affiliated organizations, or those of the publisher, the editors and the reviewers. Any product that may be evaluated in this article, or claim that may be made by its manufacturer, is not guaranteed or endorsed by the publisher.

frontiers | Frontiers in Immunology

TYPE Review
PUBLISHED 15 July 2022
DOI 10.3389/fimmu.2022.961796

OPEN ACCESS

EDITED BY
Chang Li,
Chinese Academy of Agricultural Sciences (CAAS), China

REVIEWED BY
Peisong Gao,
Johns Hopkins University, United States
Yutong Zhao,
The Ohio State University, United States

*CORRESPONDENCE
Xian-Bin Kong
kongxianbinvip@163.com
Long Yang
long yang@tjutcm.edu.cn
Gong Cheng
gongcheng@mail.tsinghua.edu.cn

†These authors have contributed equally to this work and share first authorship

SPECIALTY SECTION
This article was submitted to Molecular Innate Immunity, a section of the journal Frontiers in Immunology

RECEIVED 05 June 2022
ACCEPTED 27 June 2022
PUBLISHED 15 July 2022

CITATION
Ren Y, Miao J-M, Wang Y-Y, Fan Z, Kong X-B, Yang L and Cheng G (2022) Oncolytic viruses combined with immune checkpoint therapy for colorectal cancer is a promising treatment option.
Front. Immunol. 13:961796.
doi: 10.3389/fimmu.2022.961796

Oncolytic viruses combined with immune checkpoint therapy for colorectal cancer is a promising treatment option

Yi Ren[1†], Jia-Meng Miao[1†], Yuan-Yuan Wang[2,3†], Zheng Fan[4], Xian-Bin Kong[1*], Long Yang[2,3*] and Gong Cheng[5,6*]

[1]College of Traditional Chinese medicine, Tianjin University of Traditional Chinese Medicine, Tianjin, China, [2]Research Center for Infectious Diseases, Tianjin University of Traditional Chinese Medicine, Tianjin, China, [3]School of Integrative Medicine, Tianjin University of Traditional Chinese Medicine, Tianjin, China, [4]Department of Critical Medicine, The First Affiliated Hospital of Suzhou University, Suzhou, China, [5]Tsinghua-Peking Joint Center for Life Sciences, School of Medicine, Tsinghua University, Beijing, China, [6]Institute of Infectious Diseases, Shenzhen Bay Laboratory, Shenzhen, China

Immunotherapy is one of the promising strategies in the treatment of oncology. Immune checkpoint inhibitors, as a type of immunotherapy, have no significant efficacy in the clinical treatment of patients with pMMR/MSS/MSI-L mCRC alone. Therefore, there is an urgent need to find combination therapies that can improve the response rate of immune checkpoint inhibitors. Oncolytic viruses are a new class of cancer drugs that, in addition to directly lysing tumor cells, can facilitate the action of immune checkpoint inhibitors by modulating the tumor microenvironment and transforming "cold" tumors into "hot" ones. The combination of oncolytic viruses and immune checkpoint inhibitors is currently being used in several primary and clinical studies to treat tumors with exciting results. The combination of genetically modified "armed" OV with ICIs is expected to be one of the treatment options for pMMR/MSS/MSI-L mCRC. In this paper, we will analyze the current status of oncolytic viruses and ICIs available for the treatment of CRC. The feasibility of OV in combination with ICI for CRC will be discussed in terms of the mechanism of action of OV in treating tumors.

KEYWORDS

oncolytic viruses, immune checkpoint inhibitor, colorectal cancer, tumor microenvironment, immunotherapy

Introduction

Colorectal cancer (CRC) is one of the most common and deadly cancers in the world community. It is the second most common cancer in women and the third most common in men. In 2018, there were 1.8 million CRC cases and 880,792 deaths worldwide, and CRC incidence is increasing in people under 50 years of age (1). The standard conventional treatments for CRC are surgery, chemotherapy, and radiotherapy, but because these three approaches have therapeutic limitations, immunotherapy has emerged as one of the newer options for treating CRC. In contrast to standard treatments, immunotherapy uses the patient's immune system to fight cancer cells by modulating the innate and adaptive immune response, which overcomes the problem of specificity in tumor treatment and provides a further breakthrough in the treatment of CRC (2).

Immune checkpoint inhibitors (ICIs) are one of the popular immunotherapies for treating tumors in recent years, and they have shown exciting results in treating melanoma (3). Immune checkpoint inhibitors (ICIs) are monoclonal antibodies that activate the immune response by targeting and inhibiting immune checkpoints, including CTLA-4 and PD-1. Currently, ICIs have shown promising results in the treatment of mismatch-repair-deficient (dMMR) or high levels of microsatellite instability (MSI-H) (dMMR-MSI-H) CRC. However, ICIs have no benefit for treatment mismatch-repair-savvy (pMMR) and microsatellite stable (MSS) or low levels of microsatellite instability (MSI-L) (pMMR-MSI-L) CRC (4). Therefore, there is an urgent need to find combination therapies that can increase the response rate of pMMR/MSS/MSI-L mCRC to immune checkpoint inhibitors.

Oncolytic viruses (OVs) are a novel class of tumor therapeutic strategy to reduce tumors through preferential replication in tumor cells and stimulate host anti-tumor immunity to promote the lysis of tumors. There are many DNA and RNA viruses that can be used as OVs. At present, the viruses most commonly used in experimental cancer research are poxviruses, reoviruses, herpes simplex viruses (HSV), and adenovirus (5). The therapeutic activity of OVs is not limited to its tumor lytic activity but also includes the integrated modulation of the tumor microenvironment (TME) and immune system (6). Thus, OVs provide an ideal means to reverse immunosuppression of the tumor microenvironment and sensitize the tumor to immune checkpoint blockade (7). In addition, transgenes can be inserted into the OV genome through viral genome engineering techniques, where virally encoded gene expression can immunomodulate tumors. New OVs expressing checkpoint inhibitory antibody molecules can also be created. Through viral antibody therapy, i.e., genetic delivery of recombinant antibodies, combined with different modes of direct and indirect cancer cell killing, it can enhance the therapeutic efficacy, reduce the chance of drug resistance, and increase the local immune response to tumor cells (8).

With the marketing approval of the first oncolytic virus, Talimogene laherparepvec (T-VEC), for the treatment of advanced melanoma, oncolytic virus immunotherapy has been used in routine clinical oncology research (9). The combination of OVs with other immunotherapies, particularly with immune checkpoint inhibitors (ICIs), has shown promise as a treatment for oncology. The combination of OVs and ICIs could have a synergistic effect in increasing the response rate of tumor cells to immunotherapeutic agents, which may play an essential role in the future of clinical cancer treatment (10). This paper will analyze the oncolytic viruses that can be used to treat CRC and the current situation of ICIs in the treatment of CRC and discuss the feasibility of OVs combined with ICIs in the treatment of CRC from the mechanism of OVs in the treatment of tumor.

Oncolytic virus for treating colorectal cancer

Vaccinia virus

Vaccinia virus (VV) has a safety profile in humans as a smallpox vaccine. Recombinant VV has been used as an expression vector to enhance the tumor lytic effect and has been widely used in clinical trial studies in tumor models and patients with advanced solid cancers (11).

Researchers (12) constructed an attenuated strain of VG9 containing IL-24 (VG9-IL-24) targeting vaccinia virus. VG9-IL-24 induced specific and durable immune responses against colorectal tumors, produced enhanced killing of CRC cells, and inhibited the growth of colorectal cancer tumors, including through the induction of apoptosis in CRC cells *via* multiple apoptotic signaling pathways.

Colorectal cancer (CRC) frequently causes the spread of tumor cells within the peritoneal cavity, eventually leading to peritoneal carcinoma (PC) (13). Peritoneal metastases (PM) occur in about a quarter of CRC patients, and peritoneal metastases from CRC are considered to be the end-stage of the disease, second only to liver and lung metastases in terms of incidence, with a poor prognosis and one of the leading causes of patient death (14). A research team found that a GM-CSF carrying tumor lysing vaccinia virus JX-594 (pexastimogene devacirepvec, Pexa-Vec) effectively inhibits CRC peritoneal metastasis by selectively infecting and lysing peritoneal tumor cells and activating peritoneal dendritic cells (DCs) and CD8 T cells to restore peritoneal anti-cancer immunity (15).

Reoviruses

Oncolytic reovirus (pelareorep) is a non-enveloped dsRNA virus that selectively lyses KRAS-mutated colorectal tumor cells.

KRAS mutations are prevalent in 40-45% of colorectal cancer (CRC) patients, and treatment options are limited. One study found that (16), pelareorep preferentially induces autophagic mechanisms by up-regulating several vital autophagic proteins in KRAS mutations, which further triggers the apoptotic pathway, resulting in increased apoptosis and cell death in CRC cells. Meanwhile, it has also been demonstrated that (17) In CRC patients with KRAS mutations, pelareorep enhances immune efficacy and exerts tumor lytic effects by up-regulating the expression of surface peptides of MHC I molecules and activating CD4 and CD8 T cell populations.

HSV

Herpes simplex viruses can be classified into types I and II (HSV-1, HSV-2 for short). Related researchers have genetically modified HSV-1 to express IL-12. HSV-1 expressing IL-12 promotes the cytolytic activity of natural killer cells and cytotoxic T lymphocytes, infects and kills colorectal cancer cell lines, and promotes anti-tumor immunity (18). oHSV-2 has been shown to alter the tumor microenvironment (TME) by increasing the infiltration of immune cells (NK cells, CD8 cells, and DCs), leading the TME from an immunosuppressed state to an anti-tumor immune state, thus transforming a "cold" tumor into a "hot" one (19). Meanwhile, there is experimental evidence that (20) oHSV-2 has been shown to have anti-tumor activity in patients with metastatic rectal cancer, with better efficacy when oHSV-2 is combined with immune checkpoint inhibitors.

Adenovirus

Adenovirus is the more commonly used oncolytic virus vector, and the genome can be easily genetically modified to achieve better therapeutic results (21). At present, there are many genetically modified oncolytic adenoviruses used in the treatment of colorectal cancer. Researchers have constructed an oncolytic adenovirus (SPDD-UG) carrying SNORD44 (a C/D box snoRNA) and the GAS5 gene, which has been shown to inhibit the growth of colorectal cancer cells and induce apoptosis (22). In addition, an oncolytic adenovirus (rAd.DCN.GM) combining core proteoglycans and expressing granulocyte-macrophage colony-stimulating factor (GM-CSF) was shown to inhibit the growth and distant metastasis of colorectal cancer cells (23). In addition, a novel dual-targeted oncolytic adenovirus CD55-TRAIL combined with luteolin inhibited CRC cell proliferation while minimizing cytotoxicity to normal cells (24). A related experimental study found that adenovirus from a Non-human apes (GAd) encoding multiple neoantigens resulted in a novel GAd that effectively controlled tumor growth in mice and had a high potential for tumor eradication when combined with ICIs (25). Although the combination of adenovirus and ICIs has not yet been applied to colorectal cancer, there is still great promise in modifying adenovirus in various ways and using it in combination with ICIs to treat colorectal cancer.

Other viruses

An oncolytic measles virus (OMV) encoding IL-12 can effectively induce apoptosis in rectal colon cancer cells by activating the IL-12/IFN-c/TNF-a inflammatory response (26). Orf virus (ORFV) can rapidly mediate innate and adaptive immune responses *in vivo*, so it has been proposed as a potential oncolytic virus vector. Studies have demonstrated that ORFV strain NA1/11 can inhibit CRC growth and metastasis by inducing apoptosis in CRC cells (27). In addition, a research team (28) produced M51R genetically engineered recombinant virus from cDNA clones containing the M protein mutation to construct M51R vesicular stomatitis virus (M51R VSV), which inhibits CRC peritoneal surface spread (PSD). Combined with immune checkpoint inhibitors may enhance the oncolytic potential of M51R VSV by reversing the immunosuppressive microenvironment of the peritoneum. Coxsackievirus B3 (CVB3) strain PD effectively infected and lyse CRC cells in a mouse model of colorectal cancer and demonstrated a good safety profile (29). On this basis, the researchers generated the cDNA clone of CVB3 variant PD-0 and generated the recombinant CVB3 variant PD-H from the clone. In immunocompetent mice, PD-H showed potent oncolytic activity against colorectal cancer and prevented the development of tumor malignancy (30) (**Table 1**).

Current status of immune checkpoint inhibitors for colorectal cancer

Immune checkpoints are cell-surface proteins whose function is to control the initiation, duration, and magnitude of the immune response. Disruption of immune checkpoints is one way to inhibit tumor immune evasion and stop cancer progression. The two most clinically relevant checkpoints, CTLA4 and PD-1, act as brakes on the anti-cancer immune response. Therefore, by inhibiting PD-1 or CTLA4 checkpoints or simultaneously inhibiting PD-1 or CTLA4 checkpoints, tumor-specific T cells can be expanded and stimulated to perform anti-tumor functions (32).

Immune checkpoint inhibitors (ICIs) increase T-cell activity and the ability to kill tumor cells by inhibiting these immune checkpoint activities. At present, ICIs have been shown to have a

TABLE 1 Oncolytic virus available for colorectal cancer treatment.

Virus	Type of virus	Route of virus administration	Effect	References
VV	VG9-IL-24	i.t./i.p.	Significantly inhibits tumour growth and induces apoptosis in colorectal cancer cells	(12)
	JX-594	i.p.	Inhibition of CRC peritoneal metastasis and lysis of Peritoneal tumour cells	(15)
Reovirus	Pelareorep	i.t.	Lysis of KRAS-mutated CRC cells	(16)
	Pelareorep	Cell experiment	Promotes immune-mediated recognition and destruction of tumour cells	(17)
	RC402	p.o.	Significantly inhibits the growth of colorectal cancer tumours (combination with anti-PD-1 blockade)	(31)
HSV	Δ47/Δ34.5/IL12 HSV-1	Cell experiment	Effective in killing CRC cells	(18)
	oHSV-2	i.t.	Increased infiltration of immune cells	(19)
Adenovirus	SPDD-UG	i.t.	Inhibits CRC cell growth and induces apoptosis in CRC cells	(22)
	rAd.DCN.GM	i.t.	Significantly inhibits CRC tumour growth and distant metastasis	(23)
	CD55-TRAIL	Cell experiment/i.t.	Effective antitumour effects on CRC cells in vitro and in vivo (combination with luteolin)	(24)
Measles virus	MeVac FmIL-12	i.t.	Effective induction of apoptosis in CRC cancer cells	(26)
ORFV	NA1/11	i.t.	Inhibition of CRC growth and metastasis by induction of CRC apoptosis	(27)
VSV	M51R VSV	i.p.	Inhibited the growth of PSD in CRC	(28)
CVB3	PD	Cell experiment/i.t.	Efficient infection and lysis of CRC cells	(29)
	PD-H	i.t.	Effective tumourolytic activity against CRC	(30)

considerable improvement in the prognosis of patients with microsatellite instability-high (MSI-H)/DNA mismatch repair (dMMR) deficient (MSI-H/dMMR) tumors. In parallel, a series of clinical trials have demonstrated that patients with MSI-H/dMMR mCRC can be treated with Pembrolizumab and nivolumab monotherapy or nivolumab combined with Ipilimumab (33).

PD-1/PD-L1 inhibitors

Programmed cell death-1 (PD-1) is a transmembrane glycoprotein expressed in activated T cells, and programmed cell death ligand 1 (PD-L1) is expressed on antigen-presenting cells and tumor cells. In the tumor microenvironment, the release of cytokines (IFN-γ, ILs, TNF-α) can induce high levels of PD-L1 expression. At the same time, the binding of PD-1 to PD-L1 can induce tumor cells to evade immune surveillance by inhibiting T-cell activation and proliferation (34). Therefore, PD-1/PD-L1 inhibitors can restore the activity of T cells and their ability to kill tumor cells by blocking PD-1/PD-L1 signaling for therapeutic purposes (35).

Currently, the main PD-1 inhibitors used in clinical studies for treating colorectal cancer are Pembrolizumab and Nivolumab. Pembrolizumab is currently approved by the US Food and Drug Administration (FDA) for the first-line treatment of unresectable or metastatic colorectal cancer with high microsatellite instability or mismatch repair defects (36).

A KEYNOTE-164 clinical phase II study enrolled 124 patients with MSI-H/dMMR CRC receiving≥2 standard treatments. The results showed that in cohort A (fluoropyrimidine, oxaliplatin, and irinotecan in combination or not with anti-vascular endothelial growth factor/epidermal growth factor receptor monoclonal antibody), the ORR was 33%, including 2 CRS; In cohort B (≥ 1 previous treatment), the ORR was 33%, including 5 CRS. This study confirms the anti-tumor effects and clinical efficacy of Pembrolizumab in previously treated MSI-H/dMMR colorectal cancer patients (37). In the phase 3 KEYNOTE-177 trial, 307 MSI-H/dMMR CRC patients were enrolled in the study and randomly assigned to receive either Pembrolizumab or chemotherapy and 294 MSI-H/dMMR CRC patients (152 treated with Pembrolizumab and 142 with chemotherapy) were analyzed by HRQOL. These data further confirm the benefit of Pembrolizumab as a first-line treatment for patients with MSI-H/dMMR CRC (38).

Growing tumors show one of three patterns: (1) little or no tumor-infiltrating immune cell infiltration (“immune ignorance “). (2) the presence of intra-tumoural immune infiltration with minimal or no PD-L1 expression (“non-functional immune response”). (3) Immune infiltration that resides only around the outer edge of the tumor cell mass (“excluded infiltrate “). However, most treatment patients showed a lack of PD-L1 upregulation in tumor cells or tumor-infiltrating immune cells (39). Therefore, most cancer patients are resistant to PD-1/PD-L1 blockade. The presence of an “ immune brake” on activated T cells ensures that they will only mount an effective cytotoxic response if the antigenic stimulus

is of sufficient strength or affinity and is perceived in the context of an appropriate pro-inflammatory signal (40). Therefore, there is an urgent need to find alternative immunotherapeutic and anti-tumor approaches to use in combination with PD-1/PD-L1 inhibitors to overcome the limitations of ICIs in treating tumors.

CTLA-4 inhibitors

Cytotoxic T-lymphocyte antigen 4 (CTLA-4) is a member of the immunoglobulin-associated receptor family, and the binding of CTLA-4 to its ligand B7-2 protein inhibits T-cell proliferation activation and cytokine production while decreasing the immune response (41). Therefore, blocking CTLA-4 reactivates T cells and restores their ability to attack cancer cells. However, CTLA-4 blockers alone are ineffective in treating colorectal cancer. A clinical study showed that 47 pretreated mCRC patients treated with a CTLA-4 blocker (tremelimumab) failed to show clinically meaningful results after monotherapy (42). Therefore, combining CTLA-4 blockers with other drugs for colorectal cancer is a primary research direction.

Ipilimumab, a fully human immunoglobulin G1 monoclonal antibody capable of blocking CTLA-4, was approved by the FDA in July 2018 for the immune combination treatment of MSI-H mCRC after progression on standard chemotherapy. In a large combination immunotherapy study, the CheckMate-142 trial, 119 MSI-H/dMMR CRC patients were treated with Ipilimumab combined with the PD-1 inhibitor Nivolumab and had an investigator-assessed ORR of 55% (95% CI, 45.2-63.8) and a 12-week disease control rate of 80%. This demonstrates that Nivolumab and Ipilimumab synergistically promote T-cell anti-tumor activity through complementary mechanisms of action, which provides a clinical experimental basis for CTLA-4 inhibitors combined with PD-1 inhibitors in the treatment of MSI-H/dMMR mCRC (43). Therefore, this suggests a new strategy for the future treatment of colorectal cancer: through the complementary mechanism of dual inhibitors, block the inhibition of CTLA-4 on T cell activation in the early stage and PD-1 on T cell anti-tumor response in the later stage, improve the immune response and promote the anti-tumor immune response (44).

Other potential immune checkpoint targets in CRC

So far, only immunotherapies with two checkpoint targets, CTLA-4 and PD-L1/PD-1, have been approved for clinical use. However, most cancer patients do not respond to treatment with PD-1/PD-L1 inhibitors or CTLA-4 inhibitors. Therefore, as research progresses, several promising novel immune checkpoint targets are emerging as breakthrough points for cancer immunotherapy.

T-cell immunoglobulin and mucin-containing structural domain protein 3 (TIM-3) is a suppressive immune checkpoint molecule. TIM-3 has a suppressive effect on T-cell-induced immune responses. Blocking TIM-3 reverses T-cell dysfunction and restores anti-tumor immunity. Co-blockade of TIM-3 and PD-1 improves anti-cancer T cell responses in patients with advanced cancer (45). Increased TIM-3 expression in tumor tissue of CRC patients was positively correlated with poor prognosis and tumor progression. TIM-3 expression on CRC-infiltrating T cells in TME was significantly higher than TIM-3 expression on T cells in circulation. Furthermore, in CRC, the majority of TIM-3 expressing T cells in TME co-express PD-1 (46). A related study analyzed the expression of PD-1 and TIM-3 in patients with surgically treated stage I-III CRC. They found that CRC patients with high PD-1 and high Tim-3 expression had a worse prognosis than CRC patients with single high or double low expression. Thus, TIM-3 is a crucial mediator of CRC progression and may be a potential independent prognostic factor for CRC patients (47). Co-expression of TIM-3 and PD-1 on T cells may lead to resistance to ICIs in CRC patients. Therefore, treatment targeting Tim-3 with anti-PD-1 or other immunotherapies may provide clinical benefits for CRC patients (48).

TIGIT (T-cell immunoglobulin and immunoreceptor tyrosine motif (ITIM) structural domain) is a novel immune checkpoint. TIGIT is expressed on CD4 and CD8 T cells as well as innate lymphocytes, including NK cells and γδ T cells (49). PD-1 and CTLA-4 are predominantly expressed by tumor-infiltrating T cells and rarely by tumour-infiltrating NK cells. Therefore, using PD-L1/PD-1 and CTLA-4 inhibitors is not beneficial for NK cell failure. In contrast, blockade of TIGIT has been shown to prevent NK cell depletion and promote NK cell-dependent tumor immunity. At the same time, TIGIT, as a monotherapy, may be better able to reverse the failure of both T and NK cells (50). It has now been demonstrated that TIGIT is up-regulated in colorectal cancer with infiltrating lymphocytes, including CD3, CD4, CD8, and NK cells. By secreting TGF-β1, colorectal cancer cells can up-regulate TIGIT expression, promote CD8T cell depletion and facilitate tumor immune escape (51). Furthermore, it was found that elevated TIGIT on CD3 T cells led to functional defects and impaired glucose metabolism and that blocking TIGIT restored CD3 T cell activity and inhibited tumor growth. Thus, blocking TIGIT and restoring T-cell metabolic activity may represent immunotherapy for CRC (52).

LAG-3 is an Ig-like structural domain type I transmembrane protein with four structural domains called structural domain 1 (D1) to structural domain 4 (D4). Currently, LAG-3 is a promising therapeutic target for cancer immunotherapy. LAG-3 acts similarly to PD-1 and helps tumor cells to undergo immune escape (53). One study found that blocking both LAG-3 and PD-1 promoted T cell-mediated immune responses leading to a significant delay in tumor growth compared to anti-PD-1 antibody or anti-LAG-3 (LBL-007) treatment alone in CRC model mice. Thus, anti-LAG-3 and anti-PD-1 antibodies showed synergistic anti-tumor activity in CRC model mice. Anti-LAG-3 with anti-PD-1 could be a promising combination strategy for immunotherapy of CRC (54).

Currently, after the research results of PD-1 inhibitors and CTLA-4 inhibitors in the treatment of CRC, novel immune checkpoints such as TIM-3, TIGIT, and LAG-3 are not only potential biomarkers for diagnosis, prognosis, and survival prediction of CRC patients but also the next breakthrough point in immunotherapy for CRC. There are significant interactions between multiple immune checkpoints in the pathogenesis of CRC. Blocking one immune checkpoint alone may result in compensatory upregulation of other checkpoints. Therefore, combined blockade of multiple immune checkpoints may be a new immunotherapeutic strategy for CRC patients (55).

Mechanism of action of oncolytic viruses combined with immune checkpoint inhibitors

Immune checkpoint inhibitors are less effective in treating ''cold'' tumors

The tumor microenvironment (TME) refers to the complex multicellular environment in which tumors develop and typically includes T and B lymphocytes, tumor-associated macrophages (TAM), dendritic cells (DC), natural killer (NK) cells, neutrophils, and bone marrow-derived suppressor cells (MDSC) (56). The production of pro-inflammatory cytokines and the level of T-cell infiltration will somewhat alter the "cold" (non-T-cell inflammation) versus "hot" (T-cell inflammation) nature of TME, which closely correlates with the suppressive or supportive nature displayed during tumor development. ''hot'' tumors are characterized by molecular markers of T-cell infiltration and immune activation. "hot" tumors have a higher response rate to immunotherapy, whereas "cold" tumors show a marked T-cell deficiency or rejection (57). Many malignant tumor cells exhibit "cold" tumors. In addition to fewer infiltrating lymphocytes in TME, they exhibit low expression of PD -L1 and primary histocompatibility complex class I (MHC I) (58). Compared to "hot" tumors, immune checkpoint inhibitors have a minimal effect in treating "cold" tumors. Conversion of "cold" tumors to "hot" tumors will to some extent, increase the sensitivity of immunotherapy with immune checkpoint inhibitors. At the same time, combining relevant TME modulation therapies with checkpoint blockade is most likely to provide additional clinical benefits for patients with specific malignancies (59).

Oncolytic viruses sensitize ''cold'' tumors to immune checkpoint inhibitors by modulating TME

Oncolytic viruses are able to induce lysis of tumor cells, which releases tumor-associated antigens and neoantigens (TAAs and TANs) that can be captured by tumor-infiltrating antigen-presenting cells (APCs), resulting in increased T cell infiltration (60). Oncolytic viruses promote immunogenic cell death (ICD), leading to the release of danger-associated molecular patterns (DAMPs) such as calreticulin (CRT), high mobility group protein 1 (HMGB1), and ATP. At the same time, oncolytic viruses promote the maturation of DC cells and recruit immune effector cells to the vicinity of dead tumor cells, enhancing phagocytosis of tumor cells by local DCs and macrophages (61).

In addition to the release of DAMPs, OV-mediated cancer cell lysis is often associated with the release of various pathogen-associated molecular patterns (PAMPs), including viral components such as nucleic acids (DNA, dsRNA, ssRNA, and 5′-triphosphate RNA), proteins and capsid components. DAMPs and PAMPs are recognized by pattern recognition receptors on antigen-presenting cells (APCs) (such as DC and NK cells) and serve as "danger" and "eat me" signals. This signaling attracts more DCs to the TME, leading to increased recruitment and maturation of tumor-specific T cells into the TME (62). Thus, oncolytic viruses can activate innate and acquired immunity, increase T-cell infiltration and reverse the tumor microenvironment so that ''cold'' tumors can be effectively immunologically activated and transformed into ''hot'' tumors, thus facilitating the action of immune checkpoint inhibitors (63).

A clinical trial using transgenic herpes simplex virus type 1 (Talimogene laherparepvec) in combination with pembrolizumab in patients with advanced melanoma showed that OVs might make tumor cells more sensitive to immune checkpoint inhibitors by up-regulating PD-L1 expression (64). In addition, local injection of OVs into individual tumor sites induces a distant effect known as the "peritoneal effect". In this effect, distant uninfected tumors also experience immune-mediated rejection, inducing an inflammatory immune infiltrate (65). Thus, OVs and immune checkpoint inhibitors have complementary mechanisms of anti-tumor immunity, and the high selectivity of oncolytic viruses for tumor cells may lead to the local production of immune checkpoint inhibitors, thus providing a better safety profile for systemic administration (66) **(Figure 1).**

"Armed" recombinant oncolytic viruses enhance the efficacy of immune checkpoint inhibitors

To date, oncolytic viruses as monotherapy have provided only modest anti-tumor effects in patients. Therefore, in order to increase immune stimulation, OVs have been designed to provide therapeutic transgenes to "armed" oncolytic viruses (67). OVs can be used as a therapeutic platform by inserting transgenes into the oncolytic virus genome through viral genome engineering techniques to manipulate its structure to create a characteristic "armed" OVs. These "armed" OVs with immunostimulatory or anti-cancer transgenes can be used as

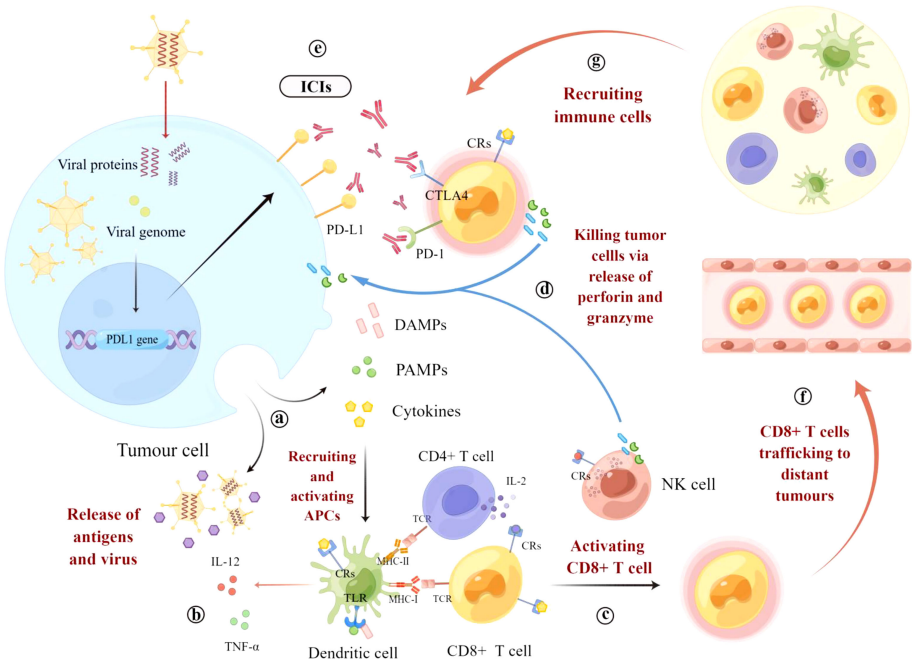

FIGURE 1
Mechanism of OVs combined with ICIs to stimulate anti-tumor immunity. **(A)** OVs enter tumor cells and undergo viral replication, leading to lysis and the release of danger-associated molecular pattern signals (DAMPs), pathogen-associated molecular patterns (PAMPs), tumor-associated antigens (TAAs), and pro-inflammatory cytokines. Viral progeny is also released, spreading to and infecting neighboring tumor cells. **(B)** These molecules recruit and activate antigen-presenting cells (APCs), such as dendritic cells (DCs), and promote the maturation of CDs through co-stimulatory markers while promoting the release of pro-inflammatory cytokines such as interleukin 12 (IL-12) and tumor necrosis factor (TNF-α) from CDs and recognition by cytokine receptors (CRs) on T cells and NK cells. **(C)** Mature dendritic cells cross-present antigens to CD4+ and CD8 + T cells *via* the major histocompatibility complex (MHC) and induce their expansion and activation. **(D)** T cells and NK cells eventually lyse tumor cells by releasing perforin, granzyme, and cytokines (IFN-γ, IL-2). **(E)** OVs infection leads to increased expression of immune checkpoint molecules such as PD-L1 and CTLA-4, thereby increasing the expression of the therapeutic targets of ICIs and sensitizing OV-infected tumor cells to ICIs. **(F)** In addition, local injection of OVs into individual tumor sites induces a distant effect, causing T cells to migrate to the site of metastatic disease, recognizing and killing distant tumor cells. **(G)** Cytokines and chemokines released in the tumor microenvironment can recruit immune cells for concerted anti-tumor activity.

monotherapy or in combination with other therapeutic modalities to reduce side effects and improve anti-tumor efficacy. If an "armed" OV is designed for systemic delivery, it could be one of the options for treating patients with metastatic tumors (68). Currently, the primary use is to genetically engineer oncolytic viruses to carry PD-1/PD-L1 antibody genes or otherwise "armed" them to enhance the sensitivity of tumor cells to ICIs.

"Armed" oncolytic viruses are carrying PD-1/PD-L1 antibody gene

Researchers built an "armed" oncolytic vaccinia virus (VV-iPDL1/GM) co-expressing PD-L1 inhibitor and GM-CSF. They found that intra-tumor injection with these engineered OVs promoted tumor infiltration of neoantigen-specific T cells while activating immune cells. VV-iPDL1/GM-secreted PD-L1 inhibitors inhibited neoantigen presentation of PD-L1 on tumor cells, leading to the systemic rejection of both the treated tumor and distant tumors. Therefore, using "armed" OVs co-expressing PD-L1 inhibitors and GM-CSF alone or combined with immune checkpoint inhibitors is a new therapeutic option for treating patients resistant to PD-1/PD-L1 blockade therapy (69). An M51R mutant vesicular stomatitis virus (VSV) has been engineered to express a single-chain antibody Fv fragment (scFv) encoded by the PD-L1 targeting antibody avelumab, a human IgG1 antibody. This novel OV effectively inhibited tumor growth in a mouse model. Thus, recombinant OVs expressing PD-1/PD-L1 antibodies are a promising agent for cancer therapy (70).

In a study, researchers encoded a humanized anti-PD-1 monoclonal antibody (anti-PD-1 monoclonal antibody) and designed a novel herpes simplex virus (HSV-aPD-1). Data from this experiment suggest that HSV-aPD-1 further improves the immune microenvironment and plays a crucial role in treating tumors that are not sensitive to ICIs or other immunotherapies (71). In addition, related studies have

developed bioengineered cell membrane nanobubbles (PD1-BCMNs) with PD-1 to carry oncolytic adenovirus virus (OA). PD1-BCMNs-OA can effectively activate tumor-infiltrating T cells and trigger a robust anti-tumor immune response. Thus, PD1-BCMNs-OA provides a clinical rationale for combining oncolytic virus therapy with immune checkpoint inhibitors (72).

"Armed" oncolytic virus enables enhanced anti-PD-1 therapy

The degree of inflammation in the tumor microenvironment affects the overall and progression-free survival rates. "Armed" OVs carrying the gene encoding inflammatory cytokines can further modify the tumor microenvironment. A study showed that a recombinant oncolytic poxvirus virus (hIL-7/mIL-12-VV) dually expressing IL-7 and IL-12 completely altered the tumor immune microenvironment by enhancing the inflammatory immune state, showing beneficial systemic anti-tumor efficacy, significantly increasing the sensitivity of solid tumors to systemic anti-PD-1 and anti-CTLA4. This combined IL-7 and IL-12 viral therapy could provide clinical benefit as a single therapy and has the potential to be effectively combined with immunotherapy for various types of solid tumors (73).

The anti-tumor efficacy of an engineered recombinant oncolytic herpes simplex virus (ONCR-177) with five transgenes was enhanced by systemic anti-PD-1 treatment. Experimental data showed that the RR of contralateral tumors treated with combination therapy was significantly enhanced by 40% RR compared with oncr-171 or anti-PD-1 monotherapy. Thus, ONCR-177 enhances tumor lysis tolerance and anti-tumor activity through activation of systemic immunity triggered by transgene expression and can be further enhanced by co-treatment with immune checkpoint inhibitors (74). It has been found that combined treatment with locally "armed" oncolytic adenovirus virus type 5 (ZD55-IL-24) and systemic PD-1 blockade resulted in synergistic suppression of locally and distantly established tumors. Local treatment with ZD55-IL-24 could help PD-1 blockade overcome the relatively low limitations of tumor immune infiltration and recognition. However, as ZD55-IL-24 must currently be administered intratumorally, it is only indicated for treating those few tumors with visible lesions such as melanoma and is challenging to use for the vast majority of tumors in clinical practice. Nonetheless, this study provides a viable experimental basis for the combination therapy of "armed" OVs (75).

In addition, a novel PD-L1 ICI with a cross-hybrid Fc region-mediated effector mechanism of IgG and IgA was designed. It is cloned as a conditionally replicating adenovirus (Ad-Cab) to limit virulence and release only into the tumor microenvironment. Ad-Cab secretes a cross-hybrid IgGA Fc fusion peptide that binds to PD-L1 binding and activates multiple immune pathways. Therefore, designing a novel ICI and expressing it with an oncolytic adenovirus could enhance tumor-killing efficacy while maintaining safety (76) (**Table 2**).

Application of oncolytic virus combined with immune checkpoint inhibitor in the treatment of colorectal cancer

Using ICIs for MSI/dMMR mCRC is a significant breakthrough in oncology. Unfortunately, the majority of mCRC patients are microsatellite stable (MSS)/DNA mismatch repair specialists (pMMR) (MSS/pMMR), and ICIs have not shown any clinical benefit in treating MSS/pMMR mCRC (77).

The oncolytic virus can enhance the response rate of tumors to immune checkpoint inhibitors. It is an ideal candidate for use in combination treatment strategies. Therefore, immune checkpoint inhibitors combined with the oncolytic virus may be a potential therapeutic option for treating MSS/pMMR mCRC.

Currently, experimental studies have shown that the use of oncolytic virus combined with immune checkpoint inhibitors has a better therapeutic effect on colorectal cancer. In an experimental study of triple immune therapy (combination of CSF-1R, OVs, and PD-1 antibodies) in a mouse model of CRC, 43% of the mice treated with the triple therapy achieved CR tumors and prolonged OS, and there was no tumor growth in 10 months from the implantation of CRC cancer cells to the end of the experiment. The researchers also observed a similar reduction in tumor load when T cells from surviving mice were treated with triple therapy and fed into the untreated CRC mouse model. Thus, this triple immune therapy therapeutic strategy could potentially overcome low T-cell infiltration and TAMs while overcoming the limitations of PD-1 immunosuppression. This could significantly improve the therapeutic efficacy of anti-PD-1 immunotherapy in colon cancer (7).

Researchers have established a telomerase-specific oncolytic adenovirus virus (OBP-301, telomerase) in which the human telomerase reverse transcriptase (hTERT) promoter element drives the expression of the viral E1A and E1B genes. This genetic modification allows OBP-301 to replicate in tumor cells and induce tumor cell-specific death selectively. In parallel, the researchers developed a CT26 *in situ* rectal tumor model with liver metastases, which was injected intra-tumorally with OBP-502 and treated in combination with PD-1 Ab. The results showed that this combination therapy inhibited liver metastases and rectal tumors. Thus, telomerase-specific oncolytic adenovirus virus led to a celiac effect by activating a systemic anti-tumor immune response, and the combination with PD-1 Ab produced a synergistic anti-tumor effect, even leading to tumor eradication (78).

TABLE 2 Modification and effects of "armed" oncolytic virus.

Modification type	"Armed"OVs	Modified features	Effect	References
Carries the PD-1/PD-L1 antibody gene	VV-iPDL1/GM	Co-expression of PD-L1 inhibitor and GM-CSF	Enhanced PD-1/PD-L1 inhibitor sensitivity	(69)
	VSV^{M51R}-PD-L1	Expression of a single-chain antibody Fv fragment encoded by the PD-L1-targeting antibody avelumab	Effective inhibition of tumour growth	(70)
	HSV-aPD-1	Encoding humanized anti-PD-1 monoclonal antibody	Improving the immune microenvironment to increase susceptibility to ICIs	(71)
	PD1-BCMNs-OA	Bioengineered cell nanomembranes carrying PD-1	Effective activation of tumour-infiltrating T cells to increase anti-tumour immune response	(72)
Carriage of other genes enables enhanced anti-PD-1 treatment	hIL-7/mIL-12-VV	Dual expression of IL-7 and IL-12	Enhancing inflammatory response to alter TME to improve anti-PD-1 and anti-CTLA-4 sensitivity	(73)
	ONCR-177	Carries five transgenes: IL12, FLT3LG, CCL4, anti-PD-1 and anti-CTLA-4	Activating systemic immunity to enhance anti-PD-1 therapy	(74)
	ZD55-IL-24	Insertion of the anti-tumour gene mda-7 and IL-24 gene	Increasing tumour immune infiltration to enhance anti-PD-1 efficacy	(75)
	Ad-Cab	Cloning from a novel PD-L1 ICI with a cross-hybrid Fc region of IgG and IgA	Activates multiple immune pathways to kill tumour cells	(76)

In addition, another trial further enhanced the sensitivity of immune checkpoint inhibitors in a mouse model of dMMR CRC by using a combination of low-dose mitomycin C (mitomycin) and oHSV. It was also found that this treatment strategy promoted the infiltration of activated conventional dendritic cells type 1 (cDC1s) into the tumor (79).

The most common route of oncolytic virus therapy is intra-tumor or intravenous administration, but its use in clinical practice is limited. Researchers have developed an orally available oncolytic reovirus, RC402, which breaks through the limitations of the use of lytic viruses in clinical treatment. Oral RC402 monotherapy significantly increased CD8+ cytotoxic T cells and decreased CD4 +CD25+Foxp3+ regulatory T cells in distant colon cancer. At the same time, the combination of RC402 and PD-1 inhibitor further inhibits colon cancer growth and enhances anti-tumor immunity within the tumor microenvironment, leading to complete tumor regression. Therefore, combining RC402 with PD-1 inhibitors could maximize the efficacy of PD-1 immune checkpoint blockade in colon cancer and trigger an effective anti-tumor immune response (31).

In a clinical trial, 15 patients with refractory colorectal cancer received intravenous oncolytic vaccinia virus Pexa-Vec (pexastimogene devacirepvec; JX-594) every 14 days. This is the first treatment for patients with refractory, metastatic colorectal cancer using repeated doses of Pexa-Vec and administered by intravenous infusion. Ten patients (67%) had imaging stable disease. This clinical trial showed safety against the vaccinia virus in patients given repeated intra-tumor doses every two weeks (80). In CRC peritoneal metastases, the efficacy of ICI monotherapy in peritoneal tumors and malignant ascites is extremely low. In contrast, intraperitoneal oncolytic vaccinia virus (JX-594) induced an intense infiltration of CD8 T cells into peritoneal tumors, reversing intraperitoneal TME and reprogramming peritoneal tumors into T-cell inflamed tumors. This study showed that when JX-594 was combined with a PD-1 inhibitor, it was able to trigger effective anti-cancer immunity and eliminate peritoneal metastases in colon cancer, allowing better control of peritoneal metastases and malignant ascites in advanced colon cancer. Therefore, combining JX-594 with ICI (anti-PD-1, anti-PD-L1, or anti-LAG-3) is a promising strategy for treating peritoneal metastases from CRC (15) (**Figure 2**).

Conclusions and challenges

In recent years, immune checkpoint inhibitors (ICIs) have become a promising strategy for treating tumors. However, in treating colorectal cancer (CRC), ICIs have shown promising results only in MSI/dMMR CRC and are very limited for treating pMMR/MSS/MSI-L mCRC. Oncolytic viruses can directly lyse tumor cells and increase T-cell infiltration by activating immunogenic cell death (ICD) and releasing danger-associated molecular patterns (DAMPs) to recruit and promote DC maturation. At the same time, OVs promote the action of immune checkpoint inhibitors by modulating the tumor microenvironment (TME) and transforming 'cold" tumors into 'hot" ones. Thus, combining oncolytic virus therapy with immune checkpoint inhibitors may break through the limitations of ICIs treatment MSS/pMMR mCRC and enhance the sensitivity of colorectal tumor cells to ICIs.

Currently, various oncolytic viruses such as vaccinia virus (VV), reoviruses, herpes simplex virus (HSV), and adenovirus have been widely used in experimental studies of colorectal cancer. Studies have demonstrated that OVs can inhibit the growth and distant metastasis of colorectal cancer cells by lysing CRC cells, inducing apoptosis, and reversing TME, and have

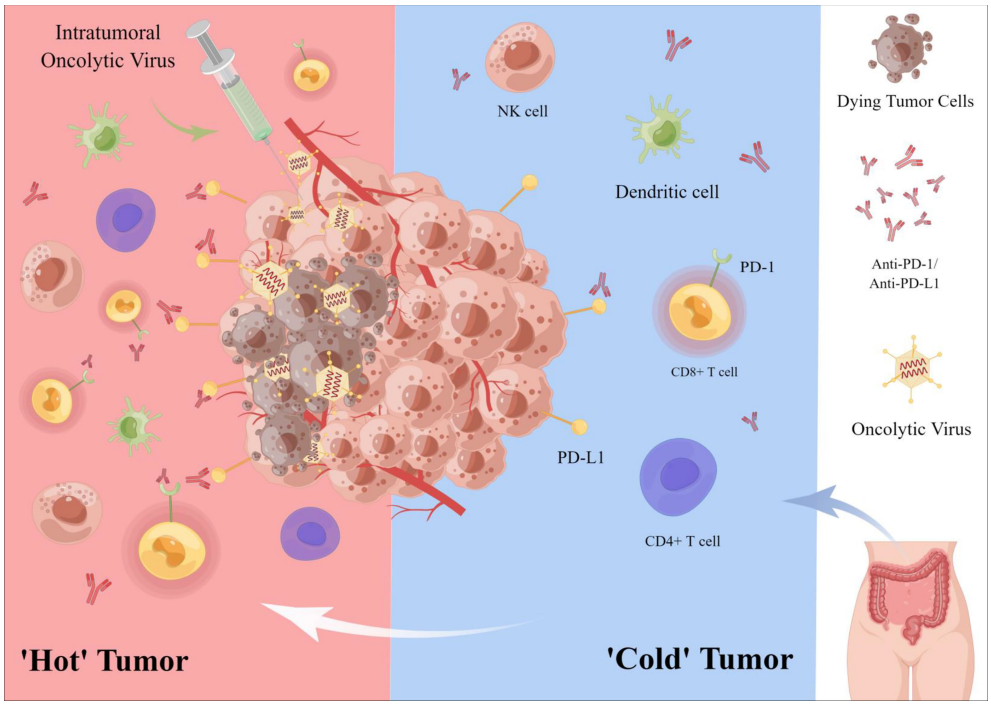

FIGURE 2
Oncolytic virus combined with immune checkpoint inhibitor in the treatment of colorectal cancer. OVs, lyse tumor cells while attracting immune cells (e.g., CD8+ T cells, NK cells) to the tumor microenvironment, thus transforming a 'cold'' tumor into a 'hot'' one to enhance the sensitivity of tumor cells to ICIs. In addition, OVs can enhance the targeted therapeutic effect of PD-1/PD-L1 inhibitors by up-regulating the expression of tumor cell immune checkpoint PD-L1.

shown exciting results in treating CRC peritoneal metastases and KRAS-mutated colorectal cancer. The combination of OVs and ICIs has become the most promising strategy for treating solid tumors today. Many researchers have used OVs as a therapeutic platform to achieve better therapeutic results, using viral genome engineering techniques to make OVs carry PD-1/PD-L1 antibody genes or other therapeutic genes, creating "armed" OVs. These "armed" OVs have a complementary mechanism to ICIs in terms of anti-tumor immunity, enhancing the targeted delivery of OVs, further increasing T-cell infiltration, and providing comprehensive regulation of TME and the immune system resulting in a more substantial anti-tumor immune response rate. Therefore, combining "armed" OVs and ICIs may be one option for treating pMMR/MSS/MSI-L mCRC.

However, although the combination of OVs and ICIs has shown therapeutic efficacy in animal models of CRC, the specific treatment and prognosis of this combination therapy for CRC patients is unclear due to the lack of clinical trial data on OVs in combination with ICIs in CRC patients. As the immune response is a complex and highly regulated biological process, the efficacy of OVs in combination with ICIs in animal models of CRC cannot be fully replicated in patients with CRC. However, the results of several animal studies and clinical trials in other solid tumors suggest that OVs and ICIs combination therapy remains a very promising strategy in treating tumors. In addition, antagonism and the occurrence of immune-related adverse events (irAEs) need to be considered when combining OVs with ICIs.

At present, it remains challenging to get OVs to every primary and metastatic tumor site to achieve the desired effect. In distant metastatic lesions with low T-cell infiltration, the therapeutic effect of OVs combined with ICIs may be minimal. Therefore, there is a need to continue the search for a more accurate and effective immunomodulatory factor to control OV-mediated anti-tumor T-cell responses (81).

In conclusion, the treatment of colorectal cancer is limited by the limited treatment strategies available. Currently, the combination of oncolytic viruses and immune checkpoint inhibitors has shown promise in several clinical trials. This strategy is expected to be a promising treatment option for colorectal cancer. It is believed that in the near future, the combination of OVs and ICIs will bring hope to pMMR/MSS/MSI-L mCRC patients through clinical trial studies.

Author contributions

Conceptualization: YR and X-BK; writing—review and editing: YR, J-MM, and Y-YW; visualization: ZF; supervision:

X-BK and LY; project administration: GC. All authors have read and agreed to the published version of the manuscript.

Funding

This research was funded by the Scientific research project of the Tianjin Education Commission, grant number 2021KJ134; Tianjin Municipal Education Commission Scientific Research Project, grant number 2019ZD11.

Acknowledgments

The figures were drawn by Figdraw (www.figdraw.com). We thank all the authors of the original work and reviewers for their time and kindness in reviewing this paper.

Conflict of interest

The authors declare that the research was conducted in the absence of any commercial or financial relationships that could be construed as a potential conflict of interest.

Publisher's note

References

1. Kanth P, Inadomi JM. Screening and prevention of colorectal cancer. *BMJ (Clinical Res ed.)* (2021) 374:n1855. doi: 10.1136/bmj.n1855

2. Johdi NA, Sukor NF. Colorectal cancer immunotherapy: options and strategies. *Front Immunol* (2020) 11:1624. doi: 10.3389/fimmu.2020.01624

3. Killock D. ICI for resected stage IV melanoma. *Nat Rev Clin Oncol* (2020) 17:450. doi: 10.1038/s41571-020-0397-8

4. Ganesh K, Stadler ZK, Cercek A, Mendelsohn RB, Shia J, Segal NH, et al. Immunotherapy in colorectal cancer: rationale, challenges and potential. *Nat Rev Gastroenterol Hepatol* (2019) 16:361–75. doi: 10.1038/s41575-019-0126-x

5. Macedo N, Miller DM, Haq R, Kaufman HL. Clinical landscape of oncolytic virus research in 2020. *J Immunother Cancer* (2020) 8:e001486. doi: 10.1136/jitc-2020-001486

6. Martin NT, Bell JC. Oncolytic virus combination therapy: killing one bird with two stones. *Mol Ther J Am Soc Gene Ther* (2018) 26:1414–22. doi: 10.1016/j.ymthe.2018.04.001

7. Shi G, Yang Q, Zhang Y, Jiang Q, Lin Y, Yang S, et al. Modulating the tumor microenvironment *via* oncolytic viruses and CSF-1R inhibition synergistically enhances anti-PD-1 immunotherapy. *Mol Ther J Am Soc Gene Ther* (2019) 27:244–60. doi: 10.1016/j.ymthe.2018.11.010

8. Kontermann RE, Ungerechts G, Nettelbeck DM. Viro-antibody therapy: engineering oncolytic viruses for genetic delivery of diverse antibody-based biotherapeutics. *MAbs* (2021) 13:1982447. doi: 10.1080/19420862.2021.1982447

9. Rehman H, Silk AW, Kane MP, Kaufman HL. Into the clinic: Talimogene laherparepvec (T-VEC), a first-in-class intratumoral oncolytic viral therapy. *J Immunother Cancer* (2016) 4:53. doi: 10.1186/s40425-016-0158-5

10. Lan Q, Xia S, Wang Q, Xu W, Huang H, Jiang S, et al. Development of oncolytic virotherapy: from genetic modification to combination therapy. *Front Med* (2020) 14:160–84. doi: 10.1007/s11684-020-0750-4

11. Guo ZS, Lu B, Guo Z, Giehl E, Feist M, Dai E, et al. Vaccinia virus-mediated cancer immunotherapy: cancer vaccines and oncolytics. *J Immunother Cancer* (2019) 7:6. doi: 10.1186/s40425-018-0495-7

12. Deng L, Yang X, Fan J, Ding Y, Peng Y, Xu D, et al. IL-24-Armed oncolytic vaccinia virus exerts potent anti-tumor effects *via* multiple pathways in colorectal cancer. *Oncol Res* (2021) 28:579–90. doi: 10.3727/096504020X15942028641011

13. Lemoine L, Sugarbaker P, van der Speeten K. Pathophysiology of colorectal peritoneal carcinomatosis: Role of the peritoneum. *World J Gastroenterol* (2016) 22:7692–707. doi: 10.3748/wjg.v22.i34.7692

14. Ceelen W, Ramsay RG, Narasimhan V, Heriot AG, De Wever O. Targeting the tumor microenvironment in colorectal peritoneal metastases. *Trends Cancer* (2020) 6:236–46. doi: 10.1016/j.trecan.2019.12.008

15. Lee YS, Lee WS, Kim CW, Lee SJ, Yang H, Kong SJ, et al. Oncolytic vaccinia virus reinvigorates peritoneal immunity and cooperates with immune checkpoint inhibitor to suppress peritoneal carcinomatosis in colon cancer. *J Immunother Cancer* (2020) 8:e000857. doi: 10.1136/jitc-2020-000857

16. Jiffry J, Thavornwatanayong T, Rao D, Fogel EJ, Saytoo D, Nahata R, et al. Oncolytic reovirus (pelareorep) induces autophagy in kras-mutated colorectal cancer. *Clin Cancer Res Off J Am Assoc Cancer Res* (2021) 27:865–76. doi: 10.1158/1078-0432.CCR-20-2385

17. Parakrama R, Fogel E, Chandy C, Augustine T, Coffey M, Tesfa L, et al. Immune characterization of metastatic colorectal cancer patients post reovirus administration. *BMC Cancer* (2020) 20:569. doi: 10.1186/s12885-020-07038-2

18. Haghighi-Najafabadi N, Roohvand F, Shams Nosrati MS, Teimoori-Toolabi L, Azadmanesh K. Oncolytic herpes simplex virus type-1 expressing IL-12 efficiently replicates and kills human colorectal cancer cells. *Microbial Pathog* (2021) 160:105164. doi: 10.1016/j.micpath.2021.105164

19. Zhang W, Hu X, Liang J, Zhu Y, Zeng B, Feng L, et al. OHSV2 can target murine colon carcinoma by altering the immune status of the tumor microenvironment and inducing antitumor immunity. *Mol Ther Oncolytics* (2020) 16:158–71. doi: 10.1016/j.omto.2019.12.012

20. Zhang B, Huang J, Tang J, Hu S, Luo S, Luo Z, et al. Intratumoral OH2, an oncolytic herpes simplex virus 2, in patients with advanced solid tumors: a multicenter, phase I/II clinical trial. *J Immunother Cancer* (2021) 9:e002224. doi: 10.1136/jitc-2020-002224

21. Niemann J, Kühnel F. Oncolytic viruses: adenoviruses. *Virus Genes* (2017) 53:700–6. doi: 10.1007/s11262-017-1488-1

22. Yuan S, Wu Y, Wang Y, Chen J, Chu L. An oncolytic adenovirus expressing SNORD44 and GAS5 exhibits antitumor effect in colorectal cancer cells. *Hum Gene Ther* (2017) 28:690–700. doi: 10.1089/hum.2017.041

23. Liu Z, Yang Y, Zhang X, Wang H, Xu W, Wang H, et al. An oncolytic adenovirus encoding decorin and granulocyte macrophage colony stimulating factor inhibits tumor growth in a colorectal tumor model by targeting pro-tumorigenic signals and *via* immune activation. *Hum Gene Ther* (2017) 28:667–80. doi: 10.1089/hum.2017.033

24. Xiao B, Qin Y, Ying C, Ma B, Wang B, Long F, et al. Combination of oncolytic adenovirus and luteolin exerts synergistic anti-tumor effects in colorectal cancer cells and a mouse model. *Mol Med Rep* (2017) 16:9375–82. doi: 10.3892/mmr.2017.7784

25. D'alise AM, Leoni G, Cotugno G, Troise F, Langone F, Fichera I, et al. Adenoviral vaccine targeting multiple neoantigens as strategy to eradicate large tumors combined with checkpoint blockade. *Nat Commun* (2019) 10:1–12. doi: 10.1038/s41467-019-10594-2

26. Wang J, Liu T, Chen J. Oncolytic measles virus encoding interleukin-12 mediated antitumor activity and immunologic control of colon cancer. *Cancer Biother Radiopharm* (2021) 36:774–82. doi: 10.1089/cbr.2019.3084

27. Chen D, Wang R, Long M, Li W, Xiao B, Deng H, et al. Identification of *in vitro* and *in vivo* oncolytic effect in colorectal cancer cells by orf virus strain NA1/11. *Oncol Rep* (2021) 45:535–46. doi: 10.3892/or.2020.7885

28. Day GL, Bryan ML, Northrup SA, Lyles DS, Westcott MM, Stewart JH. Immune effects of m51r vesicular stomatitis virus treatment of carcinomatosis from colon cancer. *J Surg Res* (2020) 245:127–35. doi: 10.1016/j.jss.2019.07.032

29. Hazini A, Pryshliak M, Brückner V, Klingel K, Sauter M, Pinkert S, et al. Heparan sulfate binding coxsackievirus b3 strain pd: a novel avirulent oncolytic

agent against human colorectal carcinoma. *Hum Gene Ther* (2018) 29:1301–14. doi: 10.1089/hum.2018.036

30. Hazini A, Dieringer B, Klingel K, Pryshliak M, Geisler A, Kobelt D, et al. Application route and immune status of the host determine safety and oncolytic activity of oncolytic coxsackievirus b3 variant pd-h. *Viruses* (2021) 13:1918. doi: 10.3390/v13101918

31. Kim C, Chon HJ, Lee HJ, Lee WS, Yang H, Kim JH, et al. Abstract 1914: orally available oncolytic reovirus, RC402, effectively promotes anti-cancer immunity and synergizes with immune checkpoint blockade in colon cancer. *Cancer Res* (2021) 81:1914–4. doi: 10.1158/1538-7445.AM2021-1914

32. Carlino MS, Larkin J, Long GV. Immune checkpoint inhibitors in melanoma. *Lancet (London England)* (2021) 398:1002–14. doi: 10.1016/S0140-6736(21)01206-X

33. Almquist DR, Ahn DH, Bekaii-Saab TS. The role of immune checkpoint inhibitors in colorectal adenocarcinoma. *BioDrugs: Clin Immunother Biopharm Gene Ther* (2020) 34:349–62. doi: 10.1007/s40259-020-00420-3

34. Wu Q, Jiang L, Li S-C, He Q-J, Yang B, Cao J. Small molecule inhibitors targeting the PD-1/PD-L1 signaling pathway. *Acta Pharmacol Sin* (2021) 42:1–9. doi: 10.1038/s41401-020-0366-x

35. Chen Y, Liu C, Zhu S, Liang X, Zhang Q, Luo X, et al. PD-1/PD-L1 immune checkpoint blockade-based combinational treatment: Immunotherapeutic amplification strategies against colorectal cancer. *Int Immunopharmacol* (2021) 96:107607. doi: 10.1016/j.intimp.2021.107607

36. Zhang X, Wu T, Cai X, Dong J, Xia C, Zhou Y, et al. Neoadjuvant immunotherapy for MSI-H/dMMR locally advanced colorectal cancer: new strategies and unveiled opportunities. *Front Immunol* (2022) 13:795972. doi: 10.3389/fimmu.2022.795972

37. Le DT, Kim TW, Van Cutsem E, Geva R, Jäger D, Hara H, et al. Phase II open-label study of pembrolizumab in treatment-refractory, microsatellite instability-high/mismatch repair-deficient metastatic colorectal cancer: keynote-164. *J Clin Oncol Off J Am Soc Clin Oncol* (2020) 38:11–9. doi: 10.1200/JCO.19.02107

38. Andre T, Amonkar M, Norquist JM, Shiu K-K, Kim TW, Jensen BV, et al. Health-related quality of life in patients with microsatellite instability-high or mismatch repair deficient metastatic colorectal cancer treated with first-line pembrolizumab versus chemotherapy (KEYNOTE-177): an open-label, randomised, phase 3 trial. *Lancet Oncol* (2021) 22:665–77. doi: 10.1016/S1470-2045(21)00064-4

39. Herbst RS, Soria J-C, Kowanetz M, Fine GD, Hamid O, Gordon MS, et al. Predictive correlates of response to the anti-PD-L1 antibody MPDL3280A in cancer patients. *Nature* (2014) 515:563–7. doi: 10.1038/nature14011

40. Zappasodi R, Merghoub T, Wolchok JD. Emerging concepts for immune checkpoint blockade-based combination therapies. *Cancer Cell* (2018) 33:581–98. doi: 10.1016/j.ccell.2018.03.005

41. Ben S, Zhu Q, Chen S, Li S, Du M, Xin J, et al. Genetic variations in the CTLA-4 immune checkpoint pathway are associated with colon cancer risk, prognosis, and immune infiltration *via* regulation of IQCB1 expression. *Arch Toxicol* (2021) 95:2053–63. doi: 10.1007/s00204-021-03040-0

42. Chung KY, Gore I, Fong L, Venook A, Beck SB, Dorazio P, et al. Phase II study of the anti-cytotoxic T-lymphocyte-associated antigen 4 monoclonal antibody, tremelimumab, in patients with refractory metastatic colorectal cancer. *J Clin Oncol Off J Am Soc Clin Oncol* (2010) 28:3485–90. doi: 10.1200/JCO.2010.28.3994

43. Overman MJ, Lonardi S, Wong KYM, Lenz H-J, Gelsomino F, Aglietta M, et al. Durable clinical benefit with nivolumab plus ipilimumab in dna mismatch repair-deficient/microsatellite instability-high metastatic colorectal cancer. *J Clin Oncol Off J Am Soc Clin Oncol* (2018) 36:773–9. doi: 10.1200/JCO.2017.76.9901

44. Ooki A, Shinozaki E, Yamaguchi K. Immunotherapy in colorectal cancer: current and future strategies. *J Anus Rectum Colon* (2021) 5:11–24. doi: 10.23922/jarc.2020-064

45. Wolf Y, Anderson AC, Kuchroo VK. TIM3 comes of age as an inhibitory receptor. *Nat Rev Immunol* (2020) 20:173–85. doi: 10.1038/s41577-019-0224-6

46. Khalaf S, Toor SM, Murshed K, Kurer MA, Ahmed AA, Abu Nada M, et al. Differential expression of TIM-3 in circulation and tumor microenvironment of colorectal cancer patients. *Clin Immunol (Orlando Fla.)* (2020) 215:108429. doi: 10.1016/j.clim.2020.108429

47. Kuai W, Xu X, Yan J, Zhao W, Li Y, Wang B, et al. Prognostic impact of pd-1 and tim-3 expression in tumor tissue in stage i-iii colorectal cancer. *BioMed Res Int* (2020) 2020:5294043. doi: 10.1155/2020/5294043

48. Klapholz M, Drage MG, Srivastava A, Anderson AC. Presence of Tim3 and PD-1 CD8 T cells identifies microsatellite stable colorectal carcinomas with immune exhaustion and distinct clinicopathological features. *J Pathol* (2022) 257:186–97. doi: 10.1002/path.5877

49. Chiang EY, Mellman I. TIGIT-CD226-PVR axis: advancing immune checkpoint blockade for cancer immunotherapy. *J Immunother Cancer* (2022) 10 e004711. doi: 10.1136/jitc-2022-004711

50. Zhang Q, Bi J, Zheng X, Chen Y, Wang H, Wu W, et al. Blockade of the checkpoint receptor TIGIT prevents NK cell exhaustion and elicits potent anti-tumor immunity. *Nat Immunol* (2018) 19:723–32. doi: 10.1038/s41590-018-0132-0

51. Li S, Ding J, Wang Y, Wang X, Lv L. CD155/TIGIT signaling regulates the effector function of tumor-infiltrating CD8+ T cell by NF-κB pathway in colorectal cancer. *J Gastroenterol Hepatol* (2022) 37:154–63. doi: 10.1111/jgh.15730

52. Shao Q, Wang L, Yuan M, Jin X, Chen Z, Wu C. TIGIT induces (CD3+) T cell dysfunction in colorectal cancer by inhibiting glucose metabolism. *Front Immunol* (2021) 12:688961. doi: 10.3389/fimmu.2021.688961

53. Maruhashi T, Sugiura D, Okazaki I-M, Okazaki T. LAG-3: from molecular functions to clinical applications. *J Immunother Cancer* (2020) 8: e001014. doi: 10.1136/jitc-2020-001014

54. Yu X, Huang X, Chen X, Liu J, Wu C, Pu Q, et al. Characterization of a novel anti-human lymphocyte activation gene 3 (LAG-3) antibody for cancer immunotherapy. *MAbs* (2019) 11:1139–48. doi: 10.1080/19420862.2019.1629239

55. Kamal AM, Wasfey EF, Elghamry WR, Sabry OM, Elghobary HA, Radwan SM. Genetic signature of CTLA-4, BTLA, TIM-3 and LAG-3 molecular expression in colorectal cancer patients: implications in diagnosis and survival outcomes. *Clin Biochem* (2021) 96:13–8. doi: 10.1016/j.clinbiochem.2021.06.007

56. Bejarano L, Jordão MJC, Joyce JA. Therapeutic targeting of the tumor microenvironment. *Cancer Discov* (2021) 11:933–59. doi: 10.1158/2159-8290.CD-20-1808

57. Duan Q, Zhang H, Zheng J, Zhang L. Turning cold into hot: Firing up the tumor microenvironment. *Trends Cancer* (2020) 6:605–18. doi: 10.1016/j.trecan.2020.02.022

58. Galon J, Bruni D. Approaches to treat immune hot, altered and cold tumours with combination immunotherapies. *Nat Rev Drug Discovery* (2019) 18:197–218. doi: 10.1038/s41573-018-0007-y

59. Kubli SP, Berger T, Araujo DV, Siu LL, Mak TW. Beyond immune checkpoint blockade: emerging immunological strategies. *Nat Rev Drug Discovery* (2021) 20:899–919. doi: 10.1038/s41573-021-00155-y

60. Malogolovkin A, Gasanov N, Egorov A, Weener M, Ivanov R, Karabelsky A. Combinatorial approaches for cancer treatment using oncolytic viruses: projecting the perspectives through clinical trials outcomes. *Viruses* (2021) 13:1271. doi: 10.3390/v13071271

61. Bommareddy PK, Shettigar M, Kaufman HL. Integrating oncolytic viruses in combination cancer immunotherapy. *Nat Rev Immunol* (2018) 18:498–513. doi: 10.1038/s41577-018-0014-6

62. Ylösmäki E, Cerullo V. Design and application of oncolytic viruses for cancer immunotherapy. *Curr Opin Biotechnol* (2020) 65:25–36. doi: 10.1016/j.copbio.2019.11.016

63. Hemminki O, Dos Santos JM, Hemminki A. Oncolytic viruses for cancer immunotherapy. *J Hematol Oncol* (2020) 13:84. doi: 10.1186/s13045-020-00922-1

64. Ribas A, Dummer R, Puzanov I, Vanderwalde A, Andtbacka RHI, Michielin O, et al. Oncolytic virotherapy promotes intratumoral T cell infiltration and improves anti-PD-1 immunotherapy. *Cell* (2017) 170:1109–19. doi: 10.1016/j.cell.2017.08.027

65. Zamarin D, Holmgaard RB, Subudhi SK, Park JS, Mansour M, Palese P, et al. Localized oncolytic virotherapy overcomes systemic tumor resistance to immune checkpoint blockade immunotherapy. *Sci Trans Med* (2014) 6:226ra232. doi: 10.1126/scitranslmed.3008095

66. Twumasi-Boateng K, Pettigrew JL, Kwok YYE, Bell JC, Nelson BH. Oncolytic viruses as engineering platforms for combination immunotherapy. *Nat Rev Cancer* (2018) 18:419–32. doi: 10.1038/s41568-018-0009-4

67. Watanabe N, Mckenna MK, Rosewell Shaw A, Suzuki M. Clinical CAR-T cell and oncolytic virotherapy for cancer treatment. *Mol Ther J Am Soc Gene Ther* (2021) 29:505–20. doi: 10.1016/j.ymthe.2020.10.023

68. Atasheva S, Shayakhmetov DM. Oncolytic viruses for systemic administration: engineering a whole different animal. *Mol Ther: J Am Soc Gene Ther* (2021) 29:904–7. doi: 10.1016/j.ymthe.2021.02.001

69. Wang G, Kang X, Chen KS, Jehng T, Jones L, Chen J, et al. An engineered oncolytic virus expressing PD-L1 inhibitors activates tumor neoantigen-specific T cell responses. *Nat Commun* (2020) 11:1395. doi: 10.1038/s41467-020-15229-5

70. Wu C, Wu M, Liang M, Xiong S, Dong C. A novel oncolytic virus engineered with PD-L1 scFv effectively inhibits tumor growth in a mouse model. *Cell Mol Immunol* (2019) 16:780–2. doi: 10.1038/s41423-019-0264-7

71. Tian C, Liu J, Zhou H, Li J, Sun C, Zhu W, et al. Enhanced anti-tumor response elicited by a novel oncolytic HSV-1 engineered with an anti-PD-1 antibody. *Cancer Lett* (2021) 518:49–58. doi: 10.1016/j.canlet.2021.06.005

72. Lv P, Chen X, Fu S, Ren E, Liu C, Liu X, et al. Surface engineering of oncolytic adenovirus for a combination of immune checkpoint blockade and virotherapy. *Biomater Sci* (2021) 9:7392–401. doi: 10.1039/D1BM00928A

73. Nakao S, Arai Y, Tasaki M, Yamashita M, Murakami R, Kawase T, et al. Intratumoral expression of IL-7 and IL-12 using an oncolytic virus increases systemic sensitivity to immune checkpoint blockade. *Sci Trans Med* (2020) 12: eaax7992.. doi: 10.1126/scitranslmed.aax7992

74. Haines BB, Denslow A, Grzesik P, Lee JS, Farkaly T, Hewett J, et al. ONCR-177, an oncolytic HSV-1 designed to potently activate systemic antitumor immunity. *Cancer Immunol Res* (2021) 9:291–308. doi: 10.1158/2326-6066.CIR-20-0609

75. Hu H-J, Liang X, Li H-L, Wang H-Y, Gu J-F, Sun L-Y, et al. Enhanced anti-melanoma efficacy through a combination of the armed oncolytic adenovirus ZD55-IL-24 and immune checkpoint blockade in B16-bearing immunocompetent mouse model. *Cancer Immunol Immunother CII* (2021) 70:3541–55. doi: 10.1007/s00262-021-02946-z

76. Hamdan F, Ylösmäki E, Chiaro J, Giannoula Y, Long M, Fusciello M, et al. Novel oncolytic adenovirus expressing enhanced cross-hybrid IgGA fc PD-L1 inhibitor activates multiple immune effector populations leading to enhanced tumor killing *in vitro*, *in vivo* and with patient-derived tumor organoids. *J Immunother Cancer* (2021) 9:e003000.. doi: 10.1136/jitc-2021-003000

77. Cohen R, Rousseau B, Vidal J, Colle R, Diaz LA, André T. Immune checkpoint inhibition in colorectal cancer: microsatellite instability and beyond. *Targeted Oncol* (2020) 15:11–24. doi: 10.1007/s11523-019-00690-0

78. Kanaya N, Kuroda S, Kakiuchi Y, Kumon K, Tsumura T, Hashimoto M, et al. Immune modulation by telomerase-specific oncolytic adenovirus synergistically enhances antitumor efficacy with anti-pd1 antibody. *Mol Ther J Am Soc Gene Ther* (2020) 28:794–804. doi: 10.1016/j.ymthe.2020.01.003

79. El-Sayes N, Vito A, Salem O, Workenhe ST, Wan Y, Mossman K. A combination of chemotherapy and oncolytic virotherapy sensitizes colorectal adenocarcinoma to immune checkpoint inhibitors in a cdc1-dependent manner. *Int J Mol Sci* (2022) 23:1754. doi: 10.3390/ijms23031754

80. Park SH, Breitbach CJ, Lee J, Park JO, Lim HY, Kang WK, et al. Phase 1b trial of biweekly intravenous pexa-vec (jx-594), an oncolytic and immunotherapeutic vaccinia virus in colorectal cancer. *Mol Ther J Am Soc Gene Ther* (2015) 23:1532–40. doi: 10.1038/mt.2015.109

81. Shi T, Song X, Wang Y, Liu F, Wei J. Combining oncolytic viruses with cancer immunotherapy: establishing a new generation of cancer treatment. *Front Immunol* (2020) 11:683. doi: 10.3389/fimmu.2020.00683

frontiers | Frontiers in Immunology

TYPE Review
PUBLISHED 25 August 2022
DOI 10.3389/fimmu.2022.971674

OPEN ACCESS

EDITED BY
Jieying Bai,
Academy of Military Medical Sciences (AMMS), China

REVIEWED BY
Wenyan Zhang,
First Affiliated Hospital of Jilin University, China
Guoli Shi,
National Institutes of Health (NIH), United States

*CORRESPONDENCE
Xianbin Kong
kongxianbinvip@163.com
Jingyan Meng
mengjy@163.com
Long Yang
long.yang@tjutcm.edu.cn
Shan Cen
shancen@imb.pumc.edu.cn

†These authors have contributed equally to this work

SPECIALTY SECTION
This article was submitted to Molecular Innate Immunity, a section of the journal Frontiers in Immunology

RECEIVED 17 June 2022
ACCEPTED 08 August 2022
PUBLISHED 25 August 2022

CITATION
Li Q, Tan F, Wang Y, Liu X, Kong X, Meng J, Yang L and Cen S (2022) The gamble between oncolytic virus therapy and IFN.
Front. Immunol. 13:971674.
doi: 10.3389/fimmu.2022.971674

The gamble between oncolytic virus therapy and IFN

Qingbo Li[1†], Fengxian Tan[2,3†], Yuanyuan Wang[2,3], Xiaohui Liu[3], Xianbin Kong[1*], Jingyan Meng[1*], Long Yang[2,3*] and Shan Cen[4*]

[1]College of Traditional Chinese medicine, Tianjin University of Traditional Chinese Medicine, Tianjin, China, [2]Research Center for Infectious Diseases, Tianjin University of Traditional Chinese Medicine, Tianjin, China, [3]School of Integrative Medicine, Tianjin University of Traditional Chinese Medicine, Tianjin, China, [4]Institute of Medicinal Biotechnology, Chinese Academy of Medical Science, Beijing, China

Various studies are being conducted on oncolytic virotherapy which one of the mechanisms is mediating interferon (IFN) production by it exerts antitumor effects. The antiviral effect of IFN itself has a negative impact on the inhibition of oncolytic virus or tumor eradication. Therefore, it is very critical to understand the mechanism of IFN regulation by oncolytic viruses, and to define its mechanism is of great significance for improving the antitumor effect of oncolytic viruses. This review focuses on the regulatory mechanisms of IFNs by various oncolytic viruses and their combination therapies. In addition, the exerting and the producing pathways of IFNs are briefly summarized, and some current issues are put forward.

KEYWORDS

oncolytic virus, IFN, signaling, oncology, tumor, cancer, immunology

1 Introduction

In recent years, research on tumor treatment by oncolytic viruses has been carried out continuously, and the related mechanism studies have been explored step by step, including direct lysis of tumor cells, inhibition of tumor angiogenesis and activation of human immunity (1). Among these mechanisms, IFN, as an active component of the human immune system, always plays an essential role in the treatment of tumors (2–4). Viruses can cause changes in IFN, as can oncolytic viruses. The release of IFN activates the human immune response through various pathways, thereby reversing the immunosuppressive state of the tumor microenvironment, which plays a positive role in tumor treatment.

There is an unstable effect of oncolytic virus therapy when applied to tumor treatment, which is very closely related to the effect of IFN. On the one hand, many tumor cells have an intact IFN pathway, which will have an immune clearance effect on the oncolytic virus (5) and cannot continue to exert therapeutic effect on tumor cells. On the other hand, the IFN secretion caused by oncolytic viruses will recruit more immune

cells, and the antiviral effect they play will undoubtedly be the extinction for oncolytic viruses, which eventually leads to making the therapeutic effect greatly reduced.

However, incomplete IFN pathway genes are present in some cells in cancer patients. It has been shown that nearly half of the 85 genes with methylation-dependent down-regulation after immortality are associated with IFN signal transduction (6), the deletion of these genes is more common in glioma, leukemia, and bladder cancer cells (7–9). Besides, pancreatic cancer, gastric cancer, hepatocellular carcinoma, and colon cancer all exhibit low expression of IFN receptors (10–14). In addition to tumor cells, many cancer patients have impaired IFN signaling in immune cells (15). Although these defects allow tumor cells to survive and can accelerate tumor cell proliferation, the absence of the IFN pathway allows the virus to escape from the immune system, thereby avoiding immune clearance and increasing the efficiency of viral tumor lysis (16). Therefore, clarifying the mechanism of action between oncolytic virus and IFN will provide a strategy for combining oncolytic virus with other therapies or modifying oncolytic virus. This will help us to properly deal with the relationship between IFN and oncolytic virus, which is very important to achieve enhanced anti-tumor effects.

In this review, it presents a 5-year review of the mechanisms of action of various oncolytic virus therapies associated with IFN. Beyond that, the mechanisms of IFN production and signaling are briefly introduced. This demonstrates the current level of research on oncolytic virus therapies in order to hopefully provide new ideas for future studies on the mechanisms regulating IFN. Of course, some of these issues need to be noted.

2 IFN generation and signals transmission

2.1 Generation of IFN

IFN was discovered in humans more than 50 years ago for its ability to elicit antiviral responses in cells (17). Currently, IFNs are classified into three types based on their sequences and cellular receptors, which including the IFNs of type I, type II and type III (18, 19). There are some differences in the pathways of production of different types of IFNs.

2.1.1 Generation of type I IFN

The type I IFN family consists of several genetically encoded members, among which IFN-α and IFN-β are well known. In fact, they can be specifically divided into 16 species, which contain 12 IFN-α isoforms, IFN-β, IFN-ϵ, IFN-κ, and IFN-ω (20–27). The production of type I IFN is induced by pathogen-associated molecular patterns (PAMPs). These PAMPs can stimulate Toll-like receptors (TLRs) located on the cell membrane or endosomal membrane (28), or cytosolic pattern recognition receptors, including nucleotide sensors such as retinoid acid-inducible gene I(RIG-I)-like receptors (RLRs) or DNA sensors, to induce IFN production (29).

Firstly, the generation of type I IFNs is dependent on the TLR pathway. TLR recognizes double-stranded RNA and single-stranded RNA or double-stranded DNA, respectively, through TLR3, 7/8, and 9 (30), which activate and mediate IFN regulatory factor (IRF) to generate type I IFN (28, 31, 32). Second, type I IFN production can also occur through a non-TLR-dependent pathway. RIG-I and melanoma differentiation-associated protein 5 (MDA5) recognize endogenous RNA (single- and double-stranded, respectively) (33) and activate IRF3 and IRF7 to generate type I IFN through a mitochondrial antiviral signaling protein (MAVS)-dependent mechanism. In addition, endogenous cytoplasmic double-stranded DNA (dsDNA)-triggered synthesis of cyclic GMP-AMP (cGAMP) activates IFN gene stimulating protein (STING), which induces IRF3 to produce type I IFN (34).

2.1.2 Generation of type II IFN

There exists only one type of type II IFN, that is IFN-γ. Diverse cells in the immune system are the primary source of its secretion, including innate-like lymphocyte populations such as innate lymphocytes (ILC) and natural killer (NK) cells, and also adaptive immune cells consisting of T helper 1 (Th1) cells and CD8 cytotoxic T lymphocytes (CTL) (35).

First of all, in innate lymphocytes, microbial infection or tissue injury activates pattern recognition receptors (PRR) as well as broadly reactive antigen receptors, which induce IFN-γ production. In addition, cytokines which consisting of interleukin (IL)-12 and IL-18 can also lead to IFN-γ production. Second, in adaptive immune cells, T-cell receptor (TCR)-mediated recognition of microbial peptides causes sustained high levels of IFN-γ production in Th1 cells and CTL. However, the mechanism of IFN-γ production differs between the two cell types, with Th1 cells producing IFN-γ associated with major histocompatibility complex (MHC) Class II molecules, whereas CTL production of IFN-γ is associated with MHC Class I molecules (35).

2.1.3 Generation of type III IFN

Type III IFN was discovered later (known as IFN-λ) and it was reported in 2003 for the first time (36, 37). It includes four kinds of IFN-λ isoforms, namely IFN-λ1 or IL-28a, IFN-λ2 or IL-28b, IFN-λ3 or IL-29, and IFN-λ4 (38–40). Similarly, viruses can mediate the expression of type III IFNs in diverse cell types (41–43).

Type III IFN is expressed in various primary human cells of the hematopoietic spectrum (44–48), in parallel with the production of large amounts of type I IFN. Meanwhile, type

III IFN is mainly produced by epithelial cells in non-hematopoietic cells (49–51). However, the exact mechanism by which it produces is not clearly explained. It has been claimed that the HSV molecular pattern is distinguished by TLR3 and TLR9 in the endosome as well as melanoma differentiation-associated gene 5 (MDA5) in the cytoplasm, which leads to the activation of nuclear factor κB (NF-κB), IRF3 and IRF7 transcription factors and their subsequent translocation to the nucleus, where they then stimulate IFN-λ gene transcription (52). In this process, the transcriptional mediator Med23 and anchoring protein repeat domain protein 1 (ANKRD1) target IRF7 and IRF3, individually, which promote the gene of type III IFN expression (53, 54).

2.2 Signal transduction of IFN

When IFN acts, it is transduced through different pathways. The three IFNs mainly signal through the Janus kinase/signal transducer and activator of transcription (JAK/STAT) pathway. There are both similarities and differences. The main differences are that the signaling of the three IFNs is carried out through the binding of different heterodimeric receptor complexes (20) (Figure 1).

Type I IFN is bound to a heterodimer of type I interferon α/β receptor 1 (IFNAR1) and IFN-α/β receptor 2 (IFNAR2) (18, 55). Signaling through the JAK/STAT pathway is the most common, which starts with phosphorylation of JAK1 and tyrosine kinase (TYK)2 and leads to phosphorylation of STAT1 as well as STAT2. Phosphorylated STATs are able to form heterodimers. The heterodimers will enter the nucleus and link with IRF9 to create the transcriptional activator IFN-stimulated gene factor (ISGF) 3. Next, ISGF3 integrates with the transcriptional enhancer called IFN-stimulated response element (ISRE), leading to transcriptional induction of ISGs (56–59). Besides this typical pathway, type I IFN can induce the expression of other genes, through STAT1 or STAT3 homodimers as well. For instance, homodimers formed by STAT1 combined with gamma activated sequence (GAS) elements that belong to different genes' promoters (60). STAT1 and STAT3 are the most frequent, but it has also been shown that in some cell types, STAT-3, -4, -5, and -6 can also be activated by interferon receptor (IFNAR), causing the next series of signaling cascades (61).

Type II IFN is bound to type II interferon gamma receptor 1 (IFNGR1) and IFN-γ receptor 2 (IFNGR2) (18, 55). The JAK/STAT pathway can be activated as well, although not in the same way as the changes in the JAK/STAT pathway caused by type I IFN. In this pathway, type II IFN can signal through ISGF3 as type I IFN does (62), causing the following series of responses. The difference is that the phosphorylation of JAK2 upon binding of type II IFN to its receptor is accompanied by allowing phosphorylation of JAK1 and IFNGR1 (63), which will recruit and phosphorylate STAT1s. Then, the homodimer formed by

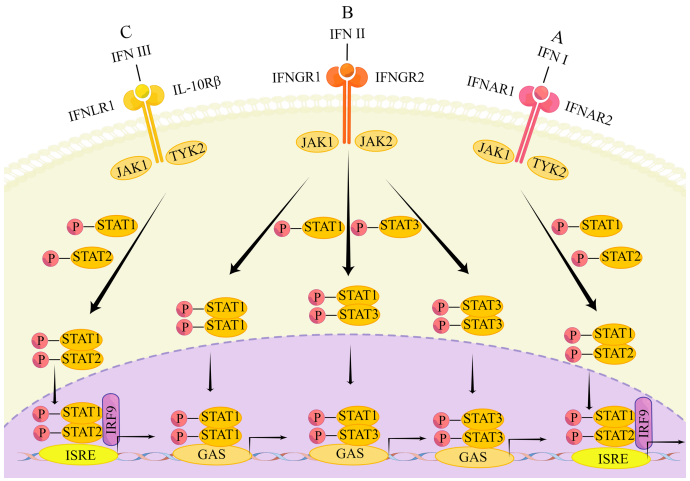

FIGURE 1
The main transduction pathway of IFN signaling. **(A)** IFN first binds to the heterodimers of IFNAR1 and IFNAR2, causing phosphorylation of JAK1 and TYK2, followed by phosphorylation of STAT1 and STAT2. Phosphorylated STATs form heterodimers that enter the nucleus and bind to IRF9 to form ISGF3, which subsequently binds to the transcriptional enhancer ISRE, triggering transcriptional induction of ISG. **(B)** Type II IFNs first bind to IFNGR1 and IFNGR2, causing phosphorylation of STAT1 and STAT2. The phosphorylated STAT forms a heterodimer that enters the nucleus and binds to IRF9 to form ISGF3. ISGF3 subsequently binds to the transcriptional enhancer ISRE, triggering the transcriptional induction of ISG. In addition, phosphorylated STAT1 homodimers, STAT3 homodimers and STAT1-STAT3 heterodimers enter the nucleus. These dimers bind to GAS elements to induce transcription factor production and initiate a second wave of gene expression; **(C)** Type III IFN binds to IFNLR1 and IL10R2, followed by the same response as the type I IFN signaling cascade.

phosphorylated STAT1 enters the nucleus, unites with the GAS element to induce transcription, inducing the generation of many transcription factors that initiate the second wave of gene expression (64). Furthermore, IFN-γ signaling can activate not only STAT1 homodimers, but also generate STAT3 homodimers and STAT1-STAT3 heterodimers. These still translocated to the nucleus to combined with the GAS element that is in the IRG gene promoter (65, 66). Apart from the above pathway, type II IFN can trigger the expression of MHCII as well, that is by inducing a different piece of genes through the function of the class II, major histocompatibility complex, transactivator (CIITA) (67).

Type III IFN is bound to interferon λ receptor 1 (IFNLR1) and IL-10 receptor 2 (IL10R2) (also known as IL-10 receptor β (IL10Rβ)) (18, 55). The induced signaling pathway is also essentially the same as that of type I IFN (36). Type III IFNs similarly form ISGF3 through phosphorylated STAT1 and STAT2, followed by binding to IRF9, which in turn triggers the expression of ISGs (42). Alternatively, type III IFN can induce the activation of STAT-3, -4, and -5 in certain cell types (68). However, the durability of ISG induction by type III IFN is demonstrated by the fact that ISGs peak later after type III IFN stimulation and persist over time. In contrast, type I IFN only induces ISG expression at an early stage and persists for a relatively short period of time (69).

Aside from the classical pathway of JAK/STAT, the three IFNs can also function in other signaling pathways, including MAPK and PI3-kinase pathways (61, 70). In addition, type I IFN can also activate and signal through the NF-κB pathway, and type II IFN can function through this pathway as well (70). Also, the bioinformatic analysis revealed the presence of NF-κB binding sites in the promoter of the type III IFN gene (68), suggesting the possibility that it also acts in the NF-κB pathway.

3 IFN and tumor treatment

IFN is able to modulate multiple pathways to achieve tumor inhibition or killing. This has been demonstrated in several experimental studies.

Under *in vitro* conditions, IFN can inhibit tumor growth through various pathways. First, IFN can affect the cell cycle of tumor cells. For example, IFNα can arrest the cell cycle of prostate cancer cells, which is achieved by upregulating endogenous inhibitors of cell cycle protein-dependent protein-dependent kinases, such as p21 (71); it has been discovered that type I IFNs can prolong the cell cycle of human breast cancer cells under *in vitro* conditions, which can suppress the growth of tumor cells (72). Second, IFN can also induce apoptosis of tumor cells. It has been shown that type I IFNs and Toll-like receptor 3 (TLR3) agonists when combined, are able to upregulate DR ligands, tumor necrosis factor-related apoptosis-inducing ligand (TRAIL), thus leading the breast tumor cell lines to be apoptotic (64). Moreover, type I IFN-induced apoptosis was connected with other ISGs, consisting of Fas, Fas ligand (FASLG), protein kinase R (PKR), and 2′-5′-oligoadenosine synthase (OAS) (64).

In the vivo environment, IFNs have been suggested to have a crucial role in tumorigenesis process. For example, in studies of 3-methylcholanthrene (MCA)-induced sarcoma models, it was found that deletion of immune cell type I and/or type II IFN signaling pathways sped up tumorigenesis and development (73, 74). Furthermore, STAT1 is thought to exert antitumor effects in transgenic mouse models of breast cancer through activation of immune and antiproliferative mechanisms (75), which is significant in type three types of IFNs signaling.

4 Molecular mechanisms by which different oncolytic virus therapies affect the IFN pathway

4.1 Vesicular stomatitis lysis virus

VSV is a prototypical member of the genus Blister virus, belonging to the family Rhabdoviridae (76). Recently, it has been extensively studied as an oncolytic agent (77). Among the IFN-related mechanisms, VSV mainly regulates IFN-induced antiviral factors, the expression of classical JAK/STAT, nuclear factor red lineage 2-related factor 2 (Nrf2), and IFN-mediated programmed cell death-ligand 1 (PD-L1) (Figure 2).

The type I IFN response is considered as an essential pathway for the development of drug resistance to VSV during tumor treatment, and tumor cells with intact or partially intact IFN signaling are resistant to viral replication (78–80). Human A375 as well as mouse B16-OVA melanoma cell lines were reported to be shielded by type I IFN and resistant to tumor lysis by wild-type VSV and VSV-GP (81)., thus preventing VSV from exerting its normal antitumor effects. VSV significantly upregulates the JAK/STAT pathway, which is an important component of the functioning of IFN. Inhibition of this link can effectively improve resistance to VSV therapy. In a preclinical trial in small cell lung cancer, the use of the JAK/STAT inhibitor lusolidin effectively increased viral replication, and the killing effect of VSV-IFN-β on tumor cells was enhanced *in vitro* conditions. Besides, it turned out that PD-L1 expression was restricted, which was also beneficial for tumor treatment. However, this combination treatment strategy did not significantly improve the survival rate of mice (82), so the safety of this combination therapy is uncertain. Additionally, this pathway was also studied in an animal experiment in melanoma, where tumor sensitivity to VSV-Δ51 was significantly increased under conditions of JAK/STAT pathway inhibition (83).

PD-L1 performs a functional role in regulating the cancer immune clearance cycle by binding to T cell-activated negative regulators, such as programmed cell death-1 (PD-1) and B7.1 (CD80) (84). In order to inhibit the killing effect on tumor cells,

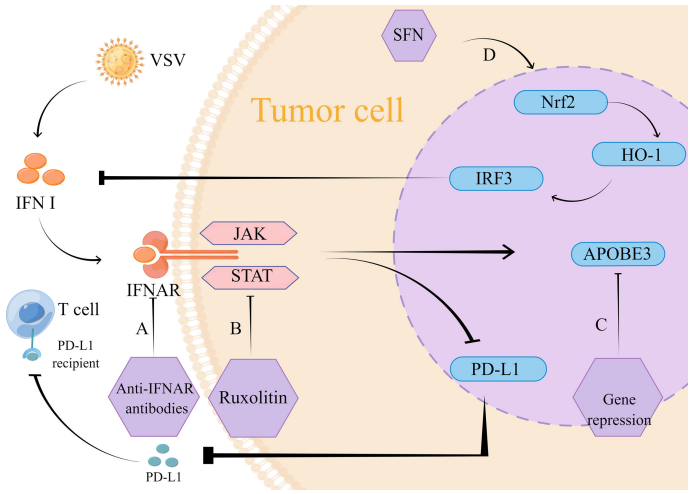

FIGURE 2
Mechanism of action of VSV therapy. **(A)** The intervention of monoclonal IFNAR antibody blocks the VSV-mediated IFN inflammatory pathway and reduces type I IFN-induced PD-L1 expression. Its low expression reduced PD-L1 binding to T cells, which thus exerted normal antitumor effects. **(B)** VSV strongly induced the JAK/STAT pathway, and inhibition of JAK/STAT using lusolidin prevented IFN-mediated antiviral response to VSV immune clearance, which promoted VSV replication and dissemination. Similarly, type I IFN-induced PD-L1 expression was reduced, thus preventing PD-L1 from binding to T cells and providing conditions for T cells to exert normal anti-tumor effects. **(C)** APOBEC3 gene expression is mediated by type I IFN, targeted inhibition of APOBEC3 gene can reduce IFN-mediated tumor resistance. **(D)** SFN through Nrf2/HO-1 pathway activates autophagy to inhibit IRF3 activity, which suppresses the type I IFN response. The inhibition of IFN response reduces the restriction of replication of VSVΔ51, so VSV exerts its normal oncolytic effect.

the combination of PD-L1 and its receptor inhibits T cells from migrating, meanwhile, the combination keeps down the T cells' proliferation as well as the release of mediators that have cytotoxic, therefore inhibition of PD-L1 expression is one of the strategies for tumor therapy. Several previous studies have shown that PD-L1 expression can be induced independently of the IFN inflammatory pathway, but is often dependent on the IRF1 pathway, a transcription factor associated with PD-L1 regulation (85–88). In contrast, according to a recent research in melanoma, VSV optimizes PD-L1 upregulation in tumors which is dependent on type I IFN expression, and in-depth studies revealed that VSV-induced type I IFN proceeds in an IFNAR-dependent manner (89). This provides an opportunity to improve the therapeutic use of VSV for tumors. In order to block the viral-mediated IFN inflammatory pathway, the monoclonal IFNAR antibody can be taken into consideration. The paper shows monoclonal IFNAR antibody can reduce PD-L1 expression which is induced by type I IFN, this will promotes immune responses with tumor-specific T cells (89). This research result provides a new target for the treatment of solid tumors.

Among the IFN-induced antiviral factors, the APOBEC cytosine deaminase family is associated with viral resistance (90), which has been demonstrated in retroviruses, herpesviruses, and hepatitis viruses, among others (91–94). In addition to being a viral limiting factor, over expression of APOBEC3 family proteins occurs in several types of cancers, so that APOBEC3 upregulation and the genomic mutations it causes to mediate therapeutic resistance are important for the prognostic profile of cancer (92, 95). In contrast, VSV, a retrovirus, is able to mediate APOBEC3 expression in tumor cells. This expression is dependent on type I IFN upregulation. This research suggests that APOBEC3 is a key gene for type I IFN stimulation and plays an influential part in the build-up of resistance to oncolytic virus therapy (96).

Nrf2 is a transcriptional regulator that maintains redox homeostasis by controlling basal and induced expression of a series of antioxidant enzymes (90). Furthermore, Nrf2 actively regulates autophagy as an essential component of the regulatory network that responses to different types of stress, including protein aggregation, nutritional deficiency, and viral infection (97). Therefore, it may also influence VSV replication and infection. A study on lung cancer and osteosarcoma showed that for drug-resistant lung cancer cells (A549) and osteosarcoma cells (U-2OS), sulforaphane (SFN) inhibited IRF3 activity by activating autophagy through the Nrf2/HO-1 pathway. This inhibited the type I IFN response and promoted VSVΔ51 replication, leading to better tumor lysis. what's more, it has shown a good safety profile in animal experiments (98).

4.2 Herpes simplex virus-1

Herpes simplex virus 1 (HSV-1) belongs to the subfamily Alphaherpesvirinae (99). Regulation of IFN by HSV and its combination therapies is achieved through multiple pathways, including STAT3-PKR-dependent antiviral responses, IRF3, and

TNF-related apoptosis-inducing ligand (TRAIL). Remarkably, there is a possibility as a potential cancer vaccine of it. (Figure 3)

Similarly, HSV still faces resistance due to innate immunity when applied. The type I IFN antiviral signaling pathway bears the brunt of viral defense in infected cells (100). Previous studies have identified protein kinase R (PKR) as a host antiviral kinase that inhibits cell proliferation and blocks the production of viral proteins, thus preventing viral replication (101). Therefore, inhibition of its expression and activation can attenuate the type I IFN-mediated antiviral response. In contrast, STAT3, as part of the type I IFN signaling pathway, can also inhibit the expression of PKR to limit the type I IFN cascade response (102–105). Similarly, protein kinase A (PKA) can also achieve this effect. Recently, it has been shown that β-blocker pretreatment inhibits the binding of catecholamines to β-adrenergic receptors, leading to a limitation of Gαs-mediated cyclic 3'-5' adenosine monophosphate (cAMP) synthesis. This limits the transient flux of intracellular cAMP to activate PKA production, whose phosphorylation to produce a variety of target proteins is necessarily affected, including β-adrenergic receptor kinase (BARK). Src kinase can be activated by BARK, thereby suppressing the activation of the important transcription factor STAT3 (106). By inhibiting this series of interferon-related responses, the antitumor efficacy of oncolytic virus T1012G is improved (107).

The IFN gene stimulating factor (STING), which is upstream of IFN production, is similar to STAT. Its mediated IFN gene stimulating factor (STING)- TANK-binding kinase 1 (TBK1)-IRF3-IFN pathway is a central cellular host defense against viral infection (108–110). However, in a preclinical study of pancreatic ductal adenocarcinoma (PDAC), it was shown that cell lines defective in the STING pathway had relatively low susceptibility to being C-REV (a type of HSV) (111). In contrast, those cell lines that capable of responsive STING pathway had relatively higher susceptibility to C-REV. This suggests that there is a correlation between STING pathway activation and resistance to C-REV, and this pathway does have an effect on oncolytic virus replication, However, data analysis revealed that it is not the main pathway affecting C-REV in human pancreatic ductal adenocarcinoma cell lines (111).

Although C-REV has no critical effect on STING, one study found that modification of HSV can act on IRF3 in the STING pathway to exert antitumor effects. Engineered HSV-1ΔN146 containing amino acids 147 to 263 of γ134.5 could efficiently replicate and lyse in malignant cells refractory to the γ134.5 null mutant. ΔN146 activated IRF3 and IFN expression, triggering immunity against the virus and the tumor. Unexpectedly, ΔN146 exposed to exogenous IFN-α was also able to replicate normally, and in a 4T1 tumor model, ΔN146 also exhibited significant inhibition of tumor growth and metastasis. Thus, ΔN146 is able

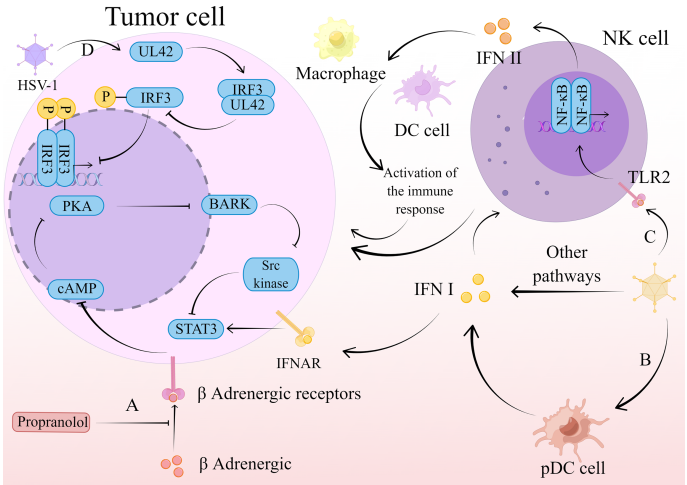

FIGURE 3
The mechanism of action of HSV-1 therapy. **(A)** Propranolol blocks β-adrenergic binding to β-adrenergic receptors, leading to a restriction of Gαs-mediated cAMP synthesis. This restriction limits the transient flux of intracellular cAMP to activate PKA production and inhibits its phosphorylation to produce BARK. activation of Src kinase is dependent on BARK, and its inhibition in turn inhibits activation of the transcription factor STAT3. This series of reactions inhibit the type I IFN-mediated antiviral response and promotes the normal replication and propagation of HSV-1, thus exerting an oncolytic effect. **(B)** HSV-1 stimulates the production of type I IFN by pDC, which activates NK cells to exert a direct killing effect on tumor cells. **(C)** HSV-1 stimulates the release of type II IFN by NK cells through the TLR2/NF-κB signaling pathway. Type II IFNs released by NK cells recruit macrophages, DC cells, and other immune cells, which act as immune agents to remove tumor cells. **(D)** The viral polymerase synthesis factor UL42 is able to interact with the host transcription factor IRF3. This interaction inhibits IRF3 phosphorylation and downstream IFN-β gene transcription, thereby suppressing IFN-β expression and thus the antiviral effect. The virus is consequently able to replicate and spread normally, exerting an oncolytic effect.

to stimulate the expression of inflammatory cytokines that do not have a serious impact on the replication of the virus in tumor cells. This can ensure to a greater extent that the oncolytic virus works (112). Furthermore, a similar effect can be achieved by causing mutations in the HSV-1 gene through the random insertion of a corruptive 1.2-kbp transposon into the viral genome. This mutation is capable of generating the viral polymerase synthesis factor UL42, which interacts with the host transcription factor IRF3 (113). The above studies suggest that genetic modification of HSV may be a new strategy to avoid immune clearance of HSV and provide a new way to enhance the effect of oncolytic virus therapy, but this may only be applicable to personalized treatment.

One of the pathways mediated by HSV-1 to generate IFN-α/β is through the stimulation of plasmacytoid dendritic cells (pDCs) (114), whose production of type I IFNs can activate NK cells (115). A current study has found that the type I IFN produced by pDCs and activated NK cells are an important link in the anti-myeloma effect of HSV-1, type I IFN has a direct cytotoxic effect on tumor cells and induces IFN to release from NK cells, thereby enhancing the killing effect of NK cells (116). In addition, type I IFNs have direct oncolytic activity against plasmacytoid tumors, where type I IFNs upregulate TRAIL expression, mitochondrial cytochrome c release, while limiting the expression of B-cell leukemia/lymphoma 2 (Bcl-2) and Bcl-XL (117). Regulation of these genes ultimately leads to apoptosis.

HSV not only acts through type I IFNs with NK cells, but also mediates type II IFNs stimulation of NK cells. Recent studies have shown that UV-oHSV2 can stimulate NK cells to secrete IFN-γ, which is achieved through the Toll-like receptor 2 (TLR2)/NF-κB signaling pathway, which activates multiple immune cells to exert anti-tumor responses (118). Furthermore, UV-oHSV2 stimulation promoted the expression of two checkpoint molecules, one located on NK cells, NKG2A, and the other on tumor cells, HLA-E. This finding predicts that anti-NKG2A may further enhance the antitumor effects occurring from UV-oHSV2 stimulation, and that anti-HLA-E treatment also has this possibility (118).

Speaking of IFN-γ, it plays an active role in the induction of apoptosis as well as tumor-infiltrating T cell recruitment. It has been shown that oHSV-1 stimulates tumor cells to secrete IFN-γ, which increases the immune activity of T cells, which is also able to enhance the activity of CD70-specific CAR T cells. This combination of specific T-cell therapy and oHSV-1 enhanced the pro-inflammatory environment and reduced anti-inflammatory factors *in vitro*, which achieved the goal of promoting tumor extinction. While this immune activation environment, this combined strategy increased the ratio of T cells and natural killer cells in the tumor microenvironment (TME) and decreased the expression of regulatory T cells as well as transforming growth factor-β1 in glioblastoma (GBM) in an *in situ* xenograft animal model. It undoubtedly brings a new therapeutic strategy for the treatment of GBM (119).

In addition, one study found that HF10 was able to prevent secondary tumors while activating anti-tumor effects. In an animal experiment with mice with squamous cell carcinoma, mice that survived HF10 treatment all showed rejection of tumors upon reactivation. Studies of systemic immunity in mice revealed that a large number of granulocytes and CD8 T cells were accumulated in the spleen at the time of HF10 application, and when co-cultured with SCC-VII cells, splenocytes released type I IFN (IFN-α and IFN-β), IFN-γ, IL-2, IL-12, and TNF-α. This suggests that mice developed anti-tumor immunity and implies that HSV has the potential for an *in situ* cancer vaccine (120).

4.3 Reovirus

MRV is a virus with double stranded RNA (dsRNA), which belongs to Reoviridae (121). Its mechanisms associated with IFN when treating tumors are mainly related to the PD-1/PD-L1 axis, STAT, and IFNAR signaling.

Similar to VSV, IFN is a key cytokine in reovirus-mediated activation of immune cell populations (122). A research found that type I and type II IFNs are able to promote PD-L1 expression in patient-derived glioma cells in a synergistic manner, while type I IFNs can induce strong expression of PD-L1 with IFN-γ, which undoubtedly has a detrimental effect on tumor treatment (123). PD-L1 binding to PD-1 prevents attack by the host's own immune system, thereby reducing T-cell activation and proliferation of cytotoxic T lymphocytes. tumor cells evade immune surveillance as a result of T-cell depletion (124, 125). In a vitro experiment, IFN-γ was the cytokine secreted after reovirus treatment of HGG cells (123). The above analysis revealed that reovirus treatment could improve the clinical outcome of brain tumor patients by activating leukocytes, enhancing T-cell infiltration into tumors and upregulating PD-L1, which prepared for later anti-PD-1 therapy. Further studies found that the addition of PD-1 blockers to reovirus enhanced systemic therapy in preclinical glioma models. These results analyze the mechanisms by which reovirus affect IFN-related pathways and provide theoretical support for the development of PD-L1 blockade combined with systemic immunoviral treatment strategies (123).

It has been noted that in a mouse model, IL-15 can be induced by type I IFN in dendritic cells (DC production) and this cytokine can activate NK cells to act (126, 127). NK cells are a type of innate lymphocyte (ILC) that, on the one hand, are able to recognize and kill infected cells as well as tumor cells, on the other hand, have an ability to induce adaptive immunity to function (128, 129).NK component of the cytotoxic machinery is triggered by type I IFN (126, 130, 131). Recent studies have shown that Reovirus are able to activate NK cells in a type I IFN -dependent manner, inducing STAT1 and STAT4 signaling in $CD56^{dim}$ as well as a subset of $CD56^{bright}$ NK cells. However, It is puzzling that MRV is dependent on type I IFN to inhibit IL-15-

induced NK cell proliferation, which may be involved with reduced AKT signaling. In *in vivo* experiments, $CD56^{bright}$ NK cells disappeared from the peripheral circulation for a brief period during the peak of the type I IFN response, which may suggest that they underwent redistribution and migrated to secondary lymphoid tissues. In combination with OV-mediated direct tumor cell killing, CD56 activation and $CD56^{bright}$ NK cells induce a spectrum of activity *via* antiviral pathways, including NK cell-mediated tumor cell killing and regulation of adaptive NK cells to lymph nodes by transport of IFN-γ-expressing CD56 (132). However, reovirus does not always depend on the type I IFN pathway for its antitumor effects. By comparing IFN-β promoter stimulator-1promoter stimulator-1 knockout (KO) mice with TLR-3 KO mice under reovirus treatment conditions, it was found that Reovirus inhibits the immunosuppressive activity of bone marrow mesenchymal stem cells in a TLR3 manner, but not in an IFN-β promoter stimulator-1 signaling-dependent manner (133).

Alternatively, the type of IFN produced by reovirus-mediated production can impact the tumor's therapeutic outcome. Studies have shown that MRV infection has a superior stimulatory effect on type III IFN production, but does not show satisfactory performance for type I IFN production. Although activation of STAT1 and STAT2 can be achieved by both type I and type III IFNs, triple-negative breast cancer cell proliferation is only sensitive to type I IFN (134). For this issue, researchers treated triple-negative breast cancer cells with a topoisomerase inhibitor that activated the DNA damage response pathway. This combination promoted the replication of the eutherian virus and enhanced cytotoxicity, achieving effective infection and killing of triple-negative breast cancer cells (134).

Again, the problem of ineffectiveness against IFN pathway-deficient tumor cells has been faced with the application of the eutherian virus. Researchers identified IFN regulatory factor 3, as a crucial transcription factor for IFN-β expression, in transformed human myeloid cells infected with tumor-selective MRV, IFN-α/β receptor (IFNAR) signaling both gradually promoted IFN I secretion from infected cells by enhancing the activation of IFN regulatory factor 3, and also promoted viral replication. However, tumors can interfere with the IFNAR pathway to maintain their own survival, and tumors that do not respond to IFNAR signaling may require other therapeutic strategies to promote adequate type I IFN secretion into the tumor microenvironment. Therefore, the parameters of eutherian virus-induced type I IFN levels need to be further explored (135).

Some viruses from the same ancestor have small genetic differences that cannot be ignored, and their effects on cell signaling and regulation of cytokine secretion may differ dramatically (136–142), which can affect antitumor effects. For example, T3D lab strains have a large variability in the regulation of RIG-I and/or IFN-dependent genes, with the least tumorigenic T3DTD strains inducing significantly higher levels compared to the most tumorigenic T3DPL strains (the difference may be a result of polymorphisms in the dsRNA-binding protein and the PKR antagonist σ3), which is crucial for the selection of the appropriate tumorigenic virus strain (143). This suggests the need to consider minor differences between viruses and to clarify the target of action when selecting combination therapies.

4.4 Newcastle disease virus

NDV belongs to the genus Aviravirus in the family Paramyxoviridae (144). The mechanism has not been extensively studied in terms of IFN-associated tumor lysis, which is associated with both type I and type II IFNs.

Similar to numerous viruses, NDV affects type I IFN (145). It is well known that type I IFN-mediated PD-L1 expression is an unfavorable factor in tumor treatment. Unexpectedly, the inflammatory response and PD-L1 upregulation induced by NDV treatment of tumors can precisely enhance the sensitivity of these tumors to PD-1/PD-L1 blockade. The strategy of intratumoral NDV injection combined with systemic PD-1 or PD-L1 blockade significantly enhances the antitumor immune effect, which provides a theoretical basis for future clinical trials (146). Further analysis revealed that this is mainly evidenced by its upregulation of PD-L1 expression in tumor cells as well as in tumor-infiltrating immune cells, which plays an important role in the development of late adaptive mechanisms of immune resistance to increased immune cell infiltration into tumors (146).

NDV infection also affects changes in type II IFN, as demonstrated in glioblastoma, colorectal and cervical cancers (147–149), and the mechanism of action needs to be further elucidated. In an animal experiment on lung cancer, it was identified that, compared to IL-4, the increase in IFN-γ concentration far exceeded its increase, IFN-γ is one of the cytokines secreted by Th1, under NDV intervention conditions (150). This indicates a shift in cellular distribution from Th2-dominant to Th1-dominant, suggesting that NDV plays a role in regulating humoral immunity and inhibiting tumor growth (148).

Naturally, genetic modification of NDV is one of the strategies to overcome the body's antiviral reflection (151). It was found that genetic modification of NDV to express influenza virus NS1 protein can improve the susceptibility of GBM to type I NDV-activated cells, resulting in better tumor

lysis (152). This viral protein can suppress the host immune response (153, 154), the virus can thus exert its antitumor effects more effectively.

4.5 Vaccinia virus

The virus of VV belongs to the genus Orthopoxvirus (OPXV) (155). Its mediated IFN exerts antitumor effects mainly related to IRF-3, JAK-STAT signaling pathway, and Th1 cells.

In the past decades, some progress has been made in the study of VV for antitumor therapy (156–159). The finding of a recent study that a recombinant VV can induce high levels of IFN while blocking the IFN-mediated antiviral response is undoubtedly an important finding. It was shown that OncoVV-WCL could achieve induction of high levels of type I IFN expression by promoting IRF-3 transcriptional activity, which could enhance the antitumor effects of oncolytic virus. Specifically, blocking the IFN-induced antiviral response is achieved through two pathways. On the one hand, OncoVV-WCL can inhibit the activity of IFN stimulatory response element (ISRE), and on the other hand, inhibition of JAK-STAT signaling pathway by OncoVV-WCL limits ISG expression (160). By these means, the virus can avoid elimination by the antiviral pathway and thus exert a normal lytic effect (160).

Another study on multiple tumors showed that vvDD-IL-23 can promote the expression and release of Th1 chemokines and some anti-tumor factors, which contained IFN-γ, as well as tumor necrosis factor-α (TNF-α), IL-2, perforin, and granzyme B (GzmB). These cytokines keep the ratio of infiltrating activated T cells CD8 and Treg to high levels, which play a therapeutic role in reversing the immunosuppressive state to achieve antitumor (161). In a clinical study, VV also acted through a similar mechanism. It was found that a classical IFN response, including the release of inflammatory cytokines/chemokines, was induced in patients who were lysing virus responders. These factors activate T cells, which can then infiltrate into the tumor to exert antitumor effects (162).

4.6 Other viruses

4.6.1 Measles virus

MV is a type of negative-stranded RNA virus that belongs to the family Paramyxoviridae, genus Morbillivirus (163). It mainly affects type I IFN to exert antitumor effects. A variety of malignant pleural mesothelioma (MPM) cell lines have a defect in antiviral type I IFN response (164), and this defect in type I IFN response is located upstream of the IFNAR. It was thought that type I IFN-deficient tumor cells sensitive to the antitumor effects of MV still participate in part of the type I IFN response though. This is achieved by relocalizing IRF3 and NF-κB in the nucleus, but the resulting ISG expression is minimal, which is very favorable for the oncolytic virus to function. Indeed, type I IFN-deficient tumor cells can induce a response that induces immunogenic death of tumor cells and additionally induces an endoplasmic reticulum stress response, enhancing the antitumor effect. At a deeper genetic level, pure deletion (HD) of all genes of type I IFN in human MPM cells leads to their sensitivity to MV virus, and HD of the type I IFN-encoding gene in MPM occurs frequently together with HD of the CDKN2A gene, it suggests a new therapeutic target (165–167). Another study using a sequential transformation model also identified reduced type 1 IFN pathway function as a significant factor in MV-mediated selectivity of transformed cytolytic tumors (168).

4.6.2 Coxsackie virus

Fewer studies have been conducted on the mechanisms by which coxsackieviruses exert tumor lysis. Recent clinical trials in non-muscle invasive bladder cancer have identified a kind of coxsackievirus, CAVATAK, that upregulates PD-L1 and lymphocyte activation gene-3 (LAG3) among the IFN-inducible genes. In parallel, this virus promotes the release of Th1-related chemokines as well as induces RIG-I. Through these pathways, it induces an inflammatory response, reverses the “cold” tumor state, has an anti-tumor effect, and shows a good biosafety profile (169).

4.6.3 Poliovirus

The neurally attenuated recombinant poliovirus PVSRIPO has also been used in oncology treatment, it has shown good efficacy in clinical trials in glioblastoma (170). Recently, researchers have explored its mechanism of action, and unlike other oncolytic viruses, PVSRIPO is insensitive to both upstream and downstream endogenous intrinsic responses to IFN triggered by MDA5 under *in vitro* conditions. Although the involvement of PRR inhibited the kinetics of PVSRIPO, PVSRIPO could still be translated in diseased cells and propagate in the cell. This occurrence may be related to the translation strategy of PVSRIPO, which prevents the body’s antiviral immune response while destroying tumor cells, and immune escape occurs (171). This property could sustain activation of the IFN response. This finding suggests that poliovirus has a significant advantage in exerting its oncolytic effect.

5 Discussions and challenges

From the above review, we can understand that a variety of viruses show the ability to activate the immune of body response, which is closely related to the IFN pathway. They reverse the immunosuppressive state in the tumor microenvironment, resulting in the production of various other cytokines and various immune cells and changing cold tumors to hot tumors. Finally, they achieve the suppressive and clearing effect on tumor cells.

For different oncolytic viruses, the pathways affecting IFN are not identical, and almost all IFN-related pathways are included, summarizing that they mainly interact with IFN through the following mechanisms: (1) PD-L1/PD-1; (2) JAK/STAT signaling pathway; (3) APOBEC cytosine deaminase family; (4) Nrf2; (5) TLR2/NF-κB signaling pathway; (6) IRF3. The elucidation of these mechanisms provides a theoretical basis for future combination therapies with various oncolytic viruses, thus providing guidance for targeted enhancement of oncolytic viral therapeutic efficacy.

At the same time, we found that oncolytic viruses are similar to other viruses. When the immunity of body is activated, it will activate the anti-virus response related to IFN, which will make the virus unable to exist in the immune microenvironment for a relatively long time. Although this can improve the biological safety of oncolytic virus therapy, it is difficult to achieve an effective anti-tumor effect for a short time. Through various ways, it can inhibit the immune clearance of oncolytic viruses, better therapeutic effect can be achieved. Here, we focus on IFNs. By summarizing, we found that researchers mainly take the following ways to achieve better anti-tumor effects: (1) Combined drugs target the inhibition sites of oncolytic viruses; (2) Genetic modification of oncolytic virus; (3) Select the appropriate strain. In addition, for tumor types with IFN deficiency, some specific defects in the IFN signaling cascade can be used as potential biomarkers, which may help identify such individual cancer patients and obtain personalized treatment (16).

Of course, there are still some problems in the study of the mechanism of action between oncolytic virus and IFNs. First, most studies are still in the preclinical stage, and their mechanisms and effects in the clinical setting are still unknown. Researchers should accelerate their studies to better benefit oncology patients. Second, due to the complexity of *in vivo* immunity, the relationship between the efficacy of viral tumor lysis and the IFNs gene has not been fully elucidated. Further studies in this area are expected in the future. In addition, many studies have used the expression level of IFNs as an indicator of antitumor effects, and the specific mechanism of its increased expression level and antitumor effects need to be further elucidated. Notably, there are few studies on type III IFN and oncolytic viruses, and it is hoped that future studies will fill this gap. Finally, the degree of research on various viruses varies greatly. Some viruses are able to activate IFN-induced antitumor immunity while avoiding immune clearance, such as PVSRIPO and HSV-1, etc. Such viruses may have more advantages in antitumor, and research on their oncolytic mechanism can be more widely carried out.

Author contributions

QL and FT: writing, editing, and visualization. YW and XL: reviewing and editing. XK: conceptualization. JM: validation. LY: supervision. SC: funding acquisition. All authors contributed to the article and approved the submitted version.

Funding

This study was supported by the Scientific research project of Tianjin Education Commission (2021KJ134), National Natural Science Foundation of China (81973728) and Science and Technology Program of Tianjin (21ZYJDJC00070).

Acknowledgments

The figures were drawn by Figdraw (www.figdraw.com).

Conflict of interest

The authors declare that the research was conducted in the absence of any commercial or financial relationships that could be construed as a potential conflict of interest.

Publisher's note

References

1. Yang L, Gu X, Yu J, Ge S, Fan X. Oncolytic virotherapy: From bench to bedside. *Front Cell Dev Biol* (2021) 9:790150. doi: 10.3389/fcell.2021.790150

2. Borden EC. Progress toward therapeutic application of interferons, 1979-1983. *Cancer* (1984) 54(11 Suppl):2770–6. doi: 10.1002/1097-0142(19841201)54:2+<2770::aid-cncr2820541425>3.0.co;2-0

3. Gresser I, Maury C, Brouty-Boyé D. Mechanism of the antitumour effect of interferon in mice. *Nature* (1972) 239(5368):167–8. doi: 10.1038/239167a0

4. Gutterman JU. Cytokine therapeutics: lessons from interferon alpha. *Proc Natl Acad Sci USA* (1994) 91(4):1198–205. doi: 10.1073/pnas.91.4.1198

5. Stetson DB, Medzhitov R. Type I interferons in host defense. *Immunity* (2006) 25(3):373–81. doi: 10.1016/j.immuni.2006.08.007

6. Kulaeva OI, Draghici S, Tang L, Kraniak JM, Land SJ, Tainsky MA. Epigenetic silencing of multiple interferon pathway genes after cellular immortalization. *Oncogene* (2003) 22(26):4118–27. doi: 10.1038/sj.onc.1206594

7. Olopade OI, Jenkins RB, Ransom DT, Malik K, Pomykala H, Nobori T, et al. Molecular analysis of deletions of the short arm of chromosome 9 in human gliomas. *Cancer Res* (1992) 52(9):2523–9.

8. Diaz MO, Ziemin S, Le Beau MM, Pitha P, Smith SD, Chilcote RR, et al. Homozygous deletion of the alpha- and beta 1-interferon genes in human leukemia and derived cell lines. *Proc Natl Acad Sci USA* (1988) 85(14):5259–63. doi: 10.1073/pnas.85.14.5259

9. Cairns P, Tokino K, Eby Y, Sidransky D. Homozygous deletions of 9p21 in primary human bladder tumors detected by comparative multiplex polymerase chain reaction. *Cancer Res* (1994) 54(6):1422–4.

10. Kondo M, Nagano H, Sakon M, Yamamoto H, Morimoto O, Arai I, et al. Expression of interferon alpha/beta receptor in human hepatocellular carcinoma. *Int J Oncol* (2000) 17(1):83–8.

11. Damdinsuren B, Nagano H, Wada H, Noda T, Natsag J, Marubashi S, et al. Interferon alpha receptors are important for antiproliferative effect of interferon-alpha against human hepatocellular carcinoma cells. *Hepatol Res Off J Japan Soc Hepatol* (2007) 37(1):77–83. doi: 10.1111/j.1872-034X.2007.00007.x

12. Saidi RF, Williams F, Silberberg B, Mittal VK, ReMine SG, Jacobs MJ. Expression of interferon receptors in pancreatic cancer: identification of a novel prognostic factor. *Surgery* (2006) 139(6):743–8. doi: 10.1016/j.surg.2005.11.010

13. Chen HM, Tanaka N, Mitani Y, Oda E, Nozawa H, Chen JZ, et al. Critical role for constitutive type I interferon signaling in the prevention of cellular transformation. *Cancer Sci* (2009) 100(3):449–56. doi: 10.1111/j.1349-7006.2008.01051.x

14. Slattery ML, Lundgreen A, Bondurant KL, Wolff RK. Interferon-signaling pathway: associations with colon and rectal cancer risk and subsequent survival. *Carcinogenesis* (2011) 32(11):1660–7. doi: 10.1093/carcin/bgr189

15. Critchley-Thorne RJ, Simons DL, Yan N, Miyahira AK, Dirbas FM, Johnson DL, et al. Impaired interferon signaling is a common immune defect in human cancer. *Proc Natl Acad Sci USA* (2009) 106(22):9010–5. doi: 10.1073/pnas.0901329106

16. Matveeva OV, Chumakov PM. Defects in interferon pathways as potential biomarkers of sensitivity to oncolytic viruses. *Rev Med Virol* (2018) 28(6):e2008. doi: 10.1002/rmv.2008

17. Isaacs A, Lindenmann J. Virus interference. i. the interferon. *Proc R Soc London Ser B Biol Sci* (1957) 147(927):258–67. doi: 10.1098/rspb.1957.0048.

18. Parker BS, Rautela J, Hertzog PJ. Antitumour actions of interferons: implications for cancer therapy. *Nat Rev Cancer* (2016) 16(3):131–44. doi: 10.1038/nrc.2016.14

19. Sprooten J, Agostinis P, Garg AD. Type I interferons and dendritic cells in cancer immunotherapy. *Int Rev Cell Mol Biol* (2019) 348:217–62. doi: 10.1016/bs.ircmb.2019.06.001

20. Walter MR. The role of structure in the biology of interferon signaling. *Front Immunol* (2020) 11:606489. doi: 10.3389/fimmu.2020.606489

21. Pestka S. The human interferon-alpha species and hybrid proteins. *Semin Oncol* (1997) 24(3 Suppl 9):S9–4-s9-17.

22. Pestka S. The interferons: 50 years after their discovery, there is much more to learn. *J Biol Chem* (2007) 282(28):20047–51. doi: 10.1074/jbc.R700004200

23. Pestka S, Krause CD, Sarkar D, Walter MR, Shi Y, Fisher PB. Interleukin-10 and related cytokines and receptors. *Annu Rev Immunol* (2004) 22:929–79. doi: 10.1146/annurev.immunol.22.012703.104622

24. Pestka S, Krause CD, Walter MR. Interferons, interferon-like cytokines, and their receptors. *Immunol Rev* (2004) 202:8–32. doi: 10.1111/j.0105-2896.2004.00204.x

25. Hardy MP, Owczarek CM, Jermiin LS, Ejdebäck M, Hertzog PJ. Characterization of the type I interferon locus and identification of novel genes. *Genomics* (2004) 84(2):331–45. doi: 10.1016/j.ygeno.2004.03.003

26. LaFleur DW, Nardelli B, Tsareva T, Mather D, Feng P, Semenuk M, et al. Interferon-kappa, a novel type I interferon expressed in human keratinocytes. *J Biol Chem* (2001) 276(43):39765–71. doi: 10.1074/jbc.M102502200

27. Hauptmann R, Swetly P. A novel class of human type I interferons. *Nucleic Acids Res* (1985) 13(13):4739–49. doi: 10.1093/nar/13.13.4739

28. Honda K, Taniguchi T. IRFs: master regulators of signalling by toll-like receptors and cytosolic pattern-recognition receptors. *Nat Rev Immunol* (2006) 6 (9):644–58. doi: 10.1038/nri1900

29. Mogensen TH. Pathogen recognition and inflammatory signaling in innate immune defenses. *Clin Microbiol Rev* (2009) 22(2):240–73. doi: 10.1128/cmr.00046-08

30. Kawasaki T, Kawai T. Toll-like receptor signaling pathways. *Front Immunol* (2014) 5:461. doi: 10.3389/fimmu.2014.00461

31. Honda K, Taniguchi T. Toll-like receptor signaling and IRF transcription factors. *IUBMB Life* (2006) 58(5-6):290–5. doi: 10.1080/15216540600702206

32. Muskardin TLW, Niewold TB. Type I interferon in rheumatic diseases. *Nat Rev Rheumatol* (2018) 14(4):214–28. doi: 10.1038/nrrheum.2018.31

33. Reikine S, Nguyen JB, Modis Y. Pattern recognition and signaling mechanisms of RIG-I and MDA5. *Front Immunol* (2014) 5:342. doi: 10.3389/fimmu.2014.00342

34. Schneider WM, Chevillotte MD, Rice CM. Interferon-stimulated genes: a complex web of host defenses. *Annu Rev Immunol* (2014) 32:513–45. doi: 10.1146/annurev-immunol-032713-120231

35. Ivashkiv LB. IFNγ: signalling, epigenetics and roles in immunity, metabolism, disease and cancer immunotherapy. *Nat Rev Immunol* (2018) 18 (9):545–58. doi: 10.1038/s41577-018-0029-z

36. Kotenko SV, Gallagher G, Baurin VV, Lewis-Antes A, Shen M, Shah NK, et al. IFN-lambdas mediate antiviral protection through a distinct class II cytokine receptor complex. *Nat Immunol* (2003) 4(1):69–77. doi: 10.1038/ni875

37. Sheppard P, Kindsvogel W, Xu W, Henderson K, Schlutsmeyer S, Whitmore TE, et al. IL-28, IL-29 and their class II cytokine receptor IL-28R. *Nat Immunol* (2003) 4(1):63–8. doi: 10.1038/ni873

38. Geoffroy K, Bourgeois-Daigneault MC. The pros and cons of interferons for oncolytic virotherapy. *Cytokine Growth factor Rev* (2020) 56:49–58. doi: 10.1016/j.cytogfr.2020.07.002

39. Onabajo OO, Muchmore B, Prokunina-Olsson L. The IFN-λ4 conundrum: When a good interferon goes bad. *J Interferon Cytokine Res Off J Int Soc Interferon Cytokine Res* (2019) 39(10):636–41. doi: 10.1089/jir.2019.0044

40. Prokunina-Olsson L, Muchmore B, Tang W, Pfeiffer RM, Park H, Dickensheets H, et al. A variant upstream of IFNL3 (IL28B) creating a new interferon gene IFNL4 is associated with impaired clearance of hepatitis c virus. *Nat Genet* (2013) 45(2):164–71. doi: 10.1038/ng.2521

41. Durbin RK, Kotenko SV, Durbin JE. Interferon induction and function at the mucosal surface. *Immunol Rev* (2013) 255(1):25–39. doi: 10.1111/imr.12101

42. Ank N, West H, Bartholdy C, Eriksson K, Thomsen AR, Paludan SR. Lambda interferon (IFN-lambda), a type III IFN, is induced by viruses and IFNs and displays potent antiviral activity against select virus infections in vivo. *J Virol* (2006) 80(9):4501–9. doi: 10.1128/jvi.80.9.4501-4509.2006

43. Donnelly RP, Kotenko SV. Interferon-lambda: a new addition to an old family. *J Interferon Cytokine Res Off J Int Soc Interferon Cytokine Res* (2010) 30 (8):555–64. doi: 10.1089/jir.2010.0078

44. Coccia EM, Severa M, Giacomini E, Monneron D, Remoli ME, Julkunen I, et al. Viral infection and toll-like receptor agonists induce a differential expression of type I and lambda interferons in human plasmacytoid and monocyte-derived dendritic cells. *Eur J Immunol* (2004) 34(3):796–805. doi: 10.1002/eji.200324610

45. Osterlund P, Veckman V, Sirén J, Klucher KM, Hiscott J, Matikainen S, et al. Gene expression and antiviral activity of alpha/beta interferons and interleukin-29 in virus-infected human myeloid dendritic cells. *J Virol* (2005) 79(15):9608–17. doi: 10.1128/jvi.79.15.9608-9617.2005

46. Lauterbach H, Bathke B, Gilles S, Traidl-Hoffmann C, Luber CA, Fejer G, et al. Mouse CD8alpha+ DCs and human BDCA3+ DCs are major producers of IFN-lambda in response to poly IC. *J Exp Med* (2010) 207(12):2703–17. doi: 10.1084/jem.20092720

47. Hillyer P, Mane VP, Schramm LM, Puig M, Verthelyi D, Chen A, et al. Expression profiles of human interferon-alpha and interferon-lambda subtypes are

ligand- and cell-dependent. *Immunol Cell Biol* (2012) 90(8):774–83. doi: 10.1038/icb.2011.109

48. Melchjorsen J, Sirén J, Julkunen I, Paludan SR, Matikainen S. Induction of cytokine expression by herpes simplex virus in human monocyte-derived macrophages and dendritic cells is dependent on virus replication and is counteracted by ICP27 targeting NF-kappaB and IRF-3. *J Gen Virol* (2006) 87(Pt 5):1099–108. doi: 10.1099/vir.0.81541-0

49. Khaitov MR, Laza-Stanca V, Edwards MR, Walton RP, Rohde G, Contoli M, et al. Respiratory virus induction of alpha-, beta- and lambda-interferons in bronchial epithelial cells and peripheral blood mononuclear cells. *Allergy* (2009) 64(3):375–86. doi: 10.1111/j.1398-9995.2008.01826.x

50. Wang J, Oberley-Deegan R, Wang S, Nikrad M, Funk CJ, Hartshorn KL, et al. Differentiated human alveolar type II cells secrete antiviral IL-29 (IFN-lambda 1) in response to influenza a infection. *J Immunol (Baltimore Md 1950)* (2009) 182 (3):1296–304. doi: 10.4049/jimmunol.182.3.1296

51. Ioannidis I, Ye F, McNally B, Willette M, Flaño E. Toll-like receptor expression and induction of type I and type III interferons in primary airway epithelial cells. *J Virol* (2013) 87(6):3261–70. doi: 10.1128/jvi.01956-12

52. Yin Y, Favoreel HW. Herpesviruses and the type III interferon system. *Virologica Sinica* (2021) 36(4):577–87. doi: 10.1007/s12250-020-00330-2

53. Griffiths SJ, Koegl M, Boutell C, Zenner HL, Crump CM, Pica F, et al. A systematic analysis of host factors reveals a Med23-interferon-λ regulatory axis against herpes simplex virus type 1 replication. *PloS Pathogens* (2013) 9(8): e1003514. doi: 10.1371/journal.ppat.1003514

54. Bilichodmath S, Nair SK, Bilichodmath R, Mangalekar SB. mRNA expression of IFN-λs in the gingival tissue of patients with chronic or aggressive periodontitis: A polymerase chain reaction study. *J Periodontol* (2018) 89(7):867–74. doi: 10.1002/jper.17-0349

55. de Weerd NA, Nguyen T. The interferons and their receptors–distribution and regulation. *Immunol Cell Biol* (2012) 90(5):483–91. doi: 10.1038/icb.2012.9

56. Lin FC, Young HA. Interferons: Success in anti-viral immunotherapy. *Cytokine Growth factor Rev* (2014) 25(4):369–76. doi: 10.1016/j.cytogfr.2014.07.015

57. Zan J, Zhang H, Gu AP, Zhong KL, Lu MY, Bai XX, et al. Yin yang 1 dynamically regulates antiviral innate immune responses during viral infection. *Cell Physiol Biochem Int J Exp Cell Physiol Biochem Pharmacol* (2017) 44(2):607–17. doi: 10.1159/000485116

58. Maney SK, Xu HC, Huang J, Pandyra AA, Ehlting C, Aguilar-Valenzuela R, et al. RAIDD mediates TLR3 and IRF7 driven type I interferon production. *Cell Physiol Biochem Int J Exp Cell Physiol Biochem Pharmacol* (2016) 39(4):1271–80. doi: 10.1159/000447832

59. Cui H, Liu Y, Huang Y. Roles of TRIM32 in corneal epithelial cells after infection with herpes simplex virus. *Cell Physiol Biochem Int J Exp Cell Physiol Biochem Pharmacol* (2017) 43(2):801–11. doi: 10.1159/000481563

60. Li SF, Gong MJ, Zhao FR, Shao JJ, Xie YL, Zhang YG, et al. Type I interferons: Distinct biological activities and current applications for viral infection. *Cell Physiol Biochem Int J Exp Cell Physiol Biochem Pharmacol* (2018) 51(5):2377–96. doi: 10.1159/000495897

61. Platanias LC. Mechanisms of type-i- and type-II-interferon-mediated signalling. *Nat Rev Immunol* (2005) 5(5):375–86. doi: 10.1038/nri1604

62. Matsumoto M, Tanaka N, Harada H, Kimura T, Yokochi T, Kitagawa M, et al. Activation of the transcription factor ISGF3 by interferon-gamma. *Biol Chem* (1999) 380(6):699–703. doi: 10.1515/bc.1999.087

63. Briscoe J, Rogers NC, Witthuhn BA, Watling D, Harpur AG, Wilks AF, et al. Kinase-negative mutants of JAK1 can sustain interferon-gamma-inducible gene expression but not an antiviral state. *EMBO J* (1996) 15(4):799–809.

64. Decker T, Kovarik P, Meinke A. GAS elements: a few nucleotides with a major impact on cytokine-induced gene expression. *J Interferon Cytokine Res Off J Int Soc Interferon Cytokine Res* (1997) 17(3):121–34. doi: 10.1089/jir.1997.17.121

65. Wesoly J, Szweykowska-Kulinska Z, Bluyssen HA. STAT activation and differential complex formation dictate selectivity of interferon responses. *Acta Biochim Polonica* (2007) 54(1):27–38.

66. Schroder K, Hertzog PJ, Ravasi T, Hume DA. Interferon-gamma: an overview of signals, mechanisms and functions. *J Leukocyte Biol* (2004) 75 (2):163–89. doi: 10.1189/jlb.0603252

67. Steimle V, Siegrist CA, Mottet A, Lisowska-Grospierre B, Mach B. Regulation of MHC class II expression by interferon-gamma mediated by the transactivator gene CIITA. *Sci (New York NY)* (1994) 265(5168):106–9. doi: 10.1126/science.8016643

68. Dumoutier L, Lejeune D, Hor S, Fickenscher H, Renauld JC. Cloning of a new type II cytokine receptor activating signal transducer and activator of transcription (STAT)1, STAT2 and STAT3. *Biochem J* (2003) 370(Pt 2):391–6. doi: 10.1042/bj20021935

69. Marcello T, Grakoui A, Barba-Spaeth G, Machlin ES, Kotenko SV, MacDonald MR, et al. Interferons alpha and lambda inhibit hepatitis c virus replication with distinct signal transduction and gene regulation kinetics. *Gastroenterology* (2006) 131(6):1887–98. doi: 10.1053/j.gastro.2006.09.052

70. Zhou Z, Hamming OJ, Ank N, Paludan SR, Nielsen AL, Hartmann R. Type III interferon (IFN) induces a type I IFN-like response in a restricted subset of cells through signaling pathways involving both the jak-STAT pathway and the mitogen-activated protein kinases. *J Virol* (2007) 81(14):7749–58. doi: 10.1128/jvi.02438-06

71. Levraud JP, Boudinot P, Colin I, Benmansour A, Peyrieras N, Herbomel P, et al. Identification of the zebrafish IFN receptor: implications for the origin of the vertebrate IFN system. *J Immunol (Baltimore Md 1950)* (2007) 178(7):4385–94. doi: 10.4049/jimmunol.178.7.4385

72. Balkwill F, Watling D, Taylor-Papadimitriou J. Inhibition by lymphoblastoid interferon of growth of cells derived from the human breast. *Int J Cancer* (1978) 22(3):258–65. doi: 10.1002/ijc.2910220307

73. Dunn GP, Bruce AT, Sheehan KC, Shankaran V, Uppaluri R, Bui JD, et al. A critical function for type I interferons in cancer immunoediting. *Nat Immunol* (2005) 6(7):722–9. doi: 10.1038/ni1213

74. Swann JB, Hayakawa Y, Zerafa N, Sheehan KC, Scott B, Schreiber RD, et al. Type I IFN contributes to NK cell homeostasis, activation, and antitumor function. *J Immunol (Baltimore Md 1950)* (2007) 178(12):7540–9. doi: 10.4049/jimmunol.178.12.7540

75. Koromilas AE, Sexl V. The tumor suppressor function of STAT1 in breast cancer. *Jak-stat* (2013) 2(2):e23353. doi: 10.4161/jkst.23353

76. Bishnoi S, Tiwari R, Gupta S, Byrareddy SN, Nayak D. Oncotargeting by vesicular stomatitis virus (VSV): Advances in cancer therapy. *Viruses* (2018) 10 (2):90. doi: 10.3390/v10020090

77. Barber GN. VSV-tumor selective replication and protein translation. *Oncogene* (2005) 24(52):7710–9. doi: 10.1038/sj.onc.1209042

78. Escobar-Zarate D, Liu YP, Suksanpaisan L, Russell SJ, Peng KW. Overcoming cancer cell resistance to VSV oncolysis with JAK1/2 inhibitors. *Cancer Gene Ther* (2013) 20(10):582–9. doi: 10.1038/cgt.2013.55

79. Patel MR, Jacobson BA, Ji Y, Drees J, Tang S, Xiong K, et al. Vesicular stomatitis virus expressing interferon-β is oncolytic and promotes antitumor immune responses in a syngeneic murine model of non-small cell lung cancer. *Oncotarget* (2015) 6(32):33165–77. doi: 10.18632/oncotarget.5320

80. Dold C, Rodriguez Urbiola C, Wollmann G, Egerer L, Muik A, Bellmann L, et al. Application of interferon modulators to overcome partial resistance of human ovarian cancers to VSV-GP oncolytic viral therapy. *Mol Ther Oncolytics* (2016) 3:16021. doi: 10.1038/mto.2016.21

81. Kimpel J, Urbiola C, Koske I, Tober R, Banki Z, Wollmann G, et al. The oncolytic virus VSV-GP is effective against malignant melanoma. *Viruses* (2018) 10 (3):108. doi: 10.3390/v10030108

82. Patel MR, Dash A, Jacobson BA, Ji Y, Baumann D, Ismail K, et al. JAK/STAT inhibition with ruxolitinib enhances oncolytic virotherapy in non-small cell lung cancer models. *Cancer Gene Ther* (2019) 26(11-12):411–8. doi: 10.1038/s41417-018-0074-6

83. Nguyen TT, Ramsay L, Ahanfeshar-Adams M, Lajoie M, Schadendorf D, Alain T, et al. Mutations in the IFNγ-JAK-STAT pathway causing resistance to immune checkpoint inhibitors in melanoma increase sensitivity to oncolytic virus treatment. *Clin Cancer Res an Off J Am Assoc Cancer Res* (2021) 27(12):3432–42. doi: 10.1158/1078-0432.Ccr-20-3365

84. Herbst RS, Soria JC, Kowanetz M, Fine GD, Hamid O, Gordon MS, et al. Predictive correlates of response to the anti-PD-L1 antibody MPDL3280A in cancer patients. *Nature* (2014) 515(7528):563–7. doi: 10.1038/nature14011

85. Loke P, Allison JP. PD-L1 and PD-L2 are differentially regulated by Th1 and Th2 cells. *Proc Natl Acad Sci United States America* (2003) 100(9):5336–41. doi: 10.1073/pnas.0931259100

86. Lee SJ, Jang BC, Lee SW, Yang YI, Suh SI, Park YM, et al. Interferon regulatory factor-1 is prerequisite to the constitutive expression and IFN-gamma-induced upregulation of B7-H1 (CD274). *FEBS Letters* (2006) 580(3):755–62. doi: 10.1016/j.febslet.2005.12.093

87. Wang X, Yang L, Huang F, Zhang Q, Liu S, Ma L, et al. Inflammatory cytokines IL-17 and TNF-α up-regulate PD-L1 expression in human prostate and colon cancer cells. *Immunol Letters* (2017) 184:7–14. doi: 10.1016/j.imlet.2017.02.006

88. Lamano JB, Lamano JB, Li YD, DiDomenico JD, Choy W, Veliceasa D, et al. Glioblastoma-derived IL6 induces immunosuppressive peripheral myeloid cell PD-L1 and promotes tumor growth. *Clin Cancer Res an Off J Am Assoc Cancer Res* (2019) 25(12):3643–57. doi: 10.1158/1078-0432.Ccr-18-2402

89. El-Sayes N, Walsh S, Vito A, Reihani A, Ask K, Wan Y, et al. IFNAR blockade synergizes with oncolytic VSV to prevent virus-mediated PD-L1 expression and promote antitumor T cell activity. *Mol Ther Oncolytics* (2022) 25:16–30. doi: 10.1016/j.omto.2022.03.006

90. Nguyen T, Nioi P, Pickett CB. The Nrf2-antioxidant response element signaling pathway and its activation by oxidative stress. *J Biol Chem* (2009) 284 (20):13291–5. doi: 10.1074/jbc.R900010200

91. Harris RS, Liddament MT. Retroviral restriction by APOBEC proteins. *Nat Rev Immunol* (2004) 4(11):868–77. doi: 10.1038/nri1489

92. Walker BA, Wardell CP, Murison A, Boyle EM, Begum DB, Dahir NM, et al. APOBEC family mutational signatures are associated with poor prognosis translocations in multiple myeloma. *Nat Commun* (2015) 6:6997. doi: 10.1038/ncomms7997

93. Sheehy AM, Gaddis NC, Choi JD, Malim MH. Isolation of a human gene that inhibits HIV-1 infection and is suppressed by the viral vif protein. *Nature* (2002) 418(6898):646–50. doi: 10.1038/nature00939

94. Suspène R, Aynaud MM, Koch S, Pasdeloup D, Labetoulle M, Gaertner B, et al. Genetic editing of herpes simplex virus 1 and Epstein-Barr herpesvirus genomes by human APOBEC3 cytidine deaminases in culture and in vivo. *J Virol* (2011) 85(15):7594–602. doi: 10.1128/jvi.00290-11

95. Roberts SA, Lawrence MS, Klimczak LJ, Grimm SA, Fargo D, Stojanov P, et al. An APOBEC cytidine deaminase mutagenesis pattern is widespread in human cancers. *Nat Genet* (2013) 45(9):970–6. doi: 10.1038/ng.2702

96. Huff AL, Wongthida P, Kottke T, Thompson JM, Driscoll CB, Schuelke M, et al. APOBEC3 mediates resistance to oncolytic viral therapy. *Mol Ther Oncolytics* (2018) 11:1–13. doi: 10.1016/j.omto.2018.08.003

97. Pajares M, Jiménez-Moreno N, García-Yagüe ÁJ, Escoll M, de Ceballos ML, Van Leuven F, et al. Transcription factor NFE2L2/NRF2 is a regulator of macroautophagy genes. *Autophagy* (2016) 12(10):1902–16. doi: 10.1080/15548627.2016.1208889

98. Olagnier D, Lababidi RR, Hadj SB, Sze A, Liu Y, Naidu SD, et al. Activation of Nrf2 signaling augments vesicular stomatitis virus oncolysis *via* autophagy-driven suppression of antiviral immunity. *Mol Ther J Am Soc Gene Ther* (2017) 25 (8):1900–16. doi: 10.1016/j.ymthe.2017.04.022

99. Zhu H, Zheng C. The race between host antiviral innate immunity and the immune evasion strategies of herpes simplex virus 1. *Microbiol Mol Biol Rev MMBR* (2020) 84(4):e00099–20. doi: 10.1128/mmbr.00099-20

100. Saha D, Wakimoto H, Rabkin SD. Oncolytic herpes simplex virus interactions with the host immune system. *Curr Opin Virol* (2016) 21:26–34. doi: 10.1016/j.coviro.2016.07.007

101. Kohlhapp FJ, Kaufman HL. Molecular pathways: Mechanism of action for talimogene laherparepvec, a new oncolytic virus immunotherapy. *Clin Cancer Res an Off J Am Assoc Cancer Res* (2016) 22(5):1048–54. doi: 10.1158/1078-0432.Ccr-15-2667

102. Ivashkiv LB, Donlin LT. Regulation of type I interferon responses. *Nat Rev Immunol* (2014) 14(1):36–49. doi: 10.1038/nri3581

103. Ho HH, Ivashkiv LB. Role of STAT3 in type I interferon responses. negative regulation of STAT1-dependent inflammatory gene activation. *J Biol Chem* (2006) 281(20):14111–8. doi: 10.1074/jbc.M511797200

104. Qin H, Niyongere SA, Lee SJ, Baker BJ, Benveniste EN. Expression and functional significance of SOCS-1 and SOCS-3 in astrocytes. *J Immunol (Baltimore Md 1950)* (2008) 181(5):3167–76. doi: 10.4049/jimmunol.181.5.3167

105. Tsai MH, Pai LM, Lee CK. Fine-tuning of type I interferon response by STAT3. *Front Immunol* (2019) 10:1448. doi: 10.3389/fimmu.2019.01448

106. Cole SW, Sood AK. Molecular pathways: beta-adrenergic signaling in cancer. *Clin Cancer Res an Off J Am Assoc Cancer Res* (2012) 18(5):1201–6. doi: 10.1158/1078-0432.Ccr-11-0641

107. Hu J, Lu R, Zhang Y, Li W, Hu Q, Chen C, et al. β-adrenergic receptor inhibition enhances oncolytic herpes virus propagation through STAT3 activation in gastric cancer. *Cell Biosci* (2021) 11(1):174. doi: 10.1186/s13578-021-00687-1

108. Ng KW, Marshall EA, Bell JC, Lam WL. cGAS-STING and cancer: Dichotomous roles in tumor immunity and development. *Trends Immunol* (2018) 39(1):44–54. doi: 10.1016/j.it.2017.07.013

109. Khoo LT, Chen LY. Role of the cGAS-STING pathway in cancer development and oncotherapeutic approaches. *EMBO Rep* (2018) 19(12):e46935. doi: 10.15252/embr.201846935

110. Ishikawa H, Barber GN. STING is an endoplasmic reticulum adaptor that facilitates innate immune signalling. *Nature* (2008) 455(7213):674–8. doi: 10.1038/nature07317

111. Morimoto D, Matsumura S, Bustos-Villalobos I, Sibal PA, Ichinose T, Naoe Y, et al. C-REV retains high infectivity regardless of the expression levels of cGAS and STING in cultured pancreatic cancer cells. *Cells* (2021) 10(6):1502. doi: 10.3390/cells10061502

112. Liu X, He B. Selective editing of herpes simplex virus 1 enables interferon induction and viral replication that destroy malignant cells. *J Virol* (2019) 93(2): e01761–18. doi: 10.1128/jvi.01761-18

113. Chapon M, Parvatiyar K, Aliyari SR, Zhao JS, Cheng G. Comprehensive mutagenesis of herpes simplex virus 1 genome identifies UL42 as an inhibitor of type I interferon induction. *J Virol* (2019) 93(23):e01446–19. doi: 10.1128/jvi.01446-19

114. Kadowaki N, Antonenko S, Lau JY, Liu YJ. Natural interferon alpha/beta-producing cells link innate and adaptive immunity. *J Exp Med* (2000) 192(2):219–26. doi: 10.1084/jem.192.2.219

115. Müller L, Aigner P, Stoiber D. Type I interferons and natural killer cell regulation in cancer. *Front Immunol* (2017) 8:304. doi: 10.3389/fimmu.2017.00304

116. Oku M, Ishino R, Uchida S, Imataki O, Sugimoto N, Todo T, et al. Oncolytic herpes simplex virus type 1 (HSV-1) in combination with lenalidomide for plasma cell neoplasms. *Br J Haematol* (2021) 192(2):343–53. doi: 10.1111/bjh.17173

117. Chen Q, Gong B, Mahmoud-Ahmed AS, Zhou A, Hsi ED, Hussein M, et al. Apo2L/TRAIL and bcl-2-related proteins regulate type I interferon-induced apoptosis in multiple myeloma. *Blood* (2001) 98(7):2183–92. doi: 10.1182/blood.v98.7.2183

118. Wang Y, Jin J, Li Y, Zhou Q, Yao R, Wu Z, et al. NK cell tumor therapy modulated by UV-inactivated oncolytic herpes simplex virus type 2 and checkpoint inhibitors. *Trans Res J Lab Clin Med* (2022) 240:64–86. doi: 10.1016/j.trsl.2021.10.006

119. Zhu G, Zhang J, Zhang Q, Jin G, Su X, Liu S, et al. Enhancement of CD70-specific CAR T treatment by IFN-γ released from oHSV-1-infected glioblastoma. *Cancer Immunol Immunother CII* (2022). doi: 10.1007/s00262-022-03172-x

120. Esaki S, Goshima F, Ozaki H, Takano G, Hatano Y, Kawakita D, et al. Oncolytic activity of HF10 in head and neck squamous cell carcinomas. *Cancer Gene Ther* (2020) 27(7-8):585–98. doi: 10.1038/s41417-019-0129-3

121. Bussiere LD, Miller CL. Reovirus and the host integrated stress response: On the frontlines of the battle to survive. *Viruses* (2021) 13(2):200. doi: 10.3390/v13020200

122. Adair RA, Scott KJ, Fraser S, Errington-Mais F, Pandha H, Coffey M, et al. Cytotoxic and immune-mediated killing of human colorectal cancer by reovirus-loaded blood and liver mononuclear cells. *Int J Cancer* (2013) 132(10):2327–38. doi: 10.1002/ijc.27918

123. Samson A, Scott KJ, Taggart D, West EJ, Wilson E, Nuovo GJ, et al. Intravenous delivery of oncolytic reovirus to brain tumor patients immunologically primes for subsequent checkpoint blockade. *Sci Trans Med* (2018) 10 (422).eaam7577. doi: 10.1126/scitranslmed.aam7577

124. Borghaei H, Paz-Ares L, Horn L, Spigel DR, Steins M, Ready NE, et al. Nivolumab versus docetaxel in advanced nonsquamous non-Small-Cell lung cancer. *New Engl J Med* (2015) 373(17):1627–39. doi: 10.1056/NEJMoa1507643

125. Tumeh PC, Harview CL, Yearley JH, Shintaku IP, Taylor EJ, Robert L, et al. PD-1 blockade induces responses by inhibiting adaptive immune resistance. *Nature* (2014) 515(7528):568–71. doi: 10.1038/nature13954

126. Nguyen KB, Salazar-Mather TP, Dalod MY, Van Deusen JB, Wei XQ, Liew FY, et al. Coordinated and distinct roles for IFN-alpha beta, IL-12, and IL-15 regulation of NK cell responses to viral infection. *J Immunol (Baltimore Md 1950)* (2002) 169(8):4279–87. doi: 10.4049/jimmunol.169.8.4279

127. Baranek T, Manh TP, Alexandre Y, Maqbool MA, Cabeza JZ, Tomasello E, et al. Differential responses of immune cells to type I interferon contribute to host resistance to viral infection. *Cell Host Microbe* (2012) 12(4):571–84. doi: 10.1016/j.chom.2012.09.002

128. Vivier E, Raulet DH, Moretta A, Caligiuri MA, Zitvogel L, Lanier LL, et al. Innate or adaptive immunity? the example of natural killer cells. *Sci (New York NY)* (2011) 331(6013):44–9. doi: 10.1126/science.1198687

129. Vidal SM, Khakoo SI, Biron CA. Natural killer cell responses during viral infections: flexibility and conditioning of innate immunity by experience. *Curr Opin Virol* (2011) 1(6):497–512. doi: 10.1016/j.coviro.2011.10.017

130. Martinez J, Huang X, Yang Y. Direct action of type I IFN on NK cells is required for their activation in response to vaccinia viral infection in vivo. *J Immunol (Baltimore Md 1950)* (2008) 180(3):1592–7. doi: 10.4049/jimmunol.180.3.1592

131. Sato K, Hida S, Takayanagi H, Yokochi T, Kayagaki N, Takeda K, et al. Antiviral response by natural killer cells through TRAIL gene induction by IFN-alpha/beta. *Eur J Immunol* (2001) 31(11):3138–46. doi: 10.1002/1521-4141(200111)31:11<3138::aid-immu3138>3.0.co;2-b

132. Wantoch M, Wilson EB, Droop AP, Phillips SL, Coffey M, El-Sherbiny YM, et al. Oncolytic virus treatment differentially affects the CD56(dim) and CD56 (bright) NK cell subsets *in vivo* and regulates a spectrum of human NK cell activity. *Immunology* (2022) 166(1):104–20. doi: 10.1111/imm.13453

133. Katayama Y, Tachibana M, Kurisu N, Oya Y, Terasawa Y, Goda H, et al. Oncolytic reovirus inhibits immunosuppressive activity of myeloid-derived suppressor cells in a TLR3-dependent manner. *J Immunol (Baltimore Md 1950)* (2018) 200(8):2987–99. doi: 10.4049/jimmunol.1700435

134. Rodríguez Stewart RM, Berry JTL, Berger AK, Yoon SB, Hirsch AL, Guberman JA, et al. Enhanced killing of triple-negative breast cancer cells by reassortant reovirus and topoisomerase inhibitors. *J Virol* (2019) 93(23):e01411–19. doi: 10.1128/jvi.01411-19

135. Oosenbrug T, van den Wollenberg DJM, Duits EW, Hoeben RC, Ressing ME. Induction of robust type I interferon levels by oncolytic reovirus requires both viral replication and interferon-α/β receptor signaling. *Hum Gene Ther* (2021) 32 (19-20):1171–85. doi: 10.1089/hum.2021.140

136. Lanoie D, Boudreault S, Bisaillon M, Lemay G. How many mammalian reovirus proteins are involved in the control of the interferon response? *Pathog (Basel Switzerland)* (2019) 8(2):83. doi: 10.3390/pathogens8020083

137. Lanoie D, Lemay G. Multiple proteins differing between laboratory stocks of mammalian orthoreoviruses affect both virus sensitivity to interferon and induction of interferon production during infection. *Virus Res* (2018) 247:40–6. doi: 10.1016/j.virusres.2018.01.009

138. Jacobs BL, Ferguson RE. The Lang strain of reovirus serotype 1 and the Dearing strain of reovirus serotype 3 differ in their sensitivities to beta interferon. *J Virol* (1991) 65(9):5102–4. doi: 10.1128/jvi.65.9.5102-5104.1991

139. Stuart JD, Holm GH, Boehme KW. Differential delivery of genomic double-stranded RNA causes reovirus strain-specific differences in interferon regulatory factor 3 activation. *J Virol* (2018) 92(9):e01947–17. doi: 10.1128/jvi.01947-17

140. Dionne KR, Galvin JM, Schittone SA, Clarke P, Tyler KL. Type I interferon signaling limits reoviral tropism within the brain and prevents lethal systemic infection. *J Neurovirol* (2011) 17(4):314–26. doi: 10.1007/s13365-011-0038-1

141. Sherry B, Torres J, Blum MA. Reovirus induction of and sensitivity to beta interferon in cardiac myocyte cultures correlate with induction of myocarditis and are determined by viral core proteins. *J Virol* (1998) 72(2):1314–23. doi: 10.1128/jvi.72.2.1314-1323.1998

142. Zurney J, Kobayashi T, Holm GH, Dermody TS, Sherry B. Reovirus mu2 protein inhibits interferon signaling through a novel mechanism involving nuclear accumulation of interferon regulatory factor 9. *J Virol* (2009) 83(5):2178–87. doi: 10.1128/jvi.01787-08

143. Mohamed A, Konda P, Eaton HE, Gujar S, Smiley JR, Shmulevitz M. Closely related reovirus lab strains induce opposite expression of RIG-I/IFN-dependent versus -independent host genes, *via* mechanisms of slow replication versus polymorphisms in dsRNA binding σ3 respectively. *PLoS Pathogens* (2020) 16(9):e1008803. doi: 10.1371/journal.ppat.1008803

144. Rahman AU, Habib M, Shabbir MZ. Adaptation of Newcastle disease virus (NDV) in feral birds and their potential role in interspecies transmission. *Open Virol J* (2018) 12:52–68. doi: 10.2174/1874357901812010052

145. Santos MR, Xavier PLP, Pires PRL, Rochetti AL, Rosim DF, Scagion GP, et al. Oncolytic effect of Newcastle disease virus is attributed to interferon regulation in canine mammary cancer cell lines. *Veterinary Comp Oncol* (2021) 19(3):593–601. doi: 10.1111/vco.12699

146. Zamarin D, Ricca JM, Sadekova S, Oseledchyk A, Yu Y, Blumenschein WM, et al. PD-L1 in tumor microenvironment mediates resistance to oncolytic immunotherapy. *J Clin Invest* (2018) 128(4):1413–28. doi: 10.1172/jci98047

147. Koks CA, Garg AD, Ehrhardt M, Riva M, Vandenberk L, Boon L, et al. Newcastle Disease virotherapy induces long-term survival and tumor-specific immune memory in orthotopic glioma through the induction of immunogenic cell death. *Int J Cancer* (2015) 136(5):E313–25. doi: 10.1002/ijc.29202

148. Mozaffari Nejad AS, Fotouhi F, Mehrbod P, Alikhani MY. Antitumor immunity enhancement through Newcastle viral oncolysate in mice model: A promising method to treat tumors. *Saudi J Biol Sci* (2021) 28(10):5833–40. doi: 10.1016/j.sjbs.2021.06.043

149. Tian L, Liu T, Jiang S, Cao Y, Kang K, Su H, et al. Oncolytic Newcastle disease virus expressing the co-stimulator OX40L as immunopotentiator for colorectal cancer therapy. *Gene Ther* (2021). doi: 10.1038/s41434-021-00256-8

150. Keshavarz M, Ebrahimzadeh MS, Miri SM, Dianat-Moghadam H, Ghorbanhosseini SS, Mohebbi SR, et al. Oncolytic Newcastle disease virus delivered by mesenchymal stem cells-engineered system enhances the therapeutic effects altering tumor microenvironment. *Virol J* (2020) 17(1):64. doi: 10.1186/s12985-020-01326-w

151. Zamarin D, Palese P. Oncolytic Newcastle disease virus for cancer therapy: old challenges and new directions. *Future Microbiol* (2012) 7(3):347–67. doi: 10.2217/fmb.12.4

152. García-Romero N, Palacín-Aliana I, Esteban-Rubio S, Madurga R, Rius-Rocabert S, Carrión-Navarro J, et al. Newcastle Disease virus (NDV) oncolytic activity in human glioma tumors is dependent on CDKN2A-type I IFN gene cluster codeletion. *Cells* (2020) 9(6):1405. doi: 10.3390/cells9061405

153. Krug RM. Functions of the influenza a virus NS1 protein in antiviral defense. *Curr Opin Virol* (2015) 12:1–6. doi: 10.1016/j.coviro.2015.01.007

154. Zamarin D, Martínez-Sobrido L, Kelly K, Mansour M, Sheng G, Vigil A, et al. Enhancement of oncolytic properties of recombinant newcastle disease virus through antagonism of cellular innate immune responses. *Mol Ther J Am Soc Gene Ther* (2009) 17(4):697–706. doi: 10.1038/mt.2008.286

155. El-Jesr M, Teir M, Maluquer de Motes C. Vaccinia virus activation and antagonism of cytosolic DNA sensing. *Front Immunol* (2020) 11:568412. doi: 10.3389/fimmu.2020.568412

156. Shen Y, Nemunaitis J. Fighting cancer with vaccinia virus: teaching new tricks to an old dog. *Mol Ther J Am Soc Gene Ther* (2005) 11(2):180–95. doi: 10.1016/j.ymthe.2004.10.015

157. Puhlmann M, Gnant M, Brown CK, Alexander HR, Bartlett DL. Thymidine kinase-deleted vaccinia virus expressing purine nucleoside phosphorylase as a vector for tumor-directed gene therapy. *Hum Gene Ther* (1999) 10(4):649–57. doi: 10.1089/10430349950018724

158. Guo ZS, Lu B, Guo Z, Giehl E, Feist M, Dai E, et al. Vaccinia virus-mediated cancer immunotherapy: cancer vaccines and oncolytics. *J Immunother Cancer* (2019) 7(1):6. doi: 10.1186/s40425-018-0495-7

159. Jia X, Chen Y, Zhao X, Lv C, Yan J. Oncolytic vaccinia virus inhibits human hepatocellular carcinoma MHCC97-h cell proliferation *via* endoplasmic reticulum stress, autophagy and wnt pathways. *J Gene Med* (2016) 18(9):211–9. doi: 10.1002/jgm.2893

160. Wang X, Zhou N, Liu T, Jia X, Ye T, Chen K, et al. Oncolytic vaccinia virus expressing white-spotted charr lectin regulates antiviral response in tumor cells and inhibits tumor growth *In vitro* and in vivo. *Mar Drugs* (2021) 19(6):292. doi: 10.3390/md19060292

161. Chen L, Chen H, Ye J, Ge Y, Wang H, Dai E, et al. Intratumoral expression of interleukin 23 variants using oncolytic vaccinia virus elicit potent antitumor effects on multiple tumor models *via* tumor microenvironment modulation. *Theranostics* (2021) 11(14):6668–81. doi: 10.7150/thno.56494

162. West EJ, Scott KJ, Tidswell E, Bendjama K, Stojkowitz N, Lusky M, et al. Intravenous oncolytic vaccinia virus therapy results in a differential immune response between cancer patients. *Cancers* (2022) 14(9):2181. doi: 10.3390/cancers14092181

163. Engeland CE, Ungerechts G. Measles virus as an oncolytic immunotherapy. *Cancers* (2021) 13(3):544. doi: 10.3390/cancers13030544

164. Achard C, Boisgerault N, Delaunay T, Roulois D, Nedellec S, Royer PJ, et al. Sensitivity of human pleural mesothelioma to oncolytic measles virus depends on defects of the type I interferon response. *Oncotarget* (2015) 6(42):44892–904. doi: 10.18632/oncotarget.6285

165. Delaunay T, Achard C, Boisgerault N, Grard M, Petithomme T, Chatelain C, et al. Frequent homozygous deletions of type I interferon genes in pleural mesothelioma confer sensitivity to oncolytic measles virus. *J Thorac Oncol Off Publ Int Assoc Stud Lung Cancer* (2020) 15(5):827–42. doi: 10.1016/j.jtho.2019.12.128

166. Yap TA, Aerts JG, Popat S, Fennell DA. Novel insights into mesothelioma biology and implications for therapy. *Nat Rev Cancer* (2017) 17(8):475–88. doi: 10.1038/nrc.2017.42

167. Jean D, Daubriac J, Le Pimpec-Barthes F, Galateau-Salle F, Jaurand MC. Molecular changes in mesothelioma with an impact on prognosis and treatment. *Arch Pathol Lab Med* (2012) 136(3):277–93. doi: 10.5858/arpa.2011-0215-RA

168. Aref S, Castleton AZ, Bailey K, Burt R, Dey A, Leongamornlert D, et al. Type 1 interferon responses underlie tumor-selective replication of oncolytic measles virus. *Mol Ther J Am Soc Gene Ther* (2020) 28(4):1043–55. doi: 10.1016/j.ymthe.2020.01.027

169. Annels NE, Mansfield D, Arif M, Ballesteros-Merino C, Simpson GR, Denyer M, et al. Phase I trial of an ICAM-1-Targeted immunotherapeutic-coxsackievirus A21 (CVA21) as an oncolytic agent against non muscle-invasive bladder cancer. *Clin Cancer Res an Off J Am Assoc Cancer Res* (2019) 25(19):5818–31. doi: 10.1158/1078-0432.Ccr-18-4022

170. Desjardins A, Gromeier M, Herndon JE2nd, Beaubier N, Bolognesi DP, Friedman AH, et al. Recurrent glioblastoma treated with recombinant poliovirus. *New Engl J Med* (2018) 379(2):150–61. doi: 10.1056/NEJMoa1716435

171. Walton RW, Brown MC, Sacco MT, Gromeier M. Engineered oncolytic poliovirus PVSRIPO subverts MDA5-dependent innate immune responses in cancer cells. *J Virol* (2018) 92(19):e00879–18. doi: 10.1128/jvi.00879-18

frontiers | Frontiers in Immunology

TYPE Review
PUBLISHED 26 August 2022
DOI 10.3389/fimmu.2022.978619

OPEN ACCESS

EDITED BY
Chang Li,
Chinese Academy of Agricultural Sciences (CAAS), China

REVIEWED BY
Hualei Wang,
Jilin University, China
Dongbo Sun,
Heilongjiang Bayi Agricultural University, China

*CORRESPONDENCE
Rui Gao
ruigao@126.com
Xianbin Kong
kongxianbinvip@163.com
Long Yang
long.yang@tjutcm.edu.cn

†The authors have contributed equally to this work

SPECIALTY SECTION
This article was submitted to Molecular Innate Immunity, a section of the journal Frontiers in Immunology

RECEIVED 26 June 2022
ACCEPTED 04 August 2022
PUBLISHED 26 August 2022

CITATION
Yi J, Miao J, Zuo Q, Owusu F, Dong Q, Lin P, Wang Q, Gao R, Kong X and Yang L (2022) COVID-19 pandemic: A multidisciplinary perspective on the pathogenesis of a novel coronavirus from infection, immunity and pathological responses. *Front. Immunol.* 13:978619. doi: 10.3389/fimmu.2022.978619

COVID-19 pandemic: A multidisciplinary perspective on the pathogenesis of a novel coronavirus from infection, immunity and pathological responses

Jia Yi[1†], Jiameng Miao[1†], Qingwei Zuo[2†], Felix Owusu[3], Qiutong Dong[1], Peizhe Lin[1], Qilong Wang[3], Rui Gao[4*], Xianbin Kong[1*] and Long Yang[2,5*]

[1]College of Traditional Chinese medicine, Tianjin University of Traditional Chinese Medicine, Tianjin, China, [2]Research Center for Infectious Diseases, Tianjin University of Traditional Chinese Medicine, Tianjin, China, [3]Institute of Traditional Chinese Medicine, Tianjin University of Traditional Chinese Medicine, Tianjin, China, [4]Institute of Clinical Pharmacology of Xiyuan Hospital, China Academy of Chinese Medical Sciences, Beijing, China, [5]School of Integrative Medicine, Tianjin University of Traditional Chinese Medicine, Tianjin, China

Coronavirus disease 2019 (COVID-19), caused by severe acute respiratory syndrome coronavirus2 (SARS-CoV-2), has spread to more than 200 countries and regions, having a huge impact on human health, hygiene, and economic activities. The epidemiological and clinical phenotypes of COVID-19 have increased since the onset of the epidemic era, and studies into its pathogenic mechanisms have played an essential role in clinical treatment, drug development, and prognosis prevention. This paper reviews the research progress on the pathogenesis of the novel coronavirus (SARS-CoV-2), focusing on the pathogenic characteristics, loci of action, and pathogenic mechanisms leading to immune response malfunction of SARS-CoV-2, as well as summarizing the pathological damage and pathological manifestations it causes. This will update researchers on the latest SARS-CoV-2 research and provide directions for future therapeutic drug development.

KEYWORDS

COVID-19, SARS-CoV-2, pathogenic mechanism, virus infected, immune pathogenesis

1 Introduction

Since the end of December 2019, a global outbreak epidemic has emerged in several countries as an acute respiratory infection caused by a previously undiscovered strain of coronavirus (1). On December 1, 2019, the first pneumonia of unknown origin was identified in Wuhan, Hubei Province, and confirmed as a new coronavirus on January 8, 2020 (2, 3). On 12 January 2020, the World Health Organization (WHO) tentatively named this virus as "2019 new coronavirus (2019-nCoV)", and on 11 February, the International Committee on Classification of Viruses officially called it "SARS -CoV-2", and on the same day WHO unified pneumonia caused by SARS-CoV-2 infection as "Coronavirus disease 2019 (COVID-19)". This pneumonia is associated with a novel strain of RNA virus from the coronavirus family. In terms of clinical manifestations, COVID-19 has a lower morbidity and mortality rate than SAS and MERS. Still, it spreads faster and more widely, and the number of infections and deaths far exceeds those of the first two viruses (4), which are highly infectious, have a long incubation period, and are prone to mutation (5). COVID-19 can lead to severe acute respiratory infections and multiple organ systems functional impairment, with 15-30% of COVID-19 patients requiring Intensive Care Unit (ICU) admission and organ function support therapy, with an overall morbidity and mortality rate of 4.3%-15% (6), with a morbidity and mortality rate of up to 61% within 28 days in critically ill patients.

Therefore, an in-depth exploration of the pathogenic mechanism of COVID-19 is crucial in achieving an accurate diagnosis, targeted therapy, vaccine development, and improved prognosis. This review provides a detailed overview of the pathogenic mechanism of the new coronavirus based on the pathogenic characteristics of the virus, the process of invasion into the human body, the dysregulation of the immune response caused, and the pathological manifestations and pathological damage of the organism, to provide clinical and scientific assistance.

2 Pathogenic characteristics and loci of action of SARS-CoV-2 virus

The main routes of transmission of SARS-CoV-2 are currently considered to be respiratory droplets and close contact (3), with the possibility of aerosol transmission (7) and vertical transmission (8) also present. Data from a clinical study of 1145 patients suggest that the severe course of COVID-19 may be closely related to its viral load during exposure (9). Therefore, studying the pathogenic characteristics of SARS-CoV-2 and its loci of action is essential to understanding the pathogenic mechanisms of the virus.

2.1 Pathogenetic characteristics of SARS-CoV-2 virus

SARS-CoV-2 is a member of the coronaviridae family, order Nestoroviridae, genus Pre-coronavirus, and is a spherical enveloped virus with a diameter of approximately 120 nm (10). Mature SARS-CoV-2 viral particles consist of a positive 5'-plus-cap and 3'-polyadenylate single-stranded RNA with a genomic sequence approximately 30,000 bases long, encoding the structural proteins nucleocapsid phosphoprotein (N), membrane glycoprotein (M), envelope (E), spines (S), and nonstructural protein (nsp) (11). Among them, it is mainly the S glycoprotein that mediates viral entry into target cells and the E and M proteins responsible for viral transcription, translation, and assembly.

The S protein consists of S1 and S2 subunits. The S1 subunit consists of the N-terminal structural domain (NTD) and the receptor binding domain (RBD), which is responsible for the direct binding of Angiotensin-converting enzyme 2 (ACE2) (12); the S2 subunit mediates the fusion of the viral envelope with the host cell membrane (13). It was shown that RBD in the SARS-CoV-2 spike-in (S) protein undergoes a specific point mutation, i.e., the asparagine is replaced by tyrosine at position 501 (N501Y) (14), and thus the N501Y S-protein binds more readily to the ACE2 receptor than the original S-protein (15). The S-protein was found to have four amino acid residues inserted at the junction of subunits S1 and S2 (PRRA) (16). This amino acid sequence can be efficiently cleaved by furin and other proteases (17), which reduce the stability of the SARS-CoV-2 S-protein, enhance viral membrane fusion and infection, and promote viral replication (18).

In addition, it has been proposed that S proteins can circulate within the Golgi and promote S protein cleavage and glycosylation, thereby infecting the plasma membrane of cells (19). Another study found that the S1/S2 cleavage site has remained constant during the human evolution of SARS-CoV-2, suggesting that it provides an adaptive advantage for the virus (14). The antiviral activity of chloroquine and its analogues are well established in the fight against SARS-CoV-2 infection (20), and clinical trials have shown that the use of some chloroquine derivatives can achieve viral reduction and improve the efficacy of the infection (21, 22). And laboratory studies have shown that its antiviral effects are attributed to multiple mechanisms, including fighting coronavirus infection by blocking the glycosylation of host receptors (23, 24), inhibiting the processing of S proteins, and suppressing the inflammatory response (25).

2.2 Action sites of SARS-CoV-2 virus

ACE2 is a metallocarboxypeptidase of the renin-angiotensin-aldosterone system (RAS) (26). The pathway of SARS-CoV-2 into host epithelial cells was mainly focused on

ACE2 (27). Accordingly, it has been found that tetracycline and doxycycline can act as inhibitors of ACE2-peg binding (28).

ACE2 is expressed in over 150 different cell types in all major human tissues and organs, and its expression levels do not vary by age, sex, or race. Immunofluorescence data showed (29) that ACE2 is expressed at higher levels in epithelial cells of the upper respiratory tract, lung, heart, kidney, testis (30), intestine, liver, pancreas, stomach, duodenum, and rectum (31), and the higher levels of ACE2 in the cilia of the nose compared to the bronchi (32) also suggest that the nose may be the initial site of viral invasion and infection.

ACE2 decreases angiotensin II (Ang II) and is a stimulator of Nicotinamide Adenine Dinucleotide Phosphate (NADPH) oxidase (33). It is a key molecule in the body's resistance to inflammation and oxidative damage in tissues triggered by SARS-CoV-2. After SARS-CoV-2 binds to the ACE2 receptor and begins to enter the cell and fuses with the viral particle-membrane, ACE2 expression will be downregulated (34), and the affinity of angiotensin II is significantly increased during infection, leading to the susceptibility of the virus in binding to ACE2 (35). It was shown that the affinity of SARS-CoV-2 to ACE2 receptor is about 10-20-fold higher than SARS-CoV (36). Therefore, based on the persistent downregulation of ACE2 expression, the overproduction of angiotensin II and activation of NADPH oxidase leads to enhanced oxidative stress mechanisms along with the release of inflammatory molecules (37), leading to the rapid progression of the disease.

In addition, cell surface phospholipid proteoglycans (HSPGs) interact with the S protein of SARS-CoV-2 (18), triggering a conformational change in the S protein RBD, and acting as a cofactor during viral endocytosis (33), which facilitates viral binding to its specific receptor (38). Basic studies suggest that HSPGs are modified by 3-OST isoform 3 but not 3-OST isoform 5, increasing S protein-mediated fusion between SARS-CoV-2 and cells, suggesting a role in virus transmission (39). In particular, HSPGs have been identified as adhesion receptors for SARS-CoV-2 infection in isolated human lung tissue explants from human lung epithelial cell nuclei *in vitro* (40).

RNA sequencing also revealed that immune cells, although not expressing ACE2, are transmembrane proteins of immunoglobulin cluster of differentiation (CD) 147, providing a pathway for the virus to enter and attack immune cells (41–43). It should be noted that one study using single-cell sequencing found that few cells in the placenta express both ACE2 and transmembrane serine proteases (TMPRSS2), thus concluding that ACE2 is not an effective route of transmission from mother to child (44). (Figure 1) Also, in combination with the replication process of new coronaviruses, the nucleoside analogue favipiravir (T-705) was found to effectively inhibit the RNA polymerase activity of RNA viruses (45). Remdesivir targets RNA-dependent RNA polymerase (RdRp) and is a nucleotide analogue. Remdesivir received emergency use authorization from the US Food and Drug Administration (FDA) and was approved as the first drug to treat patients with COVID-19 (46). The pharmacological mechanism of the drug is to interfere with the polymerization of viral RNA (47). As a broad-spectrum antiviral drug, it has significant antiviral activity against several RNA

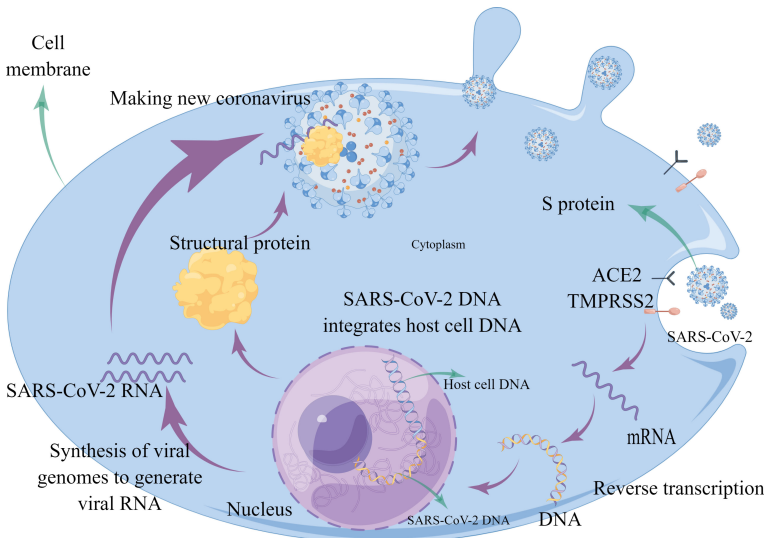

FIGURE 1
Schematic diagram showing SARS-CoV-2 injecting RNA into the host cell by binding to the ACE2 receptor on normal cells *via* the S protein. The injected RNA uses the nutrients in the host cell to replicate itself and make the structural proteins it needs. The structural proteins combine with the RNA to form a new virus.

viruses such as Ebola virus, coronavirus (48), hepatitis C virus, and human immunodeficiency virus (HIV) (49). Experimental studies have shown that the drug significantly inhibited SARS-CoV-2 virus infection in Vero E6 cells (50), while reducing viral load and pulmonary pathological changes in animal models (51), and had stronger antiviral activity in combination with interferon (52). Lopinavir/ritonavir (LPV/r) are two anti-HIV protein hydrolase inhibitor (PI) drugs that act as antiviral retroviral with a pharmacological mechanism that prevents the excision of the Gag-Poll polyprotein (53), leading to the immaturity of the virus that replicates and proliferates in the organism. Clonidine is also thought to inhibit RNA virus replication by entering the infected cells during viral RNA (54).

At the same time, studies have pointed out that papain-like protease (PLpro) and main protease (Mpro/3CLpro) are two crucial proteases produced by the new coronavirus. Therefore, inhibition of PLPro and Mpro/3CLpro can effectively inhibit virus infection and replication, and is a vital target for antiviral drug development (55). The researchers screened and evaluated the applicability of a batch of FDA-approved clinical drugs targeting PLpro to SARS-CoV-2 PLpro, and found that a naphthalene-based noncovalent inhibitor GRL0617 works by occupying and blocking the PLpro substrate-binding pockets S3 and S4 exerted a potent inhibitory activity. In addition, studies have also identified inhibitors against novel coronavirus Mpro, including boceprevir, GC-376, and calpain inhibitors II and XII, which are often mimetic peptides that mimic natural peptide substrates and covalently bind to residue C145 in Mpro to exert inhibitory effects. (56). And a study selected 47 from the list of 3987 FDA-approved drugs for *in vitro* 3CLpro enzyme inhibitor screening test, and observed that boceprevir, ombitasvir, paritaprevir, tipranavir, and micafungin showed partial inhibition, and ivermectin blocked. The 3CLpro activity of SARS-CoV-2 was more than 85%, indicating that it has the potential to inhibit the replication of SARS-CoV-2. In addition, PF-07321332, developed by Pfizer, is the first oral coronavirus-specific major protease inhibitor approved by the U.S. FDA. The FDA has approved emergency treatment for Paxlovid (PF-07321332 and ritonavir). As a protease inhibitor, PF-07321332 binds to viral enzymes and can block the activity of proteases required for the coronavirus to replicate itself. Ritonavir, an inhibitor of a key liver enzyme called CYP3A, also increased and maintained plasma concentrations of PF-07321332 when given in combination (57).

2.3 Mediating factors of SARS-CoV-2 virus invasion into cells

The consensus achieved by the current study is that the entry and spread of the SARS-CoV-2 virus depend on the host ACE2 receptor and the serine protease TMPRSS2, with possible involvement of B/L7 and furin proteases (27).

Experimental studies have shown that the S protein of the SARS-CoV-2 virus binds to the receptor, acid-dependent proteolytic cleavage (58), and is assisted by the S2 subunit to mediate the fusion of the viral membrane with the cell membrane (59), leading to cytoplasmic lysis. This process is mainly mediated by certain host proteases, including furin protease, TMPRSS2, histone B, histone L, factor Xa, and elastase (60). Bertram et al. also suggested that the coronavirus protease system is transmembrane anchored, which is essential for invasion and infection (61). As previously described, after membrane fusion and protease mediation, the S1/S2 site of the S protein will insert four amino acids, providing a motif that can be recognized and cleaved by the furin protease. The virus is then cleaved by TMPRSS2, and the viral protease system forms an unlocking and fusion catalytic structure with the type II transmembrane serine protease (TTSP) family at the cell surface and mediates rapid entry into the cell and completion of ligation within the cell (61, 62), triggering irreversible and extensive conformational changes that mediate membrane fusion (63, 64).

In addition to the associated proteases, it has been proposed that coronavirus infection increases circulating exosomes containing lung-associated autoantigens as well as viral antigens and 20S proteasomes (65). It has also been shown that SARS-CoV-2 drives host cell molecular pathways to activate cellular kinases, such as casein kinase II (CK2) and p38 mitogen-activated protein kinase (MAPK), and growth factor receptor (GFR) signaling to hijack the host protein production machinery (66) for its replication, transcription, and translation purposes.

3 Abnormalities in the body's immune response

When normal, the body's immune system can limit processes such as the entry of viruses into host cells and their replication within the host cells. The immune system has two main defense mechanisms: innate immunity and adaptive immunity. In contrast, after infection with the SARS-CoV-2 virus, the pathogen-associated molecular patterns (PAMPs) of the virus trigger specific combinations of pattern recognition receptors (PRRs) and adapter molecules, leading to an immune response adapted to the pathogen (67), resulting in abnormal immune response function and causing the associated pathological processes.

3.1 Inherent immune response dysregulation

Innate immunity is the first line of defense against infection. The main cells that perform innate immunity are mast cells, NK (natural killer cells), NKT (natural killer T cells), NHC (natural helper cells), granulocytes, macrophages, and monocytes. The organism detects coronaviruses through PRRs, which trigger an

innate immune response that effectively limits viral replication. And it helps to control or eliminate viral infections by releasing interferons (IFNs), while activating interferon-stimulated genes (ISGs) to exert direct antiviral effects and recruit antiviral immune effector cells to clear the virus (Table 1).

3.1.1 Excessive inflammatory response

Studies have shown that reduced numbers and functional failure of NK cells occur during SARS-CoV-2 infection (68, 69), and the mechanism may be closely related to the generation of reactive oxygen species (ROS) during the early stages of the immune response. In addition, Nox2 may be a key factor in the infection and development of COVID-19. It was found that the SARS-CoV-2 virus may suppress the immune response and lead to infection by activating Nox2 (NADPH oxidase 2, nicotinamide adenine dinucleotide phosphate hydrogen oxidase 2) (70). Clinical observations likewise revealed higher levels of Nox2 activation in critically ill patients with COVID-19 (37).

The main PRRs-against viruses are currently considered to be Toll-like receptors (TLRs) and RIG-I-like receptors (RLRRs), and NOD-like receptors (NLRX) (71). Among them, PRRs are present on the cytoplasmic and endosomal membranes of immune cells, and their function is to recognize foreign pathogens on the cell surface or inside. The binding of PAMPs to PRRs induces innate immune signaling (17), successively involving adaptor proteins (MYD88, TRIF, RGL-1, and MAD-5), cell membrane protein kinases (IRKs, MAPKs, and ERKs), and finally the production of transcription factors at the cell membrane (e.g., nuclear factor kappa-B, IFRs, NF-κB, and IFRs) (72). These transcription factors migrate to the nucleus and induce the expression of encoded cytokines, IFN-I, IFN-III, pro-inflammatory cytokines, and chemokines (73), which leads to a massive accumulation of neutrophils (74). Although neutrophils have an antiviral function, their secretions, cytokines, and chemokines promote the accumulation of immune cells and further produce an excessive inflammatory response (75) (Figure 2).

Glucocorticoids should be used for a short period of time, as appropriate, in patients with progressively worsening oxygenation indices, rapidly developing imaging, and over-activated inflammatory responses (76), and systemic corticosteroid use is effective in reducing mortality in critically ill patients with COVID-19 (77). The World Health Organization recommends using dexamethasone 6 mg daily for up to 10 days in patients with severe or critical COVID-19

Table 1 Summary of research progress on COVID-19 innate immune response dysregulation.

Pathological process	Mechanism	Presenters	Time
Excessive inflammatory response	ROS is associated with reduced numbers and functional failure of NK cells.	Osman; Zheng	2020
	SARS-CoV-2 suppresses immune response and causes infection through activation of Nox2.	Violi	2020
	Binding of PAMPs to PRRs induces intrinsic immune signaling.	Higashikuni	2021
	Immune signaling sequentially involves adaptor proteins (MYD88, TRIF, RGL-1 and MAD-5), cell membrane protein kinases (IRKs, MAPKs and ERKs) and finally transcription factors (e.g. nuclear factor kappa-B, IFRs, NF-κB and IFRs) are produced at the cell membrane.	Vabret	2020
	Transcription factors migrate to the nucleus and induce the expression of encoded cytokines, IFN-I, IFN-III, pro-inflammatory cytokines and chemokines.	de Wit	2016
	CRAC channel inhibitors block the release of pro-inflammatory cytokines and protect the integrity of endothelial cells.	Bruen	2022
Evasion of natural immune system recognition	Nsp16 and nsp10 induce the synthesis of viral mRNAs that mimic host cell mRNAs, thereby protecting the virus from the host intrinsic immune response.	Viswanathan	2020
	SARS-CoV-2 nsp1 causes mRNA translation shutdown in host cells and blocks RIG-I and ISG.	Higashikuni	2021
	SARS-CoV-2 inhibits interferon-induced and blocked IFN signaling and leads to decreased expression levels of toll-like receptor 7, TLR8, TLR2 and TLR4 receptors that recognize SARS-CoV-2 viral RNA, producing immune escape.	V'Kovski	2021
Interferon response dysregulation	The immune evasion mechanism of SARS-CoV-2 is also associated with the inhibition of IFN production and IFN signaling by viral proteins.	Hadjadj; Jiang	2020
	The protease of SARS-CoV-2 can directly cleave IRF3, resulting in diminished IFN production.	Moustaqil	2021
	IRF7 and IRF9 are upregulated in SARS-CoV-2 infection and severe viral load may overwhelm the IFN response and determine the outcome of the infection.	Hasan	2021
	ORF-6 acts as an antagonist of type I interferon promoting viral escape from the host intrinsic immune system.	Fiorino	2021
	Viral proteins or nucleic acids that trigger PRRs induce β-interferon TIR structural domain bridging proteins (TRIFs) and IRFs *via* TIR domain-containing junctions, thereby activating the interferon response.	Prompetchara	2020
	SARS-CoV-2 viral protein's interference with interfering with the production of IFN leads to or blocks the downstream signaling pathway following the binding of IFN to ISGs.	Bastard; Zhang	2020

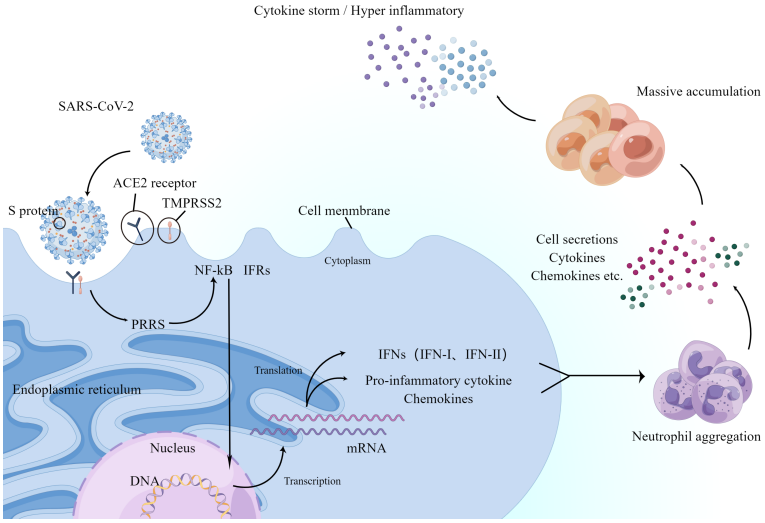

FIGURE 2
Schematic diagram showing the process by which the new coronavirus enters the human body and triggers an inflammatory response. ACE2 and TMPRSS2 play a decisive role in neo-coronavirus invasion. The major PRRs against viruses are present on the cytoplasmic and endosomal membranes of immune cells and recognize foreign viruses. After a series of processes, they finally produce transcription factors NF-κB and IFRs on the cell membrane. Next, they migrate to the nucleus and induce the expression of encoded cytokines and IFN-I and IFN-III, pro-inflammatory cytokines, and chemokines, which in turn accumulate large numbers of neutrophils. The secretion of neutrophils, cytokines, and chemokines promotes further accumulation of immune cells, producing an excessive inflammatory response or further triggering the cytokine storm mentioned below.

(78). Calcium-release-activated calcium (CRAC) channel inhibitors block the release of pro-inflammatory cytokines, protect endothelial integrity, and may be effective in treating patients with severe COVID-19 pneumonia (79).

3.1.2 Evasion of natural immune system recognition

SARS-CoV-2 viruses possess ways to escape the natural immune system, such as modifying their own viral mRNAs, inducing mRNA translation abnormalities in host cells, and blocking interferons. It was found that nsp16 and nsp10 induce the synthesis of viral mRNAs that mimic host cell mRNAs, thereby protecting the virus from the host's innate immune response (80). The spike protein of SARS-CoV-2 facilitates invasion of host cells and evades detection by host immune cells. It was found that the nsp1 of SARS-CoV-2 causes mRNA translation shutdown in host cells and blocks Retinoic acid-inducible gene I (RIG-I) and Immune Serum Globulin (ISG), key mediators of the innate immune response against viral infection (17). Furthermore, SARS-CoV-2 will inhibit interferon-induced and blocked IFN signaling and lead to decreased expression levels of toll-like receptor 7, TLR8, TLR2, and TLR4 receptors that recognize SARS-CoV-2 viral RNA, which will lead to immune escape as SARS-CoV-2 virus is not recognized by the host's immune system (81).

3.1.3 Interferon response dysregulation

IFNs are the first line of defense against viruses. It includes a series of antiviral IFN cytokines, classified into types I, II, and III according to their unique molecular structures, which trigger the expression of ISGs. ISGs exert various antiviral and other immunomodulatory functions by directly inhibiting viral replication (82), transcription, and translation through multiple mechanisms.

It is important to note that viruses (especially those infecting the lung) develop strategies to evade PRR detection and thus alter the host IFN response; for example, some viral proteins can inhibit PRRs in host cells (83). It was found that the immune evasion mechanism of SARS-CoV-2, in addition to the previously described, may also be related to the inhibition of IFN production and IFN signaling by viral proteins (84, 85). Experimental observations revealed that interferon regulatory factor (IRF) mediated signaling was not activated (86), suggesting that dysregulation of interferon response occurs during SARS-CoV-2 virus infection.

Studies suggest that although the organism produces ISGs, transcriptional processes regulated by the interferon regulators IRF3 or IRF7 are apparently absent in SARS-CoV-2 infection. And experiments have shown that the protease of SARS-CoV-2 can directly cleave IRF3 and lead to an attenuated production of IFN (87). Other experiments have shown that IRF7 and IRF9 are

upregulated in SARS-CoV-2 infection and that severe viral load may overwhelm the IFN response and determine the outcome of the infection (86), manifesting as a dysregulated IFN response. Studies suggest that Open reading frame 6 (ORF-6) acts as an antagonist of type I interferon, promoting viral escape from the host innate immune system (11).

It was found that viral proteins or nucleic acids that trigger PRRs induce β-interferon TIR structural domain bridging proteins (TRIFs) and IRFs through TIR structural domain-containing junctions, thereby activating the interferon response (88). And triggering PRRs and interferon type I pathway leads to a further oxidative stress response. Meanwhile, the SARS-CoV-2 viral protein has an inhibitory effect on IFN-I-mediated antiviral immune responses. Its interference with interfering with the production of IFN leads to or blocks the downstream signaling pathway following the binding of IFN to ISGs (89, 90), thus antagonizing the innate immune response.

3.2 Adaptive immune response dysregulation

When the organism exerts a normal adaptive immune response, the SARS-CoV-2 viral antigen is recognized, processed, and presented by antigen-presenting cells (APCs), thereby activating cellular and humoral immunity. This includes the activation of $CD4^+$ and $CD8^+$ T cell differentiation. $CD4^+$ T cells are activated and differentiate into Th1 and Th2 effector cells and other subpopulations (including Tfh cells, etc.) that recruit immune cells by secreting cytokines (including MIP-1s, INF γ, etc.) and chemokines, $CD8^+$ T cells produce substances such as Perforin, CD107a, and Granzyme B, while B cell differentiation and antibody production are stimulated, which together exert adaptive immunity to destroy the virus (58) (Table 2).

3.2.1 Dysregulated cellular immune response

Experimental studies have shown that $CD4^+$ T cells are significantly less responsive to various viral proteins such as S, N, and M proteins in SARS-CoV-2 infection (91). Clinical data showed a progressive decrease in peripheral blood $CD4^+$ T and $CD8^+$ T cells during SARS-CoV-2 infection (92). In contrast, a significant lymphocyte decrease is an important immunological marker of impending severe COVID-19 (93). Severely ill patients exhibit macrophage overreaction (also known as macrophage activation syndrome MAS) and lymphocytopenia in effective lymphocytes, including neutrophils, $CD4^+$ T cells, and NK cells (94–96).

It was found that under normal conditions, IFN-g induces the differentiation of Th0 cells into Th1 cells. In contrast, during SARS-CoV-2 infection, lower levels of IFN-g production reduce Th1 production, leading to a further attenuation of the antiviral immune response of $CD4^+$ T cells (97). In addition, Th2 cells normally produce IL4, IL-6, Il-8, IL-10, and IL-13, which suppress inflammatory responses, promote antibody responses, and inhibit Th1 cell-induced antiviral functions (98).

In COVID-19 patients, TNF-α and IFN-γ expression is reduced in $CD4^+$ T cells (99); high levels of failure markers are expressed in $CD8^+$ T cells (100); and programmed cell death protein-1 (PD-1) and T cell immunoglobulin structural domain and mucin structural domain-3 (TIM-3) expression are increased (101). T cells from patients with severe COVID-19 showed high levels of apoptosis and expression of the death receptor FAS (102),

TABLE 2 Summary of research progress on COVID-19 adaptive immune response dysregulation.

Pathological process	Mechanism	Presenters	Time
Dysregulated cellular immune response	CD4+ T cells showed significantly reduced responses to various viral proteins such as S, N and M proteins.	Grifoni	2020
	Severely ill patients exhibit macrophage overreaction (also known as macrophage activation syndrome MAS) and lymphocytopenia in effective lymphocytes, including neutrophils, CD4+ T cells, CD8+ T cells and NK cells	Giamarellos-Bourboulis; Schulte-Schrepping; Silvin; Chen	2020
	Lower levels of IFN-g production reduce Th1 production, leading to a further attenuation of the antiviral immune response of CD4+ T cells.	Han	2021
	Th2 cells normally produce IL4, IL-6, Il-8, IL-10 and IL-13, which suppress inflammatory responses and promote antibody responses and inhibit Th1 cell-induced antiviral functions.	Mahlangu	2020
	T-cell lymphopenia may be caused by pro-inflammatory cytokines and activation-induced cell death.	Bellesi; Zheng	2020
Dysregulation of humoral immune response	Helper T cells activate the differentiation of B lymphocytes in the germinal centers of lymph nodes and other lymphoid tissues and secrete pathogen-specific antibodies.	Kumar	2021
	Measurement of serological IgM and IgG titers and detection of SARS-CoV-2 NP antigen by fluorescent immunochromatography showed its high specificity and relatively high sensitivity in the early stages of infection.	Devarajan	2021
	Stalled or delayed synthesis of IgG and IgM antibodies in patients with severe COVID-19	Sun; Wang	2020

suggesting severely impaired T-cell function. It was found that in addition to the reduced number of T cells, the expression levels of T cell receptor subunits, T cell surface molecules, and their downstream signaling molecules were also severely reduced (103). In addition, SARS-CoV-2 infection also resulted in downregulation of B-cell histocompatibility complex MHC-II expression (104), which severely impaired immune function.

It should be noted that since ACE2 is not expressed in T cells, the impaired T cell response may not be due to the direct toxic effects of SARS-CoV-2 (105). It has been suggested that T-cell lymphopenia may be caused by pro-inflammatory cytokines and activation-induced cell death (69, 102).

3.2.2 Dysregulation of humoral immune response

After SARS-CoV-2 infection, cell-mediated immunity of T cells comes into play, and cytotoxic T cells recognize an attack and destroy cells containing this pathogen. Helper T cells activate the differentiation of B lymphocytes in the germinal centers of lymph nodes and other lymphoid tissues to secrete pathogen-specific antibodies (71). Studies have shown that the antibody profile against the SARS-CoV2 virus has a typical pattern of IgM and IgG production. Measurement of serological IgM and IgG titers and detecting SARS-CoV-2 nucleocapsid protein (NP) antigen by fluorescent immunochromatography showed its high specificity and relatively high sensitivity in the early stages of infection (58).

Dysregulated B-cell responses have been reported in COVID-19. Analysis of circulating B cells has shown polyclonal expansion of plasma cells and reduced memory B cells in patients with severe COVID-19 compared to patients with mild COVID-19 or healthy individuals (104, 106, 107), and synthesis of IgG and IgM antibodies also appear to be stalled or delayed (6, 108). Although studies have shown elevated anti-SARS-CoV-2 antibodies in patients with severe COVID-19 (109), their specificity and affinity appear low (110).

4 Pathological manifestations of the organism

SARS-CoV-2 viral infection causes disseminated intravascular coagulation (DIC), septic shock (111), RAS system activation, hemodynamic changes, and cellular damage by interfering with the normal function of immune function and triggering cytokine storms and bradykinin storms, which leads to a series of pathological manifestations in the organism.

4.1 Cytokine storm

Cytokine storm, also known as cytokine release syndrome, is a potentially fatal immune disease. It is characterized by the high activation of immune cells and the overproduction of large amounts of inflammatory cytokines and chemical mediators (112). It has been proposed that cytokine storm, the excessive immune response that SARS-CoV-2 infection triggers in severe cases of COVID-19 (113), is thought to be a major cause of severe disease and death in COVID-19 patients (74). Cytokine storms begin with strong activation of cytokine-secreting cells (41), and COVID-19 cytokine storms are characterized by high expression of IL-6 and TNF-α (114). The mechanism of which may be related to SARS-CoV-2 induction of cell death and thus histone release, which triggers the secretion of pro-inflammatory molecules of the interleukin-1 (IL-1) family (115), producing such IL-6, IP-10, MIP1αβ (macrophage inflammatory protein-1αβ) and MCP1 (monocyte chemotactic protein-1), and a large number of other pro-inflammatory cytokines and chemokines (116). Among them, IL-6 is an important pleiotropic pro-inflammatory mediator and a major driver of the cytokine storm. And cytokine storm is closely associated with macrophage activation syndrome (MAS). Excessive proliferation of differentiated macrophages leads to phagocytosis and hypercytosis (117, 118), which leads to systemic inflammatory abnormalities.

In addition, $CD4^+$ T lymphocytes rapidly differentiate into pathogenic T helper (Th)1 cells that produce IL-6 and GM-CSF (Granulocyte-macrophage Colony Stimulating Factor). GM-CSF plays an important role in mediating the cytokine storm (119). Subsequent induction of high levels of IL-6 and GM-CSF secretion by $CD14^+$, $CD16^+$, and monocytes (120) exacerbates the cytokine storm. Activated neutrophils can form neutrophil extracellular traps (NETs) that are involved in the pathogenesis of aseptic and nonsterile inflammation (121) and promote the development and progression of inflammation. Uncontrolled excessive inflammatory responses produce oxidative stress (imbalance between oxidants and antioxidants). Activated neutrophils and macrophages release pro-oxidant factors such as TNF-α (tumor necrosis factor-α) and release reactive oxygen species (ROS) (122–124), which in turn stimulate further cytokine production by inflammatory cells, leading to an even more intense inflammatory response (125).

In the face of the inflammatory storm generated by neo-coronavirus, it was found that timely application or combination of monoclonal antibodies can effectively reduce the rate of deterioration and mortality of neo-coronavirus pneumonia, which has broad clinical application prospects. As monoclonal antibodies against interleukin 6 receptor (IL-6), among which tocilizumab and satralizumab whose pharmacological mechanism is mainly to specifically bind to IL-6 receptor and inhibit its activation, thus inhibiting cytokine storm and reducing mortality (126), clinical studies have also confirmed that the application of this drug has significant efficacy in improving the inflammatory response in patients with COVID-19 (127). In addition, it has been shown that the administration of levilimab in patients with SARS-CoV-2

pneumonia in the absence of other signs of active infection, with or without oxygen therapy, increases the rate of sustained clinical improvement (128), that itolizumab significantly reduces the severe consequences caused by cytokine release syndrome (129), and that tocilizumab reduces the duration of hospitalization (130), the progression to mechanical ventilation (131) and the risk of transfer to the ICU (132). In addition, studies have proposed binding neutralizing antibodies to the surface of photothermal nanoparticles (NPs) to capture and inactivate novel coronaviruses. The NPs consist of a semiconductor polymer core and a biocompatible polyethylene glycol surface modified with a high-affinity neutralizing antibody. The multifunctional NP efficiently captures novel coronavirus pseudoviruses and completely blocks virus infection of host cells *in vitro* by surface-neutralizing antibodies. In addition to the virus capture and blocking functions, the NPs have a photothermal function to inactivate the virus by generating heat upon irradiation (133). The multifunctional nanoparticles also exhibit excellent biosafety *in vitro* and *in vivo*, and show satisfactory pulmonary delivery in mice. Most importantly, *in vivo* treatment with multifunctional NPs in the presence of actual novel coronaviruses was achieved, offering significantly improved therapeutic efficacy compared to soluble neutralizing antibodies and demonstrating their great potential for clinical novel coronavirus therapy. NPs are very superior to neutralizing antibodies in the treatment of actual novel coronavirus infections that occur *in vivo*. This versatile NP provides a flexible platform that can be easily adapted to other novel coronavirus antibodies and extended to new therapeutic proteins, and thus it promises to provide broad protection against the original novel coronavirus and its variants (134).

4.2 Coagulation disorders

Clinical observations have revealed alterations in hematology associated with coagulation during COVID-19 (2, 135). In most severe cases, patients develop microvascular dysfunction such as disseminated intravascular coagulation (DIC) or infectious shock (136). Thromboembolic complications are one of the main causes of morbidity and mortality in patients with COVID-19 (137).

The cause of thrombosis is an imbalance between procoagulant and anticoagulant processes. Systemic thromboembolism, including venous thromboembolism, arterial thrombosis, and thrombotic microangiopathy, is a unique and essential feature of COVID-19. In current studies, the mechanisms of coagulation disorders may also be associated with downregulation of ACE2 activity, endothelial dysfunction (138), activation of von- Willebrand factor, activation of the complement system, neutrophil extracellular traps (139), oxidative stress injury, and high inflammatory state (140) formation. These predisposes infected individuals to the activation of Virchow's triad, leading to arterial and venous thrombosis and vascular arrest anywhere in the body (141).

It has been studied that coagulation parameters, especially D-dimer levels, predict mortality in 2019 coronavirus disease and that patients with 2019 coronavirus disease have an increased risk of arterial and venous thrombosis. It has been suggested that anticoagulation (AC) is beneficial in these patients. That prophylactic AC with enoxaparin and apixaban is appropriate for treating hospitalized 2019 coronavirus disease patients with D-dimer levels >1μg/mL (142).

4.2.1 Down-regulation of ACE2 activity

As mentioned previously, the primary site of action of the SARS-CoV-2 virus is ACE2. And viral infection may lead to a decrease in ACE2 activity, resulting in elevated angiotensin II and decreased angiotensin 1-7. Angiotensin II rapidly generates reactive oxygen species mediated by NADPH oxidase and causes oxidative stress injury (143). Angiotensin 1-7 is now considered to be an important anti-inflammatory and anti-thrombotic peptide with inhibitory effects on platelet activation (144). Therefore, these will lead to RAS dysregulation, oxidative stress injury, and coagulation disorders.

4.2.2 Endothelial dysfunction

There is a strong correlation between endothelial dysfunction and thrombosis (145). Experimental studies have shown that endothelial dysfunction is a key factor in the release of the procoagulant factor fVIII (146) to generate and activate thrombus and trigger various coagulation cascades (147). This process may be associated with the endothelial expression of many prothrombotic factors and receptors. In addition, overexpression of hemagglutinin-like oxidized low-density lipoprotein receptor (LOX-1), cyclooxygenase (COX-2), and vascular endothelial growth factor (VEGF) during infection can also cause endothelial injury (148).

4.2.3 Activation of the von Willebrand factor

The underlying vascular hemophilic factor (vWF) plays a key role in COVID-19-related coagulation (149). Following endothelial injury, vWF present in the subendothelium is released, further multimerized by disulfide bonds, and exposes to the platelet-binding and collagen-binding domains (150). vWF acts as an adherent molecular glue platelet together with subendothelial collagen, activating platelet aggregation and thrombosis (151).

4.2.4 Activation of the complement system

The complement system is capable of activating the coagulation cascade through multiple mechanisms leading to vascular thrombosis. The nucleocapsid (N) protein of SARS-CoV-2 binds to mannose-binding lectin-associated serine protease (MASP)-2, which is expressed on microvessels,

leading to complement activation (121). In contrast, complement factor C3 and MAC directly activate platelets and induce platelet aggregation (152). Similarly, complement factor C5a has been shown to stimulate the expression of fibrinogen activator inhibitor 1, thereby promoting thrombosis (153).

4.2.5 Formation of neutrophil extracellular traps

NETs, also known as extra-neutrophil traps, contain various pro-thrombogenic molecules such as tissue factor, protein disulfide isomerase, factor XII, vWF, and fibrinogen (154). In addition, DNA released from extracellular NETs can directly activate platelets and lead to thrombosis. Circulating histones (major components of NETs) have also been found to activate Toll-like receptors on platelets and promote thrombin production (155).

4.3 Other pathological manifestations

Coronavirus replication can lead to lysosomal disruption, mitochondrial damage, free radical damage, disruption of membrane structure and function, destruction of mitochondria and lysosomes, cellular autolysis, and triggering ion concentration imbalance (73). Among them, reactive oxygen species (ROS) and (reactive nitrogen species) RNS may be one of the modification pathways of severe COVID-19 (156). It has been demonstrated that the downregulation of ACE2 by COVID-19 may affect the mitochondrial function of immune cells, which in turn may reduce the immune function of the host (157).

As mentioned earlier, ACE2 is an important locus for the SARS-CoV-2 virus. And one of the roles of ACE2 is to inactivate angiotensin II by converting it to angiotensin 1-7 through proteolysis, which puts ACE2 in a critical position to act as a negative regulator of the renin-angiotensin-aldosterone system (RAAS) (158) and leads to RAAS system dysfunction.

5 Pathological damage to the organism

Infection with SARS-CoV-2 will cause a range of pathological injuries such as lymphopenia, and lung tissue damage (159), such as acute respiratory distress syndrome (ARDS) and respiratory failure, sepsis-induced cardiac injury and arrhythmia (58), and multi-organ failure. Enhanced granulocyte and monocyte-macrophage infiltration are common in critically patients with COVID-19. Monocytes and macrophages are involved in and exacerbate hypersensitivity reactions (160), leading to organ damage.

5.1 Lymphoid tissue damage

Studies have shown a direct relationship between apoptosis rates and the pathogenicity and severity of COVID-19 (161). COVID-19 attacks the lymphoid tissue of the body and induces apoptosis in immune cells. During SARS-CoV-2 infection, single-cell RNA sequencing showed enrichment of SARS-CoV-2 RNA in the macrophage population of bronchoalveolar lavage samples from patients phenomenon, suggesting that the virus directly infects and attacks macrophages (162) and triggers macrophage polarization toward a pro-inflammatory phenotype (163).

Several mechanisms may exist for apoptosis, decreased expression, and functional failure of immune cells. The decrease in T-cell numbers was negatively correlated with IL-6 and TNF-α levels (164), suggesting that increased inflammatory cytokines may promote T-cell failure and apoptosis. Moreover, the IL-2 signaling pathway is inhibited, negatively regulating $CD8^+$ T cells (71) and inducing a decrease in lymphocytes. Besides, some lymphoid organs are attacked by SARS-CoV-2, which further leads to lymphocyte damage. Similarly, it has been noted that SARS-CoV-2 ORF3a induces apoptosis through the extrinsic apoptotic pathway. Caspase-8 activation/cleavage is a hallmark of the extrinsic apoptotic pathway, and SARS-CoV-2 ORF3a induces caspase-8 activation/cleavage. This process can induce epithelial apoptosis and inflammatory cytokine processing in turn, which triggers necroptotic prolapse pathway caspase-8-mediated apoptotic activation and inflammatory response, which can induce downstream immunopathogenesis in lung tissue (165).

Furthermore, elevated blood lactate levels in critically ill patients with COVID-19 inhibit lymphocyte proliferation of neutrophils with suppressive properties (e.g., granulocyte myeloid-derived suppressor cells (G-MDSCs)) (166). They may inhibit the expansion of $CD4^+$ and $CD8^+$ T lymphocytes (167).

5.2 Diffuse lung injury

Preliminary data suggest that pulmonary vascular injury and partial loss of alveolar group function are key to developing severe illness and death in patients with COVID-19 (168). Clinical data analyzed that after infection with SARS-CoV-2, most patients develop bilateral interstitial pneumonia with histology showing alveolar wall edema, protein exudates, and non-cellular focal reactive hyperplasia with vascular congestion (169), which also leads to selective death of type II pneumocytes (170). After type II pneumocyte injury, the inflammatory state will be supported by macrophage pro-inflammation (M1), cytokine release, and NF-κB support, further damaging alveolar cells in a vicious cycle (171). Loss of lung surface

active gas exchange and vascular abnormalities can lead to progressive respiratory failure. Pneumonia caused by SARS-CoV-2 leads to a rapid decrease in arterial pO2 levels measured by transcutaneous saturation (136) and hypoxemia.

Some scholars have suggested that lung tissue damage may be associated with the occurrence of NETs in large numbers of neutrophils, which in turn release toxic enzymes such as elastase (172), and secrete substances such as cationic histones. These, in addition to having direct cytotoxic effects, may also enhance infection of lung cells and thus aggravate the disease (173). In addition, oxidized phospholipids in macrophages triggering cytokine production *via* TLR4-TRIF-TRAF6 can further aggravate lung inflammation (174).

It has been found that patients with ARDS and extrapulmonary complications have significantly elevated rates of circulating pro-inflammatory cytokines, chemokines, and systemic inflammatory markers (175), suggesting that the organism is in a state of intense inflammatory response. It has been proposed that severe lung injury in COVID-19 patients is thought to result from direct viral infection and immune hyperactivation (114). (Figure 3)

One study reported that phototherapy using red and near-infrared light reduced lung inflammation and pulmonary fibrosis in mice by downregulating pro-inflammatory cytokines, upregulating IL-10 secretion from fibroblasts and lung cells, and reducing collagen deposition in the lung (176). Since lung inflammation and pulmonary fibrosis are common complications in critically ill patients with novel coronavirus infections, experiments have shown that 650 nm light-emitting diode (LED) treatment may alleviate these life-threatening problems. Compared to conventional laser excitation, 650 nm LEDs have more desirable safety properties. Under its excitation, multifunctional NPs can further inactivate the virus by assisting the photothermal function. In addition, multifunctional nanoparticles have favorable properties for pulmonary delivery and retention, which can overcome the limitation of rapid clearance of antibodies in the lung (177). The unique design of multifunctional NPs not only enables antibody-mediated neutralization to capture novel coronaviruses, but also provides a strategy to mitigate the potential risk of antibody-dependent enhancement (ADE) and new, more infectious novel coronavirus variants by inactivating the virus through direct heating. Together with efficient viral inactivation capabilities, the superior therapeutic efficacy of multifunctional NPs could be further enhanced. Future research will be conducted using site-specific binding approaches, such as site-selective click chemistry (178) that can increase surface antibody binding efficiency, control antibody binding sites and orientation and purify multifunctional nanoparticles to improve their therapeutic efficacy further.

5.3 Multiple organ injury

According to studies, COVID-19 has been shown over time to cause multi-system involvement of the cardiovascular system

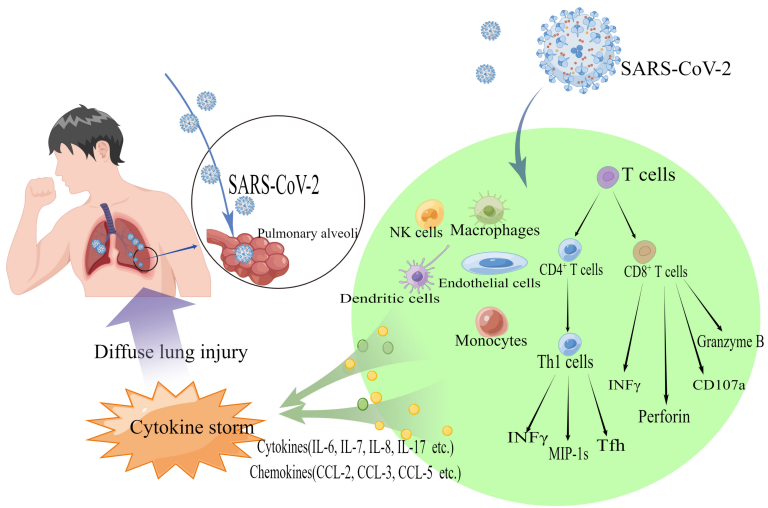

FIGURE 3
Schematic diagram showing the pathogenic mechanism of diffuse lung injury caused by 2019-nCoV. SARS-CoV-2 binds to ACE2 receptors on human alveolar epithelial cells *via* S proteins and enters the cells. NK cells, natural killer cells, macrophages, dendritic cells, monocytes, etc., release cytokines (e.g., IL-6, IL-7, IL-8, IL-17, etc.) and chemokines (e.g., CCL-2, CCL-3, CCL-5, etc.). $CD8^+$ T cells secrete substances such as Perforin, CD107a, and Granzyme B. $CD4^+$ T cells are activated and differentiate into Th1, Th2 effector cells, and other subpopulations (including Tfh cells, etc.), and also secrete cytokines (e.g., INFγ) and chemokines to recruit Immune cells are also secreted (e.g., INFγ) and chemokines are recruited, resulting in a cytokine storm that causes diffuse lung injury.

(2, 6, 179), the nervous system, the urinary system (2020), and the hematological system in addition to the respiratory and immune systems (139, 180). This is partly due to the widespread expression of ACE2 as a SARS-CoV-2 receptor in tissues and organs, and partly because SARS-CoV-2 causes a series of systemic pathological manifestations, such as cytokine storm and disorders of coagulation mechanisms (74, 181, 182).

In particular, neurological complications have become an increasingly recognized cause of morbidity and mortality in patients with COVID-19. The most common of these neurological symptoms include cerebrovascular events (183), encephalitis, Guillain-Barré syndrome, acute necrotizing encephalopathy, hemophagocytic lymphoid tissue hyperplasia, and acute ischemic cerebrovascular syndrome (184), as well as neuropsychiatric symptoms such as dizziness, sleep disturbances, cognitive deficits, delirium, hallucinations, and depression. In addition, the chronic neurological aspects of traumatic brain injury, post-stroke syndrome, long COVID-19, intractable Lyme disease, and influenza encephalopathy have close pathophysiological similarities, mainly involving positive feedback loops for TNF maintenance and activation (185), and cerebral venous sinus thrombosis (CVT) formation is also associated with infection with SARS-CoV-2 virus (139).

In addition, right ventricular (RV) dysfunction is common and correlates with poor prognosis in COVID-19 patients (186). And one experiment found that ACE2 expressed by enterocytes derived from human colon differentiation is sensitive to SARS-CoV-2 infection, revealing that IFN-c is a strong driver of epithelial cell differentiation towards the enterocyte lineage and leads to high ACE2 expression and increased susceptibility to SARS-CoV-2 (187).

In summary, the pathogenic mechanism of COVID-19 involves the combined effects of characteristic structures, genes, enzymes, and immune responses. The pathological manifestations and damage caused are manifested as a process in which the lung is the main object of damage and can cause extensive extrapulmonary partial damage as the disease progresses.

6 Conclusions and challenges

Studies on the pathogenic characteristics of neocoronaviruses and the sites of action have demonstrated that among all functional proteins of neocoronaviruses, the S protein is the main antigenic component that binds to host cell receptor proteins, promotes viral invasion of host cells, and stimulates host immune responses. ACE2 is the main receptor infection target. Serine proteases, cysteine proteases, lysosomal proteases, and other enzymes are the main proteases that activate S proteins. Therefore, the S protein can be selected as an important target for vaccine development. For clinical treatment, ACE direct injection can increase the expression of recombinant ACE2 protein and therapeutic vectors that deliver an expression of high levels of ACE2, which is used to overcome virus-induced ACE2 deficiency by increasing the expression of ACE2 protein. Alternatively, ACE inhibitors can balance ACE/ACE2 function by inhibiting the activation of S proteins through the inhibition of related enzyme activities (188). The study of viral exosomes can also be further explored to explore the possible target proteins and signaling molecules for exosomal-cell fusion, thus obtaining new ways to inhibit virus transmission.

During the immune system dysregulation caused by a new coronavirus, the virus modifies its RNA, generates an immune escape mechanism, antagonizes the immune response, and induces apoptosis of immune cells. This phenomenon suggests that viruses change by adapting to new environments, and it is speculated that a new epidemic involving coronaviruses may break out in the future. COVID-19 is highly infectious and has a long incubation period, resulting in a rampant epidemic with a complex and variable disease course, which poses a great challenge to the control of the epidemic. Up to now, no targeted vaccine or effective drug has been developed.

According to the pathogenic mechanism of neo-coronavirus, treatment is still mainly based on antiviral, anti-infective, and symptomatic supportive therapy. Many drugs have been introduced for the treatment of neo-coronavirus pneumonia; for example tetracycline and doxycycline can act as inhibitors of ACE2 binding (28); niclosamide can inhibit RNA viruses during the post-entry phase of viral RNA replication and also exhibits anti-inflammatory activity (189); chloroquine reduces the production of cytokines and damage-associated molecular patterns by interfering with the innate immune pathways of multiple immune cells, thus preventing experimental sepsis and infectious shock (190, 191). In addition, combination therapies have been introduced, such as early triple antiviral therapy with interferon beta-1b, lopinavir-ritonavir, and ribavirin, which shortens the time to viral shedding, reduces cytokine responses, relieves symptoms, and promotes the discharge of patients with mild to moderate COVID-19 (192). The discovery and study of the pathogenic mechanism of neocoronaviruses can bring the course of action of existing drugs into more explicit articulation at the cellular or molecular level to align with clinical applied medicine with more rationalized, standardized, institutionalized, and scientific research. In addition, we believe that a large number of experiments and research records can provide detailed statistics on drug efficacy, efficiency, and the number of stable cases, which can also help promote the organic combination of pathogenesis research and clinical drug action process analysis. We also suggest that a series of accurate and standardized target models may be constructed, and the criteria for clinically effective associations may be derived through model experiments. The establishment of model systems may be expected to be a reference for subsequent studies on preventing and treating other large epidemic diseases.

SASRS-CoV-2 is another highly lethal virus after SARS-CoV and MERS-CoV. COVID-19 epidemic is a major public health emergency in China and the world. The epidemic is spreading globally and the situation has been dire so far. Further experimental,

as well as clinical solutions to the currently unresolved and controversial issues, are still needed. Understanding the pathogenesis of neocoronaviruses and developing therapeutic regimens based on the complex pathogenesis of the pathological damage produced by neocoronaviruses is of great importance in response to COVID-19 and possible future epidemic viruses.

Author contributions

Conceptualization, JY, XK, QZ and FO; writing—review and editing, JY, JM, QD, QW and PL; visualization, QZ; supervision, XK and LY; project administration, RG, LY. All authors have read and agreed to the published version of the manuscript.

Funding

This research was funded by the Scientific research project of Tianjin Education Commission, grant number 2021KJ134, Tianjin Municipal Education Commission Scientific Research Project, grant number 2019ZD11, Science and Technology Program of Tianjin, China (21ZYJDJC00070), the National Key Research and Development Program of China (2019YFC1708803), and Innovation Team and Talents Cultivation Program of National Administration of Traditional Chinese Medicine (ZYYCXTD-C-202203), Scientific and technological innovation project of China Academy of Chinese Medical Sciences (Grant No. C12021A04701 to RG)

Acknowledgments

We thank all the authors of the original work and reviewers for their time and kindness in reviewing this paper. The figures were drawn by Figdraw (https://www.figdraw.com/static/index.html#/).

Conflict of interest

The authors declare that the research was conducted in the absence of any commercial or financial relationships that could be construed as a potential conflict of interest.

Publisher's note

References

1. Neuman BW, Kiss G, Kunding AH, Bhella D, Baksh MF, Connelly S, et al. A structural analysis of m protein in coronavirus assembly and morphology. *J Struct Biol* (2011) 174:11–22. doi: 10.1016/j.jsb.2010.11.021

2. Huang C, Wang Y, Li X, Ren L, Zhao J, Hu Y, et al. Clinical features of patients infected with 2019 novel coronavirus in wuhan, China. *Lancet* (2020) 395:497–506. doi: 10.1016/S0140-6736(20)30183-5

3. Zhu N, Zhang D, Wang W, Li X, Yang B, Song J, et al. A novel coronavirus from patients with pneumonia in chin. *N Engl J Med* (2020) 382:727–33. doi: 10.1056/NEJMoa2001017

4. Lee P, Kim DJ. Newly emerging human coronaviruses: Animal models and vaccine research for sars, mers, and covid-19. *Immune Netw* (2020) 20:e28. doi: 10.4110/in.2020.20.e28

5. Chan JF, Yuan S, Kok KH, To KK, Chu H, Yang J, et al. A familial cluster of pneumonia associated with the 2019 novel coronavirus indicating person-to-person transmission: a study of a family cluster. *Lancet* (2020) 395:514–23. doi: 10.1016/S0140-6736(20)30154-9

6. Wang D, Hu B, Hu C, Zhu F, Liu X, Zhang J, et al. Clinical characteristics of 138 hospitalized patients with 2019 novel coronavirus-infected pneumonia in wuhan, China. *Jama* (2020) 323:1061–9. doi: 10.1001/jama.2020.1585

7. Xia J, Tong J, Liu M, Shen Y, Guo D. Evaluation of coronavirus in tears and conjunctival secretions of patients with SARS-CoV-2 infection. *J Med Virol* (2020) 92:589–94. doi: 10.1002/jmv.25725

8. Xie P, Ma W, Tang H, Liu D. Severe COVID-19: A review of recent progress with a look toward the future. *Front Public Health* (2020) 8:189. doi: 10.3389/fpubh.2020.00189

9. Pujadas E, Chaudhry F, Mcbride R, Richter F, Zhao S, Wajnberg A, et al. SARS-CoV-2 viral load predicts COVID-19 mortality. *Lancet Respir Med* (2020) 8 (9):e70. doi: 10.1101/2020.06.11.20128934

10. Cui J, Li F, Shi ZL. Origin and evolution of pathogenic coronaviruses. *Nat Rev Microbiol* (2019) 17:181–92. doi: 10.1038/s41579-018-0118-9

11. Fiorino S, Zippi M, Gallo C, Sifo D, Sabbatani S, Manfredi R, et al. The rationale for a multi-step therapeutic approach based on antivirals, drugs and nutrients with immunomodulatory activity in patients with coronavirus-SARS2-induced disease of different severities. *Br J Nutr* (2021) 125:275–93. doi: 10.1017/S0007114520002913

12. Conceicao C, Thakur N, Human S, Kelly JT, Logan L, Bialy D, et al. The SARS-CoV-2 spike protein has a broad tropism for mammalian ACE2 proteins. *PloS Biol* (2020) 18:e3001016. doi: 10.1371/journal.pbio.3001016

13. Lu L, Liu X, Jin R, Guan R, Lin R, Qu Z. Potential roles of the renin-angiotensin system in the pathogenesis and treatment of COVID-19. *BioMed Res Int* (2020) 2020:7520746. doi: 10.1155/2020/7520746

14. Greber UF. Two years into COVID-19 - lessons in SARS-CoV-2 and a perspective from papers in FEBS letters. *FEBS Lett* (2021) 595:2847–53. doi: 10.1002/1873-3468.14226

15. Luan B, Wang H, Huynh T. Enhanced binding of the N501Y-mutated SARS-CoV-2 spike protein to the human ACE2 receptor: insights from molecular dynamics simulations. *FEBS Lett* (2021) 595:1454–61. doi: 10.1002/1873-3468.14076

16. Andersen KG, Rambaut A, Lipkin WI, Holmes EC, Garry RF. The proximal origin of SARS-CoV-2. *Nat Med* (2020) 26:450–2. doi: 10.1038/s41591-020-0820-9

17. Higashikuni Y, Liu W, Obana T, Sata M. Pathogenic basis of thromboinflammation and endothelial injury in COVID-19: Current findings and therapeutic implications. *Int J Mol Sci* (2021) 22(21):12081. doi: 10.3390/ijms222112081

18. De Pasquale V, Quiccione MS, Tafuri S, Avallone L, Pavone LM. Heparan sulfate proteoglycans in viral infection and treatment: A special focus on SARS-CoV-2. *Int J Mol Sci* (2021) 22(12):6574. doi: 10.3390/ijms22126574

19. Jennings BC, Kornfeld S, Doray B. A weak COPI binding motif in the cytoplasmic tail of SARS-CoV-2 spike glycoprotein is necessary for its cleavage,

glycosylation, and localization. *FEBS Lett* (2021) 595:1758–67. doi: 10.1002/1873-3468.14109

20. Wang M, Cao R, Zhang L, Yang X, Liu J, Xu M, et al. Remdesivir and chloroquine effectively inhibit the recently emerged novel coronavirus (2019-nCoV) *in vitro*. *Cell Res* (2020) 30:269–71. doi: 10.1038/s41422-020-0282-0

21. Gao J, Tian Z, Yang X. Breakthrough: Chloroquine phosphate has shown apparent efficacy in treatment of COVID-19 associated pneumonia in clinical studies. *Biosci Trends* (2020) 14:72–3. doi: 10.5582/bst.2020.01047

22. Gautret P, Lagier JC, Parola P, Hoang VT, Meddeb L, Mailhe M, et al. Hydroxychloroquine and azithromycin as a treatment of COVID-19: Results of an open-label non-randomized clinical trial. *Int J Antimicrob Agents* (2020) 56:105949. doi: 10.1016/j.ijantimicag.2020.105949

23. Vincent MJ, Bergeron E, Benjannet S, Erickson BR, Rollin PE, Ksiazek TG, et al. Chloroquine is a potent inhibitor of SARS coronavirus infection and spread. *Virol J* (2005) 2:69. doi: 10.1186/1743-422X-2-69

24. Zhou P, Yang XL, Wang XG, Hu B, Zhang L, Zhang W, et al. A pneumonia outbreak associated with a new coronavirus of probable bat origin. *Nature* (2020) 579:270–3. doi: 10.1038/s41586-020-2012-7

25. Guastalegname M, Vallone A. Could chloroquine/hydroxychloroquine be harmful in coronavirus disease 2019 (covid-19) treatment? *Clin Infect Dis* (2020) 71:888–9. doi: 10.1093/cid/ciaa321

26. Hornick MG, Olson ME, Jadhav AL. SARS-CoV-2 psychiatric sequelae: A review of neuroendocrine mechanisms and therapeutic strategies. *Int J Neuropsychopharmacol* (2022) 25:1–12. doi: 10.1093/ijnp/pyab069

27. Ferreira G, Blasina F, Rodríguez Rey M, Anesetti G, Sapiro R, Chavarría L, et al. Pathophysiological and molecular considerations of viral and bacterial infections during maternal-fetal and -neonatal interactions of SARS-CoV-2, zika, and mycoplasma infectious diseases. *Biochim Biophys Acta Mol Basis Dis* (2022) 1868:166285. doi: 10.1016/j.bbadis.2021.166285

28. Putics A, Filipowicz W, Hall J, Gorbalenya AE, Ziebuhr J. ADP-ribose-1"-monophosphatase: A conserved coronavirus enzyme that is dispensable for viral replication in tissue culture. *J Virol* (2005) 79:12721–31. doi: 10.1128/JVI.79.20.12721-12731.2005

29. Lei HY, Ding YH, Nie K, Dong YM, Xu JH, Yang ML, et al. Potential effects of SARS-CoV-2 on the gastrointestinal tract and liver. *BioMed Pharmacother* (2021) 133:111064. doi: 10.1016/j.biopha.2020.111064

30. Li MY, Li L, Zhang Y, Wang XS. Expression of the SARS-CoV-2 cell receptor gene ACE2 in a wide variety of human tissues. *Infect Dis Poverty* (2020) 9:45. doi: 10.1186/s40249-020-00662-x

31. Geravandi S, Mahmoudi-Aznaveh A, Azizi Z, Maedler K, Ardestani A. SARS-CoV-2 and pancreas: A potential pathological interaction? *Trends Endocrinol Metab* (2021) 32:842–5. doi: 10.1016/j.tem.2021.07.004

32. Hou YJ, Okuda K, Edwards CE, Martinez DR, Asakura T, Dinnon KH3rd, et al. SARS-CoV-2 reverse genetics reveals a variable infection gradient in the respiratory tract. *Cell* (2020) 182:429–446.e414. doi: 10.1016/j.cell.2020.05.042

33. Soto M, Dizerega G, Rodgers KE. Countermeasure and therapeutic: A(1-7) to treat acute respiratory distress syndrome due to COVID-19 infection. *J Renin Angiotensin Aldosterone Syst* (2020) 21:1470320320972018. doi: 10.1177/1470320320972018

34. Zou X, Chen K, Zou J, Han P, Hao J, Han Z. Single-cell RNA-seq data analysis on the receptor ACE2 expression reveals the potential risk of different human organs vulnerable to 2019-nCoV infection. *Front Med* (2020) 14:185–92. doi: 10.1007/s11684-020-0754-0

35. Kountouri A, Korakas E, Ikonomidis I, Raptis A, Tentolouris N, Dimitriadis G, et al. Type 1 diabetes mellitus in the sars-cov-2 pandemic: Oxidative stress as a major pathophysiological mechanism linked to adverse clinical outcomes. *Antioxidants (Basel)* (2021) 10(5):752. doi: 10.3390/antiox10050752

36. Chu H, Chan JF-W, Yuen TT-T, Shuai H, Yuan S, Wang Y, et al. Comparative tropism, replication kinetics, and cell damage profiling of SARS-CoV-2 and SARS-CoV with implications for clinical manifestations, transmissibility, and laboratory studies of COVID-19: An observational study. *Lancet Microbe* (2020) 1:e14–23. doi: 10.1016/S2666-5247(20)30004-5

37. Sindona C, Schepici G, Contestabile V, Bramanti P, Mazzon E. NOX2 activation in COVID-19: Possible implications for neurodegenerative diseases. *Medicina (Kaunas)* (2021) 57(6):604. doi: 10.3390/medicina57060604

38. Clausen TM, Sandoval DR, Spliid CB, Pihl J, Perrett HR, Painter CD, et al. SARS-CoV-2 infection depends on cellular heparan sulfate and ace2. *Cell* (2020) 183:1043–1057.e1015. doi: 10.1016/j.cell.2020.09.033

39. Tiwari V, Tandon R, Sankaranarayanan NV, Beer JC, Kohlmeir EK, Swanson-Mungerson M, et al. Preferential recognition and antagonism of SARS-CoV-2 spike glycoprotein binding to 3- O -sulfated heparan sulfate. *bioRxiv* (2020) 2020.10.08.331751. doi: 10.1101/2020.10.08.331751

40. Chu H, Hu B, Huang X, Chai Y, Zhou D, Wang Y, et al. Host and viral determinants for efficient SARS-CoV-2 infection of the human lung. *Nat Commun* (2021) 12:134. doi: 10.1038/s41467-020-20457-w

41. Azkur AK, Akdis M, Azkur D, Sokolowska M, Van De Veen W, Brüggen MC, et al. Immune response to SARS-CoV-2 and mechanisms of immunopathological changes in COVID-19. *Allergy* (2020) 75:1564–81. doi: 10.1111/all.14364

42. Hoffmann M, Kleine-Weber H, Pöhlmann S. A multibasic cleavage site in the spike protein of SARS-CoV-2 is essential for infection of human lung cells. *Mol Cell* (2020) 78:779–784.e775. doi: 10.1016/j.molcel.2020.04.022

43. Ricci D, Etna MP, Rizzo F, Sandini S, Severa M, Coccia EM. Innate immune response to SARS-CoV-2 infection: From cells to soluble mediators. *Int J Mol Sci* (2021) 22(13):7017. doi: 10.3390/ijms22137017

44. Pique-Regi R, Romero R, Tarca AL, Luca F, Xu Y, Alazizi A, et al. Does the human placenta express the canonical cell entry mediators for SARS-CoV-2? *Elife* (2020) 9:e58716. doi: 10.7554/eLife.58716

45. De Clercq E. New nucleoside analogues for the treatment of hemorrhagic fever virus infections. *Chem Asian J* (2019) 14:3962–8. doi: 10.1002/asia.201900841

46. Beigel JH, Tomashek KM, Dodd LE, Mehta AK, Zingman BS, Kalil AC, et al. Remdesivir for the treatment of covid-19 - final report. *N Engl J Med* (2020) 383:1813–26. doi: 10.1056/NEJMoa2007764

47. Lai CC, Shih TP, Ko WC, Tang HJ, Hsueh PR. Severe acute respiratory syndrome coronavirus 2 (SARS-CoV-2) and coronavirus disease-2019 (COVID-19): The epidemic and the challenges. *Int J Antimicrob Agents* (2020) 55:105924. doi: 10.1016/j.ijantimicag.2020.105924

48. Sheahan TP, Sims AC, Graham RL, Menachery VD, Gralinski LE, Case JB, et al. Broad-spectrum antiviral GS-5734 inhibits both epidemic and zoonotic coronaviruses. *Sci Transl Med* (2017) 9(396):eaal3653. doi: 10.1126/scitranslmed.aal3653

49. Tchesnokov EP, Feng JY, Porter DP, Götte M. Mechanism of inhibition of ebola virus rna-dependent rna polymerase by remdesivir. *Viruses* (2019) 11(4):326. doi: 10.3390/v11040326

50. Carothers C, Birrer K, Vo M. Acetylcysteine for the treatment of suspected remdesivir-associated acute liver failure in covid-19: A case series. pharmacotherapy. *J Hum Pharmacol Drug Ther* (2020) 40:1166–71. doi: 10.1002/phar.2464

51. Zhang L, Liu Y. Potential interventions for novel coronavirus in China: A systematic review. *J Med Virol* (2020) 92:479–90. doi: 10.1002/jmv.25707

52. Ferner RE, Aronson JK. Remdesivir in covid-19. *Bmj* (2020) 369:m1610. doi: 10.1136/bmj.m1610

53. Guan W, Lan W, Zhang J, Zhao S, Ou J, Wu X, et al. COVID-19: antiviral agents, antibody development and traditional chinese medicine. *Virologica Sin* (2020) 35:685–98. doi: 10.1007/s12250-020-00297-0

54. Rejinold NS, Piao H, Jin GW, Choi G, Choy JH. Injectable niclosamide nanohybrid as an anti-SARS-CoV-2 strategy. *Colloids Surf B Biointerfaces* (2021) 208:112063. doi: 10.1016/j.colsurfb.2021.112063

55. Mody V, Ho J, Wills S, Mawri A, Lawson L, Ebert M, et al. Identification of 3-chymotrypsin like protease (3CLPro) inhibitors as potential anti-SARS-CoV-2 agents. *Commun Biol* (2021) 4:93. doi: 10.1038/s42003-020-01577-x

56. Li J, Lin C, Zhou X, Zhong F, Zeng P, Yang Y, et al. Structural basis of the main proteases of coronavirus bound to drug candidate pf-07321332. *J Virol* (2022) 96:e0201321. doi: 10.1128/jvi.02013-21

57. Ma C, Sacco MD, Hurst B, Townsend JA, Hu Y, Szeto T, et al. Boceprevir, GC-376, and calpain inhibitors II, XII inhibit SARS-CoV-2 viral replication by targeting the viral main protease. *Cell Res* (2020) 30:678–92. doi: 10.1038/s41422-020-0356-z

58. Devarajan A, Vaseghi M. Hydroxychloroquine can potentially interfere with immune function in COVID-19 patients: Mechanisms and insights. *Redox Biol* (2021) 38:101810. doi: 10.1016/j.redox.2020.101810

59. Shang J, Ye G, Shi K, Wan Y, Luo C, Aihara H, et al. Structural basis of receptor recognition by SARS-CoV-2. *Nature* (2020) 581:221–4. doi: 10.1038/s41586-020-2179-y

60. Rahbar Saadat Y, Hosseiniyan Khatibi SM, Zununi Vahed S, Ardalan M. Host serine proteases: A potential targeted therapy for COVID-19 and influenza. *Front Mol Biosci* (2021) 8:725528. doi: 10.3389/fmolb.2021.725528

61. Bertram S, Dijkman R, Habjan M, Heurich A, Gierer S, Glowacka I, et al. TMPRSS2 activates the human coronavirus 229E for cathepsin-independent host cell entry and is expressed in viral target cells in the respiratory epithelium. *J Virol* (2013) 87:6150–60. doi: 10.1128/JVI.03372-12

62. Glowacka I, Bertram S, Müller MA, Allen P, Soilleux E, Pfefferle S, et al. Evidence that TMPRSS2 activates the severe acute respiratory syndrome coronavirus spike protein for membrane fusion and reduces viral control by the humoral immune response. *J Virol* (2011) 85:4122–34. doi: 10.1128/JVI.02232-10

63. Chen Y, Liu Q, Guo D. Emerging coronaviruses: Genome structure, replication, and pathogenesis. *J Med Virol* (2020) 92:418–23. doi: 10.1002/jmv.25681

64. Romano M, Ruggiero A, Squeglia F, Maga G, Berisio R. A structural view of sars-cov-2 rna replication machinery: Rna synthesis, proofreading and final capping. *Cells* (2020) 9(5):1267. doi: 10.20944/preprints202004.0510.v1

65. Gunasekaran M, Bansal S, Ravichandran R, Sharma M, Perincheri S, Rodriguez F, et al. Respiratory viral infection in lung transplantation induces exosomes that trigger chronic rejection. *J Heart Lung Transplant* (2020) 39:379–88. doi: 10.1016/j.healun.2019.12.009

66. Klann K, Bojkova D, Tascher G, Ciesek S, Münch C, Cinatl J. Growth factor receptor signaling inhibition prevents sars-cov-2 replication. *Mol Cell* (2020) 80:164–174.e164. doi: 10.1016/j.molcel.2020.08.006

67. Mohamed Khosroshahi L, Rokni M, Mokhtari T, Noorbakhsh F. Immunology, immunopathogenesis and immunotherapeutics of COVID-19; an overview. *Int Immunopharmacol* (2021) 93:107364. doi: 10.1016/j.intimp.2020.107364

68. Osman MS, Van Eeden C, Cohen Tervaert JW. Fatal COVID-19 infections: Is NK cell dysfunction a link with autoimmune HLH? *Autoimmun Rev* (2020) 19:102561. doi: 10.1016/j.autrev.2020.102561

69. Zheng M, Gao Y, Wang G, Song G, Liu S, Sun D, et al. Functional exhaustion of antiviral lymphocytes in COVID-19 patients. *Cell Mol Immunol* (2020) 17:533–5. doi: 10.1038/s41423-020-0402-2

70. Violi F, Oliva A, Cangemi R, Ceccarelli G, Pignatelli P, Carnevale R, et al. Nox2 activation in covid-19. *Redox Biol* (2020) 36:101655. doi: 10.1016/j.redox.2020.101655

71. Kumar A, Prasoon P, Sekhawat PS, Pareek V, Faiq MA, Kumari C, et al. Pathogenesis guided therapeutic management of COVID-19: An immunological perspective. *Int Rev Immunol* (2021) 40:54–71. doi: 10.1080/08830185.2020.1840566

72. Vabret N, Britton GJ, Gruber C, Hegde S, Kim J, Kuksin M, et al.). immunology of COVID-19: Current state of the science. *Immunity* (2020) 52:910–41. doi: 10.1016/j.immuni.2020.05.002

73. De Wit E, Van Doremalen N, Falzarano D, Munster VJ. SARS and MERS: Recent insights into emerging coronaviruses. *Nat Rev Microbiol* (2016) 14:523–34. doi: 10.1038/nrmicro.2016.81

74. Mehta P, Mcauley DF, Brown M, Sanchez E, Tattersall RS, Manson JJ. COVID-19: Consider cytokine storm syndromes and immunosuppression. *Lancet* (2020) 395:1033–4. doi: 10.1016/S0140-6736(20)30628-0

75. Neurath MF. COVID-19 and immunomodulation in IBD. *Gut* (2020) 69:1335–42. doi: 10.1136/gutjnl-2020-321269

76. Lin L, Li T. Interpretation of "Guidelines for the diagnosis and treatment of novel coronavirus (2019-nCoV)) infection by the national health commission (Trial version 5)". *Natl Med J China* (2020) 100:E001–1. doi: 10.3760/cma.j.cn112137-20200205-00199

77. Sterne J, Murthy S, Diaz JV, Slutsky AS, Villar J, Angus DC, et al. Association between administration of systemic corticosteroids and mortality among critically ill patients with covid-19: A meta-analysis. *Jama* (2020) 324:1330–41. doi: 10.1001/jama.2020.17023

78. Agarwal A, Rochwerg B, Lamontagne F, Siemieniuk RA, Agoritsas T, Askie L, et al. A living WHO guideline on drugs for covid-19. *Bmj* (2020) 370:m3379. doi: 10.1136/bmj.m3379

79. Bruen C, Al-Saadi M, Michelson EA, Tanios M, Mendoza-Ayala R, Miller J, et al. Auxora vs. placebo for the treatment of patients with severe COVID-19 pneumonia: A randomized-controlled clinical trial. *Crit Care* (2022) 26:101. doi: 10.1186/s13054-022-03964-8

80. Viswanathan T, Arya S, Chan SH, Qi S, Dai N, Misra A, et al. Structural basis of RNA cap modification by SARS-CoV-2. *Nat Commun* (2020) 11:3718. doi: 10.1038/s41467-020-17496-8

81. V'kovski P, Kratzel A, Steiner S, Stalder H, Thiel V. Coronavirus biology and replication: implications for SARS-CoV-2. *Nat Rev Microbiol* (2021) 19:155–70. doi: 10.1038/s41579-020-00468-6

82. Kim YM, Shin EC. Type I and III interferon responses in SARS-CoV-2 infection. *Exp Mol Med* (2021) 53:750–60. doi: 10.1038/s12276-021-00592-0

83. Lee HC, Chathuranga K, Lee JS. Intracellular sensing of viral genomes and viral evasion. *Exp Mol Med* (2019) 51:1–13. doi: 10.1038/s12276-019-0299-y

84. Hadjadj J, Yatim N, Barnabei L, Corneau A, Boussier J, Smith N, et al. Impaired type I interferon activity and inflammatory responses in severe COVID-19 patients. *Science* (2020) 369:718–24. doi: 10.1126/science.abc6027

85. Jiang HW, Zhang HN, Meng QF, Xie J, Li Y, Chen H, et al. SARS-CoV-2 Orf9b suppresses type I interferon responses by targeting TOM70. *Cell Mol Immunol* (2020) 17:998–1000. doi: 10.1038/s41423-020-0514-8

86. Hasan MZ, Islam S, Matsumoto K, Kawai T. SARS-CoV-2 infection initiates interleukin-17-enriched transcriptional response in different cells from multiple organs. *Sci Rep* (2021) 11:16814. doi: 10.1038/s41598-021-96110-3

87. Moustaqil M, Ollivier E, Chiu HP, Van Tol S, Rudolffi-Soto P, Stevens C, et al. SARS-CoV-2 proteases PLpro and 3CLpro cleave IRF3 and critical modulators of inflammatory pathways (NLRP12 and TAB1): Implications for disease presentation across species. *Emerg Microbes Infect* (2021) 10:178–95. doi: 10.1080/22221751.2020.1870414

88. Prompetchara E, Ketloy C, Palaga T. Immune responses in COVID-19 and potential vaccines: Lessons learned from SARS and MERS epidemic. *Asian Pac J Allergy Immunol* (2020) 38:1–9. doi: 10.12932/AP-200220-0772

89. Bastard P, Rosen LB, Zhang Q, Michailidis E, Hoffmann HH, Zhang Y, et al. Autoantibodies against type I IFNs in patients with life-threatening COVID-19. *Science* (2020) 370(6515):eabd4585. doi: 10.1126/science.abd4585

90. Zhang Q, Bastard P, Liu Z, Le Pen J, Moncada-Velez M, Chen J, et al. Inborn errors of type I IFN immunity in patients with life-threatening COVID-19. *Science* (2020) 370(6515):eabd4570. doi: 10.1126/science.abd4570

91. Grifoni A, Weiskopf D, Ramirez SI, Mateus J, Dan JM, Moderbacher CR, et al. Targets of T cell responses to sars-cov-2 coronavirus in humans with covid-19 disease and unexposed individuals. *Cell* (2020) 181:1489–1501.e1415. doi: 10.1016/j.cell.2020.05.015

92. Chen T, Wu D, Chen H, Yan W, Yang D, Chen G, et al. Clinical characteristics of 113 deceased patients with coronavirus disease 2019: Retrospective study. *Bmj* (2020) 368:m1091. doi: 10.1136/bmj.m1091

93. Chen G, Wu D, Guo W, Cao Y, Huang D, Wang H, et al. Clinical and immunological features of severe and moderate coronavirus disease 2019. *J Clin Invest* (2020) 130:2620–9. doi: 10.1172/JCI137244

94. Giamarellos-Bourboulis EJ, Netea MG, Rovina N, Akinosoglou K, Antoniadou A, Antonakos N, et al. Complex immune dysregulation in COVID-19 patients with severe respiratory failure. *Cell Host Microbe* (2020) 27:992–1000.e1003. doi: 10.1016/j.chom.2020.04.009

95. Schulte-Schrepping J, Reusch N, Paclik D, Baßler K, Schlickeiser S, Zhang B, et al. Severe COVID-19 is marked by a dysregulated myeloid cell compartment. *Cell* (2020) 182:1419–1440.e1423. doi: 10.1016/j.cell.2020.08.001

96. Silvin A, Chapuis N, Dunsmore G, Goubet AG, Dubuisson A, Derosa L, et al. Elevated calprotectin and abnormal myeloid cell subsets discriminate severe from mild COVID-19. *Cell* (2020) 182:1401–1418.e1418. doi: 10.1016/j.cell.2020.08.002

97. Han M, Ma K, Wang X, Yan W, Wang H, You J, et al. Immunological characteristics in type 2 diabetes mellitus among covid-19 patients. *Front Endocrinol (Lausanne)* (2021) 12:596518. doi: 10.3389/fendo.2021.596518

98. Mahlangu T, Dludla PV, Nyambuya TM, Mxinwa V, Mazibuko-Mbeje SE, Cirilli I, et al. A systematic review on the functional role of Th1/Th2 cytokines in type 2 diabetes and related metabolic complications. *Cytokine* (2020) 126:154892. doi: 10.1016/j.cyto.2019.154892

99. Zheng HY, Zhang M, Yang CX, Zhang N, Wang XC, Yang XP, et al. Elevated exhaustion levels and reduced functional diversity of T cells in peripheral blood may predict severe progression in COVID-19 patients. *Cell Mol Immunol* (2020) 17:541–3. doi: 10.1038/s41423-020-0401-3

100. Diao B, Wang C, Tan Y, Chen X, Liu Y, Ning L, et al. Reduction and functional exhaustion of T cells in patients with coronavirus disease 2019 (COVID-19). *Front Immunol* (2020) 11:827. doi: 10.3389/fimmu.2020.00827

101. Li M, Guo W, Dong Y, Wang X, Dai D, Liu X, et al. Elevated exhaustion levels of nk and cd8(+) t cells as indicators for progression and prognosis of covid-19 disease. *Front Immunol* (2020) 11:580237. doi: 10.3389/fimmu.2020.580237

102. Bellesi S, Metafuni E, Hohaus S, Maiolo E, Marchionni F, D'innocenzo S, et al. Increased CD95 (Fas) and PD-1 expression in peripheral blood T lymphocytes in COVID-19 patients. *Br J Haematol* (2020) 191:207–11. doi: 10.1111/bjh.17034

103. Li J, Guo M, Tian X, Wang X, Yang X, Wu P, et al. Virus-host interactome and proteomic survey reveal potential virulence factors influencing sars-cov-2 pathogenesis. *Med (N Y)* (2021) 2:99–112.e117. doi: 10.1016/j.medj.2020.07.002

104. Wilk AJ, Rustagi A, Zhao NQ, Roque J, Martínez-Colón GJ, Mckechnie JL, et al. A single-cell atlas of the peripheral immune response in patients with severe COVID-19. *Nat Med* (2020) 26:1070–6. doi: 10.1038/s41591-020-0944-y

105. Wang C, Xie J, Zhao L, Fei X, Zhang H, Tan Y, et al. Alveolar macrophage dysfunction and cytokine storm in the pathogenesis of two severe COVID-19 patients. *EBioMedicine* (2020) 57:102833. doi: 10.1016/j.ebiom.2020.102833

106. Kuri-Cervantes L, Pampena MB, Meng W, Rosenfeld AM, Ittner CAG, Weisman AR, et al. Comprehensive mapping of immune perturbations associated with severe COVID-19. *Sci Immunol* (2020) 5(49):eabd7114. doi: 10.1126/sciimmunol.abd7114

107. Mathew D, Giles JR, Baxter AE, Oldridge DA, Greenplate AR, Wu JE, et al. Deep immune profiling of COVID-19 patients reveals distinct immunotypes with therapeutic implications. *Science* (2020) 369(6508):eabc8511. doi: 10.1126/science.abc8511

108. Sun B, Feng Y, Mo X, Zheng P, Wang Q, Li P, et al. Kinetics of SARS-CoV-2 specific IgM and IgG responses in COVID-19 patients. *Emerg Microbes Infect* (2020) 9:940–8. doi: 10.1080/22221751.2020.1762515

109. Long QX, Tang XJ, Shi QL, Li Q, Deng HJ, Yuan J, et al. Clinical and immunological assessment of asymptomatic SARS-CoV-2 infections. *Nat Med* (2020) 26:1200–4. doi: 10.1038/s41591-020-0965-6

110. Robbiani DF, Gaebler C, Muecksch F, Lorenzi JCC, Wang Z, Cho A, et al. Convergent antibody responses to SARS-CoV-2 in convalescent individuals. *Nature* (2020) 584:437–42. doi: 10.1038/s41586-020-2456-9

111. Acanfora D, Acanfora C, Ciccone MM, Scicchitano P, Bortone AS, Uguccioni M, et al. The cross-talk between thrombosis and inflammatory storm in acute and long-COVID-19: Therapeutic targets and clinical cases. *Viruses* (2021) 13(10):1904. doi: 10.3390/v13101904

112. Teijaro JR, Walsh KB, Rice S, Rosen H, Oldstone MB. Mapping the innate signaling cascade essential for cytokine storm during influenza virus infection. *Proc Natl Acad Sci USA* (2014) 111:3799–804. doi: 10.1073/pnas.1400593111

113. Feng Y, Ling Y, Bai T, Xie Y, Huang J, Li J, et al. COVID-19 with different severities: A multicenter study of clinical features. *Am J Respir Crit Care Med* (2020) 201:1380–8. doi: 10.1164/rccm.202002-0445OC

114. Hu B, Huang S, Yin L. The cytokine storm and COVID-19. *J Med Virol* (2021) 93:250–6. doi: 10.1002/jmv.26232

115. Tan LY, Komarasamy TV, Rmt Balasubramaniam V. Hyperinflammatory immune response and COVID-19: A double edged sword. *Front Immunol* (2021) 12. doi: 10.3389/fimmu.2021.742941

116. Tsuchiya K. Inflammasome-associated cell death: Pyroptosis, apoptosis, and physiological implications. *Microbiol Immunol* (2020) 64:252–69. doi: 10.1111/1348-0421.12771

117. Mcgonagle D, Ramanan AV, Bridgewood C. Immune cartography of macrophage activation syndrome in the COVID-19 era. *Nat Rev Rheumatol* (2021) 17:145–57. doi: 10.1038/s41584-020-00571-1

118. Rodriguez-Smith JJ, Verweyen EL, Clay GM, Esteban YM, De Loizaga SR, Baker EJ, et al. Inflammatory biomarkers in COVID-19-associated multisystem inflammatory syndrome in children, Kawasaki disease, and macrophage activation syndrome: A cohort study. *Lancet Rheumatol* (2021) 3:e574–84. doi: 10.1016/S2665-9913(21)00139-9

119. Xu X, Han M, Li T, Sun W, Wang D, Fu B, et al. Effective treatment of severe COVID-19 patients with tocilizumab. *Proc Natl Acad Sci USA* (2020) 117:10970–5. doi: 10.1073/pnas.2005615117

120. Zhou Y, Fu B, Zheng X, Wang D, Zhao C, Qi Y, et al. Pathogenic T-cells and inflammatory monocytes incite inflammatory storms in severe COVID-19 patients. *Natl Sci Rev* (2020) 7:998–1002. doi: 10.1093/nsr/nwaa041

121. Moschonas IC, Tselepis AD. SARS-CoV-2 infection and thrombotic complications: A narrative review. *J Thromb Thrombolysis* (2021) 52:111–23. doi: 10.1007/s11239-020-02374-3

122. Fajgenbaum DC, June CH. Cytokine storm. *N Engl J Med* (2020) 383:2255–73. doi: 10.1056/NEJMra2026131

123. Zhu Z, Cai T, Fan L, Lou K, Hua X, Huang Z, et al. Clinical value of immune-inflammatory parameters to assess the severity of coronavirus disease 2019. *Int J Infect Dis* (2020) 95:332–9. doi: 10.1016/j.ijid.2020.04.041

124. Wieczfinska J, Kleniewska P, Pawliczak R. Oxidative stress-related mechanisms in SARS-CoV-2 infections. *Oxid Med Cell Longev* (2022) 2022:5589089. doi: 10.1155/2022/5589089

125. Checa J, Aran JM. Reactive oxygen species: Drivers of physiological and pathological processes. *J Inflamm Res* (2020) 13:1057–73. doi: 10.2147/JIR.S275595

126. Fu B, Xu X, Wei H. Why tocilizumab could be an effective treatment for severe COVID-19? *J Transl Med* (2020) 18:164. doi: 10.1186/s12967-020-02339-3

127. Lu CC, Chen MY, Lee WS, Chang YL. Potential therapeutic agents against COVID-19: What we know so far. *J Chin Med Assoc* (2020) 83:534–6. doi: 10.1097/JCMA.0000000000000318

128. Lomakin NV, Bakirov BA, Protsenko DN, Mazurov VI, Musaev GH, Moiseeva OM, et al. The efficacy and safety of levilimab in severely ill COVID-19 patients not requiring mechanical ventilation: Results of a multicenter randomized double-blind placebo-controlled phase III CORONA clinical study. *Inflamm Res* (2021) 70:1233–46. doi: 10.1007/s00011-021-01507-5

129. Díaz Y, Ramos-Suzarte M, Martín Y, Calderón N, Hidalgo CJ. Use of a humanized anti-CD6 monoclonal antibody (Itolizumab) in elderly patients with moderate COVID-19. *Gerontology* (2020) 66:1–9. doi: 10.1159/000512210

130. Cai Q, Yang M, Liu D, Chen J, Shu D, Xia J, et al. Experimental treatment with favipiravir for COVID-19: An open-label control study. *Eng (Beijing)* (2020) 6:1192–8. doi: 10.1016/j.eng.2020.03.007

131. Huang M, Tang T, Pang P, Li M, Ma R, Lu J, et al. Treating COVID-19 with chloroquine. *J Mol Cell Biol* (2020) 12:322–5. doi: 10.1093/jmcb/mjaa014

132. Stone JH, Frigault MJ, Serling-Boyd NJ, Fernandes AD, Harvey L, Foulkes AS, et al. Efficacy of tocilizumab in patients hospitalized with covid-19. *N Engl J Med* (2020) 383:2333–44. doi: 10.1056/NEJMoa2028836

133. Maity S, Wu WC, Tracy JB, Clarke LI, Bochinski JR. Nanoscale steady-state temperature gradients within polymer nanocomposites undergoing continuous-wave photothermal heating from gold nanorods. *Nanoscale* (2017) 9:11605–18. doi: 10.1039/C7NR04613H

134. Cai X, Chen M, Prominski A, Lin Y, Ankenbruck N, Rosenberg J, et al. A multifunctional neutralizing antibody-conjugated nanoparticle inhibits and inactivates SARS-CoV-2. *Adv Sci (Weinh)* (2022) 9:e2103240. doi: 10.1002/advs.202103240

135. Benhamou D, Keita H, Ducloy-Bouthors AS. Coagulation changes and thromboembolic risk in COVID-19 obstetric patients. *Anaesth Crit Care Pain Med* (2020) 39:351–3. doi: 10.1016/j.accpm.2020.05.003

136. Ryan C, Minc A, Caceres J, Balsalobre A, Dixit A, Ng BK, et al. Predicting severe outcomes in covid-19 related illness using only patient demographics, comorbidities and symptoms. *Am J Emerg Med* (2021) 45:378–84. doi: 10.1016/j.ajem.2020.09.017

137. Gu SX, Tyagi T, Jain K, Gu VW, Lee SH, Hwa JM, et al. Thrombocytopathy and endotheliopathy: crucial contributors to COVID-19 thromboinflammation. *Nat Rev Cardiol* (2021) 18:194–209. doi: 10.1038/s41569-020-00469-1

138. Roy D, Ghosh R, Dubey S, Dubey MJ, Benito-León J, Kanti Ray B. Neurological and neuropsychiatric impacts of COVID-19 pandemic. *Can J Neurol Sci* (2021) 48:9–24. doi: 10.1017/cjn.2020.173

139. Ghosh R, Roy D, Mandal A, Pal SK, Chandra Swaika B, Naga D, et al. Cerebral venous thrombosis in COVID-19. *Diabetes Metab Syndr* (2021) 15:1039–45. doi: 10.1016/j.dsx.2021.04.026

140. Ye Q, Wang B, Mao J. The pathogenesis and treatment of the `Cytokine storm' in COVID-19. *J Infect* (2020) 80:607–13. doi: 10.1016/j.jinf.2020.03.037

141. Manolis AS, Manolis TA, Manolis AA, Papatheou D, Melita H. COVID-19 infection: Viral macro- and micro-vascular coagulopathy and Thromboembolism/Prophylactic and therapeutic management. *J Cardiovasc Pharmacol Ther* (2021) 26:12–24. doi: 10.1177/1074248420958973

142. Billett HH, Reyes-Gil M, Szymanski J, Ikemura K, Stahl LR, Lo Y, et al. Anticoagulation in covid-19: Effect of enoxaparin, heparin, and apixaban on mortality. *Thromb Haemost* (2020) 120:1691–9. doi: 10.1055/s-0040-1720978

143. Mehta PK, Griendling KK. Angiotensin II cell signaling: Physiological and pathological effects in the cardiovascular system. *Am J Physiol Cell Physiol* (2007) 292:C82–97. doi: 10.1152/ajpcell.00287.2006

144. Santos R, Sampaio WO, Alzamora AC, Motta-Santos D, Alenina N, Bader M, et al. The ACE2/Angiotensin-(1-7)/MAS axis of the renin-angiotensin system: Focus on angiotensin-(1-7). *Physiol Rev* (2018) 98:505–53. doi: 10.1152/physrev.00023.2016

145. Yau JW, Teoh H, Verma S. Endothelial cell control of thrombosis. *BMC Cardiovasc Disord* (2015) 15:130. doi: 10.1186/s12872-015-0124-z

146. Do H, Healey JF, Waller EK, Lollar P. Expression of factor VIII by murine liver sinusoidal endothelial cells. *J Biol Chem* (1999) 274:19587–92. doi: 10.1074/jbc.274.28.19587

147. Liu S, Xu X, Kang Y, Xiao Y, Liu H.). degradation and detoxification of azo dyes with recombinant ligninolytic enzymes from aspergillus sp. with secretory overexpression in pichia pastoris. *R Soc Open Sci* (2020) 7:200688. doi: 10.1098/rsos.200688

148. Watanabe T, Barker TA, Berk BC. Angiotensin ii and the endothelium: Diverse signals and effects. *Hypertension* (2005) 45:163–9. doi: 10.1161/01.HYP.0000153321.13792.b9

149. Rand JH, Glanville RW, Wu XX, Ross JM, Zangari M, Gordon RE, et al. The significance of subendothelial von willebrand factor. *Thromb Haemost* (1997) 78:445–50. doi: 10.1055/s-0038-1657567

150. Leebeek FW, Eikenboom JC. Von Willebrand's disease. *N Engl J Med* (2016) 375:2067–80. doi: 10.1056/NEJMra1601561

151. Blair P, Rex S, Vitseva O, Beaulieu L, Tanriverdi K, Chakrabarti S, et al. Stimulation of toll-like receptor 2 in human platelets induces a thromboinflammatory response through activation of phosphoinositide 3-kinase. *Circ Res* (2009) 104:346–54. doi: 10.1161/CIRCRESAHA.108.185785

152. Subramaniam S, Jurk K, Hobohm L, Jäckel S, Saffarzadeh M, Schwierczek K, et al. Distinct contributions of complement factors to platelet activation and fibrin formation in venous thrombus development. *Blood* (2017) 129:2291–302. doi: 10.1182/blood-2016-11-749879

153. Wojta J, Huber K, Valent P. New aspects in thrombotic research: complement induced switch in mast cells from a profibrinolytic to a prothrombotic phenotype. *Pathophysiol Haemost Thromb* (2003) 33:438–41. doi: 10.1159/000083842

154. Fuchs TA, Brill A, Duerschmied D, Schatzberg D, Monestier M, Myers DDJr., et al. Extracellular DNA traps promote thrombosis. *Proc Natl Acad Sci USA* (2010) 107:15880–5. doi: 10.1073/pnas.1005743107

155. Semeraro F, Ammollo CT, Morrissey JH, Dale GL, Friese P, Esmon NL, et al. Extracellular histones promote thrombin generation through platelet-

dependent mechanisms: Involvement of platelet TLR2 and TLR4. *Blood* (2011) 118:1952–61. doi: 10.1182/blood-2011-03-343061

156. Dinicolantonio JJ, Mccarty M. Thrombotic complications of COVID-19 may reflect an upregulation of endothelial tissue factor expression that is contingent on activation of endosomal NADPH oxidase. *Open Heart* (2020) 7 (1):e001337. doi: 10.1136/openhrt-2020-001337

157. Kaundal RK, Kalvala AK, Kumar A. Neurological implications of covid-19: role of redox imbalance and mitochondrial dysfunction. *Mol Neurobiol* (2021) 58:4575–87. doi: 10.1007/s12035-021-02412-y

158. Ali M, Spinler SA. COVID-19 and thrombosis: From bench to bedside. *Trends Cardiovasc Med* (2021) 31:143–60. doi: 10.1016/j.tcm.2020.12.004

159. Barnes BJ , Adrover JM, Baxter-Stoltzfus A, Borczuk A, Cools-Lartigue J, Crawford JM, et al. Targeting potential drivers of COVID-19: Neutrophil extracellular traps. *J Exp Med* (2020) 217(6):e20200652. doi: 10.1084/jem.20200652

160. Meidaninikjeh S, Sabouni N, Marzouni HZ, Bengar S, Khalili A, Jafari R. Monocytes and macrophages in COVID-19: Friends and foes. *Life Sci* (2021) 269:119010. doi: 10.1016/j.lfs.2020.119010

161. Taghiloo S, Aliyali M, Abedi S, Mehravaran H, Sharifpour A, Zaboli E, et al. Apoptosis and immunophenotyping of peripheral blood lymphocytes in Iranian COVID-19 patients: Clinical and laboratory characteristics. *J Med Virol* (2021) 93:1589–98. doi: 10.1002/jmv.26505

162. Bost P, Giladi A, Liu Y, Bendjelal Y, Xu G, David E, et al. Host-viral infection maps reveal signatures of severe COVID-19 patients. *Cell* (2020) 181:1475–1488.e1412. doi: 10.1016/j.cell.2020.05.006

163. Shen B, Yi X, Sun Y, Bi X, Du J, Zhang C, et al. Proteomic and metabolomic characterization of covid-19 patient sera. *Cell* (2020) 182:59–72.e15. doi: 10.1016/j.cell.2020.05.032

164. Mattoo SU, Kim SJ, Ahn DG, Myoung J. Escape and over-activation of innate immune responses by sars-cov-2: two faces of a coin. *Viruses* (2022) 14 (3):530. doi: 10.3390/v14030530

165. Li S, Zhang Y, Guan Z, Li H, Ye M, Chen X, et al. SARS-CoV-2 triggers inflammatory responses and cell death through caspase-8 activation. *Signal Transduct Target Ther* (2020) 5:235. doi: 10.1038/s41392-020-00334-0

166. Felsenstein S, Herbert JA, Mcnamara PS, Hedrich CM. COVID-19: Immunology and treatment options. *Clin Immunol* (2020) 215:108448. doi: 10.1016/j.clim.2020.108448

167. Anka AU, Tahir MI, Abubakar SD, Alsabbagh M, Zian Z, Hamedifar H, et al. Coronavirus disease 2019 (COVID-19): An overview of the immunopathology, serological diagnosis and management. *Scandinavian J Immunol* (2020) 93(4):e12998. doi: 10.1111/sji.12998

168. Morris G, Bortolasci CC, Puri BK, Olive L, Marx W, O'neil A, et al. The pathophysiology of SARS-CoV-2: A suggested model and therapeutic approach. *Life Sci* (2020) 258:118166. doi: 10.1016/j.lfs.2020.118166

169. Prete M, Favoino E, Catacchio G, Racanelli V, Perosa F. SARS-CoV-2 inflammatory syndrome. Clinical features and rationale for immunological treatment. *Int J Mol Sci* (2020) 21(9):3377. doi: 10.3390/ijms21093377

170. Mason RJ. Pathogenesis of COVID-19 from a cell biology perspective. *Eur Respir J* (2020) 55(4):2000607. doi: 10.1183/13993003.00607-2020

171. Carcaterra M, Caruso C. Alveolar epithelial cell type ii as main target of sars-cov-2 virus and covid-19 development *via* nf-kb pathway deregulation: A physio-pathological theory. *Med Hypotheses* (2021) 146:110412. doi: 10.1016/j.mehy.2020.110412

172. Tang Y, Liu J, Zhang D, Xu Z, Ji J, Wen C. Cytokine storm in covid-19: The current evidence and treatment strategies. *Front Immunol* (2020) 11:1708. doi: 10.3389/fimmu.2020.01708

173. Ginsburg I, Fibach E. Polycations and polyanions in SARS-CoV-2 infection. *Med Hypotheses* (2021) 146:110470. doi: 10.1016/j.mehy.2020.110470

174. Lin C-W, Lin K-H, Hsieh T-H, Shiu S-Y, Li J-Y. Severe acute respiratory syndrome coronavirus 3C-like protease-induced apoptosis. *FEMS Immunol Med Microbiol* (2006) 46:375–80. doi: 10.1111/j.1574-695X.2006.00045.x

175. Lotfi R, Kalmarzi RN, Roghani SA. A review on the immune responses against novel emerging coronavirus (SARS-CoV-2). *Immunol Res* (2021) 69:213–24. doi: 10.1007/s12026-021-09198-0

176. Brochetti RA, Leal MP, Rodrigues R, Da Palma RK, De Oliveira LVF, Horliana A, et al. Photobiomodulation therapy improves both inflammatory and fibrotic parameters in experimental model of lung fibrosis in mice. *Lasers Med Sci* (2017) 32:1825–34. doi: 10.1007/s10103-017-2281-z

177. Koussoroplis SJ, Paulissen G, Tyteca D, Goldansaz H, Todoroff J, Barilly C, et al. PEGylation of antibody fragments greatly increases their local residence time following delivery to the respiratory tract. *J Control Release* (2014) 187:91–100. doi: 10.1016/j.jconrel.2014.05.021

178. Welch NG, Scoble JA, Muir BW, Pigram PJ. Orientation and characterization of immobilized antibodies for improved immunoassays (Review). *Biointerphases* (2017) 12:02d301. doi: 10.1116/1.4978435

179. Chen N, Zhou M, Dong X, Qu J, Gong F, Han Y, et al. Epidemiological and clinical characteristics of 99 cases of 2019 novel coronavirus pneumonia in wuhan, China: A descriptive study. *Lancet* (2020) 395:507–13. doi: 10.1016/S0140-6736(20)30211-7

180. Estrada E. Cascading from SARS-CoV-2 to parkinson's disease through protein-protein interactions. *Viruses* (2021) 13(5):897. doi: 10.3390/v13050897

181. Berlin DA, Gulick RM, Martinez FJ. Severe covid-19. *N Engl J Med* (2020) 383:2451–60. doi: 10.1056/NEJMcp2009575

182. Jose RJ, Manuel A. COVID-19 cytokine storm: The interplay between inflammation and coagulation. *Lancet Respir Med* (2020) 8:e46–7. doi: 10.1016/S2213-2600(20)30216-2

183. Karadaş Ö, Öztürk B, Sonkaya AR. A prospective clinical study of detailed neurological manifestations in patients with COVID-19. *Neurol Sci* (2020) 41:1991–5. doi: 10.1007/s10072-020-04547-7

184. Shehata GA, Lord KC, Grudzinski MC, Elsayed M, Abdelnaby R, Elshabrawy HA. Neurological complications of covid-19: Underlying mechanisms and management. *Int J Mol Sci* (2021) 22(8):4081. doi: 10.3390/ijms22084081

185. Clark IA. Chronic cerebral aspects of long covid. Post-stroke syndromes and similar states share their pathogenesis and perispinal etanercept treatment logic. *Pharmacol Res Perspect* (2022) 10:e00926. doi: 10.1002/prp2.926

186. Gibson LE, Fenza RD, Lang M, Capriles MI, Li MD, Kalpathy-Cramer J, et al. Right ventricular strain is common in intubated covid-19 patients and does not reflect severity of respiratory illness. *J Intensive Care Med* (2021) 36:900–9. doi: 10.1177/08850666211006335

187. Heuberger J, Trimpert J, Vladimirova D, Goosmann C, Lin M, Schmuck R, et al. Epithelial response to IFN-γ promotes SARS-CoV-2 infection. *EMBO Mol Med* (2021) 13:e13191. doi: 10.15252/emmm.202013191

188. Wu Y. Compensation of ACE2 function for possible clinical management of 2019-nCoV-Induced acute lung injury. *Virologica Sin* (2020) 35:256–8. doi: 10.1007/s12250-020-00205-6

189. Cairns DM, Dulko D, Griffiths JK, Golan Y, Cohen T, Trinquart L, et al. Efficacy of niclosamide vs placebo in sars-cov-2 respiratory viral clearance, viral shedding, and duration of symptoms among patients with mild to moderate covid-19: A phase 2 randomized clinical trial. *JAMA Netw Open* (2022) 5:e2144942. doi: 10.1001/jamanetworkopen.2021.44942

190. Martinson JA, Montoya CJ, Usuga X, Ronquillo R, Landay AL, Desai SN. Chloroquine modulates HIV-1-induced plasmacytoid dendritic cell alpha interferon: implication for T-cell activation. *Antimicrob Agents Chemother* (2010) 54:871–81. doi: 10.1128/AAC.01246-09

191. Yang M, Cao L, Xie M, Yu Y, Kang R, Yang L, et al. Chloroquine inhibits HMGB1 inflammatory signaling and protects mice from lethal sepsis. *Biochem Pharmacol* (2013) 86:410–8. doi: 10.1016/j.bcp.2013.05.013

192. Hung IF, Lung KC, Tso EY, Liu R, Chung TW, Chu MY, et al. Triple combination of interferon beta-1b, lopinavir-ritonavir, and ribavirin in the treatment of patients admitted to hospital with COVID-19: An open-label, randomised, phase 2 trial. *Lancet* (2020) 395:1695–704. doi: 10.1016/S0140-6736(20)31042-4

frontiers | Frontiers in Immunology

TYPE Review
PUBLISHED 17 October 2022
DOI 10.3389/fimmu.2022.1008072

OPEN ACCESS

EDITED BY
Linzhu Ren,
Jilin University, China

REVIEWED BY
Song Wang,
Fujian Agriculture and Forestry University, China
Hafiz Ullah,
Gomal University, Pakistan
Xu Tan,
Tsinghua University, China

*CORRESPONDENCE
Yang Yu
yuyang80@swmu.edu.cn
Wei Dong
dongwei@swmu.edu.cn
Changshun Bao
bcs756@126.com

†These authors have contributed equally to this work and share first authorship

SPECIALTY SECTION
This article was submitted to Molecular Innate Immunity, a section of the journal Frontiers in Immunology

RECEIVED 31 July 2022
ACCEPTED 28 September 2022
PUBLISHED 17 October 2022

CITATION
Lang R, Li H, Luo X, Liu C, Zhang Y, Guo S, Xu J, Bao C, Dong W and Yu Y (2022) Expression and mechanisms of interferon-stimulated genes in viral infection of the central nervous system (CNS) and neurological diseases.
Front. Immunol. 13:1008072.
doi: 10.3389/fimmu.2022.1008072

Expression and mechanisms of interferon-stimulated genes in viral infection of the central nervous system (CNS) and neurological diseases

Rui Lang[1,2†], Huiting Li[1†], Xiaoqin Luo[3], Cencen Liu[4], Yiwen Zhang[2], ShunYu Guo[2], Jingyi Xu[1], Changshun Bao[2,5,6,7*], Wei Dong[1*] and Yang Yu[1,3*]

[1]Key Laboratory of Medical Electrophysiology, Ministry of Education & Medical Electrophysiological Key Laboratory of Sichuan Province, (Collaborative Innovation Center for Prevention of Cardiovascular Diseases), Institute of Cardiovascular Research, Southwest Medical University, Luzhou, China, [2]Department of Neurosurgery, The Affiliated Hospital of Southwest Medical University, Luzhou, China, [3]Department of Human Anatomy and Histoembryology, School of Basic Medical Sciences, Southwest Medical University, Luzhou, China, [4]Department of Pathology, People's Hospital of Zhongjiang County, DeYang, China, [5]Sichuan Clinical Research Center for Neurosurgery, The Affiliated Hospital of Southwest Medical University, Luzhou, China, [6]Academician (Expert) Workstation of Sichuan Province, The Affiliated Hospital of Southwest Medical University, Luzhou, China, [7]Neurological diseases and brain function laboratory, The Affiliated Hospital of Southwest Medical University, Luzhou, China

Interferons (IFNs) bind to cell surface receptors and activate the expression of interferon-stimulated genes (ISGs) through intracellular signaling cascades. ISGs and their expression products have various biological functions, such as antiviral and immunomodulatory effects, and are essential effector molecules for IFN function. ISGs limit the invasion and replication of the virus in a cell-specific and region-specific manner in the central nervous system (CNS). In addition to participating in natural immunity against viral infections, studies have shown that ISGs are essential in the pathogenesis of CNS disorders such as neuroinflammation and neurodegenerative diseases. The aim of this review is to present a macroscopic overview of the characteristics of ISGs that restrict viral neural invasion and the expression of the ISGs underlying viral infection of CNS cells. Furthermore, we elucidate the characteristics of ISGs expression in neurological inflammation, neuropsychiatric disorders such as depression as well as neurodegenerative disorders, including Alzheimer's disease (AD), Parkinson's disease (PD), and amyotrophic lateral sclerosis (ALS). Finally, we summarize several ISGs (ISG15, IFIT2, IFITM3) that have been studied more in recent years for their antiviral infection in the CNS and their research progress in neurological diseases.

KEYWORDS

interferons, interferon-stimulated genes, central nervous system, interferon-stimulated gene 15, interferon-inducible tetrapeptide repeat protein 2, interferon-inducible transmembrane protein 3, viral infection, neurological diseases

10.3389/fimmu.2022.1008072

Introduction

Interferons (IFNs) are a class of antiviral cytokines that are stimulated in response to the challenge of host defenses and are crucial for mobilizing the immune response to pathogens in vertebrates. Most virus-infected cells can produce IFNs, which are secreted to bind to their receptors on autologous or other cells and initiate a signaling cascade that leads to the induction of hundreds of interferon-stimulated genes (ISGs) to promote antiviral effects (1, 2). IFNs are divided into three classes (type I, type II, and type III) based on their sequence and cellular receptors. The type I IFN family comprises members encoded by multiple genes, including 13 highly homologous subtypes of IFN-α, and the other isoforms, such as IFN-β, IFN-ϵ, IFN-κ, IFN-ω, IFN-τ, IFN-δ, and IFN-ζ (3–6). The type II IFN class only contains IFN-γ, while the type III IFN family consists of four IFN-λ molecules, including IFN-λ1(IL-29), IFN-λ2 (IL-28A), and IFN-λ3 (IL-28B), as well as IFN-λ4 (7). Type I and III IFNs are considered the classical antiviral IFNs, while type II IFN has multiple roles in the innate and adaptive immune systems (1, 2, 7–10). Additionally, type III IFNs impact antiviral activity at anatomical barriers, such as the blood-brain barrier (BBB) and epithelial cell surfaces (11). Although type I and type III IFNs induce a similar subset of ISGs, differences in cell-type specificity and signaling kinetics result in distinct responses. In general, type I IFNs activate a more robust and rapid ISG response, whereas type III IFNs induce a slower response with lower levels of ISG expression (reviewed in 2). Traditionally, IFN signaling is involved in the induction of host defense-associated ISGs through the Janus tyrosine kinase (JAK)/signal transducer and activator of transcription (STAT) signal pathway (12–14). Type I and III IFNs activate JAK1 and tyrosine kinase 2 (TYK2), resulting in cytoplasmic STAT1 and STAT2 phosphorylation (15). After phosphorylation, STAT1 and STAT2 dimerize and translocate from the cytoplasm to the nucleus, forming the IFN-stimulated gene factor 3 (ISGF3) complex with interferon regulatory factor 9 (IRF9). ISGF3 further binds to interferon stimulatory response elements (ISREs) and stimulates the transcription of ISGs (16). Type II IFN activates JAK1 and JAK2, resulting in the formation of phosphorylated STAT1 (pSTAT1) homodimers known as γ-activated factors (GAF), which translocate to the nucleus and bind to γ-activated sequences (GAS) to induce transcription of ISGs (17). Some interferon regulatory factors (IRFs) such as IRF3 can induce ISGs directly in the absence of IFN production or collaboratively with other transcription factors such as IFN regulatory factor 7 (IRF7), IRF1, and nuclear factor kappa B (NF-κB) to induce type I IFN production (17–26). In addition, some ISGs encode factors that are involved in the IFN production or response pathway through positive or negative feedback loops (27, 28). For instance, the core retinoic acid-inducible gene I (RIG-I) and melanoma differentiation-associated gene 5 (MDA5), members of the mammalian RIG-I-like receptors (RLRs), are found in the cytosol of most cell types and are powerfully activated by IFNs in a positive feedback loop of RNA virus infection (27, 29). Interferon-responsive activation of interferon-induced protein with tetrapeptide repeats 1 (IFIT1, also known as ISG56) positively regulates the expression of RIG-I, MDA5, and IFIT2 (also known as ISG54) (30). Furthermore, IFN-stimulated gene 15 (ISG15) was found to negatively regulate the IFN signaling pathway by coupling to RIG-I (31, 32).

The IFN pathway provides essential protection to the central nervous system (CNS) against viral infections. It is instrumental in immune-related diseases such as allergic reactions, chronic inflammatory diseases, autoimmune diseases, transplant rejection, viral infections, and many more (33). For example, mice with a deficiency in the IFN-I receptor subunit 1 (*Ifnar1*$^{-/-}$) are highly susceptible to various viral infections in multiple organs, including the CNS (34–36). *Ifnar1*$^{-/-}$ mice showed increased viral load after infection with Sindbis virus (SINV), and increased viral load in the CNS was associated with high susceptibility compared with wild-type (WT) mice (37). Several fatal cases of Herpes simplex encephalitis (HSE) in newborns were associated with defects in genes encoding signal transduction factors of the IFN pathway, such as Toll/interleukin-1 receptor domain-containing adaptor-inducing interferon-β (TRIF), TANK-binding kinase 1 (TBK-1), Toll-like receptor 3 (TLR3) or tumor necrosis factor receptor-associated factor 3 (TRAF3). These findings demonstrated the importance of the human IFN response to neurotropic viral infections (38–41). In addition to participating in natural immunity against viral infections, IFNs have been shown to constitute key factors in the neuroinflammatory network and make an essential contribution to the pathogenesis of neurodegenerative diseases such as Parkinson's disease (PD), Alzheimer's disease (AD), and amyotrophic lateral sclerosis (ALS) (42–45). The IFN signaling pathway was recently reported to be severely upregulated in AD patients and significantly correlated with disease severity (46–48). Activation of the IFN signaling pathway can induce the expression of hundreds of ISGs. Although ISGs are major antiviral effectors of the IFN response, the antiviral mechanisms of most ISGs have not been described until recently. The aim of this review is to provide a macroscopic overview of the characteristics of ISGs that restrict viral neural invasion and cellular expression of ISGs after viral infection of the CNS, as well as the expression characteristics of ISGs in neurological diseases (Table 1). In addition, substantial progress has been made in our understanding of individual ISGs (ISG15, IFIT2, IFITM3) in CNS viral infection and diseases in recent years (Table 1), providing an essential target for the development of novel antivirals and anti-neurological disease drugs.

TABLE 1 ISGs expression in antiviral infections, neuronal localization and neurological diseases.

ISGs	Produced by viruses and related stimuli	Specifically altered in CNS regions or cells	Neurological disorders and related models
ISG15	TMEV (49); HIV (50, 51); MHV-induced encephalitis (52);	Astrocytes and endothelial cells (49); BMECs (50); Microglia (51);	Post-traumatic brain injury ALS (53); ALS, model of cerebral ischemia, model of brain injury, model of chronic neuronal damage induced by the viral protein HIV gp120 (54); Ataxia capillaries (A-T) (55); Maternal immune activation (MIA) (56); AGS (57);
MX2	HIV (50, 51); Poly I:C (58);	BMECs (50); Microglia (51); Hippocampal dentate gyrus (58);	AGS (57);
Viperin	HIV (51); HSV-1 (59, 60); LGTV (61); TBEV (61);	Microglia (51); Neurons and astrocytes (59, 60);	AGS (57);
CH25H	HSV-1 (59, 60);	Neurons and astrocytes HSE (59, 60);	Multiple sclerosis (MS) (62);
IFITM3	SARS-CoV-2 (63); HCMV (64);	frontal cortex and choroid plexus (65);	The aging mouse (66); 5xFAD Alzheimer's disease mouse model (66);
OAS2	HSV-1 (59, 60);	Neurons and astrocytes (59, 60);	
latent RNase (RNase L)	HSV-1 (59, 60);	Neurons and astrocytes (59, 60);	
PKR	HSV-1 (59, 60);	Neurons and astrocytes (59, 60);	
IFIT1	HIV (50, 51); VSV (67); EMCV (67); HSV-1 (59, 60); JEV (68); Poly I:C (30); HCMV (69); MHV (52);	BMECs (50); Neurons and astrocytes (59, 60); Microglia (68); Astrocytes (30, 69);	
GBP5	HIV (51);	Microglia (51);	
IFIT2	JEV (68); VSV (67, 70); WNV (71); EMCV (67); Sendai virus (SeV) (72); MHV-RSA59 (73); RABV (74, 75); Poly I:C (30, 58);	Microglia (68);	
Ifi27l2a	WNV (76);		
IFP35			MS (77);
IFI27			AGS (57);
IFIT3	RABV (74);		

ISGs play an essential role in restricting viral neuroinvasion

The CNS requires a complex and coordinated immune response to prevent neurological disorders, avoid excessive immune activation and inappropriate inflammatory response, and protect against invading pathogens such as viruses. Although the CNS is immune privileged and protected from toxic substances and pathogens carried in the blood by the BBB and the blood-cerebrospinal fluid barrier (BCSFB) (78), neurotropic viruses are capable of infecting the CNS and staying there for a long time, including herpes simplex virus type 1 (HSV-1), varicella zoster virus (VZV), Japanese encephalitis virus (JEV), West Nile virus (WNV), measles, rabies virus (RABV), poliovirus, and so on (79–81). Neurotropic viruses can spread through multiple pathways to penetrate the CNS. Some viruses can enter the CNS by infecting host immune cells in the periphery and using these cells as "Trojan horses" to carry them across the BBB, or the virus can directly infect endothelial cells, disrupt the BBB, or infect peripheral neuron axons and retrograde upward through the mechanism of axonal transport of cellular cargo, such as through the olfactory pathway (33, 79, 80) (Figure 1).

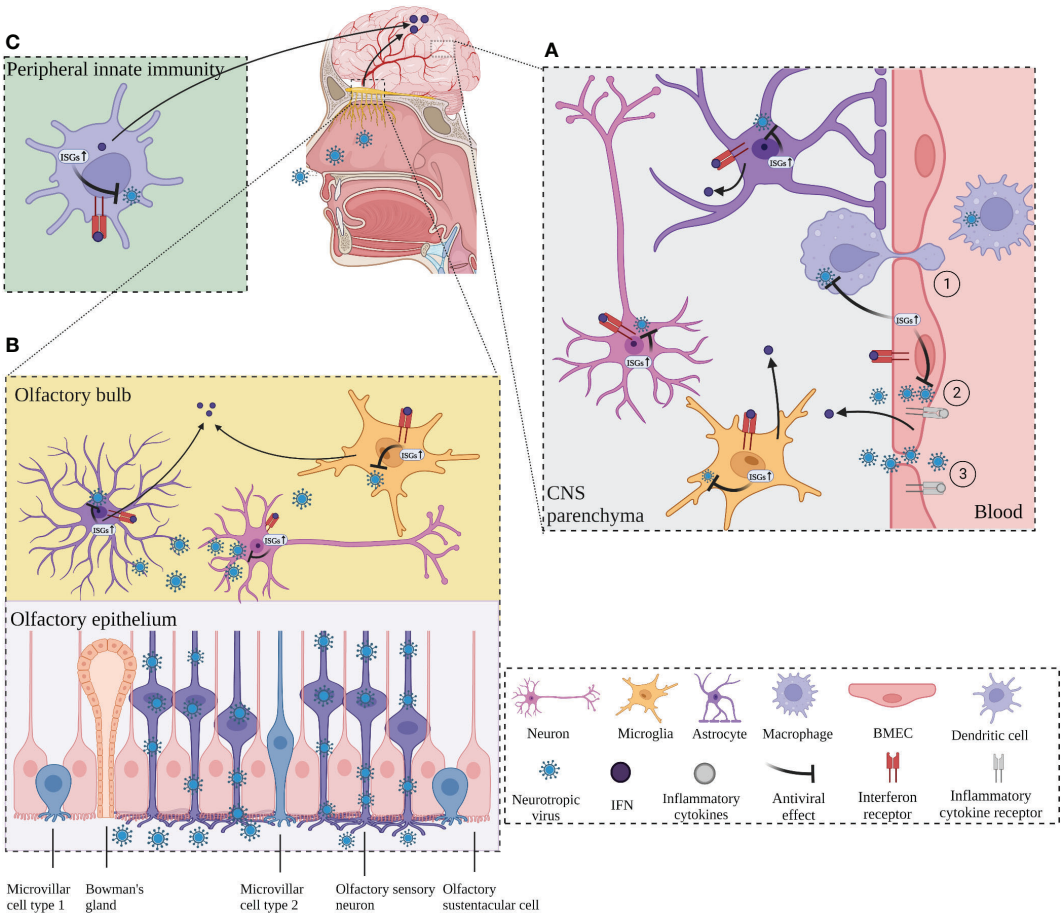

FIGURE 1
ISGs restrict viral neuroinvasion. **(A)** ISGs in BMECs, which constitute the blood-brain barrier (BBB), are activated by virus and inflammation, leading to an IFN response and activation of transcription of antiviral ISGs, followed by activation of microglia and astrocytes to release ISGs. BMECs deliver the released ISGs to macrophages to enhance the antiviral response and restrict viral invasion. ① Neurotropic virus crosses the BBB through "Trojan horse" strategy. ② Virus infects endothelial cells across the BBB. ③ Virus enters the CNS by destroying the BBB. **(B)** The virus invades the CNS retrogradely through the olfactory pathway. The virus invades the olfactory sensory neurons through the olfactory epithelium and retrogrades upward into the olfactory bulb (OB). Virus at OB activates neurons, microglia, and macrophages, which produces IFN response and induces transcription of ISGs, leading to antiviral response. Long-distance signaling of IFN at the OB activates the transcription of ISGs in the brain. **(C)** IFNs produced by peripheral antiviral response enter the CNS and activate the transcription of ISGs in advance and induces transcription of ISGs, leading to antiviral response. Long-distance signaling of IFN at the OB activates the transcription of ISGs in the brain. **(C)** IFNs produced by peripheral antiviral response enter the CNS and activate the transcription of ISGs in advance. Created with BioRender.com.

ISGs prevent viruses from crossing the BBB

The structural integrity of the BBB is critical to enable the normal neurological function of the CNS and protection from damage from inflammation, virus, and other diseases. Brain microvascular endothelial cells (BMECs) are the structural and functional basis of the BBB and play a critical role in maintaining its normal integrity. One study reported that infection of BMECs by JEV did not affect cell viability but resulted in increased permeability of the endothelial monolayer due to inflammation caused by JEV infection that inhibited the expression of tight junction (TJ) proteins in BMECs, leading to enhanced BBB permeability (81). *In vitro* experiments with cultured mouse BMECs showed that IFN-λ signaling increased transendothelial resistance, reduced viral movement across the barrier, and modulated TJ protein localization (82). In addition, IFN-λ limits the opening of the BBB by reducing the production of inflammatory cytokines in primary astrocytes and microglia and inducing activation of the JAK/STAT pathway, leading to the production of ISGs (83). Inflammation can play an indirect antiviral role while disrupting the BBB, and in an *in vitro* model of the BBB with co-culture of astrocytes and BMECs, lipopolysaccharide (LPS) promoted the expression of type I IFN signaling-related proteins such as STAT1, STAT2, ISG15, and SAMHD1 in astrocytes, TNF-α and LPS also induce the

production of ISGs (EIF2AK2, ADAR, TRIM25 and ISG15) in astrocyte cultures *in vitro* (84). BMECs have a critical function in the innate immunity of the BBB to human immunodeficiency virus (HIV) infection by causing activation of TLR3 in BMECs to induce phosphorylation of IRF3 and IRF7 (key regulators of the IFN signaling pathway) and trigger the production of endogenous IFN-β and IFN-λ, thereby significantly inhibiting viral replication (85). In addition, TLR3-activated human BMECs secrete exosomes that inhibit HIV replication by transferring antiviral factors, including several critical IFN-stimulated genes (ISG15, IFIT1, MX2) to macrophages (50). This suggests that human BMECs may help restore the antiviral status of HIV-infected macrophages, which may be a defense mechanism against neural invasion by HIV "Trojan horses" (Figure 1A).

ISGs limit viral infection in the olfactory pathway

Numerous neurotropic viruses enter the CNS through infection of peripheral nerves, including olfactory neurons and sensory or motor neurons (86). WNV can enter the CNS by infecting sensory nerve endings or olfactory neurons or through the bloodstream (87). RABV and poliovirus transmit from muscle to somatic motor neurons in the spinal cord *via* the neuromuscular junctions (NMJs) (88). Olfactory pathways play an important role in the invasion of viruses into the CNS *via* peripheral nerves (Figure 1B). Detje et al. found that blocking the type I IFN pathway promoted the spread of vesicular stomatitis virus (VSV) from the olfactory bulb (OB) to the entire CNS, while local IFN response in the OB effectively controlled viral invasion of the CNS (89). IFN-induced viperin limits the replication of Langat virus (LGTV) in the OB in a region-specific manner (61). Long-range signaling of IFN-β released from infected neurons at the OB after VSV and cytomegalovirus (CMV) infection of the nasal mucosa upregulated the expression of ISGs in uninfected brain regions (90). Similar results were obtained from another investigation, which shows that after intranasal VSV infection, IFN expressed at the OB enters the brain to activate IFIT2 transcription in advance to act as an antiviral agent (67). The accumulation of microglia around the OB and their expression of ISGs form a natural immune barrier that is instrumental in limiting the spread of VSV in the CNS and preventing fatal encephalitis (91) (Figure 1B).

ISGs are activated before viruses invade the CNS

Viral infections rapidly induce IFN in the periphery, which serves to protect most tissues from viral pathogenicity (92). Peripherally induced IFN response can induce ISGs in the brain. Peripheral IFN-α that crosses the BBB directly activates IFN-α/β receptor (IFNAR) signaling in microglia, leading to the upregulation of multiple ISGs (93, 94). As mentioned above, long-range signaling of IFN released from infected neurons at the OB after viral infection of the nasal mucosa upregulated the expression of ISGs (IFIT2, IFIT3, OAS, and MX1) in uninfected brain regions (67, 90). Lukasz et al. reported that adolescent mice injected with the viral mimic poly I:C significantly increased the expression of ISGs (IFIT2, PRKR, MX2, and IRF7) in the hippocampal dentate gyrus (58). Collectively, these findings suggest that early activation of ISGs in the CNS plays a crucial role in limiting viral infection of the CNS (Figure 1C).

Antiviral response in the CNS: Cells, ISGs, and mechanisms

The vast majority of cell types in the CNS, comprising neurons, astrocytes, oligodendrocytes, CNS-associated macrophages (CAMs), ventricular epithelial cells, and vascular endothelial cells, are responsive to IFN (95). Activation of astrocytes and microglia in the brain has an essential role in the innate immune response of the CNS to viral infection (96, 97). Different immune cells in the CNS respond to various viral stimuli. Microglia monitor the local environment and rapidly respond to widespread inflammatory stimuli, while astrocytes function as immune response cells and produce large amounts of inflammatory mediators (98). For example, during infection with Taylor mouse encephalomyelitis virus (TMEV), protein levels of ISG15 were elevated mainly in astrocytes and endothelial cells, whereas the protein levels of protein kinase R (PKR) were predominantly increased in microglia/macrophages, oligodendrocytes and neurons (49). Murine hepatitis virus (MHV) is a neurotropic coronavirus, and astrocytes and microglia produce type I IFNs (IFN-α and IFN-β), as well as interleukin (IL-6), TNF-α, IL-12, IL-1α, and IL-1β during experimental MHV infection in mice (99). HSV encephalitis (HSE) is a severe CNS infection caused primarily by HSV-1 and occasionally by HSV-2. Following infection with HSV-1, TLR2 and TLR4 are induced to activate simultaneously, and in turn, TLR2 forms a dimer with TLR1, or TLR6, which then induces IFN-β in neurons and IFN-α in astrocytes, and these IFNs subsequently induce the expression of ISGs such as viperin, CH25H (cholesterol-25-hydroxylase), oligoadenylate synthase2 (OAS2), latent RNase (RNase L), PKR, and IFIT1 (59, 60).

Microglia

Microglia, a major source of type I IFNs, exert direct antiviral effects by producing type I IFNs to stimulate the expression of ISGs or act indirectly on other cells through type I IFNs to activate the corresponding signaling pathway (100). Microglia express various pattern recognition receptors (PRRs),

10.3389/fimmu.2022.1008072

including TLRs, RNA-sensing RLRs, and cytosolic DNA sensors that are important for virus defense. PRRs recognize viral-associated molecular patterns and induce type I IFN expression in microglia (27, 101). Cyclic GMP-AMP synthase (cGAS) binds to cytoplasmic dsDNA in microglia to produce cyclic GMP-AMP (cGAMP), which activates downstream stimulator of interferon genes (STING) and ultimately activates the transcription factor IRF3. In turn, IRF3 stimulates type I IFN production, and the resulting type I IFNs bind to the heterodimeric receptor IFNAR to initiate a signaling cascade, promote nuclear translocation of heterodimeric STAT1/2, and facilitate transcriptional activation of multiple ISGs (59, 60, 67, 90, 99). Depletion of CNS microglia *via* CSF1R inactivation has higher viral loads in mice infected with WNV (TX02 strain) or VSV, with increased mortality and viral tissue loads, indicating that microglia are critical for restricting virus transmission (102, 103). The phagocytic activity of microglia recruited *via* purinergic receptor P2Y12 signaling around infected neurons play an important role in CNS antiviral immunity. Analysis of temporal lobe specimens from patients with HSV-1 encephalitis reveals that there are approximately 1–3 activated microglia around each HSV-1-positive neuron and that P2Y12-positive microglia processes extend to HSV-1-positive cells (104). In addition, the number of microglia recruited to infected neurons was significantly reduced in a P2Y12-deficient mouse model (104). Studies have shown that microglia are the main producers of type I IFNs in viral infections of the CNS. Further studies found that in the mouse model of VSV encephalitis, the infected microglia were found to produce type I IFNs, which caused both infected and uninfected microglia to upregulate the expression of IRF7 and activate innate immunity, thus limiting the trans-synaptic transmission of VSV (105). Microglia also induce IFN and ISG expression by regulating the HSPA8/DNA-PK pathway independently of STING (106). Although phagocytosis of foreign pathogens by microglia is an essential component of neuroprotective immune defense to ensure the function of healthy neurons, excessive microglia activation leads to uncontrolled inflammation that exacerbates neuronal death, causing damage to brain tissue and cells (68, 107). In mice infected with JEV, microglia activation led to uncontrolled inflammation and neuronal death (108). JEV can promote viral replication by infecting microglia and upregulating miR-146a gene expression, inhibiting NF-κB activity, blocking the antiviral JAK/STAT signaling pathway, and downregulating antiviral ISGs (IFIT1 and IFIT2) (68). Phosphorylation of IFN regulators (IRF3 and IRF7) and STAT1/3 are inhibited in HIV-infected microglia, which suppresses the expression of several key anti-HIV ISGs (ISG15, IFIT1, GBP5, MX2, and viperin) (51). Taken together, these findings suggest microglia play an essential role in antiviral defense of the CNS and contribute to explaining how the virus invades microglia and results in a persistent infection.

Astrocytes

Astrocytes have essential and significant functions in synaptic plasticity, regulation of the BBB, and maintenance of CNS homeostasis (109, 110). In viral infections, astrocytes play a key role in host defense by supporting a functional BBB, regulating glutamate homeostasis, and engaging in innate and adaptive immune response to viral infections (111). Recent studies have shown that microglia induce astrocytes proliferation through the expression of pro-inflammatory cytokines, including IL-1β, TNF, and IFN-γ (112, 113). During viral infection, astrocytes detect molecular changes in their extracellular environment and neighboring cells. Compared with microglia, astrocytes have low basal mRNA levels of PRRs and ISGs, and poorly induced *Ifn-β* mRNA following infection, but the upregulated various mRNAs in the IFN-α/β pathway of astrocytes to a higher extent than microglia, suggesting that the response of astrocytes to infection is delayed but stronger compared with that of microglia (114). Genetic astrocyte-specific deletion of the type I IFN receptor IFNAR in a mouse model of viral infection led to an increase of BBB permeability (115). Further studies revealed that abolition of astrocytic IFN-α/β signaling was followed by uncontrolled virus transmission and fatal encephalomyelitis, demonstrating the importance of the inducible IFN signaling pathway within astrocytes in limiting viral infection of the CNS (114). Imaizumi et al. reported that poly I:C upregulated the expression of IFIT2 and IFIT1 in astrocytes *via* the TLR3/IFN-β pathway and that the expression product IFIT1 positively regulated the expression of IFIT2, RIG-I, and MDA5 to enhance antiviral response (30). In addition, RNA interference (RNAi) knockdown of interferon-induced protein 35 (*IFI35*) resulted in a decrease in expression of poly I:C-induced *IFN-β*, *pStat1*, *Rig-1*, *Cxcl10*, and *Ccl5*, indicating that IFI35 may negatively regulate the astrocyte TLR3/IFN-β/pSTAT1/RIG-I/CXCL10/CCL5 axis and may partially regulate the innate immune response of astrocytes (116). Recent studies of CNS complications due to enterovirus 71 (EV71) infection have shown that in infected astrocytes, phosphorylated and non-phosphorylated STAT3 competes with STAT1 for binding to KPNA1, inhibits nuclear import of pSTAT1 and hinders the formation of the ISGF3 complex, leading to suppression of downstream ISG expression (117). Knockdown of STAT3 attenuated the suppressed IFN-mediated antiviral response to EV71 infection and led to a reduction in viral replication, demonstrating the role of STAT3 in maintaining the balance of inflammatory response in astrocytes and antiviral response in the CNS during infection (117). Borna disease virus (BDV) is a non-hemolytic RNA neurotropic virus, and replication of this virus is effectively blocked in transgenic mice expressing mouse IFN-α in astrocytes (118). Another study showed that rapid type I IFN response protected astrocytes from virus-induced cytopathic

effects upon infection with flavivirus, tick-borne encephalitis virus (TBEV), JEV, WNV, and Zika virus (ZIKV), thus limiting the spread of these viruses (119). In addition, type I and type III IFN-independent antiviral pathways were found to be involved in the control of astrocytes during ZIKV infection (120). In summary, the intrinsic structural antiviral response of astrocytes combined with rapid induction of type I IFNs is instrumental in protecting astrocytes and inhibiting viral replication in the CNS (121).

Neurons

Like microglia and astrocytes, neurons express multiple PRRs, produce innate immune cytokines such as type I IFNs following viral infection, and respond to cytokine stimulation to inhibit viral replication and increase cell survival (122–125). Previous studies have shown neuronal upregulation of key antiviral effector molecules and other ISGs in response to neurotropic virus infection, but the neurons produce a limited amount of IFN and express fewer ISGs compared with microglia (126). Delhaye et al. identified approximately 16% of IFN-producing cells corresponding to neurons, but only 3% of infected neurons produced IFN after infecting mice with two neurotropic viruses that primarily infect neurons (La Crosse virus and Theiler virus) (122). ISGs suppress viral replication by directly interrupting the viral life cycle or by stimulating the production of antiviral factors in infected and adjacent cells, but the effects vary considerably in different regions of the brain (127). Further studies have shown that the induction and response to ISGs vary considerably in diverse neuronal populations. In transgenic mice expressing IFN, the expression of typical IFN response marker MX1 was higher in CA1 and CA2 neurons in comparison with CA3 neurons in the hippocampal region (118). Lucas et al. discovered that the IFN-α-inducible protein 27 like 2A (*Ifi27l2a*), which is upregulated in the cerebellum, brainstem, and spinal cord after WNV infection, limits viral infection in these regions but not in other neurons and cells, implying that *Ifi27l2a* contributes to WNV innate immune restriction in certain cell types and tissue-specific manner (76). Furthermore, following LGTV infection in the CNS, the activity of viperin, an interferon-inducible protein that inhibits replication, effectively limits LGTV replication in the OB and brain but does not inhibit virus replication in the cerebellum (128). Viperin also reduced TBEV replication in primary cortical neurons and astrocytes *in vitro*, but not in cerebellar granule cell neurons (61).

Mutations in human TLR3 are essential in the development of human HSV-1 encephalitis (129–131). TLR3 deficiency impairs the cell-autonomous defense of IPSC-derived cortical neurons and oligodendrocytes against HSV-1 infection, but not that of trigeminal ganglion (TG) neurons, owing to TLR3 control of ISG mRNA expression levels induced in human pluripotent stem cell-derived cortical neurons but not TG neurons (132–134). It has also been reported that neurons at different developmental stages express different levels of ISGs in response to viral infection. During LACV-infected encephalitis, both LACV-infected neural precursor cells and mature neurons undergo apoptosis, but neuronal maturation increases the susceptibility of neurons to LACV-induced apoptosis because mature neurons express less ISGs compared to neural precursor cells (135). Unlike the CNS, the antiviral response of peripheral neurons, such as the dorsal root ganglion (DRG), is more dependent on the dual action of antiviral ISGs and autophagy activation. DRG produces only a small number of type I IFNs and does not effectively induce the production of ISGs (136).

Oligodendrocytes

Oligodendrocytes have been shown to be less responsive to IFN in comparison with microglia (137). Mouse oligodendrocytes have lower basal expression levels of PRRs, IFN-α/β, ISGs, and kinases and transcription factors essential for IFN-α/β signaling and displayed a later expression of ISGs by comparison to microglia. Despite the fact that infection increases the expression of ISGs in both cell types, oligodendrocytes have a more limited expression profile and absolute mRNA levels compared with microglia. This limited antiviral response is associated with the inability to upregulate IκB kinase (IkappaB kinase or IKK) and IRF7 transcripts, both of which are required for amplification of the IFN-α/β response (138).

Expression of ISGs in neurological diseases

ISGs in neuroinflammation-related diseases

Upregulation of ISGs is associated with neuroinflammation-related diseases, including neuroinflammatory diseases such as multiple sclerosis (MS) (62) and neurodegenerative diseases such as AD (46), PD (139), and ALS (54). MS patients have elevated concentrations of the bile acid precursor 25-hydroxycholesterol (25-HC) in the cerebrospinal fluid (CSF), possibly as a result of the upregulation of the ISG CH25H in macrophages (62). 25-HC is mainly synthesized from cholesterol by CH25H, and has been shown to modulate inflammatory response and oxidative stress in normal or pathological nervous systems (140, 141). Wang et al. reported that ISG15 positively correlated with the degree of neuronal damage in an animal model of ALS with no obvious signs of inflammation, a model of cerebral ischemia, a model of brain injury induced by cortical shocks, and a mouse model of chronic neuronal damage induced by the viral protein HIV gp120, with high and significantly elevated ISG15 levels in areas of

neuronal damage (54). This suggests that ISG15 may be a reliable biomarker of pathological changes in the CNS (54). Mutations in the ATM gene contribute to ataxia capillaries (A-T), a rare neurodegenerative and immunodeficiency disorder characterized by cerebellar ataxia capillaris, immunodeficiency, radiosensitivity, and cancer susceptibility. Studies have shown that in A-T, the level of ISG15 is significantly higher in the cerebellum than in the brain (55). In glucosylceramidase1 (GBA1) deficient mice (which causes Parkinson's disease alpha-synuclein pathology), IFN-β levels are elevated in neurons, and ISGs are elevated in microglia (139). IFP35 is significantly upregulated in patients with untreated MS, demonstrating that IFP35 expression levels predict disease outcome and treatment response in MS (77). TLR3, which is primarily activated in innate immunity due to viral infection and induces the production of downstream ISGs (142), has also been found to be activated in alcohol-induced brain injury (143, 144). McDonough et al. reported TLR4-dependent upregulation of ISGs in ischemia/reperfusion-induced microglia (145). Meanwhile, in an AD model, activated microglia express ISGs, and the microglia are centered around amyloid-β (Aβ) plaques and accumulate in an age-dependent manner (46). Intracerebral injection of recombinant IFN-β activated microglia and eliminated complement C3-dependent synapses. Conversely, selective IFN receptor blockade effectively reduced ongoing microglia proliferation and synapse loss in AD models, demonstrating that ISGs are associated with a reduction in synapses (46). Aicardi-Gtières syndrome (AGS) is a severe inflammatory disease mimicking congenital infection with significant IFN production, characterized by chronic CSF lymphocytosis and elevated IFN-α levels, which can lead to severe neurodevelopmental disorders, spastic dystonia, and abnormal tetraplegia (146). ISGs, such as ISG15, viperin, and IFI27, are consistently elevated in patients with AGS, and these elevated ISGs are highly correlated with disease onset and progression (57). Mutations in adenosine deaminase (ADAR1) are crucial mechanisms for the development of AGS. In ADAR1-mutant mice, the expression of ISGs in neurons and microglia is selectively activated in a patchy manner, and the expression of *Isg15* in brain neurons with ADAR1 mutation is upregulated (147). It has also been reported that conditional deletion of ADAR1, specifically in mouse neural spinal cells, leads to overall peripheral nerve depigmentation and myelin loss, and that upregulation of ISGs precedes these defects, suggesting that ISGs may be involved in the production of such defects (148). Collectively, these studies have, in part, revealed a complex relationship between the IFN signaling pathway and neuroinflammation-related diseases.

ISGs in neuropsychiatric disorders

In recent years, evidence has accumulated to show that ISGs play an important role in psychiatric symptoms caused by CNS disorders. Studies have shown an intrinsic link between type I IFN therapy and severe neuropsychiatric disorders, mainly major depression (149). Considerable evidence suggests that type I IFN is associated with psychiatric disorders, and that the production of type I IFNs as a result of TLR4 induced IRF3 activation and TLR7 induced IRF7 activation may be closely associated with IFN-mediated psychiatric disorders (93). Infant onset of RNaseT2-deficient leukoencephalopathy leads to cystic brain injury, multifocal white matter changes, brain atrophy, and severe psychomotor impairment. *Rnaset2*$^{-/-}$ mice exhibit upregulation of ISGs and IFNAR-I-dependent neuroinflammation (150). HIV-associated neurocognitive disorders (HAND) also show an upregulation of ISG15 (151). In addition, ISGs may be involved in neuronal and synaptic regulation. The upregulation of inflammatory cytokines induced by maternal immune activation (MIA) promotes ISG15 expression in the offspring's brain, leading to neuronal dendritic lesions and depression-like behavior (56). In the hippocampus, ISG15 and Ubiquitin-specific peptidase 18 (USP18) mediate IFN-α-induced reduction in neurogenesis through upregulation of ISGylation-associated proteins UBA7, UBE2L6, and HERC5 (152). Adolescent mice injected with the viral mimic poly I:C had significantly increased expression of ISGs (IFIT2, PRKR, MX2, and IRF7) in the hippocampal dentate gyrus and exhibited behavioral deficits of impulse inhibition and impaired recognition of novel objects (58). In summary, upregulation of ISGs in the CNS may regulate various cellular functions and processes, such as neuronal survival and synaptic pruning, in a brain region-dependent manner (94).

The roles of individual ISGs in CNS viral infections or neurological diseases

To date, type I IFNs remain the most potent, broad-spectrum antiviral agents. The treatment of IFN to cells induces a large set of ISGs that can prevent infection with many viral pathogens. There are currently more than 300 recognized ISGs, but the exact mechanisms of inhibiting virus replication have been identified only in a small subset of ISGs. Detailed mechanistic investigation of the functions of individual ISGs is complicated by the difficulty in dissecting particular processes in virus replication independently of one another. The responses of individual ISGs to different viral infections in different organs may also vary, and there are limited in-depth studies on the effects of individual ISGs on the nervous system. With continuous research in this field, the role of ISGs and their mechanisms are being elucidated. The following subsections summarize several representative ISGs found in viral infections and neurological diseases in recent years.

10.3389/fimmu.2022.1008072

ISG15 and ISGylation for the regulation of neurological diseases

As mentioned above, Wang et al. found that ISG15 positively correlated with the degree of neuronal injury in animal models of ALS with no obvious signs of inflammation, a model cerebral ischemia, a model of cortical shock-induced brain injury, and a mouse model of chronic neuronal injury caused by the viral protein HIV gp120, with low levels of ISG15 in unaffected areas and high levels of ISG15 in neuronal injury areas. In patients with ALS, elevated levels of ISG15 and ISGylation in the CSF were significantly higher in post-traumatic brain injury ALS compared with those in non-traumatic brain injury ALS (53). It is suggested that ISG15 may be a reliable biomarker of pathological changes in the CNS (54). In cells with mutations in ATM kinase, conjugated ISG15, but not the free form, antagonizes targeted degradation of the ubiquitin pathway, which may lead to progressive neurodegeneration in A-T patients (153). C-Type Lectin Domain Containing 16A (CLEC16A) has been shown to function in autophagy/mitochondrial autophagy and Clec16 knockdown leads to an inflammatory neurodegenerative phenotype similar to spinal cerebellar ataxia in mice. In the whole-body inducible knockout of Clec16a mice model, Clec16a expression was negatively correlated with IGS15 expression, and the expression of ISG15 in neuronal tissues was upregulated, suggesting that ISG15 may be a link between Clec16a and downstream autoimmune inflammatory processes (154). ISG15 binds to a number of key proteins and affects various pathophysiological processes in the CNS. After traumatic brain injury, ISG15 is rapidly elevated and binds covalently to myosin light chain kinase (MLCK), which may promote phosphorylation of the myosin light chain by MLCK and conversion of F-actin to stress actin, which is involved in BBB destruction by disrupting TJs, thus aggravating brain edema (155). IFN-β inhibits the MAPK signaling pathway and attenuates mechanical nociceptive hyperalgesia by elevating both free and conjugated ISG15, an effect that is increased in *ubp43*$^{-/-}$ mice lacking the key de-binding enzyme (156). Upregulation of MIA-induced inflammatory cytokines promotes ISG15 expression in the offspring brain, leading to neuronal dendritic lesions and depressive-like behavior through a mechanism of ISG15 inhibiting the ubiquitination of Rap2A by NEDD4 (an E3 ubiquitin ligase that ubiquitously inhibits Rap2A activity, leading to dendritic growth and depoliticization), thus inducing Rap2A accumulation (56). In contrast, upregulation of NEDD4 abolishes ISG15-induced dendritic damage (56). In a model of acute inflammation established by LPS-stimulated microglia, increased ISGylation maintained the stability of STAT1 and promoted a sustained immune response during inflammation (157).

IFIT2 specifically limits neurological viral infections

Interferon-induced proteins with tetratricopeptide repeats (IFIT) are prominent ISGs, induced following type I IFN- or IRF3-dependent signaling, contribute to the antiviral defense of cells by binding directly to viral RNA or by binding to eukaryotic initiation factor 3 (eIF3) and preventing eIF3 from initiating the viral translational process (158). The human IFIT gene family generally consists of four members: IFIT1, IFIT2 (ISG54, p54), IFIT3 (ISG60, p60), and IFIT5 (ISG58, p58), whereas the mouse IFIT gene family encodes for three relevant genes: IFIT1, IFIT2 and IFIT3 (ISG49, p49), which are induced during IFN signaling pathway, viral infection or other PAMP recognition and have critical roles in host antiviral defense (159, 160). IFIT1 had an antiviral effect in human cytomegalovirus (HCMV)-infected human astrocytes isolated from the fetal brain, but not in HELFs (human embryonic lung fibroblast cells) (69). Recent studies have shown that IFIT2 primarily limits viral infection and protects mice from severe morbidity and mortality following infection with RABV (75), lethal VSV (67, 70), WNV (71), and Sendai virus (SeV) (72). IFIT2 acts as an antiviral in the CNS in several ways. Both VSV and EMCV infections cause neuroinvasive disease and induce IFN-β, IFIT1, and IFIT2 in the brain. However, IFIT2 only prevents VSV invasion of the brain and not EMCV invasion of the brain, suggesting that the antiviral response of IFIT2 in the CNS is virus-specific (67). In ***Ifit2***$^{-/-}$ mice, effective VSV viral replication was restricted to the brain, and the absence of IFIT2 did not affect viral titers in other organs such as the liver or lungs, suggesting that IFIT2 can limit VSV invasion of the nervous system (67). In WNV-infected CNS, viral titers were higher in ***Ifit2***$^{-/-}$ mice compared with those in WT mice only in the OB, cerebral cortex, brainstem, cerebellum, and spinal cord, and in cells with knockdown of IFIT2, increased WNV infection was observed only in cerebellar granule cells and dendritic cells, but not in macrophages, fibroblasts, or cortical neurons (71). Overall, these data suggest that IFIT2 has a crucial role in limiting viral infection in specific regions of the brain and in specific cell types. In experiments with RABV infection of the CNS, IFIT2 exerted antiviral effects predominantly at the level of viral replication and not as a mechanism to restrict viral entry/exit or transport of RABV particles *via* axons (75). Furthermore, IFIT2 can be involved in antiviral response by inducing and enhancing innate immunity. In neurotropic coronavirus MHV-RSA59 infection, IFIT2 promoted viral clearance by facilitating microglia activation and recruitment of NK1.1 and CD4 T cells to the brain (73). Further studies have shown that IFIT2 and IFIT3 function in a complementary and synergistic manner to restrict RABV in mouse-derived neuroblastoma cells (74). In MHV-induced encephalitis, IFIT2 is a positive regulator of IFNα/β expression rather than a direct antiviral mediator, with *Ifit2*$^{-/-}$

mice showing significantly reduced expression of IFN-α/β and the downstream ISG mRNAs (*Ifit1, Isg15, and Pkr*) (52).

The role of IFITM3 in CNS infection and Alzheimer's disease

The IFN-inducible transmembrane proteins (IFITMs) form a small family of IFN-inducible proteins and have two transmembrane structural domains. The IFITMs were shown to inhibit the cellular entry step of many enveloped viruses such as influenza A, dengue, Ebola, and SARS coronavirus (161). The human IFITM family consists of four proteins, IFITM1, IFITM2, IFITM3 and IFITM5, located on chromosome 11, among them IFITM1, IFITM2 and IFITM3 are well-known ISG proteins (162). IFITMs disrupt the entry of multiple enveloped viruses, and play a role in the transport of viral particles to lysosomes for degradation (163). SARS-CoV-2 infection was recently shown to increase IFITM3 protein expression (63), and in severe SARS-CoV-2 cases, IFITM3 levels are elevated in the frontal cortex and choroid plexus (65). IFITM3 may prevent pathogenesis by limiting early replication and transmission of α-virus in the brain and spinal cord (164). In patients with Rasmussen encephalitis (RE) caused by infection with HCMV viruses, IFITM3 was detected in the neurons of brain tissue, and there was colocalization of HCMV and IFITM3, suggesting that HCMV infection may induce IFITM3 expression in neurons and that IFITM3 can effectively inhibit HCMV infection and participate in the immune response to HCMV infection in RE brain tissue (64). Further studies found that the IFITM3 single nucleotide polymorphism (SNP) rs12252 correlated with the severity of disease caused by viral infection (165–167). The rs12252-C mutant protein IFITM3 ND21 was not flexible enough to effectively prevent the fusion of the virus with the endocytic membrane, which in turn reduced the ability of the immune system to defend against viral infection. Wang et al. found that subjects carrying IFITM3 rs12252 CC genotype were at increased risk of developing RE and were associated with rapid progression of RE disease (64). In addition, the rs12252-C allele was recently reported to be associated with disease severity in patients with SARS-CoV-2 (168). In conclusion, the IFITM3 rs12252-C allele is strongly associated with the severity of some viral infectious diseases (169).

IFITM3 mRNA expression in the cortex and hippocampus is significantly positively correlated with age (ranging from 20 years to 70 years) in humans, according to genotype-tissue expression cohorts (66). IFITM3 protein levels, Aβ production (Aβ42 and Aβ40), and the amount of active IFITM3-γ-secretase were increased in the aging WT mouse brains (66). IFITM3 expression is upregulated in astrocytes and microglia in the brains of the 5xFAD Alzheimer's disease mouse model, and IFITM3 mRNA and IFITM3 protein are expressed in neurons (66). Pro-inflammatory cytokines (IFN-α or IFN-γ, IL-6, and IL-1β) increase Aβ production in neurons and astrocytes by increasing the formation of IFITM3 protein and active IFITM3-γ-secretase complexes (66). Recently, SARS-CoV-2 has been reported to increase IFITM3 protein (63), and IFITM3 levels are elevated in the frontal cortex and choroid plexus in severe SARS-CoV-2 cases (65). Hur et al. concluded that different inflammatory conditions, such as viral infection and aging, can induce the release of pro-inflammatory cytokines from astrocytes and microglia, which in turn elevate the expression of IFITM3 in neurons and astrocytes, and IFITM3 binds to active γ-secretase complexes, increasing Aβ production and increasing the risk of AD (66).

Conclusion

This review highlights the ISGs involved in resisting the neurotropic viral invasion of the CNS and the mode of activation of these ISGs in viral-infected CNS cells. Furthermore, the expression characteristics of ISGs in the development of CNS disorders are discussed. At last, we summarize in detail several mechanisms of action of individual ISGs in the CNS that have been more studied in recent years. The IFN signal pathways induce hundreds of ISGs to exert antiviral and other physiopathological effects. ISGs are a large family, and many more are still waiting to be identified. Most studies have focused on ISG as a marker of activation of the innate immune response to IFN, whereas the mechanisms of ISG in the pathophysiological response of the CNS remain unclear and need to be investigated in depth. Thus this review summarizes the current research on ISGs in CNS and indicates possible directions for future research. With the development of technologies such as CRISPR-Cas9 gene editing as well as genome-wide RNA-seq and deep proteomics (170), research on the antiviral effects of individual ISG, as well as its other functions in CNS diseases, is expected to evolve rapidly. An improved understanding of the functions of individual ISGs will facilitate the development of ISG-based therapies. Consequently, ISGs may exhibit promise as potential clinical biomarkers as well as therapeutic targets.

Author contributions

RL, YY, CB, and WD conceived the perspective of the work. RL, HL, YY, CB, and WD drafted the manuscript. HL, XL, and CL designed the figure. YZ, SG and JX assisted in collecting and organizing the literature. All authors revised and approved the final version of the manuscript. All authors contributed to the article and approved the submitted version.

Funding

This work was supported by the National Natural Science Foundation of China (31871031, 32170968, WD), the Fund of

Key Laboratory of Medical Electrophysiology in 2021 (KeyME-2021-01, YY), and China Postdoctoral Science Foundation (2021M692700, YY).

Conflict of interest

The authors declare that the research was conducted in the absence of any commercial or financial relationships that could be construed as a potential conflict of interest.

Publisher's note

References

1. Zhou J-H, Wang Y-N, Chang Q-Y, Ma P, Hu Y, Cao X. Type III interferons in viral infection and antiviral immunity. *Cell Physiol Biochem Int J Exp Cell Physiol Biochem Pharmacol* (2018) 51:173–85. doi: 10.1159/000495172

2. Lazear HM, Schoggins JW, Diamond MS. Shared and distinct functions of type I and type III interferons. *Immunity* (2019) 50:907–23. doi: 10.1016/j.immuni.2019.03.025

3. Parker BS, Rautela J, Hertzog PJ. Antitumour actions of interferons: implications for cancer therapy. *Nat Rev Cancer* (2016) 16:131–44. doi: 10.1038/nrc.2016.14

4. Sprooten J, Agostinis P, Garg AD. Type I interferons and dendritic cells in cancer immunotherapy. *Int Rev Cell Mol Biol* (2019) 348:217–62. doi: 10.1016/bs.ircmb.2019.06.001

5. Pestka S, Krause CD, Walter MR. Interferons, interferon-like cytokines, and their receptors. *Immunol Rev* (2004) 202:8–32. doi: 10.1111/j.0105-2896.2004.00204.x

6. Oritani K, Kanakura Y. IFN-? limitin: a member of type I IFN with mild lympho-myelosuppression. *J Cell Mol Med* (2005) 9:244–54. doi: 10.1111/j.1582-4934.2005.tb00353.x

7. Schoggins JW. Recent advances in antiviral interferon-stimulated gene biology. *F1000Research* (2018) 7:309. doi: 10.12688/f1000research.12450.1

8. Wells AI, Coyne CB. Type III interferons in antiviral defenses at barrier surfaces. *Trends Immunol* (2018) 39:848–58. doi: 10.1016/j.it.2018.08.008

9. Kang S, Brown HM, Hwang S. Direct antiviral mechanisms of interferon-gamma. *Immune Netw* (2018) 18:e33. doi: 10.4110/in.2018.18.e33

10. Billiau A, Matthys P. Interferon-γ: A historical perspective. *Cytokine Amp Growth Factor Rev* (2009) 20:97–113. doi: 10.1016/j.cytogfr.2009.02.004

11. Lazear HM, Nice TJ, Diamond MS. Interferon-λ: Immune functions at barrier surfaces and beyond. *Immunity* (2015) 43:15–28. doi: 10.1016/j.immuni.2015.07.001

12. Schneider WM, Chevillotte MD, Rice CM. Interferon-stimulated genes: a complex web of host defenses. *Annu Rev Immunol* (2014) 32:513–45. doi: 10.1146/annurev-immunol-032713-120231

13. Schoggins JW, Rice CM. Interferon-stimulated genes and their antiviral effector functions. *Curr Opin Virol* (2011) 1:519–25. doi: 10.1016/j.coviro.2011.10.008

14. Odendall C, Kagan JC. The unique regulation and functions of type III interferons in antiviral immunity. *Curr Opin Virol* (2015) 12:47–52. doi: 10.1016/j.coviro.2015.02.003

15. Stark GR, Darnell JEJ. The JAK-STAT pathway at twenty. *Immunity* (2012) 36:503–14. doi: 10.1016/j.immuni.2012.03.013

16. Ivashkiv LB, Donlin LT. Regulation of type I interferon responses. *Nat Rev Immunol* (2014) 14:36–49. doi: 10.1038/nri3581

17. Haque SJ, Williams BR. Identification and characterization of an interferon (IFN)-stimulated response element-IFN-stimulated gene factor 3-independent signaling pathway for IFN-alpha. *J Biol Chem* (1994) 269:19523–9. doi: 10.1016/S0021-9258(17)32200-7

18. Au-Yeung N, Horvath CM. Transcriptional and chromatin regulation in interferon and innate antiviral gene expression. *Cytokine Growth Factor Rev* (2018) 44:11–7. doi: 10.1016/j.cytogfr.2018.10.003

19. Platanitis E, Decker T. Regulatory networks involving STATs, IRFs, and NFκB in inflammation. *Front Immunol* (2018) 9:2542. doi: 10.3389/fimmu.2018.02542

20. Orzalli MH, Smith A, Jurado KA, Iwasaki A, Garlick JA, Kagan JC. An antiviral branch of the IL-1 signaling pathway restricts immune-evasive virus replication. *Mol Cell* (2018) 71:825–40.e6. doi: 10.1016/j.molcel.2018.07.009

21. Rubio D, Xu R-H, Remakus S, Krouse TE, Truckenmiller ME, Thapa RJ, et al. Crosstalk between the type 1 interferon and nuclear factor kappa b pathways confers resistance to a lethal virus infection. *Cell Host Microbe* (2013) 13:701–10. doi: 10.1016/j.chom.2013.04.015

22. Green R, Ireton RC, Gale MJ. Interferon-stimulated genes: new platforms and computational approaches. *Mamm Genome Off J Int Mamm Genome Soc* (2018) 29:593–602. doi: 10.1007/s00335-018-9755-6

23. Wang W, Xu L, Su J, Peppelenbosch MP, Pan Q. Transcriptional regulation of antiviral interferon-stimulated genes. *Trends Microbiol* (2017) 25:573–84. doi: 10.1016/j.tim.2017.01.001

24. Klotz D, Gerhauser I. Interferon-stimulated genes-mediators of the innate immune response during canine distemper virus infection. *Int J Mol Sci* (2019) 20:1620. doi: 10.3390/ijms20071620

25. Marié I, Durbin JE, Levy DE. Differential viral induction of distinct interferon-alpha genes by positive feedback through interferon regulatory factor-7. *EMBO J* (1998) 17:6660–9. doi: 10.1093/emboj/17.22.6660

26. Fujita T, Reis LF, Watanabe N, Kimura Y, Taniguchi T, Vilcek J. Induction of the transcription factor IRF-1 and interferon-beta mRNAs by cytokines and activators of second-messenger pathways. *Proc Natl Acad Sci USA* (1989) 86:9936–40. doi: 10.1073/pnas.86.24.9936

27. Goubau D, Deddouche S, Reis e Sousa C. Cytosolic sensing of viruses. *Immunity* (2013) 38:855–69. doi: 10.1016/j.immuni.2013.05.007

28. Sadler AJ, Williams BRG. Interferon-inducible antiviral effectors. *Nat Rev Immunol* (2008) 8:559–68. doi: 10.1038/nri2314

29. Takeuchi O, Akira S. Pattern recognition receptors and inflammation. *Cell* (2010) 140:805–20. doi: 10.1016/j.cell.2010.01.022

30. Imaizumi T, Numata A, Yano C, Yoshida H, Meng P, Hayakari R, et al. ISG54 and ISG56 are induced by TLR3 signaling in U373MG human astrocytoma cells: possible involvement in CXCL10 expression. *Neurosci Res* (2014) 84:34–42. doi: 10.1016/j.neures.2014.03.001

31. Kim M-J, Hwang S-Y, Imaizumi T, Yoo J-Y. Negative feedback regulation of RIG-I-Mediated antiviral signaling by interferon-induced ISG15 conjugation. *J Virol* (2008) 82:1474–83. doi: 10.1128/JVI.01650-07

32. Du Y, Duan T, Feng Y, Liu Q, Lin M, Cui J, et al. LRRC25 inhibits type I IFN signaling by targeting ISG15-associated RIG-I for autophagic degradation. *EMBO J* (2018) 37:351–66. doi: 10.15252/embj.201796781

33. McGavern DB, Kang SS. Illuminating viral infections in the nervous system. *Nat Rev Immunol* (2011) 11:318–29. doi: 10.1038/nri2971

34. Kochs G, Bauer S, Vogt C, Frenz T, Tschopp J, Kalinke U, et al. Thogoto virus infection induces sustained type I interferon responses that depend on RIG-I-Like helicase signaling of conventional dendritic cells. *J Virol* (2010) 84:12344–50. doi: 10.1128/JVI.00931-10

35. Mrkic B, Pavlovic J, Rülicke T, Volpe P, Buchholz CJ, Hourcade D, et al. Measles virus spread and pathogenesis in genetically modified mice. *J Virol* (1998) 72:7420–7. doi: 10.1128/JVI.72.9.7420-7427.1998

36. Dhondt KP, Mathieu C, Chalons M, Reynaud JM, Vallve A, Raoul H, et al. Type I interferon signaling protects mice from lethal henipavirus infection. *J Infect Dis* (2013) 207:142–51. doi: 10.1093/infdis/jis653

37. Ryman KD, Klimstra WB, Nguyen KB, Biron CA, Johnston RE. Alpha/Beta interferon protects adult mice from fatal sindbis virus infection and is an important

determinant of cell and tissue tropism. *J Virol* (2000) 74:3366–78. doi: 10.1128/JVI.74.7.3366-3378.2000

38. Casrouge A, Zhang S-Y, Eidenschenk C, Jouanguy E, Puel A, Yang K, et al. Herpes simplex virus encephalitis in human UNC-93B deficiency. *Science* (2006) 314:308–12. doi: 10.1126/science.1128346

39. Herman M, Ciancanelli M, Ou Y-H, Lorenzo L, Klaudel-Dreszler M, Pauwels E, et al. Heterozygous TBK1 mutations impair TLR3 immunity and underlie herpes simplex encephalitis of childhood. *J Exp Med* (2012) 209:1567–82. doi: 10.1084/jem.20111316

40. Pérez de Diego R, Sancho-Shimizu V, Lorenzo L, Puel A, Plancoulaine S, Picard C, et al. Human TRAF3 adaptor molecule deficiency leads to impaired toll-like receptor 3 response and susceptibility to herpes simplex encephalitis. *Immunity* (2010) 33:400–11. doi: 10.1016/j.immuni.2010.08.014

41. Sancho-Shimizu V, Pérez de Diego R, Lorenzo L, Halwani R, Alangari A, Israelsson E, et al. Herpes simplex encephalitis in children with autosomal recessive and dominant TRIF deficiency. *J Clin Invest* (2011) 121:4889–902. doi: 10.1172/JCI59259

42. Ma C, Li S, Hu Y, Ma Y, Wu Y, Wu C, et al. AIM2 controls microglial inflammation to prevent experimental autoimmune encephalomyelitis. *J Exp Med* (2021) 218:e20201796. doi: 10.1084/jem.20201796

43. Ejlerskov P, Hultberg JG, Wang J, Carlsson R, Ambjørn M, Kuss M, et al. Lack of neuronal IFN-β-IFNAR causes lewy body- and parkinson's disease-like dementia. *Cell* (2015) 163:324–39. doi: 10.1016/j.cell.2015.08.069

44. Sliter DA, Martinez J, Hao L, Chen X, Sun N, Fischer TD, et al. Parkin and PINK1 mitigate STING-induced inflammation. *Nature* (2018) 561:258–62. doi: 10.1038/s41586-018-0448-9

45. McCauley ME, O'Rourke JG, Yáñez A, Markman JL, Ho R, Wang X, et al. C9orf72 in myeloid cells suppresses STING-induced inflammation. *Nature* (2020) 585:96–101. doi: 10.1038/s41586-020-2625-x

46. Roy ER, Wang B, Wan Y-W, Chiu G, Cole A, Yin Z, et al. Type I interferon response drives neuroinflammation and synapse loss in Alzheimer disease. *J Clin Invest* (2020) 130:1912–30. doi: 10.1172/JCI133737

47. Baik SH, Kang S, Lee W, Choi H, Chung S, Kim J-I, et al. A breakdown in metabolic reprogramming causes microglia dysfunction in alzheimer's disease. *Cell Metab* (2019) 30:493–507.e6. doi: 10.1016/j.cmet.2019.06.005

48. Magusali N, Graham AC, Piers TM, Panichnantakul P, Yaman U, Shoai M, et al. A genetic link between risk for alzheimer's disease and severe COVID-19 outcomes *via* the *OAS1* gene. *Brain* (2021) 144:3727–41. doi: 10.1093/brain/awab337

49. Li L, Ulrich R, Baumgärtner W, Gerhauser I. Interferon-stimulated genes-essential antiviral effectors implicated in resistance to theiler's virus-induced demyelinating disease. *J Neuroinflamm* (2015) 12:242. doi: 10.1186/s12974-015-0462-x

50. Sun L, Wang X, Zhou Y, Zhou R-H, Ho W-Z, Li J-L. Exosomes contribute to the transmission of anti-HIV activity from TLR3-activated brain microvascular endothelial cells to macrophages. *Antiviral Res* (2016) 134:167–71. doi: 10.1016/j.antiviral.2016.07.013

51. Liu H, Zhou R-H, Liu Y, Guo L, Wang X, Hu W-H, et al. HIV Infection suppresses TLR3 activation-mediated antiviral immunity in microglia and macrophages. *Immunology* (2020) 160:269–79. doi: 10.1111/imm.13181

52. Butchi NB, Hinton DR, Stohlman SA, Kapil P, Fensterl V, Sen GC, et al. Ifit2 deficiency results in uncontrolled neurotropic coronavirus replication and enhanced encephalitis *via* impaired alpha/beta interferon induction in macrophages. *J Virol* (2014) 88:1051–64. doi: 10.1128/JVI.02272-13

53. Schwartzenburg J, Juncker M, Reed R, Desai S. Increased ISGylation in cases of TBI-exposed ALS veterans. *J Neuropathol Exp Neurol* (2019) 78:209–18. doi: 10.1093/jnen/nly129

54. Wang R-G, Kaul M, Zhang D-X. Interferon-stimulated gene 15 as a general marker for acute and chronic neuronal injuries. *Sheng Li Xue Bao* (2012) 64:577–83.

55. Kim CD, Reed RE, Juncker MA, Fang Z, Desai SD. Evidence for the deregulation of protein turnover pathways in atm-deficient mouse cerebellum: An organotypic study. *J Neuropathol Exp Neurol* (2017) 76:578–84. doi: 10.1093/jnen/nlx038

56. Hu Y, Hong X-Y, Yang X-F, Ma R-H, Wang X, Zhang J-F, et al. Inflammation-dependent ISG15 upregulation mediates MIA-induced dendrite damages and depression by disrupting NEDD4/Rap2A signaling. *Biochim Biophys Acta Mol Basis Dis* (2019) 1865:1477–89. doi: 10.1016/j.bbadis.2019.02.020

57. Wang BX, Grover SA, Kannu P, Yoon G, Laxer RM, Yeh EA, et al. Interferon-stimulated gene expression as a preferred biomarker for disease activity in aicardi-goutières syndrome. *J Interferon Cytokine Res Off J Int Soc Interferon Cytokine Res* (2017) 37:147–52. doi: 10.1089/jir.2016.0117

58. Lukasz B, O'Sullivan NC, Loscher JS, Pickering M, Regan CM, Murphy KJ. Peripubertal viral-like challenge and social isolation mediate overlapping but distinct effects on behaviour and brain interferon regulatory factor 7 expression in the adult wistar rat. *Brain Behav Immun* (2013) 27:71–9. doi: 10.1016/j.bbi.2012.09.011

59. Bansode YD, Chattopadhyay D, Saha B. Transcriptomic analysis of interferon response in toll-like receptor 2 ligand-treated and herpes simplex virus 1-infected neurons and astrocytes. *Viral Immunol* (2021) 34:256–66. doi: 10.1089/vim.2020.0238

60. Marshall C, Clark ZT, Minckler MR. Aseptic viral meningitis secondary to herpes simplex virus 2 genital infection. *Cureus* (2021) 13:14535. doi: 10.7759/cureus.14535

61. Lindqvist R, Kurhade C, Gilthorpe JD, Överby AK. Cell-type- and region-specific restriction of neurotropic flavivirus infection by viperin. *J Neuroinflamm* (2018) 15:80. doi: 10.1186/s12974-018-1119-3

62. Crick PJ, Griffiths WJ, Zhang J, Beibel M, Abdel-Khalik J, Kuhle J, et al. Reduced plasma levels of 25-hydroxycholesterol and increased cerebrospinal fluid levels of bile acid precursors in multiple sclerosis patients. *Mol Neurobiol* (2017) 54:8009–20. doi: 10.1007/s12035-016-0281-9

63. Hachim MY, Al Heialy S, Hachim IY, Halwani R, Senok AC, Maghazachi AA, et al. Interferon-induced transmembrane protein (IFITM3) is upregulated explicitly in SARS-CoV-2 infected lung epithelial cells. *Front Immunol* (2020) 11:1372. doi: 10.3389/fimmu.2020.01372

64. Wang Y-S, Luo Q-L, Guan Y-G, Fan D-Y, Luan G-M, Jing A. HCMV infection and IFITM3 rs12252 are associated with rasmussen's encephalitis disease progression. *Ann Clin Transl Neurol* (2021) 8:558–70. doi: 10.1002/acn3.51289

65. Yang AC, Kern F, Losada PM, Agam MR, Maat CA, Schmartz GP, et al. Dysregulation of brain and choroid plexus cell types in severe COVID-19. *Nature* (2021) 595:565–71. doi: 10.1038/s41586-021-03710-0

66. Hur J-Y, Frost GR, Wu X, Crump C, Pan SJ, Wong E, et al. The innate immunity protein IFITM3 modulates γ-secretase in alzheimer's disease. *Nature* (2020) 586:735–40. doi: 10.1038/s41586-020-2681-2

67. Fensterl V, Wetzel JL, Ramachandran S, Ogino T, Stohlman SA, Bergmann CC, et al. Interferon-induced Ifit2/ISG54 protects mice from lethal VSV neuropathogenesis. *PloS Pathog* (2012) 8:13. doi: 10.1371/journal.ppat.1002712

68. Sharma N, Verma R, Kumawat KL, Basu A, Singh SK. miR-146a suppresses cellular immune response during Japanese encephalitis virus JaOArS982 strain infection in human microglial cells. *J Neuroinflamm* (2015) 12:30. doi: 10.1186/s12974-015-0249-0

69. Zhang L, Wang B, Li L, Qian D-M, Yu H, Xue M-L, et al. Antiviral effects of IFIT1 in human cytomegalovirus-infected fetal astrocytes. *J Med Virol* (2017) 89:672–84. doi: 10.1002/jmv.24674

70. Fensterl V, Wetzel JL, Sen GC. Interferon-induced protein Ifit2 protects mice from infection of the peripheral nervous system by vesicular stomatitis virus. *J Virol* (2014) 88:10303–11. doi: 10.1128/JVI.01341-14

71. Cho H, Shrestha B, Sen GC, Diamond MS. A role for Ifit2 in restricting West Nile virus infection in the brain. *J Virol* (2013) 87:8363–71. doi: 10.1128/JVI.01097-13

72. Wetzel JL, Fensterl V, Sen GC. Sendai Virus pathogenesis in mice is prevented by *Ifit2* and exacerbated by interferon. *J Virol* (2014) 88:13593–601. doi: 10.1128/JVI.02201-14

73. Das Sarma J, Burrows A, Rayman P, Hwang M-H, Kundu S, Sharma N, et al. Ifit2 deficiency restricts microglial activation and leukocyte migration following murine coronavirus (m-CoV) CNS infection. *PloS Pathog* (2020) 16:e1009034. doi: 10.1371/journal.ppat.1009034

74. Chai B, Tian D, Zhou M, Tian B, Yuan Y, Sui B, et al. Murine Ifit3 restricts the replication of rabies virus both *in vitro* and *in vivo*. *J Gen Virol* (2021) 102:001619. doi: 10.1099/jgv.0.001619

75. Davis BM, Fensterl V, Lawrence TM, Hudacek AW, Sen GC, Schnell MJ. Ifit2 is a restriction factor in rabies virus pathogenicity. *J Virol* (2017) 91:00889-17. doi: 10.1128/JVI.00889-17

76. Lucas TM, Richner JM, Diamond MS. The interferon-stimulated gene Ifi27l2a restricts West Nile virus infection and pathogenesis in a cell-type- and region-specific manner. *J Virol* (2015) 90:2600–15. doi: 10.1128/JVI.02463-15

77. De Masi R, Orlando S, Bagordo F, Grassi T. IFP35 is a relevant factor in innate immunity, multiple sclerosis, and other chronic inflammatory diseases: A review. *Biology* (2021) 10:1325. doi: 10.3390/biology10121325

78. Ransohoff RM, Brown MA. Innate immunity in the central nervous system. *J Clin Invest* (2012) 122:1164–71. doi: 10.1172/JCI58644

79. Li F, Wang Y, Yu L, Cao S, Wang K, Yuan J, et al. Viral infection of the central nervous system and neuroinflammation precede blood-brain barrier disruption during Japanese encephalitis virus infection. *J Virol* (2015) 89:5602–14. doi: 10.1128/JVI.00143-15

80. Chen Z, Li G. Immune response and blood-brain barrier dysfunction during viral neuroinvasion. *Innate Immun* (2021) 27:109–17. doi: 10.1177/1753425920954281

81. Mustafá YM, Meuren LM, Coelho SVA, de Arruda LB. Pathways exploited by flaviviruses to counteract the blood-brain barrier and invade the central nervous system. *Front Microbiol* (2019) 10:525. doi: 10.3389/fmicb.2019.00525

82. Lazear HM, Daniels BP, Pinto AK, Huang AC, Vick SC, Doyle SE, et al. Interferon-λ restricts West Nile virus neuroinvasion by tightening the blood-brain barrier. *Sci Transl Med* (2015) 7:284ra59. doi: 10.1126/scitranslmed.aaa4304

83. Li Y, Zhao L, Luo Z, Zhang Y, Lv L, Zhao J, et al. Interferon-λ attenuates rabies virus infection by inducing interferon-stimulated genes and alleviating neurological inflammation. *Viruses* (2020) 12:405. doi: 10.3390/v12040405

84. Dozio V, Sanchez J-C. Profiling the proteomic inflammatory state of human astrocytes using DIA mass spectrometry. *J Neuroinflamm* (2018) 15:331. doi: 10.1186/s12974-018-1371-6

85. Li J, Wang Y, Wang X, Ye L, Zhou Y, Persidsky Y, et al. Immune activation of human brain microvascular endothelial cells inhibits HIV replication in macrophages. *Blood* (2013) 121:2934–42. doi: 10.1182/blood-2012-08-450353

86. Kalinke U, Bechmann I, Detje CN. Host strategies against virus entry *via* the olfactory system. *Virulence* (2011) 2:367–70. doi: 10.4161/viru.2.4.16138

87. Singh H, Koury J, Kaul M. Innate immune sensing of viruses and its consequences for the central nervous system. *Viruses* (2021) 13:170. doi: 10.3390/v13020170

88. Iwasaki A. Immune regulation of antibody access to neuronal tissues. *Trends Mol Med* (2017) 23:227–45. doi: 10.1016/j.molmed.2017.01.004

89. Detje CN, Lienenklaus S, Chhatbar C, Spanier J, Prajeeth CK, Soldner C, et al. Upon intranasal vesicular stomatitis virus infection, astrocytes in the olfactory bulb are important interferon beta producers that protect from lethal encephalitis. *J Virol* (2015) 89:2731–8. doi: 10.1128/JVI.02044-14

90. van den Pol AN, Ding S, Robek MD. Long-distance interferon signaling within the brain blocks virus spread. *J Virol* (2014) 88:3695–704. doi: 10.1128/JVI.03509-13

91. Wheeler DL, Sariol A, Meyerholz DK, Perlman S. Microglia are required for protection against lethal coronavirus encephalitis in mice. *J Clin Invest* (2018) 128:931–43. doi: 10.1172/JCI97229

92. Trottier MD, Lyles DS, Reiss CS. Peripheral, but not central nervous system, type I interferon expression in mice in response to intranasal vesicular stomatitis virus infection. *J Neurovirol* (2007) 13:433–45. doi: 10.1080/13550280701460565

93. Thomson CA, McColl A, Cavanagh J, Graham GJ. Peripheral inflammation is associated with remote global gene expression changes in the brain. *J Neuroinflamm* (2014) 11:73. doi: 10.1186/1742-2094-11-73

94. Aw E, Zhang Y, Carroll M. Microglial responses to peripheral type 1 interferon. *J Neuroinflamm* (2020) 17:340. doi: 10.1186/s12974-020-02003-z

95. Sorgeloos F, Kreit M, Hermant P, Lardinois C, Michiels T. Antiviral type I and type III interferon responses in the central nervous system. *Viruses* (2013) 5:834–57. doi: 10.3390/v5030834

96. Butchi NB, Du M, Peterson KE. Interactions between TLR7 and TLR9 agonists and receptors regulate innate immune responses by astrocytes and microglia. *Glia* (2009) 58:650–64. doi: 10.1002/glia.20952

97. Carroll JA, Race B, Williams K, Striebel JF, Chesebro B. Innate immune responses after stimulation with toll-like receptor agonists in ex vivo microglial cultures and an *in vivo* model using mice with reduced microglia. *J Neuroinflamm* (2021) 18:194. doi: 10.1186/s12974-021-02240-w

98. He N, Qu Y-J, Li D-Y, Yue S-W. RIP3 inhibition ameliorates chronic constriction injury-induced neuropathic pain by suppressing JNK signaling. *Aging* (2021) 13:24417–31. doi: 10.18632/aging.203691

99. Huber AK, Duncker PC, Irani DN. Immune responses to non-tumor antigens in the central nervous system. *Front Oncol* (2014) 4:328. doi: 10.3389/fonc.2014.00328

100. Chen Z, Zhong D, Li G. The role of microglia in viral encephalitis: a review. *J Neuroinflamm* (2019) 16:76. doi: 10.1186/s12974-019-1443-2

101. Paludan SR. Activation and regulation of DNA-driven immune responses. *Microbiol Mol Biol Rev MMBR* (2015) 79:225–41. doi: 10.1128/MMBR.00061-14

102. Rodríguez AM, Rodríguez J, Giambartolomei GH. Microglia at the crossroads of pathogen-induced neuroinflammation. *ASN Neuro* (2022) 14:175909142211045. doi: 10.1177/17590914221104566

103. Stonedahl S, Leser JS, Clarke P, Tyler KL. Depletion of microglia in an *Ex vivo* brain slice culture model of West Nile virus infection leads to increased viral titers and cell death. *Microbiol Spectr* (2022) 10:e00685–22. doi: 10.1128/spectrum.00685-22

104. Fekete R, Cserép C, Lénárt N, Tóth K, Orsolits B, Martinecz B, et al. Microglia control the spread of neurotropic virus infection *via* P2Y12 signalling and recruit monocytes through P2Y12-independent mechanisms. *Acta Neuropathol (Berl)* (2018) 136:461–82. doi: 10.1007/s00401-018-1885-0

105. Drokhlyansky E, Göz Aytürk D, Soh TK, Chrenek R, O'Loughlin E, Madore C, et al. The brain parenchyma has a type I interferon response that can limit virus spread. *Proc Natl Acad Sci* (2017) 114:E95–104. doi: 10.1073/pnas.1618157114

106. Malikov V, Meade N, Simons LM, Hultquist JF, Naghavi MH. FEZ1 phosphorylation regulates HSPA8 localization and interferon-stimulated gene expression. *Cell Rep* (2022) 38:110396. doi: 10.1016/j.celrep.2022.110396

107. Simmons LJ, Surles-Zeigler MC, Li Y, Ford GD, Newman GD, Ford BD. Regulation of inflammatory responses by neuregulin-1 in brain ischemia and microglial cells *in vitro* involves the NF-kappa b pathway. *J Neuroinflamm* (2016) 13:237. doi: 10.1186/s12974-016-0703-7

108. Manangeeswaran M, Ireland DDC, Verthelyi D. Zika (PRVABC59) infection is associated with T cell infiltration and neurodegeneration in CNS of immunocompetent neonatal C57Bl/6 mice. *PloS Pathog* (2016) 12:e1006004. doi: 10.1371/journal.ppat.1006004

109. Bindocci E, Savtchouk I, Liaudet N, Becker D, Carriero G, Volterra A. Three-dimensional Ca^{2+} imaging advances understanding of astrocyte biology. *Science* (2017) 356:eaai8185. doi: 10.1126/science.aai8185

110. Yoon H, Walters G, Paulsen AR, Scarisbrick IA. Astrocyte heterogeneity across the brain and spinal cord occurs developmentally, in adulthood and in response to demyelination. *PloS One* (2017) 12:e0180697. doi: 10.1371/journal.pone.0180697

111. DePaula-Silva AB, Bell LA, Wallis GJ, Wilcox KS. Inflammation unleashed in viral-induced epileptogenesis. *Epilepsy Curr* (2021) 21:433–40. doi: 10.1177/15357597211040939

112. Garber C, Vasek MJ, Vollmer LL, Sun T, Jiang X, Klein RS. Astrocytes decrease adult neurogenesis during virus-induced memory dysfunction *via* IL-1. *Nat Immunol* (2018) 19:151–61. doi: 10.1038/s41590-017-0021-y

113. Liddelow SA, Guttenplan KA, Clarke LE, Bennett FC, Bohlen CJ, Schirmer L, et al. Neurotoxic reactive astrocytes are induced by activated microglia. *Nature* (2017) 541:481–7. doi: 10.1038/nature21029

114. Hwang M, Bergmann CC. Alpha/beta interferon (IFN-α/β) signaling in astrocytes mediates protection against viral encephalomyelitis and regulates IFN-γ-dependent responses. *J Virol* (2018) 92:01901-17. doi: 10.1128/JVI.01901-17

115. Daniels BP, Jujjavarapu H, Durrant DM, Williams JL, Green RR, White JP, et al. Regional astrocyte IFN signaling restricts pathogenesis during neurotropic viral infection. *J Clin Invest* (2017) 127:843–56. doi: 10.1172/JCI88720

116. Shirai K, Shimada T, Yoshida H, Hayakari R, Matsumiya T, Tanji K, et al. Interferon (IFN)-induced protein 35 (IFI35) negatively regulates IFN-β-phosphorylated STAT1-RIG-I-CXCL10/CCL5 axis in U373MG astrocytoma cells treated with polyinosinic-polycytidylic acid. *Brain Res* (2017) 1658:60–7. doi: 10.1016/j.brainres.2017.01.018

117. Wang H, Yuan M, Wang S, Zhang L, Zhang R, Zou X, et al. STAT3 regulates the type I IFN-mediated antiviral response by interfering with the nuclear entry of STAT1. *Int J Mol Sci* (2019) 20:4870. doi: 10.3390/ijms20194870

118. Staeheli P, Sentandreu M, Pagenstecher A, Hausmann JR. Alpha/Beta interferon promotes transcription and inhibits replication of borna disease virus in persistently infected cells. *J Virol* (2001) 17:8. doi: 10.1128/JVI.75.17.8216-8223.2001

119. Watson Z, Tang S-J. Aberrant synaptic pruning in CNS diseases: A critical player in HIV-associated neurological dysfunction? *Cells* (2022) 11:1943. doi: 10.3390/cells11121943

120. Das M, Smith ML, Furihata T, Sarker S, O'Shea R, Helbig KJ. Astrocyte control of zika infection is independent of interferon type I and type III expression. *Biology* (2022) 11:143. doi: 10.3390/biology11010143

121. Lindqvist R, Mundt F, Gilthorpe JD, Wölfel S, Gekara NO, Kröger A, et al. Fast type I interferon response protects astrocytes from flavivirus infection and virus-induced cytopathic effects. *J Neuroinflamm* (2016) 13:277. doi: 10.1186/s12974-016-0748-7

122. Delhaye S, Paul S, Blakqori G, Minet M, Weber F, Staeheli P, et al. Neurons produce type I interferon during viral encephalitis. *Proc Natl Acad Sci U.S.A.* (2006) 103:7835–40. doi: 10.1073/pnas.0602460103

123. Préhaud C, Mégret F, Lafage M, Lafon M. Virus infection switches TLR-3-Positive human neurons to become strong producers of beta interferon. *J Virol* (2005) 79:12893–904. doi: 10.1128/JVI.79.20.12893-12904.2005

124. Wang J, Campbell IL. Innate STAT1-dependent genomic response of neurons to the antiviral cytokine alpha interferon. *J Virol* (2005) 79:8295–302. doi: 10.1128/JVI.79.13.8295-8302.2005

125. Samuel MA, Whitby K, Keller BC, Marri A, Barchet W, Williams BRG, et al. PKR and RNase l contribute to protection against lethal West Nile virus infection by controlling early viral spread in the periphery and replication in neurons. *J Virol* (2006) 80:7009–19. doi: 10.1128/JVI.00489-06

126. Ida-Hosonuma M, Iwasaki T, Yoshikawa T, Nagata N, Sato Y, Sata T, et al. The Alpha/Beta interferon response controls tissue tropism and pathogenicity of poliovirus. *J Virol* (2005) 79:4460–9. doi: 10.1128/JVI.79.7.4460-4469.2005

127. Oo A, Zandi K, Shepard C, Bassit LC, Musall K, Goh SL, et al. Elimination of aicardi–goutières syndrome protein SAMHD1 activates cellular innate

immunity and suppresses SARS-CoV-2 replication. *J Biol Chem* (2022) 298:101635. doi: 10.1016/j.jbc.2022.101635

128. Lindqvist R, Upadhyay A, Överby A. Tick-borne flaviviruses and the type I interferon response. *Viruses* (2018) 10:340. doi: 10.3390/v10070340

129. De Tiège X, Rozenberg F, Héron B. The spectrum of herpes simplex encephalitis in children. *Eur J Paediatr Neurol EJPN Off J Eur Paediatr Neurol Soc* (2008) 12:72–81. doi: 10.1016/j.ejpn.2007.07.007

130. Sancho-Shimizu V, Zhang S-Y, Abel L, Tardieu M, Rozenberg F, Jouanguy E, et al. Genetic susceptibility to herpes simplex virus 1 encephalitis in mice and humans. *Curr Opin Allergy Clin Immunol* (2007) 7:495–505. doi: 10.1097/ACI.0b013e3282f151d2

131. Zhang S-Y, Herman M, Ciancanelli MJ, Pérez de Diego R, Sancho-Shimizu V, Abel L, et al. TLR3 immunity to infection in mice and humans. *Curr Opin Immunol* (2013) 25:19–33. doi: 10.1016/j.coi.2012.11.001

132. Lafaille FG, Pessach IM, Zhang S-Y, Ciancanelli MJ, Herman M, Abhyankar A, et al. Impaired intrinsic immunity to HSV-1 in human iPSC-derived TLR3-deficient CNS cells. *Nature* (2012) 491:769–73. doi: 10.1038/nature11583

133. Zimmer B, Ewaleifoh O, Harschnitz O, Lee Y-S, Peneau C, McAlpine JL, et al. Human iPSC-derived trigeminal neurons lack constitutive TLR3-dependent immunity that protects cortical neurons from HSV-1 infection. *Proc Natl Acad Sci U.S.A.* (2018) 115:E8775–82. doi: 10.1073/pnas.1809853115

134. Gao D, Ciancanelli MJ, Zhang P, Harschnitz O, Bondet V, Hasek M, et al. TLR3 controls constitutive IFN-β antiviral immunity in human fibroblasts and cortical neurons. *J Clin Invest* (2021) 131:134529. doi: 10.1172/JCI134529

135. Winkler CW, Woods TA, Groveman BR, Carmody AB, Speranza EE, Martens CA, et al. Neuronal maturation reduces the type I IFN response to orthobunyavirus infection and leads to increased apoptosis of human neurons. *J Neuroinflamm* (2019) 16:229. doi: 10.1186/s12974-019-1614-1

136. Yordy B, Iijima N, Huttner A, Leib D, Iwasaki A. A neuron-specific role for autophagy in antiviral defense against herpes simplex virus. *Cell Host Microbe* (2012) 12:334–45. doi: 10.1016/j.chom.2012.07.013

137. Li J, Liu Y, Zhang X. Murine coronavirus induces type I interferon in oligodendrocytes through recognition by RIG-I and MDA5. *J Virol* (2010) 84:6472–82. doi: 10.1128/JVI.00016-10

138. Kapil P, Butchi NB, Stohlman SA, Bergmann CC. Oligodendroglia are limited in type I interferon induction and responsiveness *in vivo*. *Glia* (2012) 60:1555–66. doi: 10.1002/glia.22375

139. Vitner EB, Farfel-Becker T, Ferreira NS, Leshkowitz D, Sharma P, Lang KS, et al. Induction of the type I interferon response in neurological forms of gaucher disease. *J Neuroinflamm* (2016) 13:104. doi: 10.1186/s12974-016-0570-2

140. Dugas B, Charbonnier S, Baarine M, Ragot K, Delmas D, Ménétrier F, et al. Effects of oxysterols on cell viability, inflammatory cytokines, VEGF, and reactive oxygen species production on human retinal cells: cytoprotective effects and prevention of VEGF secretion by resveratrol. *Eur J Nutr* (2010) 49:435–46. doi: 10.1007/s00394-010-0102-2

141. Jang J, Park S, Jin Hur H, Cho H-J, Hwang I, Pyo Kang Y, et al. 25-hydroxycholesterol contributes to cerebral inflammation of X-linked adrenoleukodystrophy through activation of the NLRP3 inflammasome. *Nat Commun* (2016) 7:13129. doi: 10.1038/ncomms13129

142. Imaizumi T, Yoshida H, Hayakari R, Xing F, Wang L, Matsumiya T, et al. Interferon-stimulated gene (ISG) 60, as well as ISG56 and ISG54, positively regulates TLR3/IFN-β/STAT1 axis in U373MG human astrocytoma cells. *Neurosci Res* (2016) 105:35–41. doi: 10.1016/j.neures.2015.09.002

143. Vetreno RP, Crews FT. Adolescent binge drinking increases expression of the danger signal receptor agonist HMGB1 and toll-like receptors in the adult prefrontal cortex. *Neuroscience* (2012) 226:475–88. doi: 10.1016/j.neuroscience.2012.08.046

144. Coleman LGJ, Zou J, Crews FT. Microglial-derived miRNA let-7 and HMGB1 contribute to ethanol-induced neurotoxicity *via* TLR7. *J Neuroinflamm* (2017) 14:22. doi: 10.1186/s12974-017-0799-4

145. McDonough A, Lee RV, Noor S, Lee C, Le T, Iorga M, et al. Ischemia/Reperfusion induces interferon-stimulated gene expression in microglia. *J Neurosci Off J Soc Neurosci* (2017) 37:8292–308. doi: 10.1523/JNEUROSCI.0725-17.2017

146. Tonduti D, Fazzi E, Badolato R, Orcesi S. Novel and emerging treatments for aicardi-goutières syndrome. *Expert Rev Clin Immunol* (2020) 16:189–98. doi: 10.1080/1744666X.2019.1707663

147. Guo X, Wiley CA, Steinman RA, Sheng Y, Ji B, Wang J, et al. Aicardi-goutières syndrome-associated mutation at ADAR1 gene locus activates innate immune response in mouse brain. *J Neuroinflamm* (2021) 18:169. doi: 10.1186/s12974-021-02217-9

148. Gacem N, Kavo A, Zerad L, Richard L, Mathis S, Kapur RP, et al. ADAR1 mediated regulation of neural crest derived melanocytes and schwann cell development. *Nat Commun* (2020) 11:198. doi: 10.1038/s41467-019-14090-5

149. Neilley LK, Goodin DS, Goodkin DE, Hauser SL. Side effect profile of interferon beta-lb in MS: Results of an open label trial. *Neurology* (1996) 46:552–3. doi: 10.1212/WNL.46.2.552

150. Kettwig M, Ternka K, Wendland K, Krüger DM, Zampar S, Schob C, et al. Interferon-driven brain phenotype in a mouse model of RNaseT2 deficient leukoencephalopathy. *Nat Commun* (2021) 12:6530. doi: 10.1038/s41467-021-26880-x

151. Fields J, Dumaop W, Adame A, Ellis RJ, Letendre S, Grant I, et al. Alterations in the levels of vesicular trafficking proteins involved in HIV replication in the brains and CSF of patients with HIV-associated neurocognitive disorders. *J Neuroimmune Pharmacol Off J Soc NeuroImmune Pharmacol* (2013) 8:1197–209. doi: 10.1007/s11481-013-9511-3

152. Borsini A, Cattaneo A, Malpighi C, Thuret S, Harrison NA, Zunszain PA, et al. Interferon-alpha reduces human hippocampal neurogenesis and increases apoptosis *via* activation of distinct STAT1-dependent mechanisms. *Int J Neuropsychopharmacol* (2018) 21:187–200. doi: 10.1093/ijnp/pyx083

153. Wood LM, Sankar S, Reed RE, Haas AL, Liu LF, McKinnon P, et al. A novel role for ATM in regulating proteasome-mediated protein degradation through suppression of the ISG15 conjugation pathway. *PloS One* (2011) 6:16422. doi: 10.1371/journal.pone.0016422

154. Hain HS, Pandey R, Bakay M, Strenkowski BP, Harrington D, Romer M, et al. Inducible knockout of Clec16a in mice results in sensory neurodegeneration. *Sci Rep* (2021) 11:9319. doi: 10.1038/s41598-021-88895-0

155. Rossi JL, Todd T, Daniels Z, Bazan NG, Belayev L. Interferon-stimulated gene 15 upregulation precedes the development of blood-brain barrier disruption and cerebral edema after traumatic brain injury in young mice. *J Neurotrauma* (2015) 32:1101–8. doi: 10.1089/neu.2014.3611

156. Liu S, Karaganis S, Mo R-F, Li X-X, Wen R-X, Song X-J. IFNβ treatment inhibits nerve injury-induced mechanical allodynia and MAPK signaling by activating ISG15 in mouse spinal cord. *J Pain* (2020) 21:836–47. doi: 10.1016/j.jpain.2019.11.010

157. Przanowski P, Loska S, Cysewski D, Dabrowski M, Kaminska B. ISG'ylation increases stability of numerous proteins including Stat1, which prevents premature termination of immune response in LPS-stimulated microglia. *Neurochem Int* (2018) 112:227–33. doi: 10.1016/j.neuint.2017.07.013

158. Singh DK, Aladyeva E, Das S, Singh B, Esaulova E, Swain A, et al. Myeloid cell interferon responses correlate with clearance of SARS-CoV-2. *Nat Commun* (2022) 13:679. doi: 10.1038/s41467-022-28315-7

159. Sen GC, Fensterl V. Crystal structure of IFIT2 (ISG54) predicts functional properties of IFITs. *Cell Res* (2012) 22:1407–9. doi: 10.1038/cr.2012.130

160. Schoggins JW. Interferon-stimulated genes: roles in viral pathogenesis. *Curr Opin Virol* (2014) 6:40–6. doi: 10.1016/j.coviro.2014.03.006

161. Diamond MS, Farzan M. The broad-spectrum antiviral functions of IFIT and IFITM proteins. *Nat Rev Immunol* (2013) 13:46–57. doi: 10.1038/nri3344

162. Brass AL, Huang I-C, Benita Y, John SP, Krishnan MN, Feeley EM, et al. The IFITM proteins mediate cellular resistance to influenza a H1N1 virus, West Nile virus, and dengue virus. *Cell* (2009) 139:1243–54. doi: 10.1016/j.cell.2009.12.017

163. Huang I-C, Bailey CC, Weyer JL, Radoshitzky SR, Becker MM, Chiang JJ, et al. Distinct patterns of IFITM-mediated restriction of filoviruses, SARS coronavirus, and influenza a virus. *PloS Pathog* (2011) 7:e1001258. doi: 10.1371/journal.ppat.1001258

164. Poddar S, Hyde JL, Gorman MJ, Farzan M, Diamond MS. The interferon-stimulated gene IFITM3 restricts infection and pathogenesis of arthritogenic and encephalitic alphaviruses. *J Virol* (2016) 90:8780–94. doi: 10.1128/JVI.00655-16

165. Everitt ARThe MOSAIC Investigators, , Everitt AR, Clare S, Pertel T, John SP, et al. IFITM3 restricts the morbidity and mortality associated with influenza. *Nature* (2012) 484:519–23. doi: 10.1038/nature10921

166. Zhao X, Li J, Winkler CA, An P, Guo J-T. IFITM genes, variants, and their roles in the control and pathogenesis of viral infections. *Front Microbiol* (2019) 9:3228. doi: 10.3389/fmicb.2018.03228

167. Allen EK, Randolph AG, Bhangale T, Dogra P, Ohlson M, Oshansky CM, et al. SNP-mediated disruption of CTCF binding at the IFITM3 promoter is associated with risk of severe influenza in humans. *Nat Med* (2017) 23:975–83. doi: 10.1038/nm.4370

168. Zhang Y, Qin L, Zhao Y, Zhang P, Xu B, Li K, et al. Interferon-induced transmembrane protein 3 genetic variant rs12252-c associated with disease severity in coronavirus disease 2019. *J Infect Dis* (2020) 222:34–7. doi: 10.1093/infdis/jiaa224

169. Zhang Y-H, Zhao Y, Li N, Peng Y-C, Giannoulatou E, Jin R-H, et al. Interferon-induced transmembrane protein-3 genetic variant rs12252-c is associated with severe influenza in Chinese individuals. *Nat Commun* (2013) 4:1418. doi: 10.1038/ncomms2433

170. Schoggins JW. Interferon-stimulated genes: What do they all do? *Annu Rev Virol* (2019) 6:567–84. doi: 10.1146/annurev-virology-092818-015756

10.3389/fimmu.2022.1008072

Glossary

IFN	Interferon
ISGs	Interferon-stimulated genes
CNS	Central nervous system
BBB	Blood-brain barrier
JAK	Janus tyrosine kinase
STAT	Signal transducer and activator of transcription
ISGF3	IFN-stimulated gene factor 3
TYK2	Tyrosine Kinase 2
IRF9	Interferon regulatory factor 9 (IRF9)
ISREs	Interferon stimulatory response elements
GAF	γ-activated factors
GAS	γ-activated sequences
IRFs	Interferon regulatory factors
NF-kB	Nuclear factor k B
RIG-I	Retinoic acid-inducible gene I
MDA5	Melanoma differentiation-associated gene 5
RLRs	RIG-I-like receptors
IFIT1	Interferon-induced protein with tetrapeptide repeats 1
WT	Wild-type
SINV	Sindbis virus
HSE	Herpes simplex encephalitis
TRIF	Toll-interleukin-1 receptor domain-containing adaptor-inducing interferon-β
TBK-1	TANK-binding kinase 1
TLR3	Toll-like receptor 3
TRAF3	Tumor necrosis factor receptor-associated factor 3
AD	Alzheimer's disease
PD	Parkinson's disease
ALS	Amyotrophic lateral sclerosis
BCSFB	Blood-cerebrospinal fluid barrier
HSV-1	Herpes simplex virus type 1
VZV	Varicella-zoster virus
JEV	Japanese encephalitis virus
RABV	Rabies virus
BMECs	Brain microvascular endothelial cells
TJ	Tight junction
LPS	Lipopolysaccharide
HIV	Human immunodeficiency virus
NMJs	Neuromuscular junctions
OB	Olfactory bulb
LGTV	Langat virus
WNV	West Nile virus
VSV	Vesicular Stomatitis Virus
CMV	Cytomegalovirus

(Continued)

Continued

IFNAR	IFN-α/βreceptor
CAMs	CNS-associated macrophages
TMEV	Taylor mouse encephalomyelitis virus
PKR	Protein kinase R
MHV	Murine hepatitis virus
HSE	HSV encephalitis
CH25H	Cholesterol-25-hydroxylase
OAS	Oligoadenylate synthase
RNase L	Latent RNase
PRRs	Pattern recognition receptors
cGAS	Cyclic GMP-AMP synthase
cGAMP	Cyclic GMP-AMP
STING	Stimulator of interferon genes
RNAi	RNA interference
IFI35	Interferon-induced protein 35
EV71	Enterovirus 71
BDV	Borna disease virus
TBEV	Tick-borne encephalitis virus
ZIKV	Zika virus
Ifi27l2a	Interferon alpha-inducible protein 27 like 2A
DRG	Dorsal root ganglion
IKK	IkB kinases
MS	Multiple sclerosis
25-HC	25-hydroxycholesterol
CSF	Cerebrospinal fluid
A-T	Ataxia capillaries
GBA1	Glucosylceramidase1
AGS	Aicardi-Gtières syndrome
ADAR1	Adenosine deaminase acting on RNA1
HAND	HIV-associated neurocognitive disorders
MIA	Maternal immune activation
CLEC16A	C-Type Lectin Domain Containing 16A
MLCK	Covalently to myosin light chain kinase
HCMV	Human cytomegalovirus
HELFs	Human embryonic lung fibroblast cells
SeV	Sendai virus
IFITMs	IFN-inducible transmembrane proteins
RE	Rasmussen encephalitis
SNP	Single nucleotide polymorphism
SAMHD1	Sterile alpha motif and histidine/aspartic domain-containing protein 1
MX2	Myxovirus resistance protein 2
VSV	Vesicular stomatitis virus
KPNA1	Karyopherin-alpha1
CXCL10	C-X-C motif chemokine ligand 10
CCL5	Chemokine (C-C motif) ligand 5
IPSC	Induced pluripotent stem cells
IFP35	IFN-induced protein 35
MAPK	Mitogen-activated protein kinase

frontiers | Frontiers in Immunology

TYPE Original Research
PUBLISHED 24 November 2022
DOI 10.3389/fimmu.2022.1016545

OPEN ACCESS

EDITED BY
Chang Li,
Chinese Academy of Agricultural Sciences (CAAS), China

REVIEWED BY
Bin Zhou,
Nanjing Agricultural University, China
Gisselle N. Medina,
Agricultural Research Service (USDA), United States
Fuxiao Liu,
Qingdao Agricultural University, China
Lei Xu,
Northwest A&F University, China

*CORRESPONDENCE
Haixue Zheng
haixuezheng@163.com

†These authors have contributed equally to this work

SPECIALTY SECTION
This article was submitted to Molecular Innate Immunity, a section of the journal Frontiers in Immunology

RECEIVED 11 August 2022
ACCEPTED 26 October 2022
PUBLISHED 24 November 2022

CITATION
Dang W, Li T, Xu F, Wang Y, Yang F and Zheng H (2022) Establishment of a CRISPR/Cas9 knockout library for screening type I interferon-inducible antiviral effectors in pig cells. *Front. Immunol.* 13:1016545. doi: 10.3389/fimmu.2022.1016545

Establishment of a CRISPR/Cas9 knockout library for screening type I interferon-inducible antiviral effectors in pig cells

Wen Dang[1†], Tao Li[1†], Fan Xu[1], Yannan Wang[2], Fan Yang[1] and Haixue Zheng[1*]

[1]State Key Laboratory of Veterinary Etiological Biology, College of Veterinary Medicine, Lanzhou University, Lanzhou Veterinary Research Institute, Chinese Academy of Agricultural Sciences, Lanzhou, China, [2]Lanzhou University Second Hospital, Department of Radiology, Lanzhou, China

Diseases caused by emerging swine viruses had a great economic impact, constituting a new challenge for researchers and practicing veterinarians. Innate immune control of viral pathogen invasion is mediated by interferons (IFNs), resulting in transcriptional elevation of hundreds of IFN-stimulated genes (ISGs). However, the ISG family is vast and species-specific, and despite remarkable advancements in uncovering the breadth of IFN-induced gene expression in mouse and human, it is less characterized with respect to the repertoire of porcine ISGs and their functional annotation. Herein, with the application of RNA-sequencing (RNA-Seq) gene profiling, the breadth of IFN-induced gene expression in the context of type I IFN stimulation was explored by using IBRS-2 cell, a commonly used high-efficient cultivation system for porcine picornaviruses. By establishing inclusion criteria, a total of 359 ISGs were selected. Aiming to identify key effectors mediating type I IFN inhibition of swine viruses, a CRISPR/Cas9 knockout library of 1908 sgRNAs targeting 5' constitutive exons of 359 ISGs with an average of 5 to 6 sgRNAs per gene was constructed. Using VSV-eGFP (vesicular stomatitis virus, fused with GFP) as a model virus, a subset of highest-ranking candidates were identified, including previously validated anti-VSV genes IRF9, IFITM3, LOC100519082 and REC8, as well as several novel hits. This approach attains a high level of feasibility and reliability, and a high rate of hit identification, providing a forward-looking platform to systematically profile the effectors of type I IFN antiviral response against porcine viruses.

KEYWORDS

interferons, interferon-stimulated genes, CRISPR/Cas9, VSV-eGFP, IBRS-2

Introduction

The type I interferon (IFN) response is at the frontline in defending cells from viral pathogen invasion (1). The activation of the IFN-triggered JAK-STAT pathway results in the expression of a diverse range of gene products that serve as ultimate effectors fighting against virus replication. The genes encoding for those cellular antiviral factors are called interferon-stimulated genes (ISGs). Although hundreds of ISGs have been identified, their functional annotation with respect to antiviral potential, target specificity and concurrent mechanism-of-action is poorly characterized (2–5). Thus, it is of great need and importance to identify and characterize sets of novel ISGs for each viral species susceptible to type I IFN treatment. The follow-up endeavors to better understand the exact mechanism-of-action of newly identified ISGs have unearthed a wide range of targets for rational development of therapeutic options against virus infection.

Of note, it is estimated that approximately 10% of the genes in the human genome have the potential to be regulated by stimulation with IFNs. From decades of research, it is discovered that ISG products take on a diverse range of roles, including antiviral defense, anti-proliferative activities, and stimulation of adaptive immunity. Even though great strides into deciphering the antiviral mechanism of a select group of classic ISGs have been made, advances in profiling novel sets of antiviral effectors towards each viral species, however, have largely been limited. Previously, remarkable progress has been made using gain-of-function screening in which single ISGs were expressed and their antiviral activity was assessed against different viruses. Using expressional screening of 29 and 39 ISGs, restriction factors including Viperin, ISG20 and PKR have been identified for HCV (6), as well as IFI27, IRG1 and Viperin for neurotropic RNA viruses (7). In 2011, large-scale, fluoresce-activated, cell sorting-based overexpression screening of 389 human ISGs identified a diverse range of gene products as effectors of type I IFN antiviral response against six important human and animal viruses (8). However, gain-of-function screens are labor-intensive and clearly incapable of characterizing all relevant ISGs. Instead, loss-of-function can overcome these limitations. Loss-of-function genome-wide screen based on RNA interference (RNAi) libraries is temporarily used in identifying antiviral IFN effectors against HCV, however, drawbacks of RNAi libraries such as off-target effect hinder its wide application (9). Very recently, through genome-scale CRISPR loss-of-function screening, IFI6 was identified as an ER-resident interferon effector that blocked flavivirus replication, further potentializing CRISPR/Cas9 approach as a validated tool for screening IFN effectors (10).

To date, few studies were dedicated to examining the repertoire of ISGs in the porcine species. With the application of RNA sequencing (RNA-Seq) gene profiling, a total of 359 cellular effectors were selected as ISGs and their expression kinetics in the context of type I IFN stimulation were characterized in Instituto Biologico-Rim Suino-2 (IBRS-2) cells. Existing evidence demonstrated that IBRS-2 possessed susceptibility to the viruses of foot-and-mouth disease, swine vesicular disease, vesicular exanthema of swine, transmissible gastroenteritis, and several other viruses (11). Meanwhile, IBRS-2 cells have an aberrant RIG-I-like receptor (RLR) pathway but an intact type I IFN pathway, which facilitates the characterization of downstream antiviral effectors in the context of virus infection and IFN stimulation (12). To this aim, we constructed a CRISPR/Cas9 knockout library of 1809 unique sequences targeting 359 ISGs with an average coverage of 5 to 6 sgRNAs per gene in IBRS-2 cells. Following lentiviral delivery in IBRS-2 cells, positive selection screening identified interferon effectors crucial for blocking VSV-eGFP (Vesicular Stomatitis Virus (VSV)) replication. The highest ranking candidates included previously validated anti-VSV genes IRF9, LOC100519082 (also referred to as IFITM1), IFITM3 and REC8, as well as novel hits. This ISG-targeting CRISPR/Cas9 knockout library demonstrated a high level of consistency between type I IFNs (including two subtypes of interferon α and one subtype of interferon β) and a high rate of hit confirmation, demonstrating the promise of wide application in screening novel sets of ISGs against a panel of porcine viruses.

Materials and methods

Virus, cell lines and reagents

VSV-eGFP (Cat#: NTA-2011-ZP20; Creative Biolabs) stock was propagated in BHK-21 cell culture, titrated by 50% haemadsorbing doses (HAD_{50}) assay, aliquoted and preserved at -80°C before use. IBRS-2 and HEK 293T cells were cultured in Dulbeccos Modified Eagle Medium (DMEM) (GIBCO, Invitrogen China Limited, Shanghai, China) supplemented with 10% (v/v) fetal bovine serum (FBS) (BI, Biological Industries Israel Beit Haemek LTD., Kibbutz Beit-Haemek, Israel) and 1% (v/v) penicillin-streptomycin solution (100 I.U./mL penicillin, 5 mg/L streptomycin) (Gibco).

Recombinant human IFN-α 1b (Cat#: Z02866), IFN-α 2a (Cat#: Z03003) and IFN-β (Cat#: Z03109) were purchased from GenScript (Nanjing, China), reconstituted in PBS containing 0.1% BSA to a concentration of 10 μg/mL, and preserved at -80°C before use. Ruxolitinib (RUX) (CAS No.: 941678-49-5) (Cat#: HY-50856) was obtained from MedChemExpress (MCE), stocked at 10 mM in DMSO and preserved at -80°C before use.

RNA extraction, library preparation and sequencing

IBRS-2 cells were seeded into a 6-well plate at 1×10^6 cells per well. Following overnight culture, the plate was replenished with fresh growth medium containing 10 ng/mL of type I IFNs. At the indicated time points, cell monolayers were rinsed with

pre-cold PBS three times, and total RNA was extracted using the mirVana™ miRNA Isolation Kit (Ambion-1561) as per the manufacturer's protocol. RNA concentration was measured by UV spectrophotometry (NanoDrop™ 2000) and the RNA integrity was assessed using the Agilent 2100 Bioanalyzer System (Agilent Technologies, Santa Clara, CA, USA). The samples could be subjected to further experiment only if RNA integrity number (RIN) was greater than or equal to 7. The libraries were constructed using reagents and protocols supplied in TruSeq Stranded mRNA LTSample Prep Kit (Cat#: RS-122-2101) (Illumina, San Diego, CA, USA). Then these libraries were validated by BioAnalyzer followed by 125-bp/150-bp paired-end read sequencing on the Illumina sequencing platform (HiSeq® 2500 Sequencing Systems and HiSeq X™ Ten), as carried out by OE Biotech Co., Ltd. (Shanghai, China).

Sequence analysis

Following quality control [processing using Trimmomatic (13), removal of adapter sequences and trimming], clean reads were mapped to Sscrofa11.1 using HISAT2 with default parameters (14). Mapped reads were subsequently assembled into transcripts, with FPKM values and read counts being calculated by Cufflinks (15) and HTSeq (16), respectively. Transcript abundance was compared between mock and type I IFN-treated samples using the DESeq (version 1.24.0) R package to identify differentially expressed genes (DEGs). Inclusion criteria of a p value of < 0.05, a twofold or greater expression change and a FPKM value greater than 1 in at least one sample was set as the threshold for DEGs.

Library construction

Oligos encoding the sgRNA library with ~1908 specific sgRNA sequences targeting 359 ISGs were synthesized by a programmable microarray using the Synthesizer (GenScript, Wuhan) and cloned as a pool into lentiCRISPRv2 vector. Library quality was assessed by NGS with coverage of 100%. Following lentiviral production, IBRS-2 cells were infected with the lentiCRISPRv2-derived lentivirus at low titer (MOI = 0.05) and high titer (MOI = 0.1) for 24 h, respectively, and reseeded into growth medium containing 5 μg/mL of puromycin. Following three consecutive rounds of selective culture, approximately 4 days per round, transduced cells were subjected to further characterization of transduction efficacy.

CRISPR screening

Briefly, puromycin-selected IBRS-2 cell populations were infected with VSV-eGFP at MOI of 0.1, followed by treatment with type I IFNs for 36 h. The eGFP-positive cells that were no longer sensitive to type I IFN-mediated inhibition were harvested by fluorescent activated cell sorting (FACS). Genomic DNA was extracted from those cells, and sgRNA sequences were amplified by PCR and deep sequenced.

Lentiviral production and transduction

In order to overexpress selected top four ISGs in IBRS-2 cells, a bicistronic lentiviral vector co-expressing an ISG and the red fluorescent protein, TagRFP was constructed. Control vector co-expressing GFP/TagRFP was used in the present study. Lentiviral particles were produced by co-transfecting HEK293T cells with plasmids expressing: 1) the ISG/TagRFP proviral DNA, 2) HIV gap-pol, and 3) the vesicular stomatitis virus glycoprotein (VSV-G) in a ratio of 1:0.8:0.2, respectively. Following 6 h transfection a media change to DMEM with 3% FBS was performed. Supernatants were harvested at 48 h and 72 h, pooled, clarified by centrifugation, and stored at −80°C before use.

IBRS-2 cells were seeded into a 12 well plate at a density of 5×10^5 cells per well. Following overnight culture, cells were transduced with lentiviral particles at an MOI of 0.5. After 24 h incubation the cells were subjected to fluorescent microscopy for assessing the transduction efficiency.

VSV-eGFP infection

In order to determine the effects of top four ISGs on viral replication, vector control and ISG/TagRFP-expressing IBRS-2 cells were inoculated with VSV-eGFP at an MOI of 0.1. At 48 h post inoculation, the whole culture was freezed at −80°C and subsequently thawed at 37°C. After repeated freezing and thawing, the culture was clarified by ultracentrifugation and viral titers were measured by $TCID_{50}$ assay.

Results

VSV-eGFP is highly sensitive to type I IFN treatment

The IFN-mediated induction of hundreds of ISGs confers host cells an antiviral state against pathogen invasion (Figure 1A). The VSV replication is highly sensitive to type I IFN-induced antiviral responses (17, 18). In this regard, IBRS-2 cells pre-infected with VSV-eGFP at an MOI of 0.1 were subsequently treated with varying concentration of type I IFNs for 24 h. Virus replication was directly monitored as eGFP-positive cells by flow cytometry. As indicated, type I IFNs including IFN-α 1b, IFN-α 2a and IFN-β exerted antiviral

10.3389/fimmu.2022.1016545

activity against VSV-eGFP replication at concentrations of 10 and 100 ng/mL (Figures 1B, C). To identify the association between type I IFN-mediated inhibition and activation of the JAK-STAT pathway, VSV-eGFP-infected IBRS-2 cells were incubated with type I IFNs in combination with Ruxolitinib, a well-known JAK1 and JAK2 inhibitor. Of note, the addition of Ruxolitinib at 500 nM abolished the antiviral potential of type I IFNs and concurrently restored the VSV-eGFP replication (Figures 1B, C). Collectively, VSV-eGFP possessed sensitivity to treatment with type I IFNs. Pharmacological blocking of the JAK-STAT pathway abolished IFN inhibition and reversed VSV-eGFP replication.

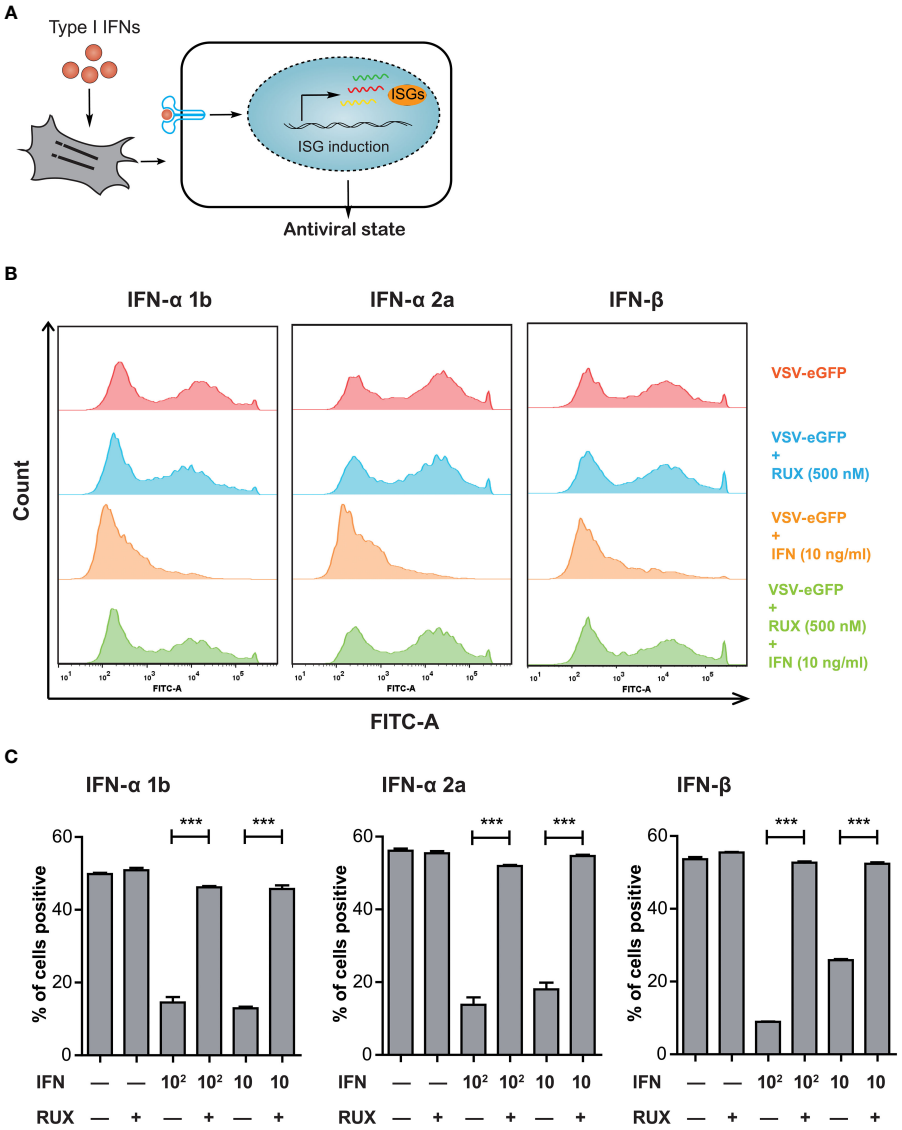

FIGURE 1
VSV-eGFP possessed a sensitivity to type I IFN-triggered antiviral response. **(A)** Treatment with exogenous type I IFNs induces the expression of hundreds of ISGs, allowing the establishment of a so-called antiviral state against pathogen invasion in host cells. **(B)** Representative Flow cytometry analysis of EGFP expression rate in VSV-eGFP-infected IBRS-2 cells mock-treated (top), treated with RUX (500 nM) (middle, upper) and IFN (10 ng/mL) (middle, lower) alone or in combination (bottom). Cells without infection were tested as a background fluorescence intensity control (not shown in the histogram). VSV-eGFP replication was effectively inhibited by type I IFN treatment but subsequently restored by supplementation of RUX. **(C)** Graphs showing Flow cytometry data analysis indicating the reversion of IFN inhibition by addition of RUX. Data are expressed as mean ± SEM. ***P < 0.001.

10.3389/fimmu.2022.1016545

RNA-Seq of type I IFN-treated IBRS-2 cells identified a list of 359 ISGs

To conduct a large-scale antiviral ISG screening, the transcriptional response to type I IFNs in IBRS-2 cells was analyzed by using RNA-Seq and inclusion criteria was established. To evaluate the kinetics of ISG expression reached by type I IFNs, a preliminary experiment was performed by challenging IBRS-2 cells with IFN-β (10 ng/mL) for 8 h, 16 h and 24 h. A simple enumeration of DEGs revealed that up-regulated DEGs achieved maximal amount by 8 h, began to decline thereafter, and reached a plateau at 16 h post treatment (Figure 2A). Conversely, several genes were significantly down-regulated over time. Given the fact that IFN-β stimulated the most up-regulated DEGs at the very early stage of treatment, an 8 h duration is reasonably regarded as the optimal incubation time for IFNs to trigger the most ISGs in IBRS-2 cells. Thus, fresh IBRS-2 cells were stimulated with IFN-α 1b (10 ng/mL) or IFN-α 2a (10 ng/mL) singly for 8 h, and subjected to RNA-Seq. Of significant note is that IFN-α 1b and IFN-α 2a were capable of inducing more up-regulated DEGs, totaling 519 and 499, respectively (Figure 2A). In addition, the pearson correlation analysis visualizing the correlation (r) values revealed a significant positive association, suggestive of a consistent pattern of gene expression among type I IFN-treated samples, albeit the fact that transcriptional response to IFN-α 1b and IFN-α 2a was more analogous (Figure 2B). As demonstrated by upset plot analysis, noticeable is the fact that

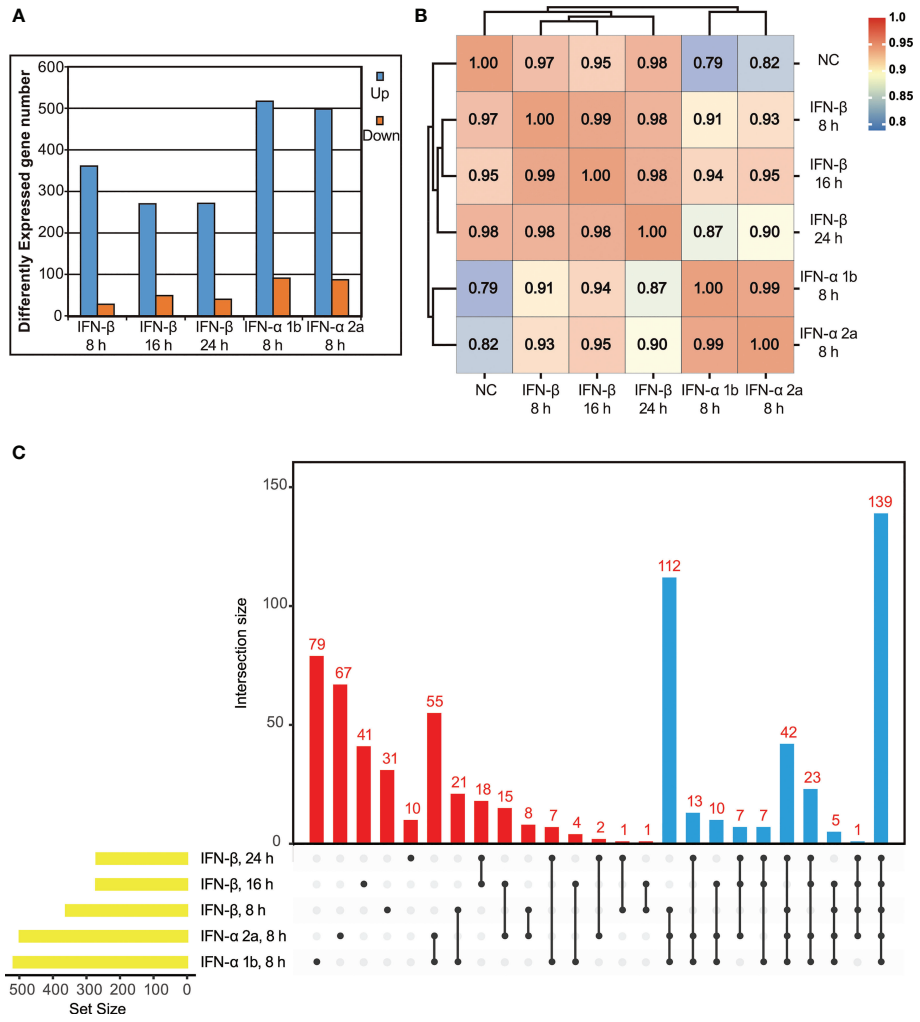

FIGURE 2
Identification of ISGs induced by exogenous type I IFNs using RNA-Seq. **(A)** Differentially expressed genes (*p* value < 0.05, twofold or more change and FPKM value greater than 1 in at least one sample) for each IFN-treated sample are depicted numerically. **(B)** Correlation matrix of all 5 IFN-treated samples (based on Pearson correlation coefficients). **(C)** Upset plot of up-regulated DEGs in IFN-treated samples. Of note, all the up-regulated DEGs in the blue bars are clustered into ISG family.

10.3389/fimmu.2022.1016545

up-regulated DEGs induced by type I IFNs overlapped considerably but were also slightly specialized, with 79 DEGs unique to IFN-α 1b, 67 DEGs unique to IFN-α 2a, and 82 DEGs unique to IFN-β (Figure 2C). Considering that among hundreds of DEGs some were not specifically induced in response to type I IFN treatment, a DEG was qualified for the ISG family only if it was consistently up-regulated in at least three or more samples across all five samples (Figure 2C, blue bars). As such, a list of 359 ISGs was compiled in the present study (Figure 3, Supplementary Table 1).

Construction and characterization of IBRS-2 knockout cell populations

Substantial efforts have been aimed at screening which ISGs are antiviral and further uncovering their mechanisms-of-action. Loss-of-function screens based on CRISPR/Cas9 are gaining increasing popularity in identifying host factors that regulate virus infection. Based on previous RNA-Seq data, we constructed a CRISPR knockout library of 1908 unique sgRNAs targeting 5' constitutive exons of 359 ISGs with an average coverage of 5 to 6 sgRNAs per gene. Following lentiviral transduction at varying MOI to attain no greater than 1 sgRNA per cell, and selective culture with puromycin (5 μg/mL) for 12 days, heterogeneous IBRS-2 knockout cell populations were harvested with high cell viability (Figure 4A). The integrity of ISG-targeting lentiCRISPR library in IBRS-2 knockout cell populations was confirmed by amplifying the sgRNA expression cassettes (Figure 4B). The scatter plot of sgRNA representation (log2 number of reads) signified that more than 98% sgRNAs from IBRS-2 knockout cell populations had representation in the plasmid pool, irrespective of the titer of lentivirus, further implying the reliability of IBRS-2 knockout cell populations (Figure 4C)

Positive selection of gene knockouts that desensitize VSV-eGFP to type I IFN treatment

To enrich for sgRNAs that rendered cells permissive to VSV-eGFP replication despite treatment with a highly suppressive dose of type I IFNs, IBRS-2 knockout cell populations were infected with VSV-eGFP (0.1 MOI) followed by subsequent treatment with IFN-α 2a at a dose of 100 ng/mL. Following 36 h treatment, a cell population permissive to VSV-eGFP replication with high eGFP-signal intensity was enriched by FACS (Figure 5A). The same procedure was applied to IFN-α 1b and IFN-β at the same dose. Following amplifying the sgRNA expression cassettes in the enriched cells, sgRNA distribution was assessed by deep sequencing (Figure 5B). As expected, a diverse range of hits from the screening, with the demonstration of the top 25 most enriched ISGs, had the potential to reconstitute the IFN signaling pathway and served as effectors of the type I IFN antiviral response towards VSV-eGFP replication (Figure 5C). Comparing the top 25 hits revealed as much as 15 overlapping genes, as displayed in Figure 5D and Table 1. Noticeable is the fact that IRF9, a key component of the type I IFN pathway, was highly ranked in the present study. Broad-acting effectors, including LOC100519082, IFITM3 and REC8 previously described as inhibitors of VSV replication elsewhere, were also on the top of the list (19, 20).

FIGURE 3
Expression levels of select ISGs in type I IFN-treated IBRS-2 cells. The font size of each ISG is directly proportional to its average fold change in type I IFN-treated IBRS-2 cells normalized to mock-treated cells. Of note, ISGs with biggest font size demonstrated highest expression levels with fold changes greater than 1000.

10.3389/fimmu.2022.1016545

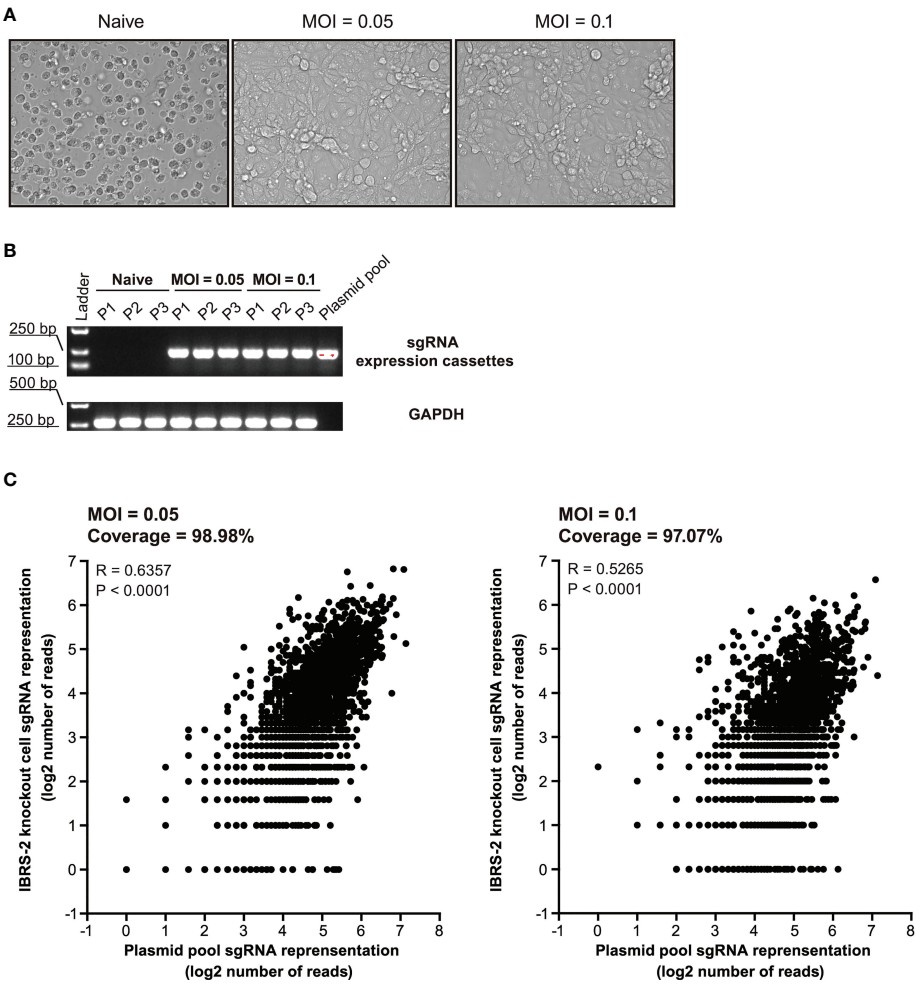

FIGURE 4
Construction and characterization of heterologous IBRS-2 knockout cell populations. **(A)** Cell morphology and growth characteristic of IBRS-2 knockout cell populations following three consecutive rounds of selective culture under the pressure of 5 μg/mL of puromycin. **(B)** Amplification of sgRNA expression cassettes using genomic DNA obtained from different passages of IBRS-2 knockout cell populations with plasmid pool as a positive control. GAPDH is used as an indicator of the input of genomic DNA. **(C)** Comparison of sgRNA representation between the plasmid pool to IBRS-2 knockout cell populations. Scatter plot of sgRNA representation between the plasmid pool to IBRS-2 knockout cell populations following three rounds of selective culture.

Validation of the screening results by using overexpression assay

To validate the screening results, lentiviral overexpression of the top four candidate antiviral ISGs was performed to determine their effects on VSV-eGFP replication. The overexpression assay relied on a bicistronic lentiviral vector co-expressing an ISG and the red fluorescent protein TagRFP (Figure 6A). Of particular, the internal ribosomal entry site (IRES) from encephalomyocarditis virus (EMCV) was used in the bicistronic vector to initiate expression of an additional TagRFP, which functioned as a reporter signal indicative of successful overexpression of target gene. To explore the availability and translational efficacy of the bicistronic vector system, cells transduced with the control vector GFP/TagRFP were subjected to fluorescent microscopy. As displayed in Figure 6B, complete co-localization of GFP and RFP was observed in control cells, suggesting that adequate gene expression from the EMCV IRES element was achieved. We observed high intensities of RFP signals in IRF9/TagRFP, REC8/TagRFP, IFITM3/TagRFP and LOC100519082/TagRFP overexpression cells, indicative of high overexpression efficiency (Figure 6C). ISG/TagRFP-expressing cells were challenged with VSV-eGFP, and viral replication was titrated by $TCID_{50}$ assay (Figure 6D). As a result, exogenous expressed IRF9 and REC8 conferred potent inhibition of VSV-eGFP replication, whereas LOC100519082 and IFITM3 only exerted moderate anti-VSV activity (Figure 6E).

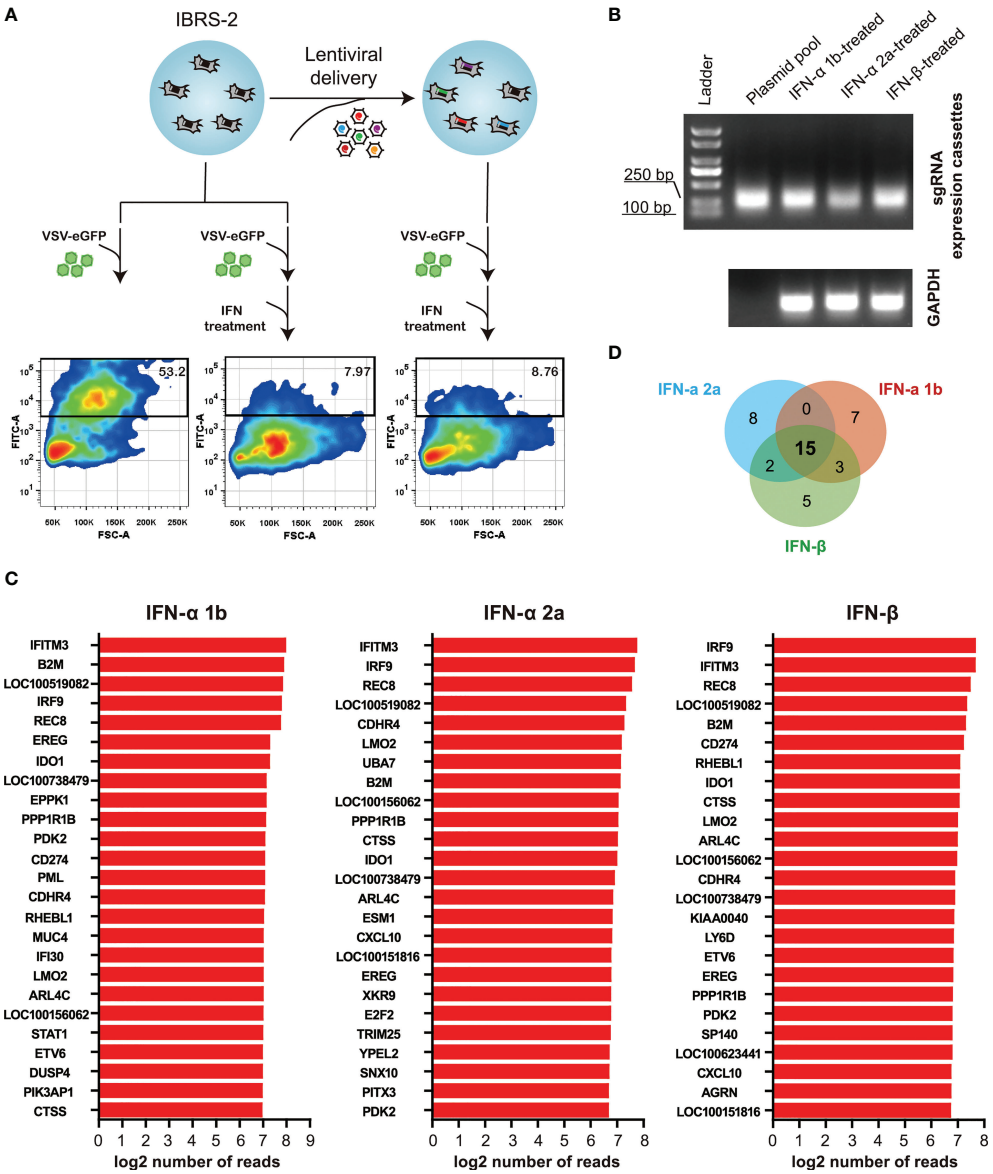

FIGURE 5
ISG-targeting CRISPR screen identifies a subset of genes as potential key effectors of the IFN response to VSV-eGFP replication. **(A)** Schematic of ISG-targeting lentiCRISPR screen to identify antiviral effectors mediating IFN-α 2a-induced antiviral response to VSV-eGFP. **(B)** Amplification of sgRNA expression cassettes in eGFP-positive IBRS-2 knockout cells. **(C)** Bar plots show the top 25 most enriched hits in the context of IFN-α 1b, IFN-α 2a and IFN-β. **(D)** Overlap between the top 25 most enriched ISGs in the context of IFN-α 1b, IFN-α 2a and IFN-β.

Discussion

The type I IFN system, resulting in the transcriptional elevation of hundreds of ISGs, constitutes the first line of defense against viral infections. The products of these ISGs exert distinct antiviral effector functions, a majority of which are still not well characterized. Meanwhile, each mammal owns a unique repertoire of ISGs, including genes conserved in all mammals and others specific to each species (21, 22). The recent efforts have been aimed at identifying the breadth of IFN-induced gene expression in a porcine cell line and constructing a validated gRNA library for CRISPR/Cas9 targeting of porcine 359 ISGs. Through extensive screening by using a model virus VSV-eGFP, several highest-ranking candidates have been enriched, including genes previously validated with anti-VSV activity and genes newly identified.

We prioritized IBRS-2 cell line above a couple of commercially available porcine cell lines in the present study.

10.3389/fimmu.2022.1016545

TABLE 1 Details of fifteen overlapping highest-ranking hits obtained from IFN-α 1b, IFN-α 2a and IFN-β.

Gene_ID	product	Family
IRF9	Interferon regulatory factor 9	IRF
IFITM3	Interferon induced transmembrane protein 3	IFITM protein family
REC8	REC8 meiotic recombination protein	kleisin family of SMC protein partners
LOC100519082	Interferon induced transmembrane protein 1	IFITM protein family
B2M	Beta-2-microglobulin	
PPP1R1B	Protein phosphatase 1 regulatory inhibitor subunit 1B	
LOC100156062	Apolipoprotein L3	Apolipoprotein L gene family
CDHR4	Cadherin related family member 4	
CTSS	Cathepsin S	Peptidase C1 family
LMO2	LIM domain only 2	
EREG	Epiregulin	Epidermal growth factor (EGF) family
IDO1	Indoleamine 2, 3-dioxygenase 1	
LOC100738479	Tripartite motif-containing protein 34	
ARL4C	ADP ribosylation factor like GTPase 4C	ADP-ribosylation factor family of GTP-binding proteins
PDK2	Pyruvate dehydrogenase kinase 2	Pyruvate dehydrogenase kinase family

Firstly, IBRS-2 cells are compromised in activation of RIG-I-like signaling pathway during virus infection. Consequently, virus stimulation is insufficient in strong and protracted induction of genes related to IFN, inflammatory, and innate immune response in IBRS-2 cells (12). Secondly, IBRS-2 cells possess an intact type I IFN pathway. Addition of exogenous type I IFNs could activate the downstream JAK-STAT pathway and result in transcriptions of ISGs (23). According to the principle of CRISPR screening strategies in Figure 5A, cells were first infected with the virus followed by IFN treatment. Thus, an aberrant RLR pathway in IBRS-2 cells could exclude the interference of endogenous IFN, inflammatory, and concurrent innate immune responses with exogenous IFN treatment, guaranteeing the accuracy of CRISPR screening to the greatest extent. Meanwhile, VSV-eGFP was applied for CRISPR screening. The VSV is a negative-sense single-stranded RNA virus. It is named as per the resultant classical vesicular lesions in affected natural hosts, such as horses, cattle, and pigs (24, 25). It is a widely used model system for virus-IFN interaction, likely due to its high sensitivity to IFN treatment (26). Although the present investigation was limited to VSV-eGFP, this library can be applied to a much wider range of viruses, such as Senecavirus A (SVA) and foot-and-mouth disease virus (FMDV) (11, 27). Infection with those viruses caused cytopathic effect (CPE) in IBRS-2 cells, yielding high titers of viral suspension.

One limitation of the present research is devoid of validation of all the top 15 hits against VSV-eGFP replication by pharmacological and genetic approaches. However, among the highest-ranking hits with generic biological effects, some were previously noted to have anti-VSV activity: (I) IRF9, a key component of the JAK-STAT pathway, functioned as a broadly acting effector against a list of viruses (28, 29). Besides, a loss-of-function screen using a small interfering RNA (siRNA) library identified IRF9 as the most significantly enriched hit responsible for the activity of IFN-α against VSV, Indiana serotype (VSV_{IND}) (30). (II) IFITM1/IFITM3 restricted VSV replication potentially through toughening the host membrane, thus preventing viral membrane fusion (19); (III) REC8 promoted the innate immune response by targeting STING and MAVS, thus constraining VSV replication (20). Noticeable is the fact that those four hits are on the top of list. Confirmation of top 4 hits *via* individual gene overexpression demonstrated the same findings, convincingly indicative of the feasibility and reliability of this knockout library. In future work, the antiviral activities and exact mechanism-of-action of novel hits need to be further characterized.

ISG products constitute a complex web of host defenses and take on a number of diverse roles. The IBRS-2 knockout cell populations contained 98% sgRNAs compared with the plasmid library, perhaps due to the fact that some sgRNAs may target ISGs essential for cell survival. Besides, ISG products exert their antiviral activity through multiple mechanisms. Many of the ISG products directly disrupt a particular step in the infection/replication cycle. For example, it is well noted that IFITM3 inhibited viral entry (31, 32). In addition, multiple ISGs (such as IRF1, IRF9 and REC8) likely conferred inhibition of viral replication by amplifying host antiviral state by stimulating IFN expression or interferon-stimulated response element (ISRE)-driven transcription (33). Conversely, several ISGs functioned as negative regulators of IFN signaling pathways and conferred cultured cells an IFN-desensitized state shortly after IFN exposure. SOCS and USP18 were two well-known ISGs that negatively regulate IFN signaling by inhibiting the JAK-STAT signaling pathway (34, 35). However, those ISGs were not highly enriched in the present screening. One of the reasons is that the intrinsic expression of ISGs in IBRS-2 is relatively low.

10.3389/fimmu.2022.1016545

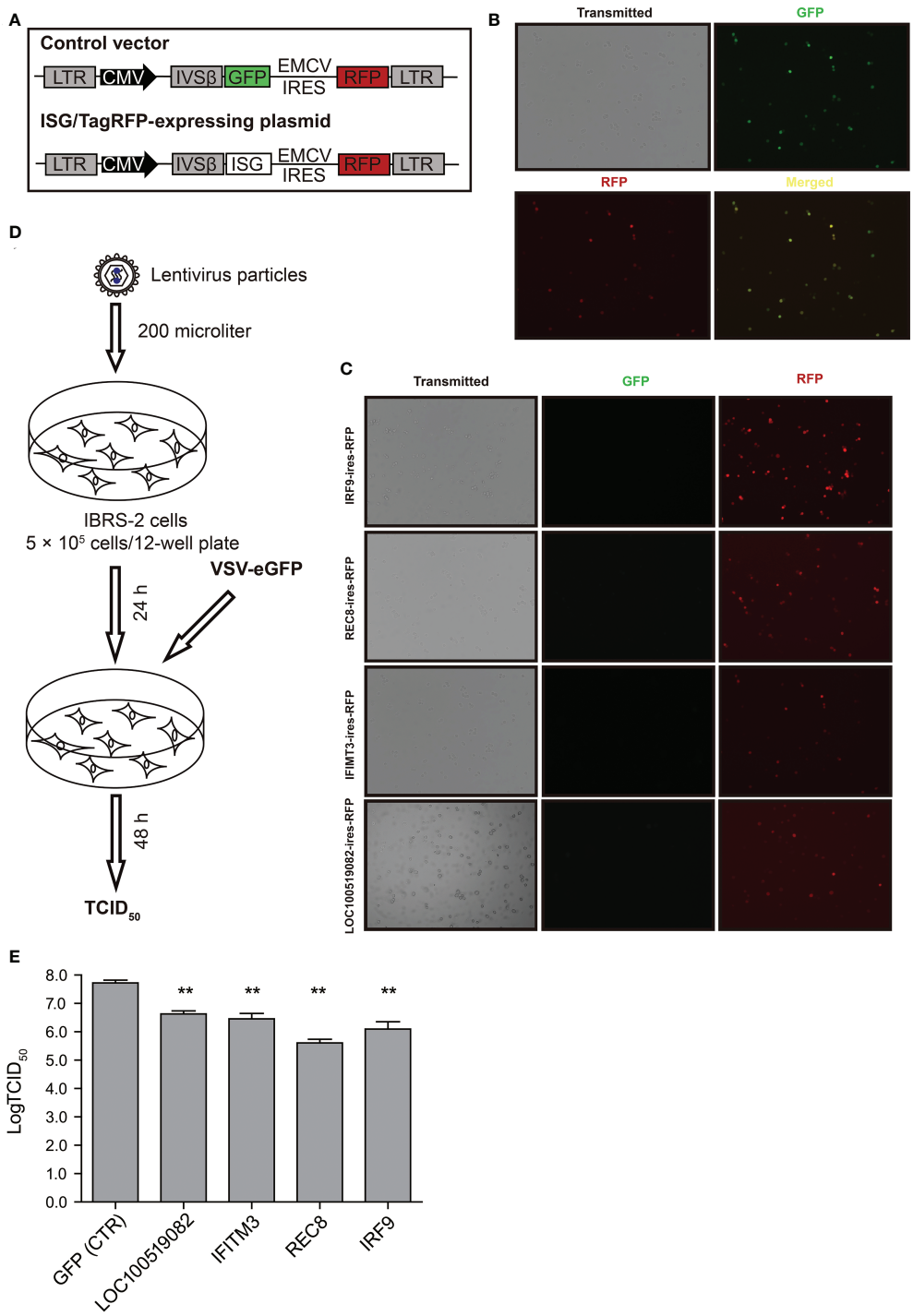

FIGURE 6
The effects of top four ISGs on VSV-eGFP replication. **(A)** Schematic representation of the gateway-compatible bicistronic lentiviral vectors used to stably overexpress ISGs. The viral backbone carries the ISG-IRES-TagRFP overexpression cassette under the CMV promoter. In parallel, control vector GFP-IRES-TagRFP was also designed. **(B)** Fluorescent micrographs of IBRS-2 cells in culture 24 h after transduction with the control vector GFP/TagRFP. **(C)** Fluorescent micrographs of IBRS-2 cells in culture 24 h after transduction with ISG/TagRFP vectors. **(D)** Schematic demonstration of workflow of transduction and virus infections. **(E)** The $TCID_{50}$ titration of VSV-eGFP titers in the vector control and ISG/TagRFP overexpression IBRS-2 cells. The experiment was repeated three times with replicate each. **P < 0.01.

Following IFN stimulation the ISG expression level increased to a level at which the cells are easy to bear.

In summary, this study presents a versatile CRISPR/Cas9 knockout library targeting 359 selected porcine ISGs with predesigned and validated sgRNAs and complete protocols for screenings. The results have expanded the ISG library in pig species and provide additional evidence that CRISPR/Cas9 system is suitable for screening novel ISGs. Furthermore, the antiviral activities of the new ISGs and their biological functions against VSV await further investigation.

Data availability statement

The data presented in the study are deposited in the Sequence Read Archive (SRA) repository, accession number PRJNA899479.

Author contributions

Conceptualization, WD, TL, and HZ. Methodology, WD, TL and FX. Software, YW and FY. Validation, WD and TL. Formal analysis, WD and TL. Data curation, WD and TL. Writing—original draft preparation, WD and TL. Writing—review and editing, WD, TL, and HZ. Visualization, FX and YW. Supervision, HZ. Project administration, WD and HZ. Funding acquisition, WD and HZ. All authors contributed to the article and approved the submitted version.

Funding

This work was funded by grants from the National Key R&D Program of China (2021YFD1800300), the State Key Laboratory of Veterinary Biotechnology (SKLVEB2021DBCG01), the Gansu Provincial Major Project for Science and Technology Development (19ZD2NA001 and 21ZD3NA001), the Central Public-interest Scientific Institution Basal Research Fund (to WD and FY), the Chinese Academy of Agricultural Science and Technology Innovation Project (CAAS-ASTIP-2022-LVRI), the Earmarked Fund for CARS-35, the Open Competition Program of Top Ten Critical Priorities of Agricultural Science and Technology Innovation for the 14th Five-Year Plan of Guangdong Province (2022SDZG02) and the Natural Science Foundation of Gansu Province (22JR5RA996).

Conflict of interest

The authors declare that the research was conducted in the absence of any commercial or financial relationships that could be construed as a potential conflict of interest.

Publisher's note

All claims expressed in this article are solely those of the authors and do not necessarily represent those of their affiliated organizations, or those of the publisher, the editors and the reviewers. Any product that may be evaluated in this article, or claim that may be made by its manufacturer, is not guaranteed or endorsed by the publisher.

Supplementary material

The Supplementary Material for this article can be found online at: https://www.frontiersin.org/articles/10.3389/fimmu.2022.1016545/full#supplementary-material

References

1. Chow KT, Gale MJr. SnapShot: Interferon signaling. *Cell* (2015) 163:1808–1808.e1. doi: 10.1016/j.cell.2015.12.008

2. Schoggins JW, Rice CM. Interferon-stimulated genes and their antiviral effector functions. *Curr Opin Virol* (2011) 1:519–25. doi: 10.1016/j.coviro.2011.10.008

3. Schoggins JW, Wilson SJ, Panis M, Murphy MY, Jones CT, Bieniasz P, et al. A diverse range of gene products are effectors of the type I interferon antiviral response. *Nature* (2011) 472:481–5. doi: 10.1038/nature09907

4. Schneider WM, Chevillotte MD, Rice CM. Interferon-stimulated genes: a complex web of host defenses. *Annu Rev Immunol* (2014) 32:513–45. doi: 10.1146/annurev-immunol-032713-120231

5. Crosse KM, Monson EA, Beard MR, Helbig KJ. Interferon-stimulated genes as enhancers of antiviral innate immune signaling. *J Innate Immun* (2018) 10:85–93. doi: 10.1159/000484258

6. Jiang D, Guo H, Xu C, Chang J, Gu B, Wang L, et al. Identification of three interferon-inducible cellular enzymes that inhibit the replication of hepatitis c virus. *J Virol* (2008) 82:1665–78. doi: 10.1128/JVI.02113-07

7. Cho H, Proll SC, Szretter KJ, Katze MG, Gale MJr., Diamond MS. Differential innate immune response programs in neuronal subtypes determine susceptibility to infection in the brain by positive-stranded RNA viruses. *Nat Med* (2013) 19:458–64. doi: 10.1038/nm.3108

8. Shalem O, Sanjana NE, Hartenian E, Shi X, Scott DA, Mikkelson T, et al. Genome-scale CRISPR-Cas9 knockout screening in human cells. *Science* (2014) 343:84–7. doi: 10.1126/science.1247005

9. Zhao H, Lin W, Kumthip K, Cheng D, Fusco DN, Hofmann O, et al. A functional genomic screen reveals novel host genes that mediate interferon-alpha's effects against hepatitis c virus. *J Hepatol* (2012) 56:326–33. doi: 10.1016/j.jhep.2011.07.026

10. Richardson RB, Ohlson MB, Eitson JL, Kumar A, McDougal MB, Boys IN, et al. A CRISPR screen identifies IFI6 as an ER-resident interferon effector that blocks flavivirus replication. *Nat Microbiol* (2018) 3:1214–23. doi: 10.1038/s41564-018-0244-1

11. House JA, House C, Llewellyn ME. Characteristics of the porcine kidney cell line IB-RS-2 clone D10 (IB-RS-2 D10) which is free of hog cholera virus. *In Vitro Cell Dev Biol* (1988) 24:677–82. doi: 10.1007/BF02623605

12. Zhang X, Yang F, Li K, Cao W, Ru Y, Chen S, et al. The insufficient activation of RIG-I-Like signaling pathway contributes to highly efficient replication of porcine picornaviruses in IBRS-2 cells. *Mol Cell Proteomics* (2021) 20:100147. doi: 10.1016/j.mcpro.2021.100147

13. Bolger AM, Lohse M, Usadel B. Trimmomatic: a flexible trimmer for illumina sequence data. *Bioinformatics* (2014) 30:2114–20. doi: 10.1093/bioinformatics/btu170

14. Kim D, Langmead B, Salzberg SL. HISAT: a fast spliced aligner with low memory requirements. *Nat Methods* (2015) 12:357–60. doi: 10.1038/nmeth.3317

15. Trapnell C, Williams BA, Pertea G, Mortazavi A, Kwan G, van Baren MJ, et al. Transcript assembly and quantification by RNA-seq reveals unannotated transcripts and isoform switching during cell differentiation. *Nat Biotechnol* (2010) 28:511–5. doi: 10.1038/nbt.1621

16. Anders S, Pyl PT, Huber W. HTSeq–a Python framework to work with high-throughput sequencing data. *Bioinformatics* (2015) 31:166–9. doi: 10.1093/bioinformatics/btu638

17. D'Agostino PM, Amenta JJ, Reiss CS. IFN-beta-induced alteration of VSV protein phosphorylation in neuronal cells. *Viral Immunol* (2009) 22:353–69. doi: 10.1089/vim.2009.0057

18. Berger Rentsch M, Zimmer G. A vesicular stomatitis virus replicon-based bioassay for the rapid and sensitive determination of multi-species type I interferon. *PloS One* (2011) 6:e25858. doi: 10.1371/journal.pone.0025858

19. Perreira JM, Chin CR, Feeley EM, Brass AL. IFITMs restrict the replication of multiple pathogenic viruses. *J Mol Biol* (2013) 425:4937–55. doi: 10.1016/j.jmb.2013.09.024

20. Chen S, Liu Q, Zhang L, Ma J, Xue B, Li H, et al. The role of REC8 in the innate immune response to viral infection. *J Virol* (2022) 96:e0217521. doi: 10.1128/jvi.02175-21

21. Shaw AE, Hughes J, Gu Q, Behdenna A, Singer JB, Dennis T, et al. Fundamental properties of the mammalian innate immune system revealed by multispecies comparison of type I interferon responses. *PloS Biol* (2017) 15:e2004086. doi: 10.1371/journal.pbio.2004086

22. Rusinova I, Forster S, Yu S, Kannan A, Masse M, Cumming H, et al. Interferome v2.0: an updated database of annotated interferon-regulated genes. *Nucleic Acids Res* (2013) 41:D1040–6. doi: 10.1093/nar/gks1215

23. Chinsangaram J, Koster M, Grubman MJ. Inhibition of l-deleted foot-and-mouth disease virus replication by alpha/beta interferon involves double-stranded RNA-dependent protein kinase. *J Virol* (2001) 75:5498–503. doi: 10.1128/JVI.75.12.5498-5503.2001

24. Bishnoi S, Tiwari R, Gupta S, Byrareddy SN, Nayak D. Oncotargeting by vesicular stomatitis virus (VSV): Advances in cancer therapy. *Viruses* (2018) 10(2):90. doi: 10.3390/v10020090

25. Betancourt D, Ramos JC, Barber GN. Retargeting oncolytic vesicular stomatitis virus to human T-cell lymphotropic virus type 1-associated adult T-cell leukemia. *J Virol* (2015) 89:11786–800. doi: 10.1128/JVI.01356-15

26. Stark GR, Kerr IM, Williams BR, Silverman RH, Schreiber RD. How cells respond to interferons. *Annu Rev Biochem* (1998) 67:227–64. doi: 10.1146/annurev.biochem.67.1.227

27. Chapman WG, Ramshaw IA. Growth of the IB-RS-2 pig kidney cell line in suspension culture and its susceptibility to foot-and-mouth disease virus. *Appl Microbiol* (1971) 22:1–5. doi: 10.1128/am.22.1.1-5.1971

28. Blaszczyk K, Olejnik A, Nowicka H, Ozgyin L, Chen YL, Chmielewski S, et al. STAT2/IRF9 directs a prolonged ISGF3-like transcriptional response and antiviral activity in the absence of STAT1. *Biochem J* (2015) 466:511–24. doi: 10.1042/BJ20140644

29. Kraus TA, Lau JF, Parisien JP, Horvath CM. A hybrid IRF9-STAT2 protein recapitulates interferon-stimulated gene expression and antiviral response. *J Biol Chem* (2003) 278:13033–8. doi: 10.1074/jbc.M212972200

30. Kueck T, Bloyet LM, Cassella E, Zang T, Schmidt F, Brusic V, et al. Vesicular stomatitis virus transcription is inhibited by TRIM69 in the interferon-induced antiviral state. *J Virol* (2019) 93(24)::e01372-19. doi: 10.1128/JVI.01372-19

31. Schoggins JW. Recent advances in antiviral interferon-stimulated gene biology. *F1000Res* (2018) 7:309. doi: 10.12688/f1000research.12450.1

32. Chemudupati M, Kenney AD, Bonifati S, Zani A, McMichael TM, Wu L, et al. From APOBEC to ZAP: Diverse mechanisms used by cellular restriction factors to inhibit virus infections. *Biochim Biophys Acta Mol Cell Res* (2019) 1866:382–94. doi: 10.1016/j.bbamcr.2018.09.012

33. Kane M, Zang TM, Rihn SJ, Zhang F, Kueck T, Alim M, et al. Identification of interferon-stimulated genes with antiretroviral activity. *Cell Host Microbe* (2016) 20:392–405. doi: 10.1016/j.chom.2016.08.005

34. Hong XX, Carmichael GG. Innate immunity in pluripotent human cells: attenuated response to interferon-beta. *J Biol Chem* (2013) 288:16196–205. doi: 10.1074/jbc.M112.435461

35. Makowska Z, Duong FH, Trincucci G, Tough DF, Heim MH. Interferon-beta and interferon-lambda signaling is not affected by interferon-induced refractoriness to interferon-alpha *in vivo*. *Hepatology* (2011) 53:1154–63. doi: 10.1002/hep.24189

frontiers | Frontiers in Immunology

TYPE Original Research
PUBLISHED 30 November 2022
DOI 10.3389/fimmu.2022.1007718

OPEN ACCESS

EDITED BY
Chang Li,
Chinese Academy of Agricultural Sciences (CAAS), China

REVIEWED BY
Renfeng Li,
Virginia Commonwealth University, United States
José (Pepe) Alcami,
Carlos III Health Institute (ISCIII), Spain
Yutong Zhao,
The Ohio State University, United States
Dan Lu,
Peking University, China

*CORRESPONDENCE
Dongrong Yi
dongrong.yi@imb.pumc.edu.cn
Long Yang
long.yang@tjutcm.edu.cn
Shan Cen
shancen@imb.pumc.edu.cn

†These authors have contributed equally to this work

SPECIALTY SECTION
This article was submitted to Molecular Innate Immunity, a section of the journal Frontiers in Immunology

RECEIVED 30 July 2022
ACCEPTED 11 November 2022
PUBLISHED 30 November 2022

CITATION
An N, Ge Q, Shao H, Li Q, Guo F, Liang C, Li X, Yi D, Yang L and Cen S (2022) Interferon-inducible SAMHD1 restricts viral replication through downregulation of lipid synthesis. *Front. Immunol.* 13:1007718. doi: 10.3389/fimmu.2022.1007718

Interferon-inducible SAMHD1 restricts viral replication through downregulation of lipid synthesis

Ni An[1†], Qinghua Ge[1†], Huihan Shao[1], Quanjie Li[1], Fei Guo[2], Chen Liang[3], Xiaoyu Li[1], Dongrong Yi[1*], Long Yang[4*] and Shan Cen[1*]

[1]Institute of Medicinal Biotechnology, Chinese Academy of Medical Science, Beijing, China, [2]Institute of Pathogen Biology, Chinese Academy of Medical Science, Beijing, China, [3]Lady Davis Institute for Medical Research and McGill AIDS Centre, Jewish General Hospital, Montreal, QC, Canada, [4]Research Center for Infectious Diseases, Tianjin University of Traditional Chinese Medicine, Tianjin, China

Background: Type I interferon (IFN) inhibits virus infection through multiple processes. Recent evidence indicates that IFN carries out its antiviral activity through readjusting of the cellular metabolism. The sterile alpha motif and histidine-aspartate domain containing protein 1 (SAMHD1), as an interferon-stimulated gene (ISG), has been reported to inhibit a number of retroviruses and DNA viruses, by depleting dNTPs indispensable for viral DNA replication. Here we report a new antiviral activity of SAMHD1 against RNA viruses including HCV and some other flaviviruses infection.

Methods: Multiple cellular and molecular biological technologies have been used to detect virus infection, replication and variation of intracellular proteins, including western blotting, qRT-PCR, Gene silencing, immunofluorescence, etc. Besides, microarray gene chip technology was applied to analyze the effects of SAMHD1 overexpression on total expressed genes.

Results: Our data show that SAMHD1 down-regulates the expression of genes related to lipid bio-metabolic pathway, accompanied with impaired lipid droplets (LDs) formation, two events important for flaviviruses infection. Mechanic study reveals that SAMHD1 mainly targets on HCV RNA replication, resulting in a broad inhibitory effect on the infectivity of flaviviruses. The C-terminal domain of SAMHD1 is showed to determine its antiviral function, which is regulated by the phosphorylation of T592. Restored lipid level by overexpression of SREBP1 or supplement with LDs counteracts with the

10.3389/fimmu.2022.1007718

antiviral activity of SAMHD1, providing evidence supporting the role of SAMHD1-mediated down-regulation of lipid synthesis in its function to inhibit viral infection.

Conclusion: SAMHD1 plays an important role in IFN-mediated blockade of flaviviruses infection through targeting lipid bio-metabolic pathway.

KEYWORDS

SAMHD1, lipid droplets (LDs), SREBP1, HCV, interferon

Introduction

Viral replication is a high energy-consuming process that totally counts on host metabolism. Therefore, viruses have evolved to hijack and regulate synthesis of proteins, nucleic acids, and lipids to serve their infection and replication. To combat virus infection, the host has developed a highly complicated immunity system to monitor and maintain a normal metabolic process. Interferon (IFN) signaling, as an important member of innate immunity, enhances and induces a good deal of interferon-stimulated genes (ISGs) to restrain viral infection. Besides directly targeting viral component, they also join in the regulation of cellular metabolism, both of which produce inhibitive effects on viral infection. Recent studies have illuminated the specific roles of ISGs in adjusting cellular metabolism to contain viral infection. Several of these ISGs, the sterile alpha motif and histidine-aspartate domain containing protein 1 (SAMHD1), spermidine/spermine acetyltransferase 1 (SAT-1), cholesterol-25-hydroxylase (CH25H), and indoleamine-2,3-dioxygenase (IDO1), exert antiviral activity against multiple viruses by manipulating different metabolic pathways (1). For instance, CH25H is able to transfer cholesterol to the oxysterol 25-hydroxycholesterol that represents a well-defined regulator of sterol biosynthesis, thus exerting its antiviral activity (2). Upregulation of SAT-1 by IFNs results in downregulation of polyamine, thereby suppressing replication of polyamine-dependent viruses (3). Deprivation of L-tryptophan by IFN-inducible IDO1 results in a strong blockade of viral protein synthesis (4).

As a homologous gene of mouse Mg11, SAMHD1 gene was originally discovered in human dendritic cells (5). Subsequently, more studies indicated that SAMHD1 could be upregulated by different types of IFNs in various cells, especially in resting CD4+ T cells and myeloid cells (6). A recent study reveals that SAMHD1 possesses dNTP hydrolase activity and catalyzes the transformation of deoxynucleoside triphosphates to inorganic triphosphate and deoxynucleoside (7). The structure of SAMHD1 protein mainly comprises a sterile alpha motif (SAM), a histidine aspartic acid-containing domain (HD), and a C-terminus domain (8). The HD domain of SAMHD1 is the most important part for maintaining the oligomeric state of dNTPase, enhancing nucleic acid interaction and exerting antiviral activity (9). Depletion of dNTPs required for viral DNA synthesis was regarded as the main antiviral mechanism. Thereby, a wide range of retroviruses and DNA viruses, including HIV, T cell leukemia virus type 1, HBV, HSV-1, and vaccinia virus, were sensitive to the suppression of SAMHD1 (10–13). Although some experimental results prove that the anti-HIV-1 activity of SAMHD1 is closely related to intracellular dNTP levels, exogenous addition of dNTP does not completely relieve the inhibitory effect of SAMHD1 and restore the replication of HIV-1, indicating that SAMHD1 is likely to have a dNTPase-independent antiviral mechanism. Consistent with this notion, the phosphorylation of SAMHD1 at Threonine 592 located in the C-terminus peptide significantly affects the antiviral capacity, but not the dNTPase domain of SAMHD1 (14). Therefore, the mechanism underlying the antiviral activity of SAMHD1 awaits further investigation.

The life cycle of the flavivirus is closely related with the host lipids that are involved in viral entry, RNA replication, and assembly (15). Because they lack their own machinery to execute lipid synthesis, flaviviruses have to hijack host lipids to complete their intracellular replication. They also enhance cholesterol and fatty acid (FA) synthesis to generate viral membranes and produce ATP, suggesting that such viruses could manipulate lipid synthesis (16, 17). LDs are ER-related organelles associated with diverse cellular processes including lipid trafficking, immunity, cellular signaling, and virus replication (18–20). Lysosomes degrade LDs to release stored lipids for energy supply, which is effectively and efficiently hijacked by flaviviruses to support their own replication (21). Therefore, it is conceivable that type I IFN signaling may regulate FA and cholesterol synthesis and thereby prevent the infection of flavivirus and other viruses that depend on lipid synthesis. In agreement with this, 25-hydroxycholesterol (25-HC), a secreted IFN-induced protein, exhibits its wide-ranging antiviral functions through inhibiting sterol regulatory element binding protein (SREBP1) activation (22). SREBP1 is involved in

enhancing cholesterol production by increasing the intake of LDL and synthesis of cholesterol (23).

In this work, we provide evidence showing that SAMHD1 plays a new role in negatively regulating both SREBP1 expression and LD formation, impairs HCV RNA replication, and inhibits the infectivity of HCV and other flavivirus. This work suggests that SAMHD1 may act as an innate immune effector to restrict flaviviridae family and other lipid-dependent viruses.

Materials and methods

Plasmid construction

Full-length SAMHD1 cDNA and the cDNA fragment encoding SAMHD1 truncations (base pairs 1–582, 45–626, and 112–626 of SAMHD1 cDNA) with Myc tag sequences were cloned into the pcDNA4.0 vector (Invitrogen) using the *Kpn*I and *Eco*RI restriction sites. SAMHD1 point mutations (T592A and T592D) were generated by using a site-directed mutagenesis kit (SBS). The plasmid of infectious HCV DNA clone (JFH1) was kindly offered by Takaji Wakita. The HCV 5' untranslated region (UTR) and 3'UTR sequences were cloned into the 5'-terminus and 3'-terminus of the Renilla luciferase reporter gene, respectively, to construct a reporter gene translation system mediated by HCV IRES. The primers were designed as follows: for 5'UTR, 5'-CCCAAGCTTAC CTGCCCCTAATAGGGGCG-3'/5'-CGGGATCCGTTGGTGTTT CTTTTGGT-3'; for Rluc, 5'-CGGGATCCATGACCAGCAAGG TGTACGA-3'/5'-CCGCTCGAGTTACTGCTCGTTCTTCA GCA-3'; for 3'UTR, 5'-CCGCTCGAGAGCGGCACACACTAGGT ACA-3'/5'-GGGCCCACATGATCTGCAGAGAGACC-3'; and for T7-Rluc, 5'-TAATACGACTCACTATAGGACCTGCCCCTAA TAGGGGCG-3'/5'-CCGCTCGAGTTACTGCTCGTTCTT CAGCA-3'.

Cell culture and transfection

All cells including Huh7.5.1 cells (kept in our lab), Huh7 cells (kept in our lab), Vero cells (CCL-81; ATCC), Huh7 cell line containing the JFH1-derived subgenomic replicon (JFH1; HCV subtype 2a) (kept in our lab), and HEK293T cells (CRL-11268; ATCC) were cultured in Dulbecco's modified Eagle's medium (DMEM) (Gibco) with 10% fetal bovine serum (FBS) at 37°C with 5% CO_2. Plasmids and mRNA were respectively transfected into cells with Lipofectamine 2000 (Invitrogen) and Vigofect (Vigorous) in line with the manufacturer's instructions.

Production of JFH1 HCVcc

JFH1 (HCV subtype 2a) mRNA was produced by using an *in vitro* RNA transcription kit (Ambion) according to the manufacturer's instructions and then transfected into Huh7.5.1 cells with Lipofectamine RNAi Max (Invitrogen). At 72 hpt, culture supernatants were collected for cell debris removement and further concentration and then stored at −80°C. The 50% tissue culture infective dose ($TCID_{50}$) of the HCV stock was determined by gradient dilution assay and immunofluorescence staining.

Virus infections

A total of 5×10^5 per well of Huh7.5.1 cells (or SAMHD1-KD Huh7.5.1 cells) were seeded into six-well plates for 24 h before transfection with pSAMHD1. At 48 hpt, JFH1 HCVcc was used to infect cells overexpressing SAMHD1 at an MOI = 0.2. After 72 h of incubation, cells were harvested for virus (or host) proteins or RNA analysis and supernatants were used for progeny virus analysis. Vero cells were used to infect cells with Japanese encephalitis virus (JEV) (SA14-14-2) or dengue virus 2 (DENV2) (Tr1751). JEV RNA and DENV2 titer were respectively measured by qRT-PCR and plaque assay to determine their own infection level.

Western blotting

Cells were lysed in cell lysis solution (Pierce) on ice for 1 h and centrifuged at 12,000 rpm for 5 min to remove cell debris. The supernatants were subjected to SDS-PAGE. Proteins were then transferred to a 0.45-μm polyvinylidene difluoride (PVDF) membrane and labeled with specific antibodies. The antibodies used in this subject were as follows: anti-MYC (9E10, 1:1,000), anti-HA (H9658, 1:1,000), anti-FLAG (F1804, 1:1,000), and anti-beta-actin (A2066, 1:1,000) were from Sigma; anti-SAMHD1 (ab67820, 1:1,000), anti-NS3 (ab65407, 1:1,000), and anti-Core (ab2740, 1:1,000) were from Abcam; anti-SREBP-1 (39940, 1:1,000) was from Active Motif; HRP-conjugated goat anti-mouse (ZSGB-Bio, catalog ZB2305, 1:5,000) and goat anti-rabbit (ZSGB-Bio, catalog ZB2301, 1:5,000) were secondary antibodies.

Gene silencing

siRNAs were transfected into Huh7.5.1 cells seeded into six-well plates by using LipofectamineTM RNAimax (Invitrogen, catalog 13778-150) at the concentration of 50 pmol/well. siRNAs were purchased from JSTBIO; siNT: target sequences 5′-UUC UCC GAA CGU GUC ACG UTT- 3′ and 5′-ACG UGA CAC GUU CGG AGA ATT- 3′; SAMHD1 siRNA: target sequences 5′- CCU CGU CCG AAU CAU UGA UTT -3′ and 5′-AUC AAU GAU UCG GAC GAG GTT -3′.

qRT-PCR

Virus RNA or cellular RNA was isolated with TRIzol reagents (Invitrogen) according to the manufacturer's protocols. Quantification of viral RNA was measured by the use of the one-step SYBR PrimeScript RT-PCR kit (Takara). The primer pair (5′-GCGTTAGTATGAGTGTCGTG-3′ and 5′-TCGCAAGCACCCTATCAG-3′) amplifies the 5′ UTR of HCV. The primer pair (5′-ACAATCATGGCAAACGACAA-3′ and 5′-CTTCTCGTTGTGGGCTTCTC-3′) was used to detect JEV RNA. Glyceraldehyde-3-phosphate dehydrogenase (GAPDH) RNA were selected as an internal control to normalize viral RNA through amplifying with primers 5′-ATCATCCCTGCCTCTACTGG-3′ and 5′-GTCAGGTCCAC CACTGACAC-3′.

Progeny virus analysis

After HCVcc infection, part of the culture medium was collected for qRT-PCR or ELISA tests. qRT-PCR analysis was used to quantify copies of HCV RNA extracted from 200 µl of culture medium by RNA extraction kit (Tiandz), and JFH1 mRNA transcribed *in vitro* was set as the standard substance. Some culture medium was directly applied for ELISA (Laibo Bio) to detect HCV core protein released in supernatants. To measure the infection level of progeny virus, 1 ml of culture medium was incubated with naïve Huh7.5.1 cells seeded in six-well plates for another 72 h. Then, cells were harvested for qRT-PCR and immunofluorescence staining to detect HCV RNA and protein symbolizing the infection level of progeny virus.

Immunofluorescence staining

Cells were firstly fixed in 4% paraformaldehyde and permeabilized with 0.2% Triton X-100 at room temperature. After washing three times with 1× PBS, cells were incubated with primary antibodies for 1 h at room temperature with gentle shaking, then followed by adding Alexa Fluor-conjugated secondary antibodies [donkey anti-mouse antibody (Alexa Fluor 488) and donkey anti-rabbit antibody (Alexa Fluor 555)] for another 1 h after washing. DAPI was used to stain nuclei. Images were recorded with a PerkinElmer Ultra View VoX confocal imaging system.

Gene chip

The data analysis of gene expression profiling chip is performed by using the Rosetta Resolver System for data preprocessing and Cluster analysis was carried out using Eisen S Laboratory Cluster 3.0 and the TreeView software (http://rana.lbl.gov/EisenSoftware.htm). Principal component analysis (PCA) with ArrayTrack (http://edkb.fda.gov/webstart/arraytrack/), the DAVID 6.7 online database (http://david.abcc.ncifcrf.gov/), and the KEGG pathway database (http://www.genome.jp/kegg/) were used to express change that is greater than twofold that from the genetic analysis of signaling pathways.

Total cellular cholesterol analysis

Huh7.5.1 cells were seeded in six-well plates and subsequently transfected with or without pSAMHD1. After 24 h, cells were lysed with hypotonic buffer (25 mM Tris-HCl, 5 mM EDTA, 1 mM dithiothreitol, and protease inhibitor cocktail, pH 7.4) and homogenized with a 22-gauge needle. The sample supernatants were collected by centrifugation at 3,000 rpm for 10 min. Total cellular cholesterol was detected by using an Amplex Red Cholesterol Assay Kit (ThermoFisher Scientific) according to the manufacturer's instructions.

High content screening

Prior to high content screening (HCS) platform analysis, HCV core protein and SAMHD1 protein in cells were labeled with fluorescence according to immunofluorescence staining. The correlation of fluorescence intensity between SAMHD1 and HCV core protein was detected by the CellInsight CX5 HCS platform (Thermo Fisher Scientific) with a ×10 objective. HCS Studio™ cell analysis software was applied to quantify proteins based on their own signal intensity. A limit was typically set on cells without SAMHD1 overexpressing.

Construction of the SAMHD1 knock out Huh7.5.1 cell line

SgRNAs targeting SAMHD1 were designed and cloned into the lentiCRISPRv2 backbone. The sgRNA oligos were shown as follows: SAMHD1 sense: caccgCGGAAGGGGTGTTTG AGGGG and antisense: aaacCCCCTCAAACACCCCTTCCGc. The oligos were annealed (5 min at 95°C; 2 min at 85°C; 2 min at 65°C; 2 min at 45°C; 2 min at 25°C) and ligated into lentiCRISPRv2 by the *Bsm*BI restriction site. HEK293T cells were transfected with lentiCRISPRv2-sgRNA targeting SAMHD1, pVSVG, and psPAX2 to produce lentivirus, and then lentivirus containing lentiCRISPRv2-sgRNA targeting SAMHD1 was used to infect Huh7.5.1 cells in the presence of 2 µg/ml puromycin. After 2–4 weeks of monoclonal selection, the level of endogenous SAMHD1 expression was monitored by Western blotting.

mRNA decay assay

Huh7.5.1 cells seeded in six-well plates were transfected with plasmid expressing SAMHD1 or pcDNA4.0 set as a control for 24 h, and then 5 μg/ml actinomycin D was added into culture medium for the next 12 h. After treatment with actinomycin D, cells were harvested at five consecutive time points (0, 3, 6, 9, and 12 h) for RNA extraction and qRT-PCR analysis. SREBP1 mRNA abundance was detected by a primer pair (5′-GCGCAGAT CGCGGAGCCAT-3′ and 5′-CCCTGCCCCACTCCCAGCAT-3′) and normalized to GAPDH mRNA. Curves were fitted to mRNA signal and time by linear regression. mRNA half-lives were calculated using the following equation: t1/2 = ln(2)/k, where k is the elimination rate constant.

Dual-luciferase reporter gene assay

A predicted regulatory region of a 5′ flanking sequence (−1,500 bp to +55 bp) of SREBP1 was cloned into a pGL3-Basic vector containing a firefly luciferase reporter gene (Promega, Madison, Wisconsin, USA) by the *Kpn* I and *Hind* III restriction sites. The empty pGL3-Basic vector was used as the negative control. The phRL-TK vector containing a Renilla luciferase reporter gene (Promega, Madison, Wisconsin, USA) was used as internal reference in the Dual-luciferase Reporter Assay System. HEK293T cells seeded in six-well plates were co-transfected with 800 ng of SAMHD1 plasmid, 800 ng of the pGL3-Basic-SREBP1 promoter, and 20 ng of phRL-TK by Lipofectamine 2000. pcDNA4.0 was set as a control. After 48 h, cells were lysed and the luciferase activities in cell lysates was monitored by a Dual Luciferase Assay kit (Vazyme, Nanjing, China). The relative luciferase activities are shown as a ratio of the firefly luciferase activity to that of the Renilla luciferase.

Statistical analysis

All results are shown as the mean ± standard deviation (SD). A two-tailed, unpaired Student's *t*-test in the GraphPad Prism software was used for statistical analysis. Statistical significance between two groups was marked as follows: $p < 0.05$ (*), $p < 0.01$ (**), and $p < 0.001$ (***). "n.s." stands for "not significant".

Results

SAMHD1 negatively regulates fatty acid synthesis of the cell

To investigate the role of SAMHD1 in regulating host gene expression, we performed genome-wide gene expression profile analysis of SAMHD1-overexpressing Huh7.5.1 and control cells using microarray gene chip technology, and identified approximately 153 differentially expressed genes ($p < 0.01$, log2 fold change [FC] > 1) (Supplementary Table S1). GO pathway enrichment analysis of the differentially expressed genes revealed upregulated mRNAs mainly related to the pathways of cytokine–cytokine interaction, MAPK signaling and chemotactic signaling, and the downregulated mRNAs found in metabolic pathways such as FAs, amino acid metabolism, and terpenoid synthesis.

Since lipid synthesis was reported to participate in host immune and viral replication, we next focus on the investigation of the inhibitory effect of SAMHD1 on expression of genes related to FA metabolism. In agreement with the results of gene expression profile analyses, quantification RT-PCR analysis showed that the expression of SAMHD1 resulted in significant reduction in mRNA abundance of several genes related to the FA bio-metabolic pathway and cholesterol synthesis, including SREBP1, SCD5, and ELOVL6 (Figure 1A; Table S2). Interestingly, SREBP1 mRNA was the most reduced among them, which encodes a key lipid transcription factor that controls gene expression relevant to FA synthesis. In line with the decreased level of SREBP1 mRNA, the expression of endogenous SREBP1 at the protein level was significantly reduced in the presence of SAMHD1 (Figure 1B). To further assess the downregulation of endogenous SREBP1 mRNA by SAMHD1, we applied mRNA decay assay and Dual-luciferase reporter gene assay to measure the impact of SAMHD1 on the stability of mRNA and promoter activity. Figure 1B indicates that SREBP1 mRNA had a shorter half-life under the condition of SAMHD1 overexpression, whereas the promoter activity of SREBP1 mRNA was insensitive to exogenous SAMHD1 (Figure 1C). This suggests that SAMHD1 reduces the level of SREBP1 mRNA through impairing the stability of mRNA but not mRNA transcription, which contributes to the decrease of SREBP1 protein. Accordingly, the exogenous expression of SAMHD1 significantly downregulates the total level of intracellular cholesterol to approximate 25%–35% of the control group (Figure 1D). Furthermore, the immunofluorescence assay revealed that lipid droplets (LDs) were significantly reduced about 50% in the SAMHD1-expressing cells compared with that of control cells (Figures 1E, F). These results together suggest an important function of SAMHD1 in negatively regulating cholesterol synthesis and the formation of LDs.

The antiviral activity of SAMHD1 against flaviviruses

More evidence indicated the involvement of cellular LDs at different steps of the life cycle of flaviviruses. The inhibitory effect of SAMHD1 on the formation of LDs presented herein inspires us whether SAMHD1 restricts the replication of HCV

10.3389/fimmu.2022.1007718

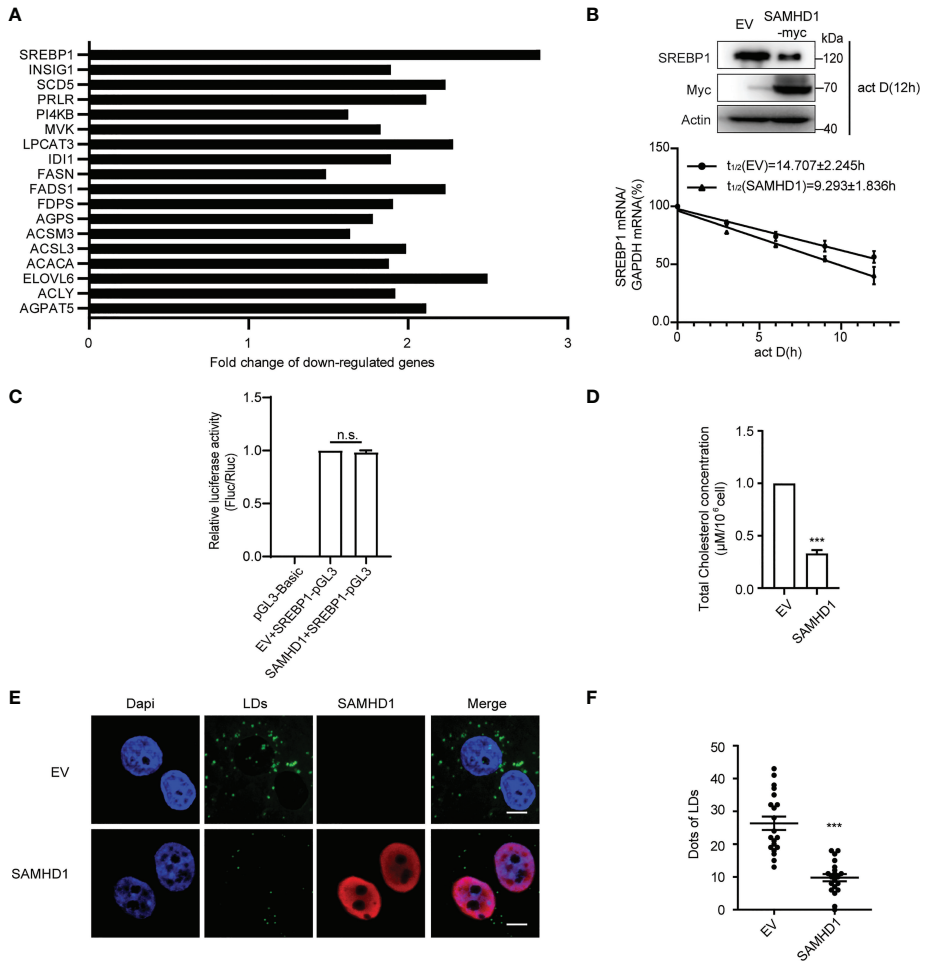

FIGURE 1
SAMHD1 negatively regulates fatty acid synthesis of cell. **(A)** Plasmid expressing SAMHD1 was transfected into Huh7.5.1 cells for 48 h, pcDNA4.0 was set as a control, and then cells were applied for quantification of genes associated with lipid metabolism by qRT-PCR analysis. The relative changes in gene expression were analyzed by using the $2^{-\Delta\Delta CT}$ method (Livak method). **(B)** mRNA decay assay was applied to measure the level of SREBP1 mRNA in SAMHD1-overexpressing cells at five consecutive time points (0, 3, 6, 9, and 12 h) in the presence of 5 μg/ml actinomycin D Decay of SREPBP1 mRNA is depicted after normalization to GAPDH mRNA and mRNA half-lives are calculated (mean values ± SD; *n* = 3). The expression of endogenous SREBP1 and extrogenous SAMHD1 proteins at 12 h post-addition of actinomycin D was analyzed by Western blotting. **(C)** HEK392t cells were transfected with plasmid encoding SAMHD1-myc (or pcDNA4.0), pGL3-Basic-SREBP1 promoter, and phRL-TK for 48 h; promoter activities were indicated as a ratio of Firefly luciferase/Renilla luciferase. Data are shown as mean values ± SD (*n* = 3). Values of the EV +SREBP1-pGL3 group arbitrarily set to 1. **(D)** Huh7.5.1 cells were transfected with pSAMHD1 or empty vector for 48 h. Cell lysates were objected to total cholesterol analysis. Data are presented as mean ± SD (*n* = 3). **(E)** SAMHD1 suppresses the formation of LDs. Huh7.5.1 cells with SAMHD1 overexpressing were analyzed by immunofluorescence staining. LDs, SAMHD1, and nucleus were respectively stained with BODIPY493/503 (green), anti-myc antibody (red), and DAPI (blue). Representative images are shown. Bars, 5 μm. **(F)** LD signals were statistical analyzed for 20 randomly selected cells by the use of Image-Pro Plus 7.0C software and plotted as a histogram. Data are shown as mean ± SD. ns, not significant; ***P<0.001.

and other flaviviruses. To address it, we investigated the replication of HCV and several flaviviruses, including JEV and DENV in SAMHD1-expressing cells, which were determined by viral genomic RNA (for HCV and JEV) or virus titer (for DENV). As shown in Figure 2, SAMHD1 exhibited different inhibitory effects on the replication of HCV, JEV, and DENV. These results suggest that SAMHD1 may serve as an innate immunity factor to control flavivirus infection. It is worth noting that overexpression of SAMHD1 had no influence on the replication of influenza A virus and enterovirus EV71 (data not shown), suggesting the specificity of its antiviral activity.

SAMHD1 inhibits HCV replication

To further understand the antiviral mechanism of SAMHD1, we investigated the effect of SAMHD1 on viral gene expression and production of HCV. Huh7.5.1 cells

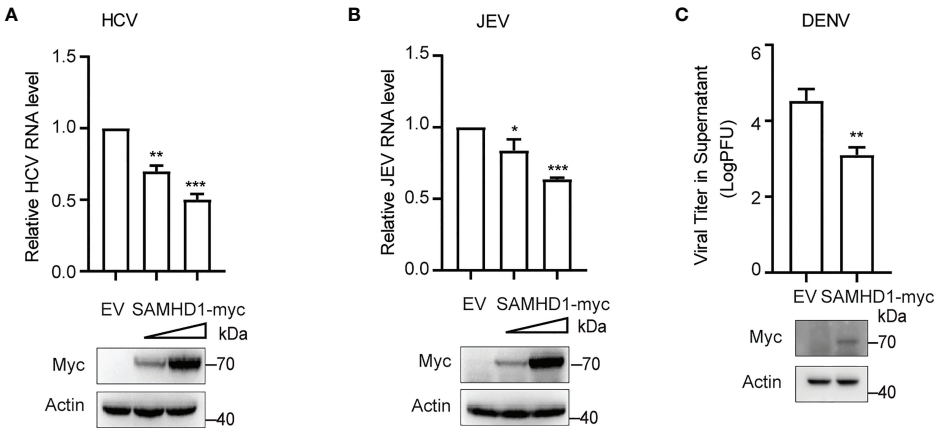

FIGURE 2
SAMHD1 inhibits the flavivirus infection. Normal Huh7.5.1 cells were transfected with plasmid encoding N-terminal myc-tagged SAMHD1 or pcDNA4.0 for 24 h followed by infection with **(A)** JFH1 HCVcc (MOI = 0.2), **(B)** JEV (MOI = 0.2), and **(C)** DENV (MOI = 0.2), respectively. At 48 hpi, total cellular RNA was isolated by using Trizol reagent for qRT-PCR analysis. HCV and JEV infection levels were evaluated by viral RNA in cells, and viral titer analysis was used for measurement of DENV infection level. Cell lysates were analyzed by Western blotting to determine expression levels of SAMHD1 and β-actin proteins. Data are shown as mean ± SD and depicted as histogram representative of three independent experiments. *P<0.05; **P<0.01, and ***P<0.001.

transiently expressing N-terminal myc-tagged SAMHD1 were infected with JFH1 HCVcc (MOI = 0.2), followed by quantification of cellular viral protein and RNA level and virus production, using immunoblot and qRT-PCR, respectively. These results showed that overexpressing SAMHD1 exhibited a similar inhibitory effect (approximately 50% inhibition at a higher level of SAMHD1) on viral protein (Figure 3A) and RNA (Figure 3B) levels and virus production (Figure 3C). This suggests that SAMHD1 mainly targets the early step of HCV replication, and impaired virus production most likely is a result of the reduction of viral gene expression. We further examined the anti-HCV activity of SAMHD1 by immunostaining HCV capsid protein in the infected cells. Data of HCS showed significant inhibition of HCV core expression in the SAMHD1-positive cells (Figure 3D), and quantification analysis revealed that almost 60% core protein expression was inhibited at the highest SAMHD1 protein level (Figure 3E). We also noticed that approximately only 70% of the cells expressed SAMHD1, which shows a significant inhibition of HCV core expression by SAMHD1, and also indicates a probable underestimation of the anti-HCV capacity of SAMHD1 shown by the results in Figures 3A-C.

Besides testing the antiviral activity of SAMHD1 overexpression, we also examine the anti-HCV activity of endogenous SAMHD1. SAMHD1 protein expression was strongly induced by IFN-α2b in the Huh7.5.1 cell line and successfully depleted by use of two different small interfering RNAs (siRNAs) (Figure 4A). To further confirm the anti-HCV activity of endogenous SAMHD1, we applied these siRNAs targeting SAMHD1 to a Huh7 cell line containing JFH1 subgenomic replicon, followed by the quantification of HCV NS3 and core proteins and RNA level, using immunoblot and qRT-PCR. As Figure 4B shows, knockdown of SAMHD1 led to the increase of NS3 and core protein expression and 36% elevation of HCV RNA level, which strongly displayed the inhibition of endogenous SAMHD1. To further confirm the antiviral activity of endogenous SAMHD1, we constructed a SAMHD1 knockout Huh7.5.1 cell line by CRISPR-Cas9 technology and infected with JFH1 HCVcc, followed by detection of progeny virus through qRT-PCR, ELISA, and immunofluorescence analysis. As Figures 4C-E show, depletion of endogenous SAMHD1 profoundly rescued HCV RNA proteins released in culture medium by threefold and elevated the infection level of progeny virus. Extrogenous expression of SAMHD1 in SAMHD1-KO Huh7.5.1 cells exhibited a stronger inhibition (approximately 70% inhibition at a higher level of SAMHD1) than in normal Huh7.5.1 cells, which suggests endogenous SAMHD1 indeed possesses antiviral activity. Taken together, both extrogenous and endogenous SAMHD1 are able to negatively regulate the HCV replication.

The C-terminus of SAMHD1 is required for its anti-HCV activity

To determine the domains of SAMHD1 involved in its antiviral activity, we analyzed the inhibitory effect of three SAMHD1 truncations on HCV replication, which consist of residues 45–626, 112–626, and 1–582, representing removal of nuclear localization signal (NLS), SAM, and C-terminal

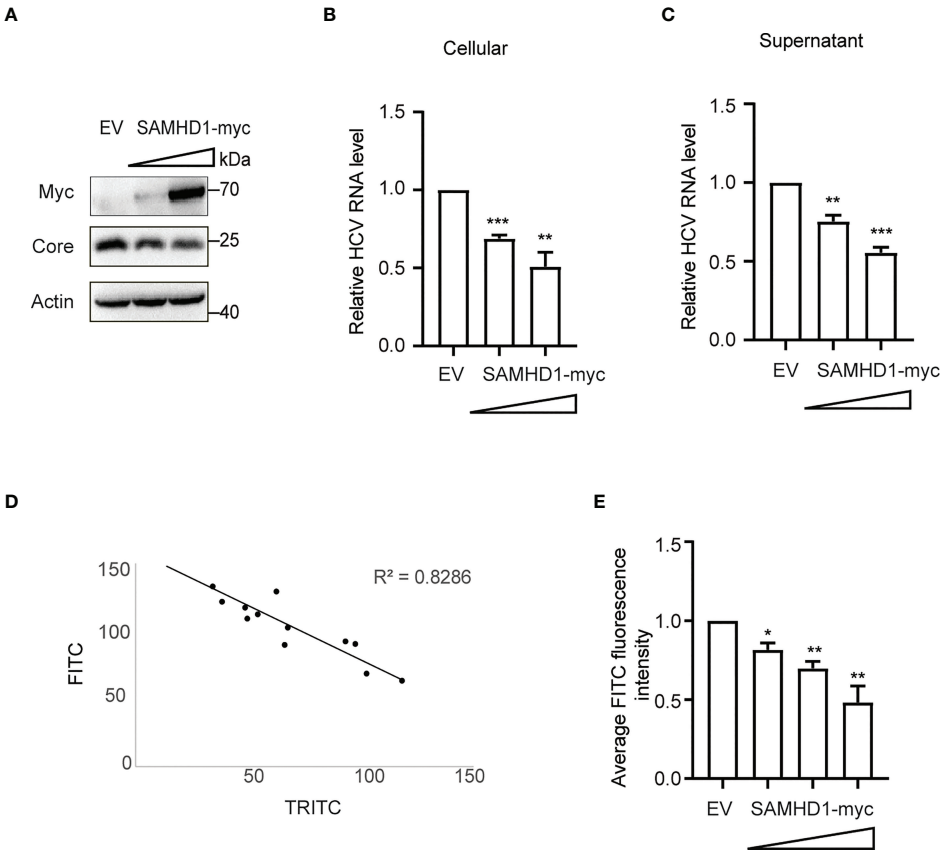

FIGURE 3
Extrogenous SAMHD1 inhibits HCV replication. Huh7.5.1 cells with extrogenous SAMHD1 overexpression were infected with JFH1 HCVcc (MOI = 0.2) for 48 h. **(A)** Cell lysates were detected by Western blotting to analyze the expression levels of SAMHD1 and HCV core proteins. β-actin was used as a sample loading control. **(B)** Levels of HCV RNA in cells were evaluated by qRT-PCR. **(C)** Levels of infectious progeny viruses in culture supernatants were tested by infecting naïve Huh7.5.1 cells, followed by qRT-PCR analysis of HCV RNA in cells at 72 hpi. All of the data are representative of three independent experiments. For panels **(B, C)** data of SAMHD1 groups are normalized to the control group, whose value is set to 1. **(D)** Huh7.5.1 cells with extrogenous SAMHD1 overexpressing infected with JFH1 HCVcc and processed by immunofluorescence staining. The correlation between fluorescence intensity of SAMHD1 (TRITC) and HCV core proteins (FITC) was detected by high content screening. **(E)** Data of the inhibition on average fluorescence intensity of HCV core protein by different concentrations of extrogenous SAMHD1 are plotted as a histogram. The value of the control group is arbitrarily set to 1 (mean values ± SD; *n* = 3). *P<0.05; **P<0.01, and ***P<0.001.

domains, respectively. Huh7.5.1 cells were transfected with plasmid coding for these truncations, followed by HCV infection. Results of Western blotting showed that, similar to wild-type SAMHD1, the expression of 45–626 and 112–626 but not 1–582 truncations significantly reduced the expression of the HCV core protein, which was verified by a twofold reduction in HCV RNA level determined by qRT-PCR (Figure 5A), suggesting the importance of SAMHD1 C-terminus in its anti-HCV activity.

It is worth noting that SAMHD1 is regulated by phosphorylation of its C-terminal domain at Thr-592, which annihilates its antiviral function yet has only a small effect on its phosphohydrolase activity. In order to study the relationship between the phosphorylation of Thr-592 and its antiviral activity, we mutated 592 T to A (not phosphorylated) or D (phosphomimetic), and transfected them into Huh7.5.1 cells using SAMHD1 as a positive control followed by infection with JFH1 HCVcc. Interestingly, we found that when we mutated the threonine at position 592 of SAMHD1 to alanine (T→A), which could not be phosphorylated, the expression of core protein was further reduced compared to the wild-type SAMHD1 group (Figure 5B). The antiviral effect of SAMHD1 disappeared after we permanently phosphorylated the threonine at position 592 of SAMHD1 to alanine (T→D), indicating that T592 phosphorylation significantly reduced the antiviral effect of SAMHD1.

To rule out the impact of endogenous SAMHD1 and accentuate the antiviral activities of SAMHD1 truncations and mutants, we transfected plasmids expressing SAMHD1 truncations and mutants in SAMHD1-KO Huh7.5.1 cells

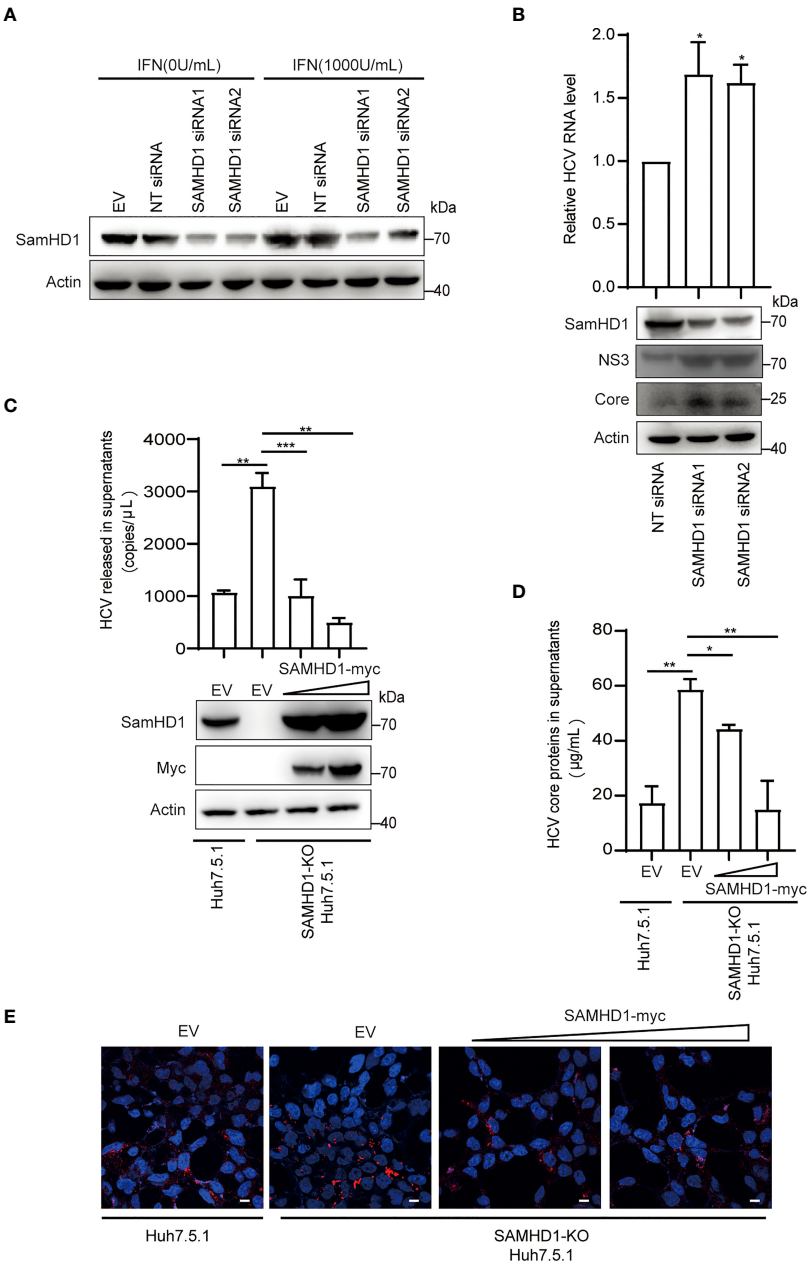

FIGURE 4
Endogenous SAMHD1 participates in HCV inhibition. **(A)** Huh7.5.1 cells were transfected with 50 pmol/ml siRNAs targeting SAMHD1 or non-targeting siRNA (NT siRNA) for 24 h, and followed by the addition of IFN-α2b (1,000 U/ml) for another 48 h. Cell lysates were analyzed by Western blotting to determine the expression level of endogenous SAMHD1 protein. **(B)** Huh7 cells containing JFH1 subgenomic replicon were transfected with two different siRNAs targeting SAMHD1 for 48 h, and then a part of cells was harvested for measurement of HCV structural or non-structural proteins (core and NS3) by Western blotting. The other part of the cells was applied for total RNA extraction and qRT-PCR analysis. Values are shown as means ± SD (n = 3) and the value of the control group is set to 1. **(C–E)** A SAMHD1 knockout Huh7.5.1 cell line constructed by CRISPR-Cas9 technology was used to transfect plasmid expressing SAMHD1 and incubated with JFH1 HCVcc for an additional 48 h; normal Huh7.5.1 cells and pcDNA4.0 were respectively treated as cell control and plasmid control, and HCV RNA and HCV core proteins in culture medium were quantified by qRT-PCR **(C)** and ELISA **(D)**. Data are representative of three independent experiments and shown as a histogram. Expression of endogenous and extrogenous SAMHD1 proteins was verified by Western blotting. Cell culture medium containing progeny virus was incubated with naïve Huh7.5.1 cells for an additional 72 h and detected HCV core proteins by immunofluorescence staining. Representative images are shown (cells > 10), Bars, 5 μm **(E)**. *P<0.05; **P<0.01, and ***P<0.001.

10.3389/fimmu.2022.1007718

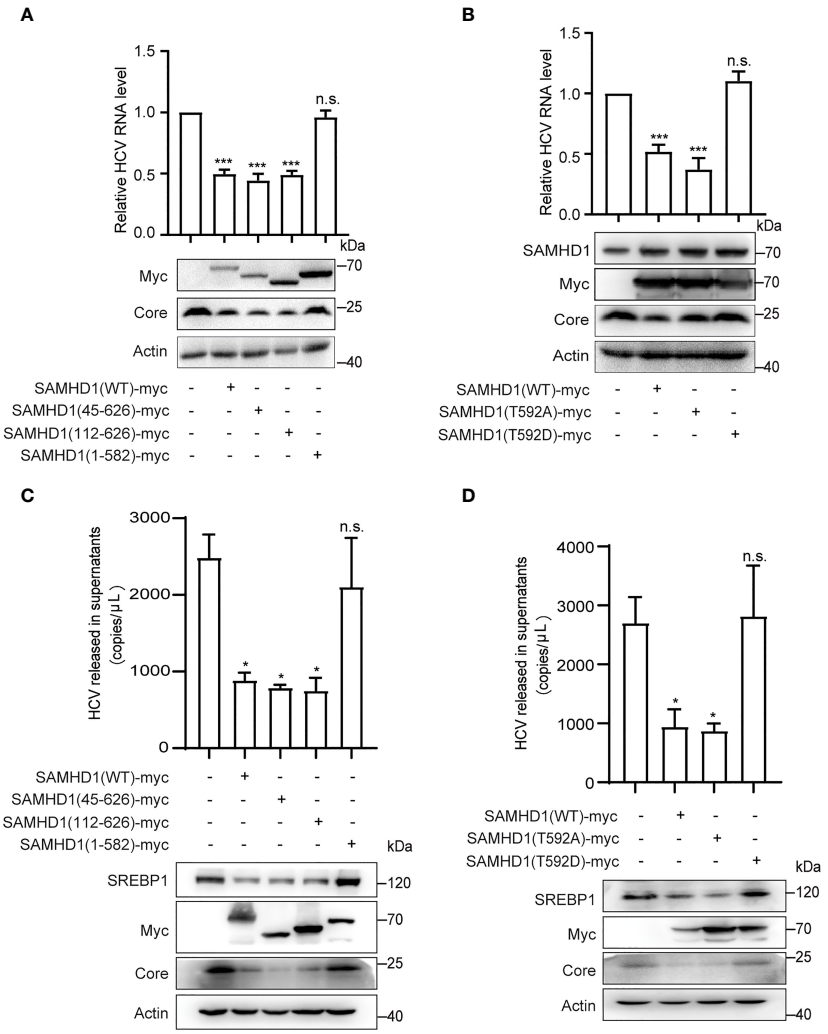

FIGURE 5
The C-terminus of SAMHD1 is essential for its anti-HCV activity. **(A, B)** Normal Huh7.5.1 cells were respectively transfected with plasmids expressing SAMHD1 truncations [SAMHD1(45–626), SAMHD1(112–626), and SAMHD1(1–582)] **(A)** or SAMHD1 mutants [SAMHD1(T592A) and SAMHD1(T592D)] **(B)**, and followed by infection with JFH1 HCVcc for 48 h. Cell lysates were examined by Western blotting to determine the expression of SAMHD1 and HCV proteins. Replication levels of HCV RNA in infected cells were isolated and quantified by qRT-PCR. **(C, D)** SAMHD1-KO Huh7.5.1 cells were respectively transfected with plasmids expressing SAMHD1 truncations [SAMHD1(45–626), SAMHD1(112–626), and SAMHD1(1–582)] **(C)** and SAMHD1 mutants [SAMHD1(T592A) and SAMHD1(T592D)] **(D)** and infected with JFH1 HCVcc for 48 h. HCV RNA in culture medium was isolated and quantified by qRT-PCR. Cells were harvested for detection of protein expression by Western blotting. All data are representative of three independent experiments and shown as mean ± SD. ns, not significant; *P<0.05, and ***P<0.001

followed by infection with JFH1 HCVcc. Consistent with the anti-HCV activities in normal Huh7.5.1 cells, only 1–582 truncation and T592D mutant totally lost their inhibition on HCV replication; in addition, they also exerted little effect on SREBP1 protein expression, suggesting a strong correlation between the downregulation of SREBP1 and the inhibition of HCV replication by SAMHD1 (Figures 5C, D).

To reinforce such correlation, we also explored functions of SAMHD1 truncations in the formation of LDs by immunofluorescence analysis. Compared with wild-type SAMHD1, 45–626 and 112–626 truncations that are able to inhibit HCV replication reduced the amounts of LDs, whereas the 1–582 truncation weakly obstructed LD formation (Figure S1). These data together provide robust evidence on the role of SAMHD1 in SREBP1 downregulation and LD decrease, which are correlated with their antiviral functions.

SAMHD1 impairs RNA replication of HCV

Furthermore, we found that overexpressing SAMHD1 in the Huh7 replicon cell line also resulted in inhibition on HCV NS3 expression (Figure 6A). This provides evidence supporting that SAMHD1 mainly affects viral gene expression at the stage of

10.3389/fimmu.2022.1007718

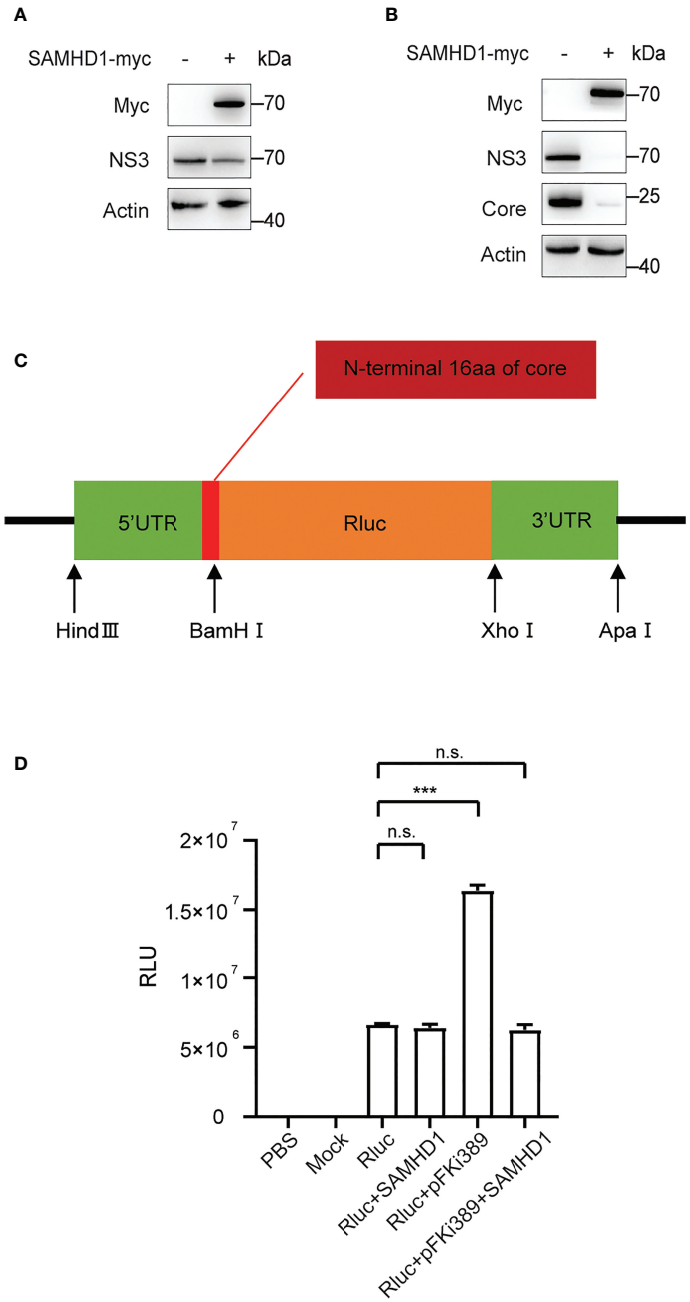

FIGURE 6
Effect of SAMHD1 on HCV replication and translation. **(A)** Huh7 replicon cells were transfected with plasmid expressing SAMHD1 for 48 h. Cell lysates were analyzed by Western blotting to determine the expression level of NS3 protein. Data are representative of three independent experiments. **(B)** Huh7.5.1 cells were co-transfected with plasmid of SAMHD1 and JFH1 HCVcc RNA transcripted *in vitro*. At 48 h post-transfection, HCV NS3 and core proteins in cells were detected by Western blotting to determine inhibition on HCV replication by SAMHD1. This experiment has been repeated three times. **(C)** Schematic presentation of HCV IRES-mediated luciferase reporter system. **(D)** pFKi389 containing all non-structural proteins was co-transfected with or without pSAMHD1-myc into Huh7.5.1 cells; after 24 h incubation, all cells of test groups but not control groups were transfected with HCV IRES-mediated luciferase mRNA for another 24 h. The values of Renilla luciferase (RLU) activity were measured and used to assess translation or replication level of HCV RNA under circumstances of SAMHD1 overexpression. Data are indicated as mean ± SD (n = 3). ns, not significant; ***P<0.001.

transcription or (and) translation. In agreement with the hypothesis, we observed a similar inhibition of viral NS3 and core expression by SAMHD1 in cells transfected with *in vitro* transcripted HCV genomic RNA (Figure 6B), which warrants no entry step-involved viral gene expression.

To validate the above hypothesis, we cloned the HCV 5'UTR and 3'UTR into the upstream and downstream of the Renilla luciferase reporter gene, respectively, to construct a reporter gene translation system mediated by HCV IRES (Figure 6C). The system contains the complete HCV 5'UTR and 3'UTR and mimics the HCV replication process by providing HCV nonstructural proteins in trans. We obtained the mRNA of Renilla luciferase containing HCV IRES by *in vitro* transcription and then transfect ion into Huh7.5.1 cells with SAMHD1 or pFKi389 (a replicon that contains all non-structural proteins from NS3 to NS5B), or co- transfection of SAMHD1 and pFKi389, and investigated the mRNA levels by testing the luciferase activity (Figure 6D). The results showed that the RLU reading of the Rluc+pFKi389 group was doubled compared with the Rluc group, indicating that the luciferase reporter system could be transactivated to mimic HCV RNA replication. First, we found that the expression of SAMHD1 had no significant effect on RLU readings in the absence of HCV nonstructural proteins, suggesting that SAMHD1 does not affect the IRES-mediated translation. However, SAMHD1 drastically reduced the RLU reading when the luciferase reporter system is transactivated. The above results further confirm that SAMHD1 does not affect the IRES-mediated translation process but inhibits the RNA replication process, thereby inhibiting the expression of viral proteins.

Supplementary lipid counteracts the anti-HCV activity of SAMHD1

To explore if the anti-HCV effect of SAMHD1 is related to its ability to decrease intracellular dNTPs, we examined whether recruitment of dNTPs would rescue HCV replication in SAMHD1-transfected Huh7 replicon cells. Results showed that expression levels of HCV proteins did not increase when compared with that of the control group (Figure 7A), suggesting that the antagonism of SAMHD1 on HCV infection is not achieved by reducing intracellular dNTP levels, and other mechanisms may exist.

It was previously reported in the literature that HCV infection can activate the expression of SREBPs, FA synthetase (FASN), and other genes involved in the lipid synthesis and transportation. Inhibition of the activity of SREBPs and FASN blocks the replication of HCV RNA and the production of infectious virus particles. SAMHD1 inhibits the expression of SREBP1, which probably results in inhibiting HCV RNA replication. Based on the above conjecture, we co-transfected the SAMHD1 and SREBP1 plasmids in Huh7.5.1 cells or SAMHD1-KO Huh7.5.1 cells followed by infection with JFH1 HCVcc to observe whether the inhibitory effect of SAMHD1 on HCV changed. As expected, the results of our Western blotting and qRT-PCR assays further confirmed that the supplementary SREBP1 plasmid counteracts the anti-HCV activity of SAMHD1 (Figures 7B, C). A similar result was obtained when rescuing LD s (Figures 7D, E). Without interference of endogenous SAMHD1, the level of HCV production in the presence of extrogenous SAMHD1 proteins rescued by extrogenous expression of SREBP1 or addition of LDs was more obvious ly observed (Figures 7F, G), which suggests that SAMHD1 suppresses the host cholesterol and FA biosynthesis pathways by downregulating the expression of SREBP1 to inhibit HCV replication.

Discussion

Innate immunity is at the forefront of cellular defense that monitors and recognizes viruses and is characterized by IFN stimulation. SAMHD1 is discovered early as an antiviral ISG, widely existing in eukaryotes and prokaryotes, and highly homologous. At present, the study of the antiviral function of SAMHD1 mainly focuses on retrovirus and some DNA virus, and few studies focus on other kinds of virus (24, 25). Our work expands the antiviral spectrum of SAMHD1 to RNA virus including HCV, JEV, and DENV, suggesting that SAMHD1 has evolved to negatively regulate a wide range of different pathogenic viruses, thus playing a crucial function in innate immunity. We note that SAMHD1 moderately inhibits HCV or JEV compared with HIV or other DNA viruses. One possibility is that these viruses evolved a partial resistance to SAMHD1 during a long evolutionary process (26). The other possibility is that some other host factors induced by type1 IFN, such as CypA, assist in the formation of HCV replicase complex or guard HIV nucleic acids from cytosolic sensors, which counters the inhibition of SAMHD1 (27).

SAMHD1 significantly enhances the antiviral immune response and regulates the IFN-induced inflammatory response involved in the host–virus defense system (28–30). At present, SAMHD1 is considered to restrict HIV-1 reverse transcription by hydrolyzing the majority of cellular dNTPs below the concentration needed for efficient catalysis by viral enzymes through its dNTPase activity. The addition of exogenous dNTPs or knockdown of SAMHD1 partially reverses such inhibition (31). Moreover, HIV Vpx also accelerates ubiquitination of SAMHD1 and is marked for proteasomal degradation (6, 32). However, this strategy of protecting host from virus infection through depletion of dNTPs hardly explains the entirety of SAMHD1's antiviral functionality (33). Our work suggests a new antiviral strategy of SAMHD1 through impairing lipid synthesis independent of decreasing dNTP pools, providing new evidence supporting the multi-antiviral activities of SAMHD1.

The phosphorylation of SAMHD1 at T592 has been shown to be involved in multiple cellular processes, including tetramer association, cell cycle phase and dissociation, expedited regulatory

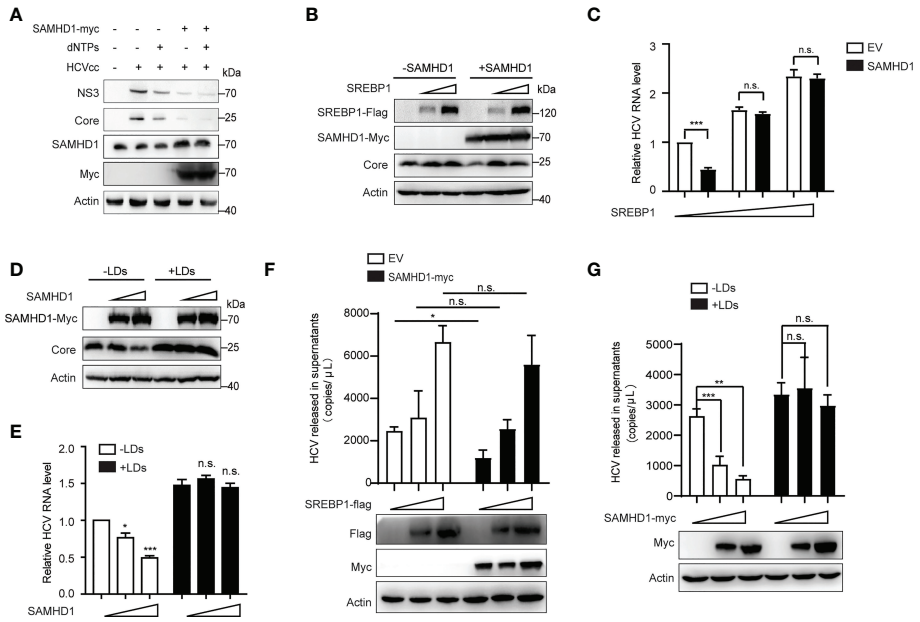

FIGURE 7
Supplementary lipid rescues HCV replication inhibited by SAMHD1. **(A)** pSAMHD1-myc or pcDNA4.0 was transfected into Huh7 replicon cells with or without the addition of 10 μM dNTPs and cultured for 48 h. Expression levels of HCV core and NS3 proteins were determined by Western blotting (n = 3). **(B)** Plasmids encoding SREBP1-flag were co-transfected with pSAMHD1-myc into Huh7.5.1 cells and followed by infection with JFH1 HCVcc (MOI = 0.2) for an additional 72 h. Expression of HCV core protein detected by Western blotting was used to evaluate the HCV replication level. **(C)** HCV RNA in cells was isolated for qRT-PCR analysis. Cells in the control group were transfected with the same amount of empty vector. Values of qRT-PCR are shown as means ± SD (n = 3) and the value of the control group is set to 1. **(D)** Huh7.5.1 cells were transfected with pSAMHD1-myc followed by infection with JFH1 HCVcc (MOI = 0.2) in the presence of 100 μg/ml LDs for an additional 72 h. Expression of HCV core protein in cells detected by Western blotting was used to measure HCV infection level. **(E)** HCV RNA in cells was extracted for qRT-PCR analysis. Data are representative of three independent experiments and shown as means ± SD. **(F)** Plasmids encoding SREBP1-flag were transfected into SAMHD1-KO Huh7.5.1 cells with or without extrogenous SAMHD1 expression and followed by infection with JFH1 HCVcc (MOI = 0.2) for an additional 72 h. HCV RNA in culture medium was isolated for qRT-PCR analysis. Values of qRT-PCR are shown as means ± SD (n = 3). Expression of extrogenous proteins was detected by Western blotting. **(G)** SAMHD1-KO Huh7.5.1 cells were transfected with pSAMHD1-myc followed by infection with JFH1 HCVcc (MOI = 0.2) in the presence of 100 μg/ml LDs for an additional 72 h. Progeny virus RNA in supernatants was extracted for qRT-PCR analysis. Data are representative of three independent experiments and shown as means ± SD. Expression of extrogenous proteins was analyzed by Western blotting. ns, not significant; *P<0.05, **P<0.01, and ***P<0.001.

nucleotide release, and antiviral activity. All types of IFNs share activation of SAMHD1 *via* dephosphorylation at T592 (14, 34, 35). Similarly, our work showed that T592 phosphorylation significantly reduced the anti-HCV effect of SAMHD1. These results together suggest the crucial role of this key site in IFN-mediated innate immunity against different viruses.

IFNs are multifunctional cytokines that widely manipulate intracellular processes to defend virus infection. There is no doubt that viruses may participate in manipulating the cholesterol and FA synthesis to support their replication (36). Viral replication is a high-energy-demanding process; thus, they modulate not only FAs but also cholesterol to provide ATP and use lipids for their nucleic acid production (36–38). Recent studies have shown that an antiviral pathway of IFN seems to be related to impairment of lipid biosynthesis (39). Studies subsequently indicate that IFN can directly inhibit transcription and expression of SREBPs *via* IFNAR1 or stimulate a series of ISGs to realize the inhibition of lipid synthesis (40). We surprisingly discover that SAMHD1 possesses such function of downregulation of lipid production likely through restraining SREBP1 transcription. The inhibition of whole lipid metabolism contributes to the reduction of LDs. Such a cascade of reactions caused by SAMHD1 finally leads to the crush of HCV RNA replication. This discovery has been regarded as a participant in innate immunity and extensively addressed the biochemical functions of SAMHD1. Collectively, SAMHD1 impairing lipid metabolism for viral inhibition is considered as a fresh supplement for cellular innate immunity regulated by IFN.

Data availability statement

The original contributions presented in the study are included in the article/Supplementary Material. Further inquiries can be directed to the corresponding authors.

Author contributions

SC, LY, and DY conceptualized and supervised the study. QL, XL, FG, and CL performed formal analysis and carried out the investigation. NA, QG, and HS performed the main experiments. SC and DY wrote the original draft and reviewed the manuscript. All authors contributed to the article and approved the submitted version.

Funding

This work was supported by the National Natural Science Foundation of China 81902075 (to DY) and CAMS Innovation Fund for Medical Sciences 2021-I2M-1-038 (to SC), 2021-I2M-1-030 (to QL), and 2021-I2M-1-043 (to XL).

Conflict of interest

The authors declare that the research was conducted in the absence of any commercial or financial relationships that could be construed as a potential conflict of interest.

Publisher's note

Supplementary material

The Supplementary Material for this article can be found online at: https://www.frontiersin.org/articles/10.3389/fimmu.2022.1007718/full#supplementary-material

SUPPLEMENTARY FIGURE 1
Effects of SAMHD1 truncations on the formation of LDs. Huh7.5.1 cells with extrogenous SAMHD1 truncations [SAMHD1(45–626), SAMHD1(112–626), and SAMHD1(1–582)] overexpressing were measured by immunofluorescence staining. LDs, SAMHD1, and nucleus were respectively stained with BODIPY493/503 (green), anti-myc antibody (red), and DAPI (blue). Representative images are shown. Bars, 5 μm.

SUPPLEMENTARY TABLE 1
Genome-wide gene expression profile analysis of SAMHD1 overexpressing Huh7.5.1 cells

SUPPLEMENTARY TABLE 2
Description of genes associated with lipid metabolism in Figure 1A.

References

1. Fritsch SD, Weichhart T. Effects of Interferons and Viruses on Metabolism. *Front Immunol* (2016) 7:630. doi: 10.3389/fimmu.2016.00630

2. Blanc M, Hsieh WY, Robertson KA, Kropp KA, Forster T, Shui G, et al. The Transcription Factor Stat-1 Couples Macrophage Synthesis of 25-Hydroxycholesterol to the Interferon Antiviral Response. *Immunity* (2013) 38 (1):106–18. doi: 10.1016/j.immuni.2012.11.004

3. Mounce BC, Poirier EZ, Passoni G, Simon-Loriere E, Cesaro T, Prot M, et al. Interferon-Induced Spermidine-Spermine Acetyltransferase and Polyamine Depletion Restrict Zika and Chikungunya Viruses. *Cell Host Microbe* (2016) 20 (2):167–77. doi: 10.1016/j.chom.2016.06.011

4. Mellor AL, Munn DH. Ido Expression by Dendritic Cells: Tolerance and Tryptophan Catabolism. *Nat Rev Immunol* (2004) 4(10):762–74. doi: 10.1038/nri1457

5. Li N, Zhang W, Cao X. Identification of Human Homologue of Mouse Ifn-Gamma Induced Protein from Human Dendritic Cells. *Immunol Lett* (2000) 74 (3):221–4. doi: 10.1016/s0165-2478(00)00276-5

6. Laguette N, Sobhian B, Casartelli N, Ringeard M, Chable-Bessia C, Ségéral E, et al. Samhd1 Is the Dendritic- and Myeloid-Cell-Specific Hiv-1 Restriction Factor Counteracted by Vpx. *Nature* (2011) 474(7353):654–7. doi: 10.1038/nature10117

7. Powell RD, Holland PJ, Hollis T, Perrino FW. Aicardi-Goutieres Syndrome Gene and Hiv-1 Restriction Factor Samhd1 Is a Dgtp-Regulated Deoxynucleotide Triphosphohydrolase. *J Biol Chem* (2011) 286(51):43596–600. doi: 10.1074/jbc.C111.317628

8. Qiao F, Bowie JU. The Many Faces of Sam. *Science's STKE Signal transduction knowledge Environ* (2005) 2005(286):re7. doi: 10.1126/stke.2862005re7

9. Aravind L, Koonin EV. The Hd Domain Defines a New Superfamily of Metal-Dependent Phosphohydrolases. *Trends Biochem Sci* (1998) 23(12):469–72. doi: 10.1016/s0968-0004(98)01293-6

10. Goldstone DC, Ennis-Adeniran V, Hedden JJ, Groom HC, Rice GI, Christodoulou E, et al. Hiv-1 Restriction Factor Samhd1 Is a Deoxynucleoside Triphosphate Triphosphohydrolase. *Nature* (2011) 480(7377):379–82. doi: 10.1038/nature10623

11. Sliva K, Martin J, Von Rhein C, Herrmann T, Weyrich A, Toda M, et al. Interference with Samhd1 Restores Late Gene Expression of Modified Vaccinia Virus Ankara in Human Dendritic Cells and Abrogates Type I Interferon Expression. *J Virol* (2019) 93(22):e01097-19. doi: 10.1128/JVI.01097-19

12. Kim ET, White TE, Brandariz-Núñez A, Diaz-Griffero F, Weitzman MD. Samhd1 Restricts Herpes Simplex Virus 1 in Macrophages by Limiting DNA Replication. *J Virol* (2013) 87(23):12949–56. doi: 10.1128/jvi.02291-13

13. Wing PA, Davenne T, Wettengel J, Lai AG, Zhuang X, Chakraborty A, et al. A Dual Role for Samhd1 in Regulating Hbv Cccdna and Rt-Dependent Particle Genesis. *Life Sci alliance* (2019) 2(2):e201900355. doi: 10.26508/lsa.201900355

14. Cribier A, Descours B, Valadão AL, Laguette N, Benkirane M. Phosphorylation of Samhd1 by Cyclin A2/Cdk1 Regulates Its Restriction Activity toward Hiv-1. *Cell Rep* (2013) 3(4):1036–43. doi: 10.1016/j.celrep.2013.03.017

15. Martín-Acebes MA, Vázquez-Calvo Á, Saiz JC. Lipids and Flaviviruses, Present and Future Perspectives for the Control of Dengue, Zika, and West Nile Viruses. *Prog Lipid Res* (2016) 64:123–37. doi: 10.1016/j.plipres.2016.09.005

16. Mackenzie JM, Khromykh AA, Parton RG. Cholesterol Manipulation by West Nile Virus Perturbs the Cellular Immune Response. *Cell Host Microbe* (2007) 2(4):229–39. doi: 10.1016/j.chom.2007.09.003

17. Soto-Acosta R, Mosso C, Cervantes-Salazar M, Puerta-Guardo H, Medina F, Favari L, et al. The Increase in Cholesterol Levels at Early Stages after Dengue Virus Infection Correlates with an Augment in Ldl Particle Uptake and Hmg-Coa Reductase Activity. *Virology* (2013) 442(2):132–47. doi: 10.1016/j.virol.2013.04.003

18. Singh R, Kaushik S, Wang Y, Xiang Y, Novak I, Komatsu M, et al. Autophagy Regulates Lipid Metabolism. *Nature* (2009) 458(7242):1131–5. doi: 10.1038/nature07976

19. Saka HA, Valdivia R. Emerging Roles for Lipid Droplets in Immunity and Host-Pathogen Interactions. *Annu Rev Cell Dev Biol* (2012) 28:411–37. doi: 10.1146/annurev-cellbio-092910-153958

20. Rambold AS, Cohen S, Lippincott-Schwartz J. Fatty Acid Trafficking in Starved Cells: Regulation by Lipid Droplet Lipolysis, Autophagy, and

Mitochondrial Fusion Dynamics. *Dev Cell* (2015) 32(6):678–92. doi: 10.1016/j.devcel.2015.01.029

21. Walther TC, Farese RVJr.. Lipid Droplets and Cellular Lipid Metabolism. *Annu Rev Biochem* (2012) 81:687–714. doi: 10.1146/annurev-biochem-061009-102430

22. Zhou RH, Yao M, Lee TS, Zhu Y, Martins-Green M, Shyy JY. Vascular Endothelial Growth Factor Activation of Sterol Regulatory Element Binding Protein: A Potential Role in Angiogenesis. *Circ Res* (2004) 95(5):471–8. doi: 10.1161/01.Res.0000139956.42923.4a

23. Horton JD, Goldstein JL, Brown MS. Srebps: Activators of the Complete Program of Cholesterol and Fatty Acid Synthesis in the Liver. *J Clin Invest* (2002) 109(9):1125–31. doi: 10.1172/JCI15593

24. Gramberg T, Kahle T, Bloch N, Wittmann S, Müllers E, Daddacha W, et al. Restriction of Diverse Retroviruses by Samhd1. *Retrovirology* (2013) 10(1):1–12. doi: 10.1186/1742-4690-10-26

25. Hollenbaugh JA, Gee P, Baker J, Daly MB, Amie SM, Tate J, et al. Host Factor Samhd1 Restricts DNA Viruses in Non-Dividing Myeloid Cells. *PloS Pathog* (2013) 9(6):e1003481. doi: 10.1371/journal.ppat.1003481

26. Mohamed A, Bakir T, Al-Hawel H, Al-Sharif I, Bakheet R, Kouser L, et al. Hiv-2 Vpx Neutralizes Host Restriction Factor Samhd1 to Promote Viral Pathogenesis. *Sci Rep* (2021) 11(1):20984. doi: 10.1038/s41598-021-00415-2

27. Cobos Jiménez V, Booiman T, de Taeye SW, van Dort KA, Rits MA, Hamann J, et al. Differential Expression of Hiv-1 Interfering Factors in Monocyte-Derived Macrophages Stimulated with Polarizing Cytokines or Interferons. *Sci Rep* (2012) 2:763. doi: 10.1038/srep00763

28. Rice GI, Bond J, Asipu A, Brunette RL, Manfield IW, Carr IM, et al. Mutations Involved in Aicardi-Goutières Syndrome Implicate Samhd1 as Regulator of the Innate Immune Response. *Nat Genet* (2009) 41(7):829–32. doi: 10.1038/ng.373

29. Behrendt R, Schumann T, Gerbaulet A, Nguyen LA, Schubert N, Alexopoulou D, et al. Mouse Samhd1 Has Antiretroviral Activity and Suppresses a Spontaneous Cell-Intrinsic Antiviral Response. *Cell Rep* (2013) 4(4):689–96. doi: 10.1016/j.celrep.2013.07.037

30. Maelfait J, Bridgeman A, Benlahrech A, Cursi C, Rehwinkel J. Restriction by Samhd1 Limits Cgas/Sting-Dependent Innate and Adaptive Immune Responses to Hiv-1. *Cell Rep* (2016) 16(6):1492–501. doi: 10.1016/j.celrep.2016.07.002

31. Lahouassa H, Daddacha W, Hofmann H, Ayinde D, Logue EC, Dragin L, et al. Samhd1 Restricts the Replication of Human Immunodeficiency Virus Type 1 by Depleting the Intracellular Pool of Deoxynucleoside Triphosphates. *Nat Immunol* (2012) 13(3):223–8. doi: 10.1038/ni.2236

32. Hrecka K, Hao C, Gierszewska M, Swanson SK, Kesik-Brodacka M, Srivastava S, et al. Vpx Relieves Inhibition of Hiv-1 Infection of Macrophages Mediated by the Samhd1 Protein. *Nature* (2011) 474(7353):658–61. doi: 10.1038/nature10195

33. Mauney CH, Hollis T. Samhd1: Recurring Roles in Cell Cycle, Viral Restriction, Cancer, and Innate Immunity. *Autoimmunity* (2018) 51(3):96–110. doi: 10.1080/08916934.2018.1454912

34. Wittmann S, Behrendt R, Eissmann K, Volkmann B, Thomas D, Ebert T, et al. Phosphorylation of Murine Samhd1 Regulates Its Antiretroviral Activity. *Retrovirology* (2015) 12:103. doi: 10.1186/s12977-015-0229-6

35. Pauls E, Jimenez E, Ruiz A, Permanyer M, Ballana E, Costa H, et al. Restriction of Hiv-1 Replication in Primary Macrophages by Il-12 and Il-18 through the Upregulation of Samhd1. *J Immunol (Baltimore Md 1950)* (2013) 190(9):4736–41. doi: 10.4049/jimmunol.1203226

36. Yu Y, Clippinger AJ, Alwine JC. Viral Effects on Metabolism: Changes in Glucose and Glutamine Utilization During Human Cytomegalovirus Infection. *Trends Microbiol* (2011) 19(7):360–7. doi: 10.1016/j.tim.2011.04.002

37. Robinzon S, Dafa-Berger A, Dyer MD, Paeper B, Proll SC, Teal TH, et al. Impaired Cholesterol Biosynthesis in a Neuronal Cell Line Persistently Infected with Measles Virus. *J Virol* (2009) 83(11):5495–504. doi: 10.1128/jvi.01880-08

38. Zheng YH, Plemenitas A, Fielding CJ, Peterlin BM. Nef Increases the Synthesis of and Transports Cholesterol to Lipid Rafts and Hiv-1 Progeny Virions. *Proc Natl Acad Sci United States America* (2003) 100(14):8460–5. doi: 10.1073/pnas.1437453100

39. Blanc M, Hsieh WY, Robertson KA, Watterson S, Shui G, Lacaze P, et al. Host Defense against Viral Infection Involves Interferon Mediated Down-Regulation of Sterol Biosynthesis. *PloS Biol* (2011) 9(3):e1000598. doi: 10.1371/journal.pbio.1000598

40. Brown MS, Goldstein JL. The Srebp Pathway: Regulation of Cholesterol Metabolism by Proteolysis of a Membrane-Bound Transcription Factor. *Cell* (1997) 89(3):331–40. doi: 10.1016/s0092-8674(00)80213-5

Frontiers in Immunology

Explores novel approaches and diagnoses to treat immune disorders. The official journal of the International Union of Immunological Societies (IUIS) and the most cited in its field, leading the way for research across basic, translational and clinical immunology.

Discover the latest Research Topics

See more →

Frontiers

Avenue du Tribunal-Fédéral 34
1005 Lausanne, Switzerland
frontiersin.org

Contact us

+41 (0)21 510 17 00
frontiersin.org/about/contact